

2013-01-01

Geology and Geochemistry of the Sierra Blanca Rare Earth Complex, Sierra Blanca, Texas

Nicole Kyger

University of Texas at El Paso, n.kyger@gmail.com

Follow this and additional works at: https://digitalcommons.utep.edu/open_etd



Part of the [Geology Commons](#)

Recommended Citation

Kyger, Nicole, "Geology and Geochemistry of the Sierra Blanca Rare Earth Complex, Sierra Blanca, Texas" (2013). *Open Access Theses & Dissertations*. 1857.

https://digitalcommons.utep.edu/open_etd/1857

This is brought to you for free and open access by DigitalCommons@UTEP. It has been accepted for inclusion in Open Access Theses & Dissertations by an authorized administrator of DigitalCommons@UTEP. For more information, please contact lweber@utep.edu.

GEOLOGY AND GEOCHEMISTRY OF THE SIERRA BLANCA RARE
EARTH COMPLEX, SIERRA BLANCA, TEXAS

NICOLE KYGER

Department of Geological Sciences

APPROVED:

Philip C. Goodell, Ph.D., Chair

Nicholas E. Pingitore, Ph.D.

Josiah M. Heyman, Ph.D.

Benjamin C. Flores, Ph.D.
Dean of the Graduate School

Copyright ©

by

Nicole Kyger

2013

GEOLOGY AND GEOCHEMISTRY OF THE SIERRA BLANCA RARE
EARTH COMPLEX, SIERRA BLANCA, TEXAS

by

NICOLE KYGER, BA Summa Cum Laude, University of Colorado

THESIS

Presented to the Faculty of the Graduate School of
The University of Texas at El Paso
in Partial Fulfillment
of the Requirements
for the Degree of

MASTER OF SCIENCE

Department of Geological Sciences
THE UNIVERSITY OF TEXAS AT EL PASO

May 2013

ACKNOWLEDGEMENTS

This thesis would not have been possible without the assistance of many people.

I would like to acknowledge and thank my thesis committee for their time, patience and efforts; Dr. Phil Goodell, Dr. Nick Pingitore, Dr. Josiah Heyman. I appreciate your time and support in this endeavor. Without the enthusiasm and support of Dr. Goodell I may have never become interested in the rare earth elements and the unique deposit of Sierra Blanca, TX. Thank you for all your input, advice, and support during the time it took to complete this thesis. To my husband, Robert Kyger, for his continued support and belief in my capabilities, you have my eternal gratitude; I could not have completed this without you covering my six. My father, Dr. Bernhard Free piqued my interest in geology at a young age and without his support I may not have returned to attempt a master's degree, thank you is not enough for all you have done. I would like to thank Dan Gorski, Stanley Korzeb, and Texas Rare Earth Resources for financial assistance, sample analysis, and for allowing me access to the laccoliths and data. Thank you, Richard Morris, for always reminding me to measure first and wave my arms later, and I will never forget that when things do not go according to plan "It's a drill program". Clay Newton and Zachary Black of Gustavson Associates offered advice in the early stages that helped further my research and writing. Life in Sierra Blanca was made much more enjoyable by Jamie and Ricky May and Joe and Sharon Tammen who offered access to their ranch, good food, and allowed me to stay at the guest house whenever necessary.

ABSTRACT

With an increasing standard of living comes an increase in demand for high tech goods, environmentally friendly (green) and military technologies, and the inherent need to procure the necessary raw materials. Demand for the rare earth elements (REE) is on the rise, and there is no foreseeable decline in the need for accessible deposits. Between 2010 and present, the United States Congress has heard numerous reports on the importance of REE, and in 2012 the Department of Defense(DoD)declared REE a critical resource, with implications for national security. The Sierra Blanca laccoliths, 150 kilometers southeast of El Paso, TX represent a potential low grade/high tonnage deposit that is especially interesting due to the high heavy rare earth content. Previous work has suggested that the Sierra Blanca laccoliths offer a unique opportunity to explore and develop a domestic source of this critical resource

Thorough geologic mapping of the laccoliths has allowed previously unmapped structures and contacts to be associated with geochemical data from whole rock and trace analyses of 70 rhyolite surface samples. Detailed information about the concentration, zoning, and dispersion of REE are incorporated into a characterization of the deposit, showing an enrichment of REE throughout the laccoliths, with late stage enrichment through the action of F-rich fluids evident at the contact and fracture zones. Yttrifluorite is the major REE bearing mineral, with minor amounts of xenotime and bastnäsite being found primarily on Round Top Mountain. The Sierra Blanca laccoliths represent a new REE deposit type, and with an understanding of the geology and geochemistry associated with the Sierra Blanca REE deposit, this research creates a basis for future exploration in the search for domestic sources of this critical resource.

TABLE OF CONTENTS

ACKNOWLEDGEMENTS	iv
ABSTRACT	v
TABLE OF CONTENTS.....	vi
LIST OF TABLES.....	viii
LIST OF FIGURES	ix
INTRODUCTION.....	11
Location.....	16
Geology- Regional	18
Geology - Local	21
Previous Work	24
STATEMENT OF PROBLEM.....	28
Objective	30
METHODS.....	31
Geological Mapping.....	32
Cross-Sections	35
Remote Sensing and Geophysics.....	36
Sampling.....	39
Geochemical Analysis.....	41
Statistical Analysis.....	43
DATA.....	46
Geological Maps and Cross-Sections	46
Geochemical Distribution Maps	50
Element distribution across profiles.....	69
Sample Data.....	84
Petrological Diagrams	89
Statistics	95
DISCUSSION.....	103
Geology	103
Geochemistry	105

CONCLUSIONS	108
Future Work.....	110
REFERENCES	111
APPENDIX I: ABBREVIATIONS USED	115
APPENDIX II: SAMPLE LOCATION	116
APPENDIX III: CONSTITUENT MAPS	117
APPENDIX IV: RATIO MAPS	148
APPENDIX V: HISTOGRAMS	181
APPENDIX VI: CORRELATION COEFFICIENTS	305
APPENDIX VII: SCATTERGRAMS	341
APPENDIX VIII: FACTOR ANALYSIS	352
VITA.....	355

LIST OF TABLES

Table 1.1: Abundance of common ore metals in igneous rocks in ppm (modified after Guilbert and Park, 1986)	13
Table 1.2: Average crustal abundance of Elements indicated in weight % and in ppm for less abundant elements (modified after Mason and Moore, 1982)	13
Table 3.1: Methods used to accomplish objectives of study.....	31
Table 3.3: Sample Identification and labeling	40
Table 3.4: Elements and Oxides analyzed (from ALS Geochemistry Service Schedule 2013)	41
Table 3.6: Removed samples and outliers	43
Table 3.7: List of removed and retained constituents.....	45
Table 3.8: Statistical analyses performed on geochemical data collected from each laccolith	45
Table 4.1: Sample location, number collected	84
Table 4.2: Element Quantity by location (REE in bold).....	84
Table 4.3: Oxide Quantity by Location	84
Table 4.4: Rhyolite outliers: elements (ppm).....	85
Table 4.5: Rhyolite outliers: major oxide components (wt. %)	86
Table 4.6: Chemical composition (wt. %) of SB Laccoliths compared to average of topaz rhyolites (adapted from Christiansen, et al., 1983).....	86
Table 4.7: Comparison of average REE in weathered and fresh samples	87
Table 4.8: Eu/Eu* calculation (from GCDToolkit, Janoušek, et al., 2006).....	87
Table 4.9: Standard Statistics for REE: Little Blanca, Little Round Top, Round Top	95
Table 4.10: Standard Statistics for REE: Rhyolite outliers.....	96
Table 4.11: Means of elements and oxides by location (trace elements in ppm, oxides in weight %, REE in bold)	97
Table 4.12: Factor analysis and loading scores	102

LIST OF FIGURES

Fig. 1.1: Periodic table of the elements, showing the lanthanide series (REE) in light blue (http://www.iupac.org).....	12
Fig. 1.2: Location of the Sierra Blanca laccoliths	17
Fig. 1.3: Regional Tectonic and Physiographic features (modified after Muehlberger, 1980; Carciumaru and Ortega, 2008; Ortega and Carciumaru, 2010)	19
Fig. 1.4: Detail of Geologic Atlas of Texas, Van Horn-El Paso Sheet (Revised 1983)	20
Fig. 1.5: Stratigraphic Column: Descriptions modified after http://mrdata.usgs.gov/geology ; Hulse, et al. 2012.	21
Fig. 1.6: Massive fluorite (purple) in heavily brecciated zone at the rhyolite/limestone contact. Exposure in a prospect trench on the north flank of Round Top. Tag is approximately 10cm. (Photo: N. Kyger) ..	23
Fig. 1.7: Detail of the Albritton and Smith (1965) geologic map, showing of the Sierra Blanca laccoliths (Kf: Finlay Limestone; Kw: Rocks of Washita age; Tds Dikes and sills; Tr: Rhyolite and rhyolite porphyry; QTb: Basin deposits Qc: Older colluvium; Qm: Madden Gravel; Qba: Balluco Gravel; Qa: Alluvium)	24
Fig. 1.8: Test adit on northwest flank of Round Top. (Photo: N. Kyger)	26
Fig. 3.1: Typical terrain on the flanks of the Sierra Blanca laccoliths. (Photo: N. Kyger).....	32
Fig. 3.2: Abrupt change in slope and typical scree slope associated with it (Photo: N. Kyger)	33
Fig. 3.3: Historical image of (left to right) Round Top, Little Round Top and Little Blanca. Differences in color are indicative of inferred contact and faults (Image: Google Earth TM).....	36
Fig. 3.4: Alteration zones (left) and enhanced structure (right)	37
Fig. 3.5: Geology and inferred faults superimposed upon aeromagnetic survey image.....	38
Fig. 3.6: Location of samples collected for analysis. Quitman Stock is to south of image	39
Fig. 3.7: Location of removed samples and outliers showing proximity to contact or faults	44
Fig. 4.1: Geological map of the Sierra Blanca Laccoliths with cross-sections, focusing on Little Blanca, Little Round Top, and Round Top.....	46
Fig. 4.2: Geological Cross sections of the laccoliths: A) Little Blanca, B) Little Round Top, C) Round Top.....	49
Fig. 4.3: F distribution	50
Fig. 4.4: Y distribution.....	51
Fig. 4.5: La distribution	52
Fig. 4.6: Ce distribution	53
Fig. 4.7: Dy distribution.....	54
Fig. 4.8: Lu distribution	55
Fig. 4.9: U distribution.....	56
Fig. 4.10: Na ₂ O distribution	57
Fig. 4.11: Al ₂ O ₃ distribution	58
Fig. 4.12: P ₂ O ₅ distribution	59
Fig. 4.13: SiO ₂ distribution	60
Fig. 4.14: K ₂ O/SiO ₂	61
Fig. 4.15: Na ₂ O/SiO ₂	62
Fig. 4.16: La/Yb ratio distribution.....	63
Fig. 4.17: La/F ratio distribution	64
Fig. 4.18: Ce/Yb ratio distribution.....	65
Fig. 4.19: Nd/Yb ratio distribution	66
Fig. 4.20: La/Lu ratio distribution	67

Fig. 4.21: Map showing increasing Eu/Eu* magnitude from SB-LB-LRT-RT	68
Fig. 4.22: Samples projected onto plane of profile – Little Blanca: Inferred Fault, Contact.....	69
Fig. 4.23: La profile – Little Blanca: Inferred Fault, Contact	70
Fig. 4.24: Gd profile – Little Blanca: Inferred Fault, Contact	71
Fig. 4.25: Lu profile – Little Blanca: Inferred Fault, Contact.....	72
Fig. 4.26: La/Lu ratio profile – Little Blanca	73
Fig. 4.27: Samples projected onto plane of profile – Little Round Top: Inferred Fault, Contact.....	74
Fig. 4.28: La profile – Little Round Top: Inferred Fault, Contact	75
Fig. 4.29: Gd profile – Little Round Top: Inferred Fault, Contact.....	76
Fig. 4.30: Lu profile – Little Round Top: Inferred Fault, Contact	77
Fig. 4.31: La/Lu ratio profile – Little Round Top	78
Fig. 4.32: Samples projected onto plane of profile – Round Top: Inferred Fault, Contact	79
Fig. 4.33: La profile – Round Top: Inferred Fault, Contact.....	80
Fig. 4.34: Gd profile – Round Top: Inferred Fault, Contact.....	81
Fig. 4.35: Lu profile – Round Top: Inferred Fault, Contact	82
Fig. 4.36: La/Lu ratio profile – Round Top	83
Fig. 4.37: Increasing Eu anomaly magnitude.....	88
Fig. 4.38: Petrological classification of samples based on geochemistry (Pink: Sierra Blanca, Red: Little Blanca, Green: Round Top, Blue: Little Round Top)	89
Fig. 4.39: Geotectonic classification of the Sierra Blanca rhyolites (Pink: Sierra Blanca, Red: Little Blanca, Green: Round Top, Blue: Little Round Top)	90
Fig. 4.40: Alumina saturation plot (Pink: Sierra Blanca, Red: Little Blanca, Green: Round Top, Blue: Little Round Top)	91
Fig. 4.41: REE chondrite normalized spider diagram of average REE for all laccoliths (Pink: Sierra Blanca, Red: Little Blanca, Green: Round Top, Blue: Little Round Top)	92
Fig. 4.42: Major oxide components of Sierra Blanca	93
Fig. 4.43: Major oxide components of Little Blanca.....	93
Fig. 4.44: Major oxide components of Little Round Top	94
Fig. 4.45: Major oxide components of Round Top	94
Fig. 4.46: Histogram of Dy for A) Little Blanca, B) Little Round Top, C) Round Top	99
Fig. 4.47: Scattergram of La-vs.-F and La-vs.-Y showing LREE enrichment on Little Blanca.....	100
Fig. 4.48 Scattergram of Lu -vs. - F and Lu - vs. - Y showing HREE enrichment of Little Round Top and Round Top, and relative HREE depletion of Little Blanca	101
Fig. 5.1: Tectonic schematic of the emplacement of the Sierra Blanca laccoliths.	104

INTRODUCTION

The rare earth elements (REE) comprise the Lanthanide series on the periodic table of elements, from lanthanum (La, atomic number 57) to lutetium (Lu, atomic number 71). The elements scandium and yttrium are often included with the REE due to their association with REE deposits and chemical similarity (Figure 1.1). Chemically, REE are incompatible trace elements, with decreasing ionic radius as atomic number increases from La to Lu, a similar outer electron orbit configuration, and are unsuitable in size or charge to the cation sites of common minerals. REE are classified as lithophile, and in an equilibrium system of minerals and coexisting silicate melt, are preferentially partitioned into melt (Long, *et al.*, 2010; <http://ocw.mit.edu>). The REE can be separated by mass into the light rare earths (LREE/Cerium group: La – Sm,) and the heavy rare earths (HREE/ Yttrium group: Eu – Lu). Rocks or magma showing enrichment in the REE are called fertile, while those showing strong depletion in REE are depleted (Alberède, 2003; Gambogi and Cordier, 2010). With stories of China's stranglehold on REE production and national security issues becoming commonplace, REE have gone from being a relatively obscure topic to one that is recognized by the general public, and discussed in the national and international media (Humphries, 2012). The first REE were discovered and described in Sweden in the late 18th century (Gschneidner, 1987), and it was not until the latter half of the 20th century that the lanthanide series was fully described (Spedding, 1961). The rare earth elements have numerous high-tech applications, such as, environmentally friendly “green” technologies, and military systems (computers, cell phones, LCD televisions, hybrid car batteries, wind turbines, missile targeting systems, and night vision equipment), and as a result, are in continuous demand. As the standard of living increases across the globe, the demand for products using REE is rising, and consequently, interest in discovering new, domestic sources is growing (Grasso, 2012).

1 H hydrogen [1.007; 1.008]	2 He helium 4.003	IUPAC Periodic Table of the Elements															
3 Li lithium [6.938; 6.997]	4 Be beryllium 9.012	Key: atomic number Symbol name standard atomic weight										5 B boron [10.80; 10.83]	6 C carbon [12.00; 12.02]	7 N nitrogen [14.00; 14.01]	8 O oxygen [15.99; 16.00]	9 F fluorine 19.00	10 Ne neon 20.18
11 Na sodium 22.99	12 Mg magnesium 24.31	13 Al aluminium 26.98	14 Si silicon [28.08; 28.09]	15 P phosphorus 30.97	16 S sulfur [32.05; 32.07]	17 Cl chlorine [35.44; 35.46]	18 Ar argon 39.96										
19 K potassium 39.10	20 Ca calcium 40.08	21 Sc scandium 44.96	22 Ti titanium 47.87	23 V vanadium 50.94	24 Cr chromium 52.00	25 Mn manganese 54.94	26 Fe iron 55.85	27 Co cobalt 58.93	28 Ni nickel 58.69	29 Cu copper 63.55	30 Zn zinc 65.38(2)	31 Ga gallium 69.72	32 Ge germanium 72.63	33 As arsenic 74.92	34 Se selenium 78.96(3)	35 Br bromine 79.90	36 Kr krypton 83.80
37 Rb rubidium 85.47	38 Sr strontium 87.62	39 Y yttrium 88.91	40 Zr zirconium 91.22	41 Nb niobium 92.91	42 Mo molybdenum 95.94(2)	43 Tc technetium	44 Ru ruthenium 101.1	45 Rh rhodium 102.9	46 Pd palladium 106.4	47 Ag silver 107.9	48 Cd cadmium 112.4	49 In indium 114.8	50 Sn tin 118.7	51 Sb antimony 121.8	52 Te tellurium 127.6	53 I iodine 126.9	54 Xe xenon 131.3
55 Cs caesium 132.9	56 Ba barium 137.3	57-71 lanthanoids	72 Hf hafnium 178.5	73 Ta tantalum 180.9	74 W tungsten 183.8	75 Re rhenium 186.2	76 Os osmium 190.2	77 Ir iridium 192.2	78 Pt platinum 195.1	79 Au gold 197.0	80 Hg mercury 200.6	81 Tl thallium [204.3; 204.4]	82 Pb lead 207.2	83 Bi bismuth 209.0	84 Po polonium	85 At astatine	86 Rn radon
87 Fr francium	88 Ra radium	89-103 actinoids	104 Rf rutherfordium	105 Db dubnium	106 Sg seaborgium	107 Bh bohrium	108 Hs hassium	109 Mt meitnerium	110 Ds darmstadtium	111 Rg roentgenium	112 Cn copernicium		114 Fl flerovium		116 Lv livermorium		
57 La lanthanum 138.9	58 Ce cerium 140.1	59 Pr praseodymium 140.9	60 Nd neodymium 144.2	61 Pm promethium	62 Sm samarium 150.4	63 Eu europium 152.0	64 Gd gadolinium 157.3	65 Tb terbium 158.9	66 Dy dysprosium 162.5	67 Ho holmium 164.9	68 Er erbium 167.3	69 Tm thulium 168.9	70 Yb ytterbium 173.1	71 Lu lutetium 175.0			
89 Ac actinium	90 Th thorium 232.0	91 Pa protactinium 231.0	92 U uranium 238.0	93 Np neptunium	94 Pu plutonium	95 Am americium	96 Cm curium	97 Bk berkelium	98 Cf californium	99 Es einsteinium	100 Fm fermium	101 Md mendelevium	102 No nobelium	103 Lr lawrencium			

Fig. 1.1: Periodic table of the elements, showing the lanthanide series (REE) in light blue (<http://www.iupac.org>)

While REE are not actually rare, cerium, with an average concentration of 60 ppm in the Earth's crust, is similar to zinc in crustal abundance (Gambogi and Cordier, 2010), it is uncommon to find them in concentrations high enough to be considered an economically recoverable deposit (Table 1.1 and Table 1.2).

Table 1.1: Abundance of common ore metals in igneous rocks in ppm (modified after Guilbert and Park, 1986)

Element	Mafic Rocks	Granitic Rocks	Element	Mafic Rocks	Granitic Rocks
Li	16	40	Ag	0.1	0.04
Be	1	5	Cd	0.2	0.12
Ti	12,000	1600	Sn	1.5	3
V	225	42	Sb	0.6	0.2
Cr	180	15	Ce	20	96
Mn	1750	500	Ta	0.8	4
Co	47	3	W	0.8	1.9
Ni	145	7	Au	0.004	0.004
Cu	90	15	Hg	0.09	0.08
Zn	120	50	Tl	0.2	1.8
As	2	1.5	Pb	7	20
Se	0.05	0.05	Bi	0.007	0.01
Zr	120	185	Th	3.5	17.5
Nb	20	20	U	0.75	3.3
Mo	1.45	1.2	S	300	350

Table 1.2: Average crustal abundance of Elements indicated in weight % and in ppm for less abundant elements (modified after Mason and Moore, 1982)

Element	Crustal Abundance	Element	Crustal Abundance
H	0.14%	Rh	0.005
Li	20	Pd	0.01
Be	2.8	Ag	0.07
B	10	Cd	0.2
C	200	In	0.1
N	20	Sn	2
O	46.60%	Sb	0.2
F	625	Te	0.01
Na	2.83%	I	0.5
Mg	2.09%	Cs	3
Al	8.13%	Ba	0.04%
Si	27.72%	La	30
P	0.10%	Ce	60
S	260	Pr	8.2
Cl	130	Nd	28
K	2.59%	Sm	6.0

Element	Crustal Abundance	Element	Crustal Abundance
Ca	3.63%	Eu	1.2
Sc	22	Gd	5.4
Ti	0.44%	Tb	0.9
V	135	Dy	3.0
Cr	100	Ho	1.2
Mn	0.09%	Er	2.8
Fe	5.00%	Tm	0.5
Co	25	Yb	3.4
Ni	75	Lu	0.5
Cu	55	Hf	3
Zn	70	Ta	2
Ga	15	W	1.5
Ge	1.5	Re	0.001
As	1.8	Os	0.005
Se	0.05	Ir	0.001
Br	2.5	Pt	0.01
Rb	90	Au	0.004
Sr	375	Hg	0.08
Y	33	Tl	0.5
Zr	165	Pb	13
Nb	20	Bi	0.2
Mo	1.5	Th	7.2
Ru	0.01	U	1.8

Until 1948, REE were produced from placer deposits in India and Brazil. In the 1950s, vein deposits (monazite) in South Africa were a major source of REE. From the 1960s – 1980s Mountain Pass, CA was the premier global producer of LREE (Rose, 1960; Gambogi and Cordier, 2010; Long et al, 2010). Today China dominates production of REE, producing 97% of global REE resources, while the United States had zero mine production in 2010 and 2011 (<http://minerals.usgs.gov/minerals/pubs/>).

Global economics and national security interests are important considerations in the development of domestic REE supplies, the necessity of increasing our knowledge of REE deposits, and understanding under what conditions an economically viable concentration of REE is likely to be found. The most common forms of REE deposit that are being exploited today include; carbonatites (LREE -

Mountain Pass, CA, LREE and HREE – Bayan Obo, Mongolia) and high-grade pegmatites (Strange Lake, QC). In 2010, the United States Geological Survey published a report on domestic REE deposits and the global perspective, discussing the REE deposits found in the U.S., but failed to include the potential Sierra Blanca REE complex (Long, et. al., 2010). As early as 1991 the idea of low-grade, high tonnage deposits as economically viable had been recognized (Černý, 1991). The Sierra Blanca laccoliths represent such a deposit, and previous studies of the area have indicated that the rare earth enrichment, especially of the HREE, of the Sierra Blanca laccoliths may possibly justify further exploration and mining of the deposit (Rubin, et al, 1987b; Price, et al., 1990; Hulse, et al., 2012).

Exploration drilling conducted by Texas Rare Earth Resources (www.trer.com) began in the summer of 2011 on Round Top, with plans to expand to Little Round Top and Little Blanca if warranted. With the rising interest in REE, a better knowledge of the geological and geochemical constraints on REE deposits will be necessary to the successful exploration for, and development of, said deposits. The study of the Sierra Blanca laccoliths will help in creating a better understanding of the factors that may control REE enrichment in a low-grade, high tonnage deposit.

LOCATION

The Sierra Blanca laccoliths lie approximately 100 km southeast of El Paso, in the Trans-Pecos region of west Texas. The laccoliths are five shallow rhyolite intrusions that are exposed just north of the Quitman Mountains and the town of Sierra Blanca, TX, and (clockwise from west) are named Round Top, Little Round Top, Little Blanca Mountain, Triple Hill and Sierra Blanca (Fig. 1.2). The Trans-Pecos region is bounded on the east by the Pecos River, and covers roughly 51000 km² in the westernmost portion of Texas. Physiographically, the region is the Texas extent of the Basin and Range province, with elevations ranging from a low of 305m at the mouth of the Pecos River, to a high of 2667m at Guadalupe Peak (Powell, 1980). The U.S. portion of the Chihuahuan Desert lies in the Trans-Pecos region of west Texas and portions of southern New Mexico (Lloyd, et al., 1980; Baddock, et al., 2011), and the region exhibits the typical flora and fauna of the Chihuahuan Desert. Climate ranges from semi-arid to arid in the high desert, with precipitation dictated by elevation. Average annual precipitation is 304mm, the majority of which falls in the late summer monsoon months (July – September). Summer temperatures range from 29° to 35°C, and winter temperatures from -3° to 0°C, with elevation playing a large role in temperature variation. Desert grassland is the most common vegetation type, with desert shrub grading into open woodland in the highest elevations of the Davis and Guadalupe Mountains (Lloyd, et al. 1980; Baddock, et al., 2011). Due to low precipitation, the majority of the region is given over to extensive grazing, and agriculture is limited to irrigated areas along the Rio Grande River.

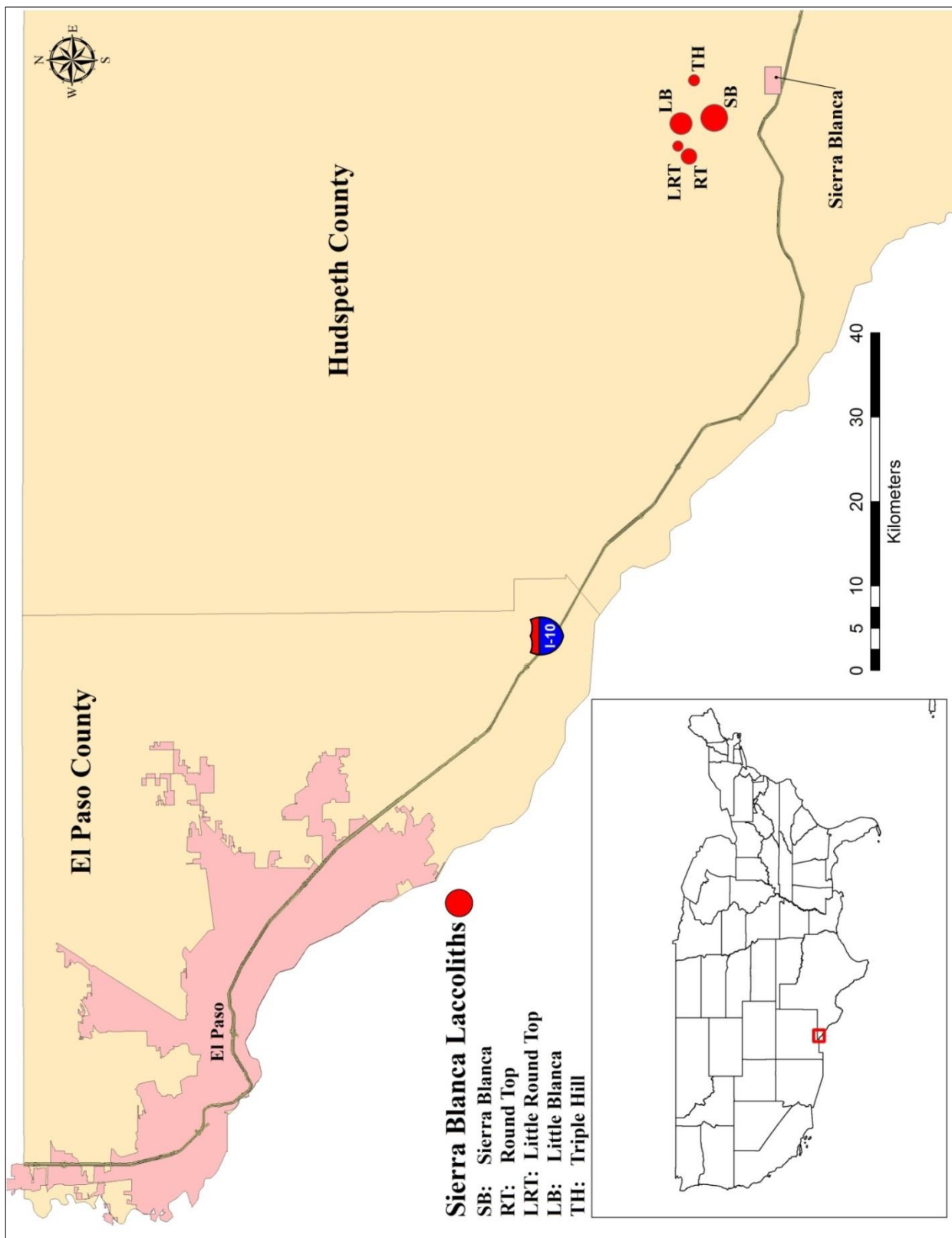


Fig. 1.2: Location of the Sierra Blanca laccoliths

GEOLOGY- REGIONAL

The Sierra Blanca laccoliths lie on the boundary between a rigid structural platform to the north, and a mobile geosynclinal belt to the south – the Diablo Plateau and Chihuahua Trough. This intra-continental boundary, the Texas Lineament, is sharply defined in the area between the Sierra Blanca laccoliths and the northern Quitman Mountains (Fig. 1.3), extending on a northwest trend (Albritton and Smith, 1965; Muelberger, 1980; Shannon and Goodell, 1986; Carciumaru and Ortega, 2008). The Texas Lineament is an ancient belt of fracture that represents the southwestern edge of the North American Craton, and forms the northwestern boundary of the Chihuahua Trough (Albritton and Smith, 1965; Ortega and Carciumaru, 2010). The Chihuahua Trough is a Mesozoic age, deep sedimentary basin characterized by numerous deformational events. Laramide deformation in the region dates from the late Cretaceous to Eocene (85 – 36Ma), with stratigraphic evidence for Laramide effects best preserved in the Big Bend area, where five distinct orogenic pulses are recorded (Muehlberger, 1980; Carciumaru and Ortega, 2008). Post-Laramide leveling of the region was followed by widespread, silicic, ignimbritic volcanism in late Eocene and early Oligocene, with a major period of volcanic activity from 40 – 31.5 Ma (Muehlberger, 1980; Matthews and Adams, 1986; Gilmer, et. al. 2003). The onset of Rio Grande rifting from 30 to 18 Ma is associated with an initial phase of increased volcanism in the region (Ortega and Carciumaru, 2010). The Northern Quitman Mountains caldera (Fig. 1.3) is superimposed across the Laramide deformed Paleozoic and Mesozoic marine strata of the Chihuahua Trough, and is located at the northeastern limit of thrust faults of the Chihuahua Trough (Hobbs and Hoffer, 1980; Murry, 1980).

There is no proof that the Sierra Blanca peaks are co-magmatic with the northern Quitman Mountains, however Barker (1980), proposed that dikes and sills in the Finlay Mountains, 10km west of

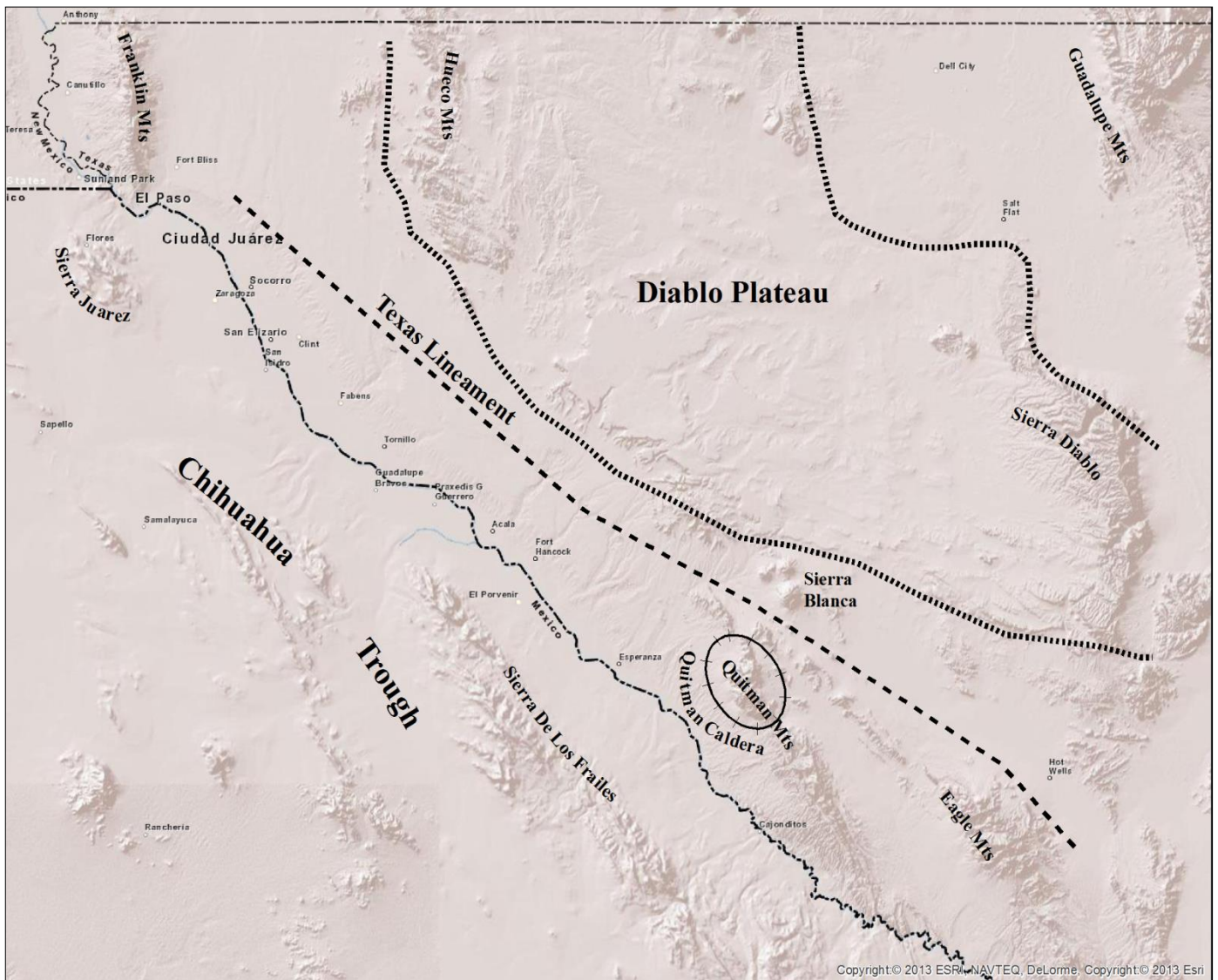


Fig. 1.3: Regional Tectonic and Physiographic features (modified after Muehlberger, 1980; Carciumaru and Ortega, 2008; Ortega and Carciumaru, 2010)

the Sierra Blanca laccoliths are petrographically similar to mafic, plagioclase-rich rocks of the dioritic intrusions on the Sierra Blanca laccoliths, suggesting that the Finlay Mountains, Sierra Blanca laccoliths, and northern Quitman Mountains may all be underlain by the same large pluton, or very similar plutons. McNulty (1980) postulated that magmatic resurgence associated with the Quitman Mountains caldera may have been the source of magma which produced the Sierra Blanca laccoliths, and Matthews and Adams (1986) suggest that the spatial and temporal proximity of the Sierra Blanca laccoliths with the Quitman Mountain igneous series (Fig. 1.4) indicate co-magmatism. Shannon and Goodell (1986) rule

out a crystal fractionation magmatic link between the Quitman Mountains caldera and the Sierra Blanca laccoliths, proposing instead that the proximity of the laccoliths and the Quitman Mountains igneous complex to the Texas Lineament, and their location on the eastern flank of the Rio Grande rift, may indicate two different sources of magma.

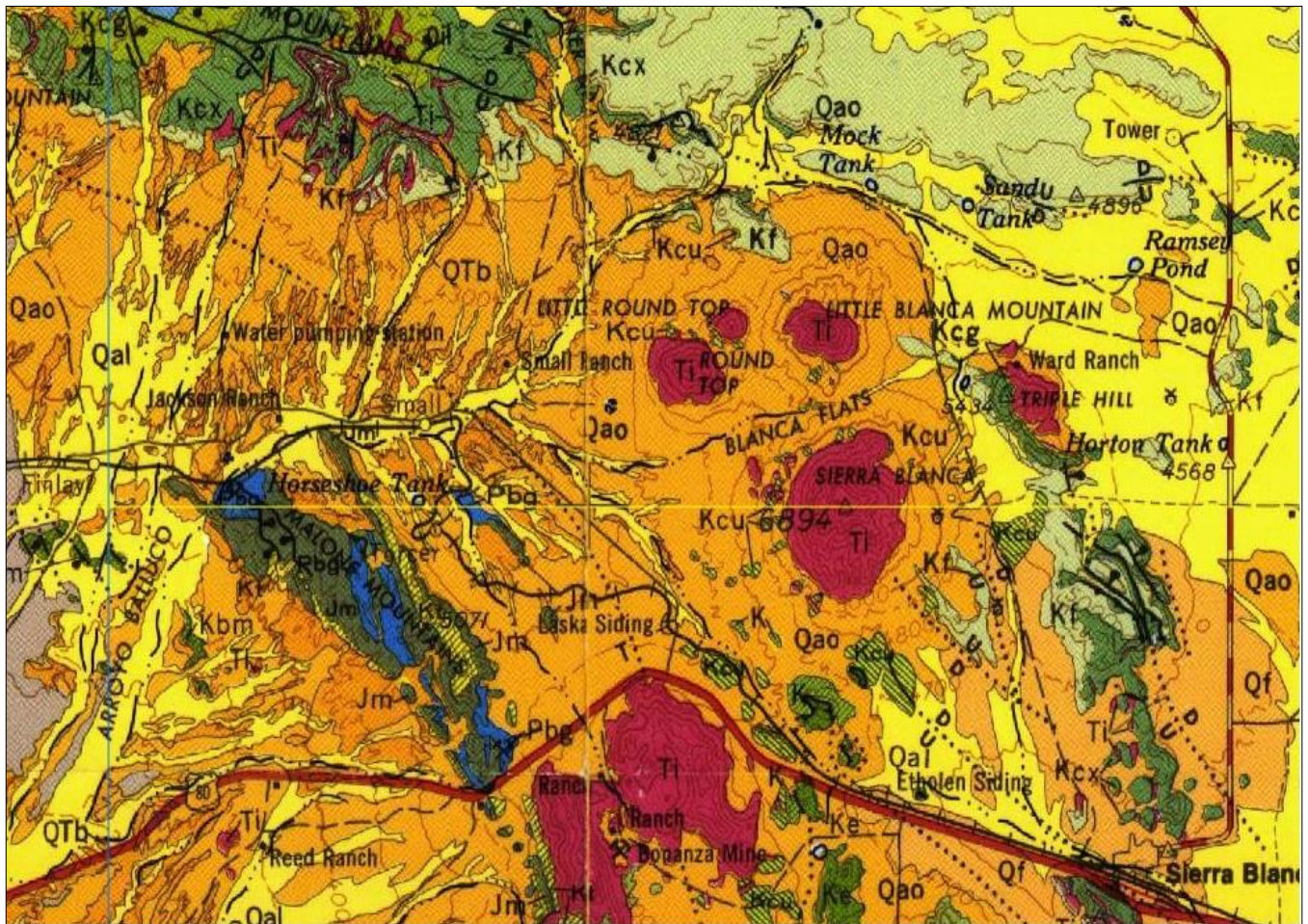


Fig. 1.4: Detail of Geologic Atlas of Texas, Van Horn-El Paso Sheet (Revised 1983)

GEOLOGY - LOCAL

The Sierra Blanca laccoliths are five shallow, fine-grained, locally porphyritic, Tertiary rhyolites intruded into Cretaceous sedimentary rocks (Fig. 1.4) composed of transgressive clastics and neritic carbonates (McAnulty 1980), deposited on the southern edge of the Diablo Plateau and the northern edge of the Chihuahua Trough (Fig. 1.3). Albritton and Smith (1965), summarize the sedimentary strata as the Washita Formation – undivided. McAnulty (1980) subdivides the Washita Group into the Espy Limestone, Del Rio Formation, and Buda Limestone (Fig. 1.5).

Quaternary	Colluvium	Sand to boulder-sized, angular to sub-angular clasts of rhyolite and limestone
	Quitman Mountains Caldera Volcanics	High-K, calc-alkaline, metaluminous to peraluminous trachytes, quartz trachytes, rhyolites. 35.9 ± 0.6 m.y. (Matthews and Adams, 1986)
	Sierra Blanca Rhyolites	Fine-grained, aphanitic to porphyritic. Light grey to red. Quartz phenocrysts. 36.2 ± 0.6 m.y. (Matthews and Adams, 1986)
Tertiary	Diorite	Hornblende-porphyry diorite intrusion. 40.6 ± 1.1 m.y. (Matthews and Adams, 1986)
Cretaceous	Buda	Light brownish-grey to grey, thin bedded, nodular limestone
	Del Rio	Medium grey, calcareous to gypsiferous nodular marl and marly limestone. Siltstone lenses, pyrite common.
	Espy	Dark grey to blueish limestone, interbedded with sandstone and sandy shale
	Benevides	Fine-grained, greyish pink to pale red, calcareous quartz sandstone.
	Finlay	Grey, fine-grained limestone, some cherty beds, siltstone and sandstone near base.

Fig. 1.5: Stratigraphic Column: Descriptions modified after <http://mrdata.usgs.gov/geology>; Hulse, et al. 2012.

The petrological classification of the Sierra Blanca laccoliths remains a matter of debate, and the laccoliths have been variously described as peraluminous (Price et al., 1990), metaluminous (this paper), and analogous to peralkaline topaz rhyolites (Shannon, 1986). The laccoliths are composed of fine-grained, intrusive, locally porphyritic rhyolite. Sierra Blanca Peak is a uniform, leucocratic, rhyolitic porphyry with conspicuous quartz and potassium feldspar phenocrysts (0.4 – 1.0 mm) in aphanitic groundmass, with some biotite phenocrysts (Rubin et al., 1987a). Little Blanca, Little Round Top, and Round top are aphanitic rhyolites showing slight banding (Albritton, 1965). The rhyolite is strongly depleted in Ti, Fe, Mg and P, and enriched in Be, U, and REE (Barker, 1980; McAnulty, 1980; Rubin et al., 1987a). The rhyolite is found in five different colors according to the degree of alteration present: grey, red, pink, tan, and brown. The pink and red colors are produced by the replacement of magnetite by hematite; brown and tan rhyolites show goethite or limonite replacement of the iron (Hulse, et. al., 2012). Tan and brown rhyolites are most common in fractured zones, and may represent hydrothermal or groundwater alteration. REE have been found to be most common in the grey and pink rhyolites (Hulse, et. al., 2012). Data also suggests a late stage hydrothermal event resulting in extreme REE enrichment in fractured zones (this paper and A. Gomez, in prep.). Sill-like bodies of diorite (0.5 – 5m thick) intrude the sedimentary rocks on the flanks of the laccoliths, generally the shale units, and the rhyolite intruded the Cretaceous strata along pre-existing diorite intrusions (McAnulty, 1980; Price et al., 1990). The diorite has been dated to between 40.6 ± 1.0 ma and 48 ma based upon four whole rock, K-Ar dates (Matthews and Adams, 1986), while K-Ar dating places Sierra at $36 \text{ Ma} \pm 0.6$ (Henry, et. al., 1986; Matthews and Adams, 1986; Rubin, et. al., 1990).

Fluorite occurrences are numerous and widespread in the limestone surrounding the laccoliths, near the contact (Fig. 1.6), and in highly fractured and brecciated zones. Strongly fluoritized shales and

marls indicate that the hydrothermal fluids associated with the intrusion were rich in fluorine, or the result of an F-rich vapor phase (McAnulty 1980, Price, et al., 1990).



Fig. 1.6: Massive fluorite (purple) in heavily brecciated zone at the rhyolite/limestone contact. Exposure in a prospect trench on the north flank of Round Top. Tag is approximately 10cm. (Photo: N. Kyger)

On the slopes of the mountains, mass wasting by slump and landslide are the dominant features (McAnulty, 1980). Albritton and Smith (1965), McAnulty (1980), and Rubin, et al. (1987a) have noted indications that the laccoliths were emplaced at shallow depth, the sedimentary strata domed over the intrusive bodies, and that the present slopes of the mountains approximate the original contours of the intrusive bodies.

PREVIOUS WORK

The geology of the Sierra Blanca area remained relatively unknown until the mid-19th century when initial mapping and studies of the geology along the Rio Grande were carried out as part of the United States and Mexican Boundary Survey, however, it was not until the early 1900's that comprehensive geological reports and maps became available. The USGS professional paper, *Geology of the Sierra Blanca Area, Hudspeth County, Texas* (Albritton and Smith, 1965), is the seminal study of the regional geology, and remains one of the most informative papers on the geology of the region (Fig. 1.7).

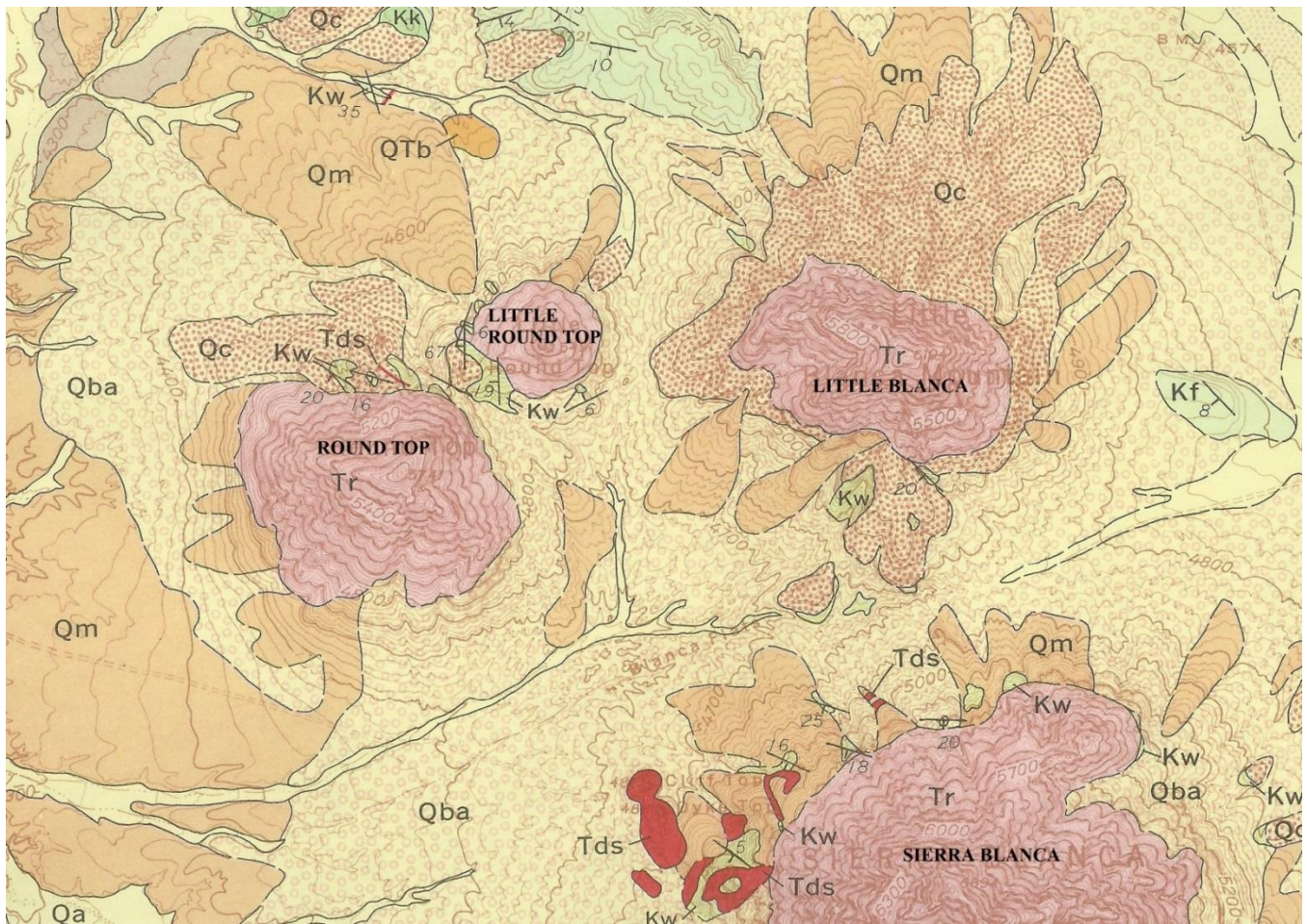


Fig. 1.7: Detail of the Albritton and Smith (1965) geologic map, showing of the Sierra Blanca laccoliths (Kf: Finlay Limestone; Kw: Rocks of Washita age; Tds Dikes and sills; Tr: Rhyolite and rhyolite porphyry; QTb: Basin deposits Qc: Older colluvium; Qm: Madden Gravel; Qba: Balluco Gravel; Qa: Alluvium)

Previous academic work and mining exploration shows a continuous interest in the potential economic value of the Sierra Blanca laccoliths. McAnulty (1974) investigated the fluorspar deposits of Texas, including preliminary details about the Sierra Blanca laccoliths. Later work (McAnulty, 1980; Shannon, 1986; Shannon and Goodell, 1986) focused on the geology and mineralization of the Sierra Blanca peaks. Barker (1980) included the Sierra Blanca intrusive cluster in his study of the igneous rocks of the Sierra Blanca area, introducing five new analyses of the rhyolites, and suggesting that the similarities between the Sierra Blanca cluster, the northern Quitman Mountains, and the Finlay Mountains, indicate a single, or very similar sources of magma. Later studies of the Quitman-Sierra Blanca igneous complex (Shannon, 1986; Shannon and Goodell, 1986), have ruled out a co-magmatic link between the North Quitman Stock and the Sierra laccoliths, postulating instead a long-lived system progressing from differentiation of lower crustal melts to crystal fractionation of upper-mantle melts. The geochemistry and age of the Sierra Blanca and Finlay Mountain intrusions were further refined by Shannon (1986) , Shannon and Goodell (1986), and Matthews and Adams (1987), with the addition of detailed geochemical characterization, thirty-three new major and trace element analyses, fourteen lanthanide determinations, one new Rb-Sr, and four new K-Ar age dates. Rubin et al. (1987a) investigated the presence of cryolite, Li-rich micas, rutilated quartz, trace element enrichment, and depletion in Mg, Ca, and Ti relative to calc-alkaline rhyolites on Round Top laccolith as evidence of pegmatitic vapor phase crystallization. The presence of cryolite and high HREE enrichment differentiate the laccoliths from chemically similar topaz-bearing rhyolites. Further studies indicate that the rhyolites were emplaced in a continental arc setting during a compressive stage, indicated by the east-northeast trend of veins and dikes throughout the region, and a change in the chemistry of magmas from calc-alkalic in western Mexico, to alkali in Texas (Price et. al., 1990; Ortega and Carciumaru, 2010).

The economic potential of the Sierra Blanca laccoliths was realized as early as 1974 by McAnulty during his study of the fluorspar deposits. Murry (1980) discusses the economic potential of

the area, focusing on the Quitman caldera and its associated hydrothermal veins and contact metasomatic skarn deposits, while the potential Be and REE deposits of the Sierra Blanca laccoliths have been discussed by numerous researchers of the region (Shannon, 1986; Shannon and Goodell, 1986; Rubin et al., 1987a; 1987b; Price et al., 1990). The Be and trace element enrichment of the rhyolites led to exploration and drilling, from 1984-85, by the Cabot Corporation. Beryllium was found to be hosted by the fluorspar deposits in the Buda Limestone, extending weakly into the rhyolite in the contact zones (Rubin, et. al., 1990). In 1986 the Round Top property was joint ventured to Cypress Beryllium Corporation (later Cypress Sierra Blanca, Inc.), and a 340 meter test adit was driven into the northern flank of Round Top Mountain (Fig. 1.8).



Fig. 1.8: Test adit on northwest flank of Round Top. (Photo: N. Kyger)

Due to the poor economic conditions of the early 1990s, the difficulty of finding a ready market for beryllium oxide, and the monopoly on beryllium production held by Brush Wellman, the project was abandoned, and the Sierra Blanca laccoliths remained largely untouched until 2008 (S. Korzeb, pers. commun.). The extreme enrichment of the laccoliths in trace elements and REE, reported by several authors (McAnulty, 1980; Matthews and Adams, 1986; Shannon, 1986; Shannon and Goodell, 1986; Rubin et. al., 1987a, 1987b; Price et. al., 1990) indicates that the laccoliths represent a potential high-tonnage, low-grade resource of rare metals, and in June 2011, Texas Rare Earth Resources began exploration drilling for REE on Round Top (Texas Rare Earth Resources: [www. trer.com](http://www.trer.com)), with plans to expand to Little Round Top and Little Blanca if conditions warrant.

STATEMENT OF PROBLEM

The difficulty of locating an economically viable REE deposit lies principally in the rarity of a sufficiently concentrated amount of recoverable REE within the host rock. The Sierra Blanca laccoliths represent a unique, potential low-grade/high-tonnage REE deposit that was overlooked in the 2010 USGS report on domestic REE deposits. The laccoliths are dissimilar to other known deposits (Mountain Pass, USA; Bayan Obo, China), and no current deposit model exists to describe them. The Sierra Blanca laccoliths are analogous to topaz rhyolites, and this similarity alone makes the laccoliths economically interesting because of the association of topaz rhyolites with volcanogenic beryllium, tin, uranium, and fluorite deposits (Burt, et al., 1982; Christiansen, et al., 1983). Previous exploration (1984 – 1990s) confirmed Be and U enrichment, especially on Round Top, and more recent (2011 – 2012) exploration for REE indicates that the Sierra Blanca laccoliths hold the potential of being a low grade/large tonnage REE deposit.

The Sierra Blanca laccoliths are trace element enriched (Shannon, 1986; Price, 1990, 2004) rhyolites, in a tectonic setting (along a rift, during an extensional tectonic regime) analogous to topaz rhyolites, but showing an uncharacteristic enrichment in HREE. The location of the laccoliths on the Texas Lineament, proximity across the lineament from the Quitman Mountains Caldera and position over the Precambrian shoulder of the Rio Grande Rift, a longer history of regional compression and extension may all play a role in the unusual HREE enrichment of the rhyolites. The close spatial and temporal proximity of the laccoliths to the Quitman Mountains Caldera has been previously examined, concluding that notwithstanding the similarities between the Quitman, Finlay, and Sierra Blanca mountains (Murry, 1980); a co-magmatic link can be ruled out (Shannon, 1986; Shannon and Goodell, 1986). Despite the lack of a co-magmatic link, the magmas of both bodies may have originated from the same heat event, but from two slightly different source magmas (Shannon and Goodell, 1986). The existence of an enriched cratonic block has been postulated as a possible contributor to the enrichment in

large ion lithophiles (LIL), high field strength (HFS) elements, REE, and fluorine (P. Goodell, pers. commun.). Igneous activity associated with crustal extension may have remobilized these chemicals within the enriched cratonic block, and the resulting magma composition and magmatic processes along rift shoulders may be characteristic of the low-grade/high tonnage type deposit that the Sierra Blanca laccoliths represent (P. Goodell, in prep.)

Future exploration for REE has much to gain from a characterization of the distinctive features of the Sierra Blanca laccoliths. A detailed study of the geology and geochemistry of the Sierra Blanca laccoliths will increase the understanding of the formation of the deposit, the extent of mineralization, and will allow for the characterization of a new deposit type.

OBJECTIVE

Characterization of the Sierra Blanca laccoliths through a synthesis of field and laboratory work will yield information that may be applied to other regions of interest, and to develop future exploration criteria for similar deposits. Geological and geochemical features of the laccoliths can be extrapolated to other, similar regions, guiding the initial exploratory work necessary to the development of an economically viable deposit. The main objective of this study is to describe the geology and geochemistry of the potential low-grade/ high-tonnage REE deposit in the Sierra Blanca laccoliths, in a manner that can in turn be used to further exploration for REE in similar environments. To determine what characterizes this deposit, it is the objective of the researcher to examine the laccoliths in a series of steps:

1. Update the geological map of the region of interest.
2. Collect surface samples for whole rock and trace element analyses.
3. Incorporate geochemical data from surface samples into maps and cross-sections for spatial analyses.
4. Determine the extent of differences in the dispersion and zoning of REE between and within the laccoliths.
5. Complete a geological and geochemical comparison of the laccoliths.

METHODS

The description of the Sierra Blanca laccoliths will be undertaken using a combination of field work and laboratory analysis. Field activities will include mapping (paper and GIS) and sampling. Geophysical data will be briefly touched upon as a method of verifying field observations. Laboratory analyses will include assays of major and trace elements. Geochemical and statistical analysis will be used to examine the collected field and laboratory data. Table 3.1 shows the questions the study proposes to examine, and the tools that will be used to answer them.

Table 3.1: Methods used to accomplish objectives of study

	<i>Field Mapping (Paper and GIS)</i>	<i>Whole Rock Analysis</i>	<i>Trace Element Analysis</i>	<i>Cross Sections</i>	<i>Geophysical Data and remote sensing</i>	<i>Geochemical and statistical analysis</i>
1. How does the geology of the different laccoliths compare?	X	X	X	X	X	X
2. What is the role of geological structure in the dispersion and zoning of REE	X	X	X	X	X	X
3. How does the geochemistry of the different laccoliths compare?	X	X	X	X		X

GEOLOGICAL MAPPING

Mapping of the Sierra Blanca laccoliths combined both field mapping and remote sensing. Field mapping took place over the period of roughly one year, from July 2011 to June 2012, and was used to update the Albritton and Smith (1965) geological map of the Sierra Blanca laccoliths (Fig. 1.7) and includes greater detail about contacts, geological structures, and outcrops, as well as sample locations. Contacts and visible structures were mapped on paper at a scale of 1:3000, as well as being recorded using a handheld global positioning system (GPS) unit. In the field, mapping was accomplished with the aid of USGS 7.5 minute topographical maps, and a Garmin 62STC GPSmap unit. Data collected with the GPS are in NAD 1983, Universal Transverse Mercator (UTM), Zone 13N. Sample locations were marked on the paper map in the field, and later verified using the GPS coordinates that were collected at the same time. An attempt was made to collect linear track features with the GPS, in the hopes of using them to follow structures and the visible or inferred contact. Due to the nature of the terrain (Fig. 3.1), these tracks were not an accurate depiction of linear features, and were not used in mapping.



Fig. 3.1: Typical terrain on the flanks of the Sierra Blanca laccoliths. (Photo: N. Kyger)

As the contact is largely covered by colluvium, it was often necessary to infer the contact using float. The area on the map that marked the transition between a mixture of limestone and rhyolite colluvium to one composed solely of rhyolite was judged to represent the general location of the contact. In the prospect trenches on the flanks of the laccoliths the contact is often visible, and a projected line drawn from that contact shows that inferring the contact using float gives a reasonable location for the actual contact. In addition to the contact, a series of faults were mapped. The location of the faults was inferred from abrupt changes in topography and the scree slopes that often accompany it (Fig. 3.2). Geophysical data was used to confirm the location of the inferred faults.



Fig. 3.2: Abrupt change in slope and typical scree slope associated with it (Photo: N. Kyger)

Contacts, faults and sample sites mapped in the field were transferred to a 1:24000 USGS topographical map, and the paper map was digitized using ESRI ArcView, creating various GIS layers (Table 3.2).

Samples located on the map via GPS coordinates are linked to geochemical data to enable spatial analysis of the major and trace elements using ArcView.

Table 3.2: GIS Layers

<i>Layer Name</i>	<i>Description</i>
Geology	Lithology, contacts
Hudspeth.sid	Digital raster graphic mosaic of Hudspeth county, Tx.
Faults	Inferred faults, as verified by other remote sensing methods
Samples	GPS location of samples including all geochemical data

CROSS-SECTIONS

Cross-sections of each laccolith were created using A-Prime Software's CrossView for ArcGIS. The cross-sections were chosen to pass within 200 meters of multiple samples that are near to the contact with the country rock to those farthest away from the contact (Fig. 4.1). The samples were then projected onto the plane of the cross-section profile. In some cases samples are shown as above the profile (Fig. 4.24) due to the fact that the cross-sections do not necessarily go through the highest elevation of the laccolith. The cross-sections also incorporate geologic features (Fig. 4.2) to help determine the possible role of structure in the dispersion of REE in the bodies of the laccoliths. None of the cross sections postulate on the location of a feeder, but it has been hypothesized that the large positive magnetic anomaly present in the valley between the laccoliths (Fig. 3.5) may represent the feeder (S. Korzeb, pers. commun.). Detritus around a deep drill hole located in this area however, includes mostly diorite (90+ %) and limestone, indicating that the area may instead be underlain with diorite. Information on this drill hole has not been located by the author, or by TRER, who is interested in the assay results from said hole.

REMOTE SENSING AND GEOPHYSICS

Data collected through remote sensing (aerial photography, ASTER imagery) were studied to confirm the location of contacts and structures that are discernible in the images. Using historical imagery available on Google Earth TM, it was found that the vegetation and color differences apparent in the historical images could be used to delineate structures and contacts (Fig. 3.3). Advanced Spaceborne Thermal Emission and Reflection Radiometer (ASTER) imagery, in conjunction with geological maps, has been shown to be a powerful tool in mapping outcrops that relate to local lithology (Gomez et al., 2005). The very near infra-red (VNIR) band can provide information about alteration zones, which are a common source of rare earth elements (Hunt, 1977), while the thermal infra-red (TIR) wavelength can be used to distinguish silicates and carbonates (Salisbury et al., 1987).



Fig. 3.3: Historical image of (left to right) Round Top, Little Round Top and Little Blanca. Differences in color are indicative of inferred contact and faults (Image: Google Earth TM).

Various combinations of the bands (wavelengths) are used to identify different characteristics of the surface being studied. ASTER imagery of the Sierra Blanca, TX region, obtained and processed by the author to characterize alteration zones (Fig. 3.4) was compared to field data, geologic maps, and aerial photos, to further verify the location of inferred geological structures.

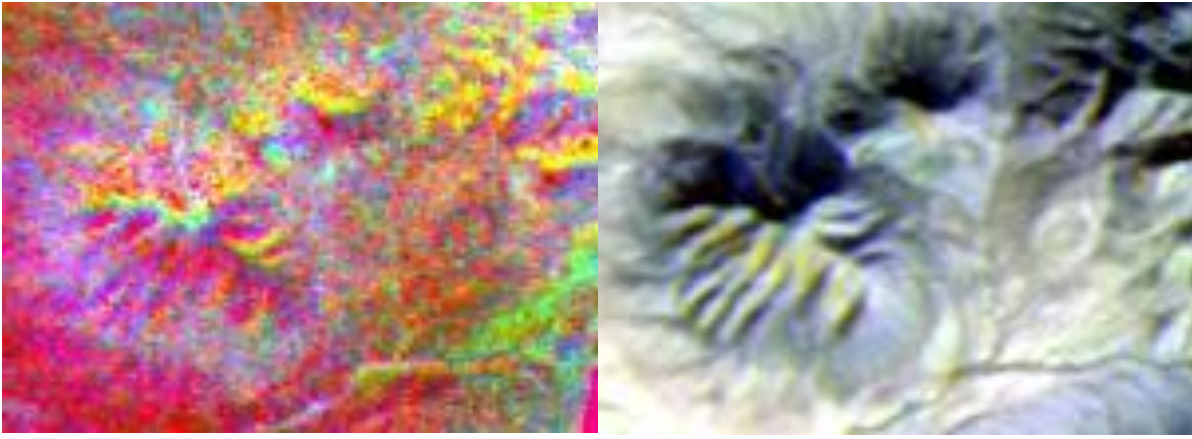


Fig. 3.4: Alteration zones (left) and enhanced structure (right)

Geophysical data, in the form of an aeromagnetic survey conducted by TRER, was of particular interest in confirming the presence of obscured structures. Geological features were compared to the magnetic anomalies and it was found that areas of low magnetic signature correlate with colluvium and sedimentary rocks, while high magnetic signatures are associated with the igneous intrusive bodies (rhyolite, diorite, mafic dikes). Faults that were inferred based upon abrupt changes in surface topography are shown to follow equally abrupt changes in magnetic signature, and in some cases follow pronounced linear features evident in the aeromagnetic survey image (Fig. 3.5).

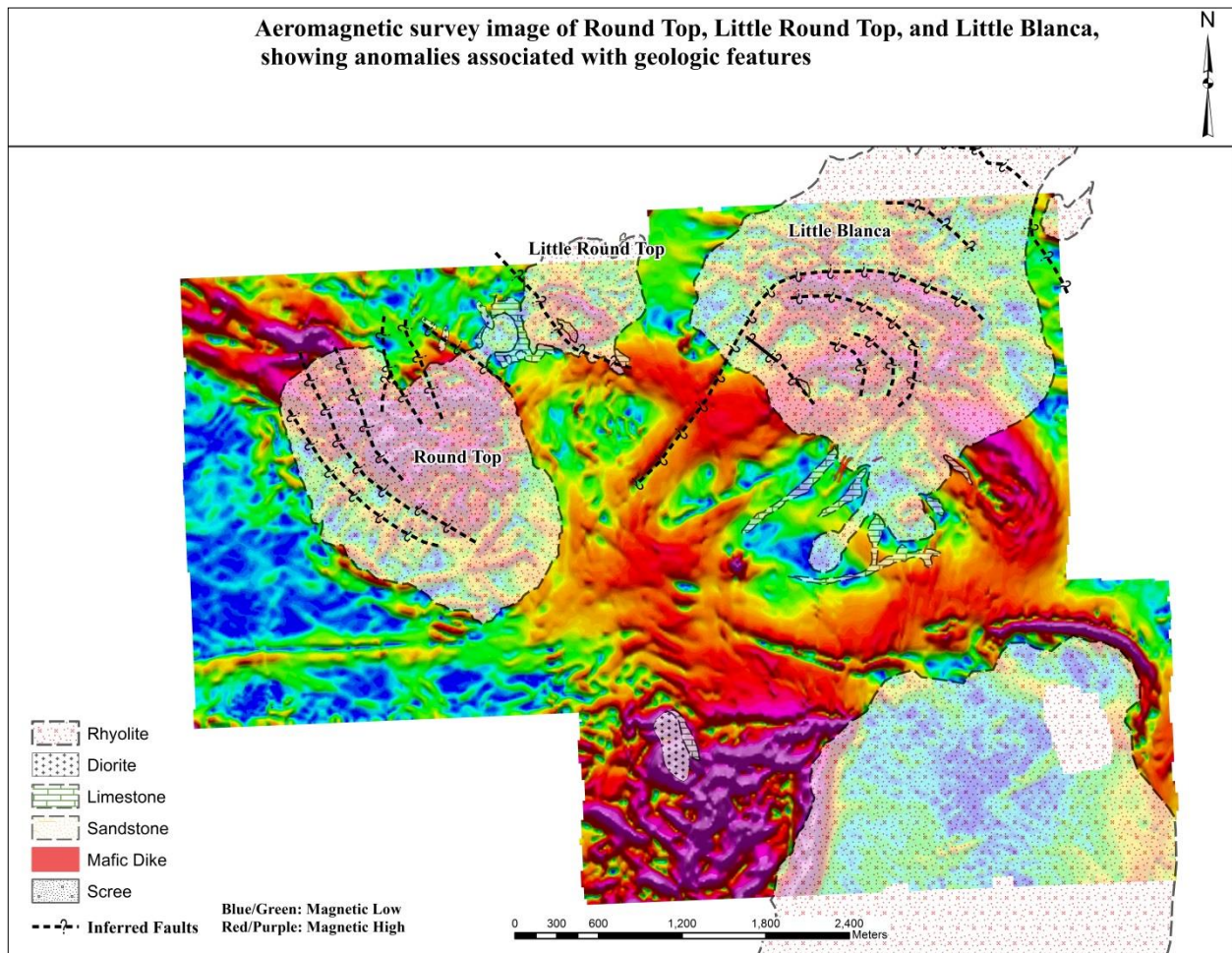


Fig. 3.5: Geology and inferred faults superimposed upon aeromagnetic survey image.

SAMPLING

Samples were collected between June 2011 and July 2012 from Round Top, Little Round Top, Little Blanca, Sierra Blanca, and the outcrops of dike material just west of Sierra Blanca (Fig. 3.6, Table 3.3), and include surface samples, samples taken from newly exposed rocks along drill roads, the Sierra Blanca quarry (RCL Rocks) and prospect trenches. The majority of the samples come from the northern three laccoliths (Round Top, Little Round Top, and Little Blanca); those with the highest concentration of REE and of most interest as a potentially economic deposit.

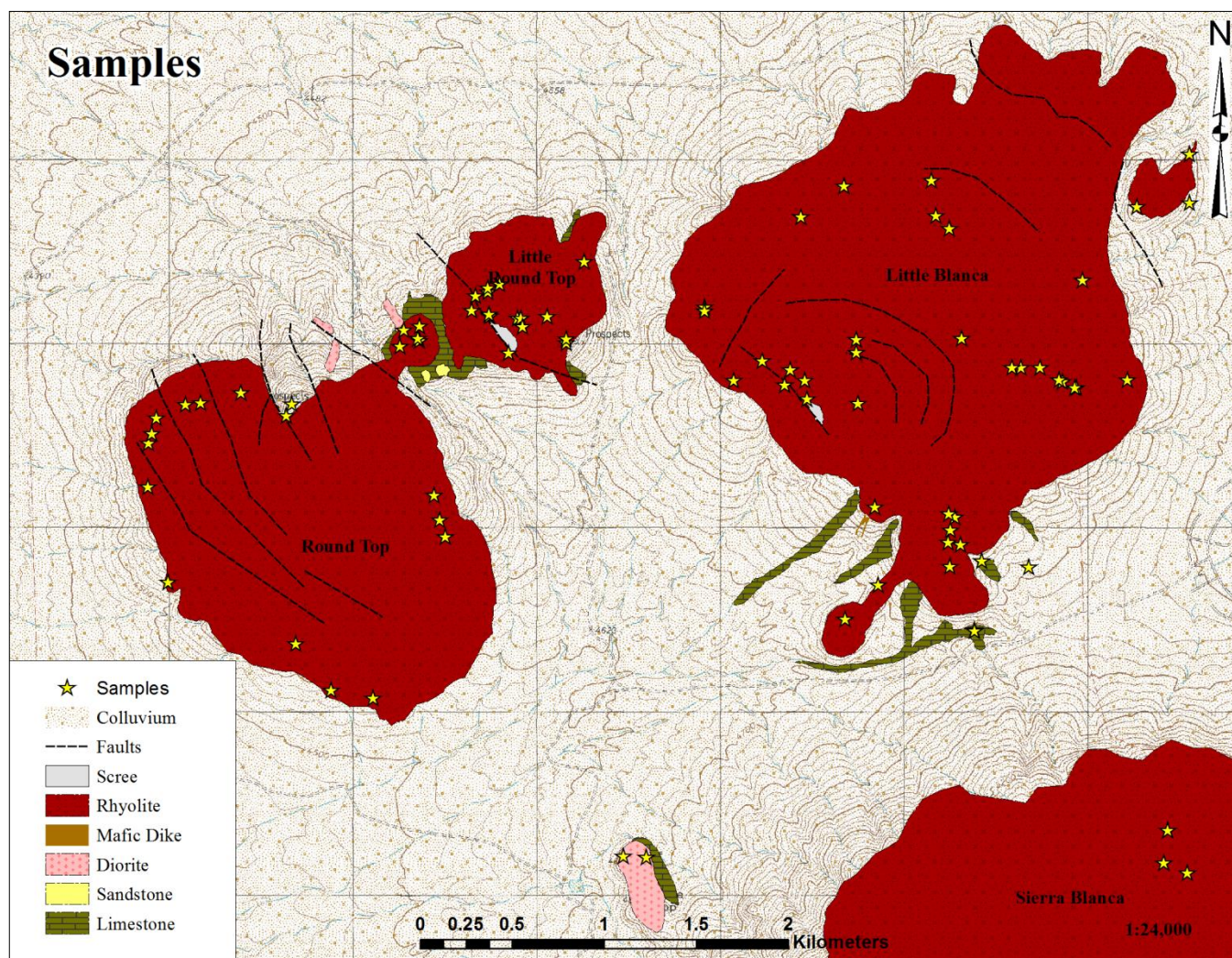


Fig. 3.6: Location of samples collected for analysis. Quitman Stock is to south of image

Every attempt was made to take surface samples from larger outcrops to allow the weather rind to be removed, producing a less weathered, “fresh” sample. In cases where this was not possible due to the nature of the sample or outcrop, this was noted in the field notebook. Approximately 1.5 to 2 kilograms of sample were collected and placed into labeled bags while still in the field. Samples are identified by mountain and by number, as shown in Table 3.3. Samples taken in May and June of 2011 were not taken by the author, and are labeled with initials-number, and the letter “S” (ie. LB-1S). Later samples taken by the author are labeled simply by initial and number (LB1). This discontinuity in sample labeling occurred because the early samples were collected by Stanley Korzeb and were not initially counted with surface samples for this project. It was decided to keep later labeling the same as it is in field notebooks to avoid confusion, rather than change it to reflect a continuum from the early TRER samples.

Table 3.3: Sample Identification and labeling

	<i>Round Top (RT)</i>	<i>Little Round Top (LRT)</i>	<i>Little Blanca (LB)</i>	<i>Sierra Blanca (SB)</i>	<i>Other (DD- Diorite Dike, MD-Mafic Dike, QS – Quitman Stock)</i>
Collected by author	RT 12 5 3 - RT 12 5 4 RT 12 6 1 - RT 12 6 3	LRT1-LRT14	LB1-LB31	SB2 – SB5	DD2 – DD3 MD1, QS2
Collected by S. Korzeb	RT201, 226, 231,233, 251, 252, 262, 287, RT334 – RT337	LRT-2S – LRT- 8S	LB-1S LB-10S	– SB-RCL-1	

GEOCHEMICAL ANALYSIS

Samples were sent to ALS Laboratories in Reno, Nevada, and analyzed in accordance with the ME-MS81d package, which includes rare earth and trace elements using Inductively Coupled Plasma – Mass Spectroscopy (ICP-MS), and the whole rock package using Inductively Coupled Plasma – Atomic Emission Spectroscopy (ICP-AES). Fluorine (F) content was analyzed using fusion-ion chromatography. Table 3.4 indicates which elements are tested for, and the range in which they can be detected. Further information about the analysis methods are available on the ALS Global website; www.alsglobal.com.

Table 3.4: Elements and Oxides analyzed (from ALS Geochemistry Service Schedule 2013)

	Analytes	Range (ppm)	Analytes	Range (ppm)	Analytes	Range (ppm)	Analytes	Range (ppm)
Trace Elements	Ba	0.5-10000	Hf	0.2-10000	Sn	1-10000	W	1-10000
	Ce	0.5-10000	Ho	0.01-1000	Sr	0.1-10000	Y	0.5-10000
	Cr	10-10000	La	0.5-10000	Ta	0.1-2500	Yb	0.03-1000
	Cs	0.01-10000	Lu	0.01-1000	Tb	0.01-1000	Zr	2-10000
	Dy	0.05-1000	Nb	0.2-2500	Th	0.05-1000		
	Er	0.03-1000	Nd	0.1-10000	Tl	0.5-1000		
	Eu	0.03-1000	Pr	0.03-1000	Tm	0.01-1000		
	Ga	0.1-1000	Rb	0.2-10000	U	0.05-1000		
	Gd	0.05-1000	Sm	0.03-1000	V	5-10000		
Whole Rock	SiO ₂	0.01-100%	MgO	0.01-100%	TiO ₂	0.01-100%	BaO	0.01-100%
	Al ₂ O ₃	0.01-100%	Na ₂ O	0.01-100%	MnO	0.01-100%	LOI	0.01-100%
	Fe ₂ O ₃	0.01-100%	K ₂ O	0.01-100%	P ₂ O ₅	0.01-100%		
	CaO	0.01-100%	Cr ₂ O ₃	0.01-100%	SrO	0.01-100%		

The geochemical data collected from the laccoliths is used to characterize the individual laccoliths, determine if REE enrichment is consistent within and between the individual laccoliths, to identify possible zoning, and to postulate a differentiation sequence. Isotopic analysis is beyond the range of this study, and remains a future area of interest. Munazzim Ali, PhD candidate at the University of Texas at El Paso is currently undertaking isotopic studies and further dating of the Sierra Blanca area in order to further our knowledge of the laccoliths.

STATISTICAL ANALYSIS

Statistical analysis of trace element and whole rock analyses using IBM SPSS to quantitatively compare the different laccoliths was based on a selection of rhyolite samples from Sierra Blanca, Little Blanca, Little Round Top, and Round Top.

Eighty-eight (88) samples were collected between June 2011 and July 2012, and include rhyolites, diorites, and limestone. To facilitate the comparison of the laccoliths, the samples were filtered to create a database that includes only the rhyolites. Samples that were consistently outliers with anomalously high or low values were also removed from the final database (Table 3.8).

Table 3.6: Removed samples and outliers

Sample	Rock Type
LB11, RT12 5 4	Limestone
LRT8, DD1, DD2	Diorite
LRT-8S, LB-5S, RT201, RT226, RT231, RT233, RT251RT252, RT262, RT287, RT334–RT337,	Unknown - possibly rhyolite breccias
LB18, MD1	Mafic dike
QS2	Granodiorite
SB-RCL-1	Crusher Fines- RCL Quarry

It was found that many of the outliers were located near the contact or inferred faults (Fig. 3.7)

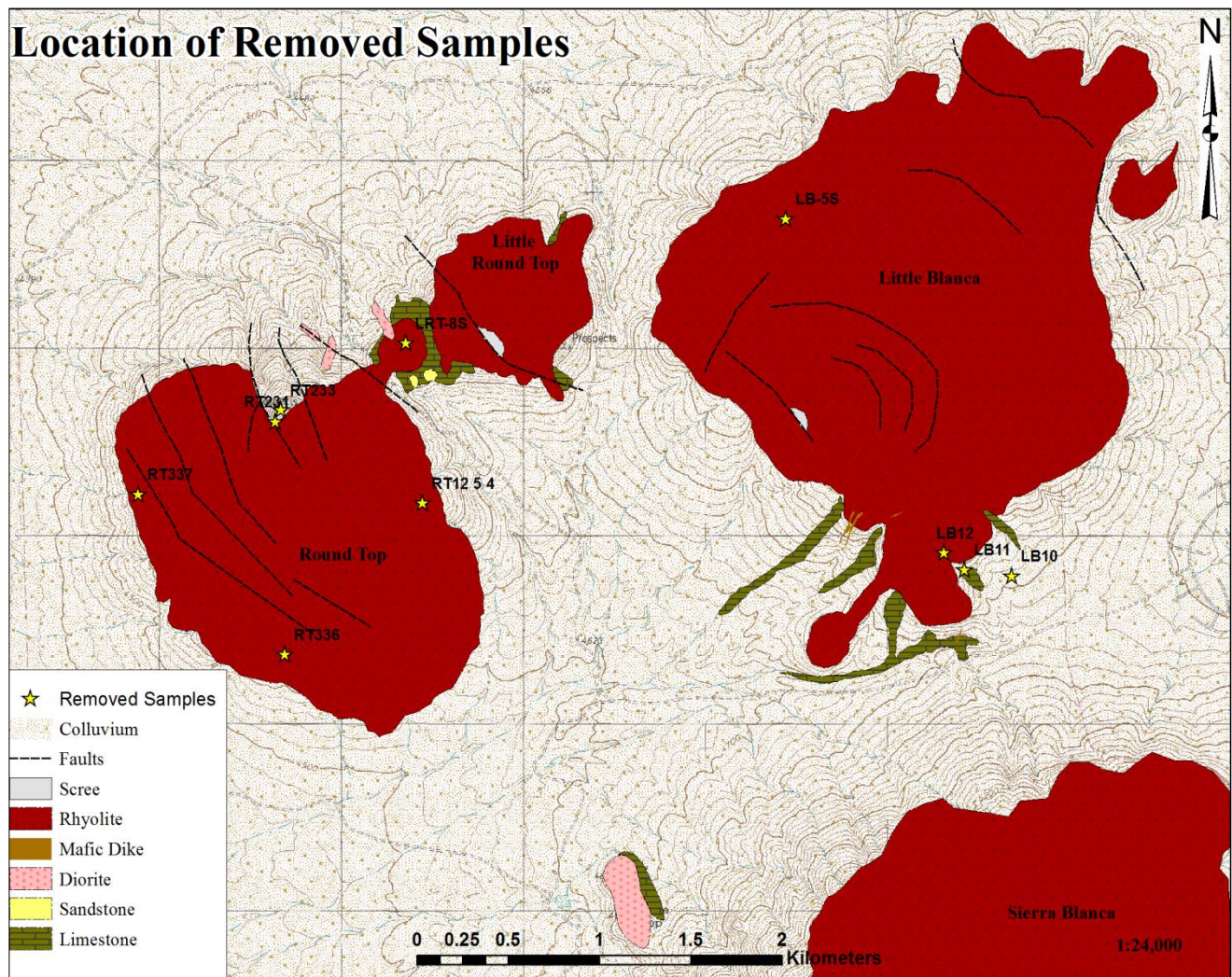


Fig. 3.7: Location of removed samples and outliers showing proximity to contact or faults

The final database was separated by laccolith, and constituents were filtered so only the relevant constituents remained. Relevant constituents are considered to be those of economic importance to an REE deposit. Constituents with an extremely low abundance were removed (Table3.7).

Table 3.7: List of removed and retained constituents

<i>Removed Constituents</i>	<i>Retained Constituents</i>
As, Cu, Pb, Ag, Co, Cr, Ni, V, W, MgO, Cr ₂ O ₃ , TiO ₂ , MnO	Ba, Be, Ce, Cs, Dy, Er, Eu, F, Ga, Gd, Hf, Ho, La, Lu, Mo, Nb, Nd, Pr, Rb, Sm, Sn, Sr, Ta, Tb, Th, Tl, Tm, U, Y, Yb, Zn, Zr, SiO ₂ , Al ₂ O ₃ , Fe ₂ O ₃ , CaO, Na ₂ O, K ₂ O, P ₂ O ₅ , SrO, BaO

Data was separated by laccolith, and univariate, bivariate and multivariate analyses were run on Little Blanca, Little Round Top, and Round Top. Table 3.8 shows what analyses were performed.

Table 3.8: Statistical analyses performed on geochemical data collected from each laccolith

	<i>Analysis</i>
Univariate	Standard statistics Histograms
Bivariate	Correlations Scatter Diagrams
Multivariate	Factor analysis

DATA

The following data represents results reviewed in the discussion portion of this thesis. Complete collections of the data can be found in the appendices.

GEOLOGICAL MAPS AND CROSS-SECTIONS

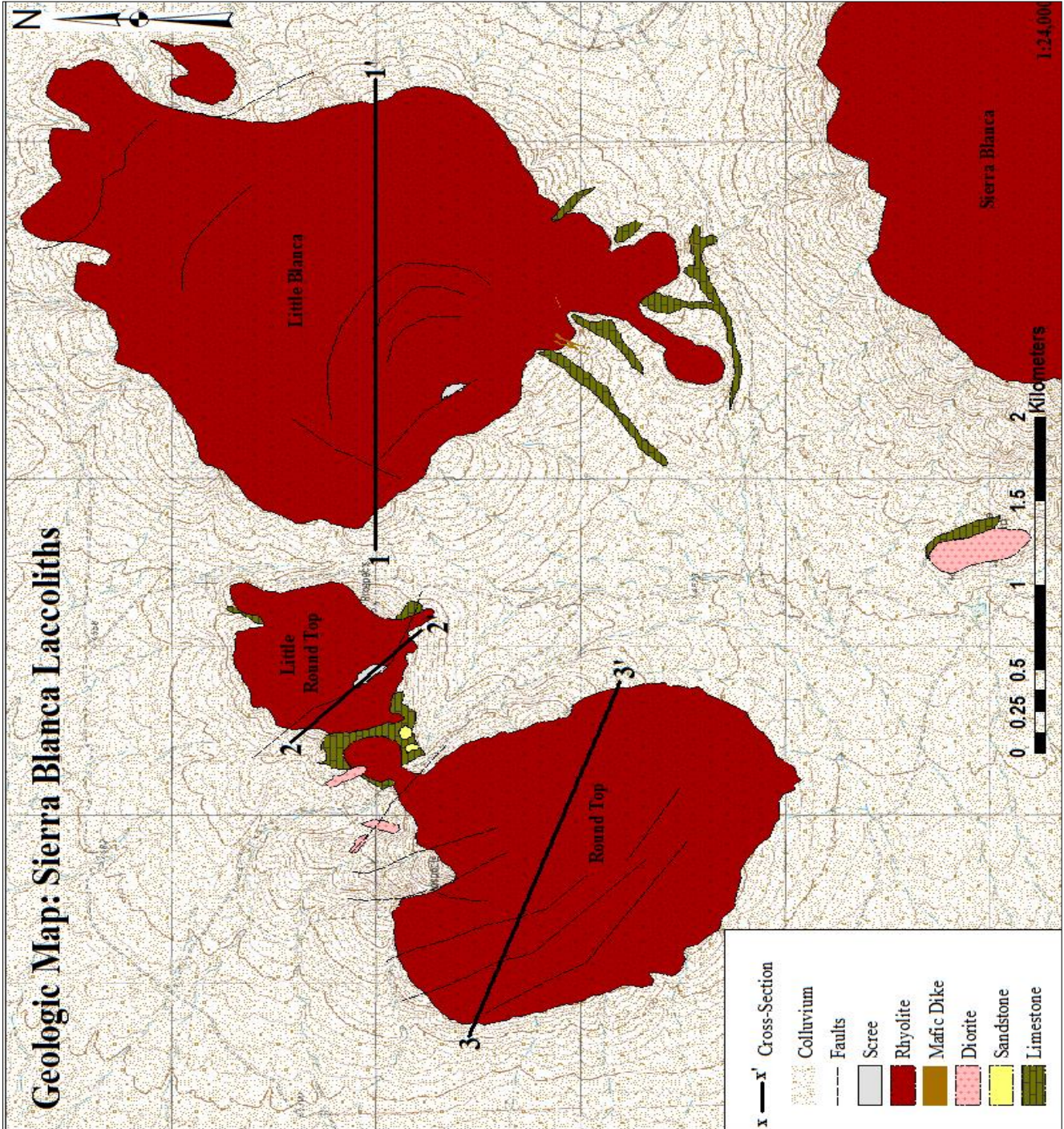
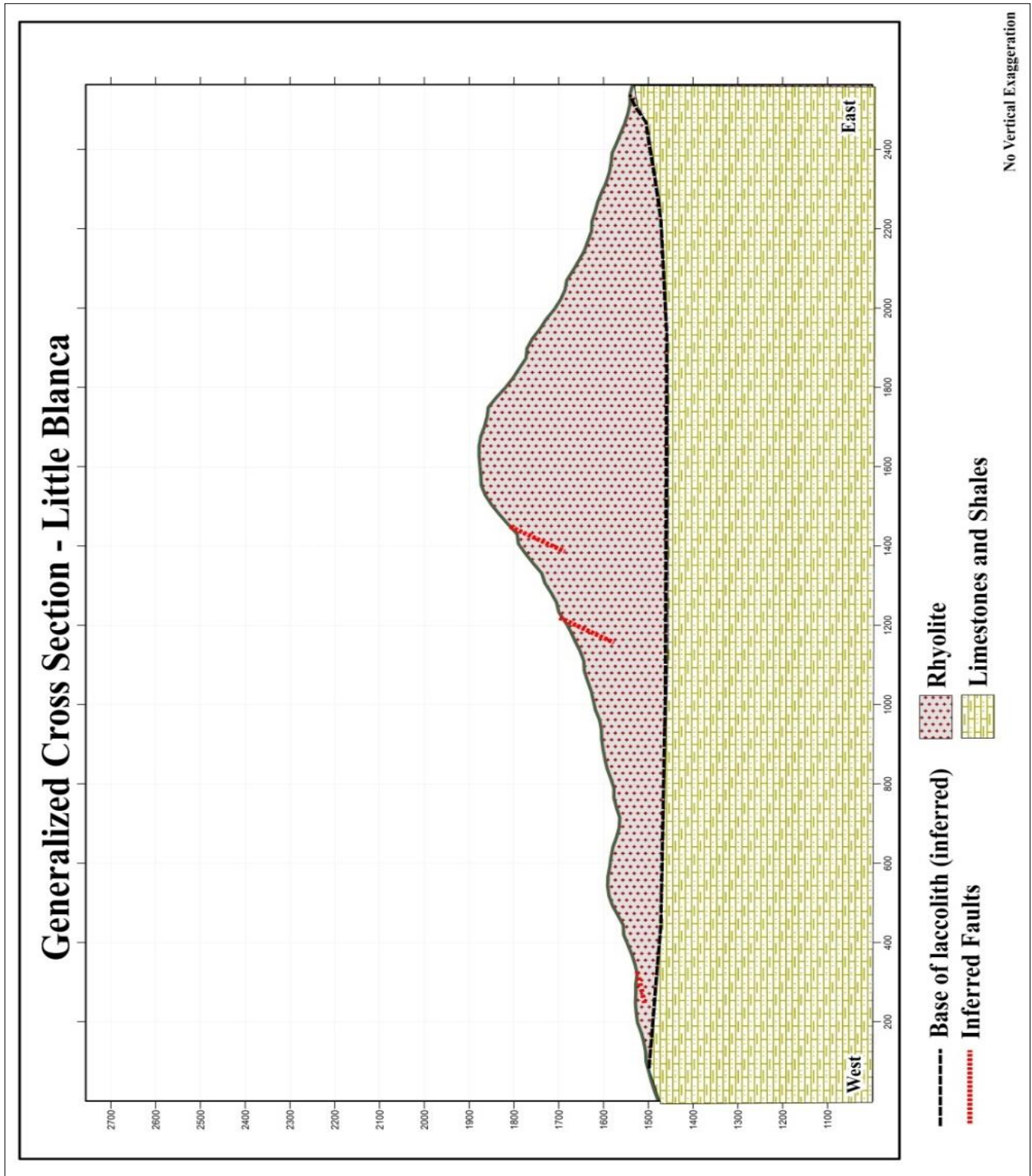
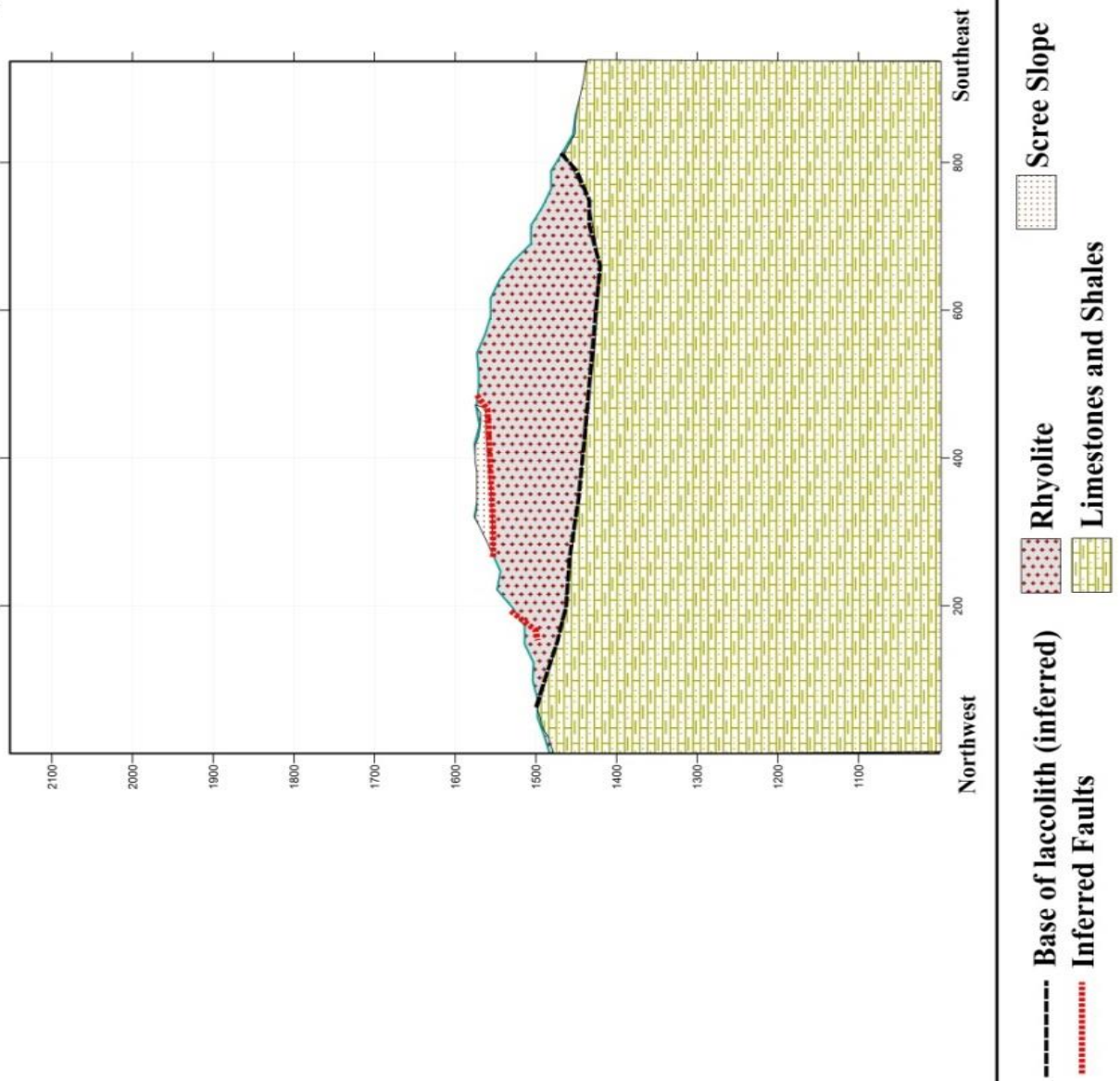


Fig. 4.1: Geological map of the Sierra Blanca Laccoliths with cross-sections, focusing on Little Blanca, Little Round Top, and Round Top.



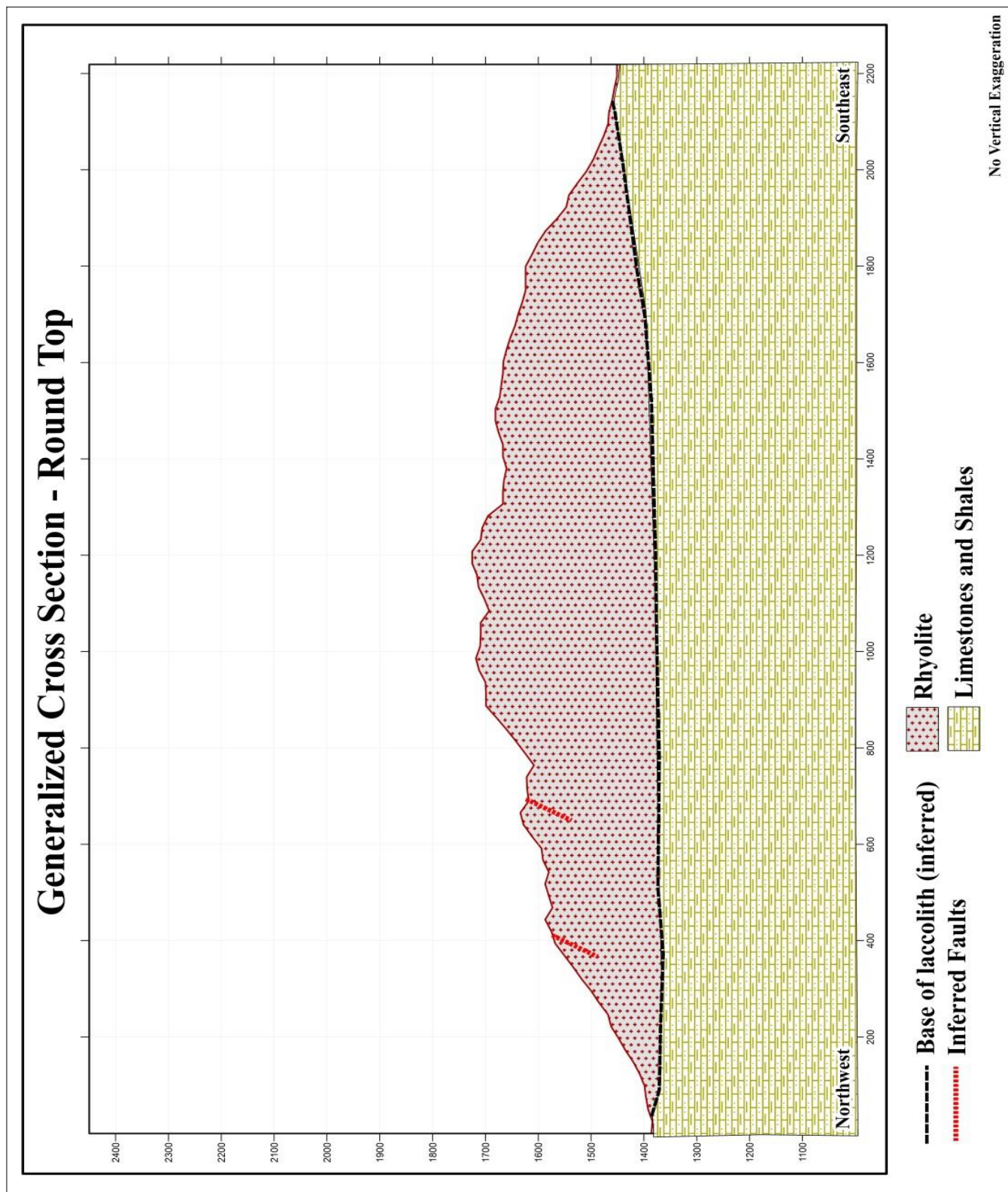
A) Geological cross section of Little Blanca (units: meters)

Generalized Cross Section - Little Round Top



No Vertical Exaggeration

B) Geological cross section of Little Round Top (units: meters)



C) Geological cross section of Round Top (units: meters)

Fig. 4.2: Geological Cross sections of the laccoliths: A) Little Blanca, B) Little Round Top, C) Round Top.

GEOCHEMICAL DISTRIBUTION MAPS

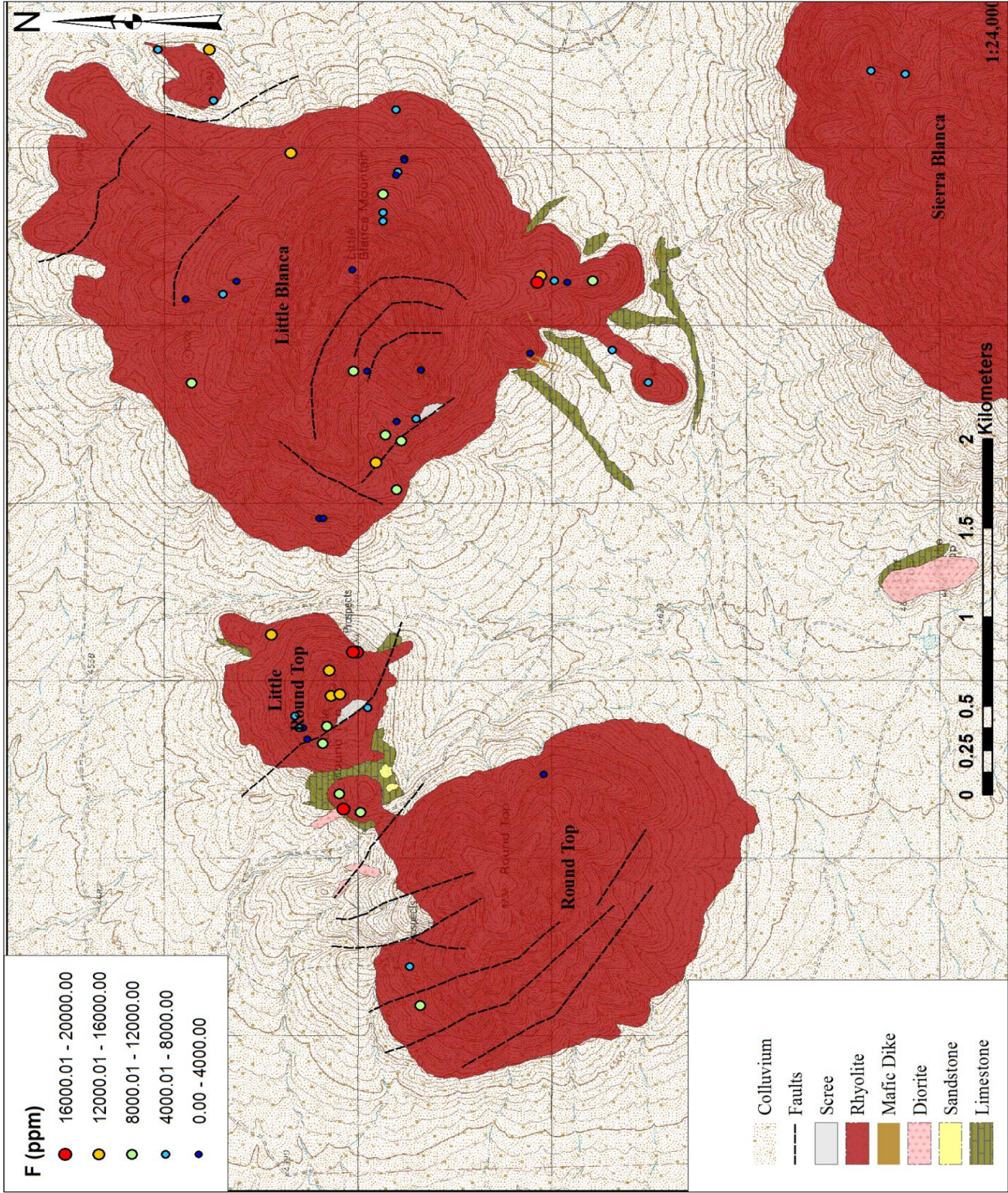
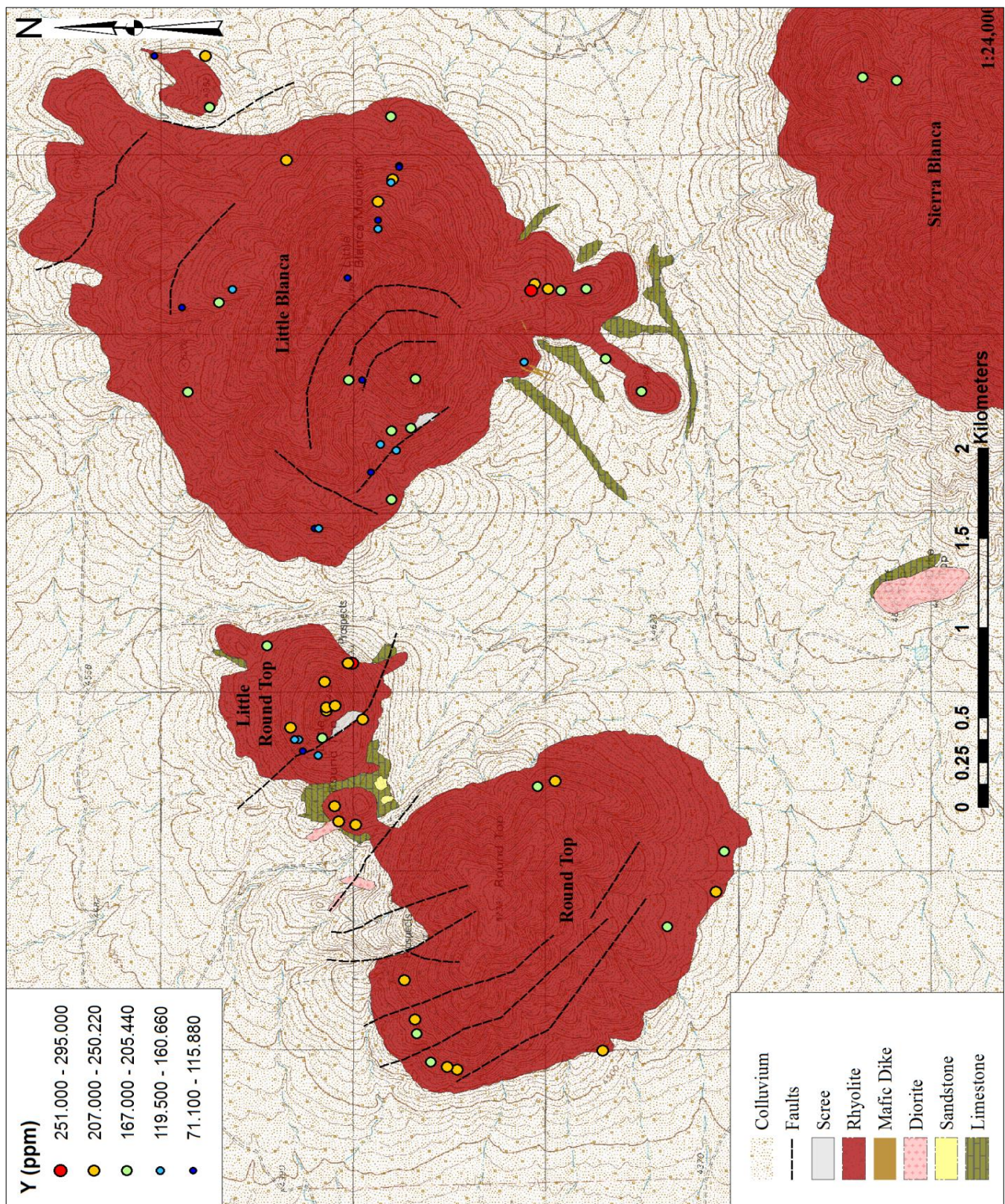


Fig. 4.3: F distribution



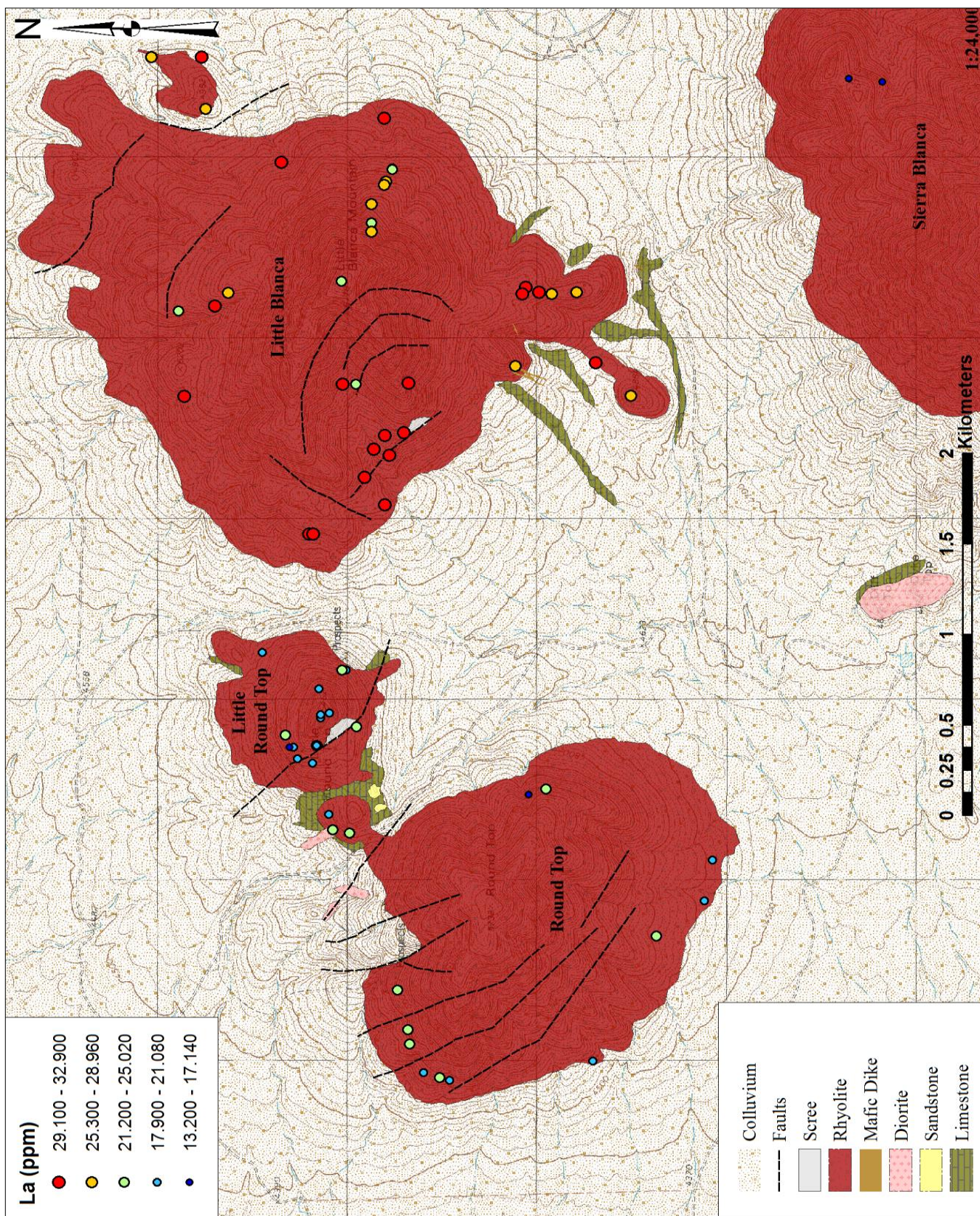


Fig 4.5: La distribution

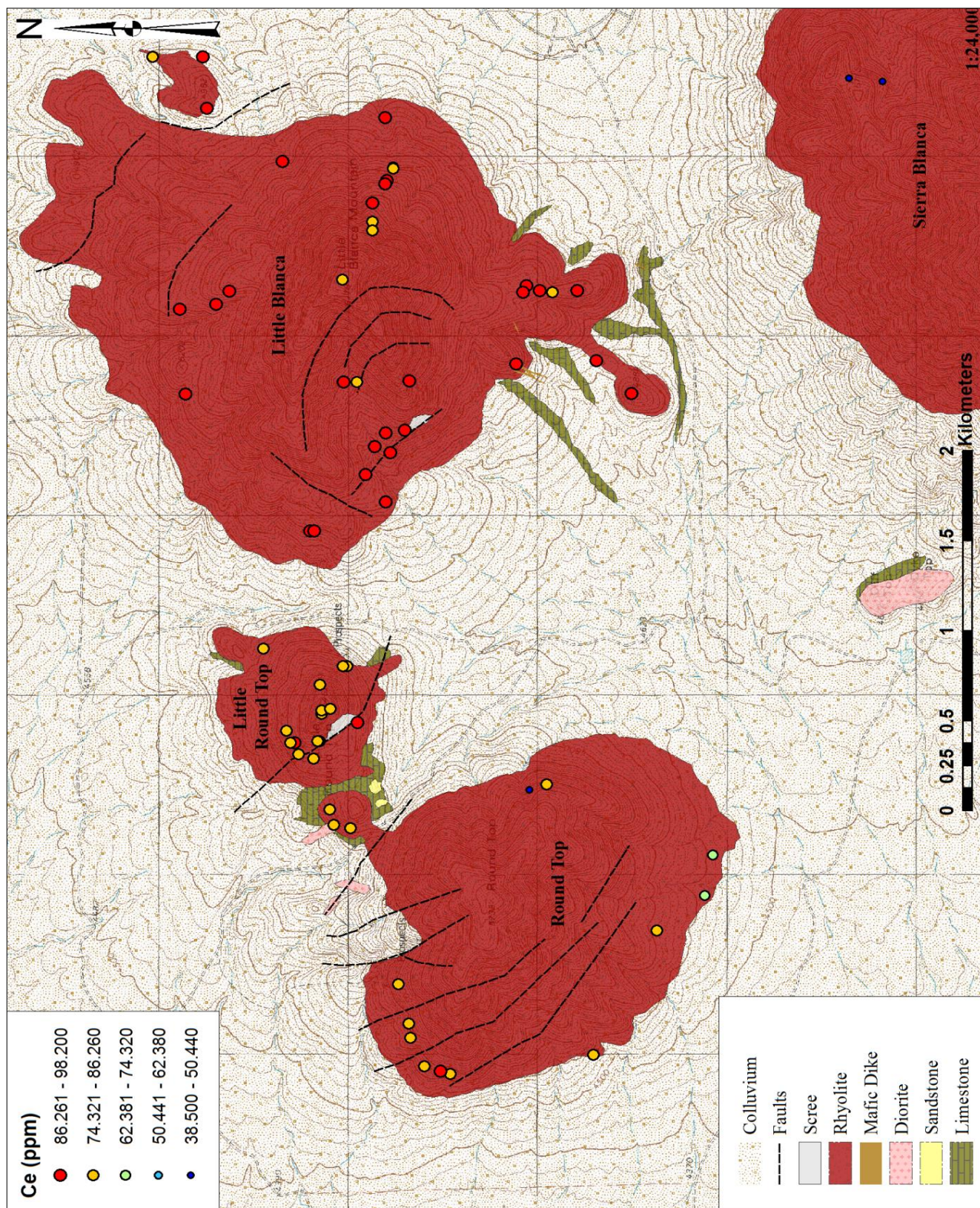


Fig. 4.6: Ce distribution

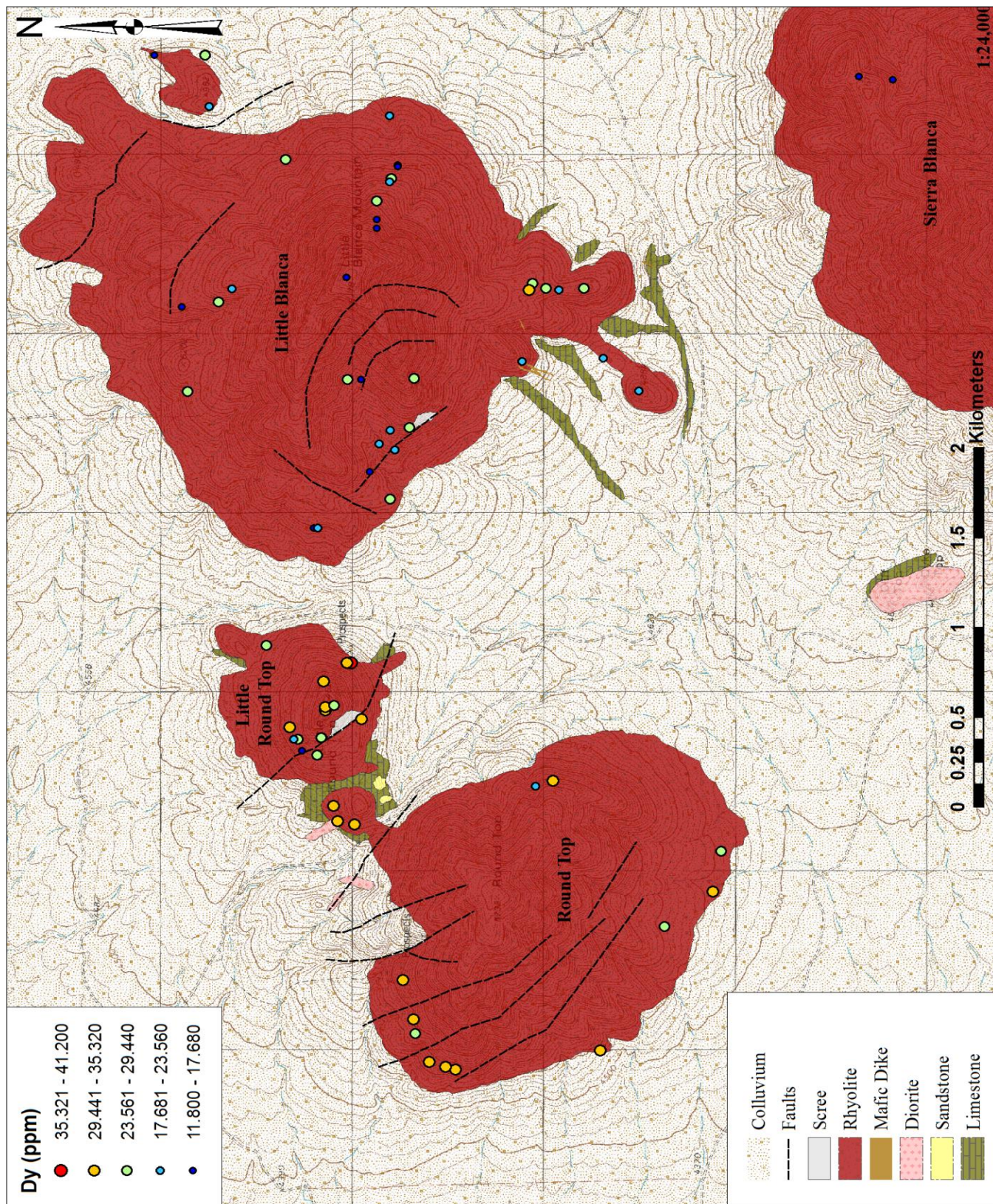


Fig. 4.7: Dy distribution

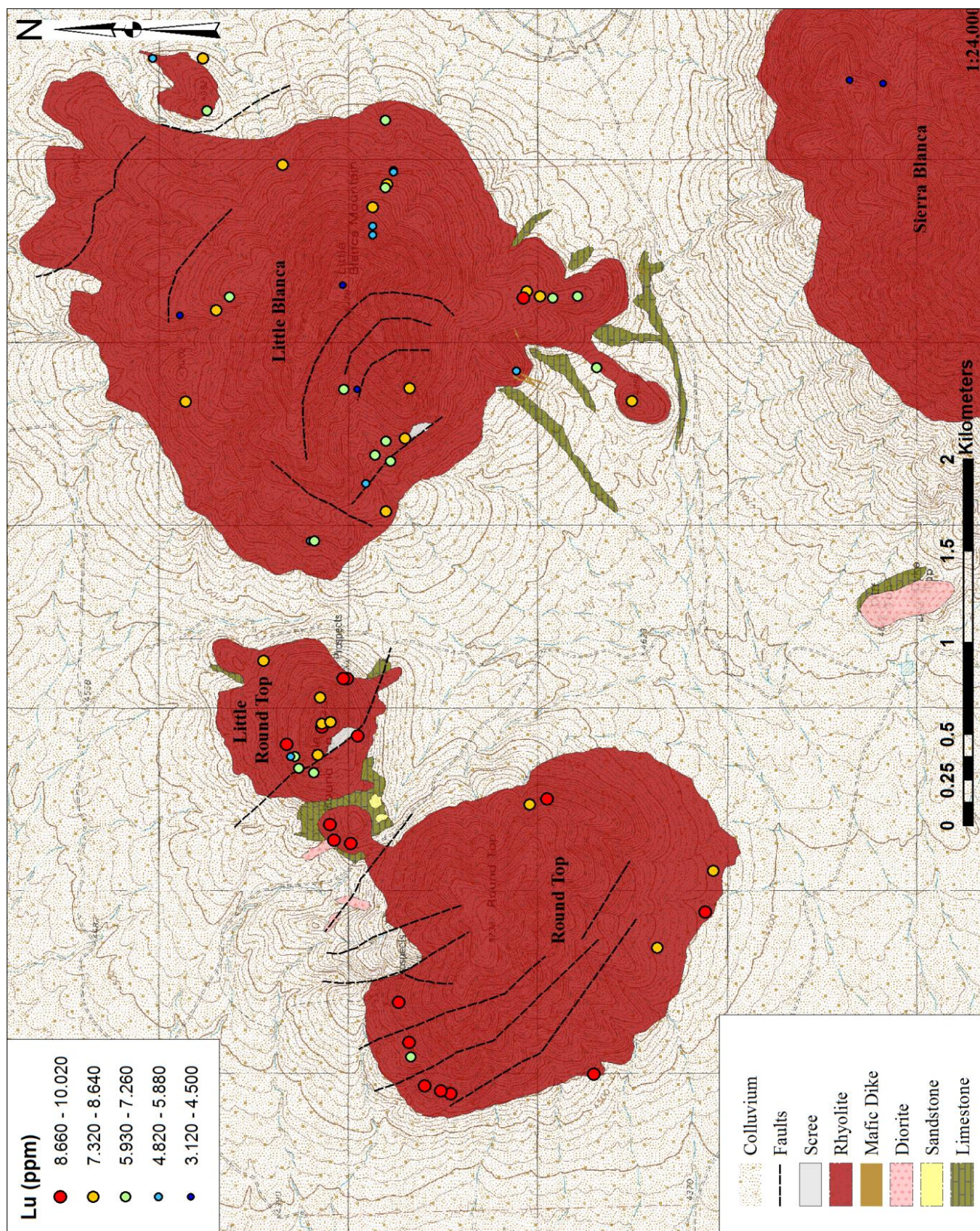


Fig. 4.8: Lu distribution

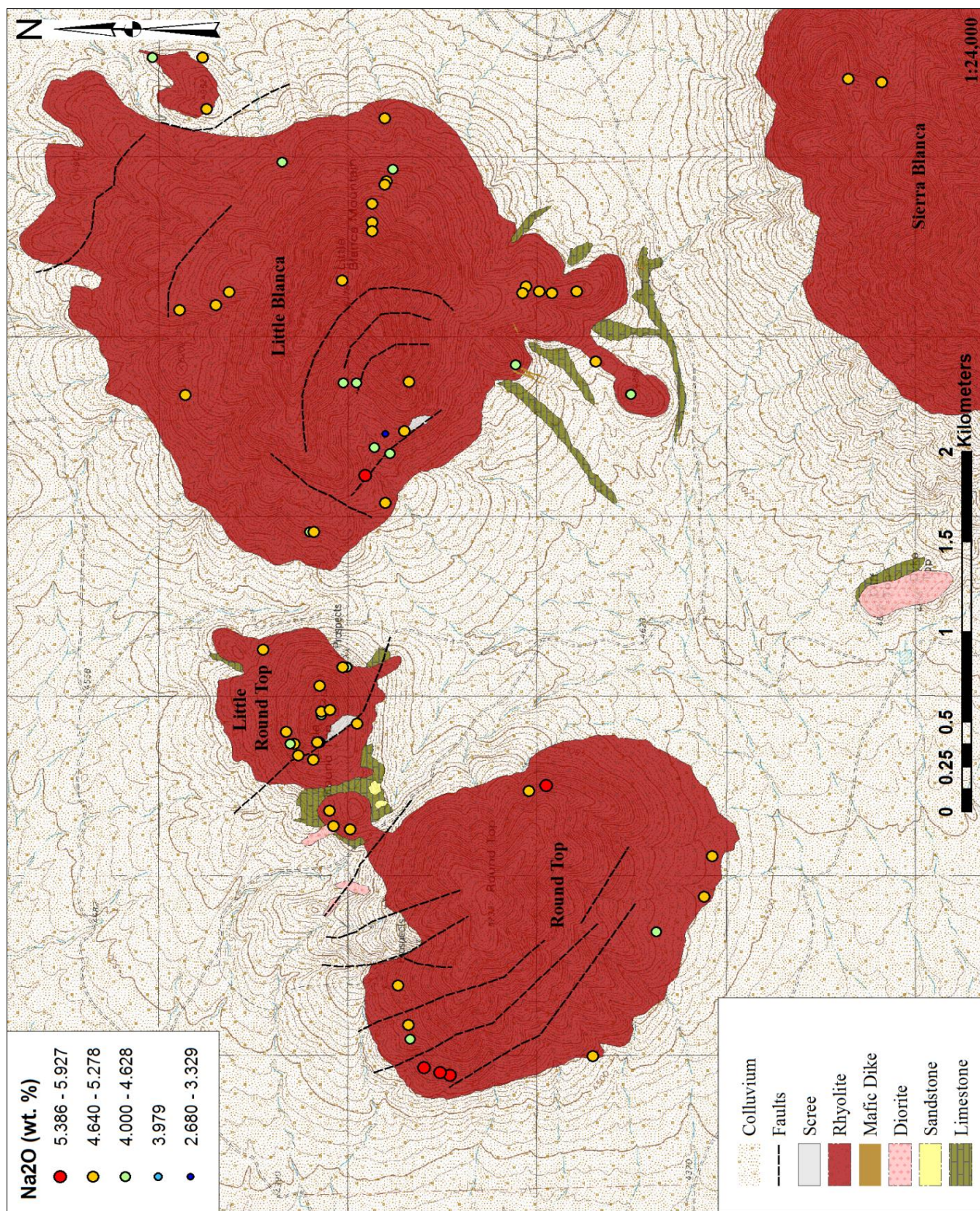


Fig. 4.10: Na₂O distribution

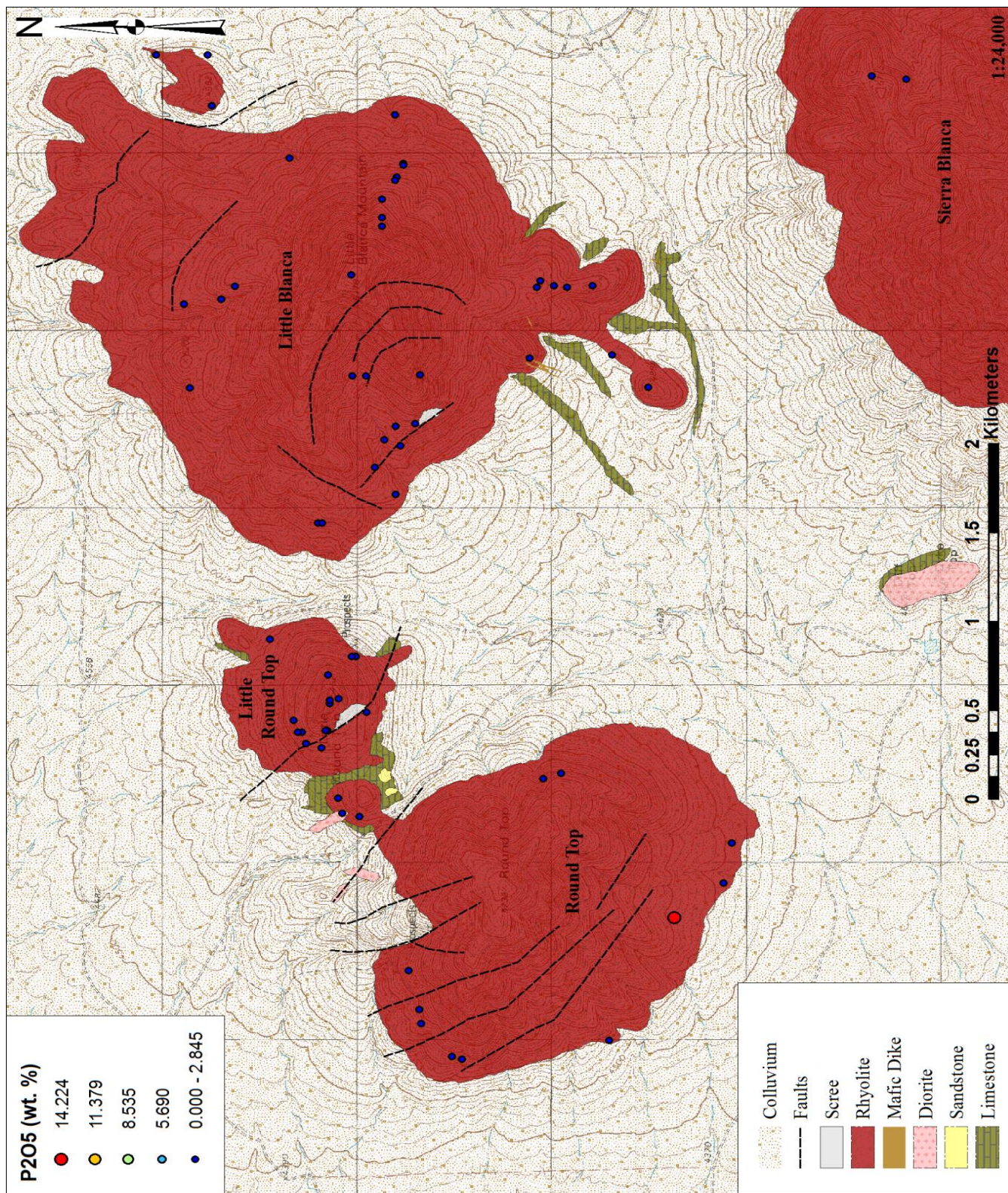


Fig. 4.12: P₂O₅ distribution

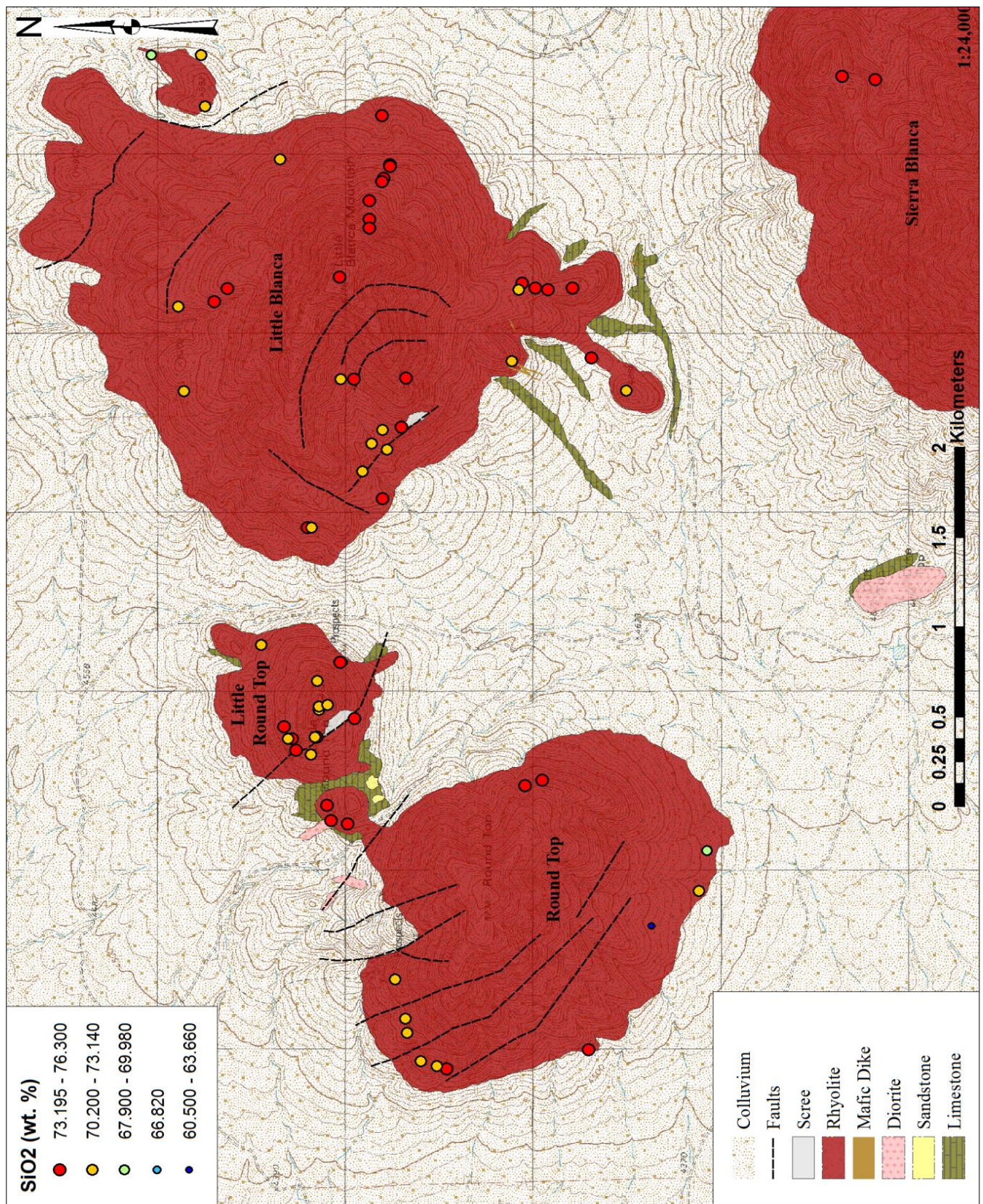


Fig. 4.13: SiO₂ distribution

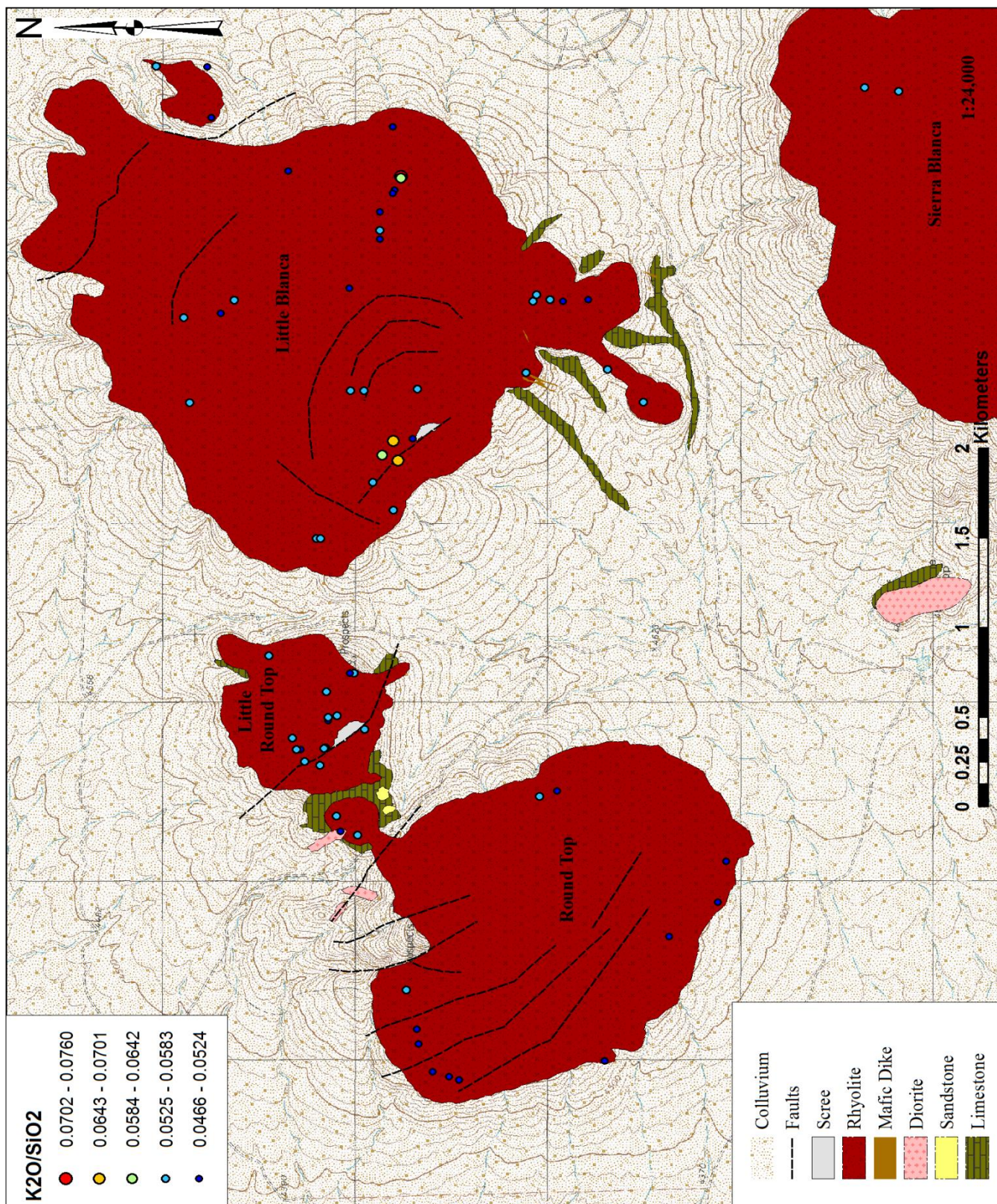


Fig. 4.14: K₂O/SiO₂

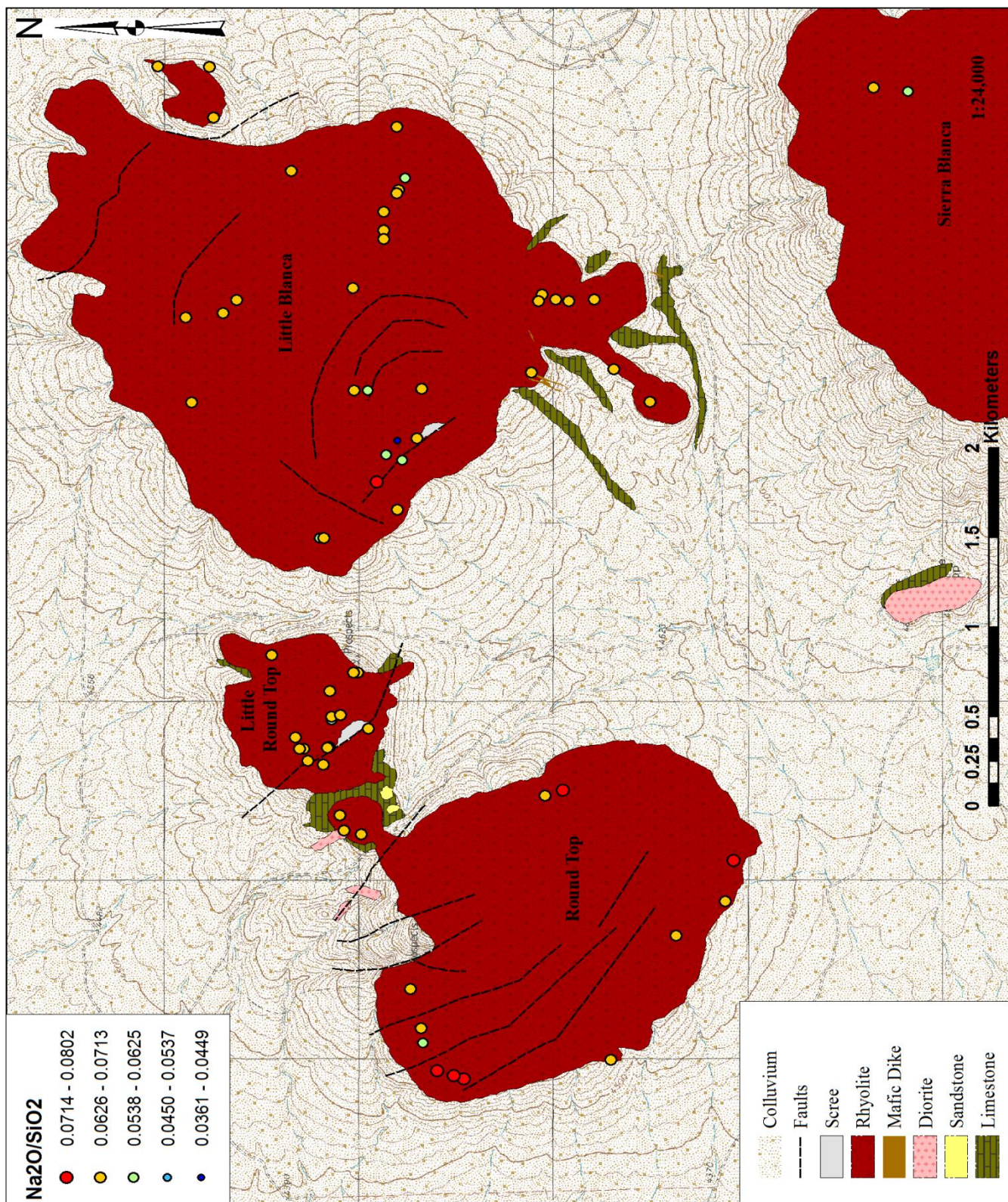


Fig. 4.15: Na₂O/SiO₂

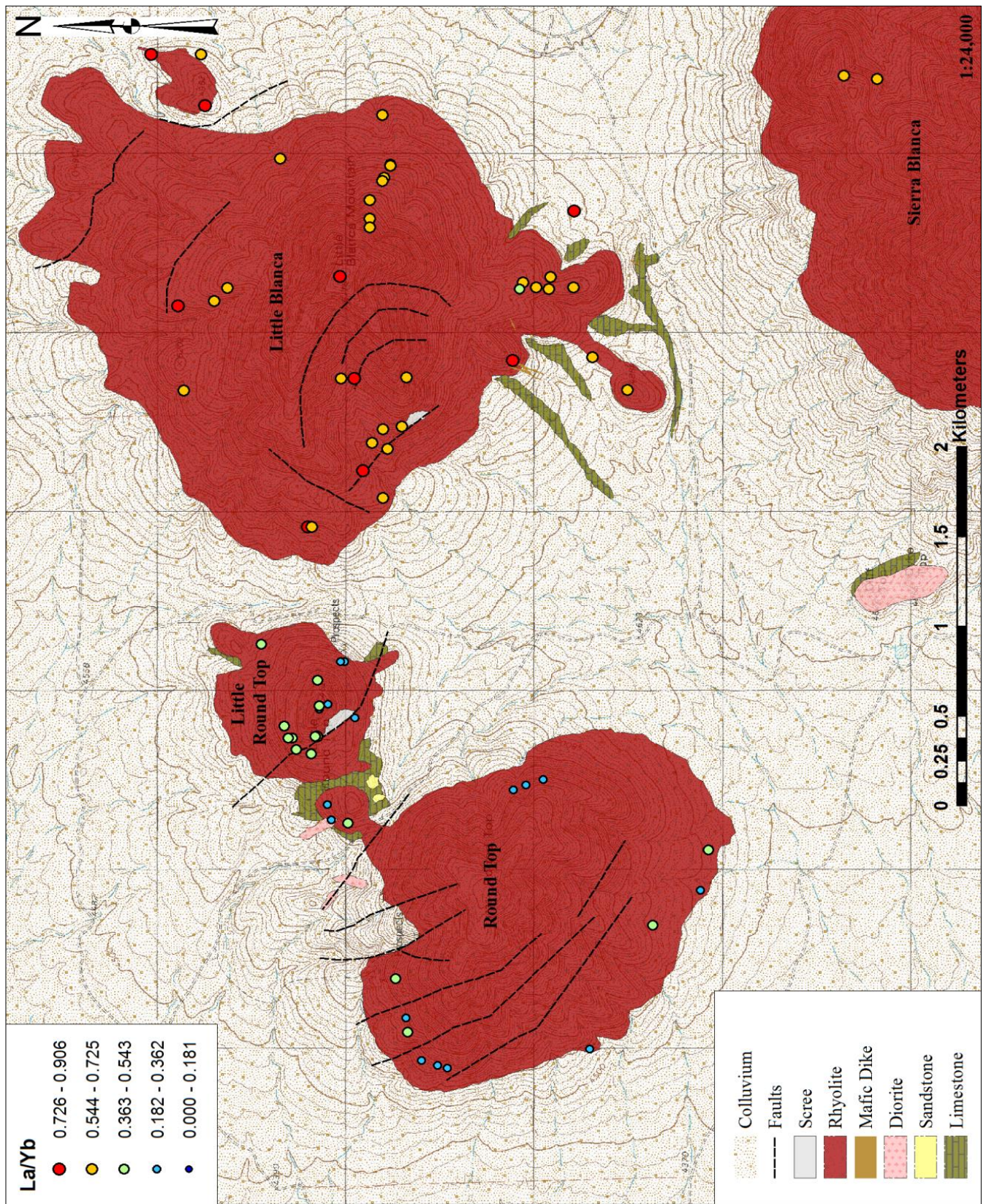


Fig. 4.16: La/Yb ratio distribution

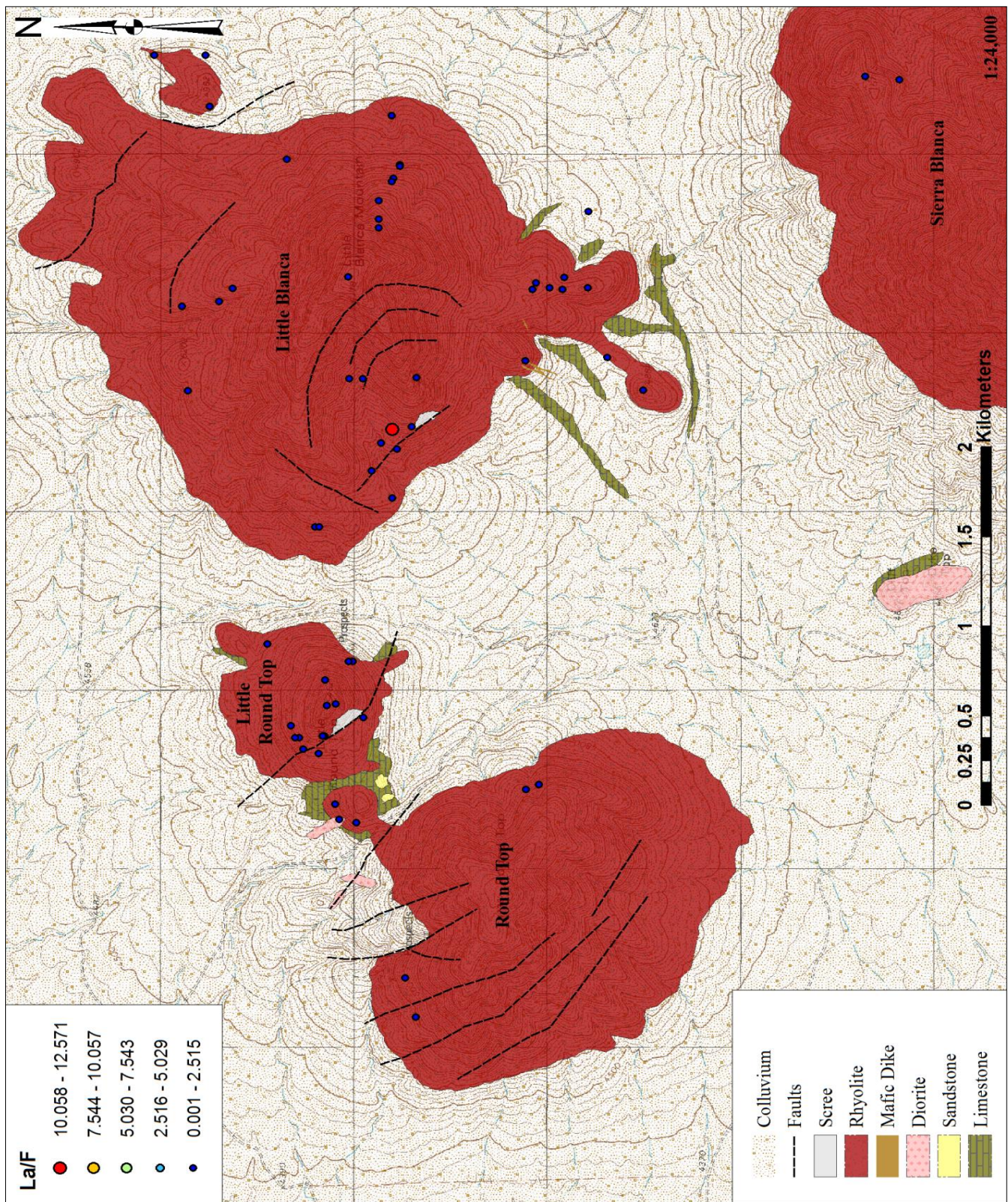


Fig. 4.17: La/F ratio distribution

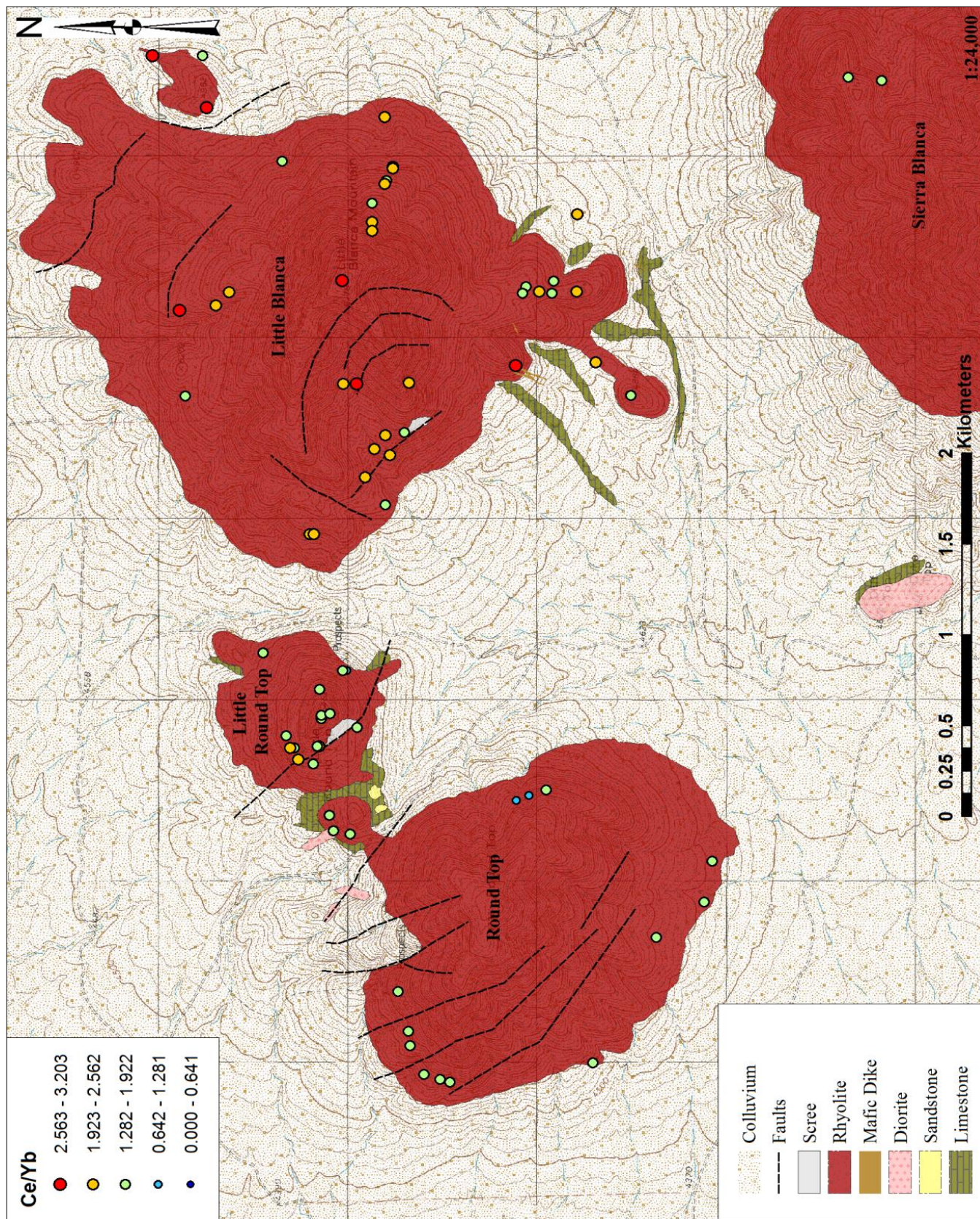


Fig. 4.18: Ce/Yb ratio distribution



Fig. 4.19: Nd/Yb ratio distribution

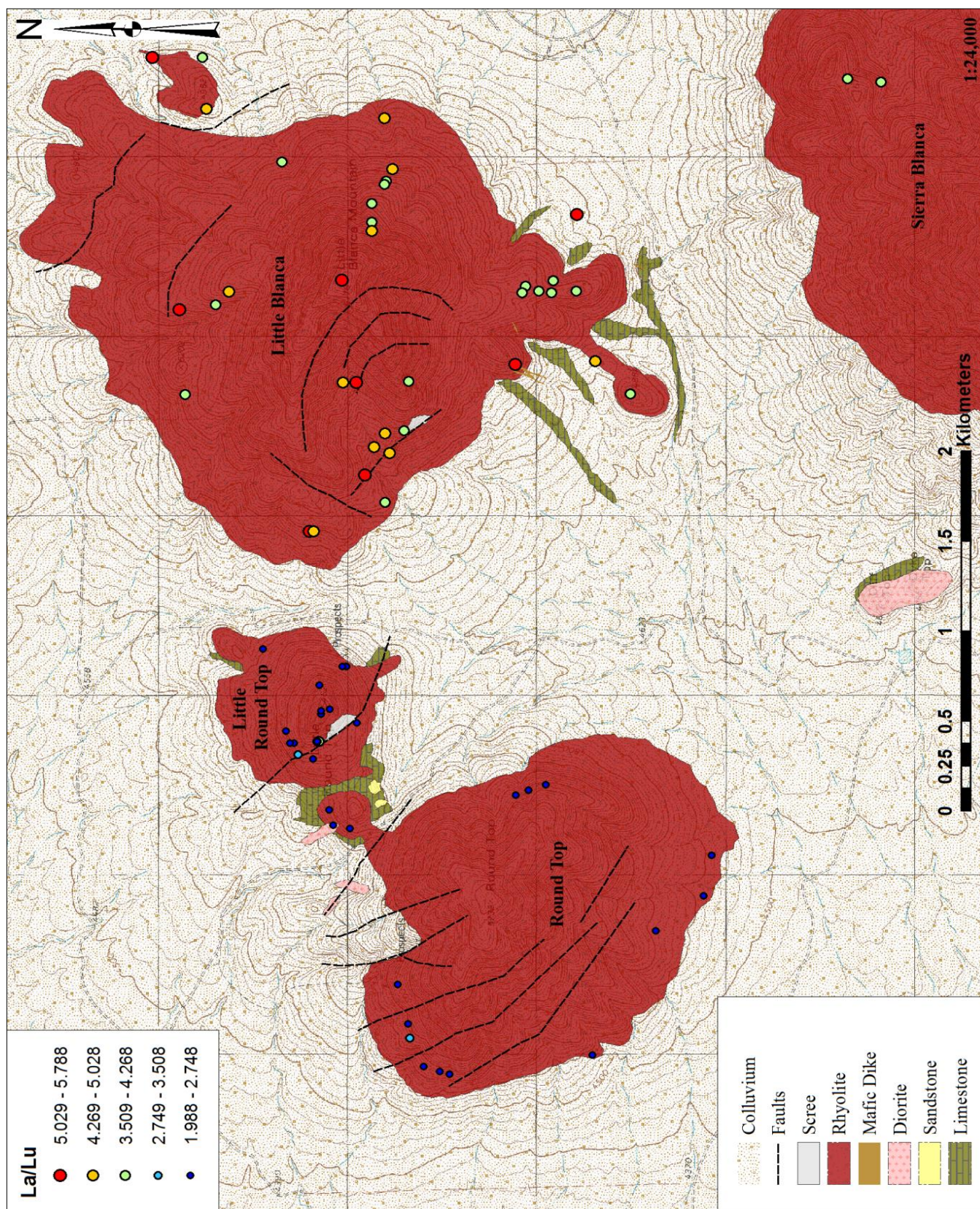


Fig. 4.20: La/Lu ratio distribution

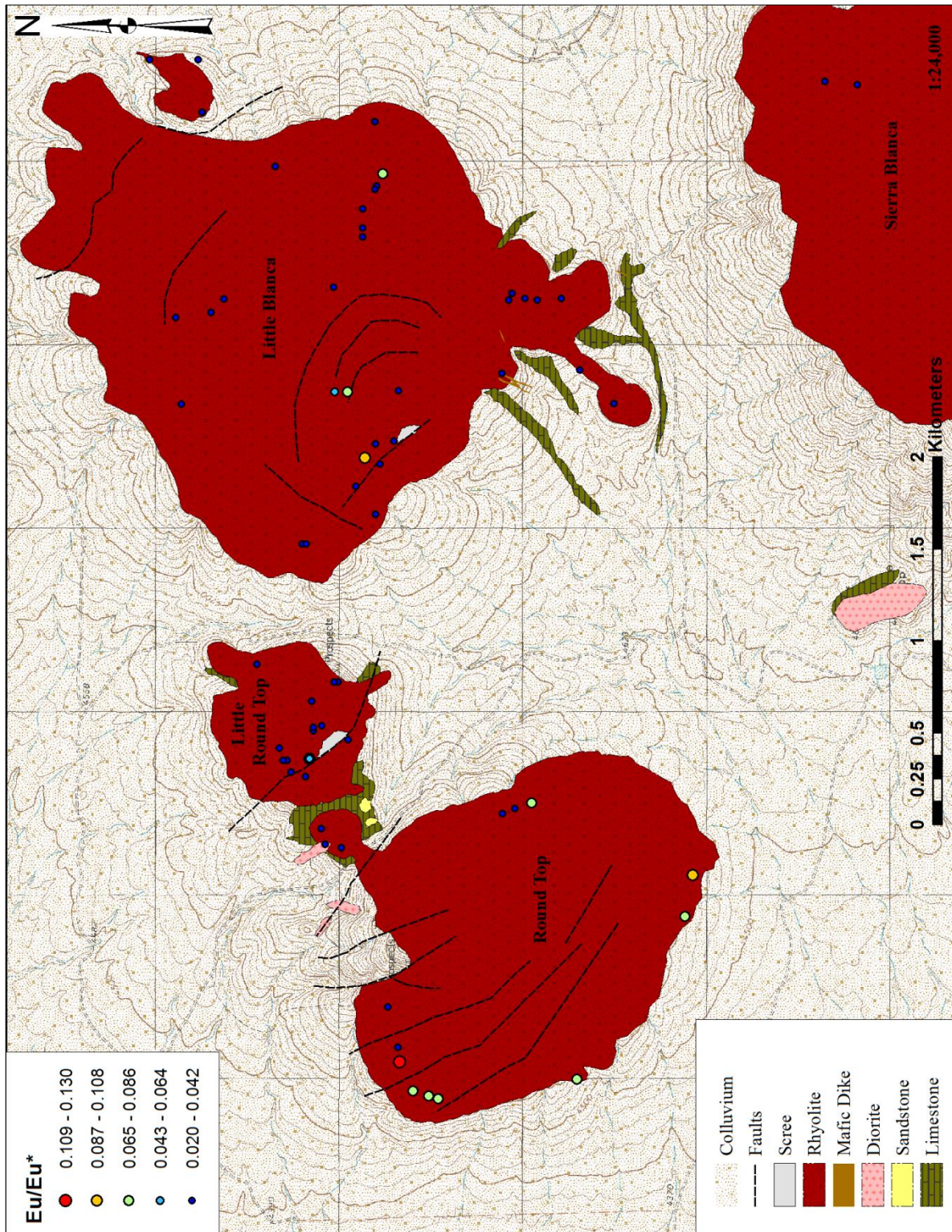


Fig. 4.21: Map showing increasing Eu/Eu^* magnitude from SB-LB-LRT-RT

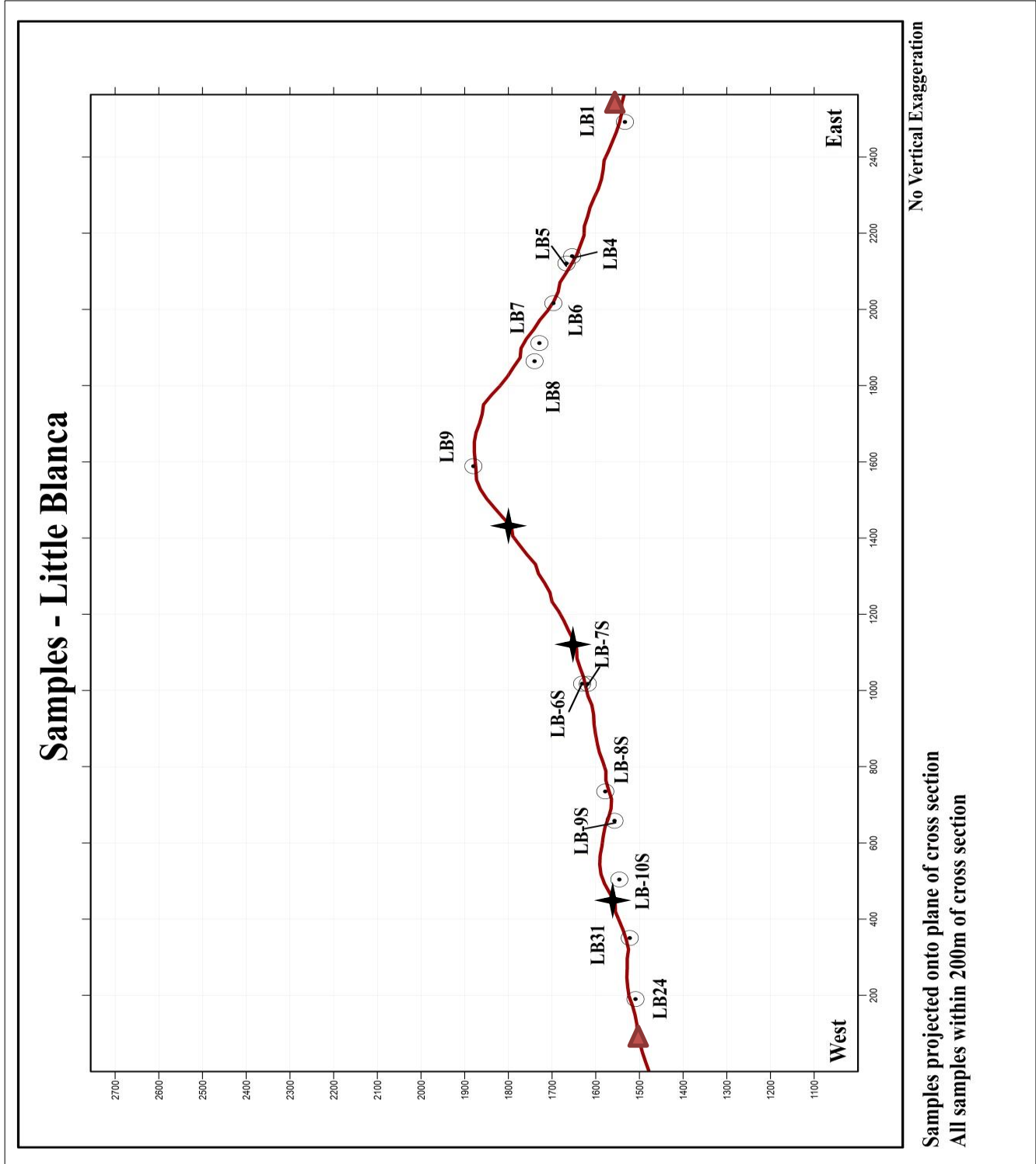


Fig. 4.22: Samples projected onto plane of profile – Little Blanca: ★ Inferred Fault, ▲ Contact

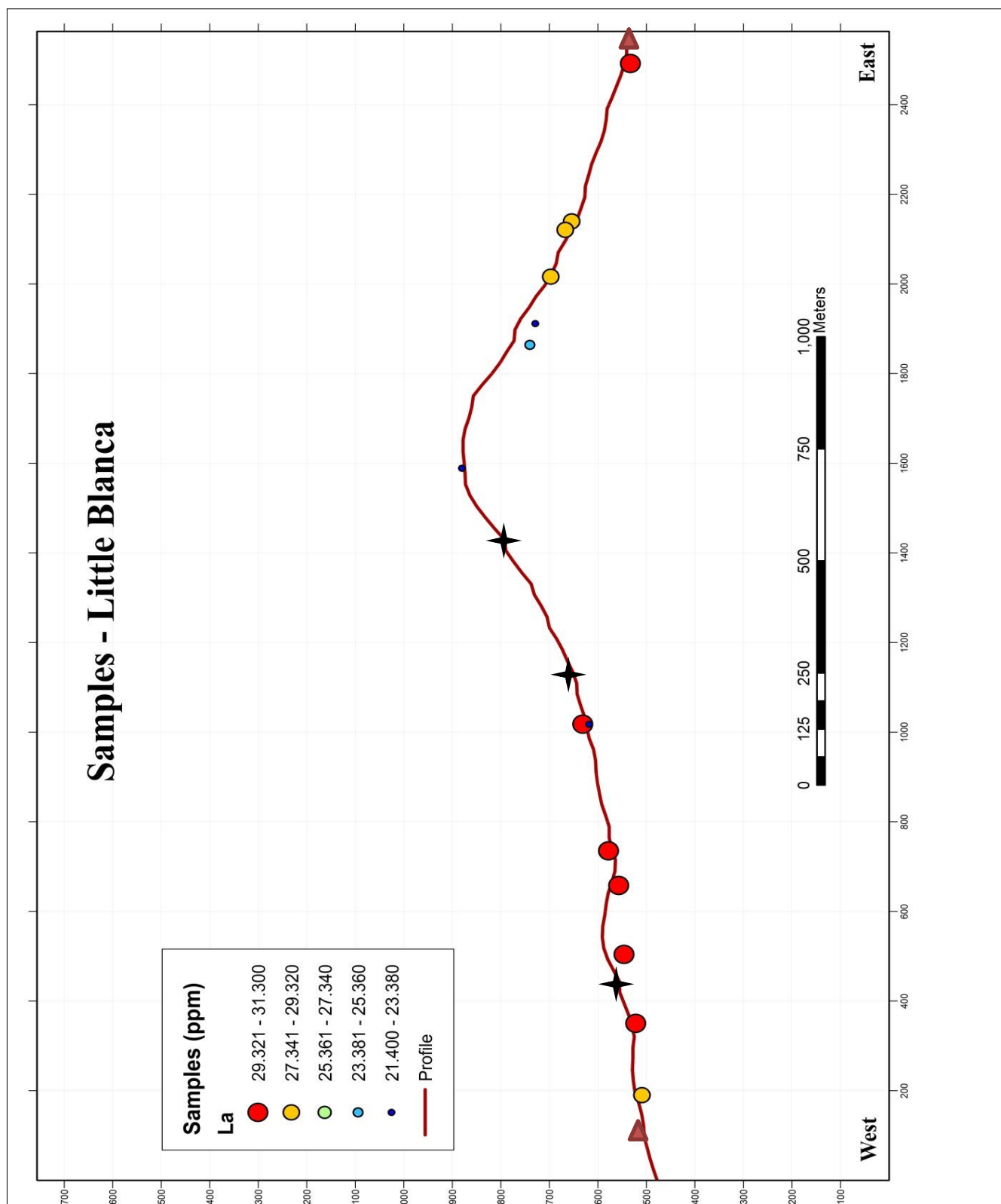


Fig. 4.23: La profile – Little Blanca: ★ Inferred Fault, ▲ Contact

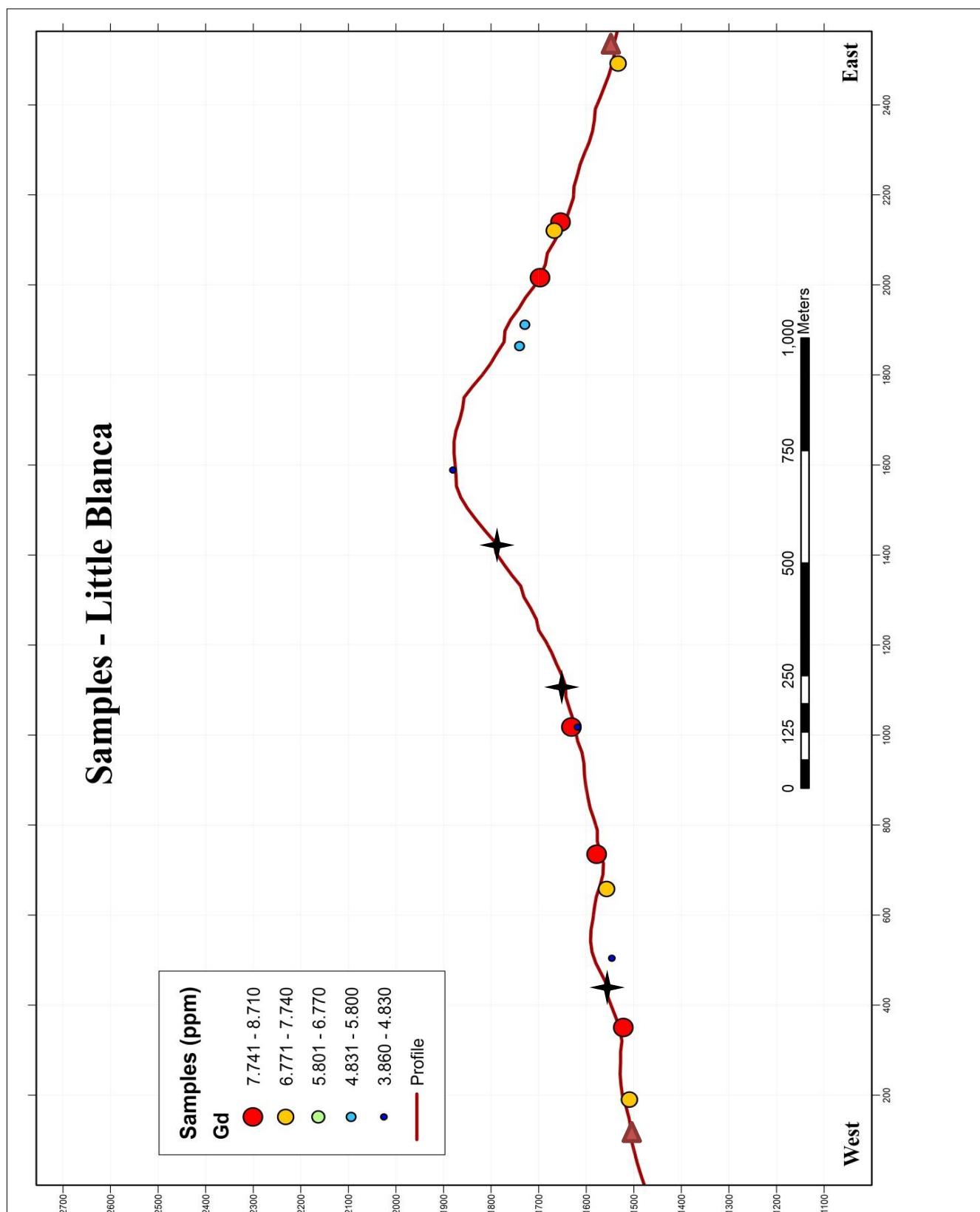


Fig. 4.24: Gd profile – Little Blanca: ★ Inferred Fault, ▲ Contact

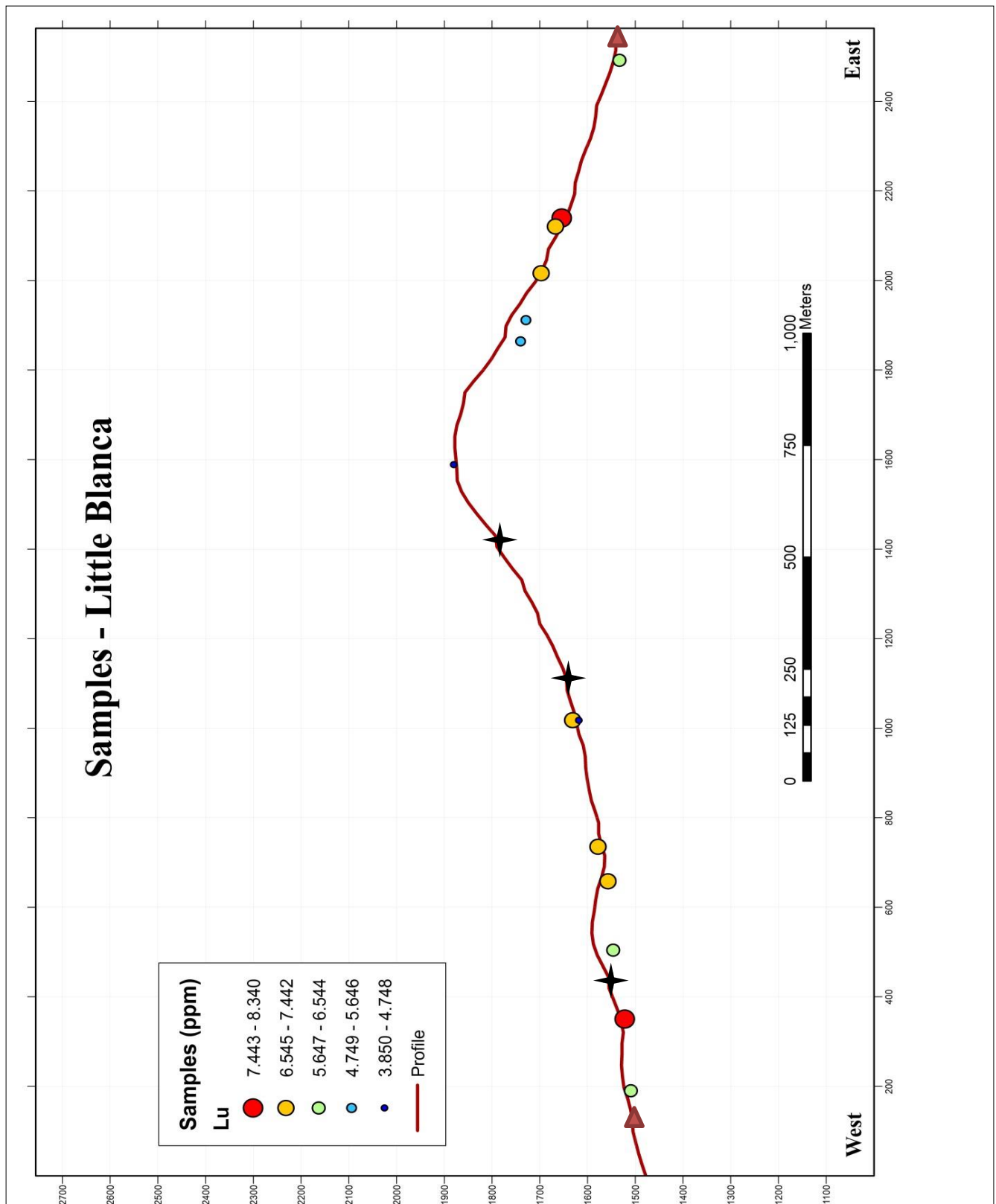


Fig. 4.25: Lu profile – Little Blanca: ★ Inferred Fault, ▲ Contact

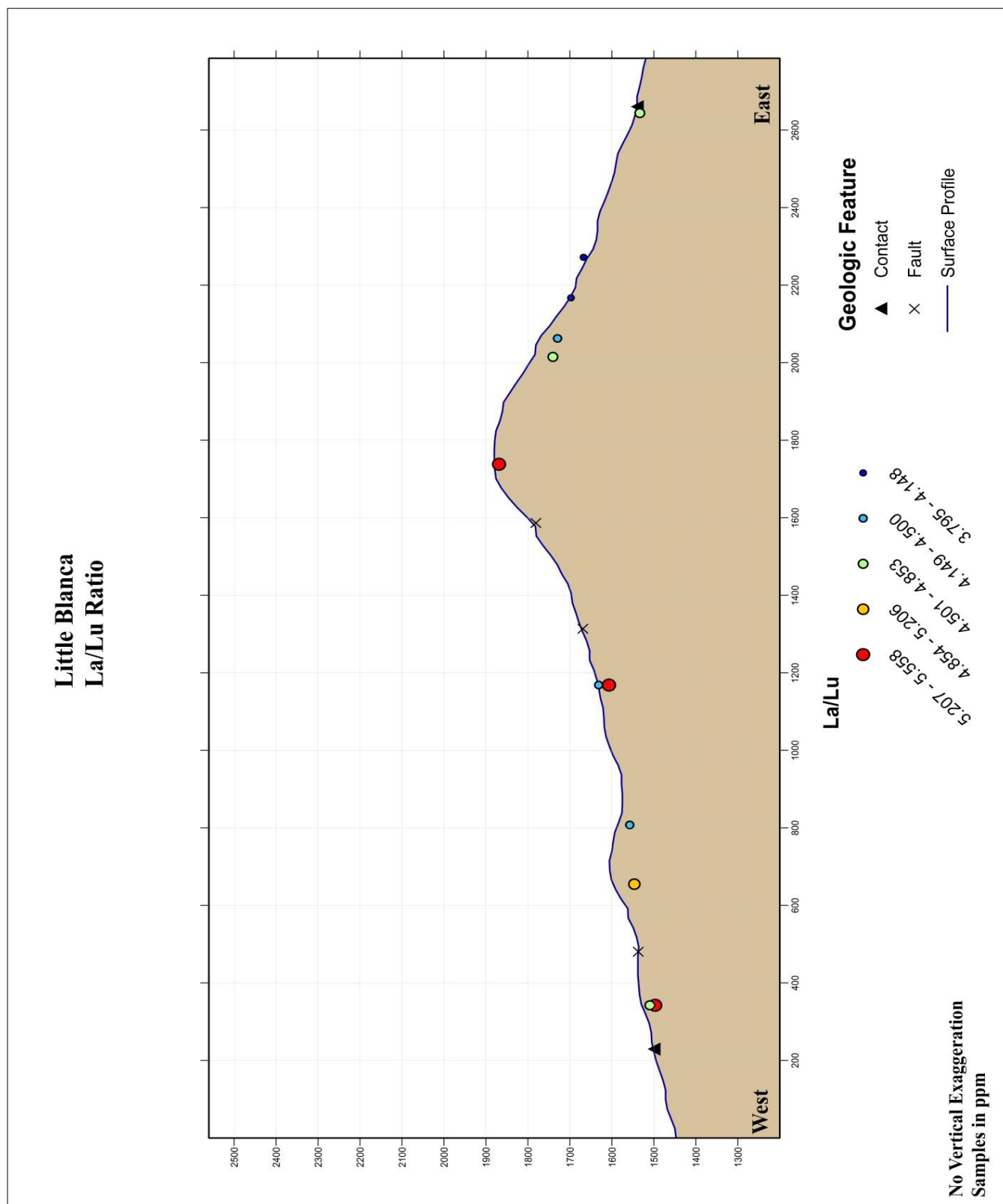


Fig. 4.26: La/Lu ratio profile – Little Blanca

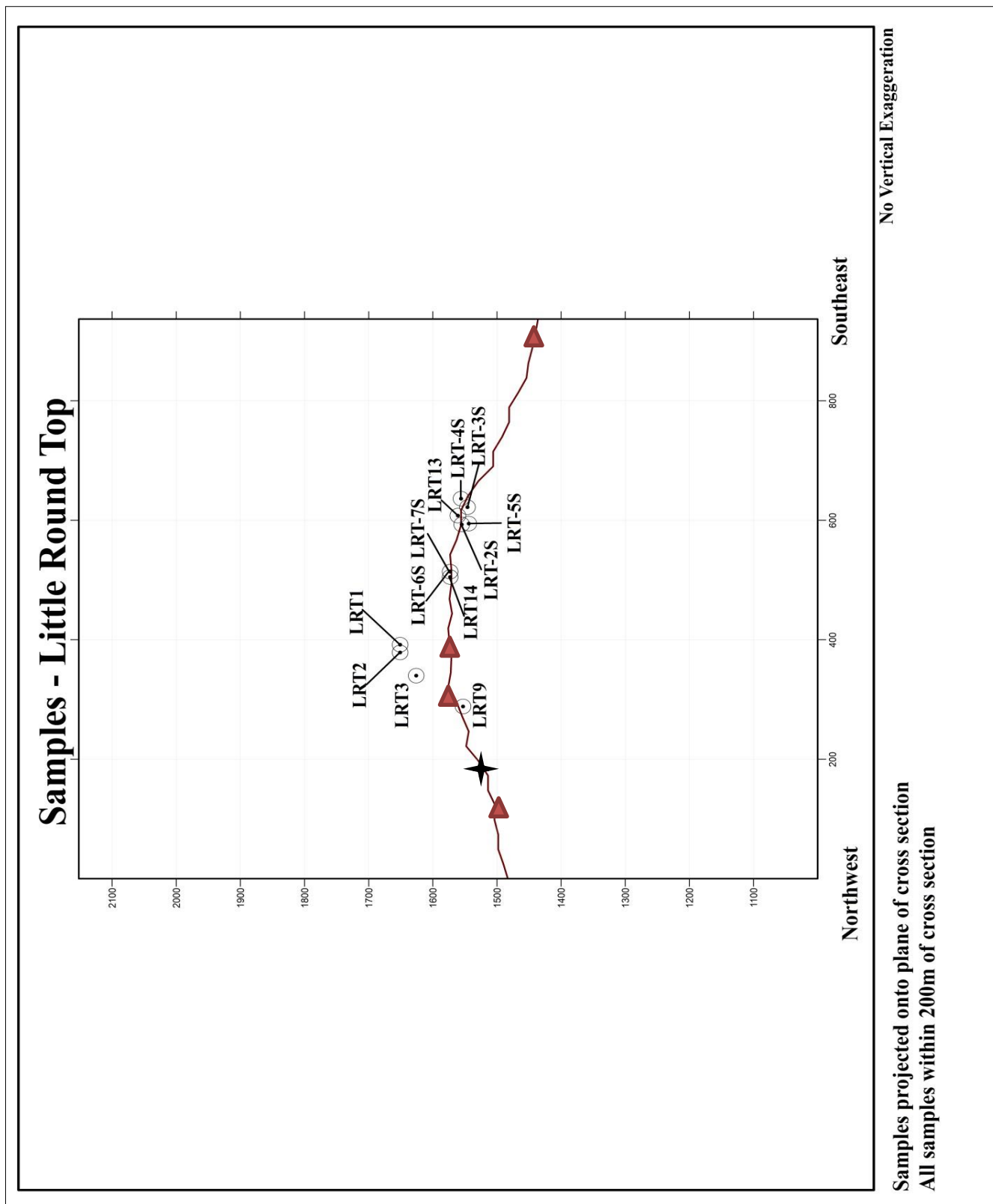


Fig. 4.27: Samples projected onto plane of profile – Little Round Top: ★ Inferred Fault, ▲ Contact

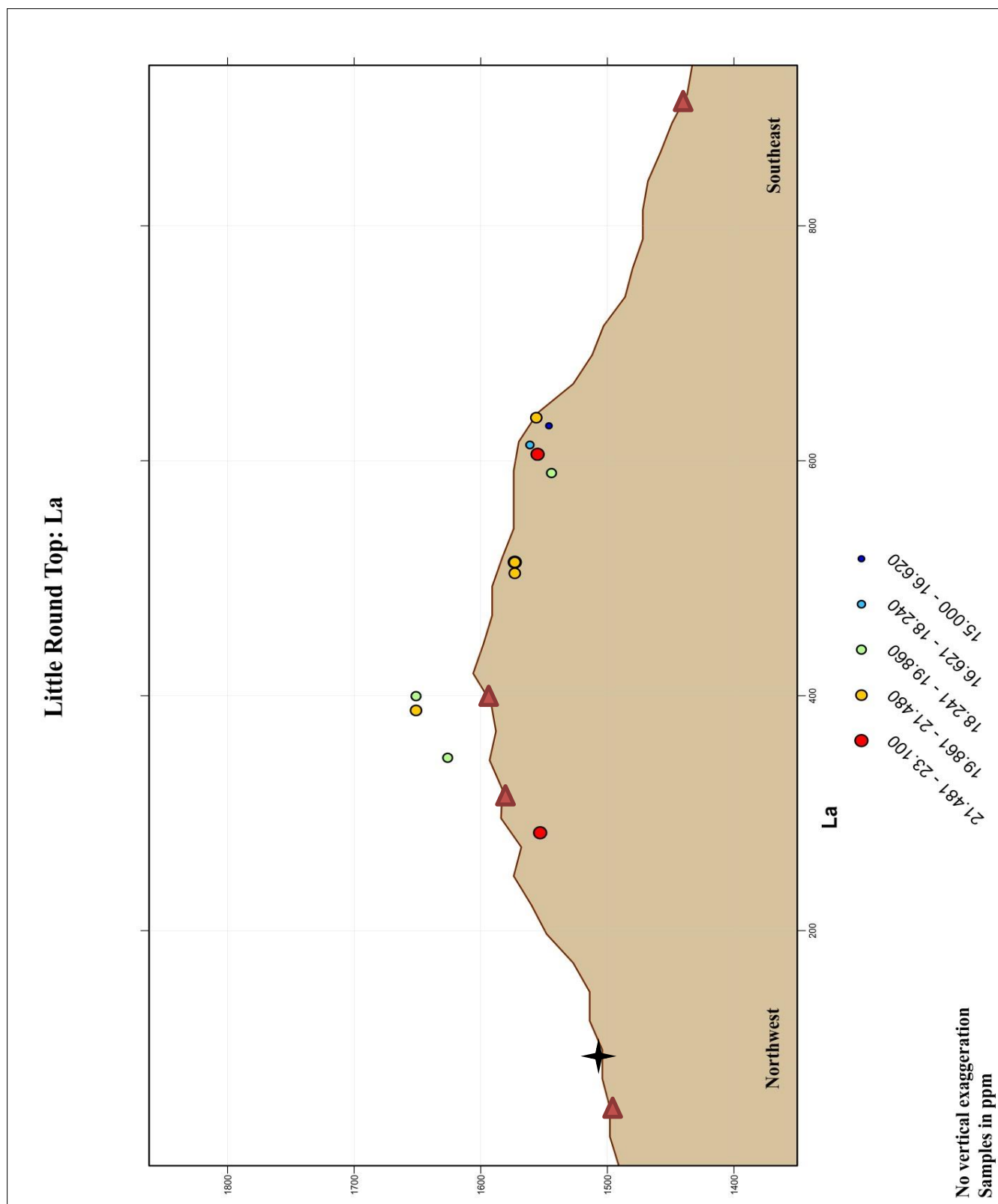


Fig. 4.28: La profile – Little Round Top: ★ Inferred Fault, ▲ Contact

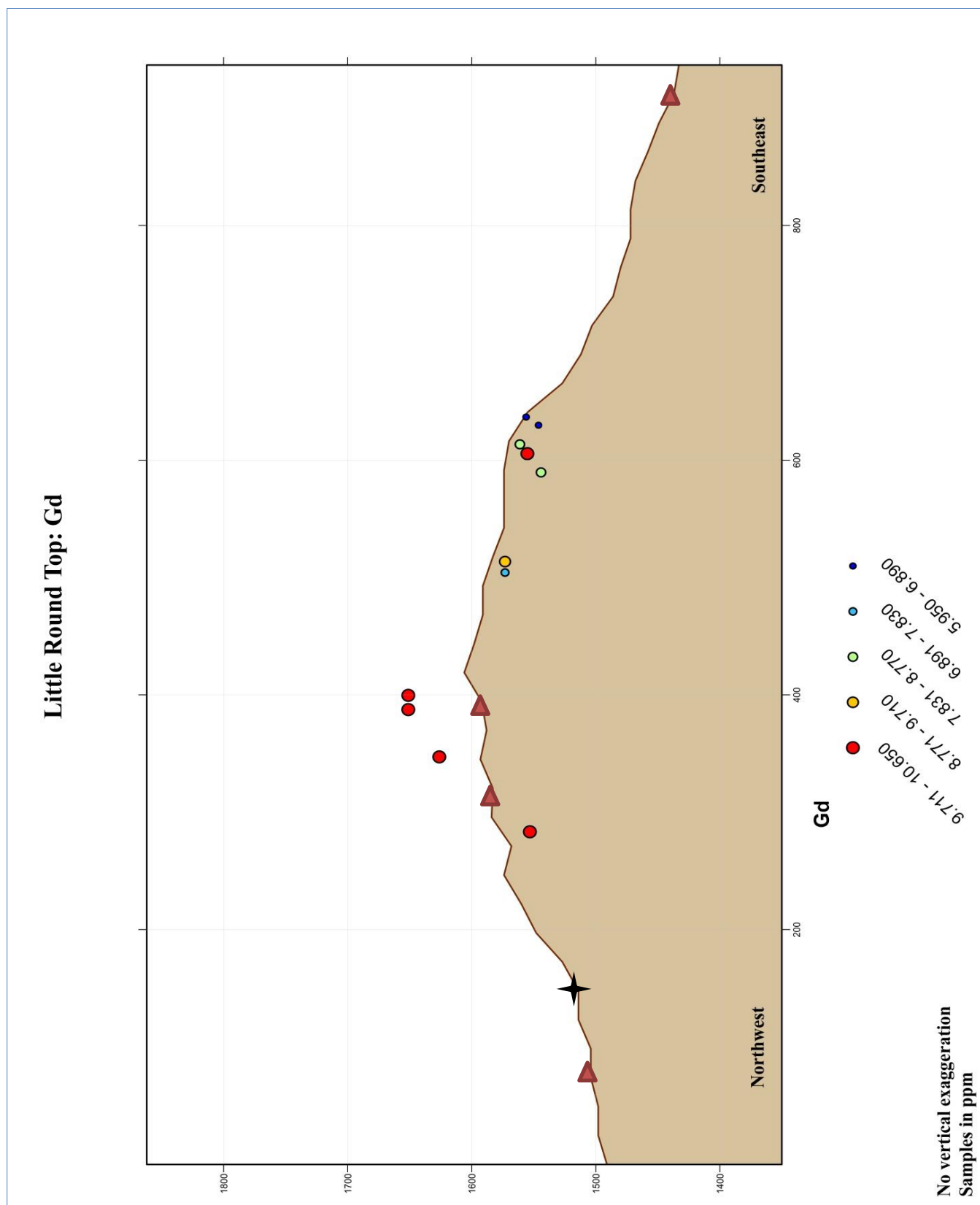


Fig. 4.29: Gd profile – Little Round Top: ★ Inferred Fault, ▲ Contact

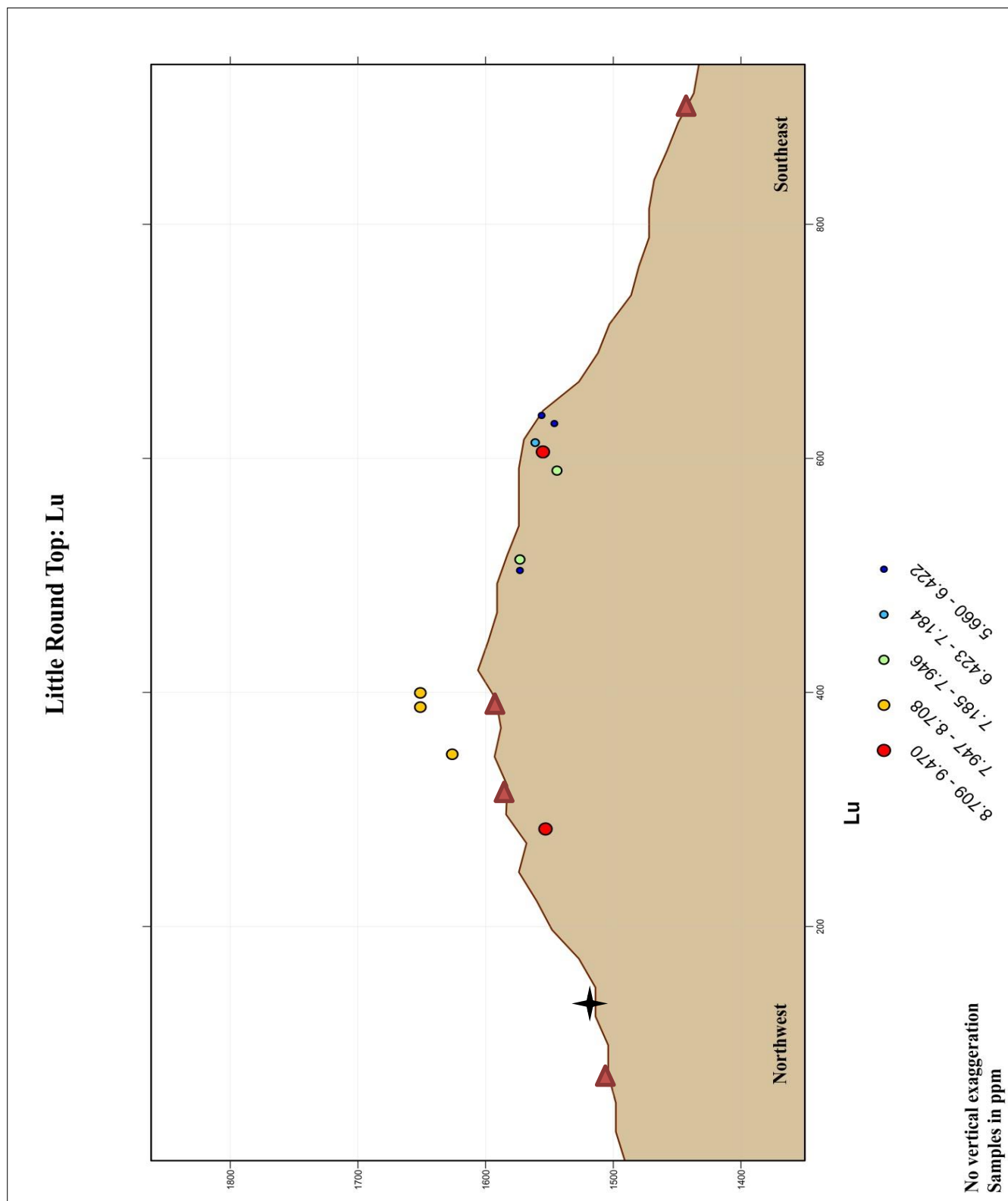


Fig. 4.30: Lu profile – Little Round Top: ★ Inferred Fault, ▲ Contact

Little Round Top La/Lu Ratio

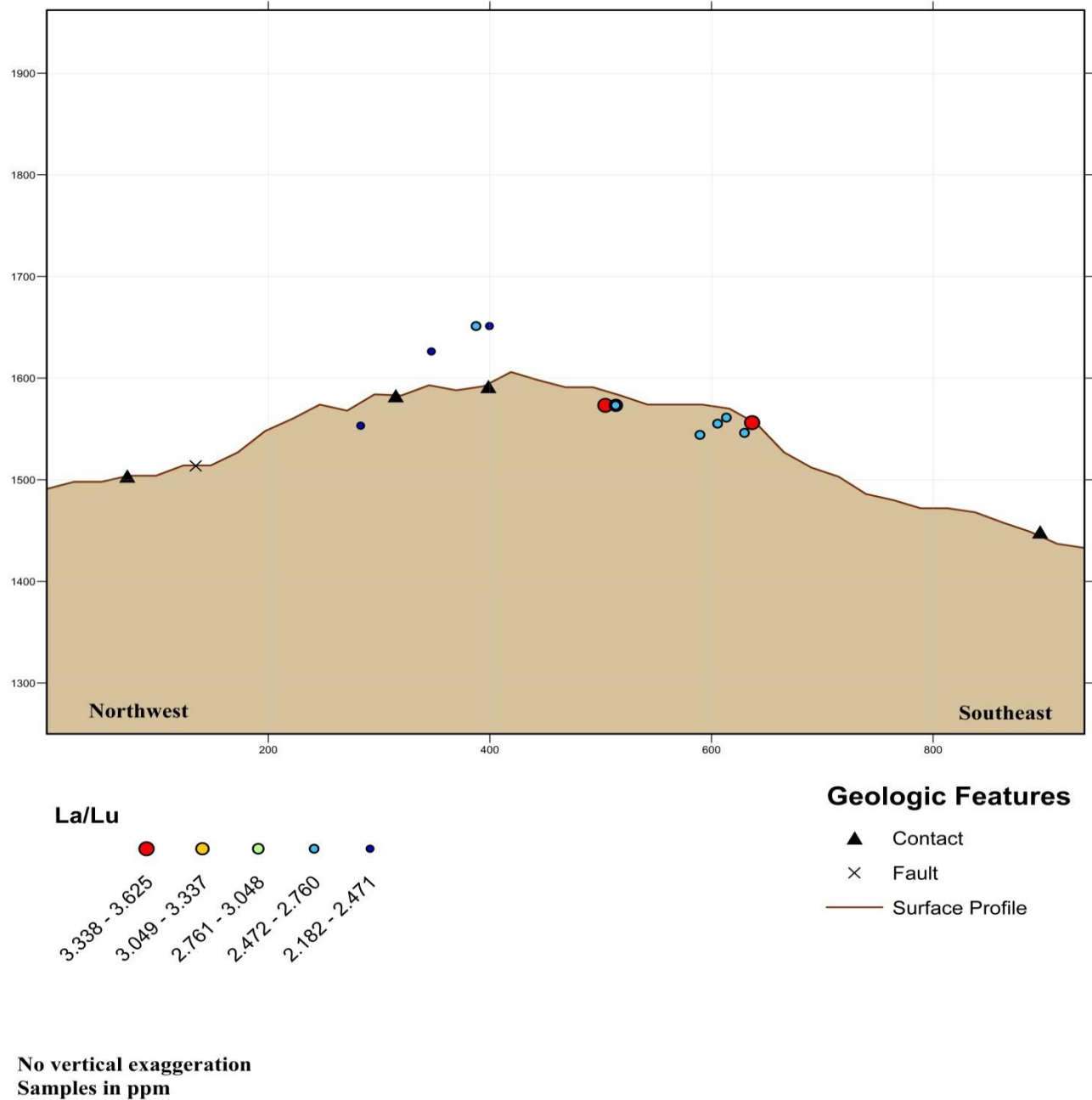


Fig. 4.31: La/Lu ratio profile – Little Round Top

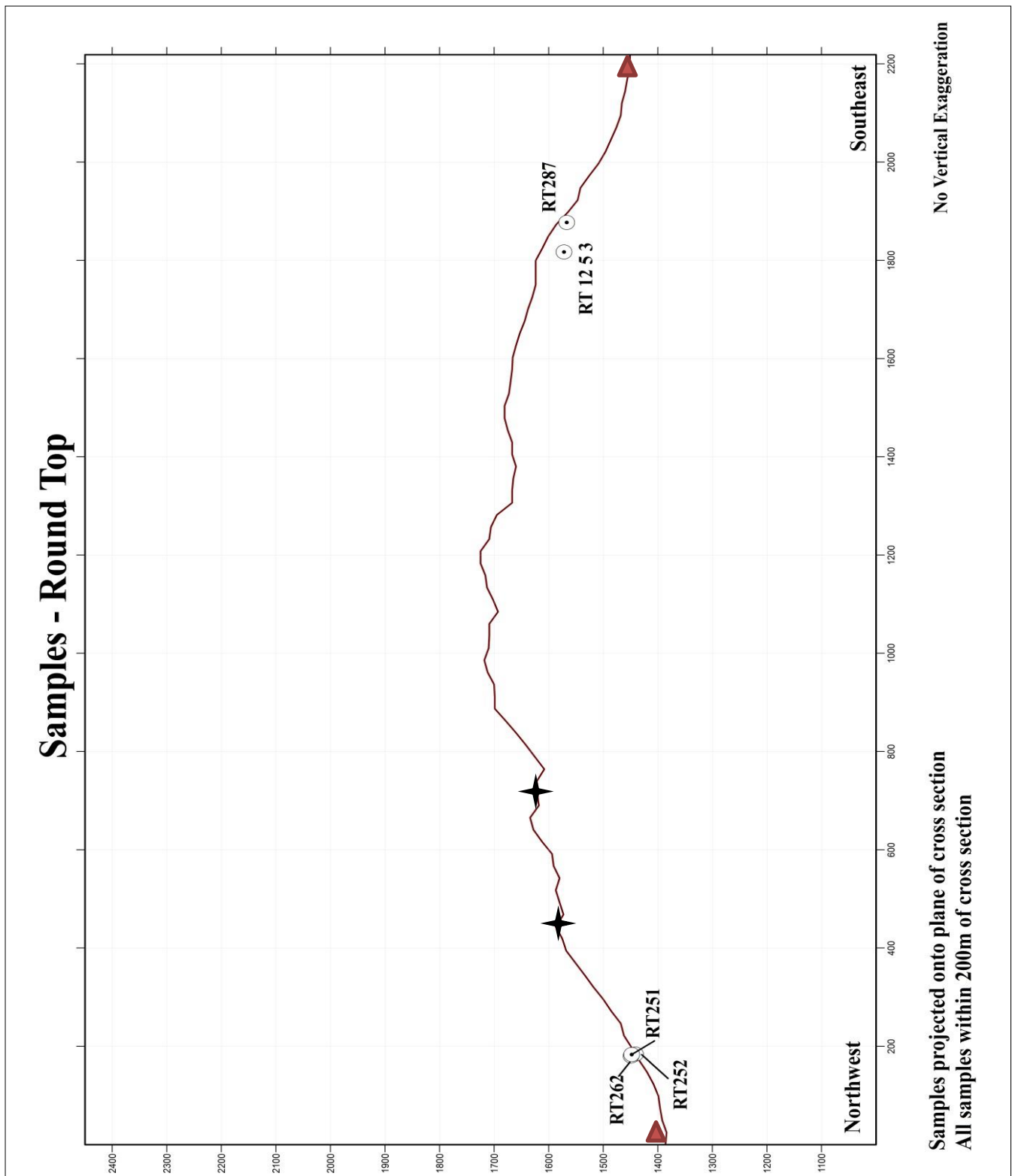


Fig. 4.32: Samples projected onto plane of profile – Round Top: ★ Inferred Fault, ▲ Contact

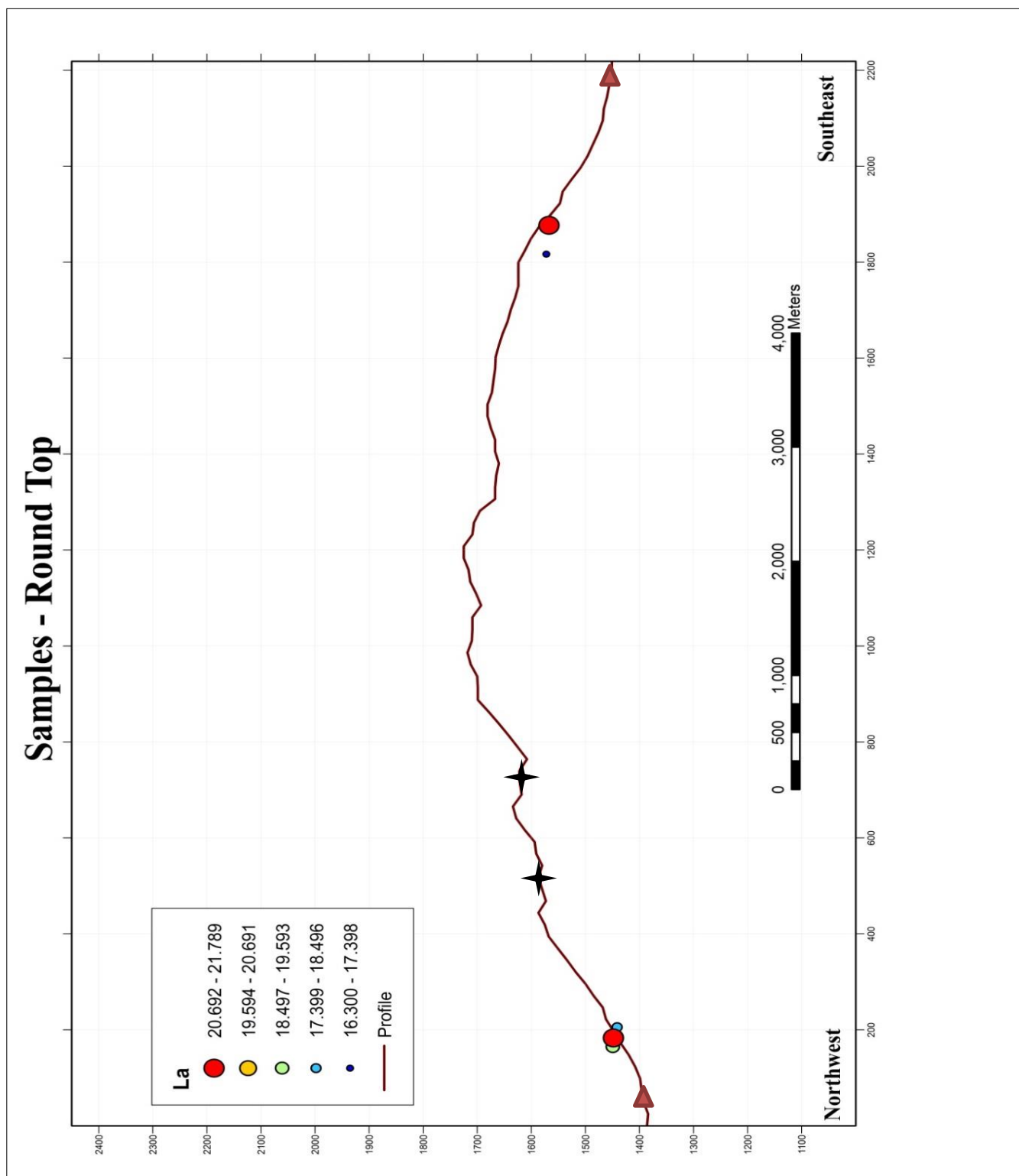


Fig. 4.33: La profile – Round Top: ★ Inferred Fault, ▲ Contact

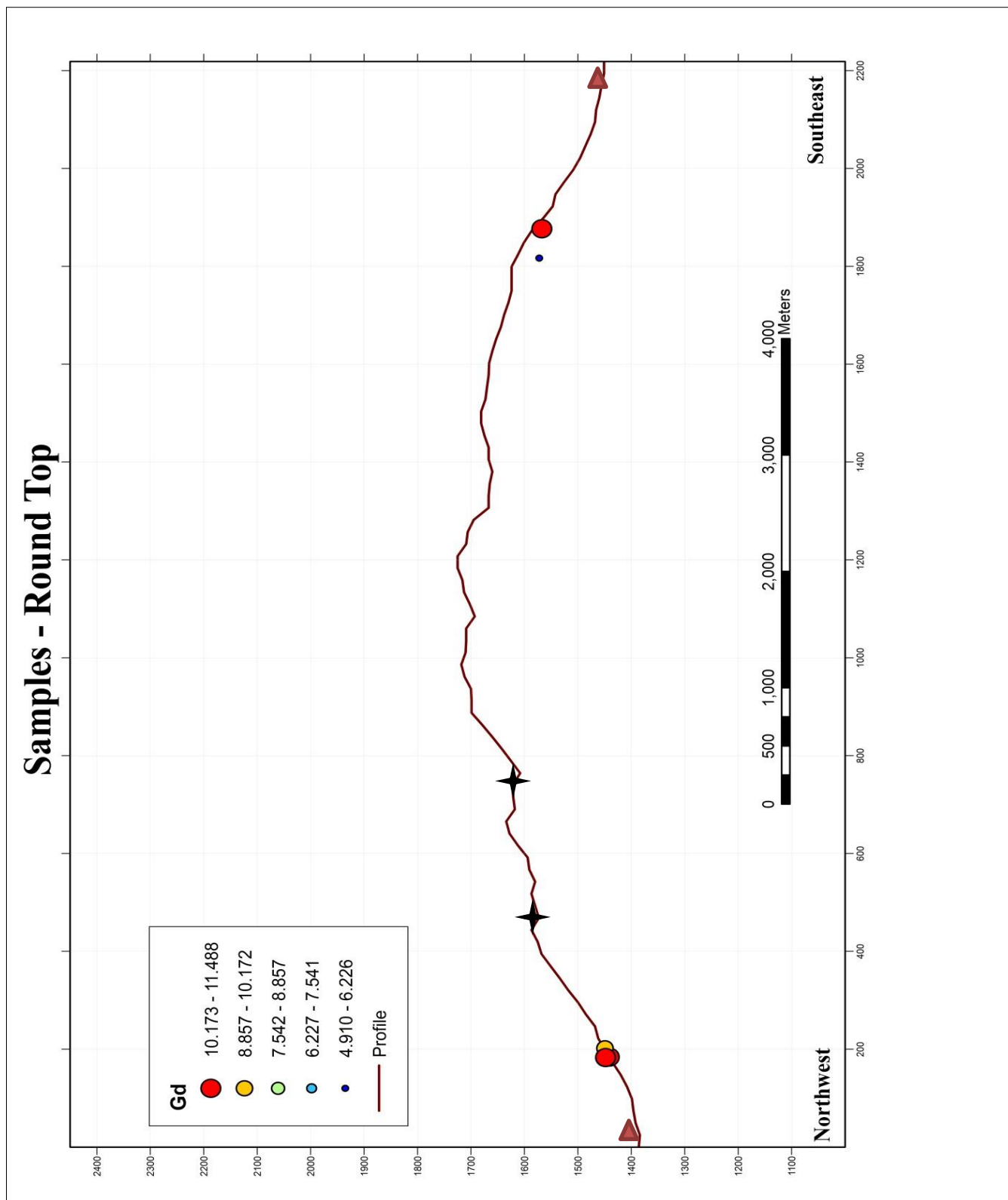


Fig. 4.34: Gd profile – Round Top: ★ Inferred Fault, ▲ Contact

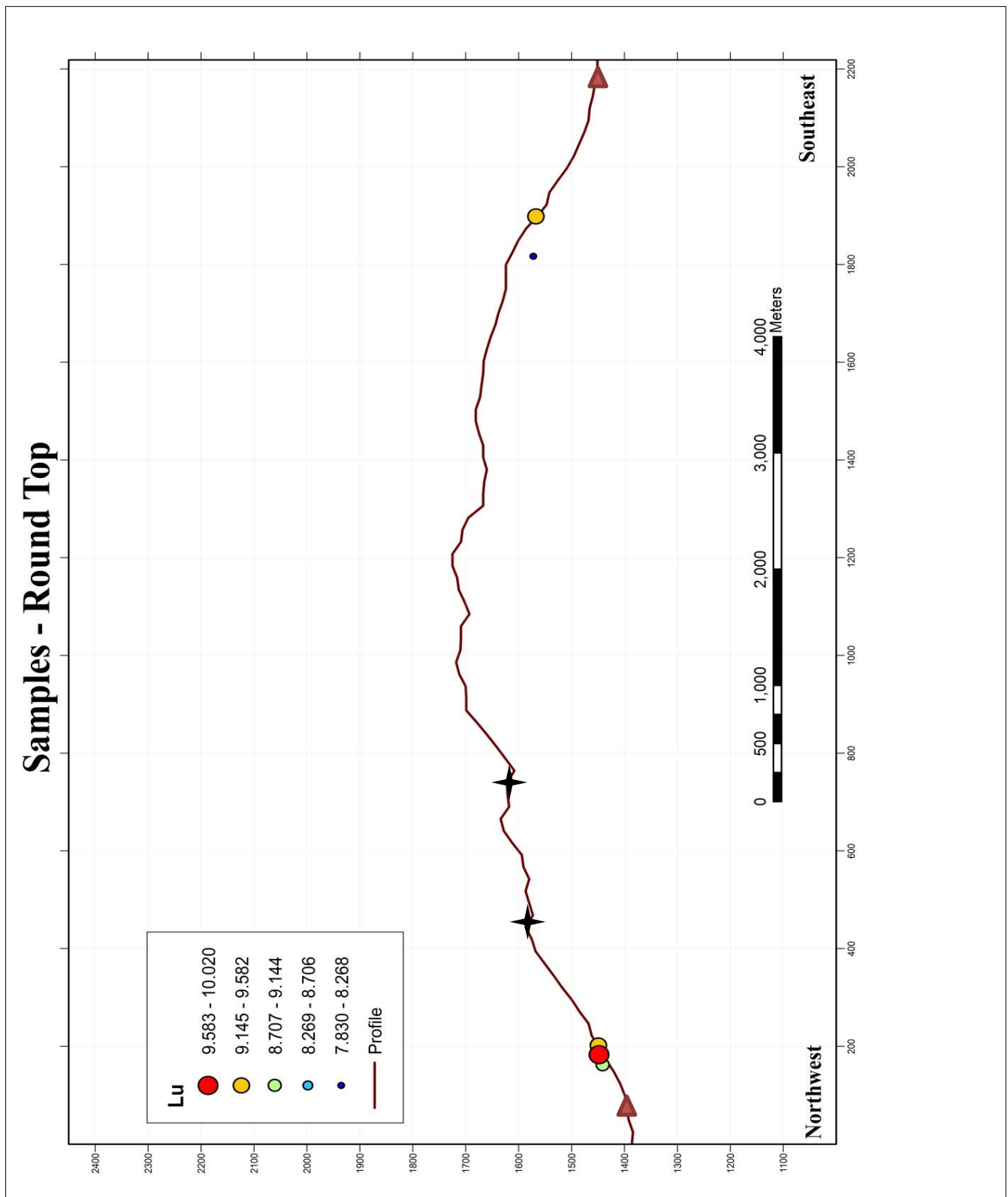


Fig. 4.35: Lu profile – Round Top: ★ Inferred Fault, ▲ Contact

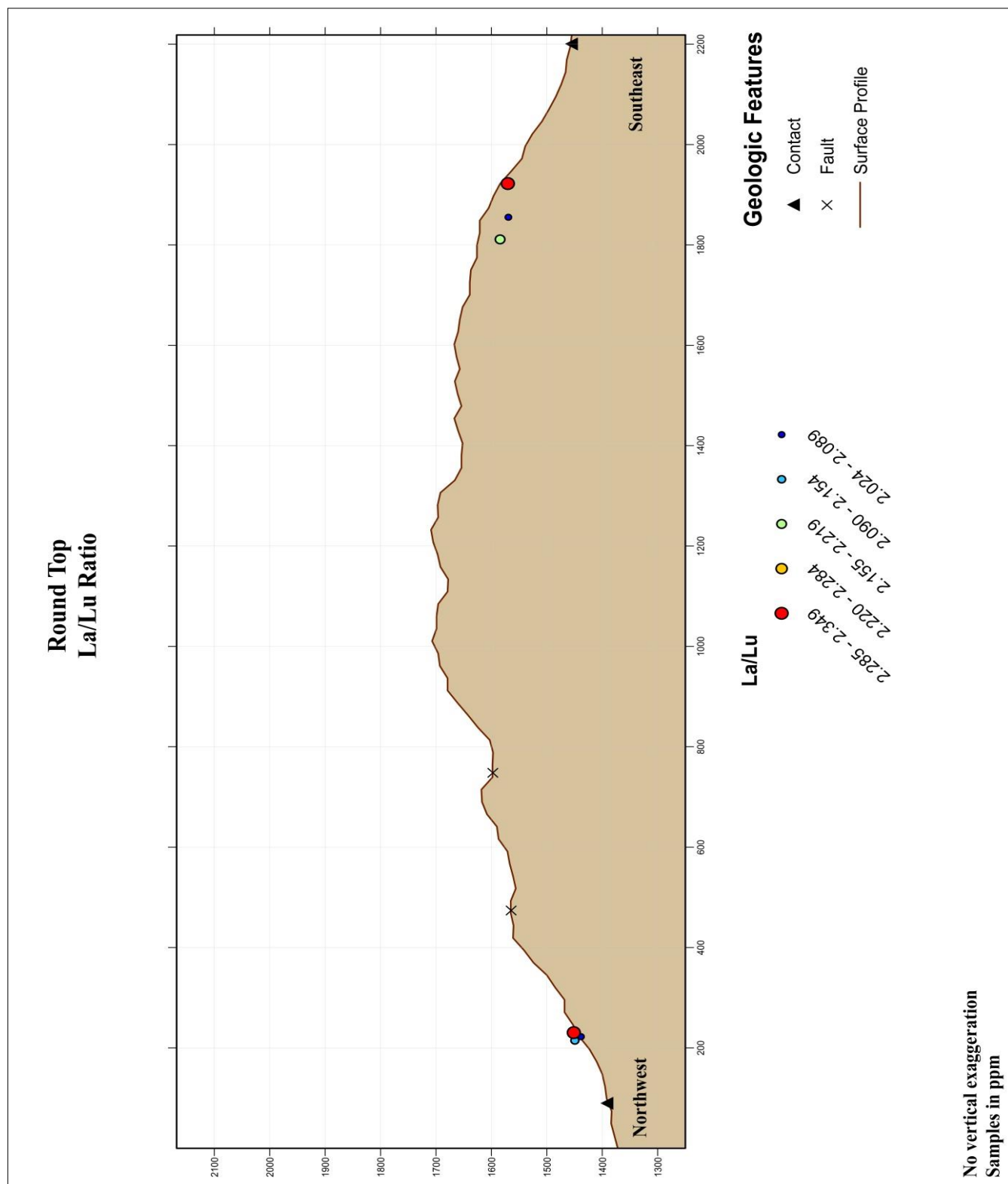


Fig. 4.36: La/Lu ratio profile – Round Top

SAMPLE DATA

Table 4.1: Sample location, number collected

<i>Location</i>	<i>Number of Samples</i>
Sierra Blanca	5
Little Blanca	42
Little Round Top	21
Round Top	17
Northern Quitman Stock	1
Diorite Outcrops	2
Total Samples	88

Table 4.2: Element Quantity by location (REE in bold).

	<i>Round Top</i>	<i>Little Round Top</i>	<i>Little Blanca</i>	<i>Sierra Blanca</i>
High	Eu , Sr,	Ba, Ce , Cs, Dy , Er , F, Ga, Hf, Ho , Lu , Mo, Nb, Nd , Pr , Sm , Sn, Ta, Tb , Th, Tm , U, Yb , Zn, Zr	Be, La , Tl,	Gd , Y
Low			Gd, Nd, Rb, Sm, Y,	Ba, Be, Ce, Cs, Dy, Er, Eu, F, Ga, Hf, Ho, La, Lu, Mo, Nb, Pr, Rb, Sn, Sr, Ta, Tb, Th, Tl, Tm, U, Yb, Zn, Zr

Table 4.3: Oxide Quantity by Location

	<i>Round Top</i>	<i>Little Round Top</i>	<i>Little Blanca</i>	<i>Sierra Blanca</i>
High	CaO, P ₂ O ₅ , SrO	BaO, Fe ₂ O ₃ , Na ₂ O		Al ₂ O ₃ , K ₂ O, SiO ₂
Low	Al ₂ O ₃ , SiO ₂	Na ₂ O, K ₂ O		BaO, CaO, BaO, Fe ₂ O ₃ , P ₂ O ₅ , SrO

Table 4.4: Rhyolite outliers: elements (ppm)

Sample	LB10	LB12	LRT-8S	LB-5S	RT336	RT337	RT231	RT233	Crustal Average
Ba	195.500	110.000	25.300	66.000	29.329	1.750	2.444	0.556	320
Be									1.5
Ce	89.100	71.400	59.300	8.400	76.257	32.250	32.467	31.967	37.5
Co	1.800	0.375	0.375	1.200	8.757	33.338	33.211	32.956	25
Cr	40.000	10.000	10.000	0.750					100
Cs	55.300	17.250	38.900	11.600	39.893	0.224	0.262	0.241	1.8
Cu	3.750	3.750	3.750	3.750	11.414	79.825	76.989	75.856	55
Dy	17.700	29.300	23.000	1.090	28.364	10.721	11.317	11.089	3.6
Er	19.400	29.400	25.100	0.830	40.571	88.613	87.067	85.111	2.2
Eu	0.410	0.090	0.080	0.160	1.476	8.295	8.304	8.040	1.15
F	4110.000	20000.000	3230.000	29.100					579.239
F wt. %	0.411	10.400	0.323	0.003					0.058
Ga	66.500	59.300	66.800	1.800	66.400	20.238	20.478	19.789	17
Gd	7.020	10.100	6.690	0.910	9.997	8.915	9.670	9.854	3.45
Hf	73.900	60.600	90.600	0.900	75.671	1.125	4.444	1.667	3.35
Ho	4.400	7.340	5.790	0.260	59.983	413.750	391.444	393.111	0.77
La	30.700	25.500	16.800	5.100	21.329	29.138	29.689	27.789	17
Lu	5.790	6.700	7.830	0.130	8.567			1.778	0.315
Mo	3.000	1.500	1.500	2.000	35.571	260.125	320.556	287.667	1
Nb	305.000	258.000	369.000	2.000	310.857	10.139	11.210	10.778	11.5
Nd	27.200	24.000	21.500	4.400	261.357	1613.125	1778.889	1892.222	18
Ni	9.000	3.750	3.750	3.750	1.571	10.614	11.650	11.072	75
Pb	184.000	147.000	256.000	61.000	195.571	145.375	141.444	135.333	13
Pr	9.380	8.670	8.020	1.100	10.640	97.738	69.267	66.767	4.45
Rb	1780.000	966.000	1740.000	32.800	1355.971	67.663	66.700	64.533	45
Sm	7.440	8.540	7.600	0.910	9.177	3.714	3.839	3.663	3.7
Sn	125.000	96.000	147.000	1.000	126.000	187.313	189.556	183.722	2.5
Sr	39.700	657.000	25.400	2840.000	98.886	5.763	5.089	4.722	292.5
Ta	54.900	45.800	62.500	0.200	63.794	7.460	7.796	7.760	1.05
Tb	2.170	3.560	2.520	0.160	10.073	51.225	63.678	63.289	0.58
Th	153.500	130.000	168.500	1.610	142.714				4.55
Tl	5.500	2.400	5.400	0.375	14.457	10.625	84.111	10.889	0.36
Tm	4.560	6.080	5.720	0.130	37.689	231.250	242.889	235.778	0.32
U	26.400	56.700	29.800	99.900	40.300	56.250	58.944	58.811	1.165
V	16.000	21.000	6.000	12.000	92.286	561.250	680.222	702.556	135
W	5.000	4.000	9.000	1.000	185.429	1078.375	1051.444	1073.333	1.5
Y	129.000	257.000	149.500	11.100	186.200	74.475	72.911	73.144	20
Yb	37.000	45.100	50.200	0.900	49.786	13.031	13.078	13.183	2.1
Zn	488.000	474.000	477.000	8.000	482.474	1.541	1.581	1.527	76.5
Zr	950.000	760.000	1040.000	29.000	884.723	0.189	0.391	0.238	111.5

Table 4.5: Rhyolite outliers: major oxide components (wt. %)

Sample	LB10	LB12	LRT-8S	LB-5S	RT336	RT337	RT231	RT233	Crustal Average
SiO ₂	74.900	60.200	72.800	7.400	62.601	0.090	0.117	0.117	58.2
Al ₂ O ₃	12.550	10.650	12.700	1.380	11.936	5.468	4.949	4.989	15.85
Fe ₂ O ₃	1.780	1.100	1.580	0.780	2.166	3.608	3.803	3.867	
CaO	0.750	17.100	0.230	62.100	1.047	0.020	0.018	0.016	6.9
MgO	0.100	0.150	0.150	0.600	0.117	0.058	0.077	0.112	
Na ₂ O	4.550	4.960	4.690	0.210	4.000	0.004	0.010	0.011	3.15
K ₂ O	3.490	2.380	4.080	0.250	3.213	0.009	0.010	0.010	1.49
Cr ₂ O ₃	0.008	0.008	0.008	0.008					
TiO ₂	0.040	0.010	0.020	0.060	0.019				
MnO	0.060	0.060	0.060	0.020	0.181	1.588	1.571	1.337	
P ₂ O ₅	0.060	0.010	0.010	0.090	14.224	100.063	98.544	98.556	0.2
SrO	0.008	0.090	0.008	0.350	0.011	11901.250	1.111	1.111	
BaO	0.020	0.010	0.008	0.010	0.003	6.250	12778.889	10775.556	

Table 4.6: Chemical composition (wt. %) of SB Laccoliths compared to average of topaz rhyolites (adapted from Christiansen, et al., 1983)

	<i>Sierra Blanca Complex</i>	<i>Average Topaz Rhyolites</i>
SiO ₂	72.695	76.0
TiO ₂	0.017	0.6
Al ₂ O ₃	13.052	13.0
Fe ₂ O ₃	1.513	1.0
MnO	0.065	0.06
MgO	0.093	0.08
CaO	1.205	0.6
Na ₂ O	4.757	4.0
K ₂ O	3.881	4.8
P ₂ O ₅	0.217	0
F	0.996	0.3

Table 4.7: Comparison of average REE in weathered and fresh samples

	<i>La</i>	<i>Ce</i>	<i>Pr</i>	<i>Nd</i>	<i>Sm</i>	<i>Eu</i>	<i>Gd</i>
Weathered	24	81.04	9.288	24.38	8.29	0.094	8.314
Fresh	23.725	76.25	9.0875	25.95	9.065	0.095	9.125
	<i>Tb</i>	<i>Dy</i>	<i>Ho</i>	<i>Er</i>	<i>Tm</i>	<i>Yb</i>	<i>Lu</i>
Weathered	2.856	24.7	6.33	26.17	5.71	47.06	7.412
Fresh	2.9025	24.275	6.06	25.2625	5.4375	43.7	6.84

Table 4.8: Eu/Eu* calculation (from GCDToolkit, Janoušek, et al., 2006)

<i>Sample</i>	<i>Eu/Eu*</i>	<i>Sample</i>	<i>Eu/Eu*</i>	<i>Sample</i>	<i>Eu/Eu*</i>	<i>Sample</i>	<i>Eu/Eu*</i>
LB1	0.04	LRT1	0.04	LB13	0.03	RT12 5 3	0.03
LB-1S	0.03	LRT2	0.03	LB14	0.03	RT12 6 1	0.04
LB2	0.04	LRT-2S	0.03	LB15	0.03	RT12 6 2	0.04
LB-2S	0.03	LRT3	0.03	LB16	0.03	RT12 6 3	0.04
LB3	0.08	LRT-3S	0.04	LB17	0.03	RT201	0.07
LB-3	0.03	LRT4	0.03	LB19	0.03	RT226	0.13
LB4	0.04	LRT-4S	0.03	LB20	0.03	RT251	0.07
LB-4S	0.04	LRT5	0.04	LB21	0.03	RT252	0.07
LB5	0.03	LRT-5S	0.04	LB22	0.03	RT262	0.07
LB6	0.03	LRT6	0.03	LB23	0.03	RT287	0.07
LB-6S	0.05	LRT-6S	0.09	LB24	0.03	RT334	0.09
LB7	0.04	LRT7	0.03	LB25	0.03	RT335	0.07
LB-7S	0.07	LRT-7S	0.05	LB26	0.03	SB2	0.02
LB8	0.03	LRT9	0.04	LB27	0.03	SB3	0.02
LB-8S	0.04	LRT10	0.04	LB28	0.03	SB4	0.02
LB9	0.04	LRT11	0.03	LB29	0.03	SB5	0.02
LB-9S	0.03	LRT12	0.03	LB30	0.03		
LB10	0.17	LRT13	0.03	LB31	0.03		
LB-10S	0.03	LRT14	0.04				

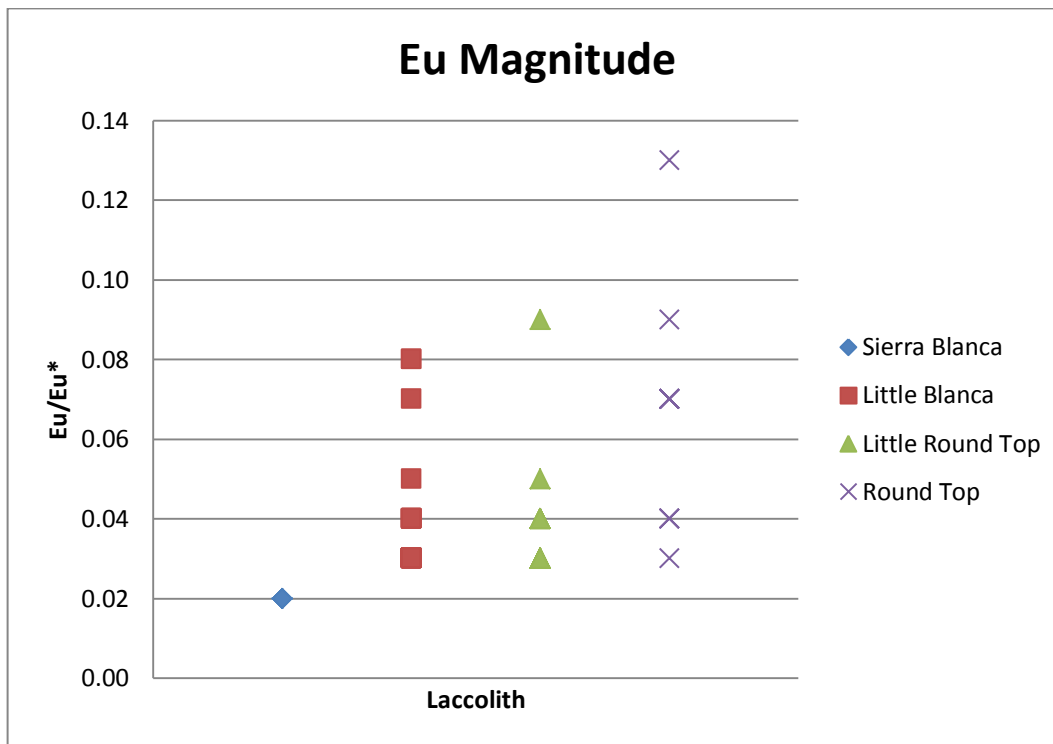
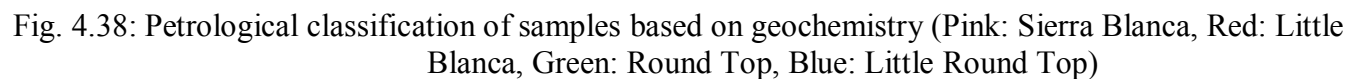


Fig. 4.37: Increasing Eu anomaly magnitude

(Calculated using GCDToolkit; Janoušek et al., 2006).



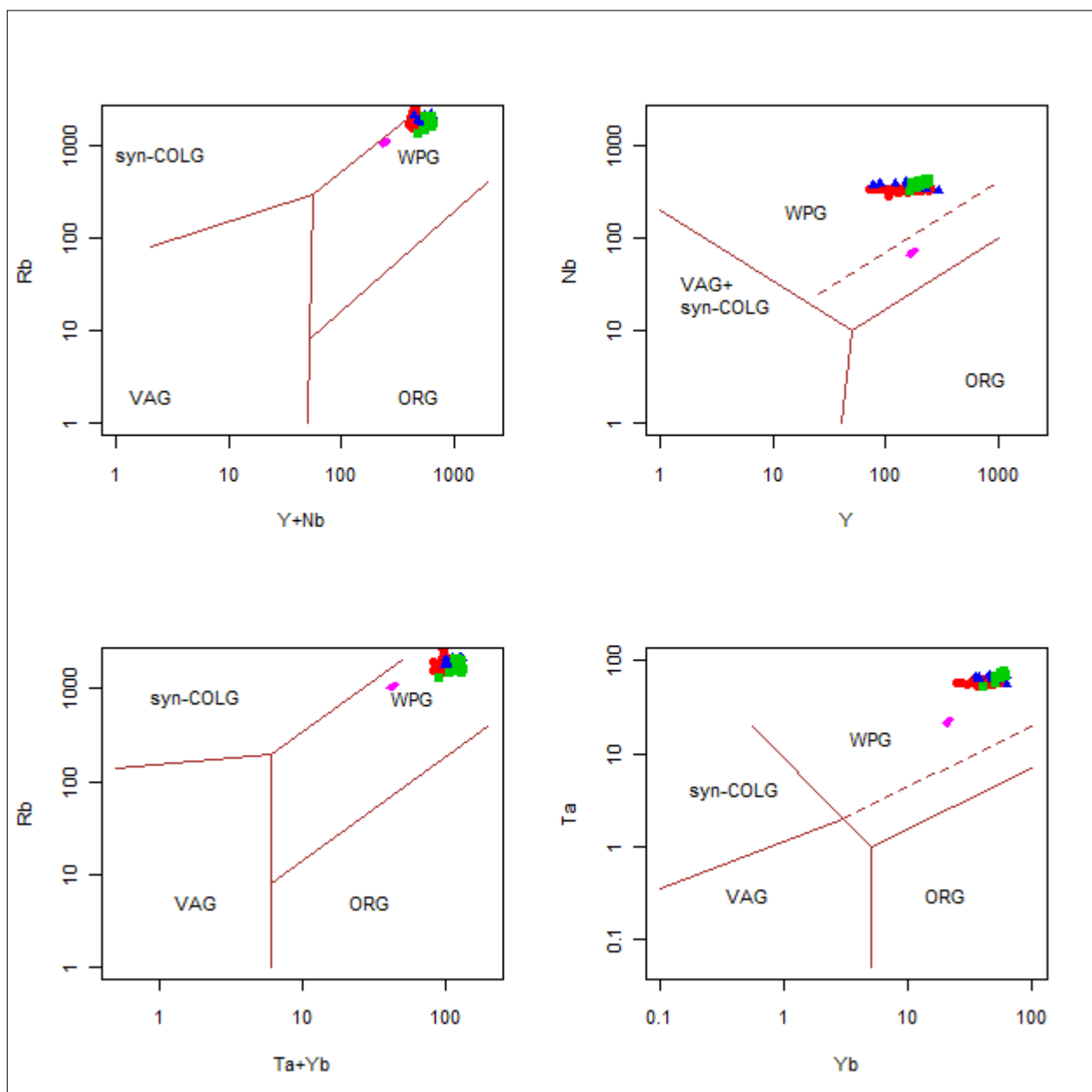


Fig. 4.39: Geotectonic classification of the Sierra Blanca rhyolites (Pink: Sierra Blanca, Red: Little Blanca, Green: Round Top, Blue: Little Round Top)

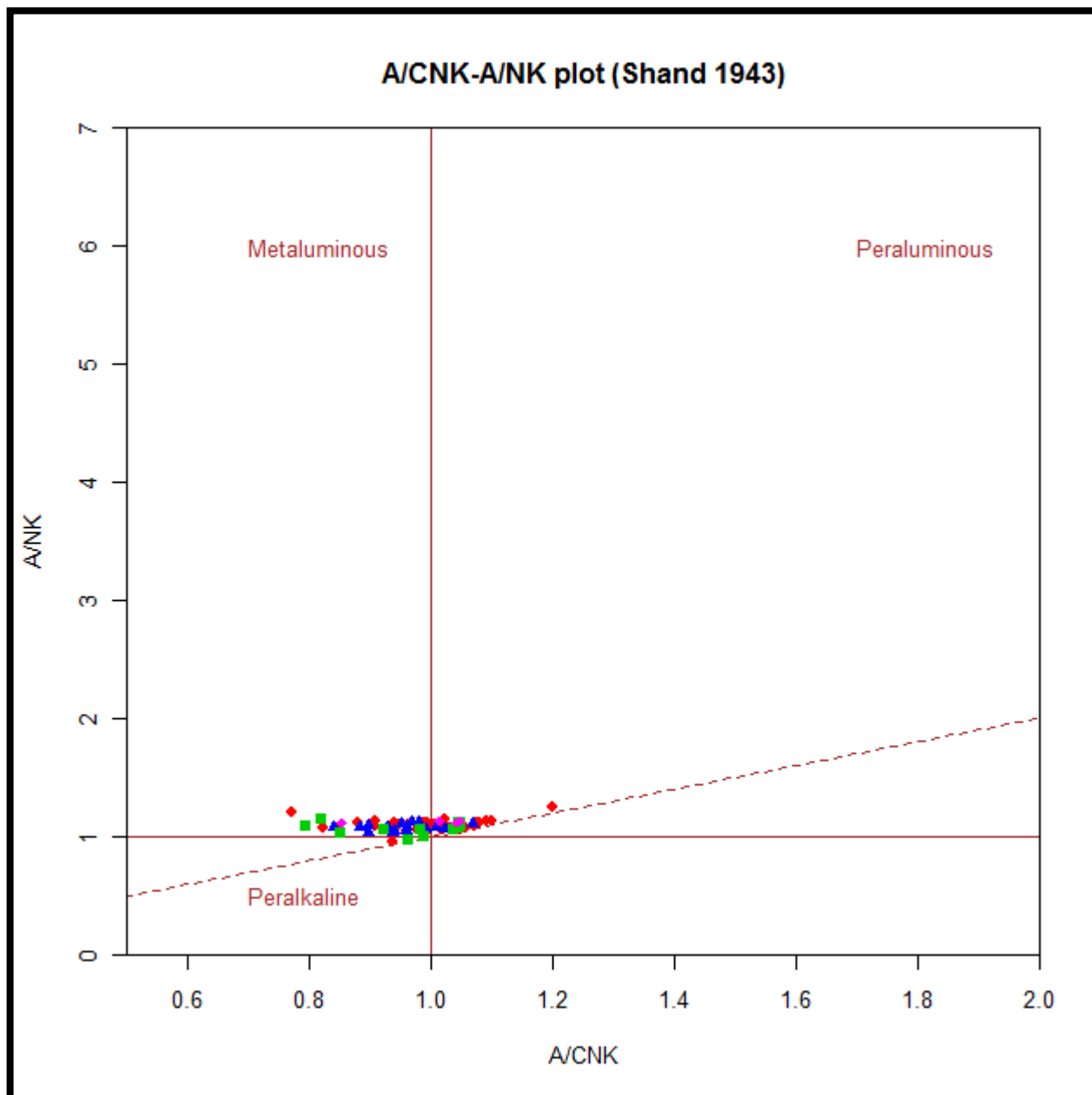


Fig. 4.40: Alumina saturation plot (Pink: Sierra Blanca, Red: Little Blanca, Green: Round Top, Blue: Little Round Top)

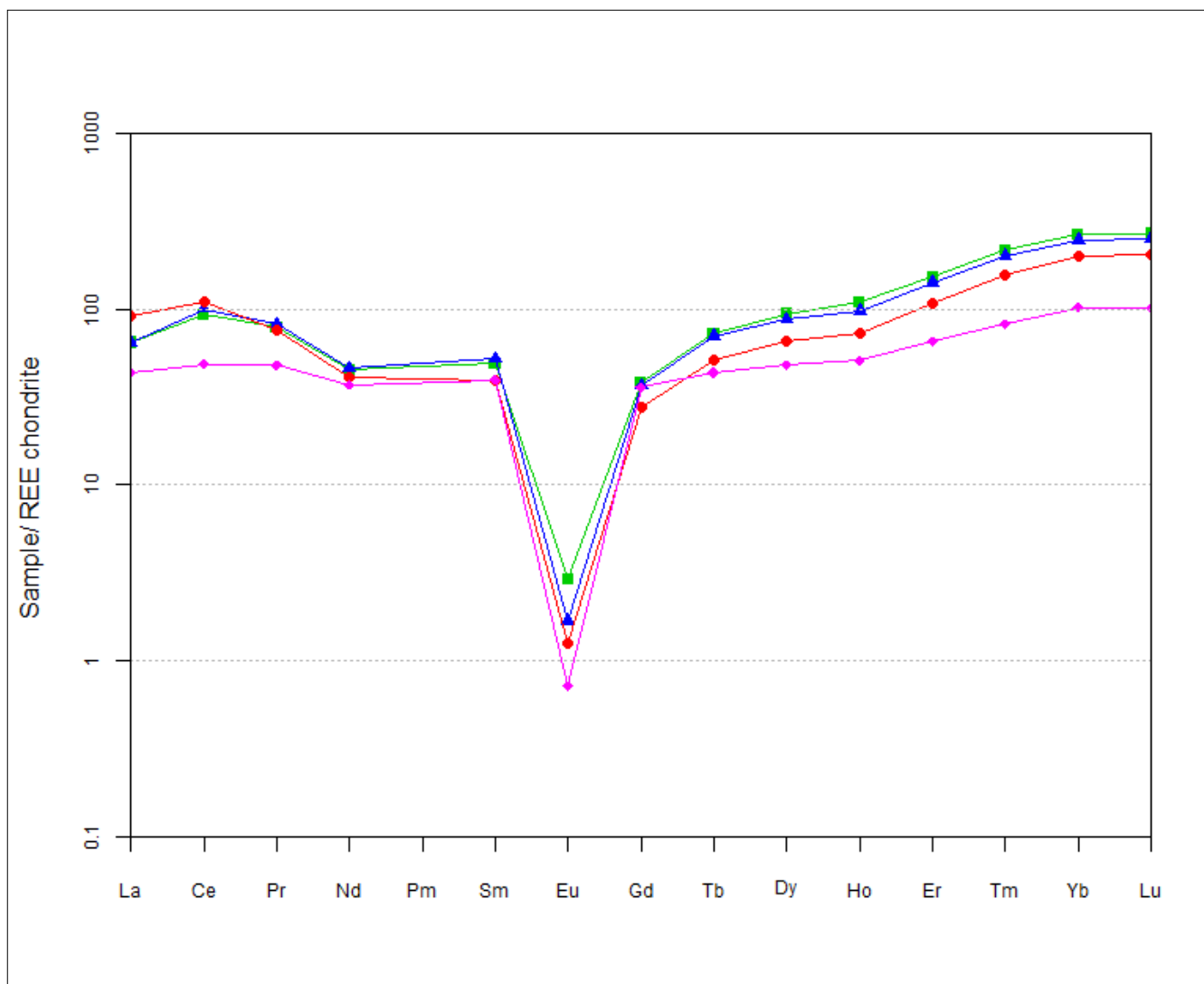


Fig. 4.41: REE chondrite normalized spider diagram of average REE for all laccoliths (Pink: Sierra Blanca, Red: Little Blanca, Green: Round Top, Blue: Little Round Top)

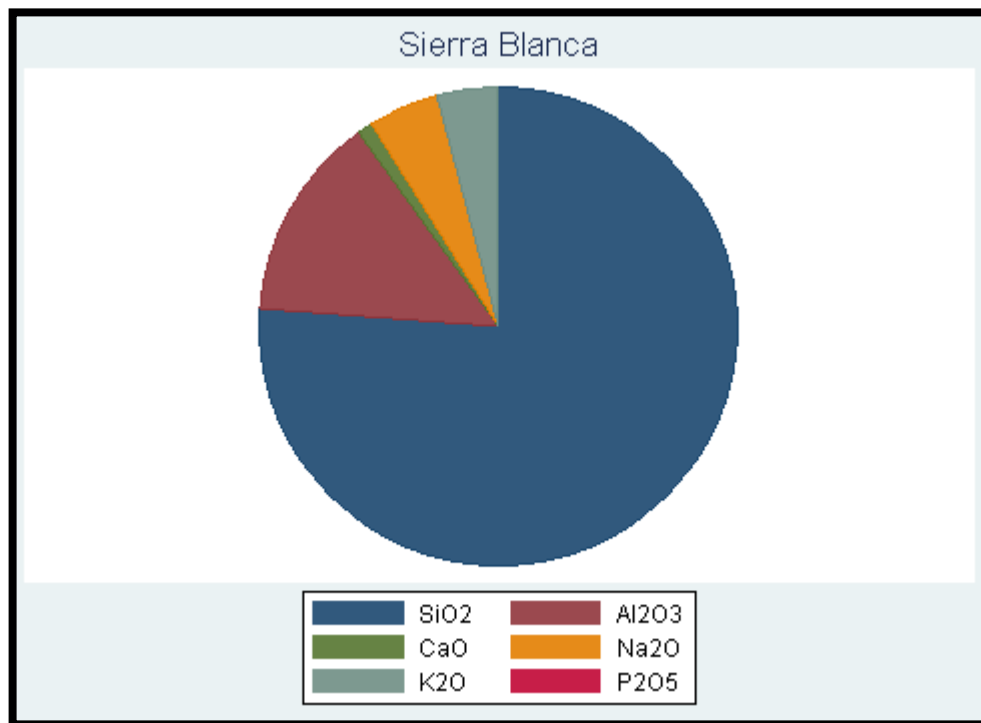


Fig. 4.42: Major oxide components of Sierra Blanca

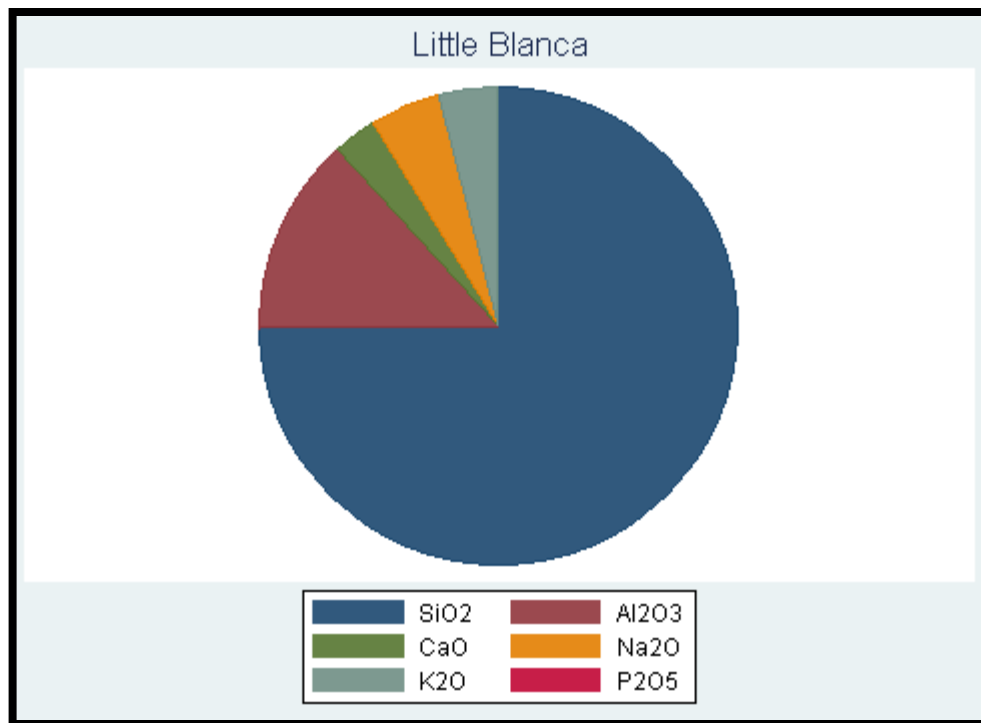


Fig. 4.43: Major oxide components of Little Blanca

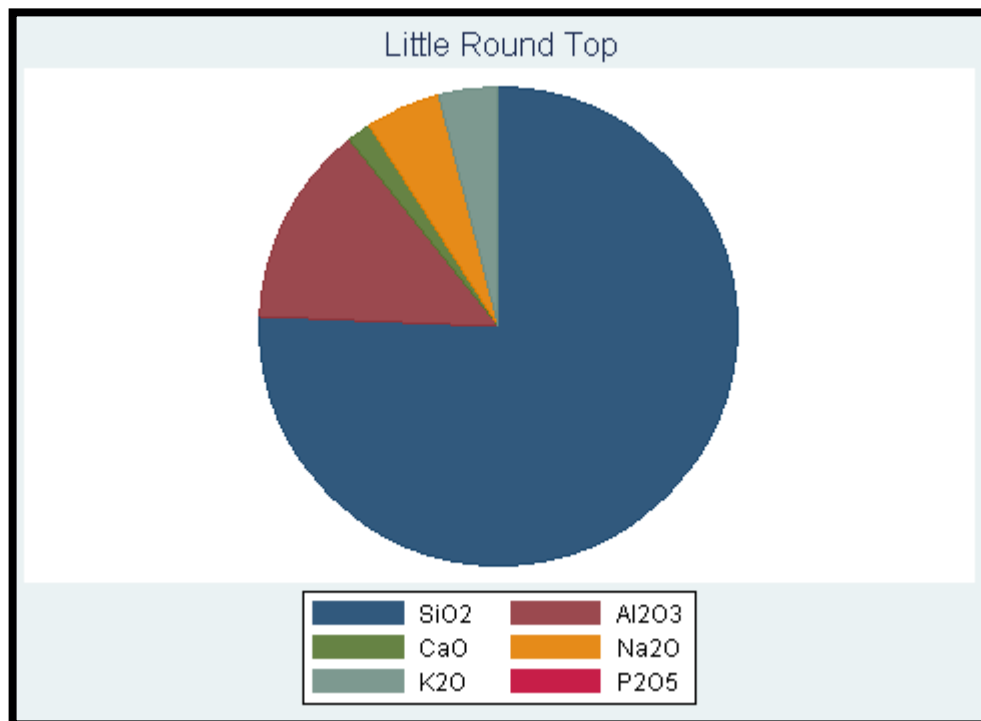


Fig. 4.44: Major oxide components of Little Round Top

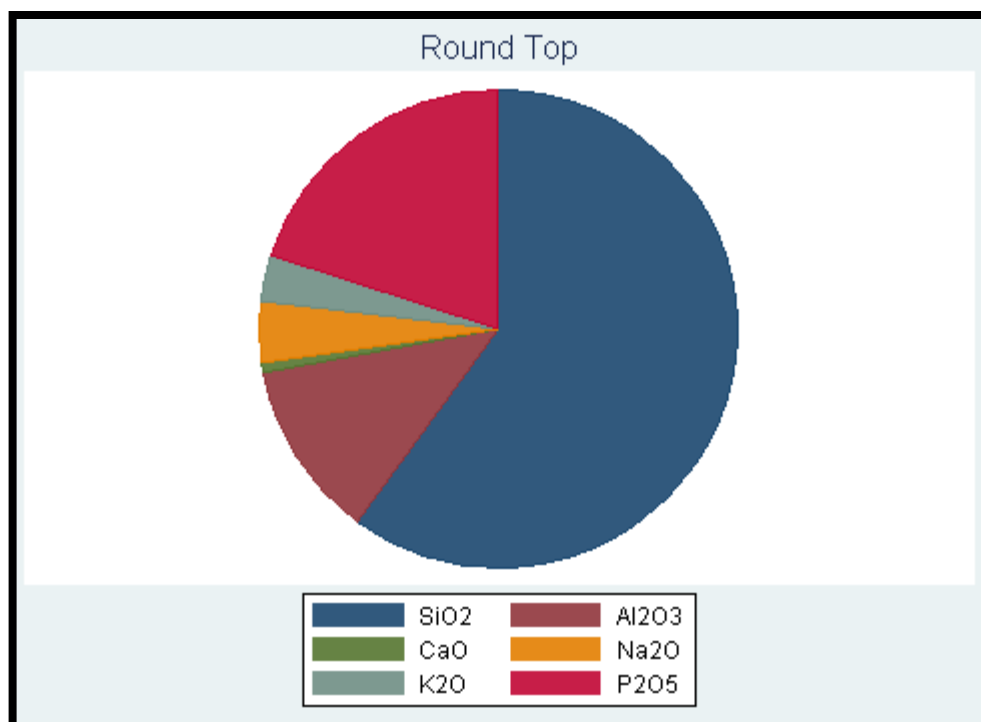


Fig. 4.45: Major oxide components of Round Top

STATISTICS

Univariate Statistics

Table 4.9: Standard Statistics for REE: Little Blanca, Little Round Top, Round Top

<i>Little Blanca REE</i>	<i>N</i>	<i>Minimum</i>	<i>Maximum</i>	<i>Mean</i>	<i>Standard Deviation</i>
La	38	6.600	278.000	78.10789	69.498775
Ce	38	67.800	98.200	88.76053	7.289368
Pr	38	5.780	11.250	9.32289	1.302669
Nd	38	14.600	30.000	24.51316	3.647077
Sm	38	4.290	9.930	7.74579	1.475115
Eu	38	0.050	0.410	0.09289	0.055649
Gd	38	3.860	10.300	7.30447	1.731437
Tb	38	1.350	3.610	2.47289	0.607809
Dy	38	11.800	31.000	21.34342	5.234387
Ho	38	2.850	7.750	5.34158	1.321035
Er	38	12.350	34.300	22.98816	5.562877
Tm	38	2.830	7.360	5.14053	1.159611
Yb	38	25.000	58.000	42.30000	8.321512
Lu	38	3.850	8.870	6.59632	1.246531

<i>Little Round Top REE</i>	<i>N</i>	<i>Minimum</i>	<i>Maximum</i>	<i>Mean</i>	<i>Standard Deviation</i>
La	19	15.000	23.100	20.08947	1.864840
Ce	19	75.400	87.000	81.09474	3.382056
Pr	19	7.290	11.350	10.06684	0.941370
Nd	19	19.600	31.700	27.67895	2.867748
Sm	19	6.990	12.050	10.16421	1.201126
Eu	19	0.080	0.250	0.12316	0.036976
Gd	19	5.950	12.850	9.53053	1.724437
Tb	19	2.100	4.670	3.32526	0.0669306
Dy	19	16.800	41.200	28.27895	6.036885
Ho	19	3.850	10.100	7.00000	1.614796
Er	19	16.900	42.800	29.77368	6.790422
Tm	19	4.020	8.700	6.49842	1.341124
Yb	19	35.300	63.300	51.84211	8.659312
Lu	19	5.660	9.730	8.11526	1.331033

<i>Round Top REE</i>	<i>N</i>	<i>Minimum</i>	<i>Maximum</i>	<i>Mean</i>	<i>Standard Deviation</i>
La	13	16.300	22.500	20.09257	1.9829872
Ce	13	44.600	88.089	75.09020	12.601706
Pr	13	5.510	11.550	9.71237	1.582405
Nd	13	13.100	261.357	45.07946	65.173782
Sm	13	4.040	11.275	9.53608	1.899613
Eu	13	0.050	1.476	0.31012	0.361386
Gd	13	4.910	11.650	9.92516	1.733571
Tb	13	2.010	10.073	3.96626	1.917671
Dy	13	21.500	35.144	30.14943	4.034906
Ho	13	6.080	59.983	11.86209	14.487297
Er	13	24.100	40.571	32.63688	4.159490
Tm	13	5.423	37.689	9.36241	8.542682
Yb	13	41.367	62.237	55.38048	5.873796
Lu	13	6.570	10.020	8.70632	0.928650

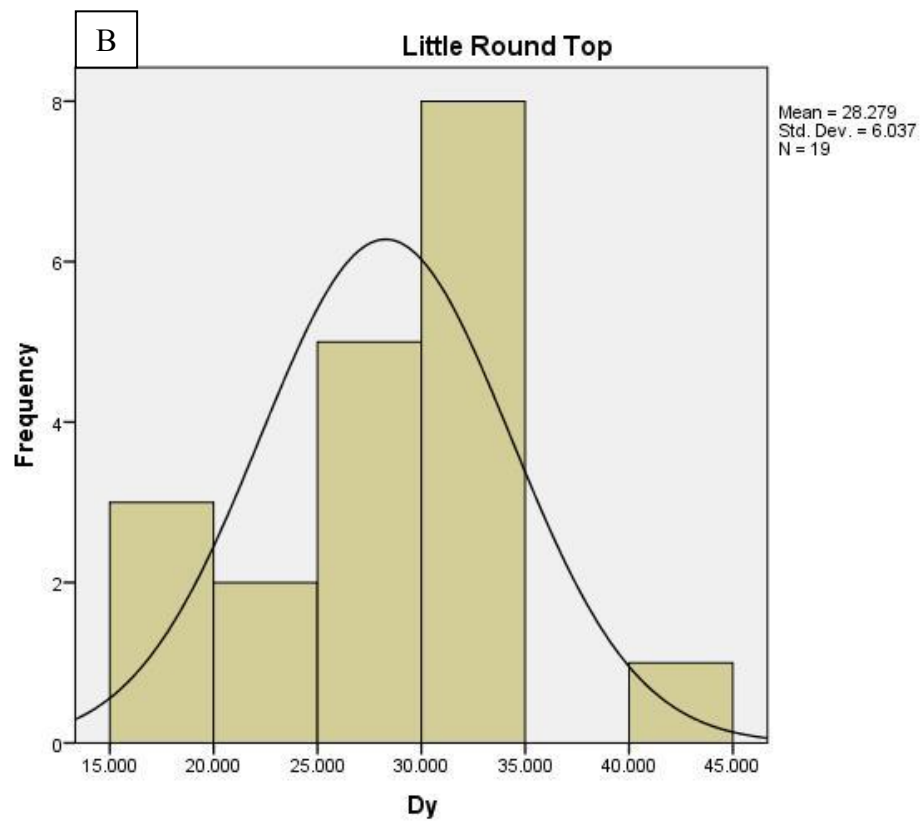
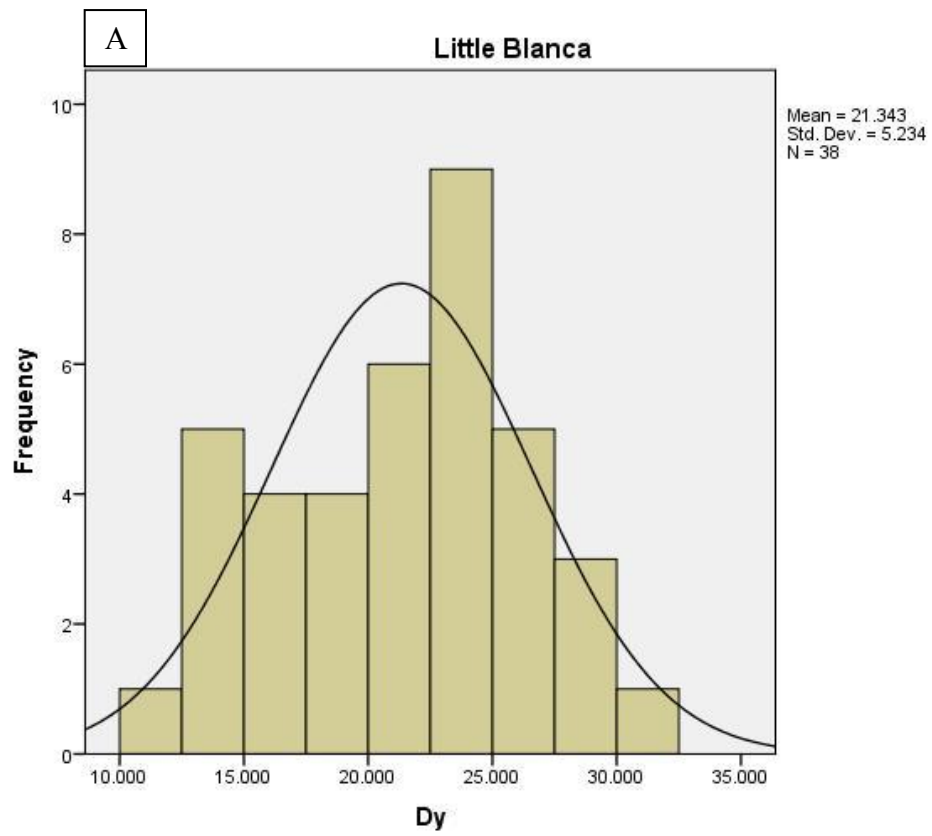
Table 4.10: Standard Statistics for REE: Rhyolite outliers

<i>Rhyolite Outliers</i>	<i>N</i>	<i>Minimum</i>	<i>Maximum</i>	<i>Mean</i>	<i>Standard Deviation</i>
La	8	5.100	30.700	23.255	8.717839
Ce	8	8.400	89.100	50.143	27.879271
Pr	8	1.100	97.738	33.948	37.665165
Nd	8	4.400	1892.222	702.837	883.612145
Sm	8	0.910	9.177	5.610	2.957569
Eu	8	0.080	8.304	3.357	4.047017
Gd	8	0.910	10.100	7.895	3.124085
Tb	8	0.160	63.678	24.584	29.214615
Dy	8	1.090	29.300	16.573	9.821683
Ho	8	0.260	413.750	159.510	199.682576
Er	8	0.830	88.613	47.011	34.874303
Tm	8	0.130	242.889	95.512	117.469429
Yb	8	0.900	50.200	27.785	19.788801
Lu	6	0.130	8.567	5.132	3.412970

Table 4.11: Means of elements and oxides by location (trace elements in ppm, oxides in weight %, REE in bold)

	<i>Round Top (n = 5)</i>	<i>Little Round Top (n = 21)</i>	<i>Little Blanca (n = 40)</i>	<i>Sierra Blanca (n = 5)</i>	<i>Crustal Abundance (ppm) *</i>
Ba	78.320	140.438	80.253	17.600	320.000
Be	14.680	20.640 ¹	49.780 ²	7.650 ³	1.500
Ce	65.220	79.171	86.605	49.060	37.500
Cs	40.738	76.714	48.791	19.230	1.800
Dy	23.938	26.884	21.096	18.190	3.600
Er	25.678	28.237	22.722	15.880	2.200
Eu	0.346	0.212	0.096	0.062	1.150
F	4712.000	9345.500 ¹	6966.539	4542.444	573.239
Ga	61.780	68.981	68.708	48.100	17.000
Gd	8.618	9.202	7.193	10.808	3.450
Hf	71.480	85.038	74.235	11.960	3.350
Ho	6.178	6.648	5.284	4.296	0.770
La	21.560	20.533	27.668	16.740	17.000
Lu	6.926	7.729	6.464	3.728	0.315
Mo	2.000	2.667	2.250	1.700	1.000
Nb	319.520	358.795	322.450	71.620	11.500
Nd	25.420	27.605	23.998	26.500	18.000
Pr	8.808	9.862	9.104	6.922	4.450
Rb	1634.620	1839.024	1853.095	1035.800	45.000
Sm	7.888	9.856	7.580	9.084	3.700
Sn	117.800	140.143	124.800	45.800	2.500
Sr	318.060	166.505	173.488	50.080	292.500
Ta	54.560	62.347	56.665	22.380	1.050
Tb	2.702	3.165	2.439	2.410	0.580
Th	149.488	170.535	155.478	53.440	4.550
Tl	5.375	5.605	5.774	3.160	0.360
Tm	5.464	6.167	5.067	3.056	0.320
U	25.318	35.715	34.665	11.844	1.165
Y	176.160	182.238	165.050	204.000	20.000
Yb	45.364	49.389	41.538	24.260	2.100
Zn	418.400	481.714	464.800	156.200	76.500
Zr	920.000	1046.667	937.500	122.400	111.500
Al ₂ O ₃	11.304	13.171	12.715	13.7300	15.850
BaO	0.011	0.020	0.011	0.008	
CaO	4.888	1.712	2.925	1.694	6.900
Fe ₂ O ₃	1.738	1.849	1.473	1.004	
K ₂ O	3.986	3.808	3.846	4.052	1.490
Na ₂ O	3.986	4.843	4.550	4.576	3.150
P ₂ O ₅	0.058	0.055	0.027	0.010	0.200
SiO ₂	68.480	71.419	71.230	71.720	58.200
SrO	0.038	0.022	0.024	0.010	

¹ n = 20, ² n = 10, ³ n = 4 *Average from Table 1.2 references



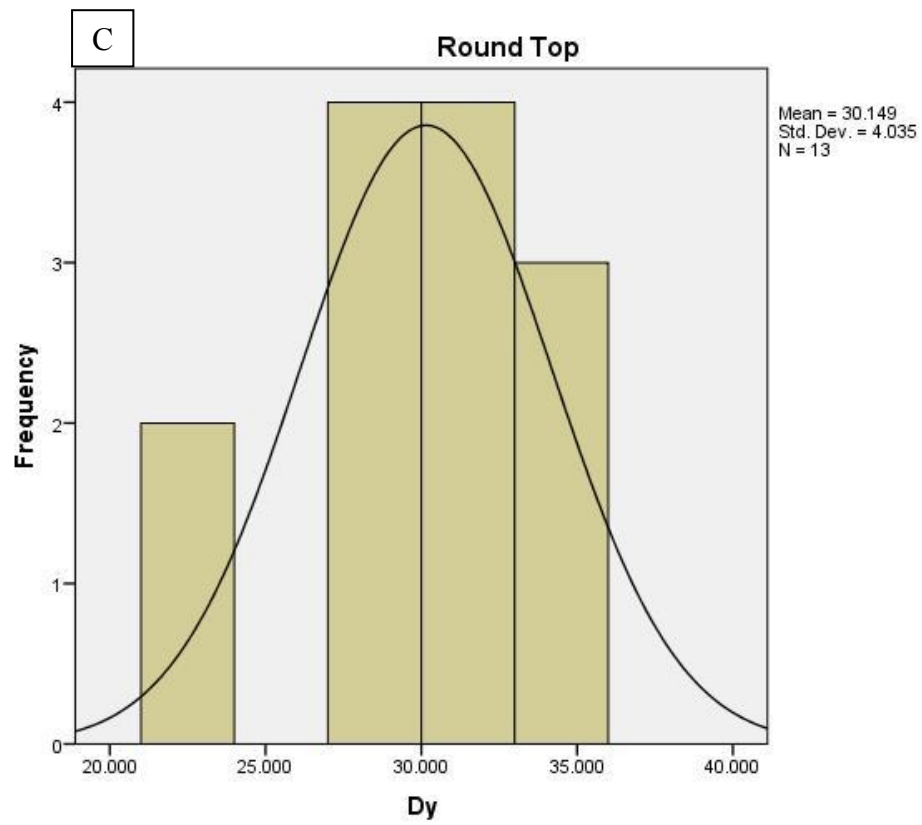


Fig. 4.46: Histogram of Dy for A) Little Blanca, B) Little Round Top, C) Round Top

Bivariate Statistics

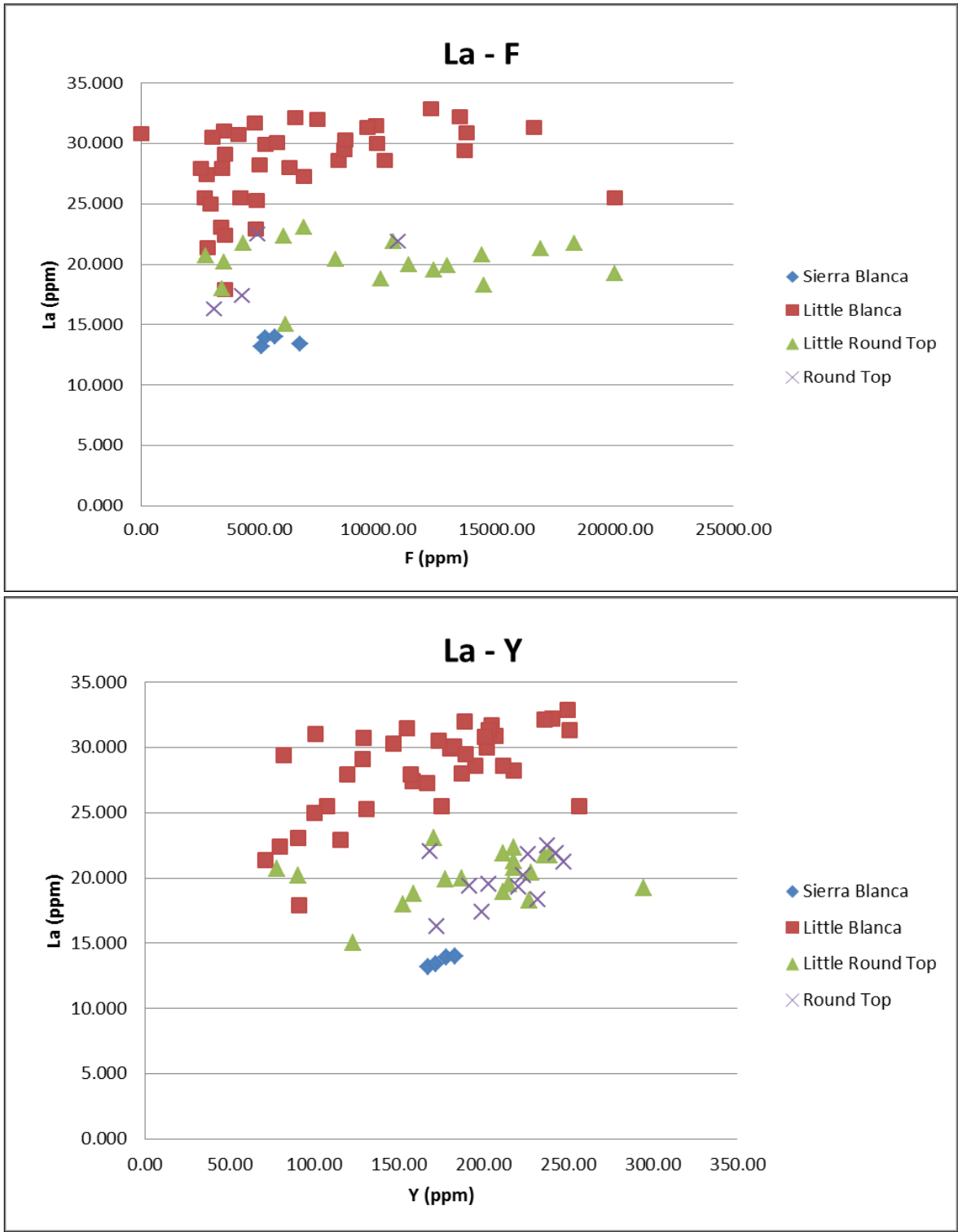


Fig. 4.47: Scattergram of La-vs.-F and La-vs.-Y showing LREE enrichment on Little Blanca

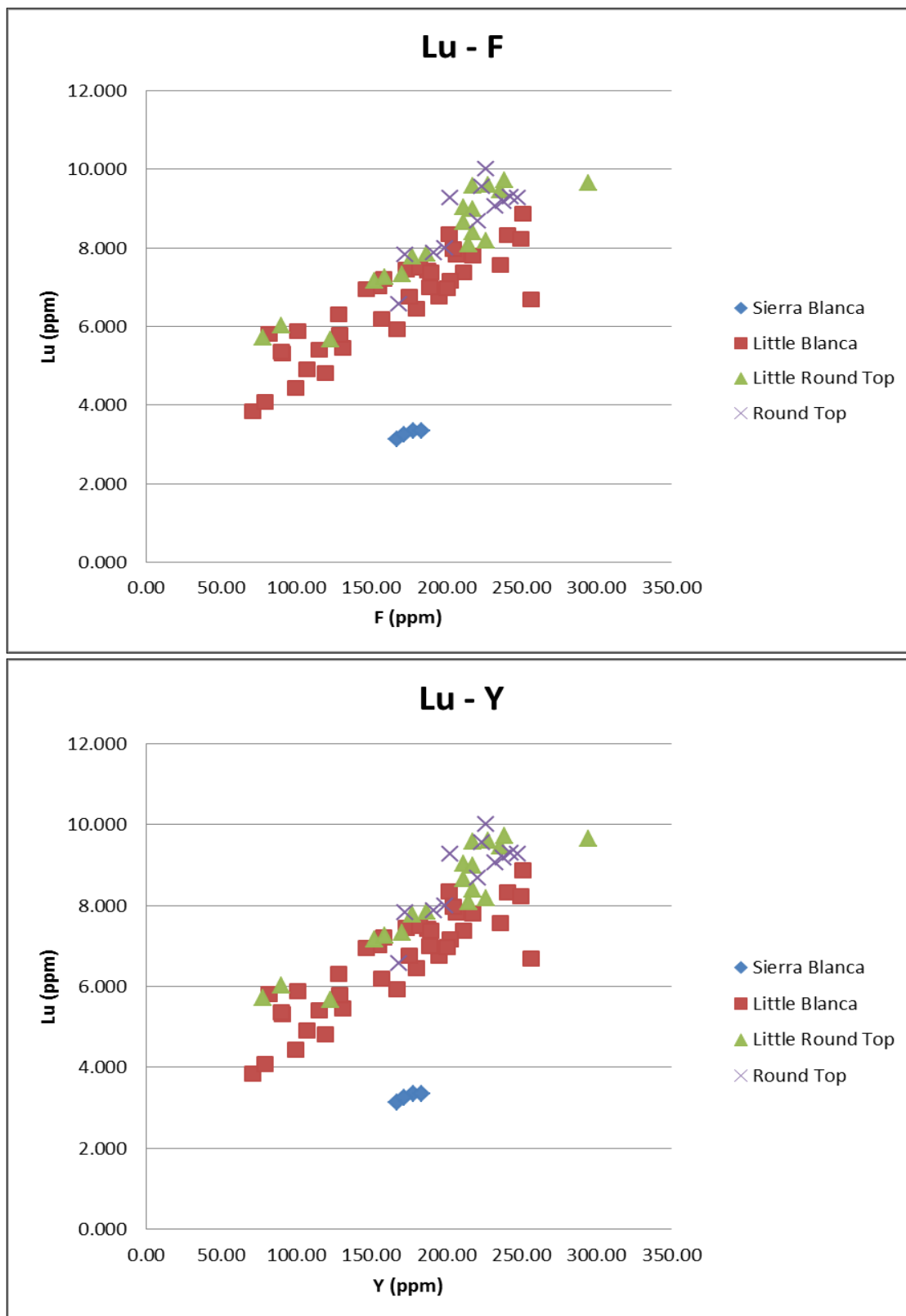


Fig. 4.48 Scattergram of Lu –vs. - F and Lu – vs. – Y showing HREE enrichment of Little Round Top and Round Top, and relative HREE depletion of Little Blanca

Multivariate Statistics

Table 4.12: Factor analysis and loading scores

	1	2	3	4	5	6	7	8	9
Little Blanca	Sm .939 Tm .882 Er .875 Tb .862 Ho .848 Dy .839 Gd .826 Lu .822 Y .814 F .802 Nd .800 Pr .749 SrO .747	Na ₂ O .907 Th .737 Zr .659	Ce .566 Pr .390 La .389 Rb .370 Cs .363 Eu .355 Nd .343 Tl .262 Nb .240 Sn .235 Zn .224 Sm .208	Al ₂ O ₃ .586 La .469 Ba .453 Fe ₂ O ₃ .443 Ga .437 Pr .432 Nd .398 F .300	La .835 Pr .792 Nd .734 Sm .482 Eu .451 Sr .437 SrO .407	Th .479 Zr .405 Sn .378 Hf .375 Rb .347 Fe ₂ O ₃ .298 Tl .275 F .223 SrO .204 Nd .218	Ta .420 U .412 SiO ₂ .404 BaO .360 La .359 Th .312 Na ₂ O .260 Pr .257 P ₂ O ₅ .219 Nd .218	CaO .338 SiO ₂ .332 Ce .276 Al ₂ O ₃ .243 F .225 Zr .223 Be .203 Fe ₂ O ₃ .202 Sr .196 K ₂ O .132 Na ₂ O .126 Tl .106 La .100	U .392 Fe ₂ O ₃ .347 P ₂ O ₅ .253 CaO .192 Mo .140 Eu .129 Sm .121
Little Round Top	Zr .961 K ₂ O .949 SiO ₂ = Rb .943 Ga .931 Hf .925 Tl .915 Ta .877 Sn .848 Ce .841 Th .822 Zn .782 Fe ₂ O ₃ .701	Lu .807 Sm .801 Yb .778 Nd .763 Pr .738 Tm .723 La .701 Er .677 Tb .651 Ho .650 Gd .646 Y .636 Dy .628	BaO .783 La .597 P ₂ O ₅ .596 Ba .567 Pr .564 Nd .522 Eu .509 Cs .284	P ₂ O ₅ .605 Be .556 Fe ₂ O ₃ .536 Zn .462	Mo .947 Cs .431 Th .315	Cs .671 Ba .230 F .354	Sr .354 P ₂ O ₅ .314 Na ₂ O .146 Be .116 F = Fe ₂ O ₃ .115 Mo .109	F .186 Ba .175 Zn .163 Ce .115	N/A
Round Top	K ₂ O .978 Nb .971 Zr .964 Al ₂ O ₃ .954 Rb .933 SiO ₂ .901 Th .888 Ga .865 Hf .853 Na ₂ O .838 F .814 Sn .760	Er .921 Lu .878 Dy .859 Y .814 Pr .726	Sr .750 Sm .689 Ce .638 Gd .578 Pr .564 La .542 Zn .533	Bao .908 Ba .799 La .426	Be .700 Mo .396 Zn .309 Ba .261 SiO ₂ .240 Ga .238	Ba .432 U .313 BaO .224 Dy .212	Gd .225 U .145 Sm = Nb .122 SrO .120 Mo .114 Ta .112 Be .109 Ba = Hf .105	N/A	N/A

DISCUSSION

GEOLOGY

The rhyolites of the Sierra Blanca laccoliths intrude the Cretaceous sediments of the Washita Group (undivided), often along pre-existing fractures created by an earlier diorite intrusion (Price, et al., 1990). Previous mapping (Fig. 1.4 and 1.7) limits the rhyolite/colluvium contact to the exposed, upper portions (above 1524m) of the laccoliths. The recently completed, field-derived geological map of the laccoliths expands upon features originally mapped by Albritton and Smith (1965), with the inclusion of newly mapped mafic dikes on the southern flank of Little Blanca and an additional diorite outcrop to the northwest of the small knob between Little Round Top and Round Top (Fig. 4.1). The location of the contact between the intrusions and sedimentary country rock was more closely defined, increasing the areal extent of the laccolith bodies at the surface. Generalized topographical cross-sections of the laccoliths (Fig. 4.2) indicate a trace of the inferred faults that are not extrapolated to depth due to a lack of data. The location of the feeder for the laccoliths remains unknown, though it has been postulated that it is located in the approximate center of the valley dividing the laccoliths. Examination of the magnetic anomaly map (Fig 3.5) indicates a magnetic high in the approximate center of the laccoliths, and it has been proposed that this may be indicative of a feeder (Stanley Korzeb, pers. commun.).

The lithological character of the laccoliths is that of a fine-grained, felsic, alkali rhyolite (Fig. 4.32). Geotectonic classification of the laccoliths (Fig. 4.39) shows them to be within plate granites (WPG). Based upon the Shand (1943) classification by molar alkali versus alumina content, where $Al_2O_3 > (CaO + Na_2O + K_2O)$ is peraluminous, and $Al_2O_3 < (CaO + Na_2O + K_2O)$ and $Al_2O_3 > (Na_2O + K_2O)$ is metaluminous, the Sierra Blanca rhyolites range from metaluminous to slightly peraluminous (Fig. 4.40), contrary to previous work (Price et al., 1990) that indicates the rhyolites are peraluminous. According to the plot they are not peralkaline, but lie just above the boundary. The felsic nature of the rhyolites is evident in the high SiO_2 content (Table 4.11, and Figs 4.42- 4.45), within and between the laccoliths (Fig. 4.13). Na_2O is only slightly above, while Al_2O_3 is below, that of crustal average (Table

4.11). Fig. 5.1 is a simplified tectonic schematic depicting the emplacement of the Sierra Blanca laccoliths in the stable block. Heat associated with the Rio Grande Rift caused more rapid melting of the felsic stable block, resulting in the younger age of the laccoliths. Differences in the magmatic source result in the geological and geochemical variations seen on either side of the Texas Lineament.

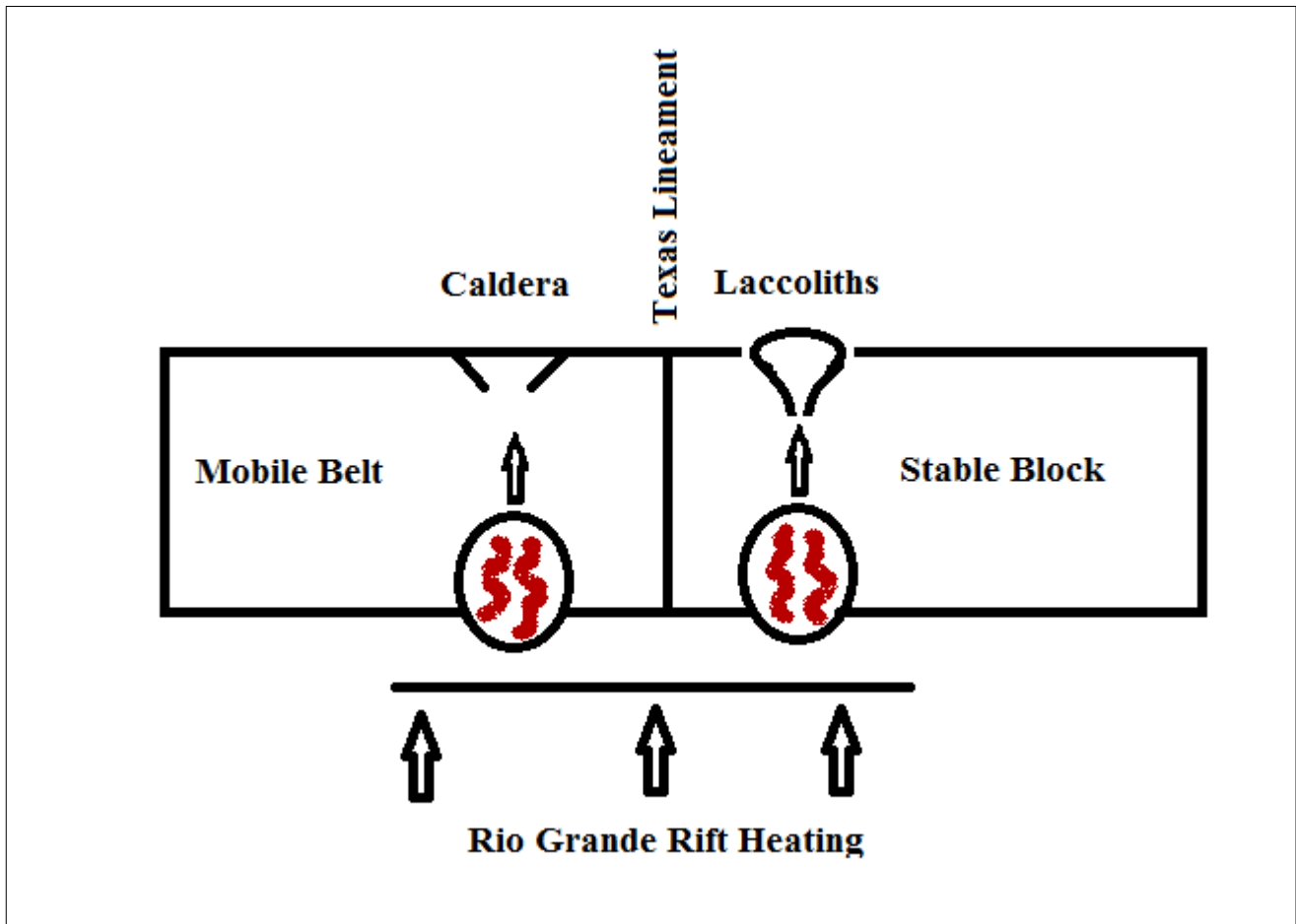


Fig. 5.1: Tectonic schematic of the emplacement of the Sierra Blanca laccoliths.

GEOCHEMISTRY

The tectonic setting and geochemistry of the laccoliths are in many ways analogous to topaz rhyolites, as shown in Fig. 1.3 and Table 4.6, but show a unique enrichment in HREE (Table 4.11, Fig. 4.41), uncharacteristic of a typical topaz rhyolite (Price, 2004). In comparison to crustal average (Table 4.11), all four laccoliths show enrichment in the REE. A comparison of “fresh” to weathered samples indicates that weathering has little to no effect on REE concentration (Table 4.7). The greatest enrichment of HREE (Table 4.2) is evident on Little Round Top. Little Blanca shows greater enrichment in LREE (Table 4.2, Fig. 4.47), with an increase in enrichment in HREE evident on Little Round Top and Round Top. The LREE enrichment of Little Blanca, and its relative depletion in HREE can be seen in the corresponding HREE enrichment of Little Round Top and Round Top, as evident in scattergrams of La and Lu compared to F (Figs. 4.47 and 4.48). Only Sierra Blanca shows little to no change in enrichment pattern, and remains the least REE enriched of the laccoliths (Figs. 4.4 – 4.8).

While overall enrichment is high in comparison to crustal averages, it can be seen in Figs. 4.22 – 4.36 that REE enrichment is not homogeneous over the laccoliths and shows changes along the profiles. These and other data (Amed Gomez, in prep.) suggest a late stage, F-rich, hydrothermal event. Ratios of the LREE La (Fig. 4.16), Ce (Fig. 4.18), and Nd (Fig. 4.19) to the HREE Yb show little to no change within the laccoliths. On Little Blanca, as distance from the inferred contact increases, REE concentrations decline. Sample LB9 (Figs. 4.20 – 4.23), consistently shows the lowest values in REE concentration. These areas are marked by intensely fractured rhyolite, areas where the circulation of fluids is facilitated by the fractures. A comparison of outlier data (Table 4.4 and 4.5) with drill data from Round Top, documents the increased REE enrichment in fracture zones through late stage fluid actions.

A marked Eu depletion, as is seen in the Sierra Blanca laccoliths, is indicative of plagioclase-involved differentiation under low oxygen fugacity (Kemp, et al., 2005). Eu/Eu^* magnitude is the hypothetical value of Eu if no Eu^{+2} was taken up by plagioclase (Winter, 2010). Table 4.6 and Fig. 4.19 show the Eu/Eu^* magnitude, indicating an increase in magnitude as one progresses through Sierra

Blanca, Little Blanca, Little Round Top, to Round Top. The HREE enrichment pattern (from least to greatest: SB-LB-LRT-RT) substantiates this. Silica content also decreases from Sierra Blanca to Round Top, following the same pattern.

An examination of F and Y, elements commonly associated with REE, shows that the Sierra Blanca laccoliths are enriched in both with respect to crustal average (Table 4.11, Figs. 4.3 and 4.4). Ratios of the REE to F show no discernible pattern, either with distance from the contact or proximity to inferred faults. Ratios of the REE to Y show slight increases near inferred faults on Little Blanca and Little Round Top. F shows a slightly increased concentration at contacts and in the vicinity of inferred faults on Little Round Top (Fig. 4.3), while Y shows a relatively even dispersion across the laccoliths (Fig. 4.4).

The small sample size of the data precludes the justification for factor analysis. In spite of this, past experience demonstrates that it can be useful in a suggestive manner. Factor analysis of the different laccoliths indicates a strong correlation between REE, F and Y (Table 4.12). HREE are most often associated with Y, while F is found with both LREE and HREE. A comparison of major oxide components on the laccoliths (Fig. 4.42 – 4.45) demonstrates the high silica, sodium and aluminum content of the rhyolites, as well as the low P_2O_5 content of Sierra Blanca, Little Blanca, and Little Round Top. The increased P_2O_5 of Round Top may be associated with xenotime or monazite. Based upon elements and their loading value in each factor, data suggests that the mineralogical components of the laccoliths include; bastnäsite - $(La,Ce)(CO_3)F$ or $(Y,Ce)(CO_3)F$, cryolite - Na_3AlF_6 , thorite - $(Th,U)SiO_4$, xenotime - $(Yb, Y, HREE)PO_4$, yttrocerite - $(Ca,Y,Ce)F_{2+x}$, and yttrifluorite - $(Ca_{1-x}Y_x)F_{2+x}$. Silicate rock components, Na_2O , Al_2O_3 , and SiO_2 , are evident in factors 7, 8, and 9 on Little Blanca, and factor 1 on Little Round Top and Round Top. A greater amount of LREE are associated with the rock components on Little Blanca, as is U. Th, possibly thorite, may be associated with factor 7 on Little Blanca and factor 1 on Little Round Top. Round top shows HREE loading high on factor 2, with LREE loading on factor 3, which may be associated with bastnäsite. Cryolite (Na_3AlF_6) may be associated with factors 1 on Round Top. The association of cryolite with REE deposits has been noted in various studies

(Bowden et al., 1979; Gramenitskii and Shchekina, 2005). Price, et al. (1990), postulate that the presence of cryolite on the laccoliths is evidence for vapor phase crystallization.

CONCLUSIONS

1. The Sierra Blanca laccoliths represent a unique deposit of REE, partly analogous to topaz rhyolites, yet demonstrating an unusual enrichment in HREE.
2. The regional tectonic setting, associated with the Texas Lineament, the Rio Grande rift extensional regime, and the associated magmatism are postulated to be factors in the emplacement of the REE-enriched rhyolites. The emplacement of the Sierra Blanca rhyolites takes place in the stable block near the stable block/mobile belt boundary.
3. REE enrichment of the rhyolites is consistent throughout the Sierra Blanca laccoliths at levels well above crustal average.
4. Enrichment in the HREE and incompatible trace elements Be, F, Rb, Y, Zr, Nb, Sn, U, indicates possible economic potential beyond that of a REE deposit.
5. The laccoliths show zoning of the REE, from enrichment of LREE on Little Blanca to HREE on Little Round Top and Round Top.
6. Internal zonation of each laccolith does not take place. Superimposition by conclusion 7 does take place.
7. A late stage enrichment along fractured zones through the action of F-rich liquids is indicated by the higher concentration of F and associated REE, as identified by outliers.
8. REE are found in association with Y and F throughout the laccoliths. Factor analysis suggests the following mineralogy. Yttrocerite and yttrofluorite are the main REE bearing minerals, and the data supports their distribution throughout the laccoliths, whereas xenotime and bastnäsite are minor REE bearing mineral components, with xenotime only in Round Top.
9. Prior data indicates the differentiation sequence of the laccoliths as SB-LB-RT-LRT. Examination of the Eu/Eu^* magnitude as it changes across the laccoliths demonstrates

that Round Top exhibits the least amount of differentiation in comparison to the other laccoliths. This technique results in a differentiation sequence of RT-LRT-LB-SB. Resolving this remains a controversy.

FUTURE WORK

1. How can geophysical techniques be used to their best advantage? Verification of the location, depth, and orientation of feeders, faults and contacts would reveal more detail about structural roles in REE enrichment.
2. What is the source of the magma and the REE? The source of HREE in the Sierra Blanca laccoliths has not been adequately explained. Enrichment in HREE is possible through the dissolution of xenotime, garnet or zircon in the mantle. A detailed petrological study being undertaken by M. Ali utilizing isotope analysis to address these hypotheses and will enhance the body of knowledge surrounding this and other REE deposits.
3. Can the age of the laccoliths be more closely determined? The age of the Sierra Blanca laccoliths is based on a single K-Ar date. K-Ar dating has limitations for laccoliths, and dating using different isotopes would allow the genesis of the laccoliths to be further constrained.
4. What is the near-surface/ upper crustal differentiation sequence? Petrologic literature contains numerous additional suggested differentiation indicators which can be applied in the area.
5. Can cryolite be used as indicator of HREE? The association of cryolite with HREE is as yet not well understood. Studies indicate that cryolite is associated with REE deposits containing HREE, suggesting that it may act as an indicator mineral for HREE.

REFERENCES

1. Albritton, C.C., Jr., and Smith, J.F., Jr., 1965, Geology of the Sierra Blanca Area, Hudspeth County, Texas: US Geological Survey Professional Paper 479.
2. Baddock, M.C., Gill, T.E., Bullard, J.E., Dominguez Acosta, M. and Rivera, N.I., 2011, Geomorphology of the Chihuahuan Desert based on potential dust emissions: *Journal of Maps*, v. 2011, p. 249-259.
3. Barker, D. S., 1980, Cenozoic igneous rocks, Sierra Blanca area, Hudspeth County, Texas, *In* P. W. Dickerson, J. M. Hoffer, J. F. Callender, Eds., *Trans-Pecos Region Southeastern New Mexico and West Texas*, New Mexico Geological Society Guidebook, 31st Field Conference, Trans-Pecos Region: University of New Mexico, Albuquerque, p. 219-223.
4. Bowden, P., Bennett, J.N., Whitley, J.E., Moyes, A. B., 1979, Rare earths in Nigerian Mesozoic granites and related rocks: *Physics and Chemistry of the Earth*, v.11, p. 479-491.
5. Burt, D.M., Sheridan, M.F., Bikun, J.V., Christiansen, E.H., 1982, Topaz Rhyolites – Distribution, Origin, and Significance for Exploration: *Economic Geology*, v. 77, p. 1818-1836.
6. Carciumaru, D., Ortega, R., 2008, Geologic structure of the northern margin of the Chihuahua trough: Evidence for controlled deformation during Laramide Orogeny: *Boletín de la Sociedad Geológica Mexicana*, v.60, p. 43-69.
7. Černý, P., 1991, Rare-element Granitic Pegmatites. Part I: Anatomy and Internal Evolution of Pegmatitic Deposits: *Geoscience Canada*, v. 18, p. 49-67.
8. Christiansen, E.H., Burt, D.M., Sheridan, M.F., and Wilson, R.T., 1983, The petrogenesis of topaz rhyolites from the western United States: *Contributions to Mineralogy and Petrology*, v. 83, p. 1-16.
9. Gambogi, J., and Cordier, D.J., 2010, *Rare Earths: 2010 Minerals Yearbook*, U.S. Department of the Interior, U.S. Geological Survey.
10. Gilmer, A.K., Kyle, J.R., Connelly, J.N., Mathur, R.D., Henry, C.D., 2003, Extension of Laramide magmatism in southwestern North America into Trans-Pecos Texas: *Geology*, v. 31, p. 447 – 450.
11. Gomez, C., Delacourt, C., Allemand, P., Ledru, P., Wackerle, R., 2005. Using ASTER remote sensing data set for geological mapping, in *Namibia: Physics and Chemistry of the Earth*, v. 30, p. 97-108.
12. Gramenitskii, E. N., Shchekina, T. I., 2005, Behavior of Rare Earth Elements and Yttrium during the Final Differentiation Stages of Fluorine-Bearing Magmas: *Geochemistry International*, v. 43, no. 1, p. 39-52.
13. Grasso, V.B., 2012, *Rare Earth Elements in National Defense: Background, Oversight Issues, and Options for Congress*. Congressional Research Service Report for Congress, R41744.
14. Gschneidner KA, Cappellen, ed. 1987, *1787–1987 Two hundred Years of Rare Earths*”. Rare Earth Information Center, IPRT, North-Holland
15. Guilbert, J.M., Park, C.F. Jr, 1986, *The Geology of Ore Deposits*: Long Grove, Waveland Press Inc., 985 p.

16. Henry, C.D., McDowell, F.W., Price, J.G., and Smyth, R.C., 1986, Compilation of potassium-argon ages of Tertiary igneous rocks, Trans Pecos Texas: Bureau of Economic Geology Geological Circular 86-2, University of Texas at Austin.
17. Hobbs, T. M.C., and Hoffer, J.M., 1980, The Square Peak Volcanic Series, Northern Quitman Mountains, Hudspeth County, Texas, *in* Dickerson, P.W., Hoffer, J.M., Callender, J.F., Eds., Trans-Pecos Region Southeastern New Mexico and West Texas: New Mexico Geological Society Guidebook, 31st Field Conference, Trans-Pecos Region, p.231-235.
18. Hulse, D.E., Newton, M. C. III, Malhotra, D., Black, Z. J., 2012: NI 43-101 Preliminary Economic Assessment Round Top Project Sierra Blanca, Texas, Gustavson Associates, Lakewood, CO, 146 p.
19. Humphries, M., 2012, Rare Earth Elements: The Global Supply Chain, Congressional Research Service Report for Congress, R41347.
20. Hunt, G.R., 1977. Spectral signatures of particulate minerals in the visible and near infrared. *Geophysics* 42. 501-513.
21. Janoušek, V., Farrow, C.M. & Erban, V., 2006, Interpretation of whole-rock geochemical data in igneous geochemistry: introducing Geochemical Data Toolkit (GCDkit): *Journal of Petrology*, v. 47(6), p. 1255-1259.
22. Kemp, A.I.S., Wormald, R.J., Whitehouse, M.J., Price, R.C., 2005, Hf isotopes in zircon reveal contrasting sources and crystallization histories for alkaline to peralkaline granites of Temora, southeastern Australia: *Geology*, v. 33, no. 10, p. 797-800.
23. Lloyd, W.J., Schmidt, R.H. Jr., 1980: Land Use in the Basin and Range Topographic Province of Trans-Pecos Texas, *in* Dickerson, P.W., Hoffer, J.M., Callender, J.F., Eds., Trans-Pecos Region Southeastern New Mexico and West Texas: New Mexico Geological Society Guidebook, 31st Field Conference, Trans-Pecos Region, p. 305-310.
24. Long, K.R., Van Gosen, B.S., Foley, N.K., Cordier, D., 2010, Principle Rare Earth Elements Deposits of the United States – A Summary of Domestic Deposits and a Global Perspective: Scientific Investigations Report 2010-5220. U.S. Department of the Interior, U.S. Geological Survey.
25. Mason, B., and Moore, C.B., 1982, Principles of geochemistry; John Wiley and Sons, Inc., New York, 344 p.
26. Matthews, W.K. III, Adams, J.A.S., 1986, Geochemistry, Age, and Structure of the Sierra Blanca and Finlay Mountain Intrusions, Hudspeth County, Texas, *In* Price, J.G., Henry, C.D., Parker, D.F., Barker, D.S., Eds., *Igneous Geology of Trans-Pecos Texas*, Bureau of Economic Geology Guidebook 23, University of Texas at Austin, p. 225-226.
27. McAnulty, W. N., 1974, Fluorspar in Texas: The University of Texas at Austin Bureau of Economic Geology Handbook 3, 31 p.
28. McAnulty, W. N., 1980, Geology and Mineralization of the Sierra Blanca Peaks, Hudspeth County, Texas. *In* P. W. Dickerson, J. M. Hoffer, J. F. Callender, Eds., Trans-Pecos Region Southeastern New Mexico and West Texas, New Mexico Geological Society Guidebook, 31st Field Conference, Trans-Pecos Region, University of New Mexico, Albuquerque, p. 263-266.

29. Muehlberger, W.R., 1980, Texas lineament revisited, *In* P. W. Dickerson et al., Eds., Trans-Pecos Region Southeastern New Mexico and West Texas, New Mexico Geological Society Guidebook, 31st Field Conference, Trans-Pecos Region, University of New Mexico, Albuquerque, p. 113-121.
30. Murry, D.H., 1980, Mineralization in the Northern Quitman Mountains, Hudspeth County, Texas. *In* P. W. Dickerson et al., Eds., Trans-Pecos Region Southeastern New Mexico and West Texas, New Mexico Geological Society Guidebook, 31st Field Conference, Trans-Pecos Region, University of New Mexico, Albuquerque, p. 267- 270.
31. Ortega, R., and Carciumaru, D., 2010, Tectonic Inversions in the Northern Bend of the Chihuahua Trough: International Journal of Geology, v. 4, p. 14-22.
32. Price, J.G., 2004, I Never Met a Rhyolite I Didn't Like – Some of the Geology in Economic Geology; SEG Newsletter, No. 57, p. 1-13.
33. Price, J.G., Rubin J.N., Henry, C.D., Pinkston, T.L., Tweedy, S.W., Koppenaar, D.W., 1990, Rare-metal enriched peraluminous rhyolites in a continental arc, Sierra Blanca area, Trans-Pecos Texas; Chemical modification by vapor-phase crystallization, *in* Stein, H.J., and Hannah, J.L., eds., Ore-bearing granite systems; Petrogenesis and mineralizing processes: Geological Society of America Special Paper 246, p. 103-120.
34. Rose, E.R., 1960, Rare Earths of the Grenville Sub-Province Ontario and Quebec, GSC Report Number 59-10. Ottawa: Geological Survey of Canada Department of Mines and Technical Surveys.
35. Rubin, J.N., Price, J.G., Henry, C.D., Kyle, J.R., 1990, Geology of the Beryllium-Rare Earth Element Deposits at Sierra Blanca, West Texas, *in* Kyle, J.J., Thompson, T.B., eds., Industrial Mineral Resources of the Delaware Basin, Texas and New Mexico: Guidebook Prepared for Society of Economic Geologists Field Conference – 24 -27 October 1990, p. 191-203.
36. Rubin J.N., Price, J.G., Henry, C.D., Koppenaar, D.W., 1987a, Cryolite-bearing and rare metal-enriched rhyolite, Sierra Blanca Peaks, Hudspeth County, Texas. *American Mineralogist*, v. 72, p. 1122-1130.
37. Rubin, J. N., Price, J.G., Henry, C.D., Pinkston, T.L., Tweedy, S.W., Koppenaar, D.W., Peterson, S.B., Harlan, H.M., Miller, W.T., Thompson, R.J., Grabowski, R.B., Laybourn, D.P., Schrock, G.E., Johnson, A., Staes, D.G., Gaines, R.V., Miller, F.H., 1987b, Mineralogy of Beryllium Deposits Near Sierra Blanca, Texas: Bureau of Mines / Minerals yearbook area reports: domestic 1987, Volume 2, p. 601-614.
38. Salisbury, J.W., Walter, L.S., Vergo, N., 1987, Mid-infrared (2.1-2.5 μ m) Spectra of Minerals: United States Geological Survey, Open File Report, pp. 87-263.
39. Shand, J.S., 1943, Eruptive Rocks: Their genesis, composition and classification, with a chapter on meteorites: New York and London, J. Wiley and Sons, Inc., 444p.
40. Shannon, W.M., and Goodell, P.C., 1986, Lithogeochemistry of Intrusive Rocks of the Quitman-Sierra Blanca Igneous Complex, Hudspeth County, Texas: *In* Jonathan, J.G., Price, G., Henry, C.D., Parker, D.F., Barker, D.S., Eds., Igneous Geology of Trans-Pecos Texas: Bureau of Economic Geology Guidebook 23, University of Texas at Austin, p. 225-226.

41. Shannon, W.M., 1986, Lithogeochemical Characterization of Intrusive Rocks Comprising the Quitman-Sierra Blanca Igneous Complex, Hudspeth County, Texas. M. S. Thesis, University of Texas at El Paso.
42. Spedding F., Daane, A.H., 1961, The Rare Earths: New York and London, John Wiley & Sons, Inc.
43. United States Geological Survey, Mineral Commodity Summaries, 2013, Rare Earths (http://minerals.usgs.gov/minerals/pubs/commodity/rare_earth/mcs-2013-raree.pdf).
44. Winter, J.D., 2010, Principles of Igneous and Metamorphic Petrology, Second Edition: New York, Prentice and Hall, 702p.

APPENDIX I: ABBREVIATIONS USED

Abbreviations used

CA:	Crustal Abundance
DD:	Diorite Dike
HREE:	Heavy Rare Earth Elements (Tb – Lu)
LB:	Little Blanca
LREE:	Light Rare Earth Elements (La – Gd)
LRT:	Little Round Top
MD:	Mafic Dike
ppb:	Parts per billion
ppm:	Parts per million
QS:	Quitman Stock
REE:	Rare Earth Elements
RT:	Round Top
SB:	Sierra Blanca

APPENDIX II: SAMPLE LOCATION

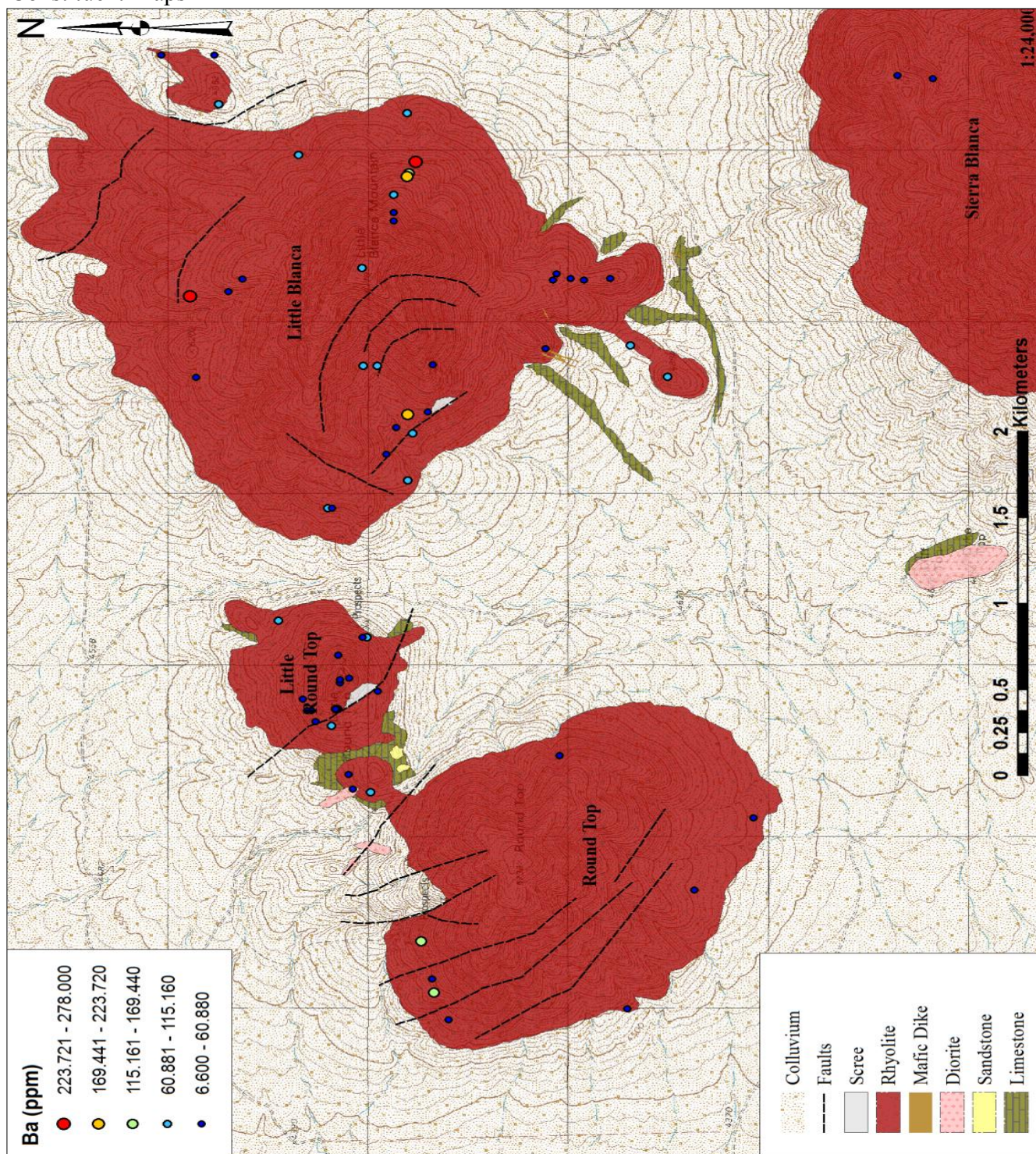
Sample Locations

Table 3.3 Sample Locations (GCS NAD83)

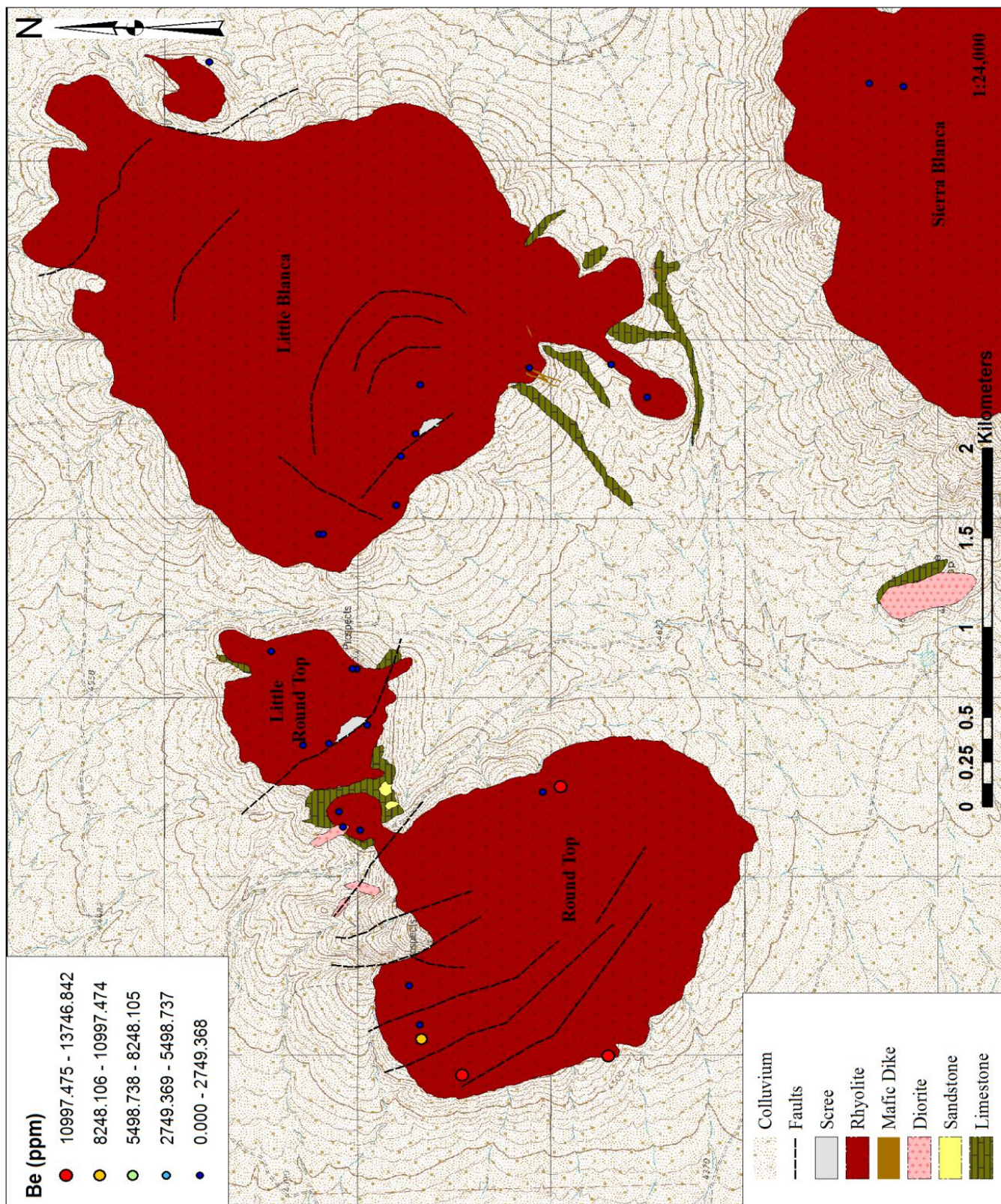
<i>Sample</i>	<i>Longitude</i>	<i>Latitude</i>	<i>Sample</i>	<i>Longitude</i>	<i>Latitude</i>
LB1	-105.42900	31.28260	LB16	-105.43920	31.27460
LB2	-105.43190	31.28220	LB17	-105.43910	31.27340
LB3	-105.43200	31.28220	LB18	-105.43770	31.27030
LB4	-105.43270	31.28250	LB19	-105.42550	31.29130
LB5	-105.43290	31.28260	LB20	-105.42550	31.29370
LB6	-105.43400	31.28320	LB21	-105.42850	31.29110
LB7	-105.43510	31.28320	LB22	-105.43160	31.28750
LB8	-105.43560	31.28320	LB23	-105.45320	31.28610
LB9	-105.43850	31.28460	LB24	-105.45320	31.28590
LB10	-105.43460	31.27340	LB25	-105.44510	31.27080
LB11	-105.43730	31.27370	LB26	-105.44320	31.27250
LB12	-105.43850	31.27450	LB27	-105.44340	31.27630
LB13	-105.43883	31.27582	LB28	-105.44440	31.28140
LB14	-105.43920	31.27600	LB29	-105.44730	31.28160
LB15	-105.43910	31.27520	LB30	-105.44860	31.28230
LB31	-105.45150	31.28250			
LB-1S	-105.43921	31.28999	LB-2S	-105.43999	31.29062
LB-3S	-105.44027	31.29235	LB-4S	-105.44524	31.29206
LB-5S	-105.44771	31.29055	LB-6S	-105.44450	31.28452
LB-7S	-105.44450	31.28389	LB-8S	-105.44746	31.28251
LB-9S	-105.44827	31.28304	LB-10S	-105.44989	31.28346
LRT1	-105.46390	31.28550	LRT2	-105.46370	31.28550
LRT3	-105.46360	31.28510	LRT4	-105.46220	31.28560
LRT5	-105.47060	31.28410	LRT6	-105.46950	31.28510
LRT7	-105.47040	31.28490	LRT8	-105.46950	31.28440
LRT9	-105.46440	31.28380	LRT10	-105.46110	31.28430
LRT11	-105.46110	31.28450	LRT12	-105.46010	31.28830
LRT13	-105.46560	31.28680	LRT14	-105.46550	31.28560
LRT-2S	-105.46492	31.28718	LRT-3S	-105.46560	31.28698
LRT-4S	-105.46629	31.28659	LRT-5S	-105.46652	31.28588
LRT-6S	-105.46552	31.28570	LRT-7S	-105.46552	31.28569
LRT-8S	-105.46959	31.28449			
RT12 5 3	-105.46830	31.27560	RT12 5 4	-105.46860	31.27680
RT12 6 1	-105.48200	31.28130	RT12 6 2	-105.47970	31.28180
RT12 6 3	-105.468583	31.27619	RT201	-105.483796	31.272468
RT252	-105.484959	31.279305	RT262	-105.484501	31.280539
RT287	-105.467971	31.274759	RT334	-105.47206	31.266828
RT335	-105.474456	31.267216	RT336	-105.4765	31.269472
RT337	-105.484995	31.277155	RT231	-105.4771	31.28068
RT233	-105.476782	31.281244	RT226	-105.482845	31.281209
RT251	-105.484783	31.279764			
SB2	-105.42680	31.25890	SB3	-105.42680	31.25890
SB4	-105.42660	31.26050	SB5	-105.42660	31.26050
SB-RCL-1	-105.42548	31.25841			
MD1	-105.43769	31.27024	QS2	-105.49126	31.21241
DD2	-105.45641	31.25908	DD3	-105.45772	31.25913

APPENDIX III: CONSTITUENT MAPS

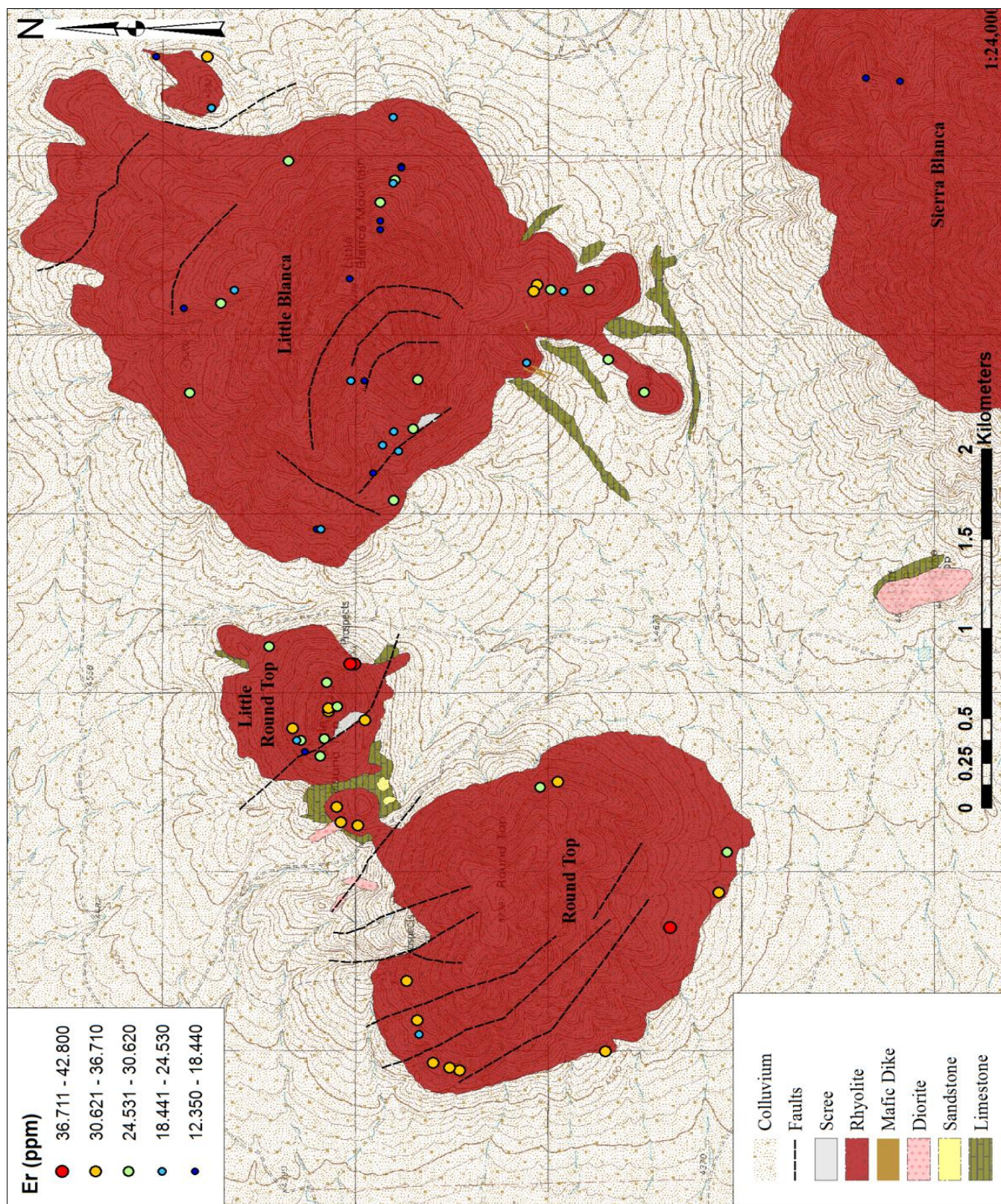
Constituent Maps



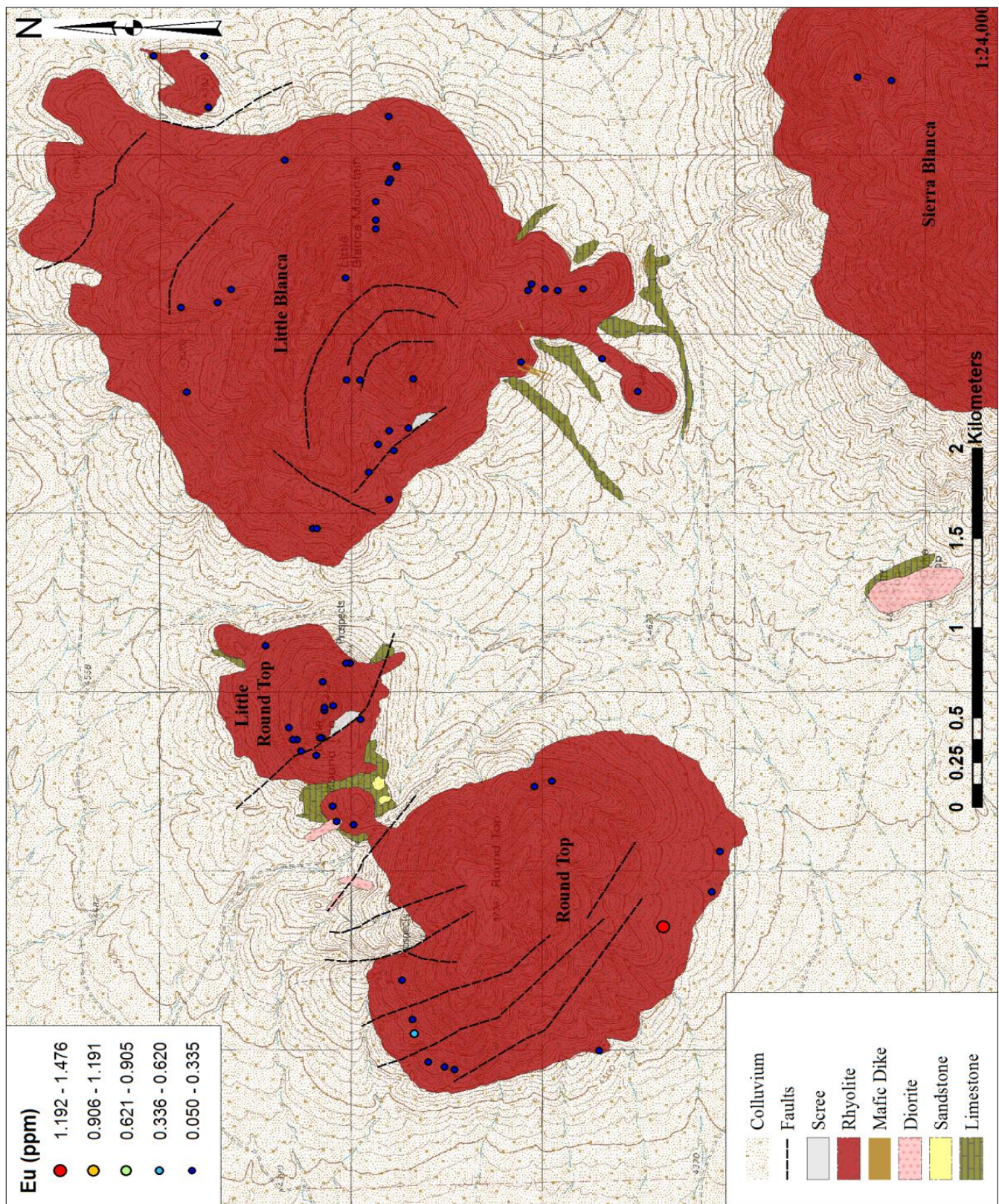
Barium



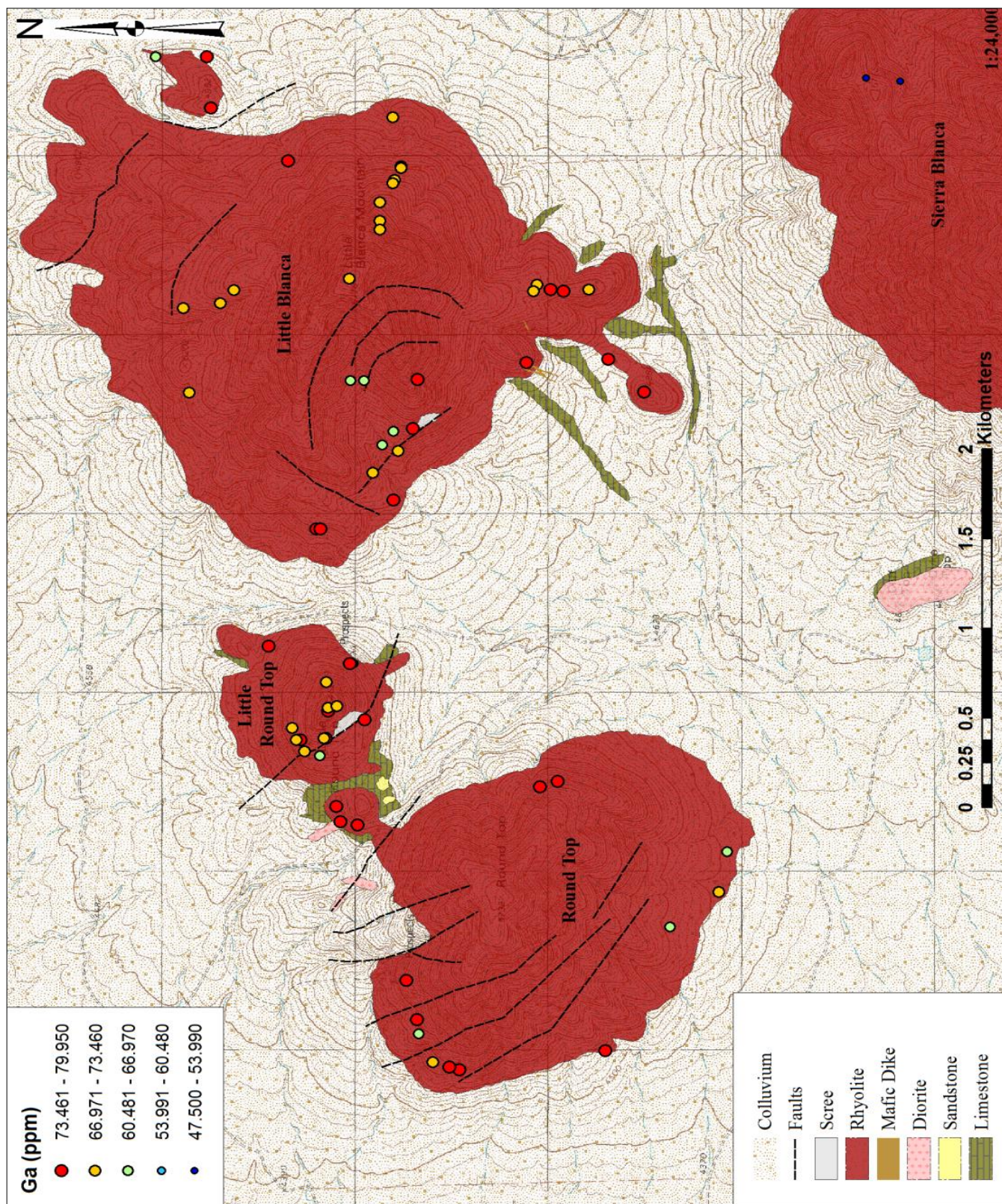
Beryllium



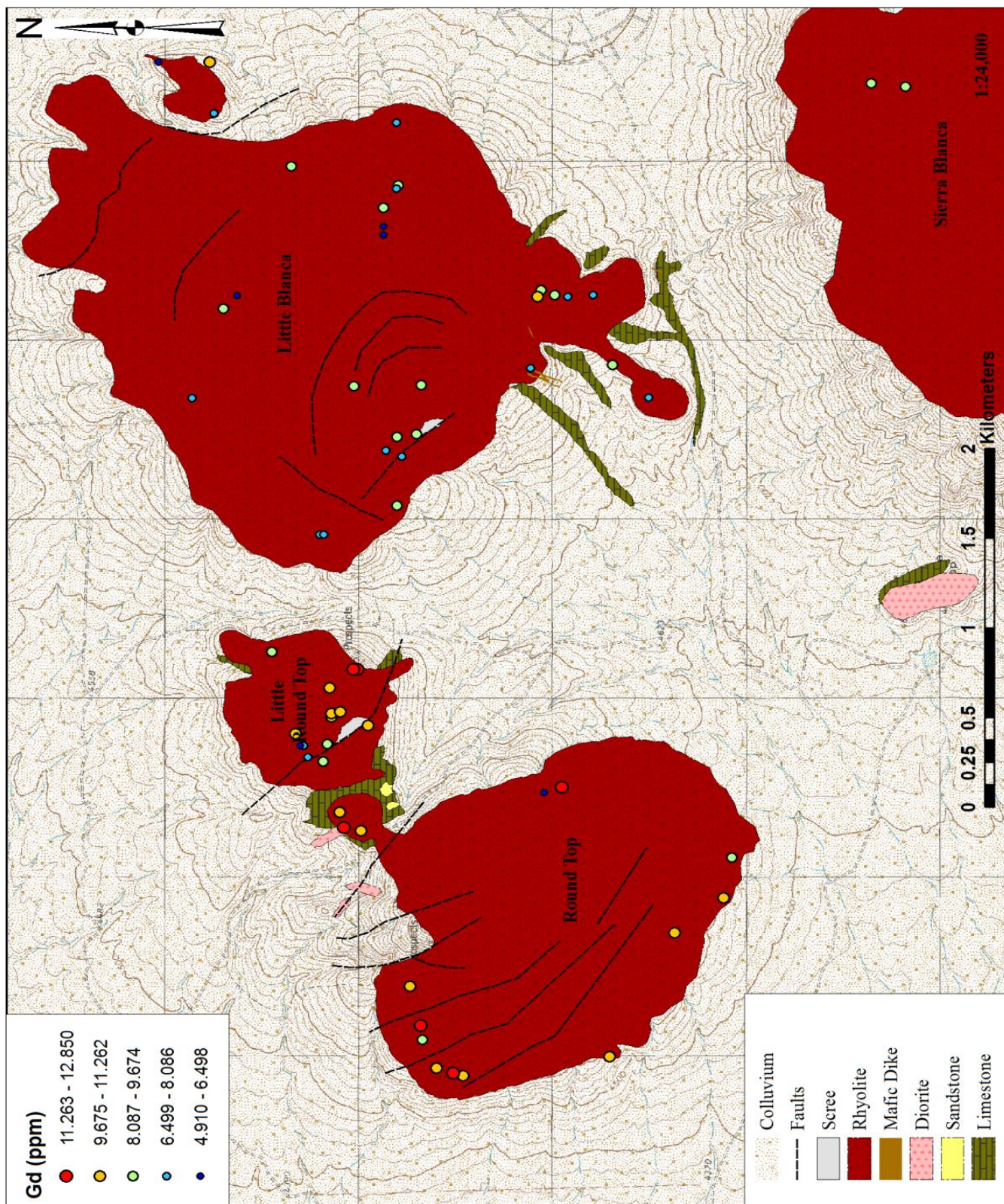
Erbium



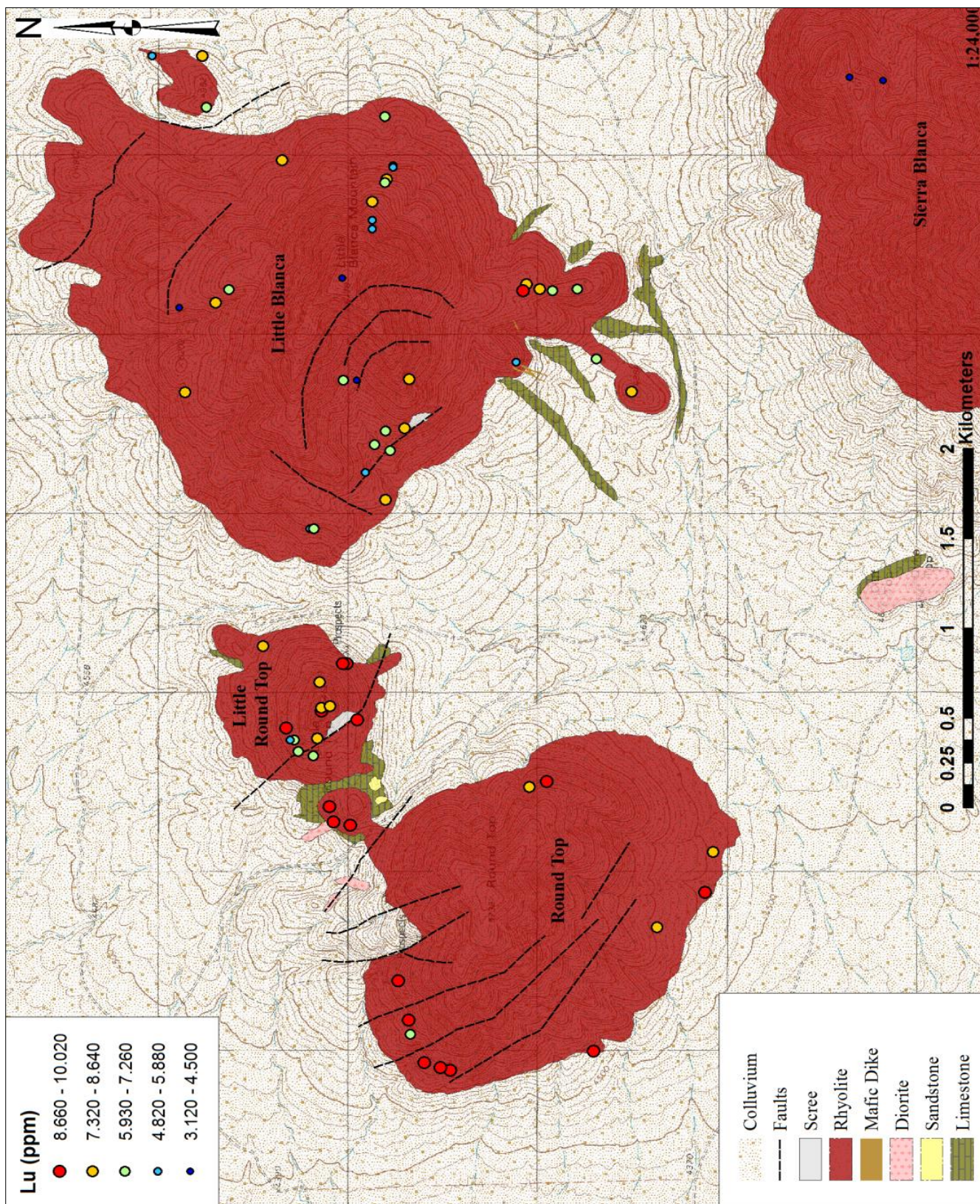
Europium



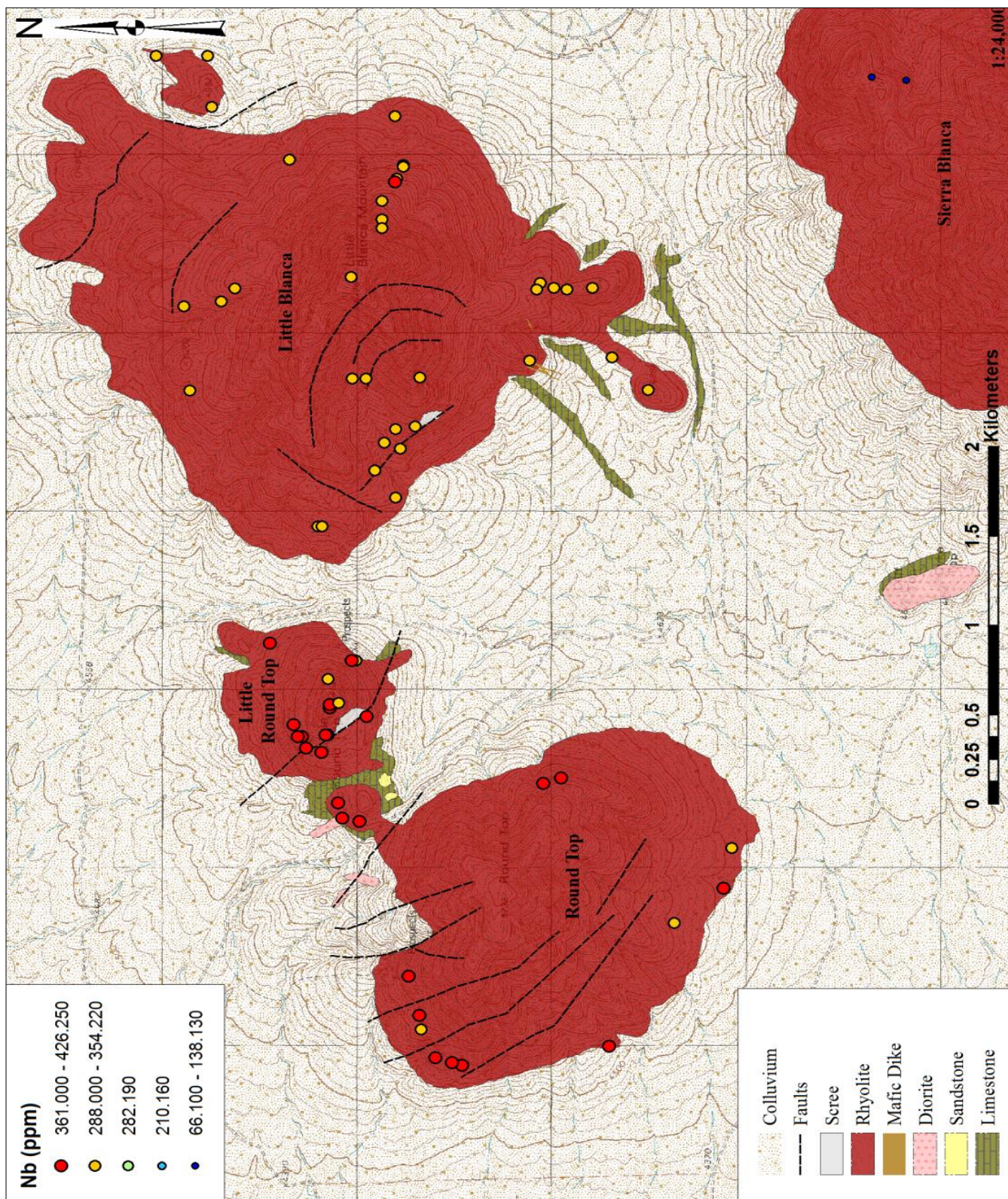
Gallium



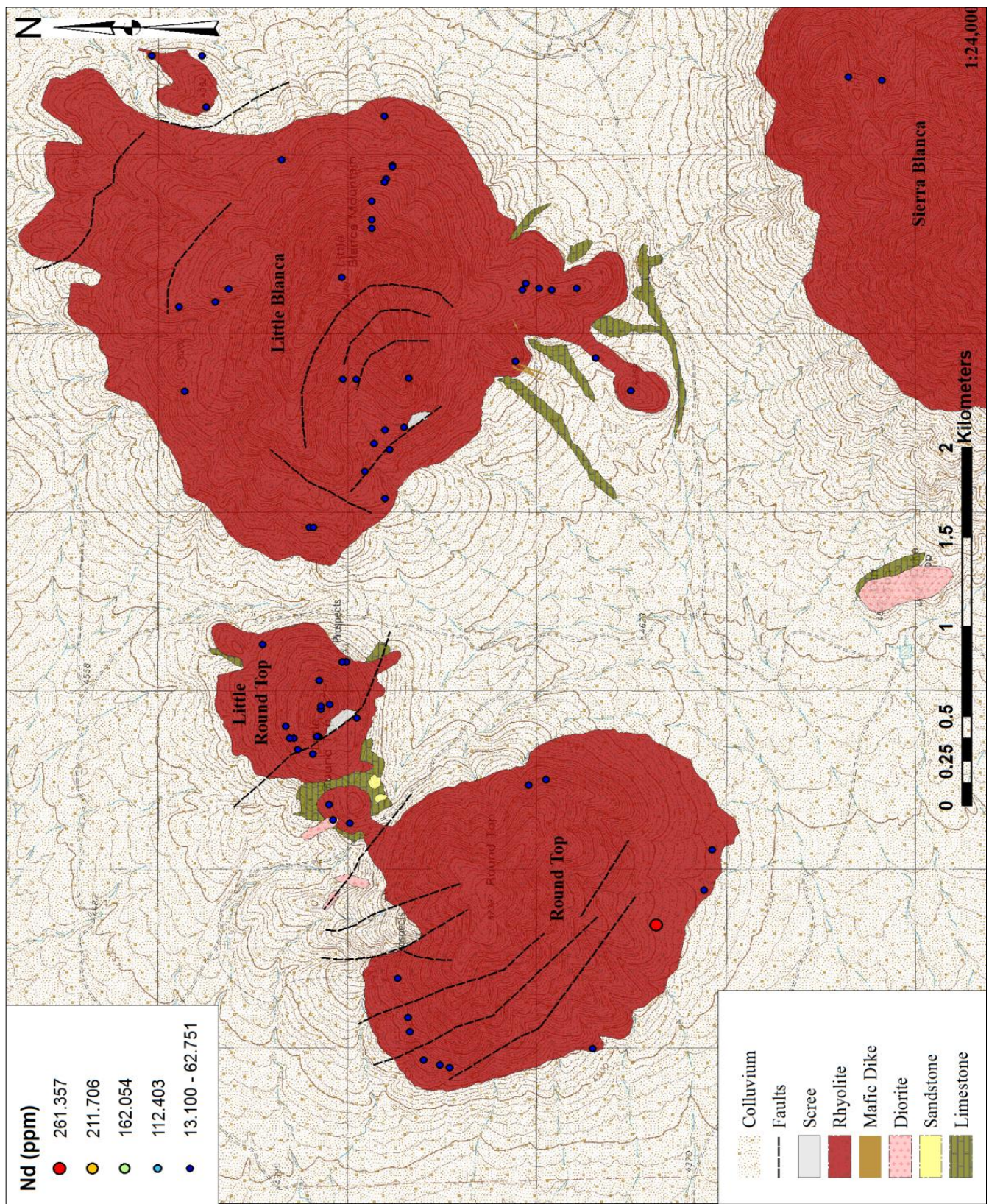
Gadolinium



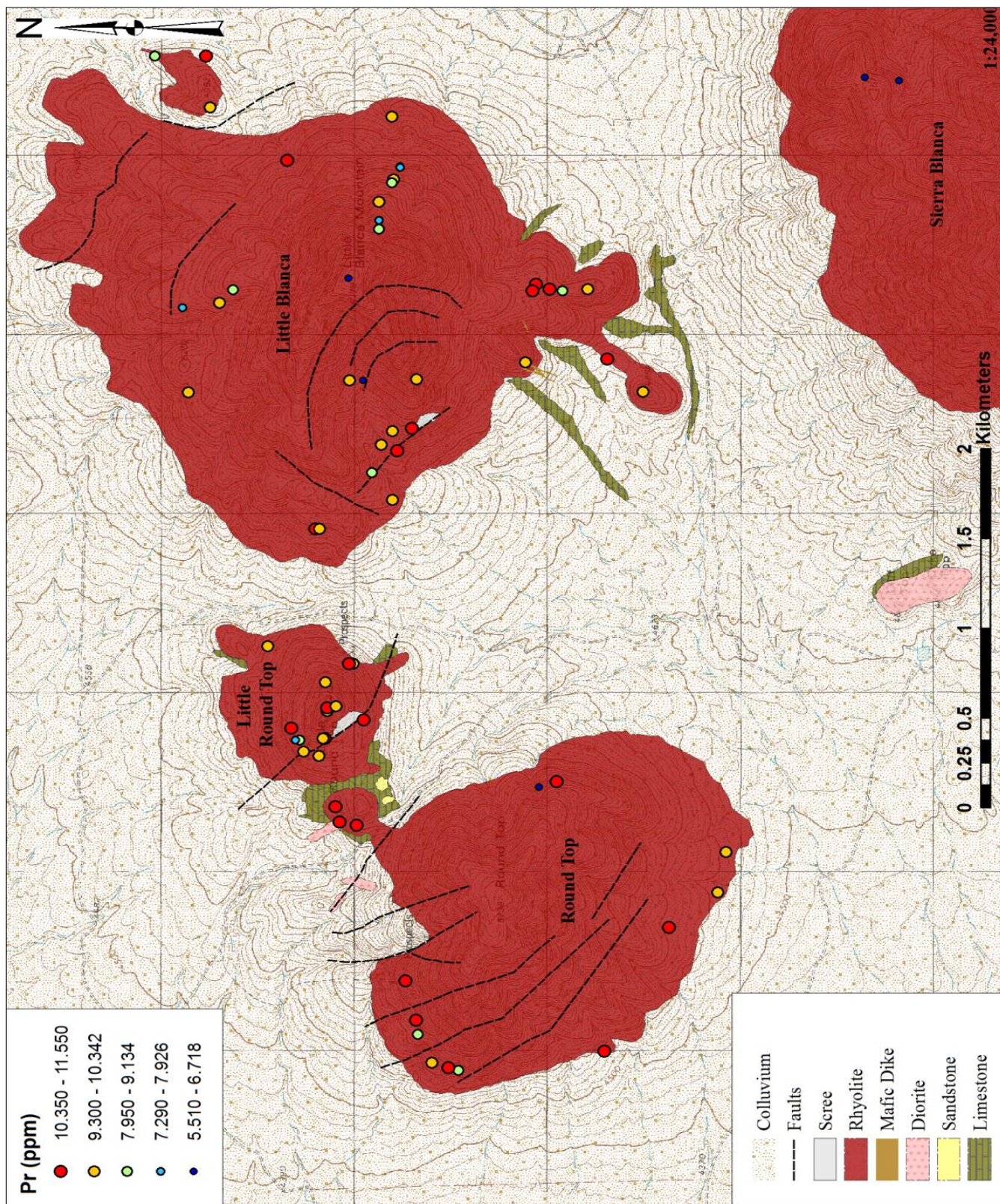
Lutetium



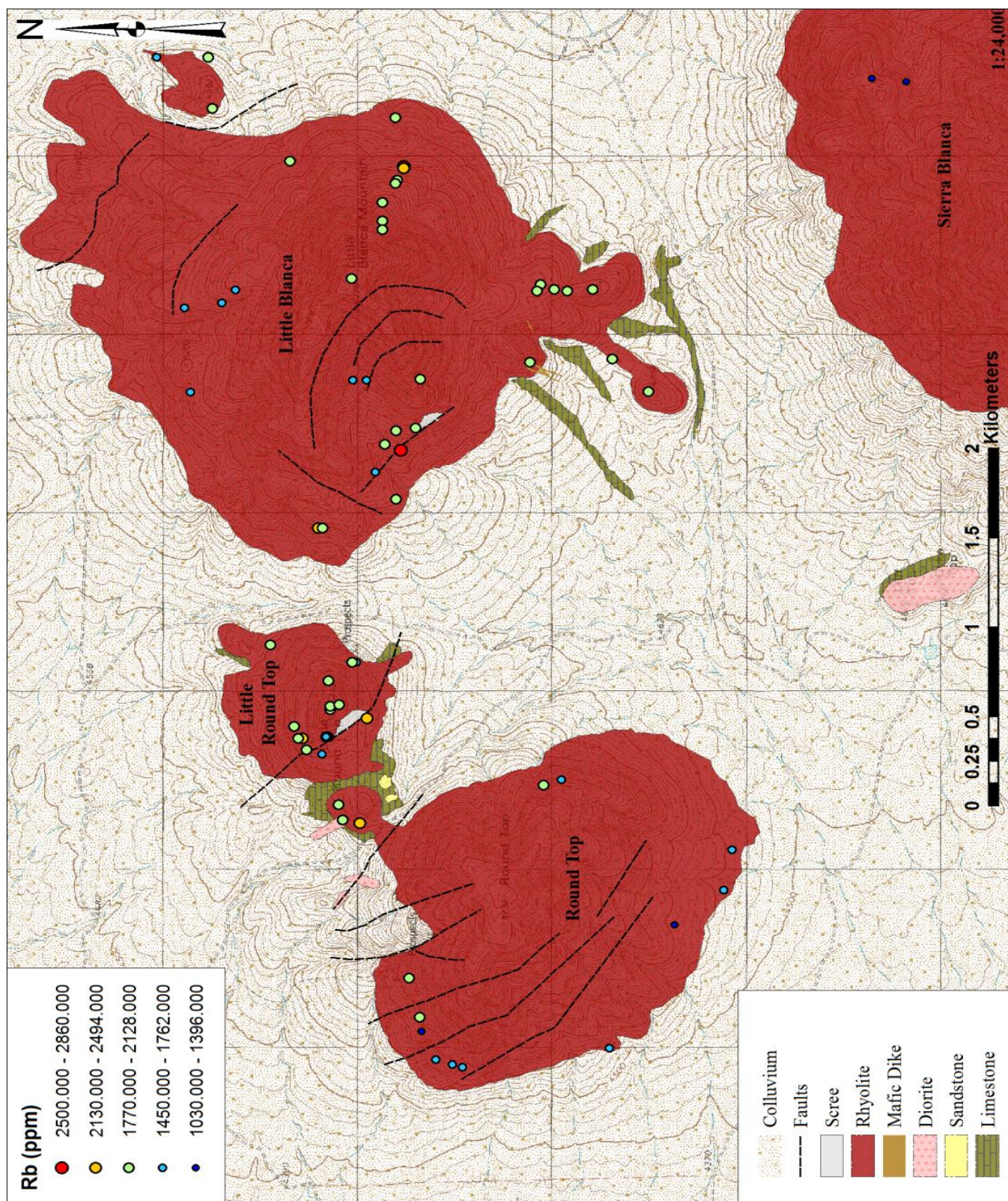
Niobium



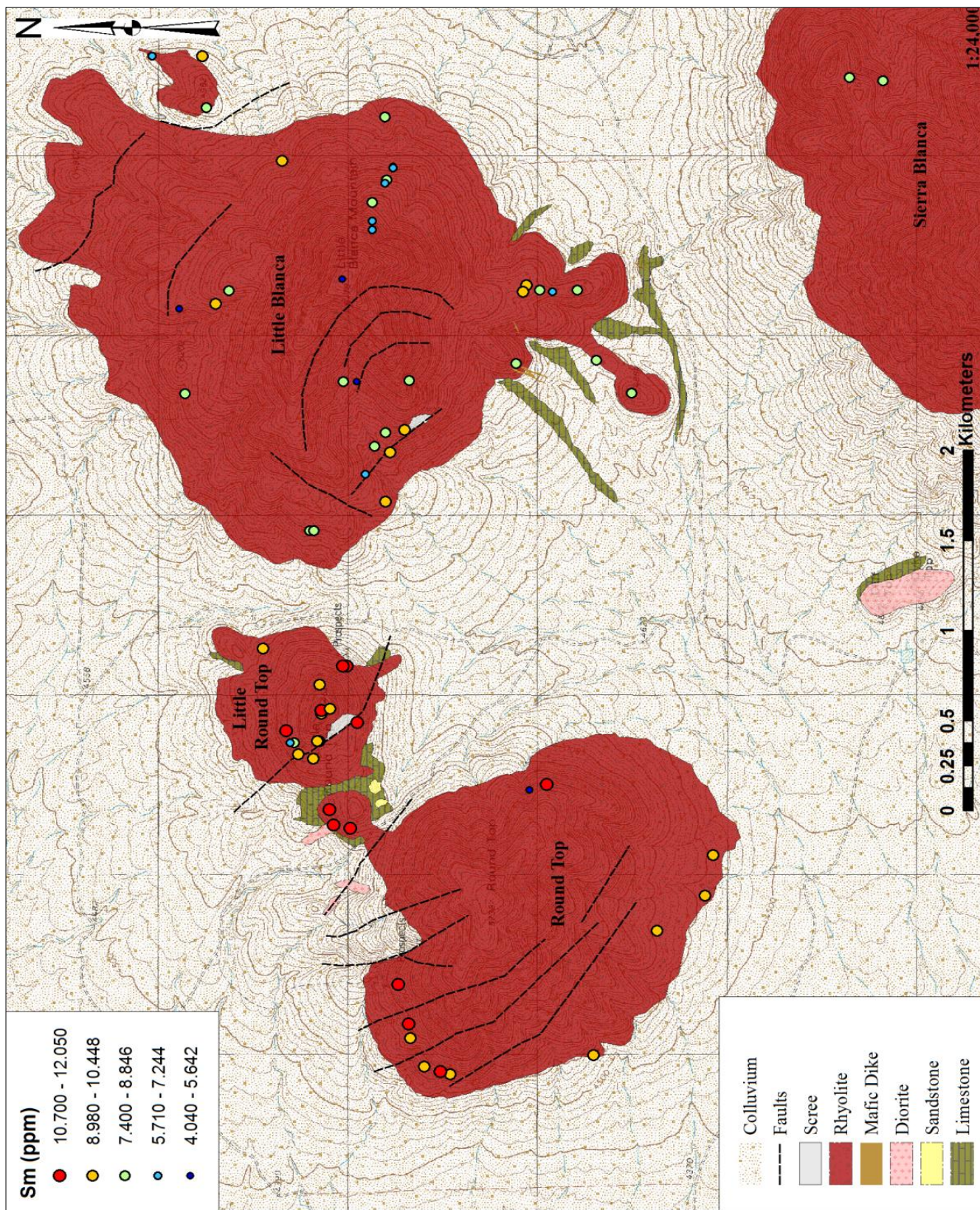
Neodymium



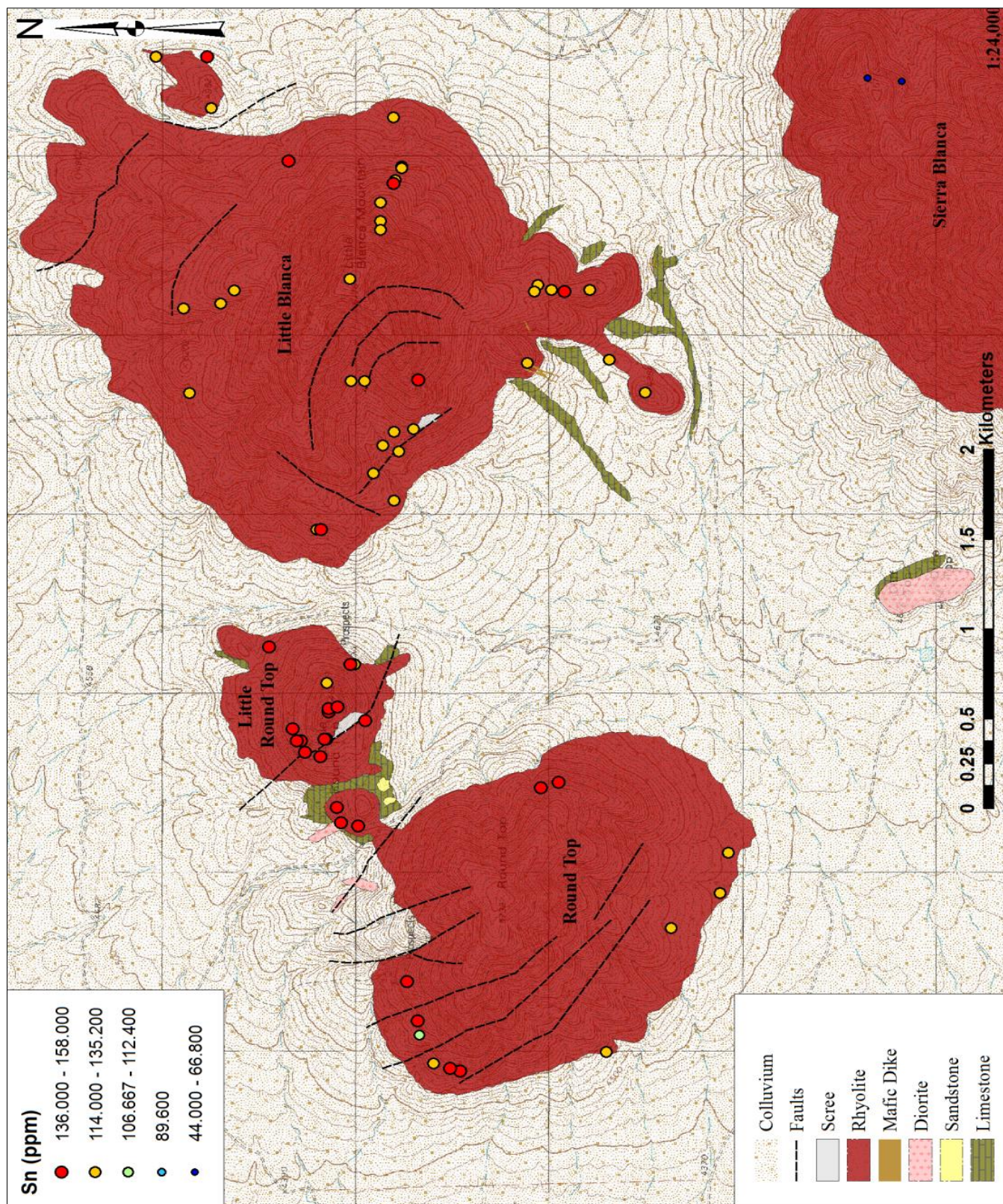
Praseodymium



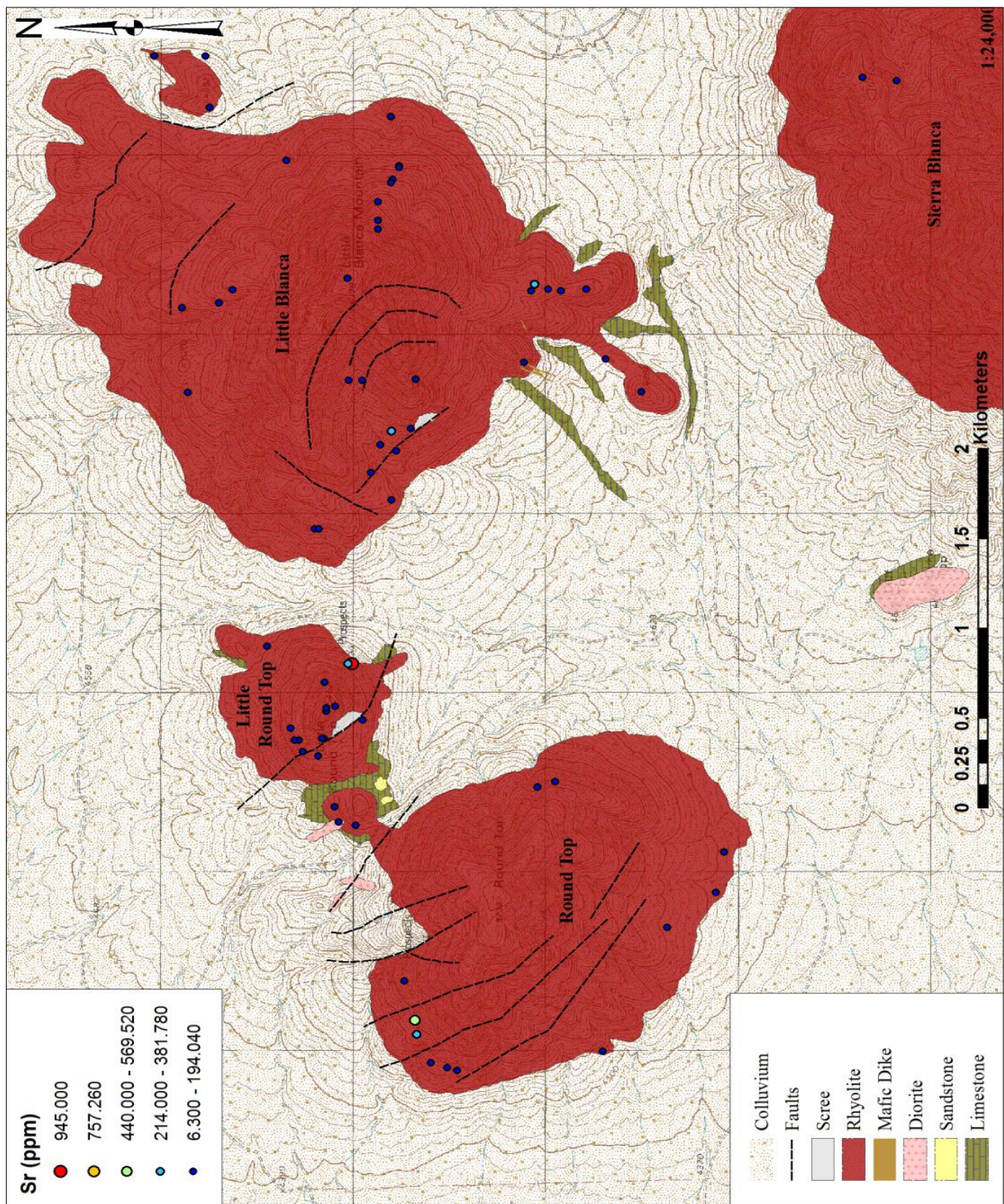
Rubidium



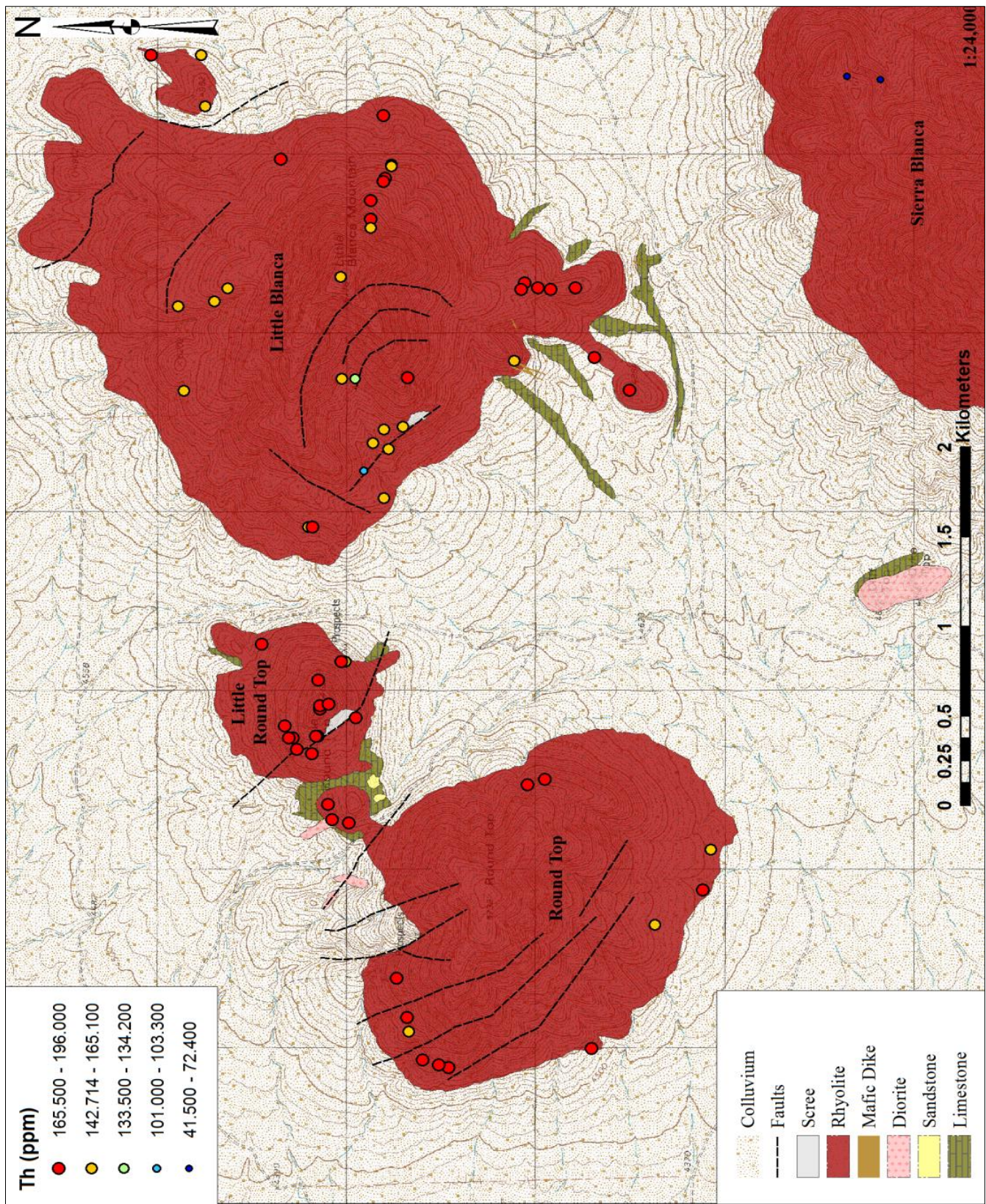
Samarium



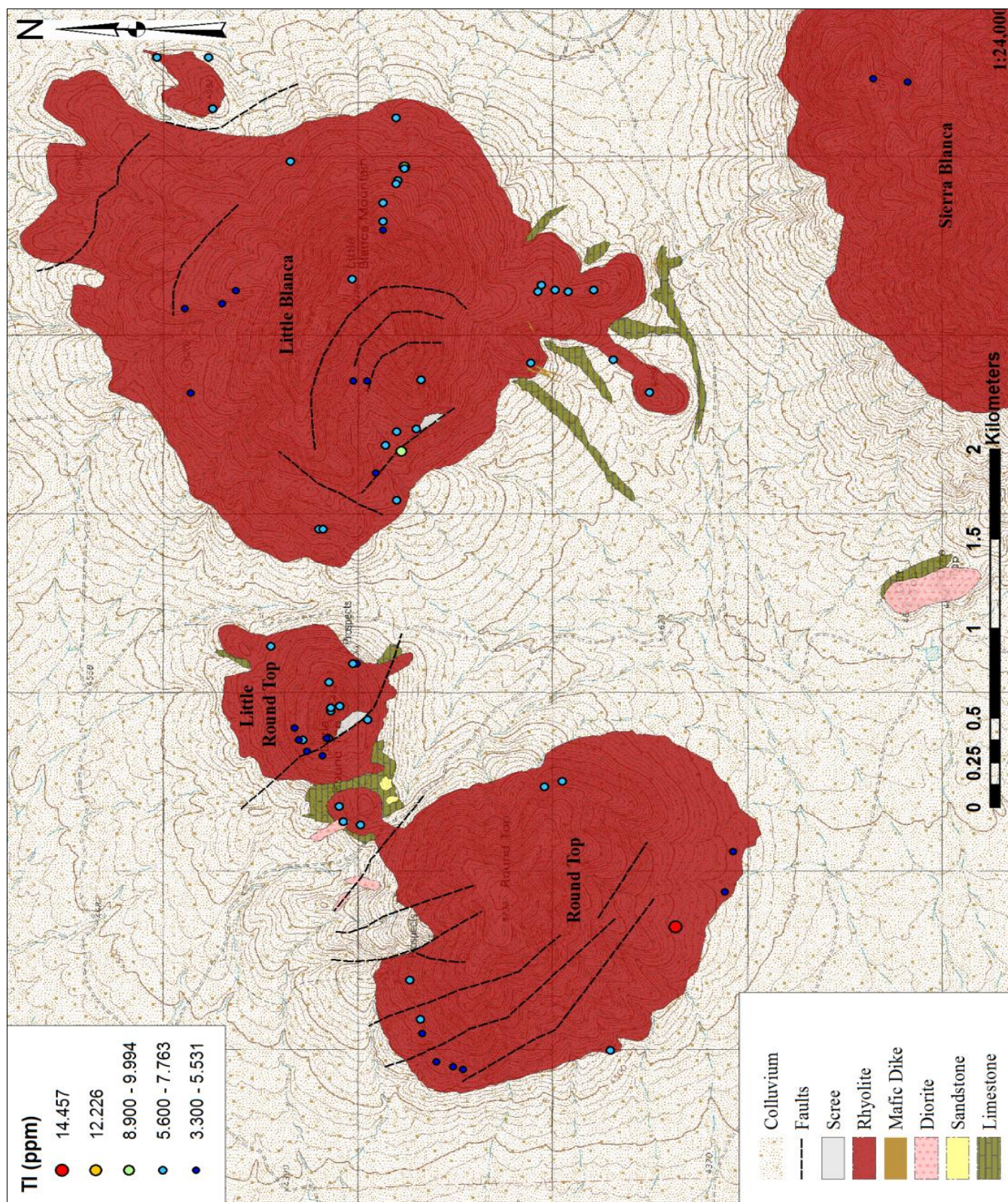
Tin



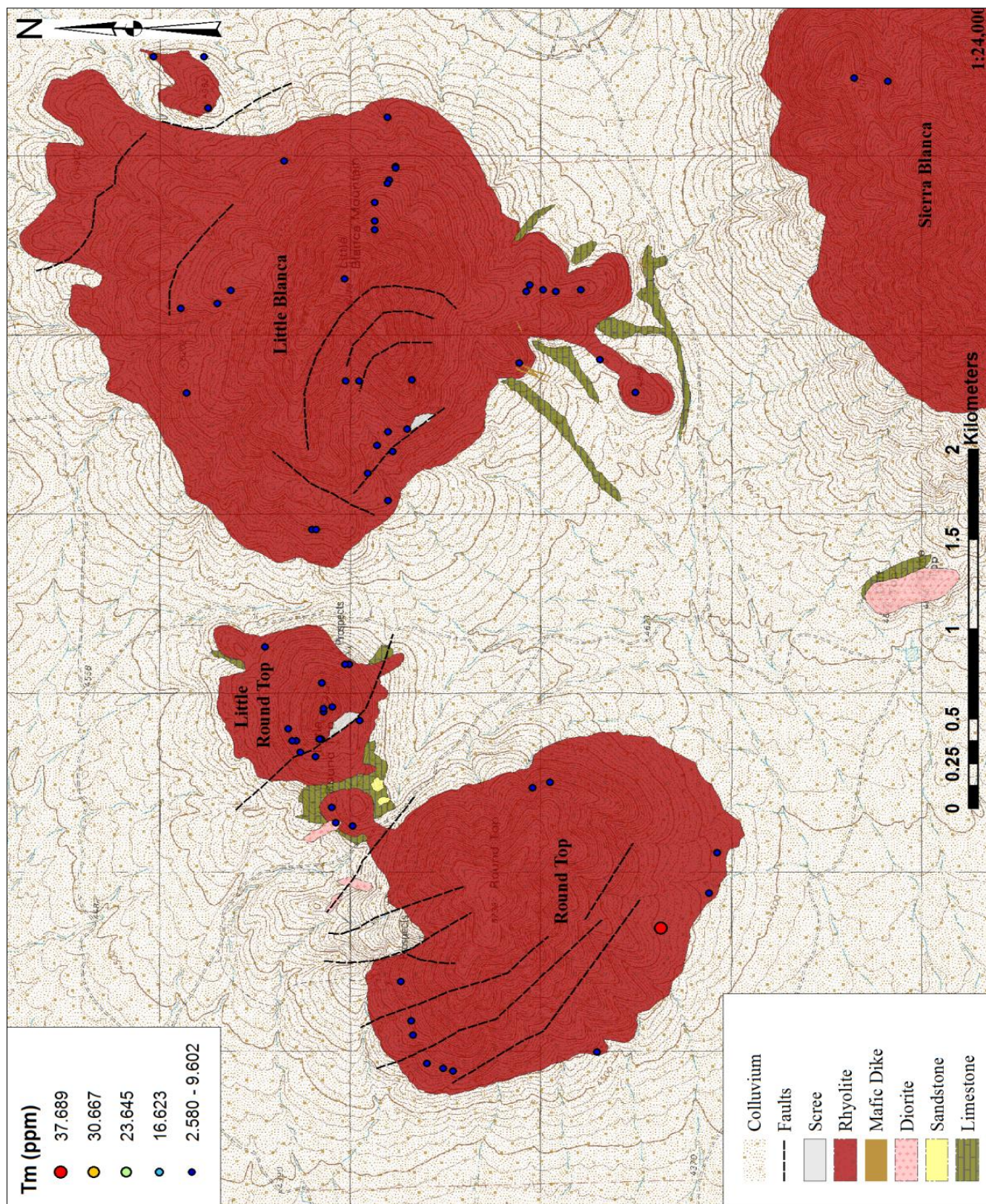
Strontium



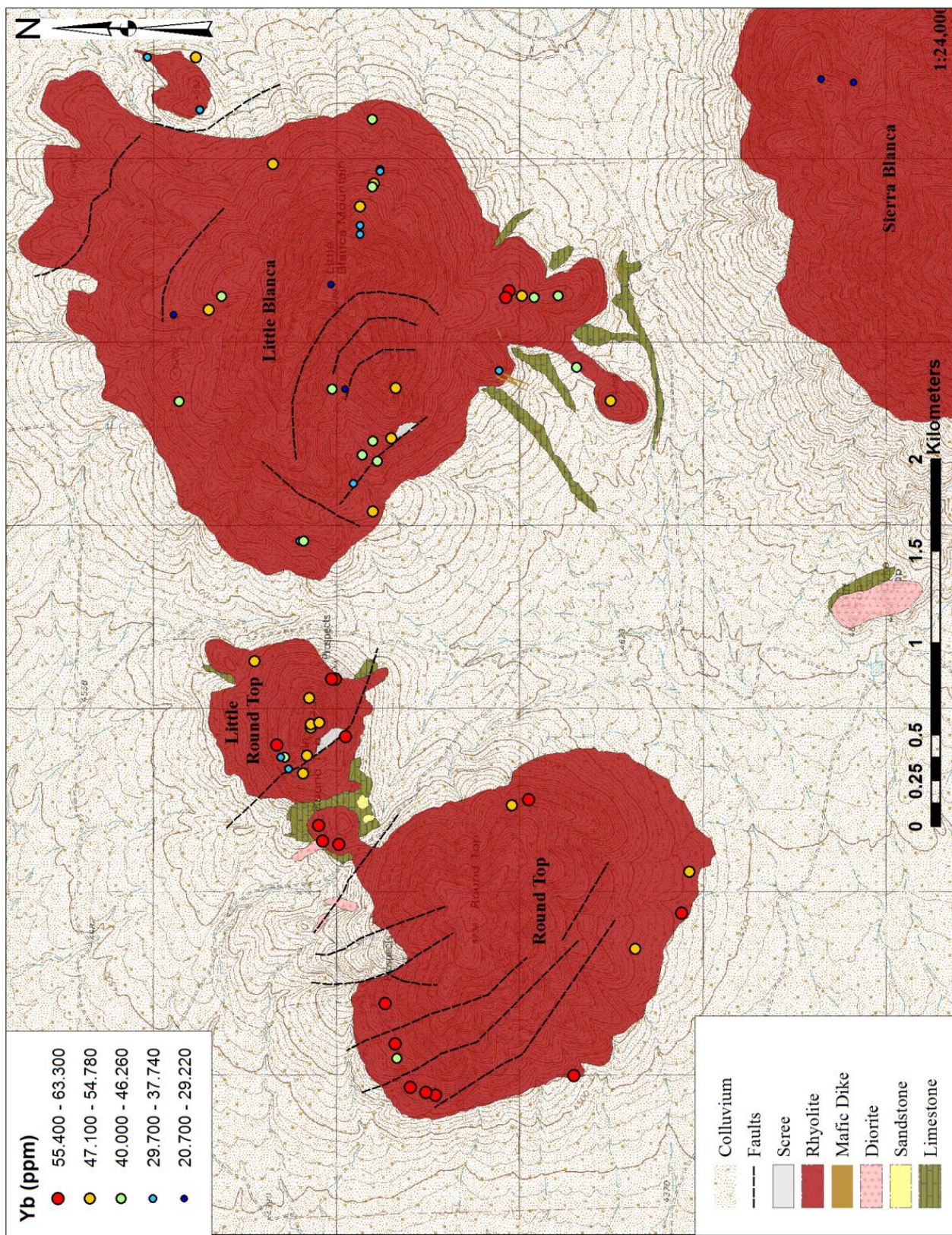
Thorium



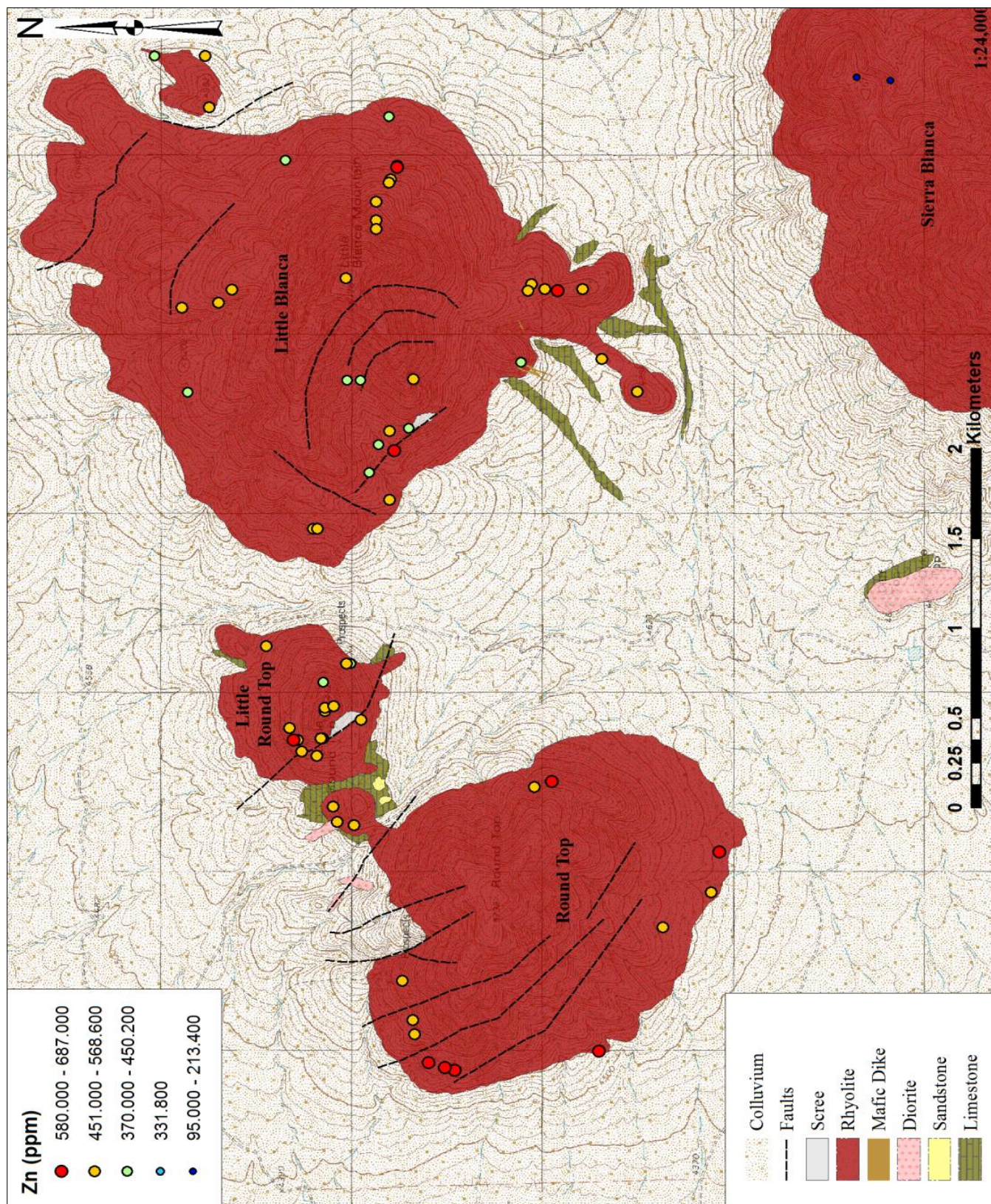
Thallium



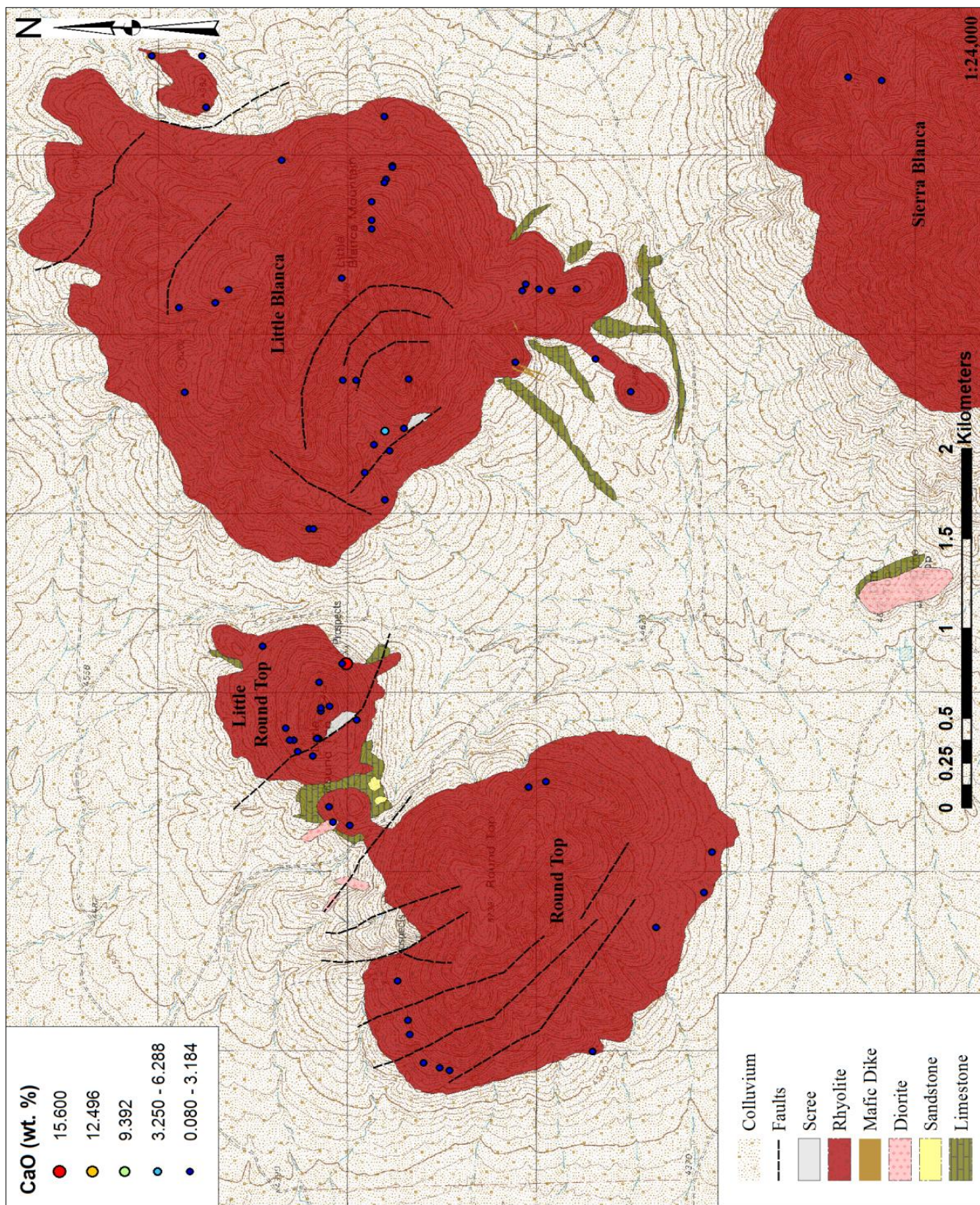
Thulium



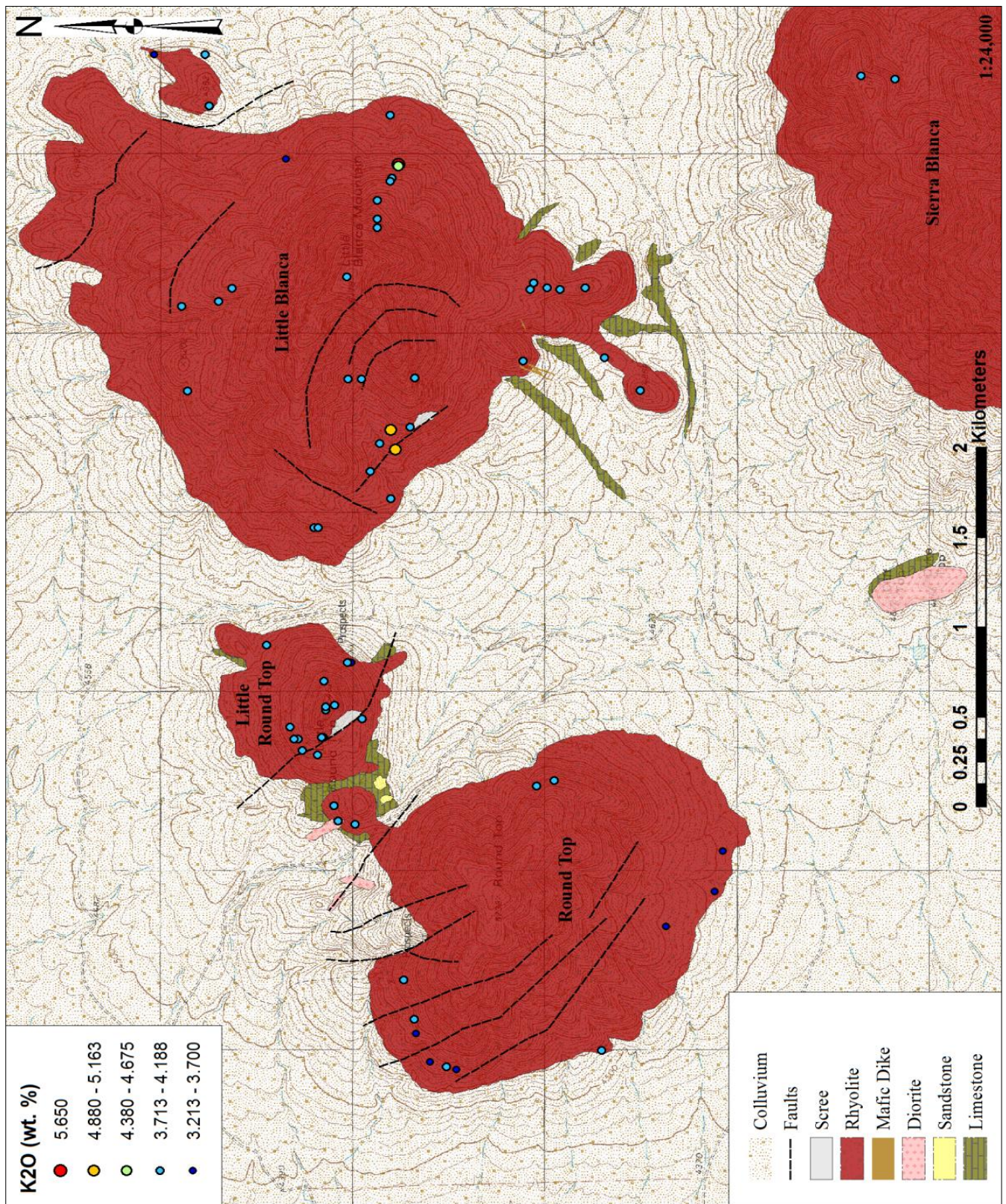
Ytterbium



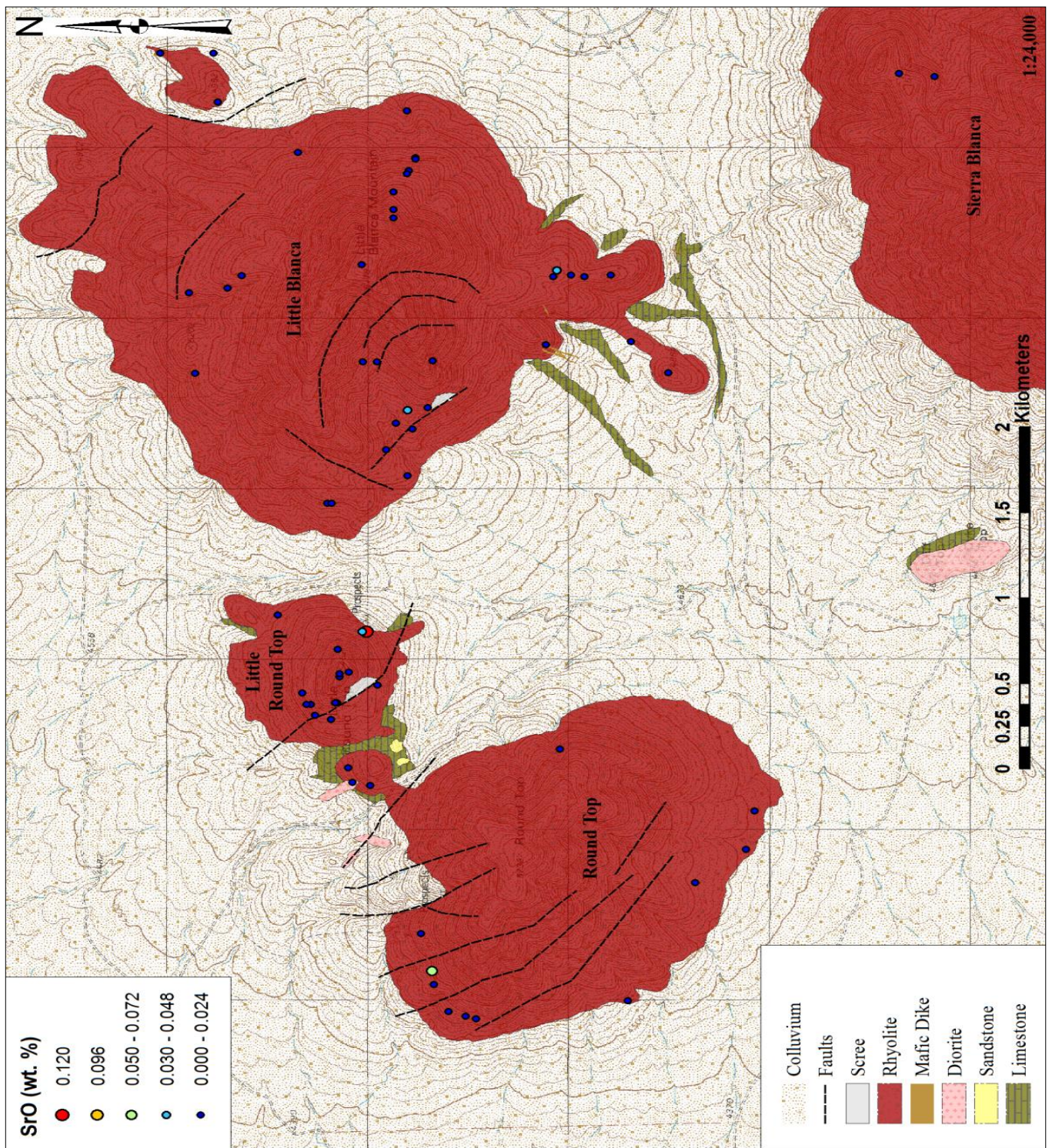
Zinc



Calcium Oxide



Potassium Oxide



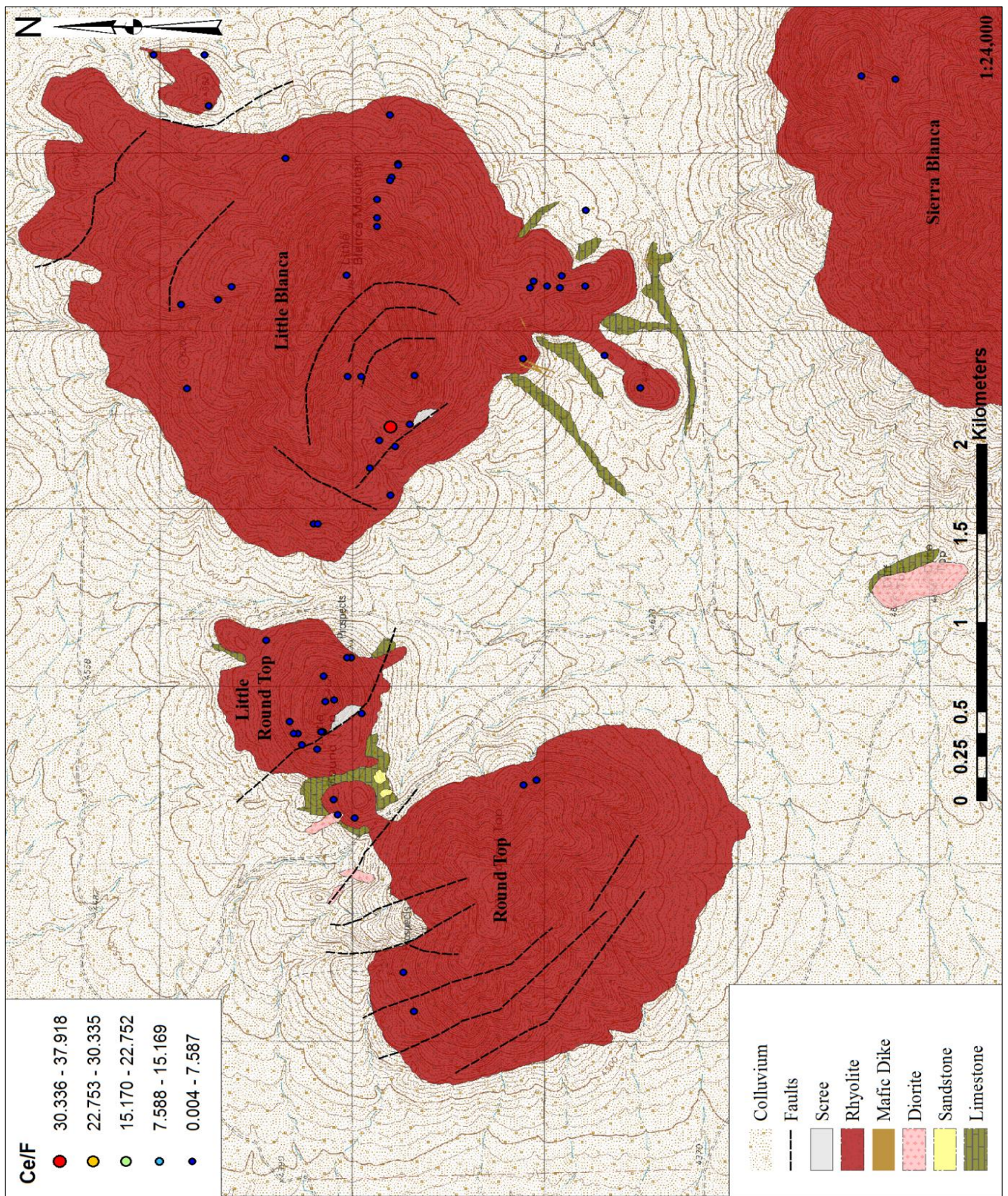
Strontium Oxide

APPENDIX IV: RATIO MAPS

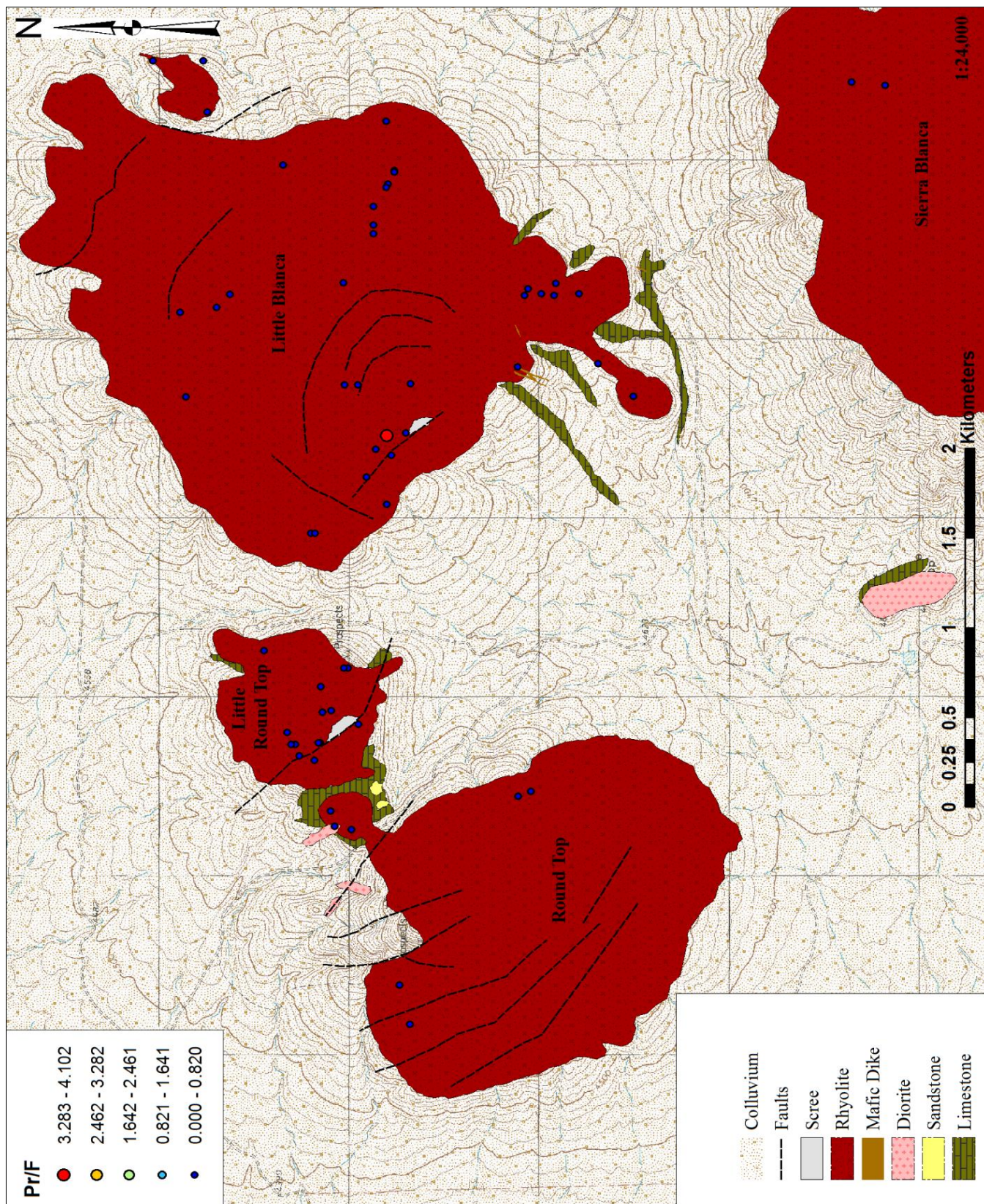
Ratio Maps



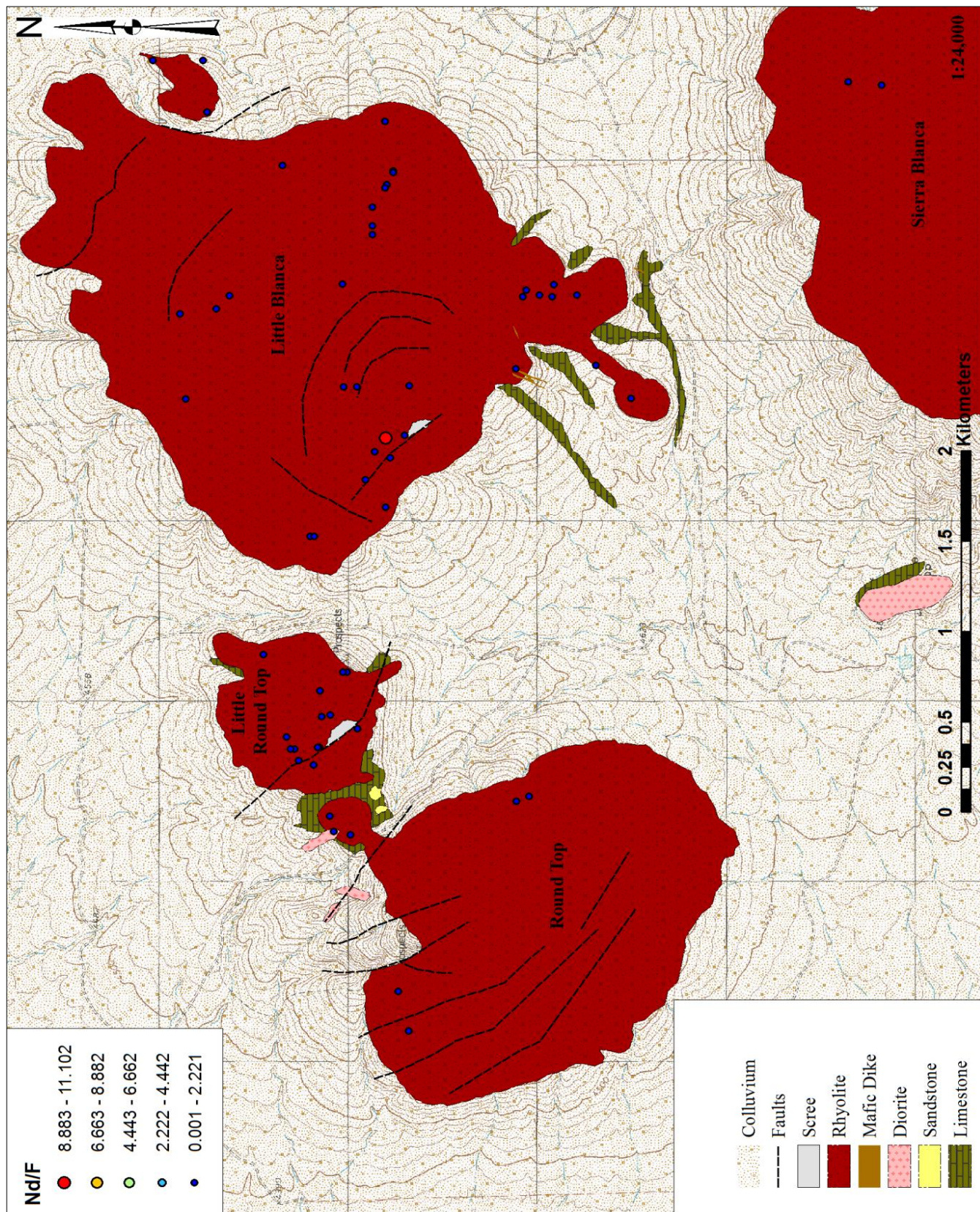
La/F



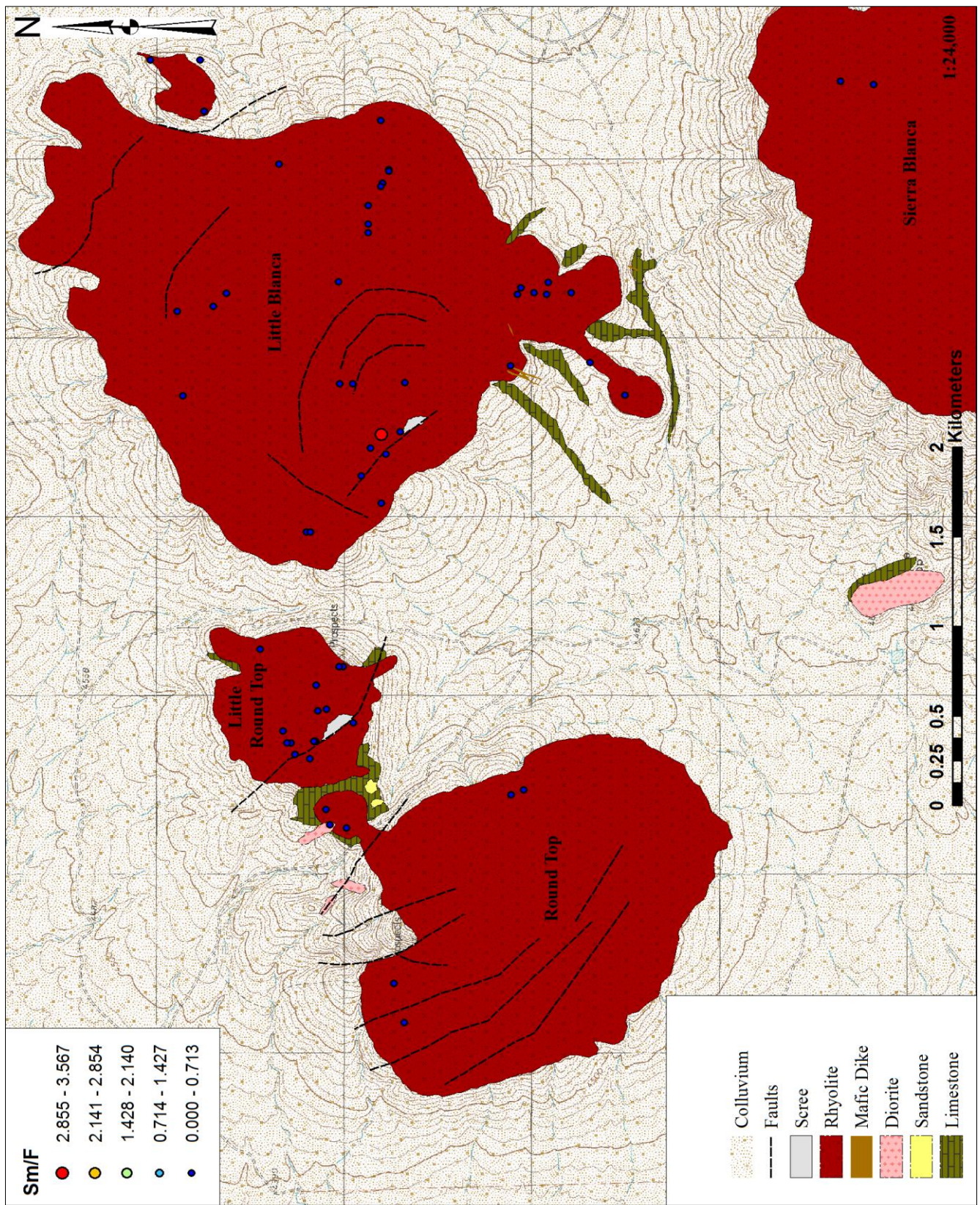
Ce/F



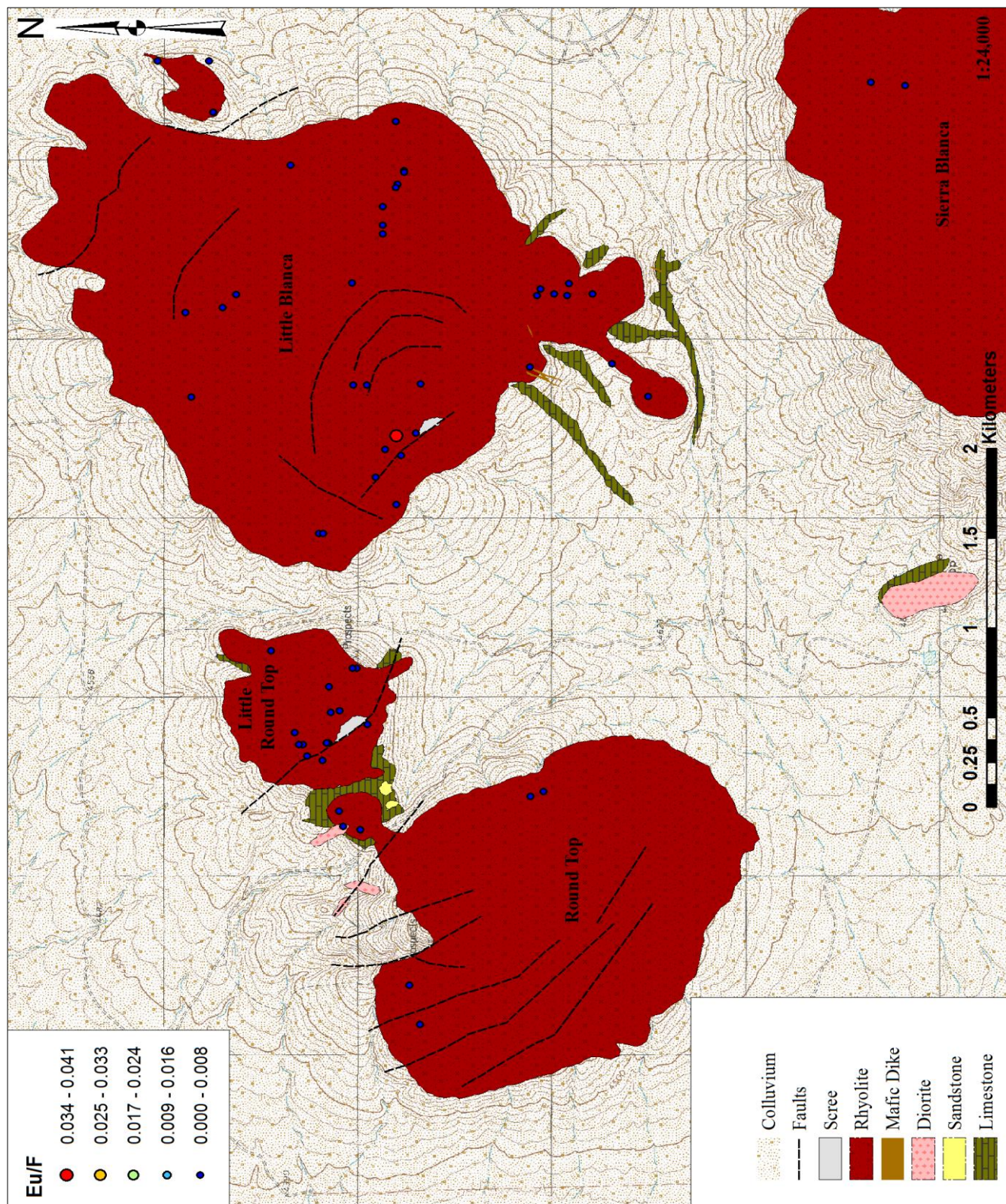
Pr/F



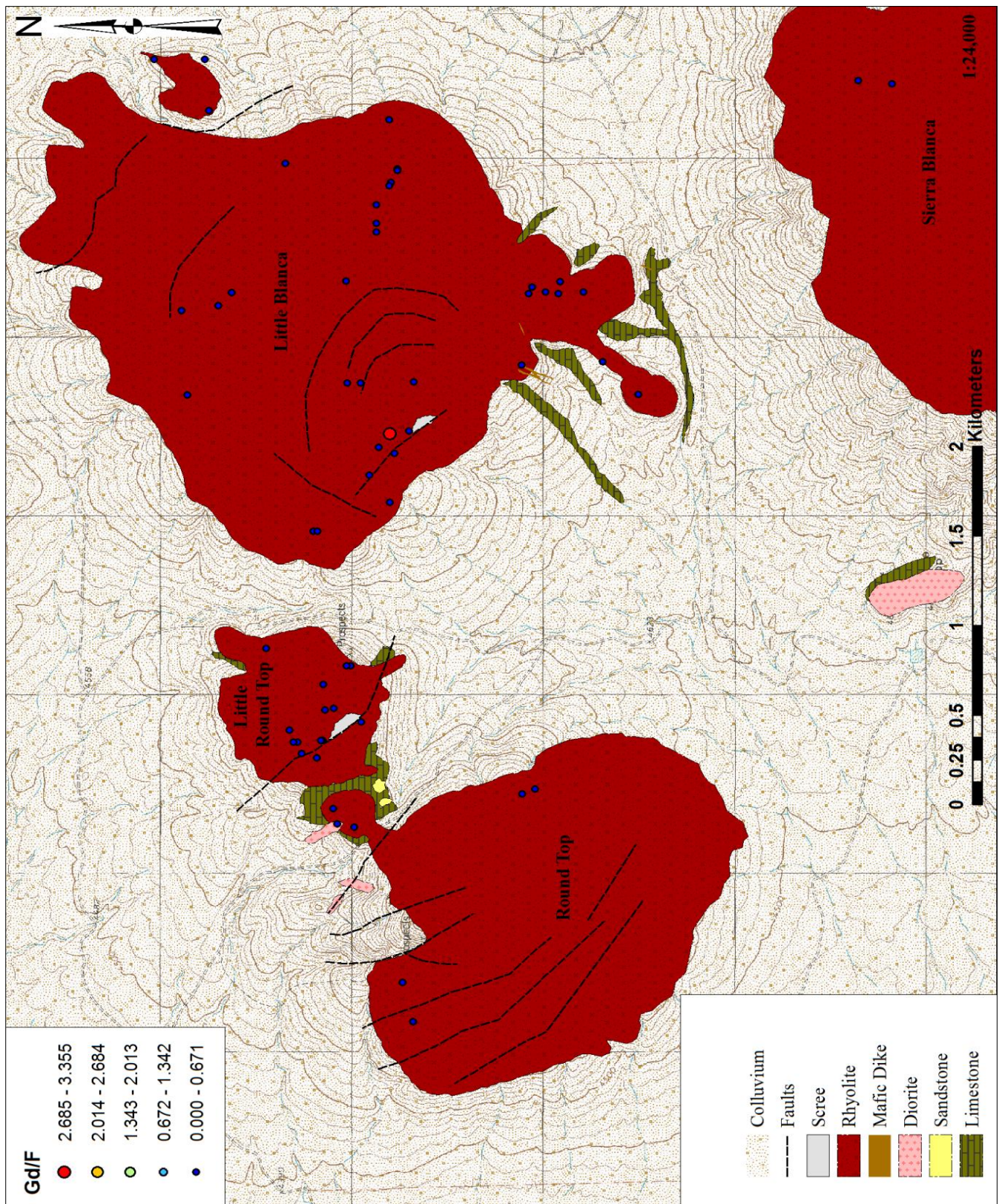
Nd/F



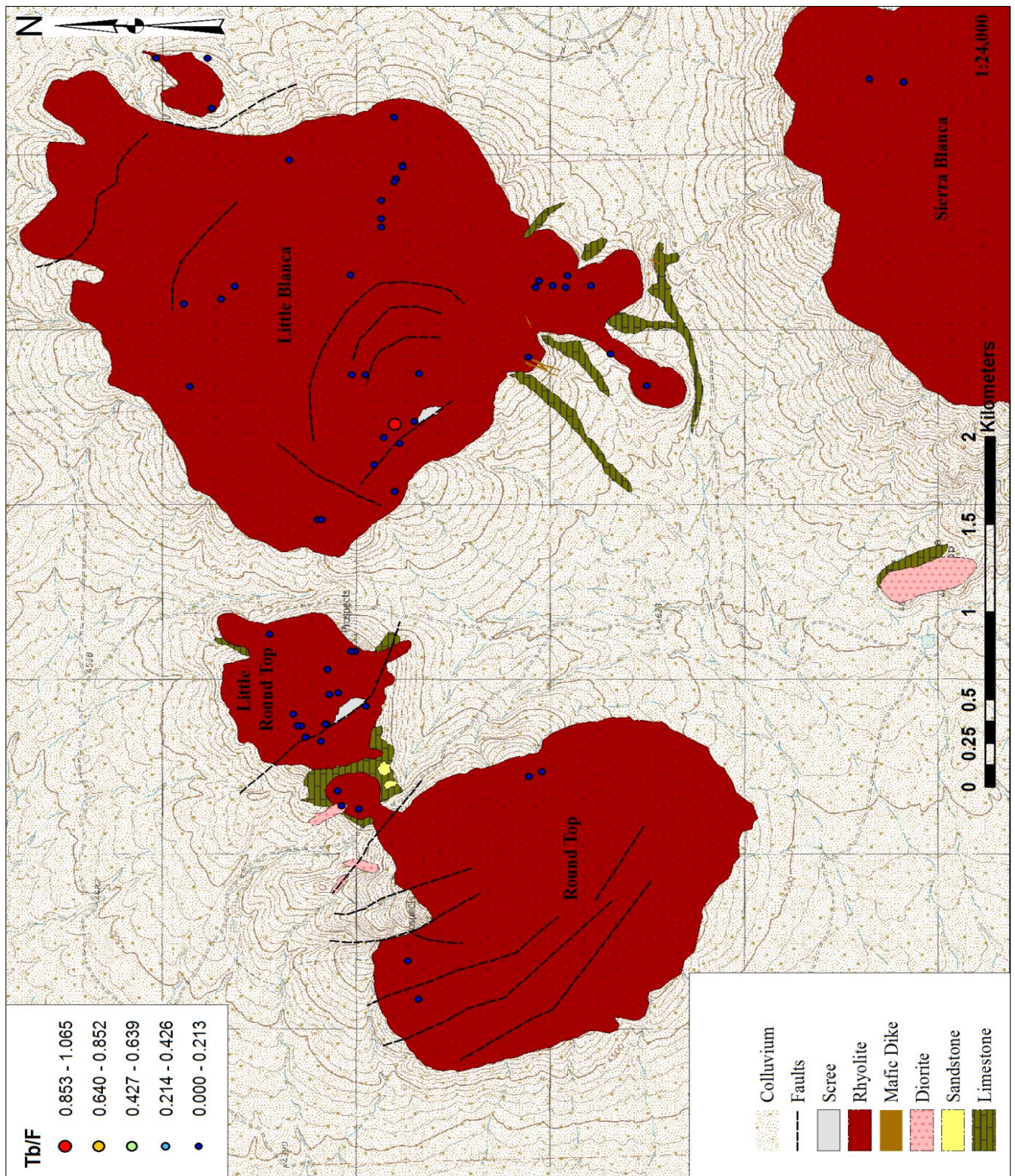
Sm/F



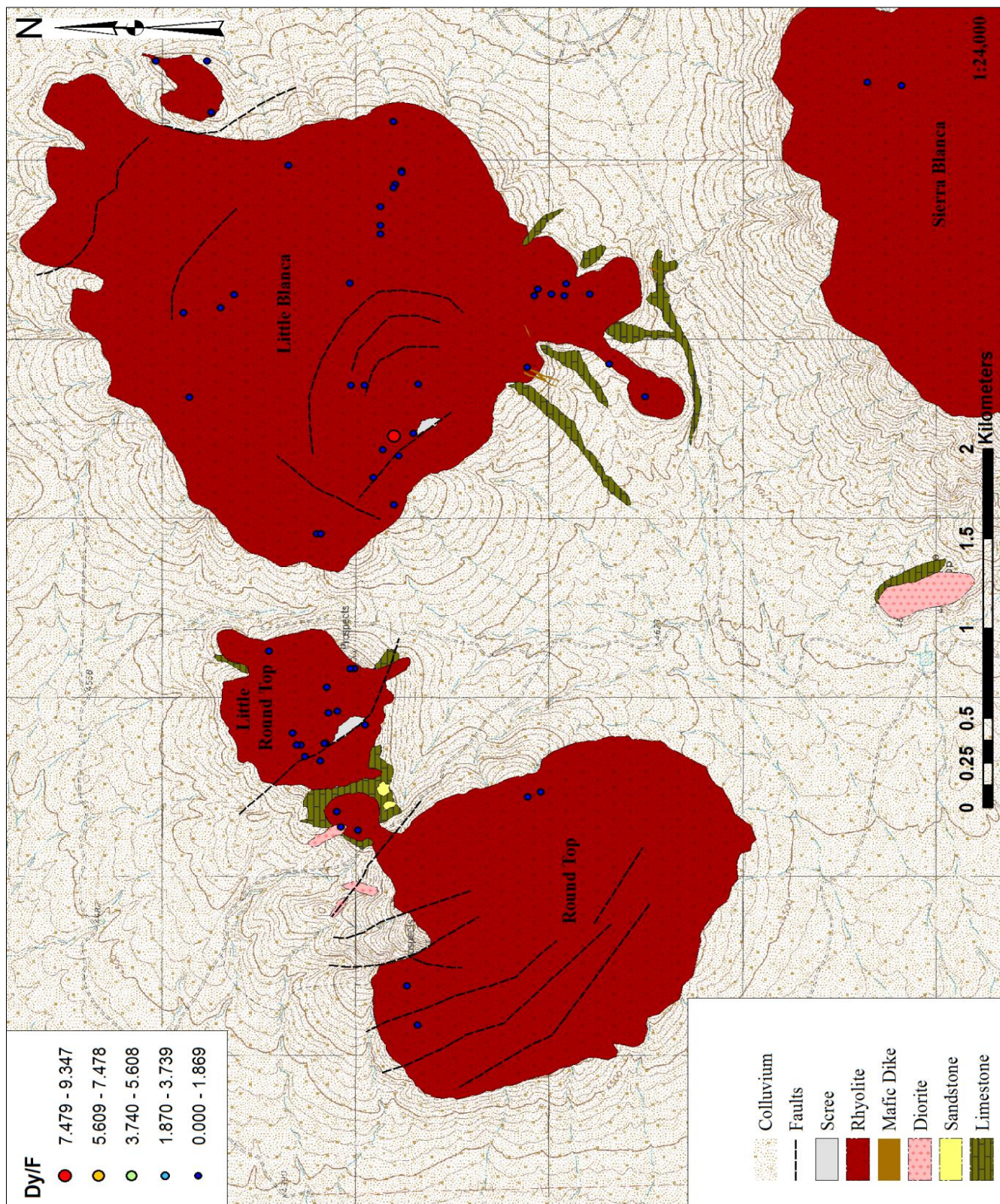
Eu/F



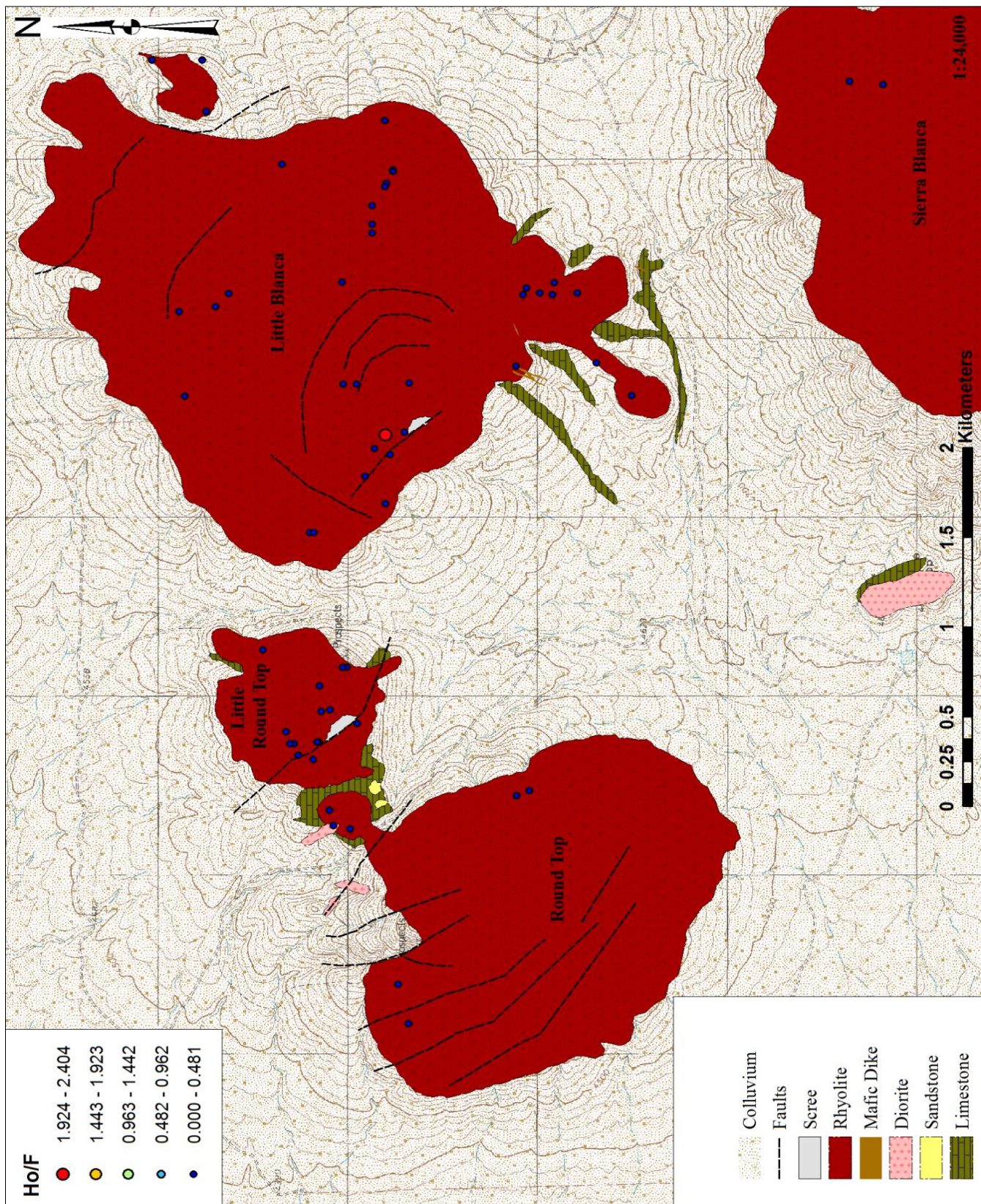
Gd/F



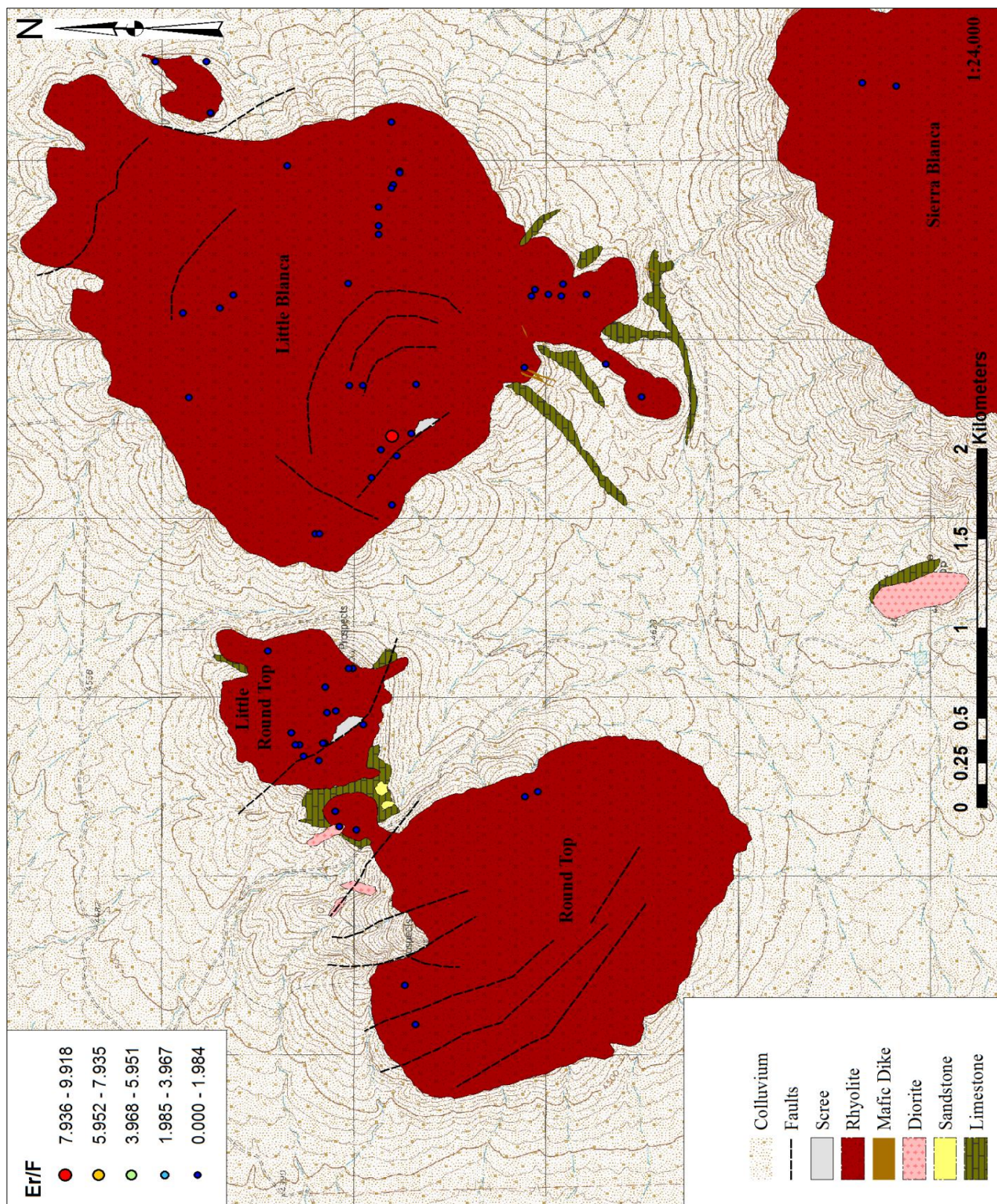
Tb/F



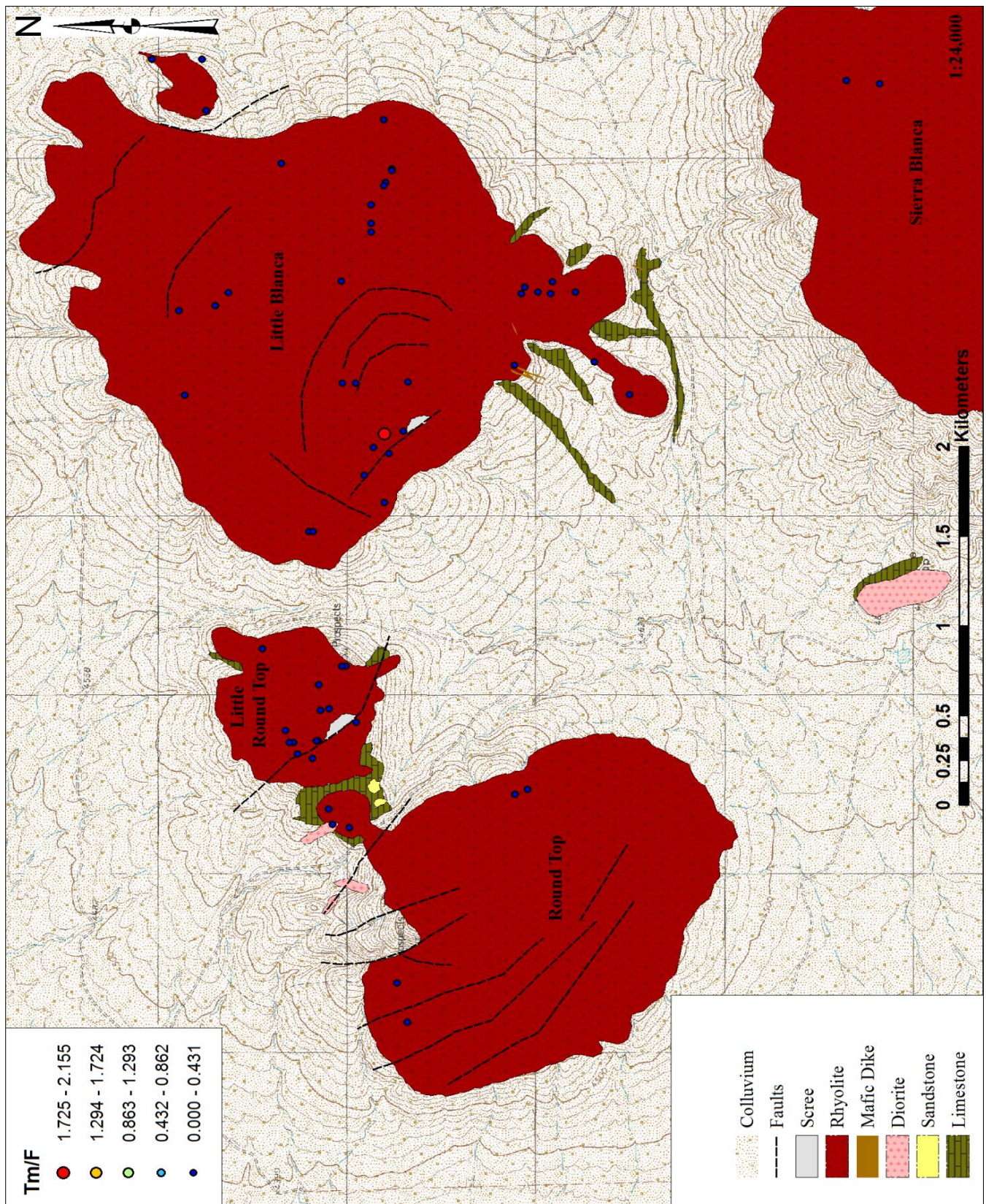
Dy/F



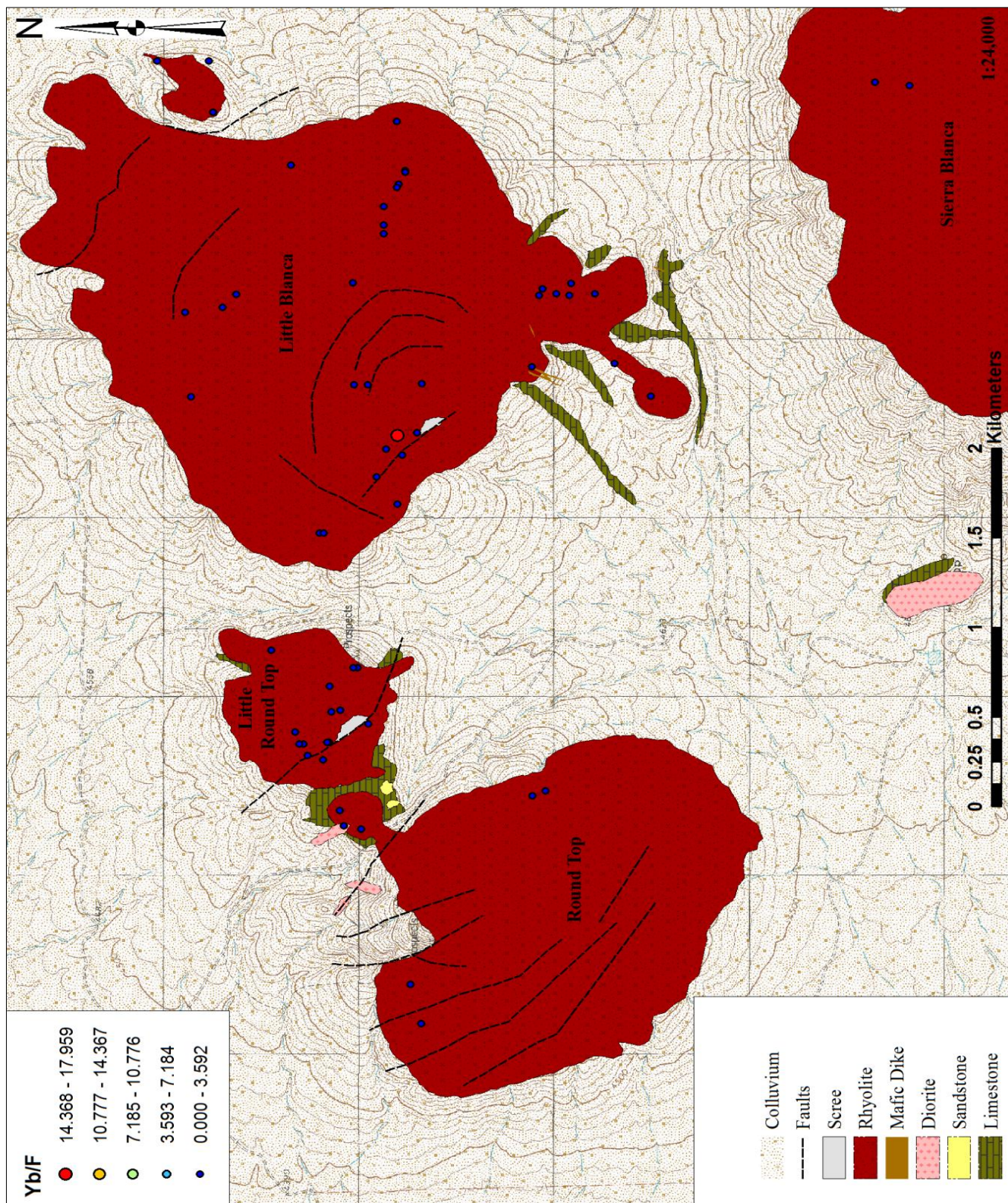
Ho/F



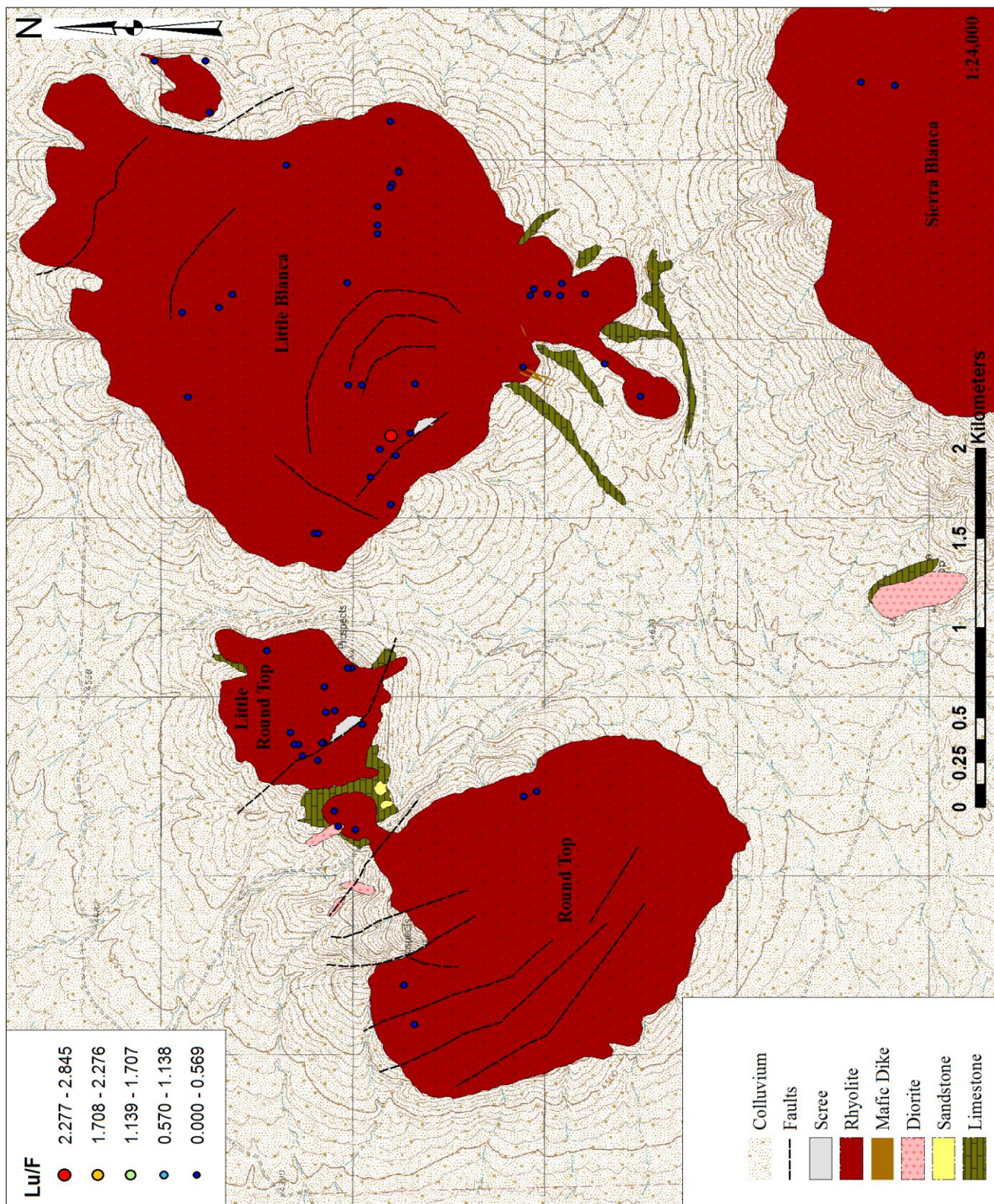
Er/F



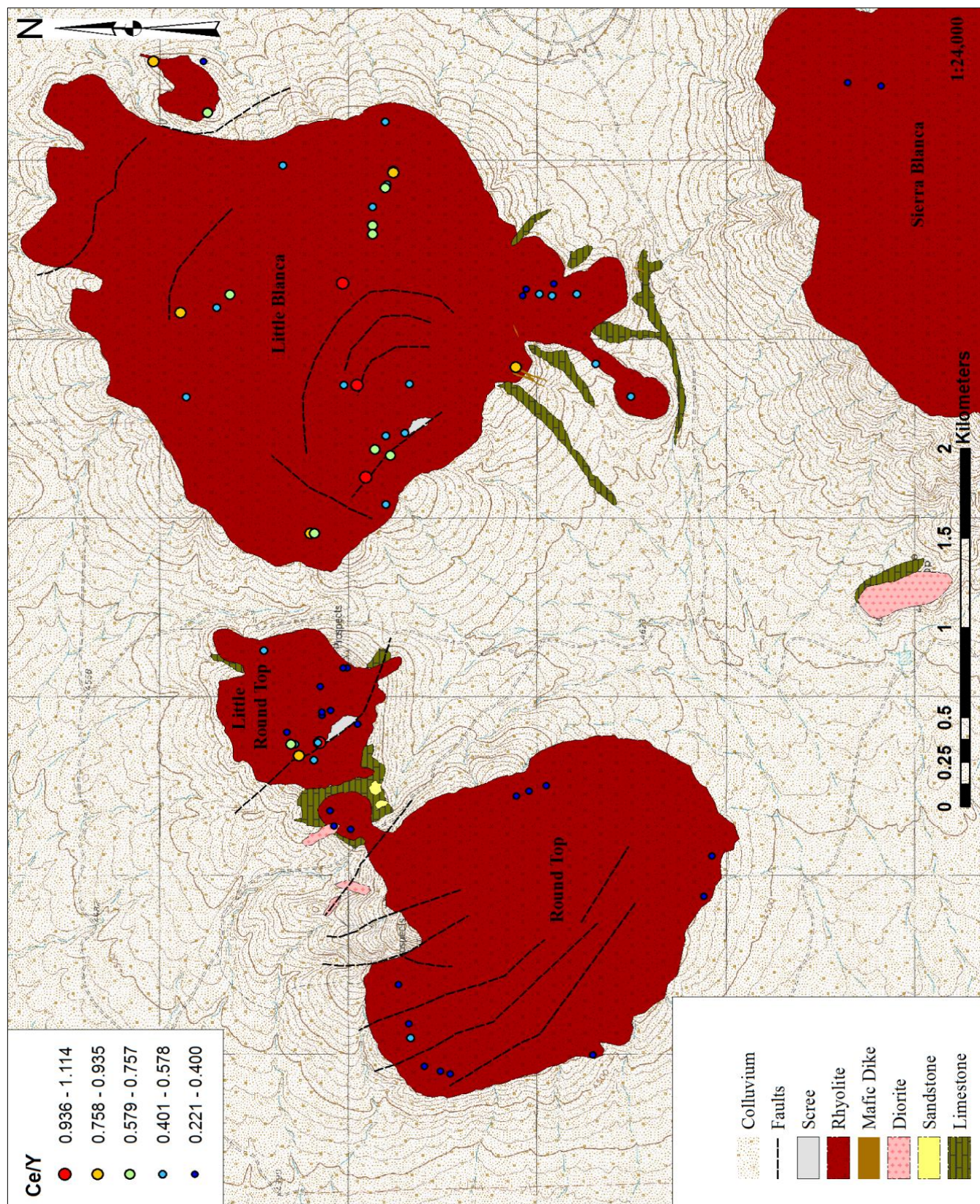
Tm/F



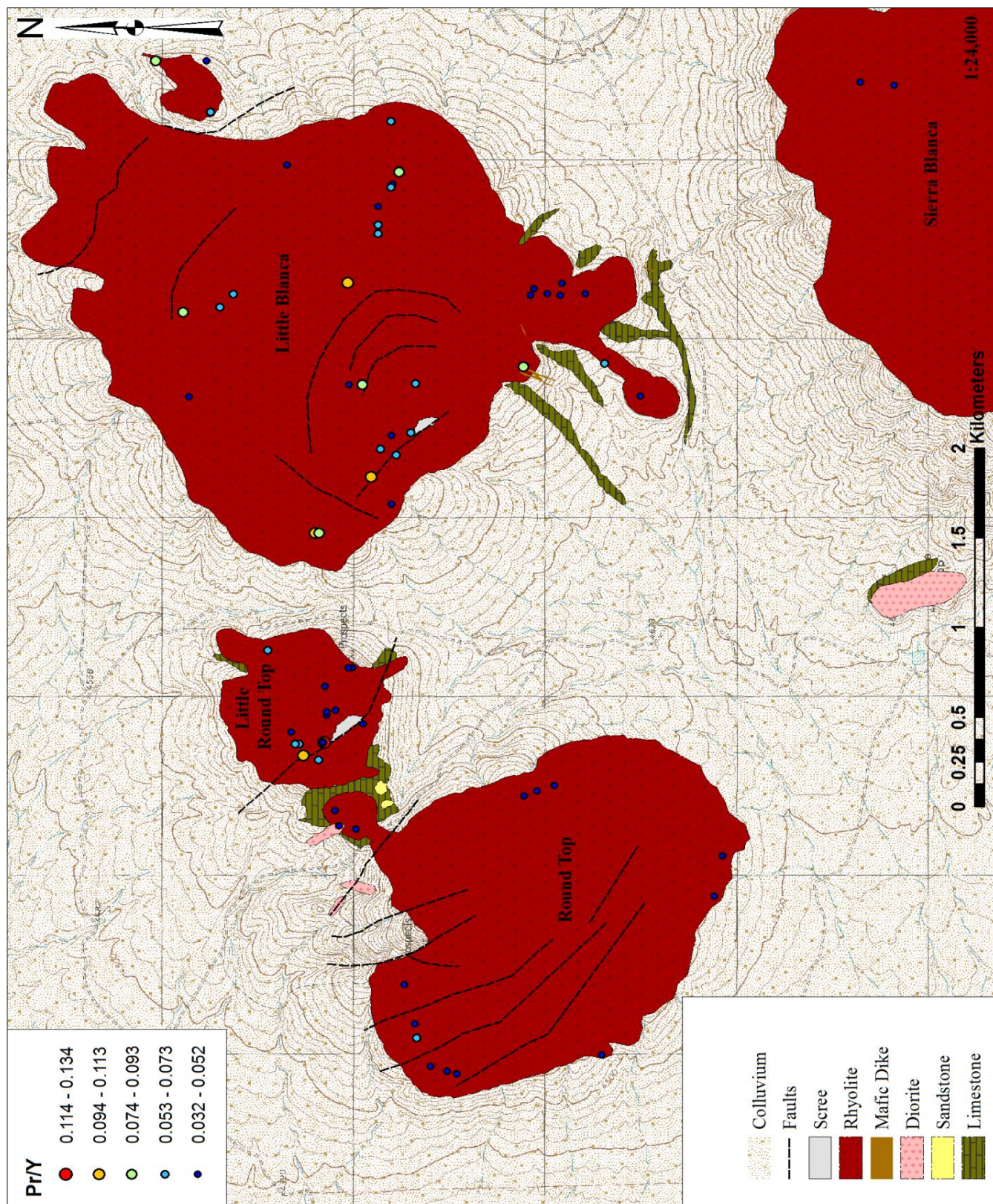
Yb/F



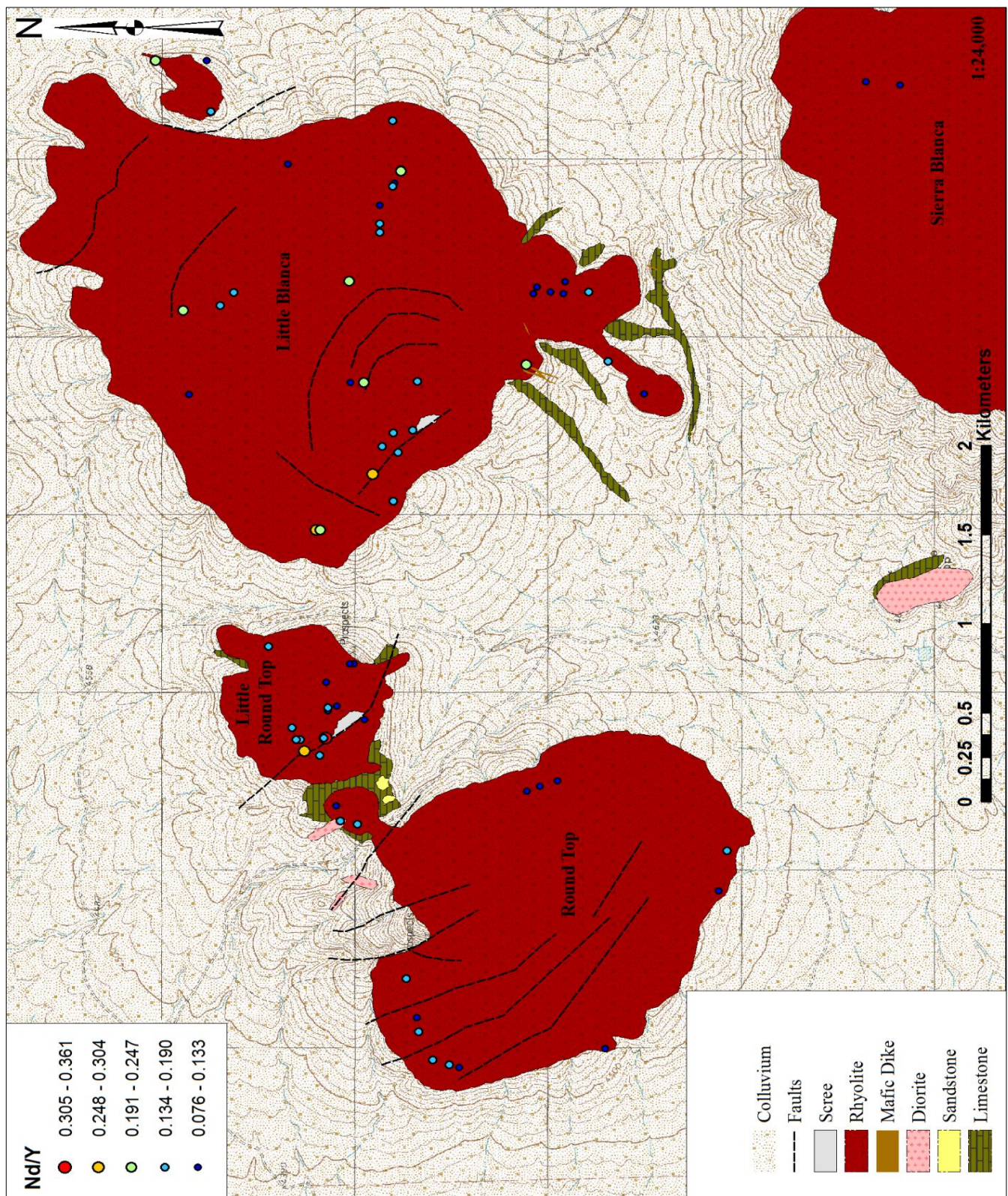
Lu/F



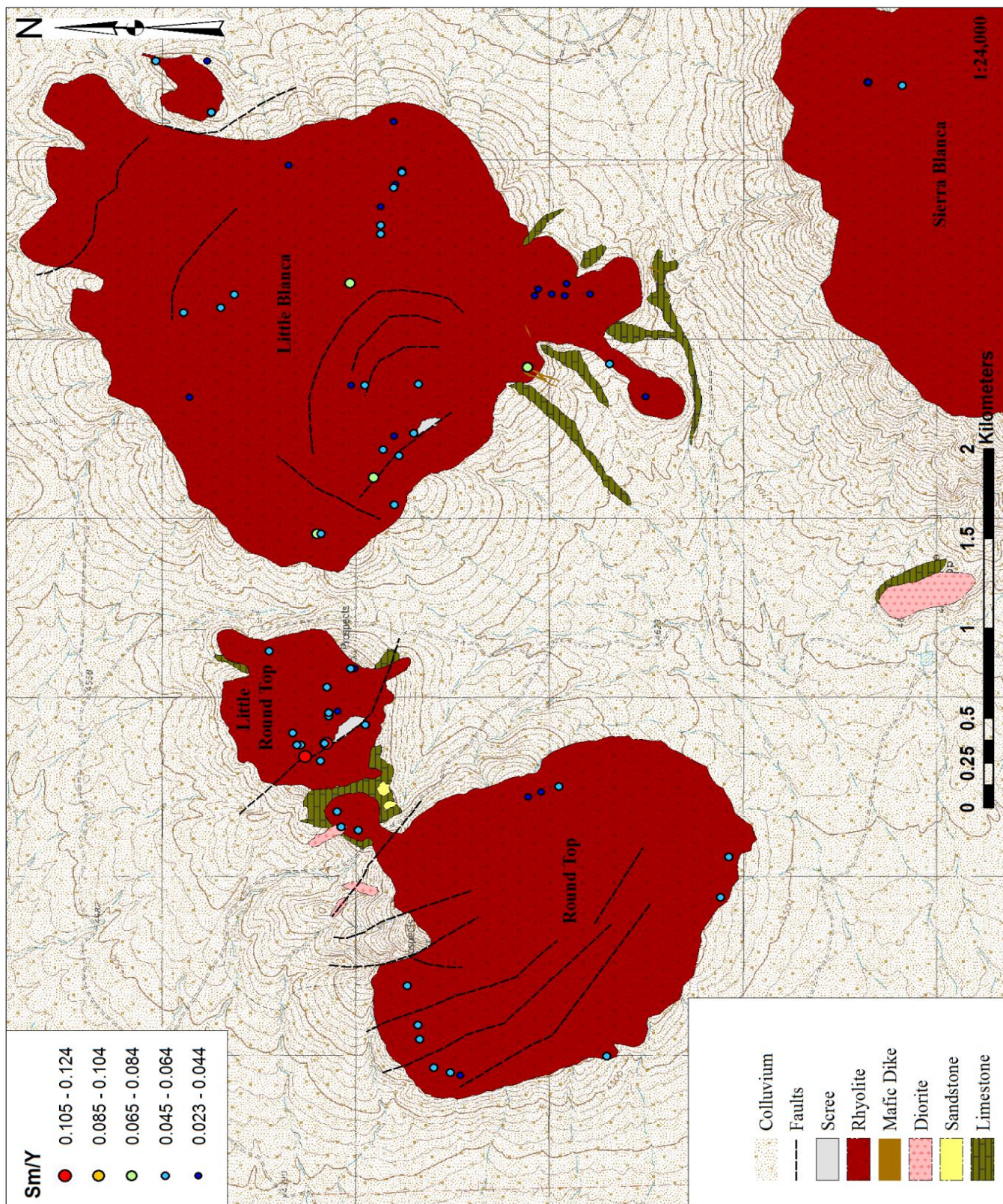
Ce/Y



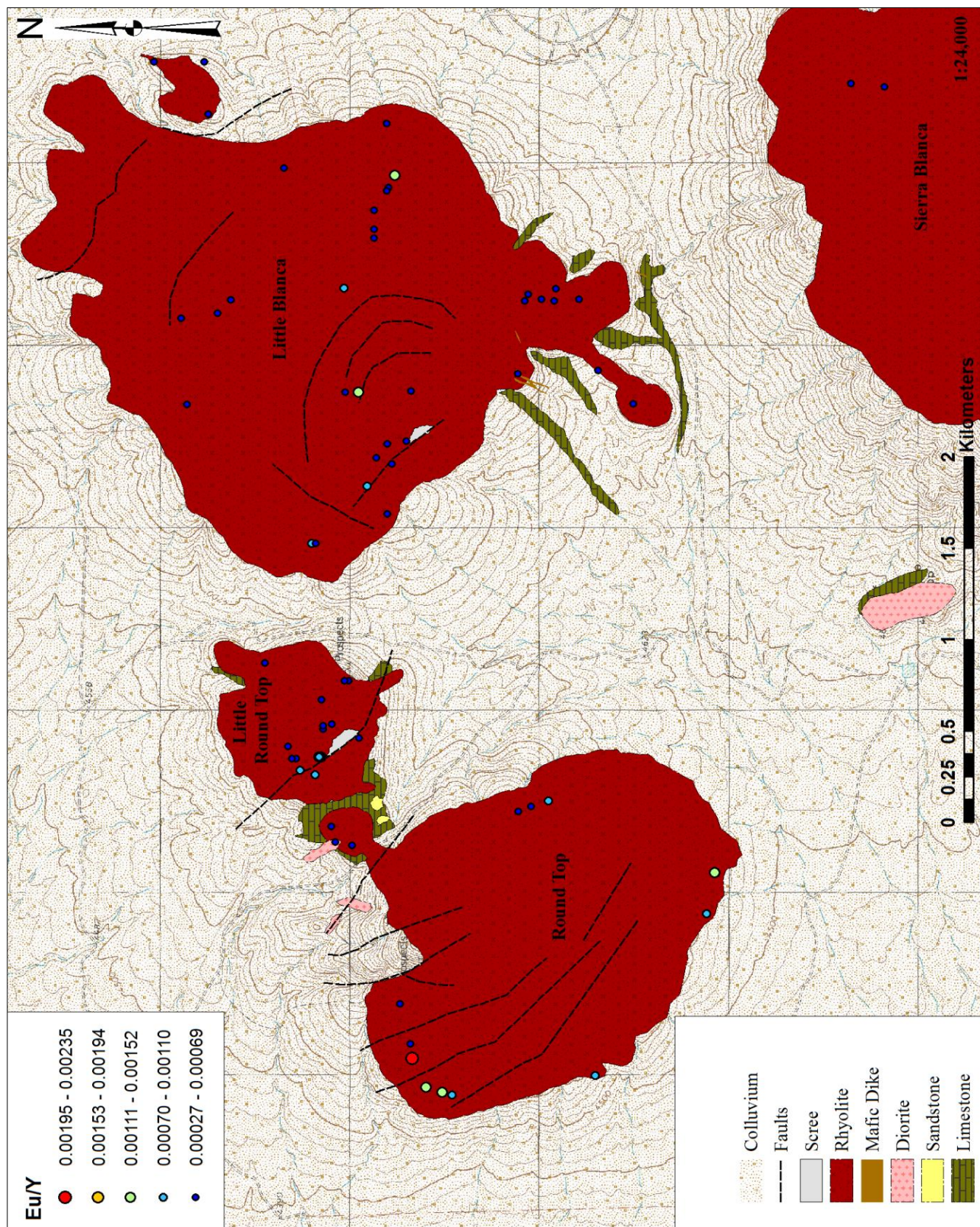
Pr/Y



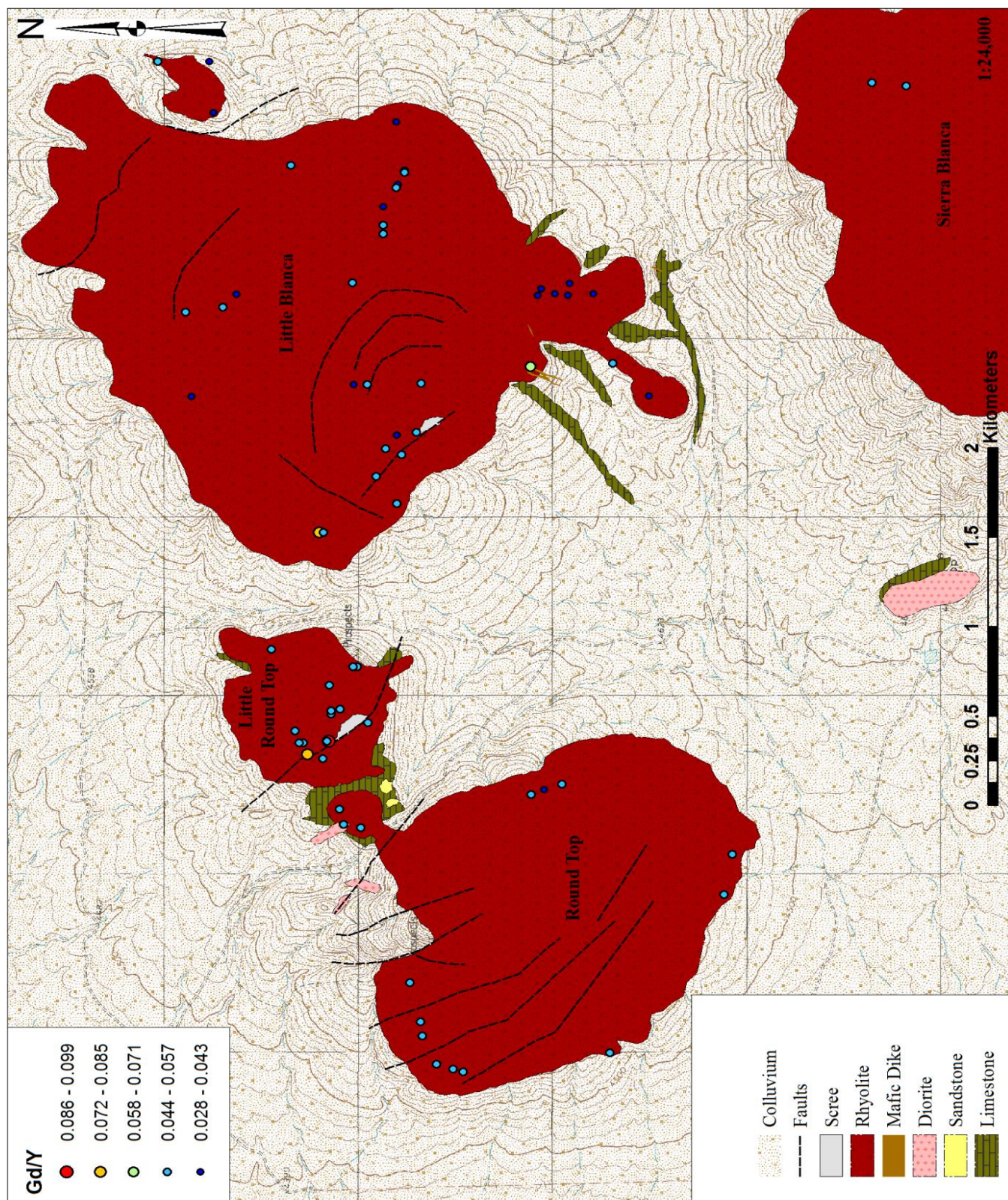
Nd/Y



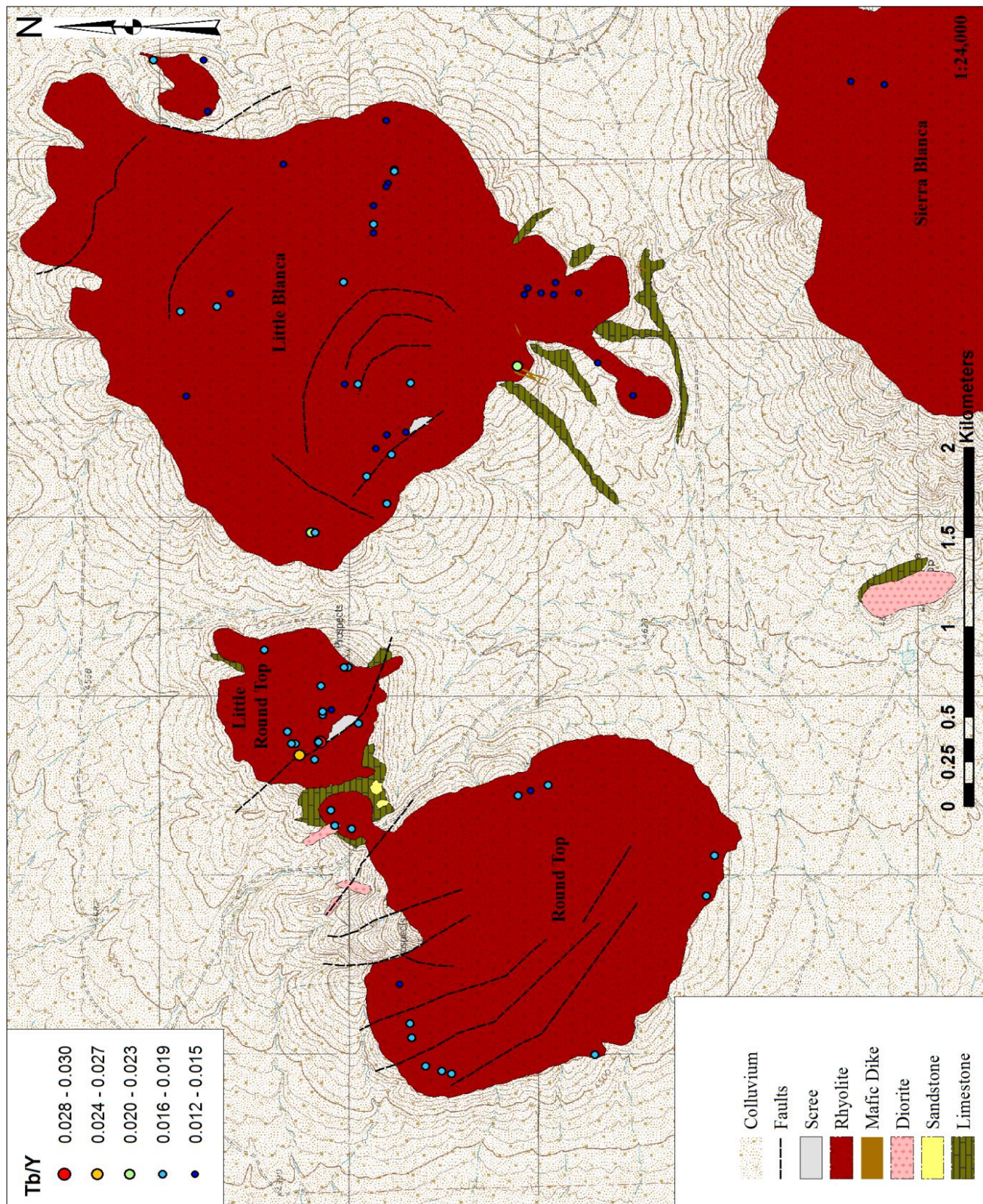
Sm/Y



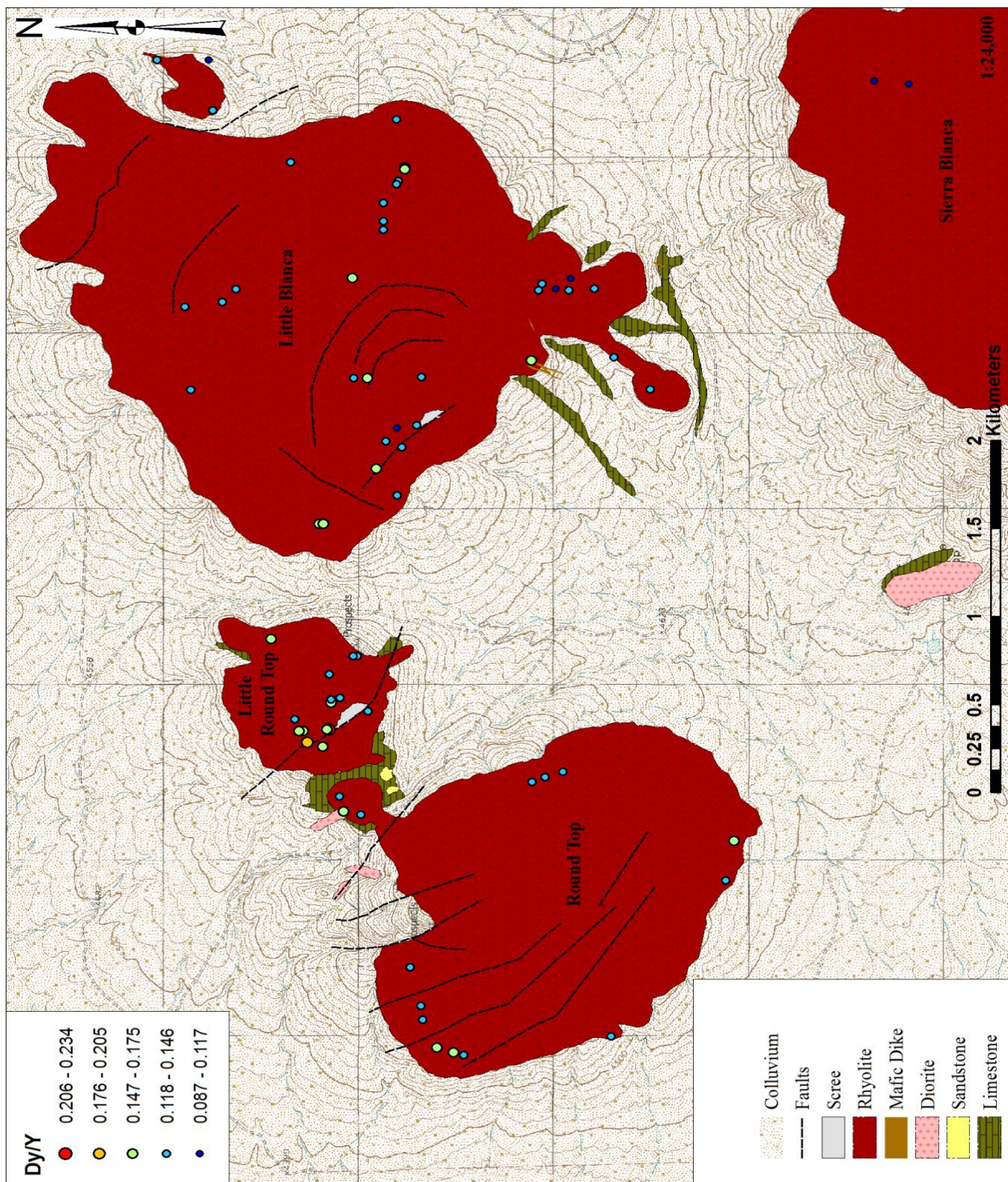
Eu/Y



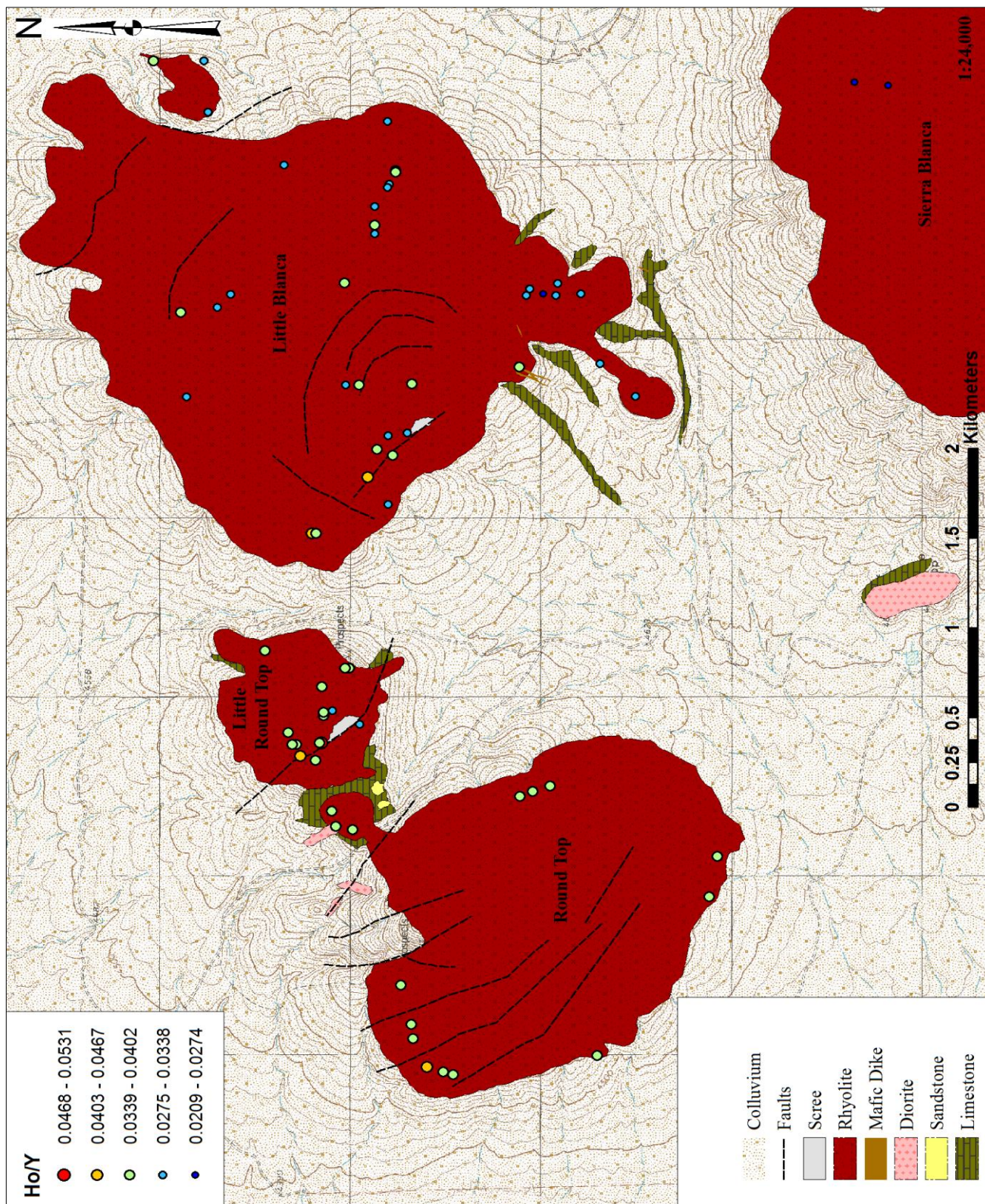
Gd/Y



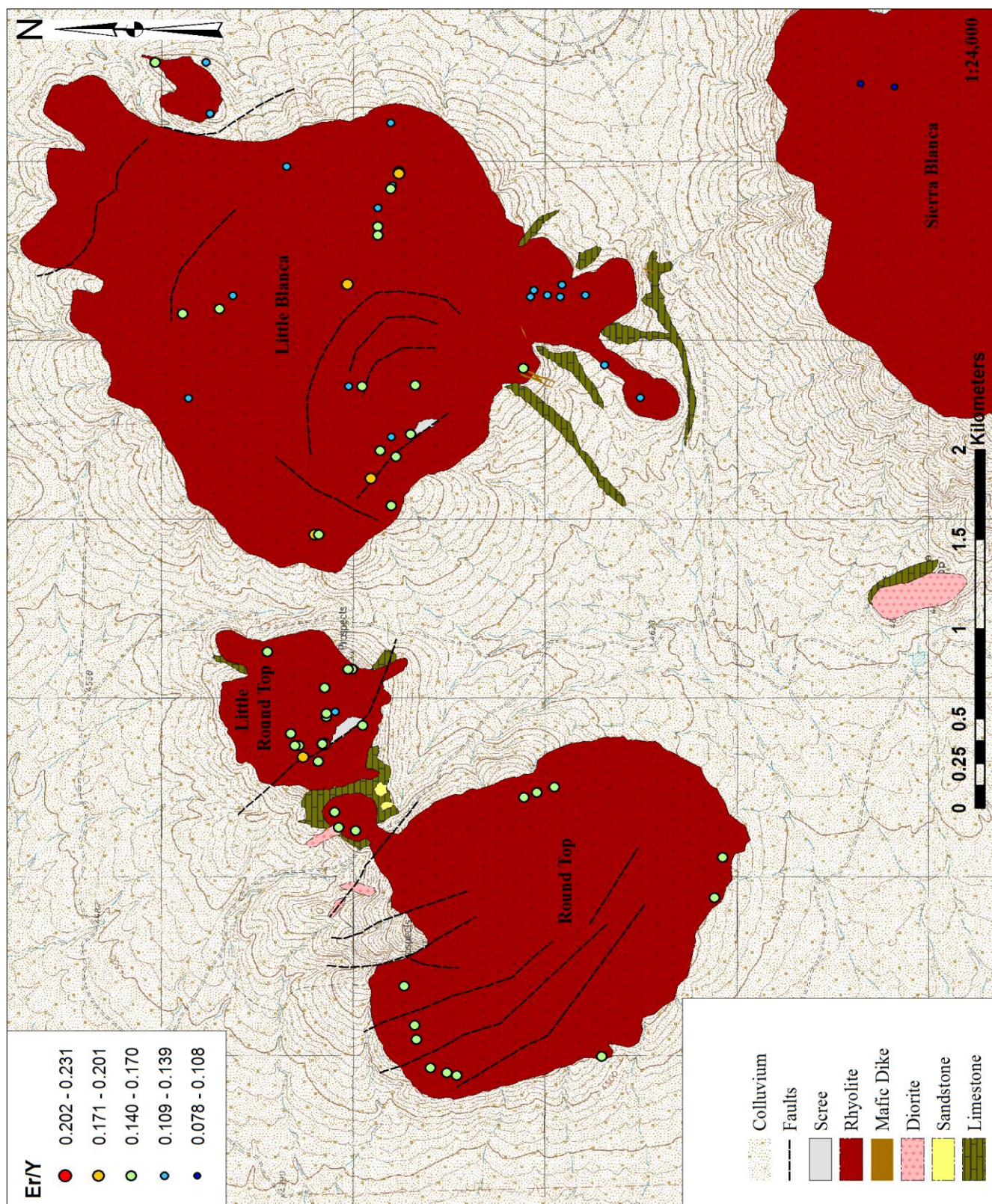
Tb/Y



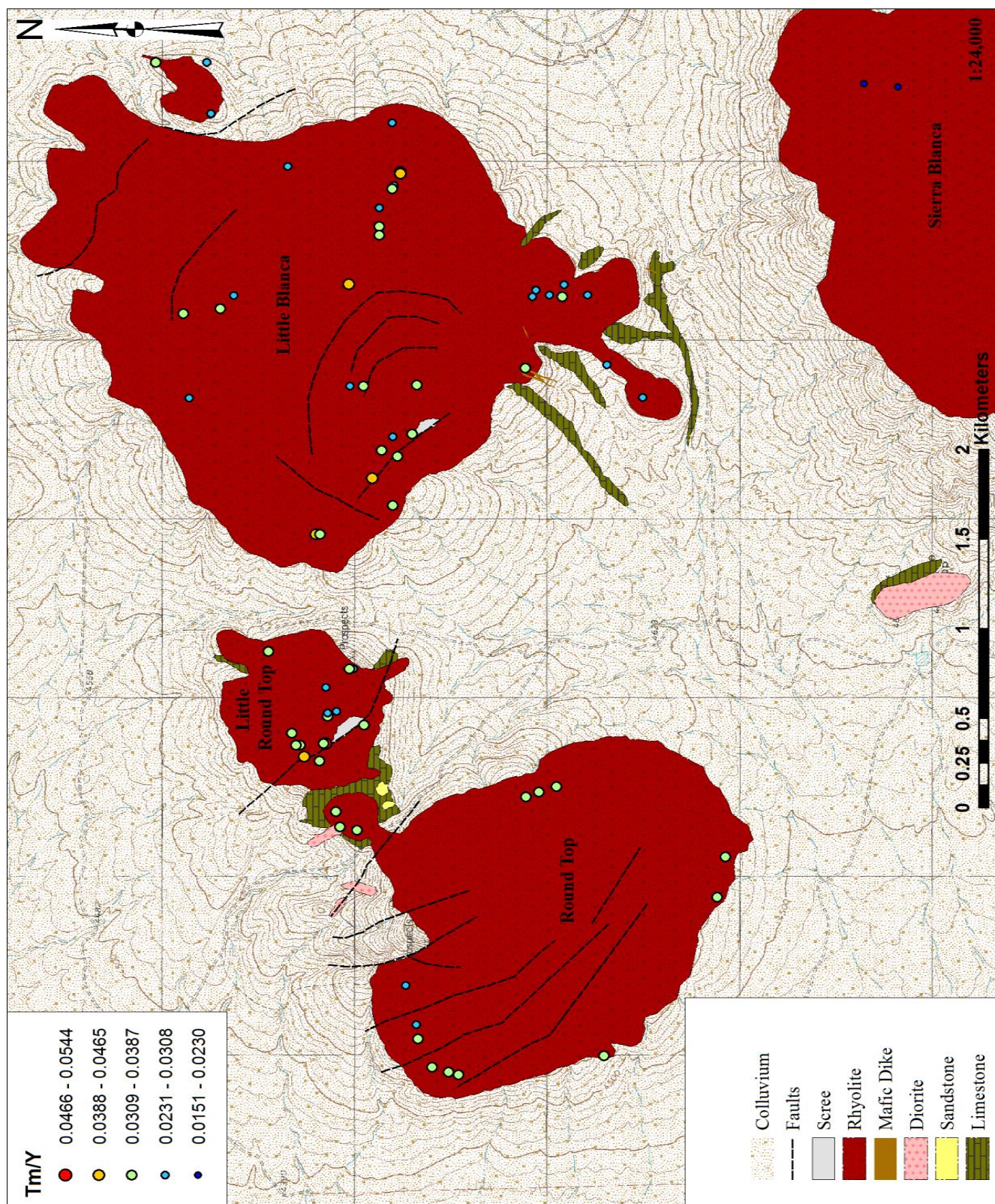
Dy/Y



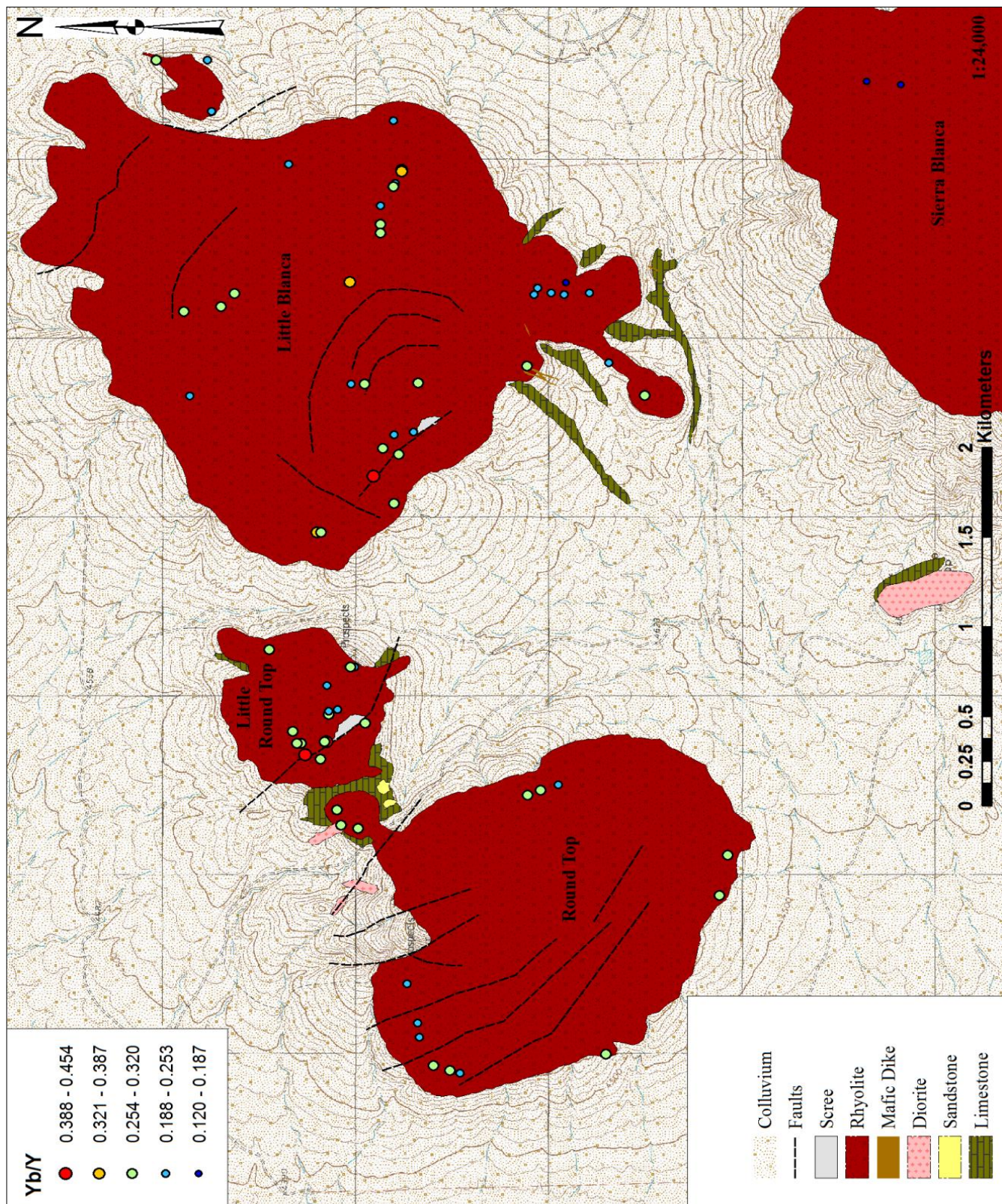
Ho/Y



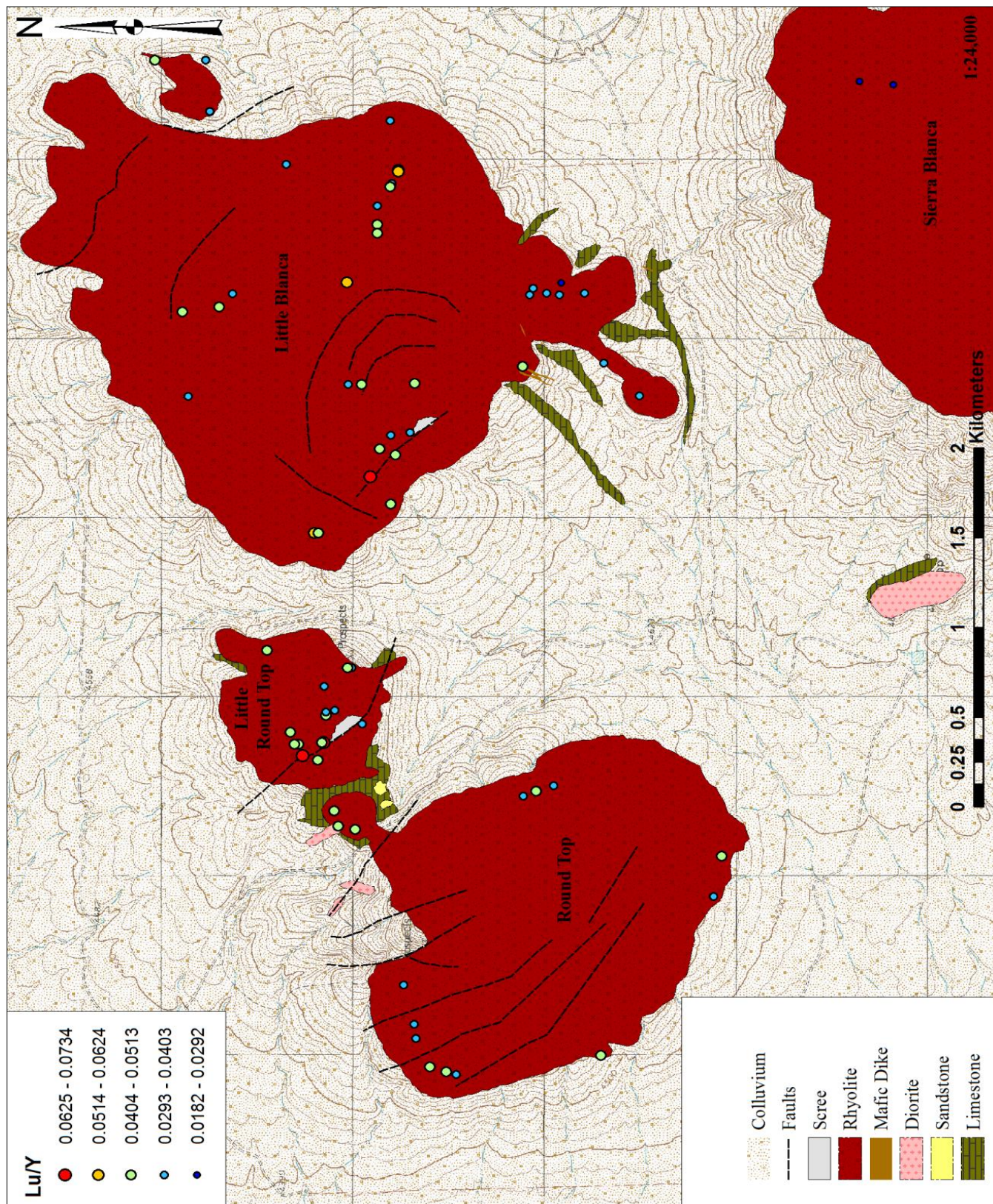
Er/Y



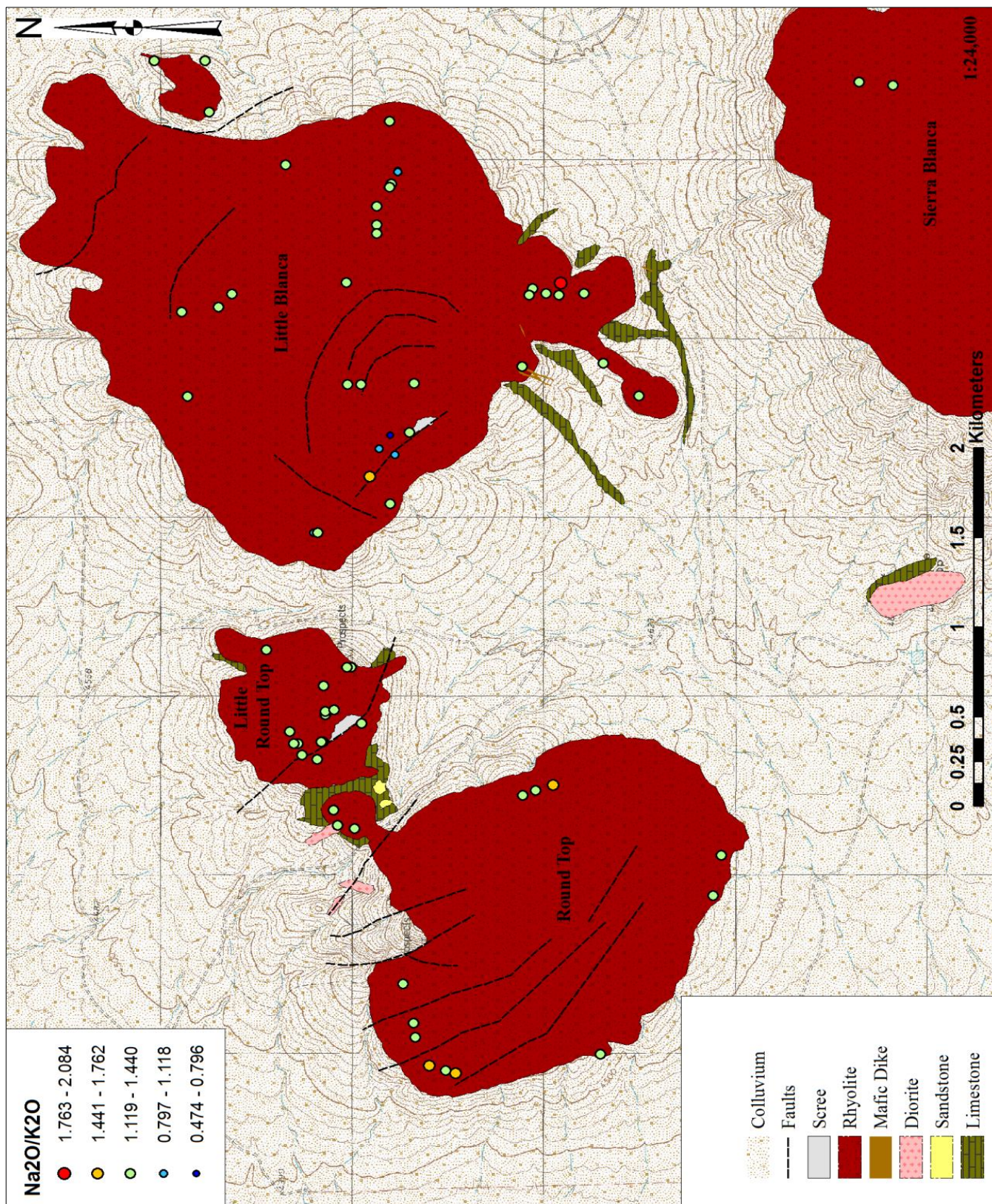
Tm/Y



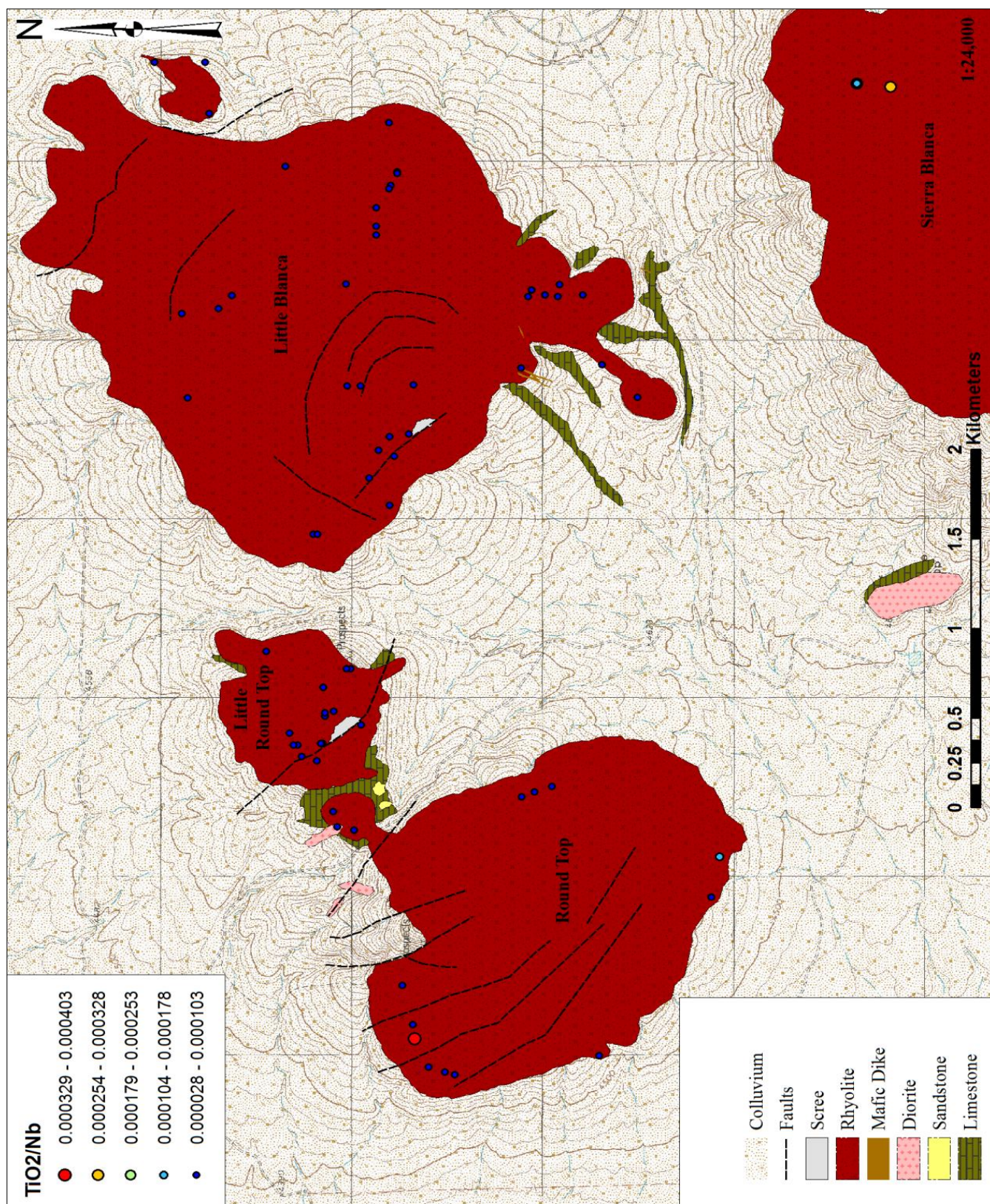
Yb/Y



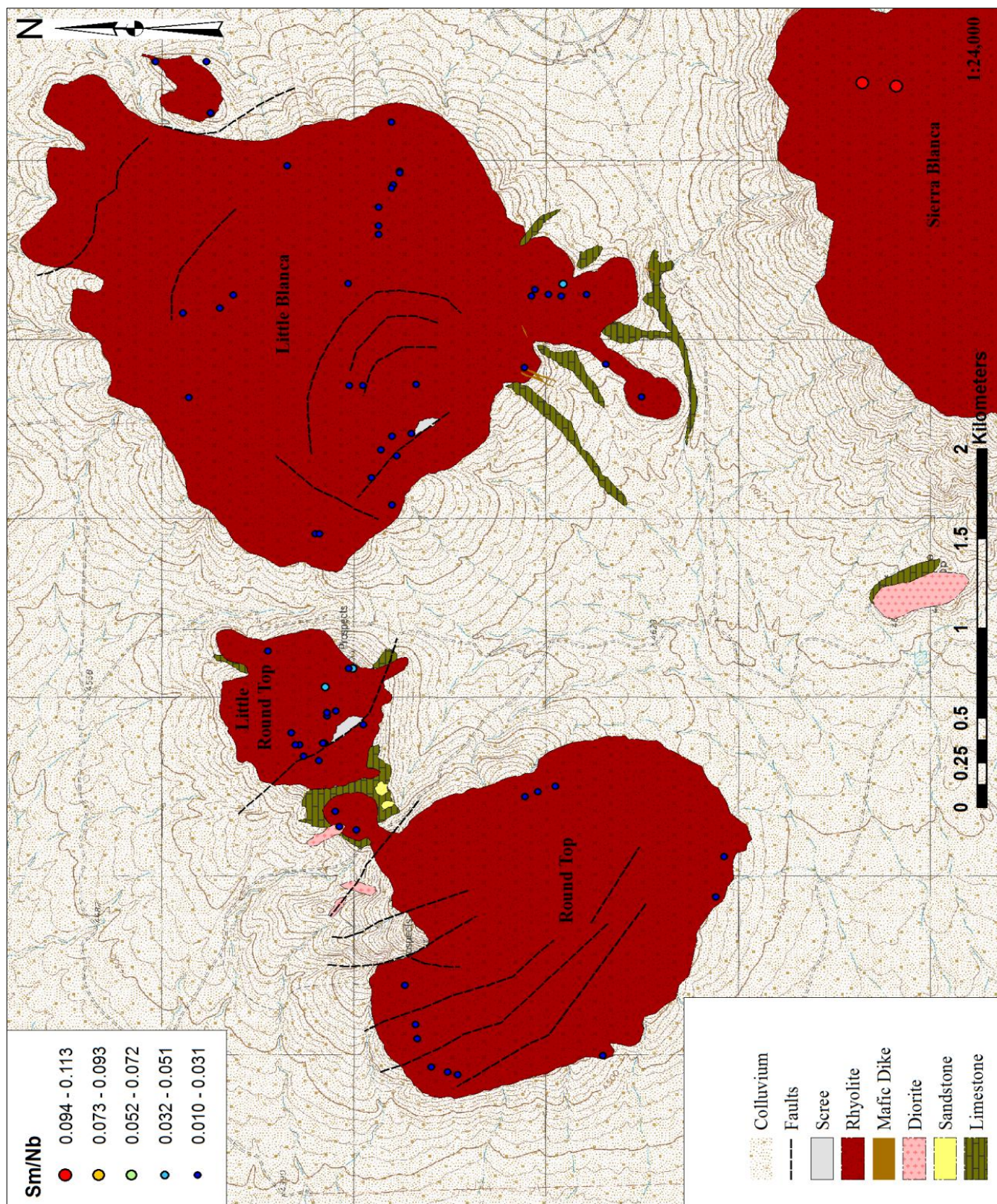
Lu/Y



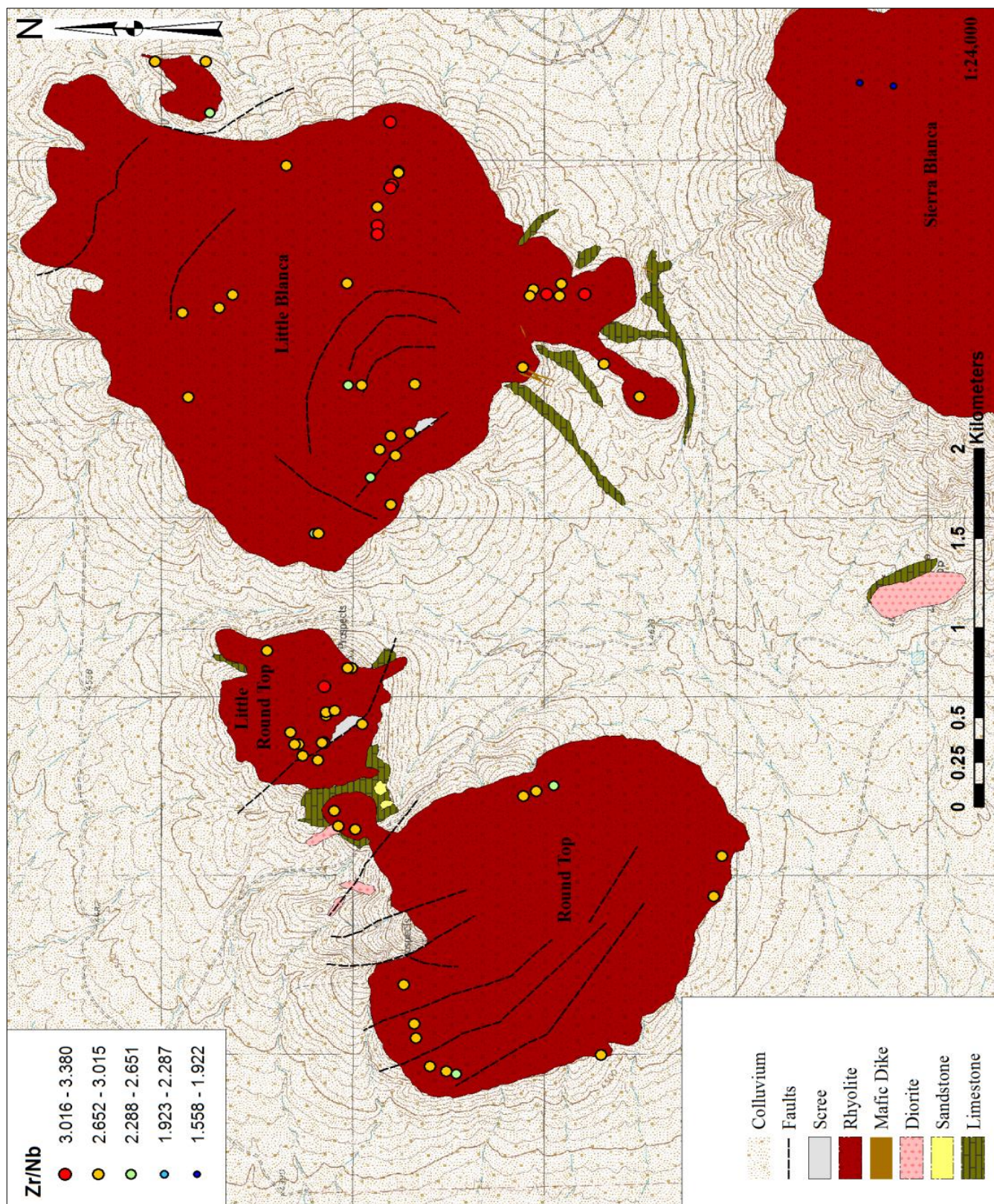
Na₂O/K₂O



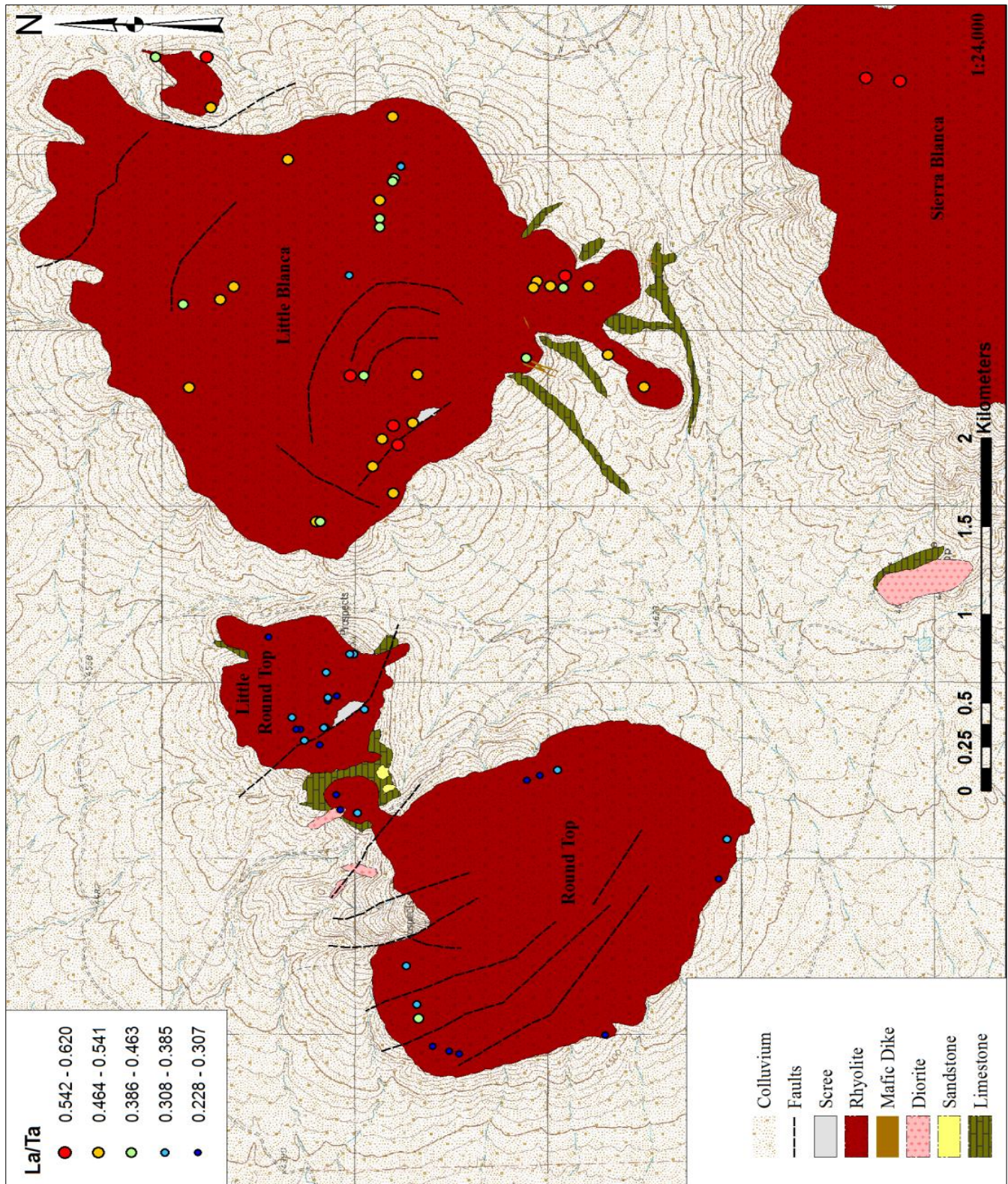
TiO₂/Nb



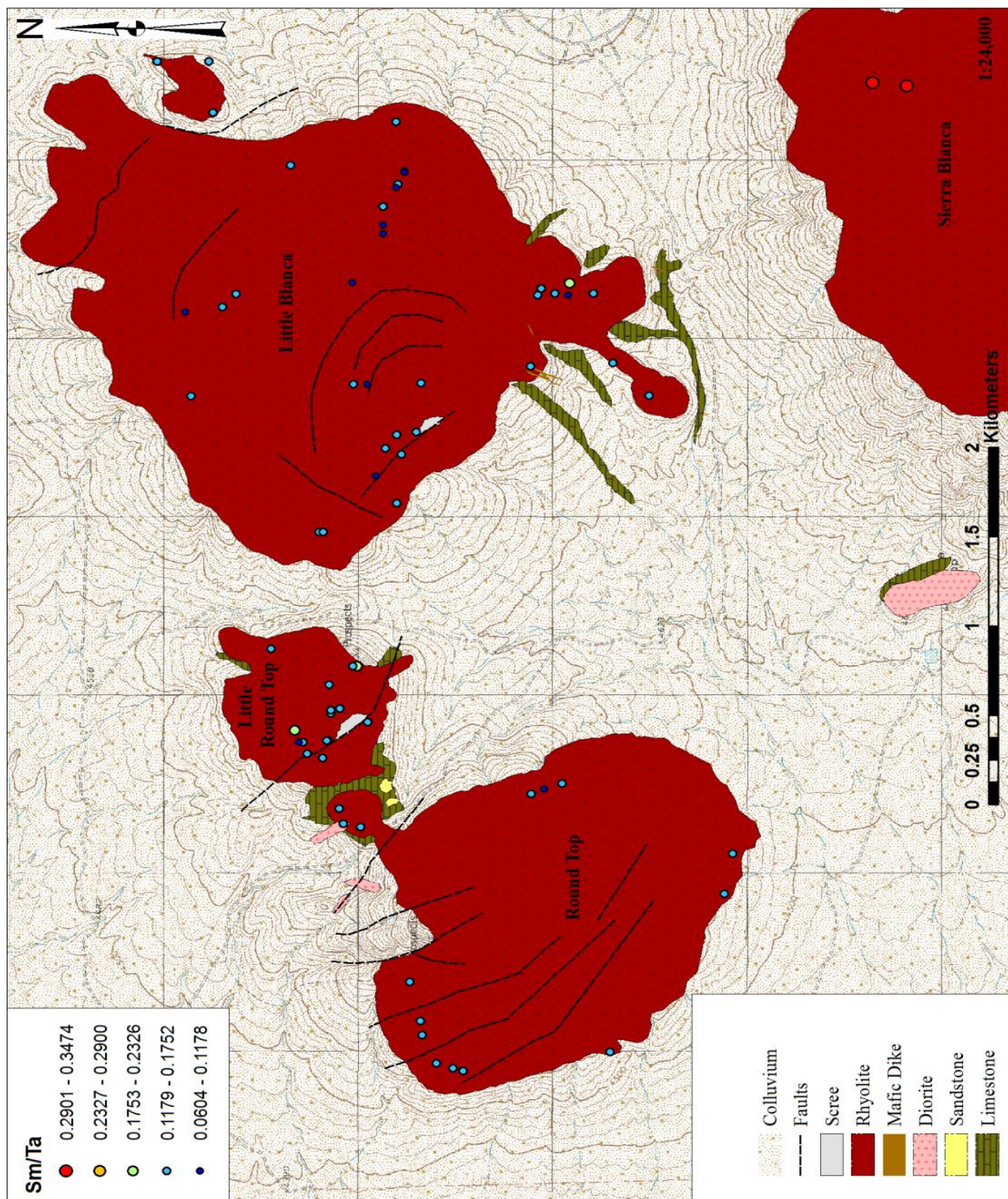
Sm/Nb



Zr/Nb



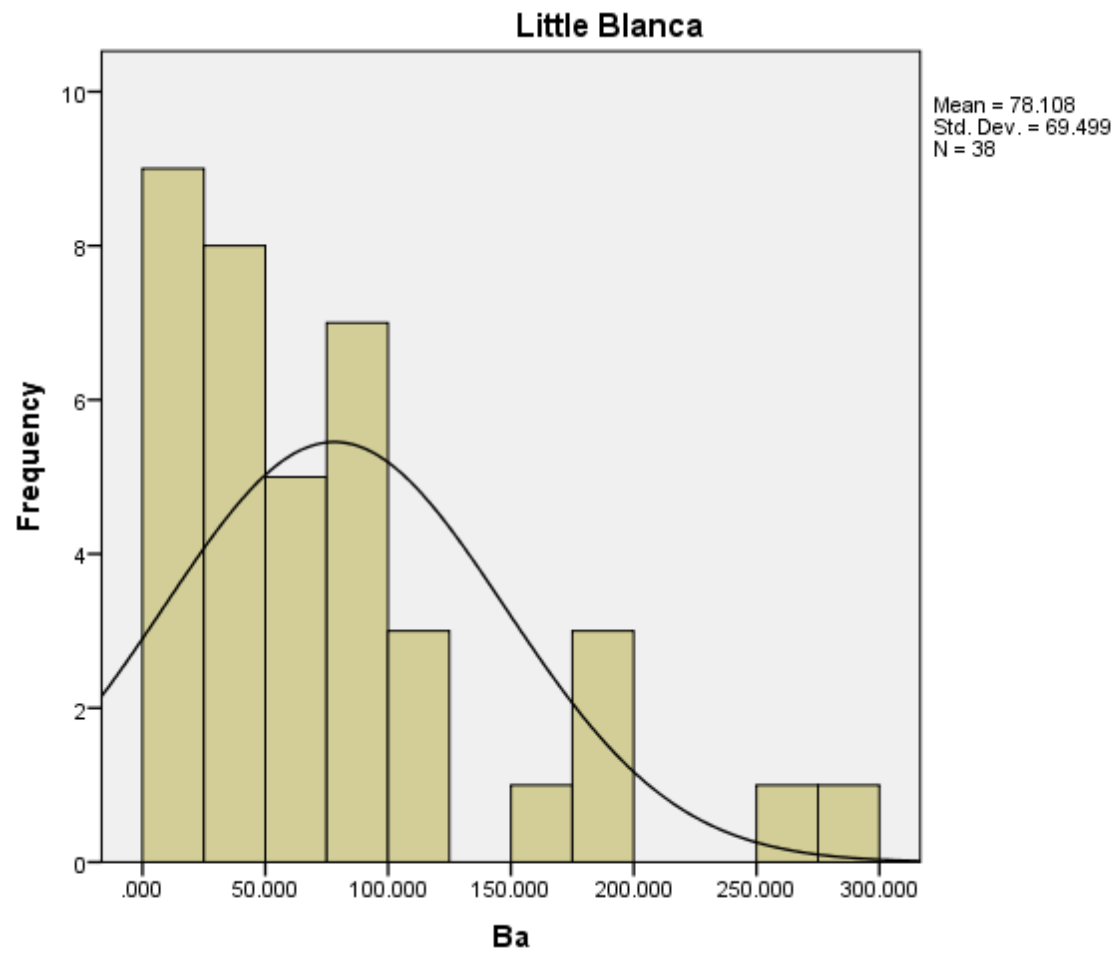
La/Ta

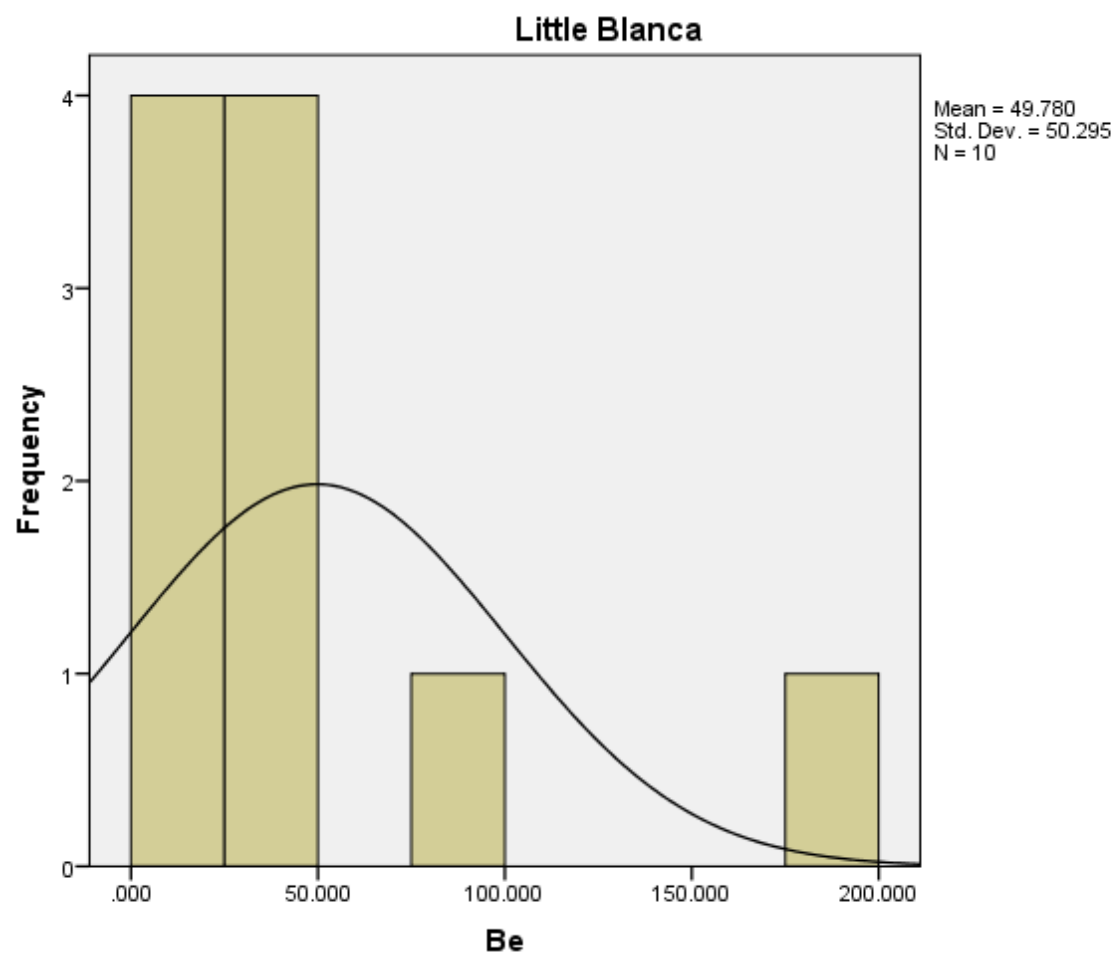


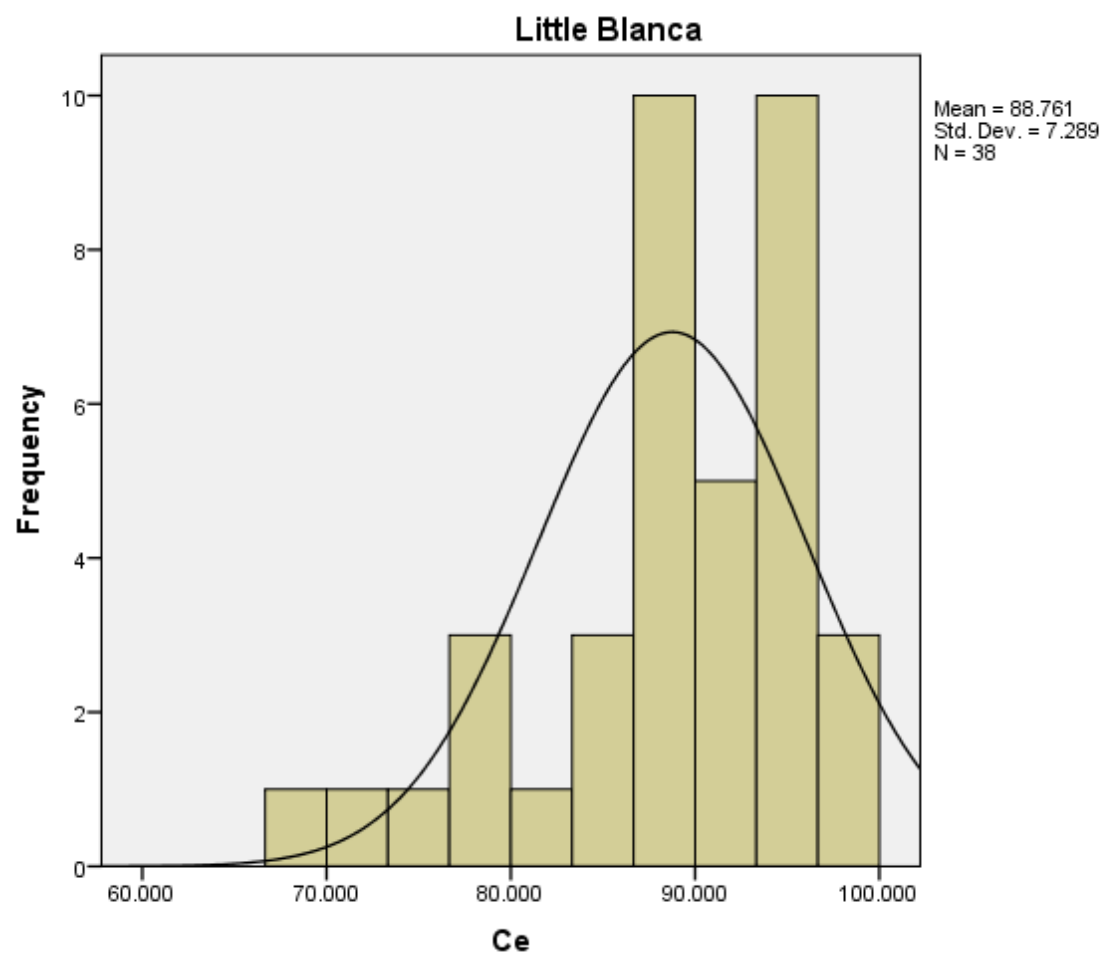
Sm/Ta

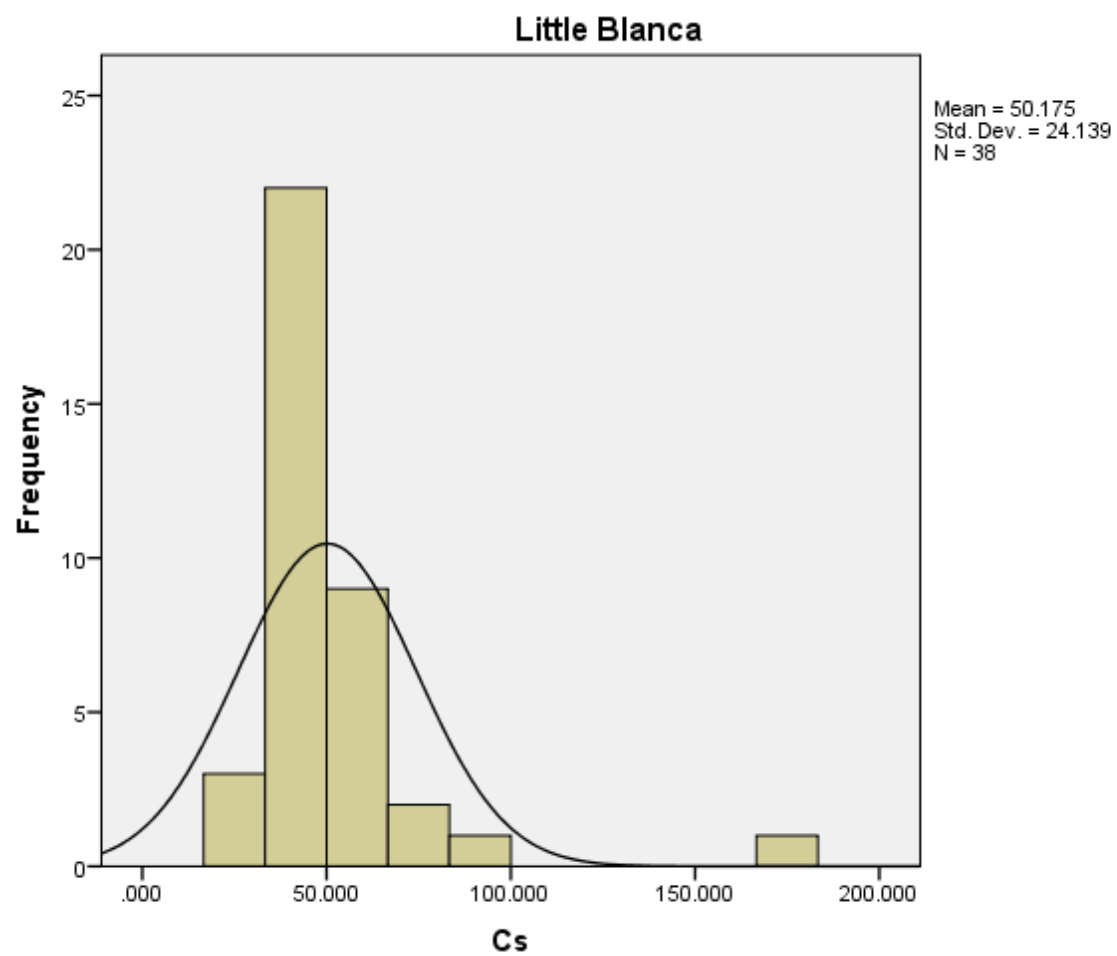
APPENDIX V: HISTOGRAMS

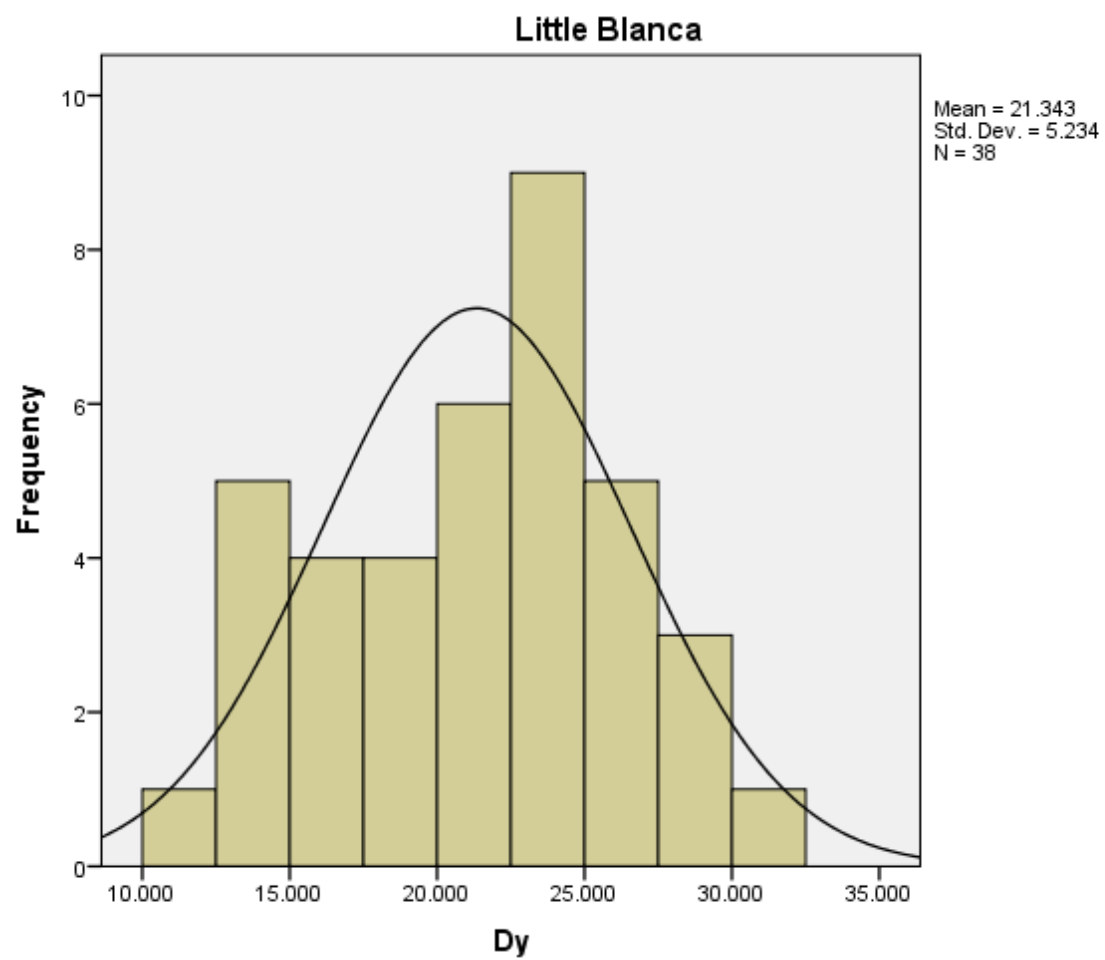
Histograms: Little Blanca

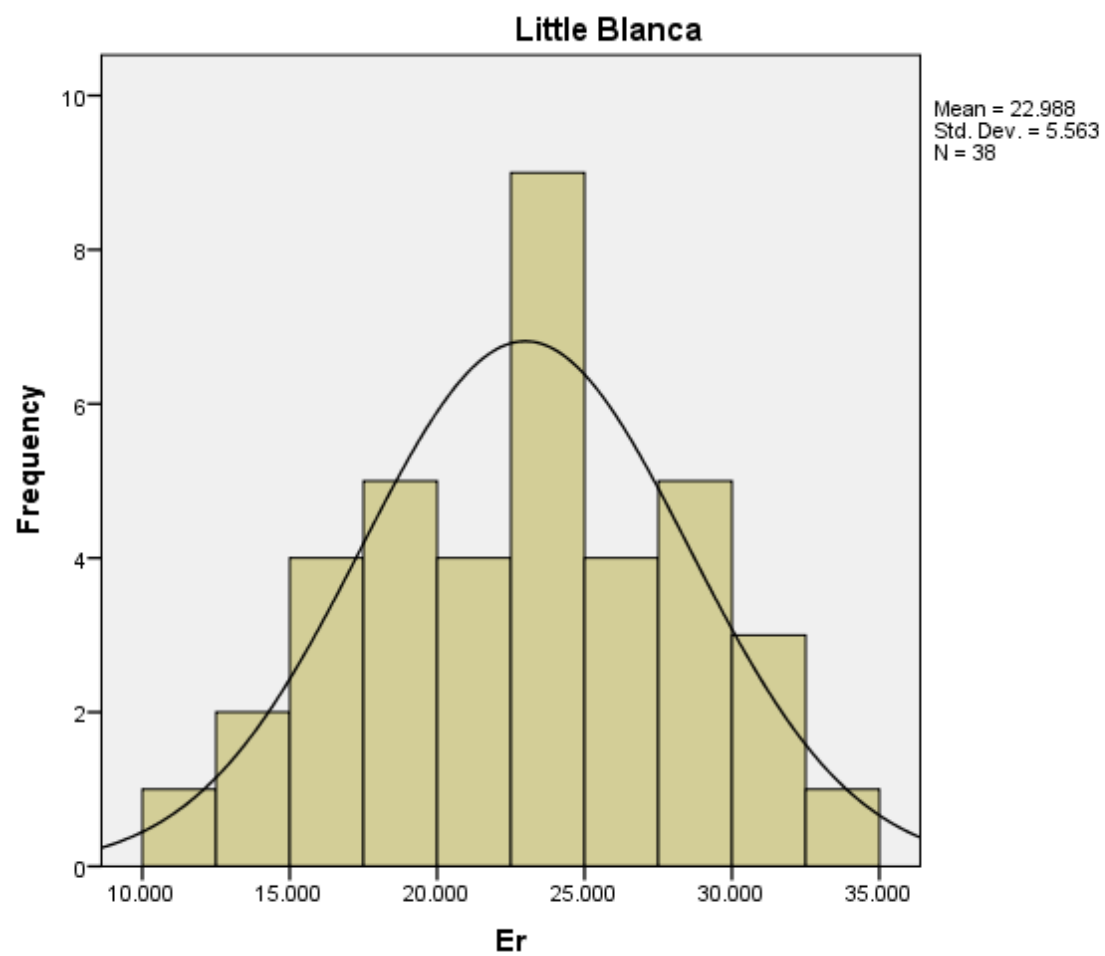


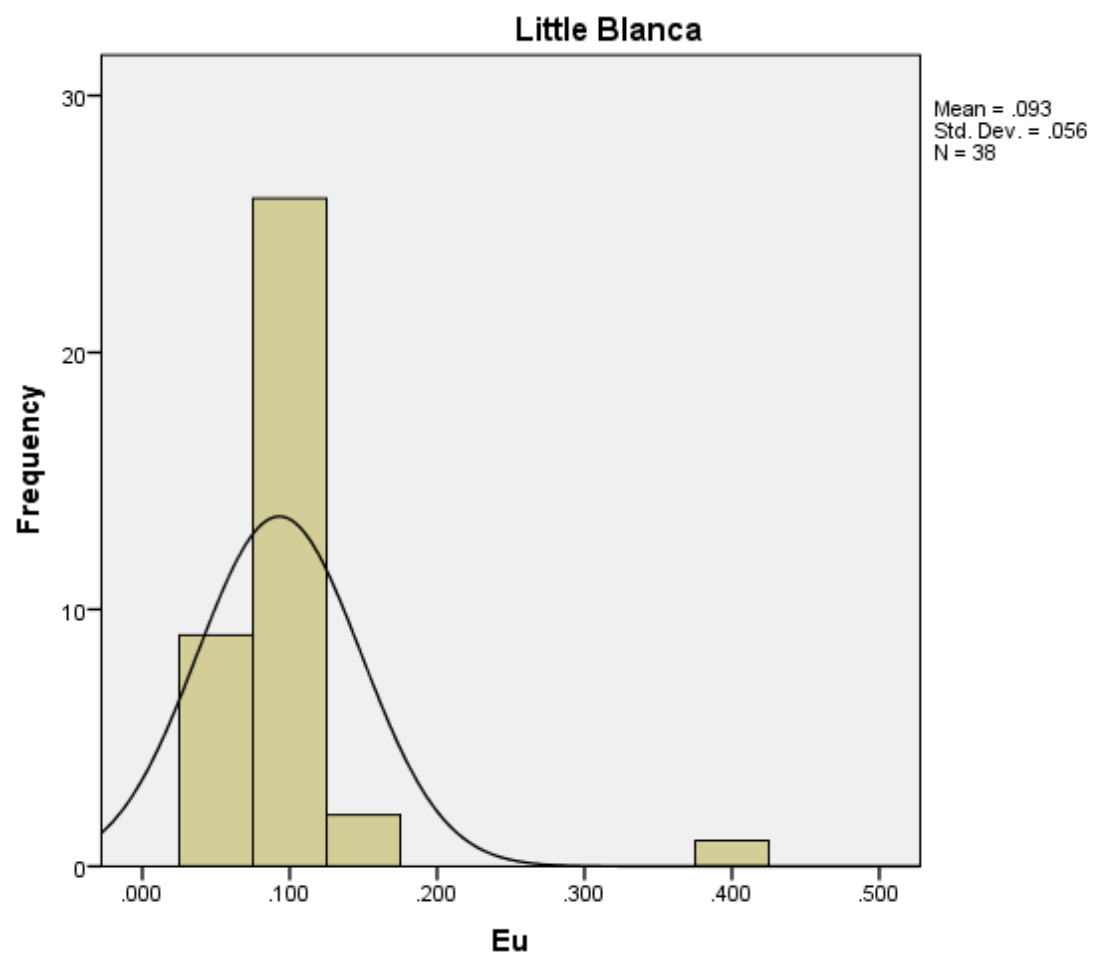


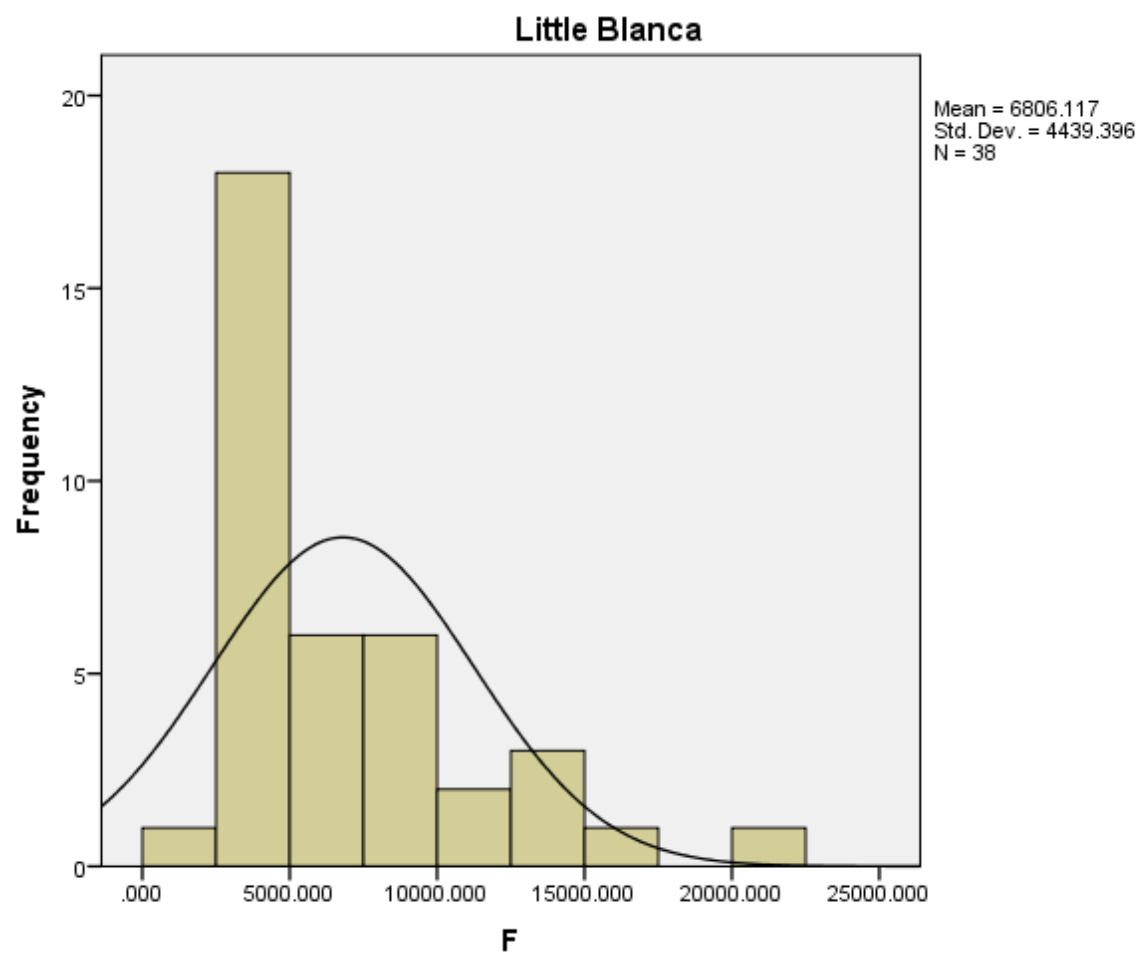


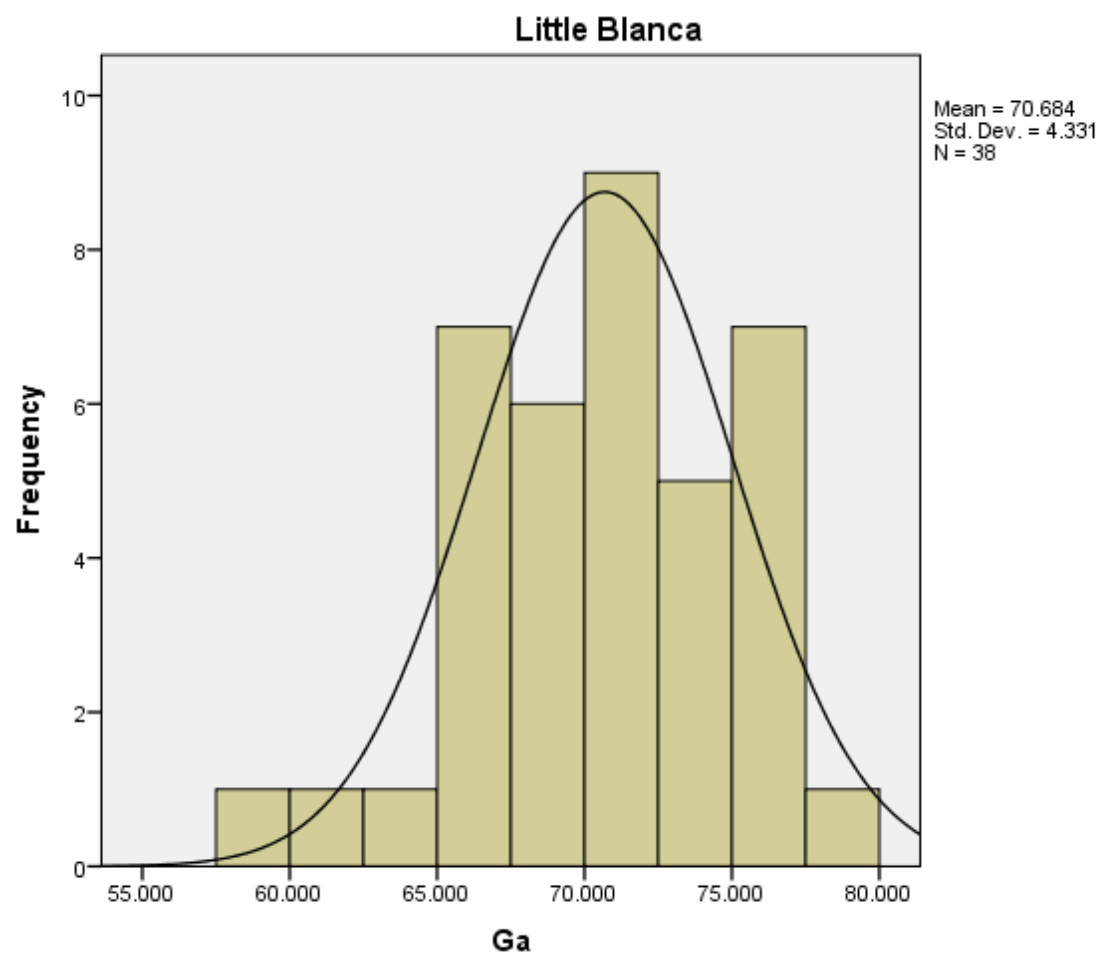


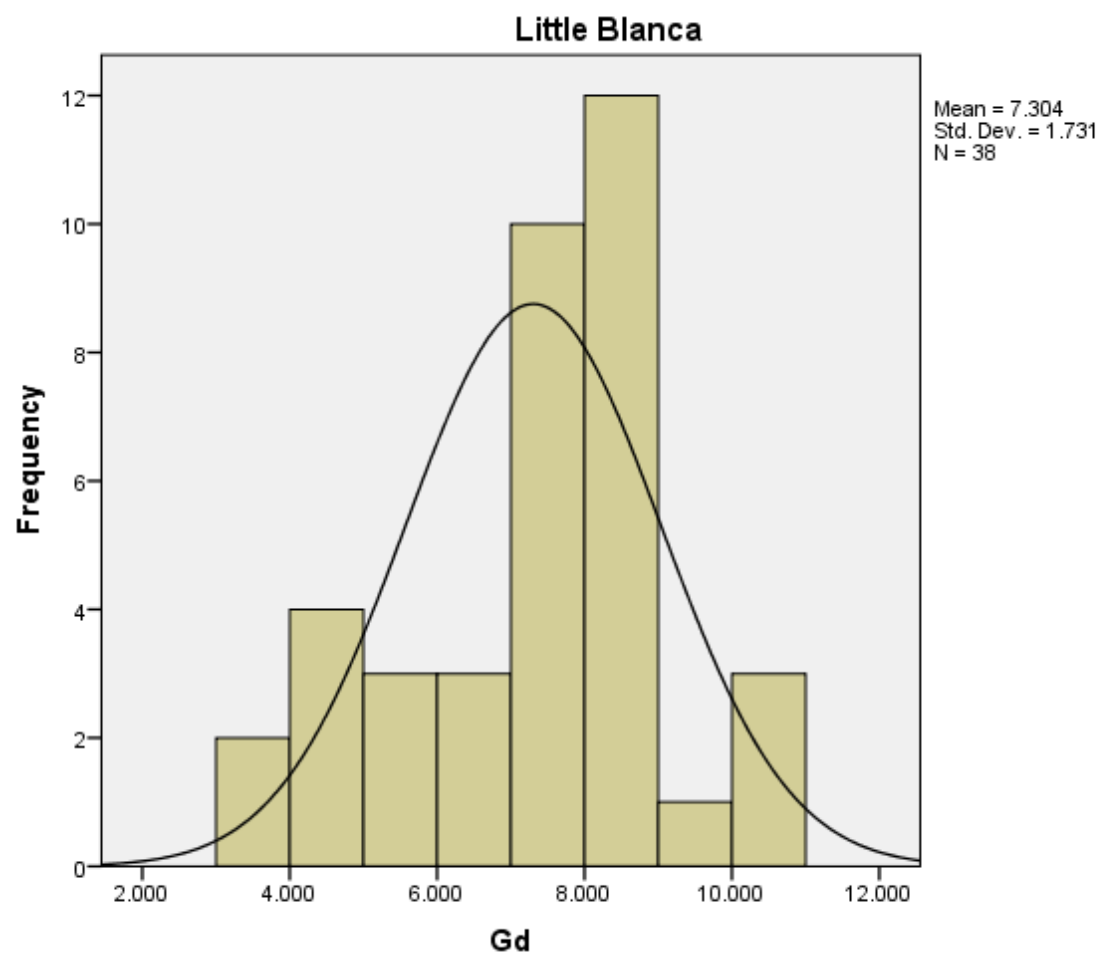


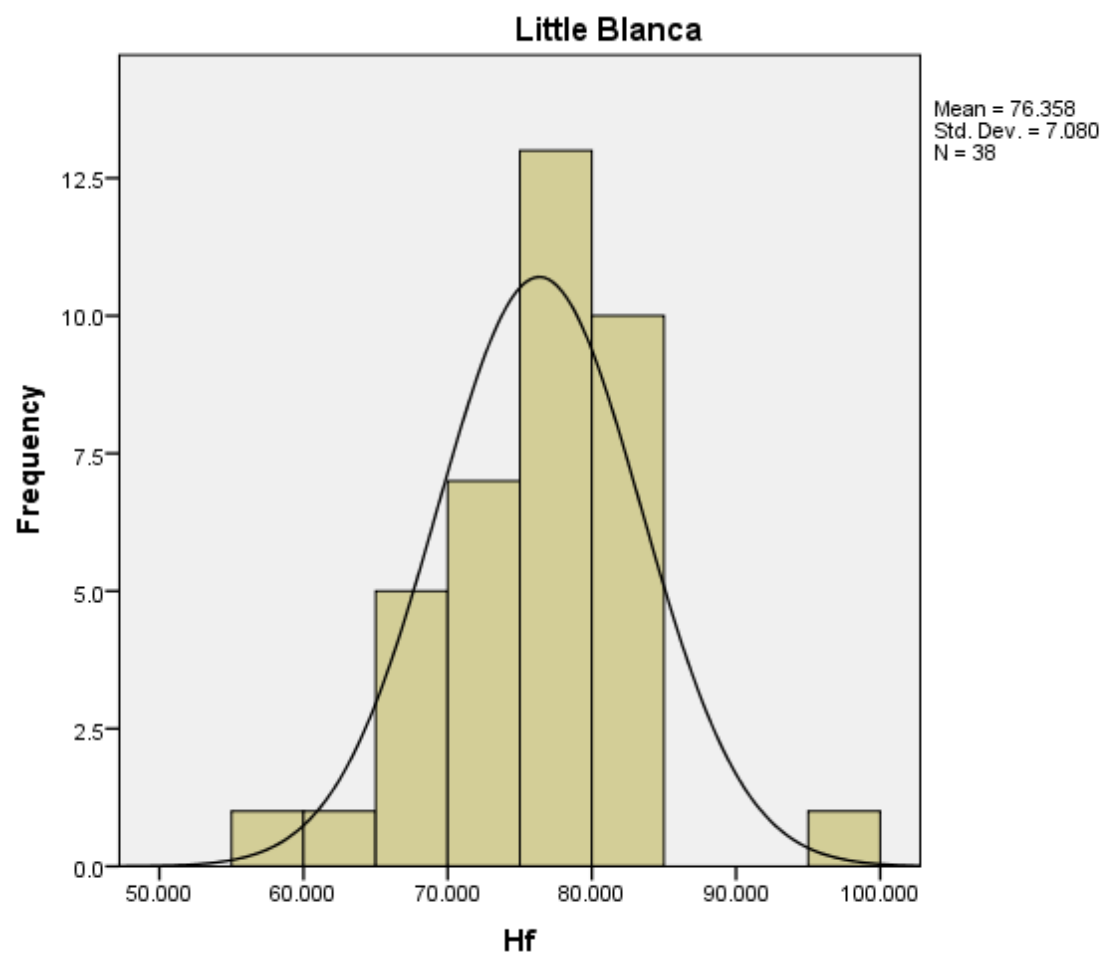


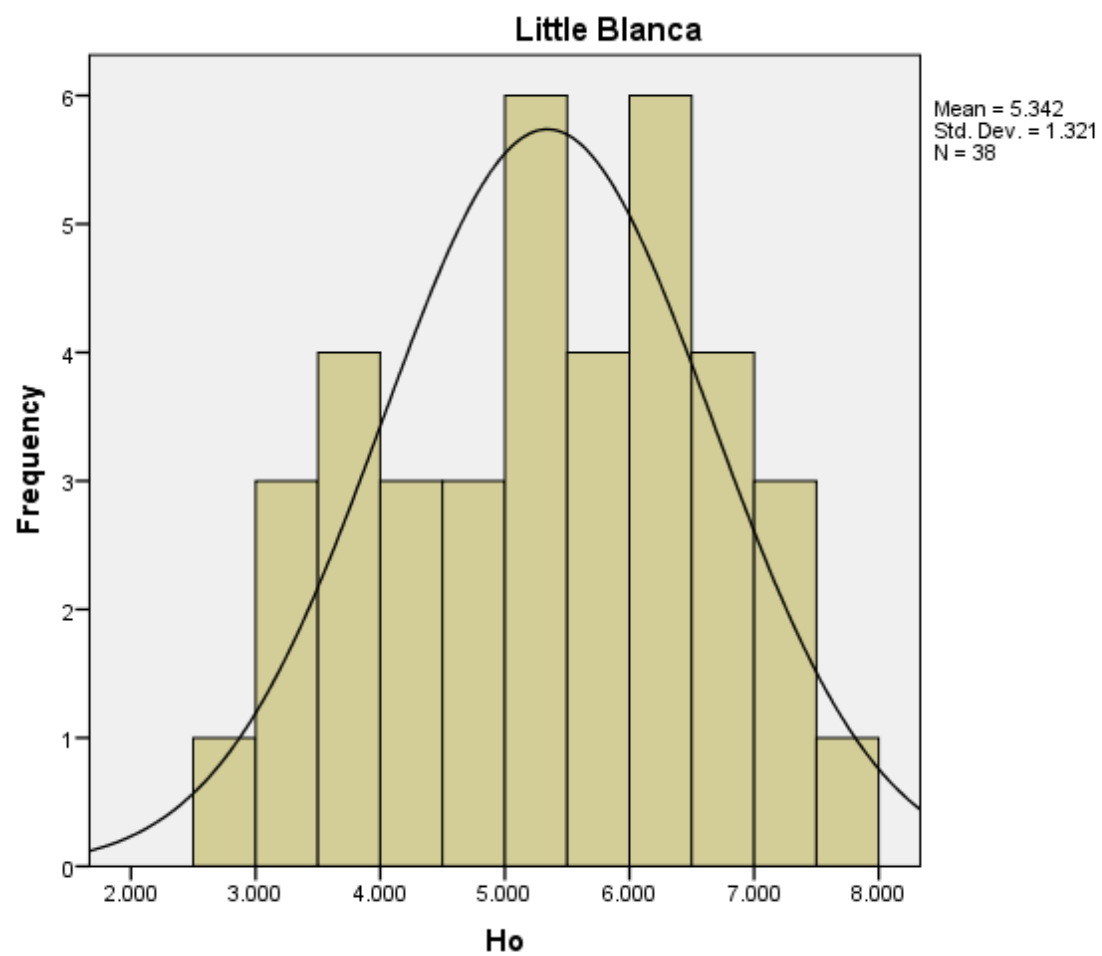


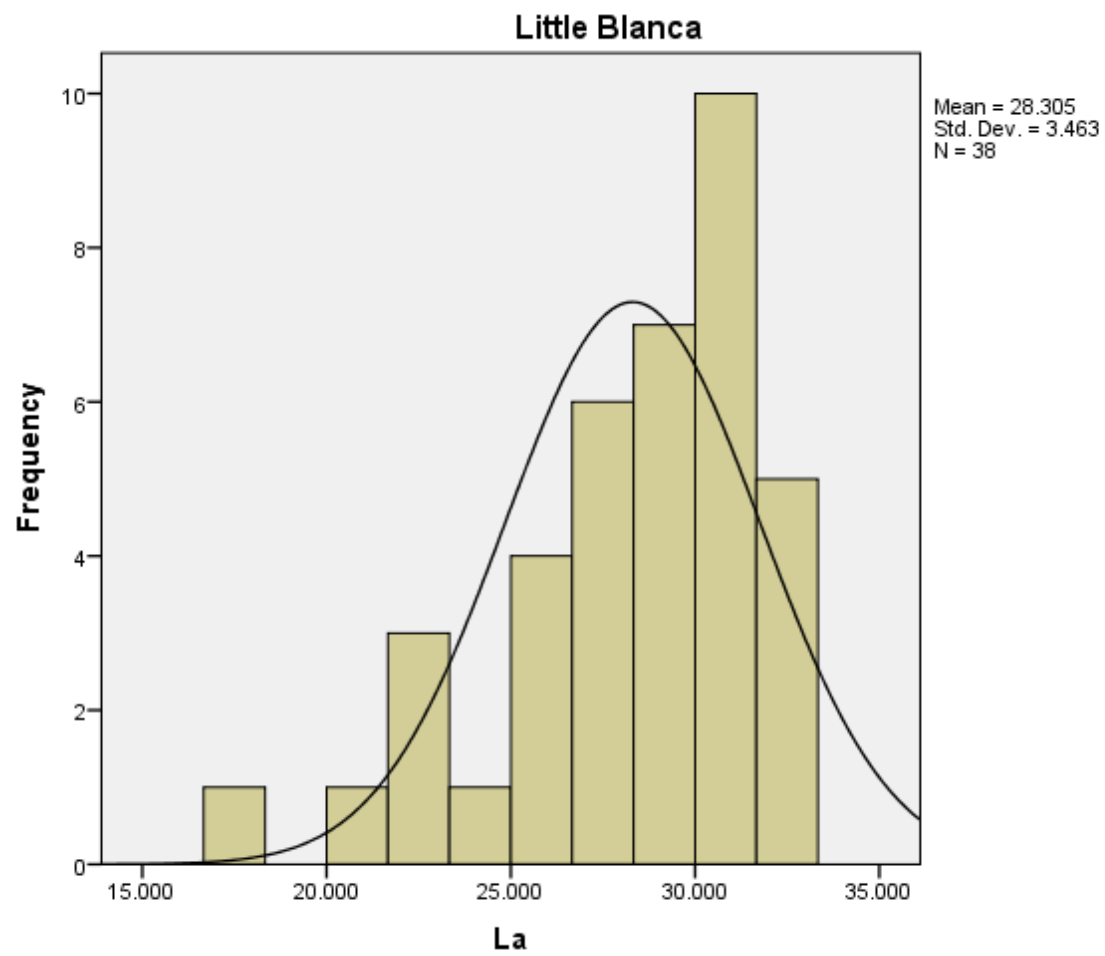


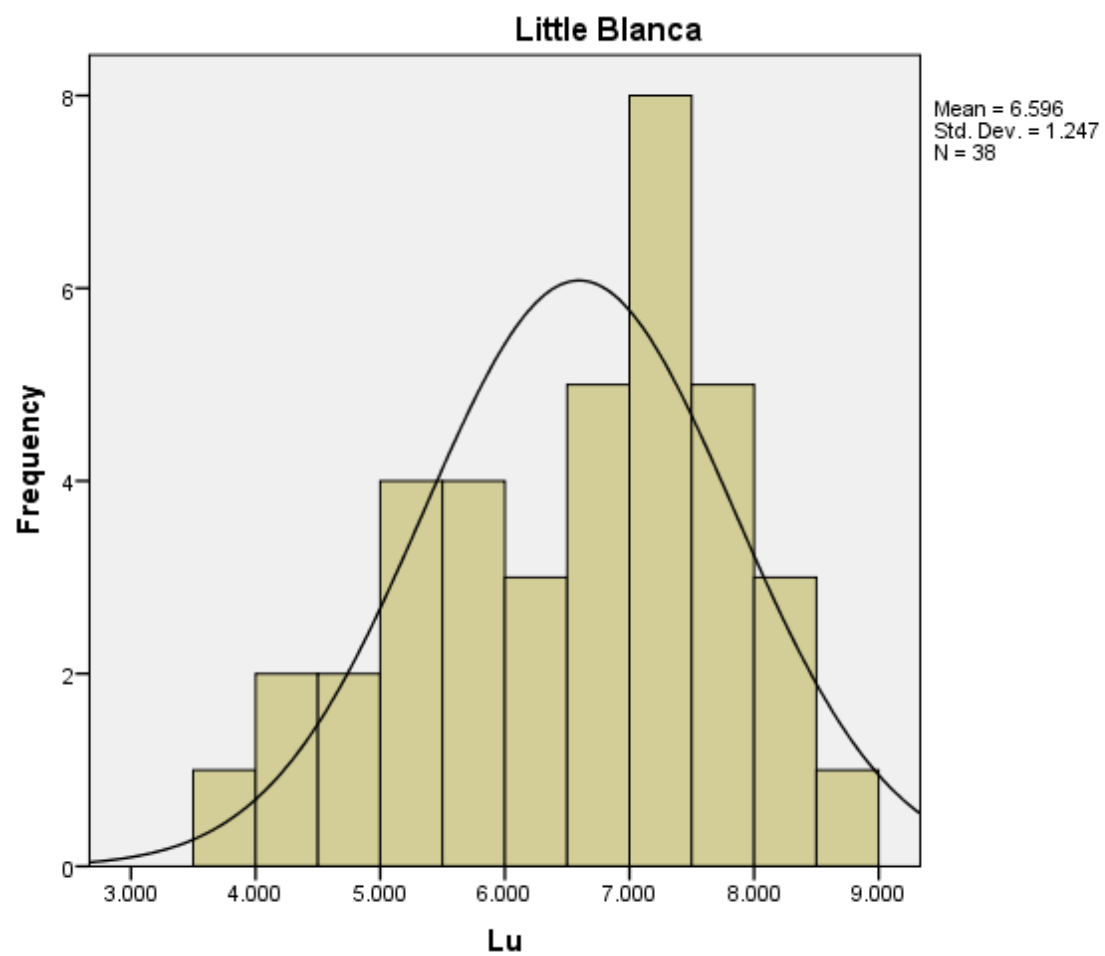


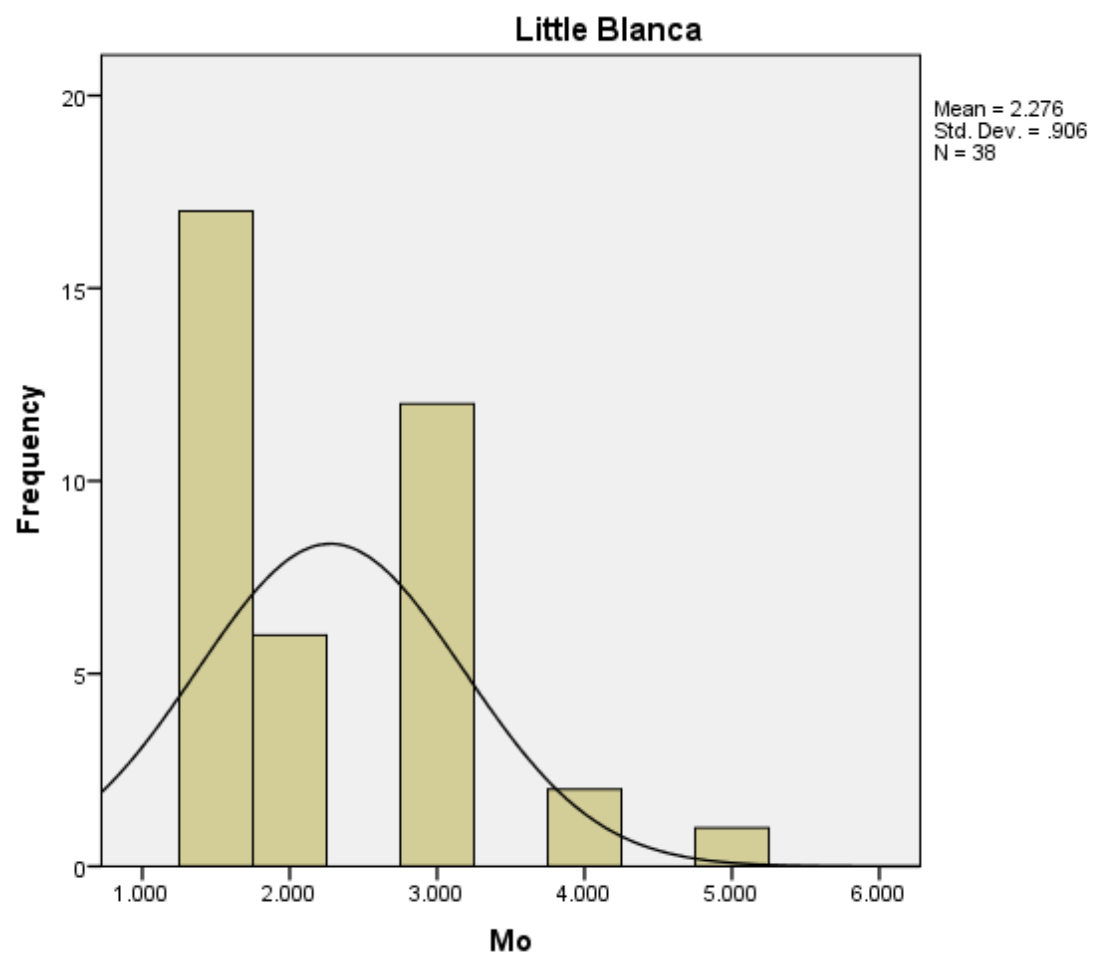


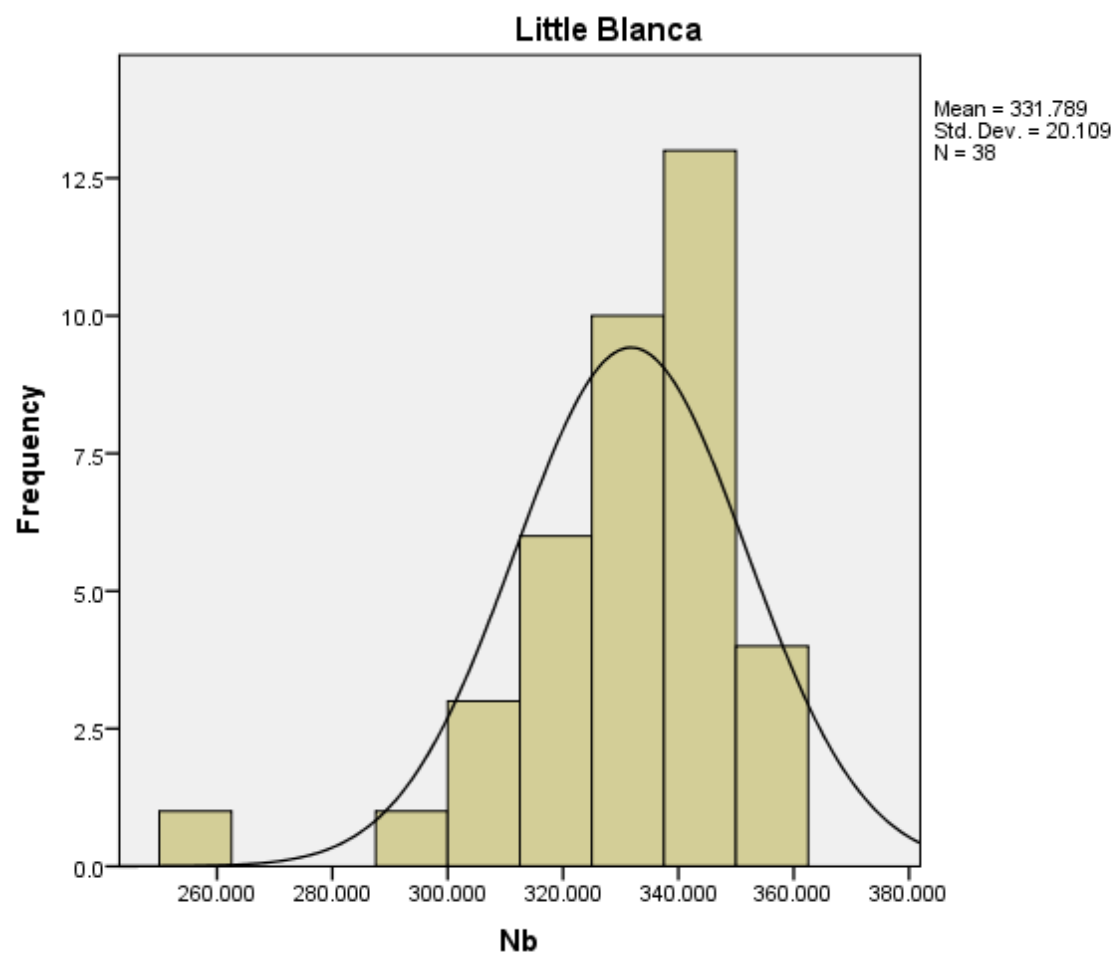


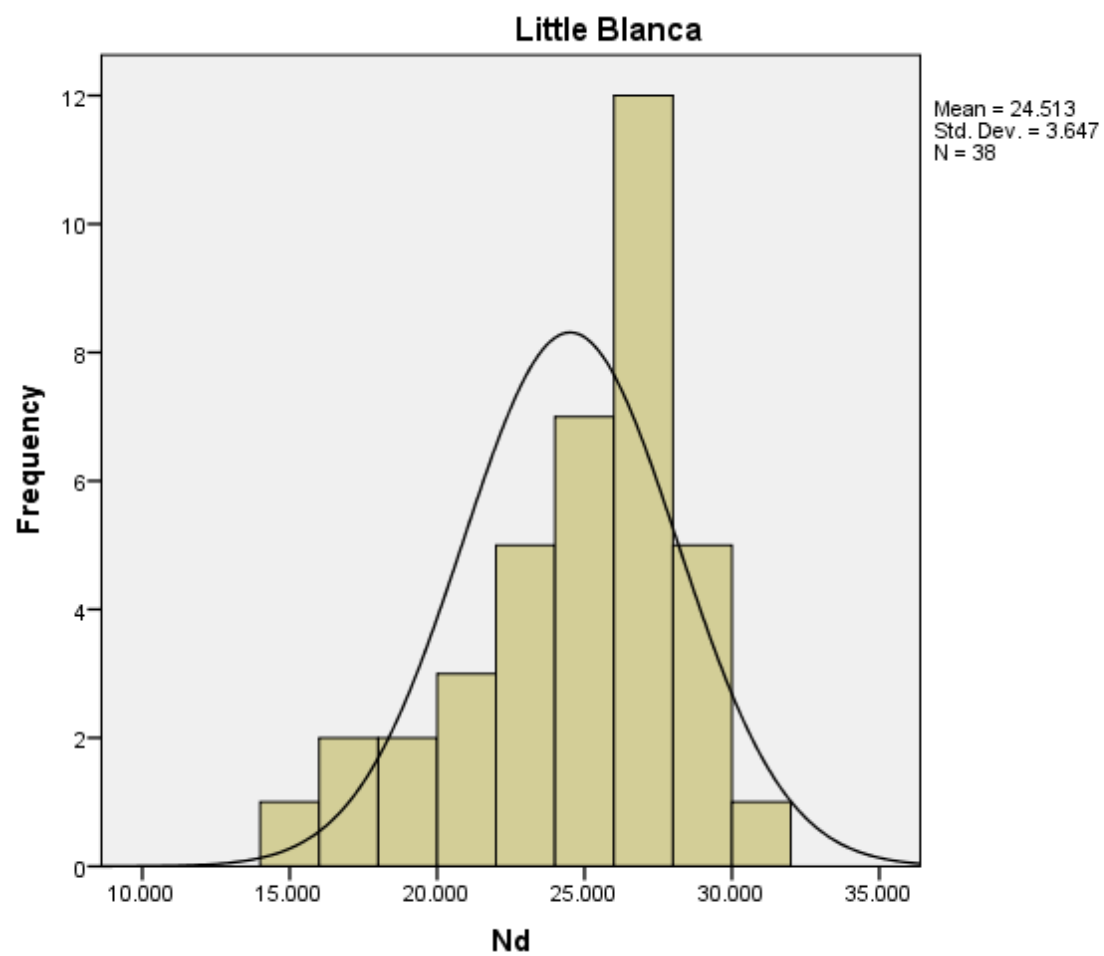


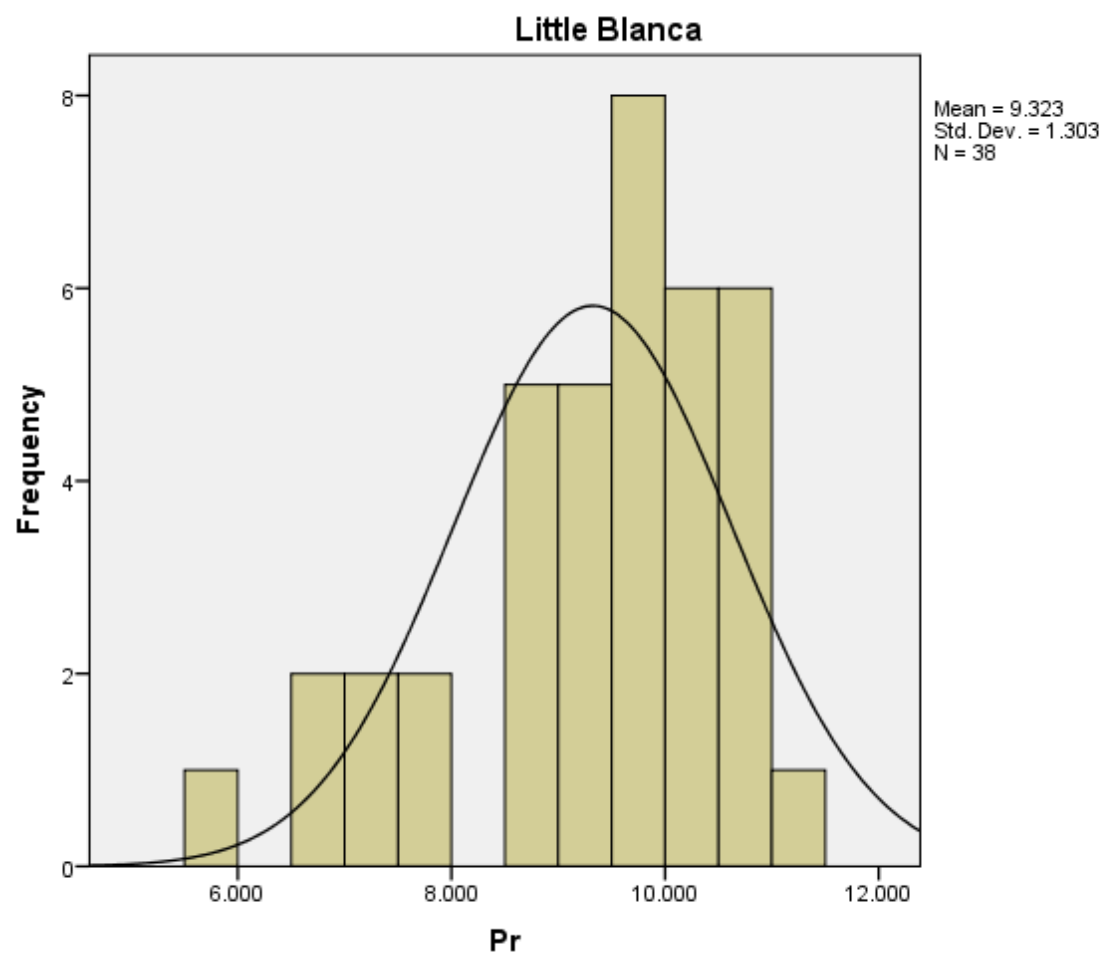


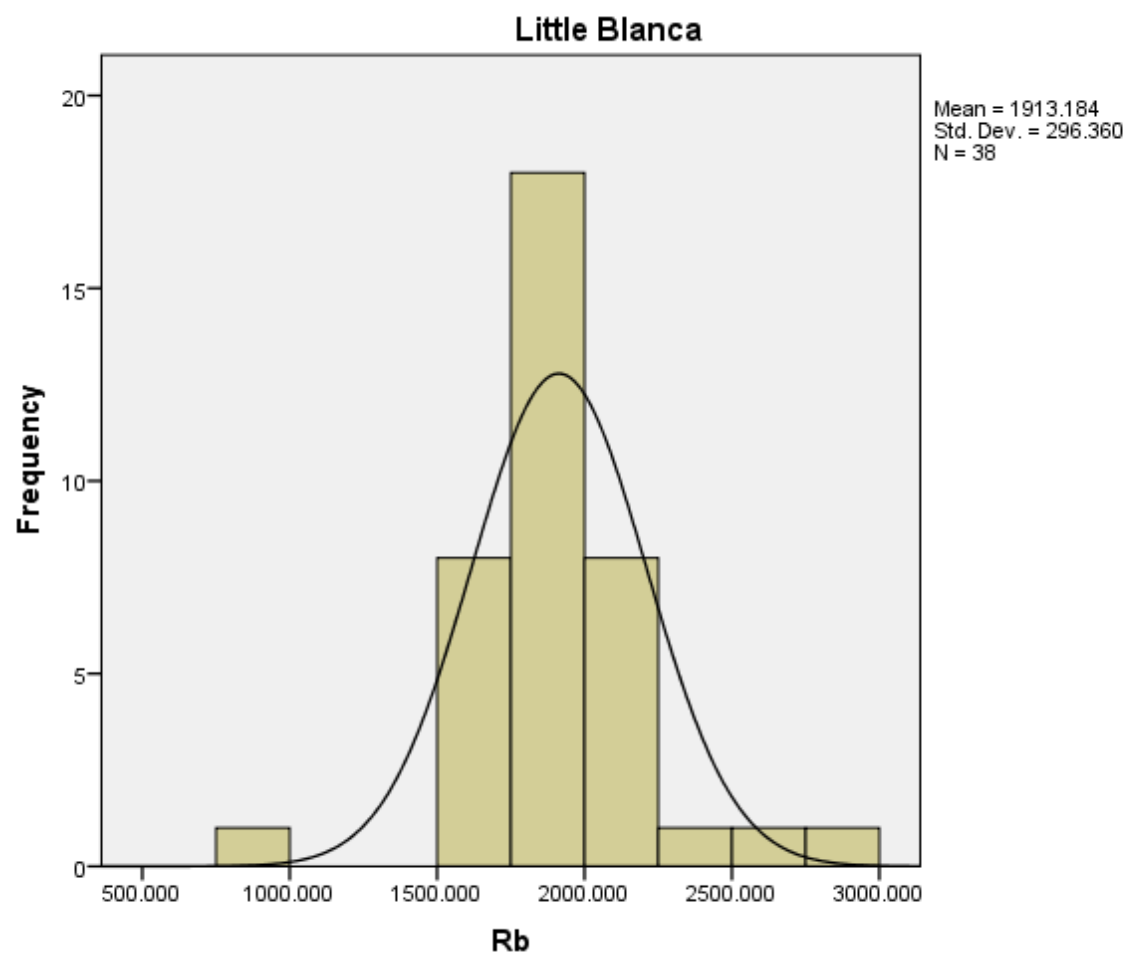


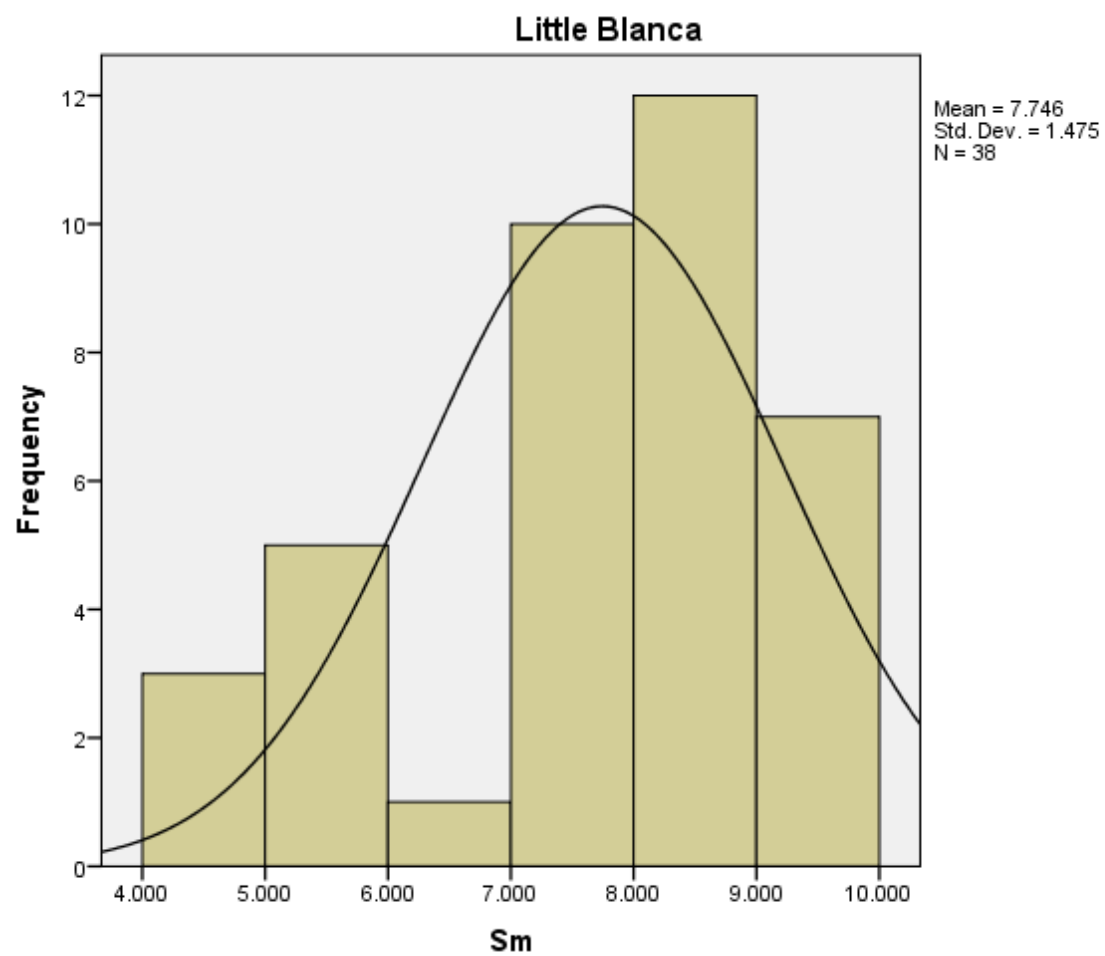


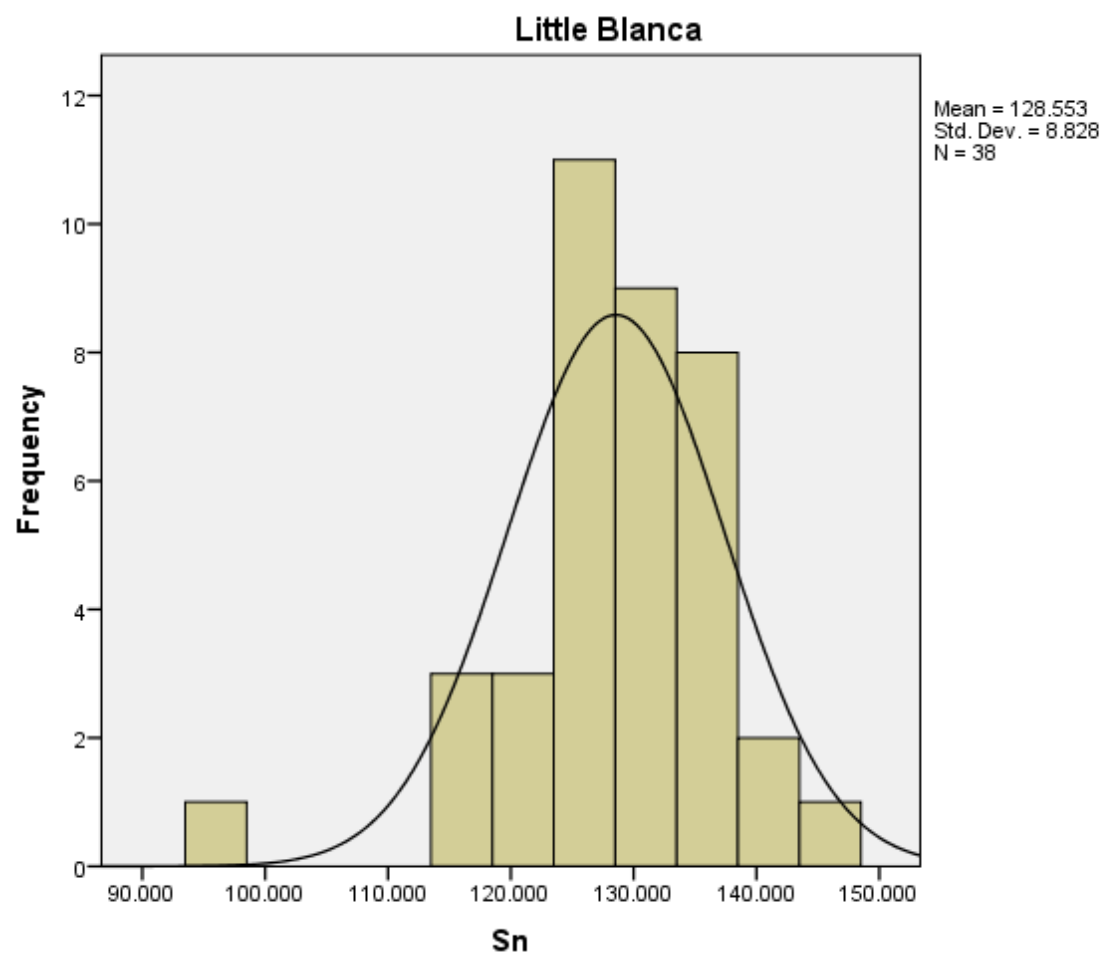


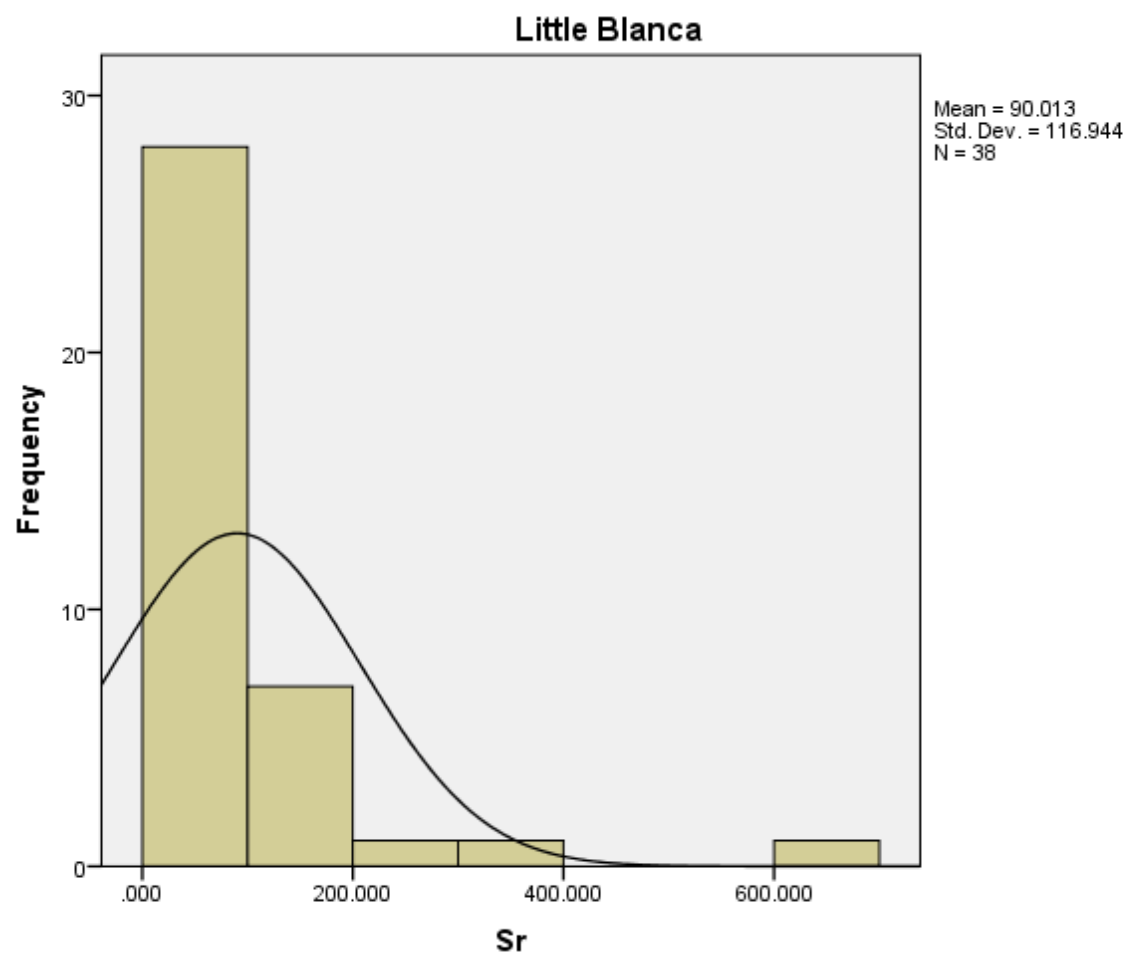


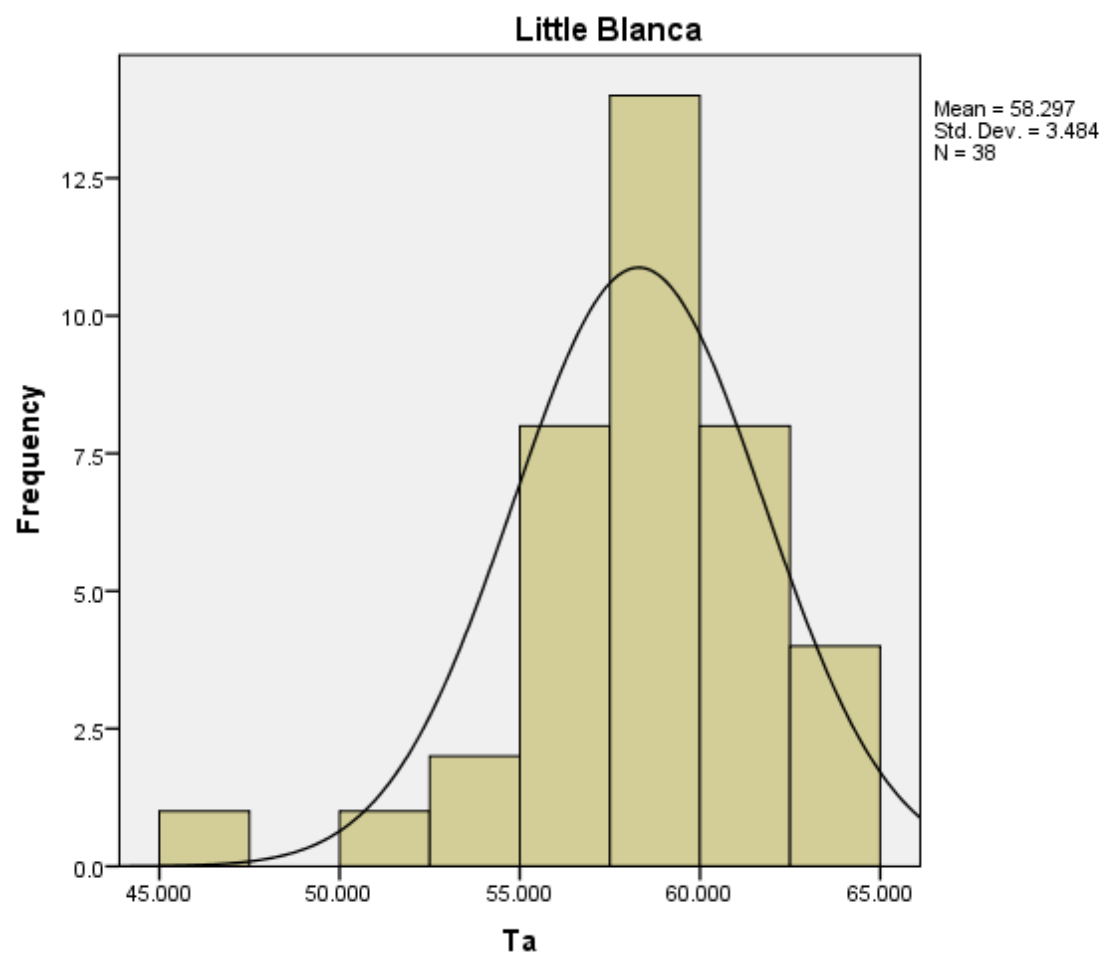


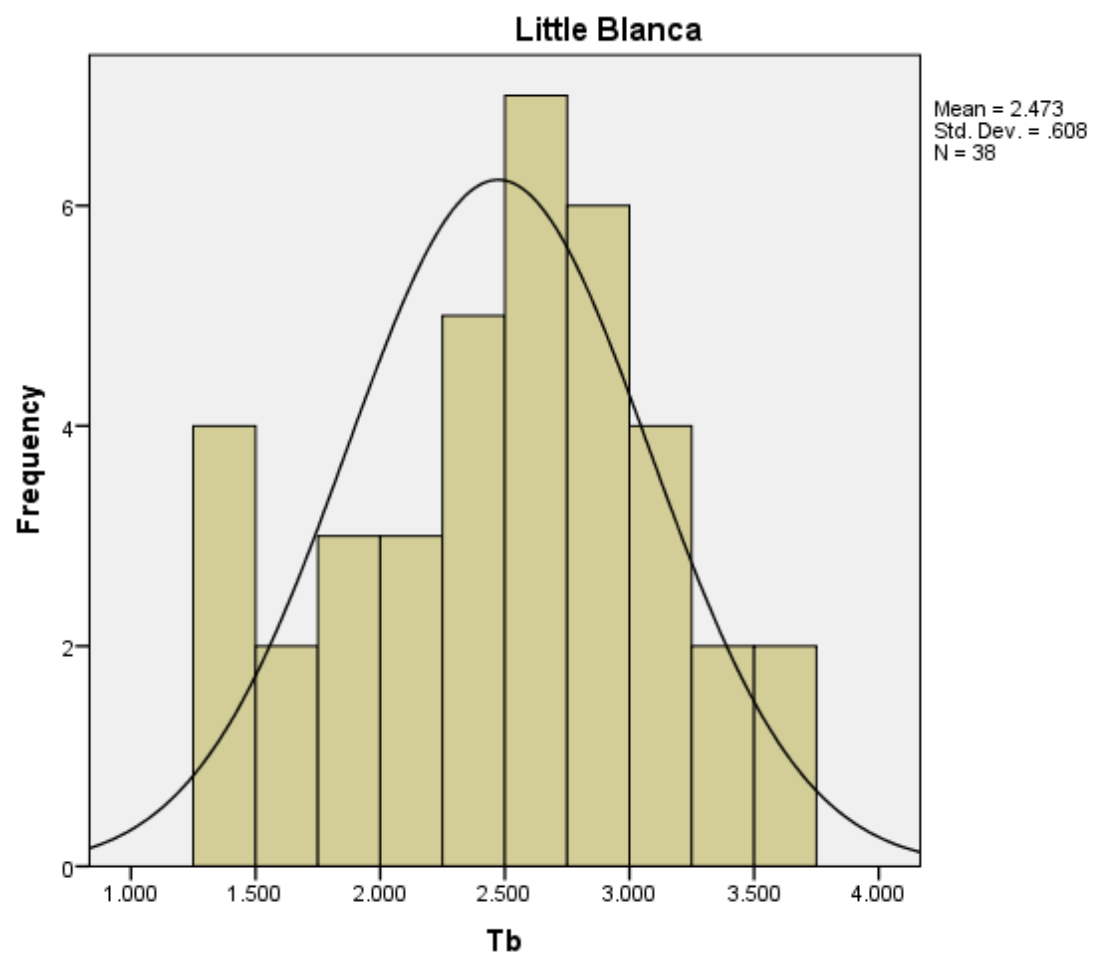


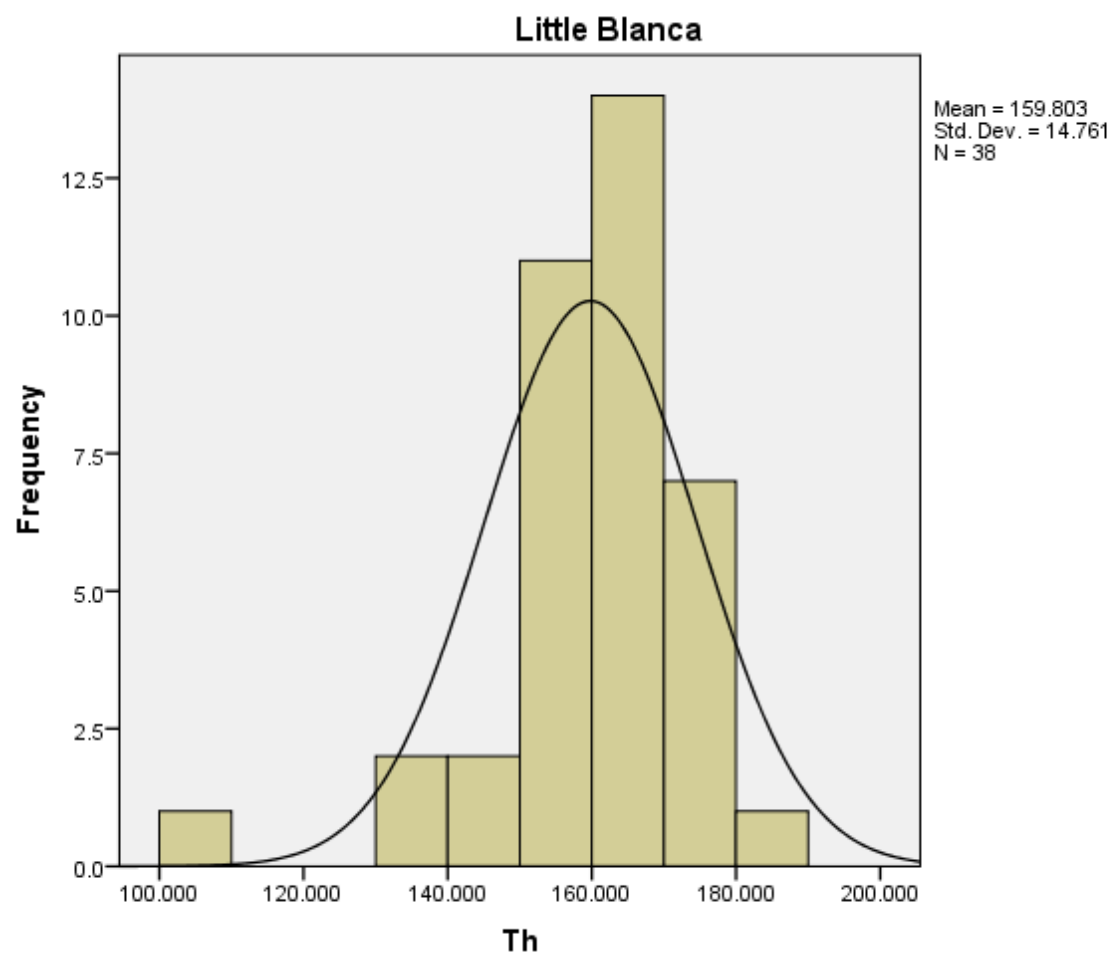


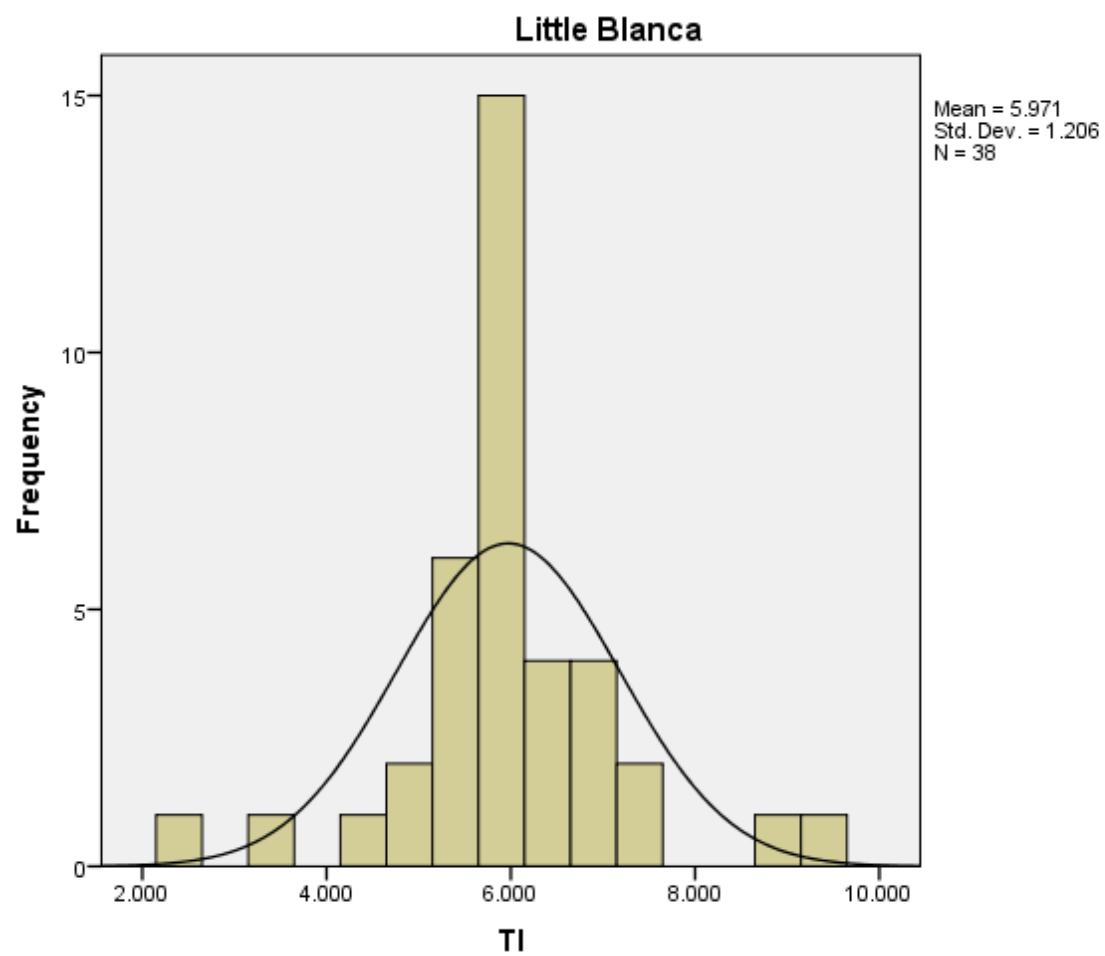


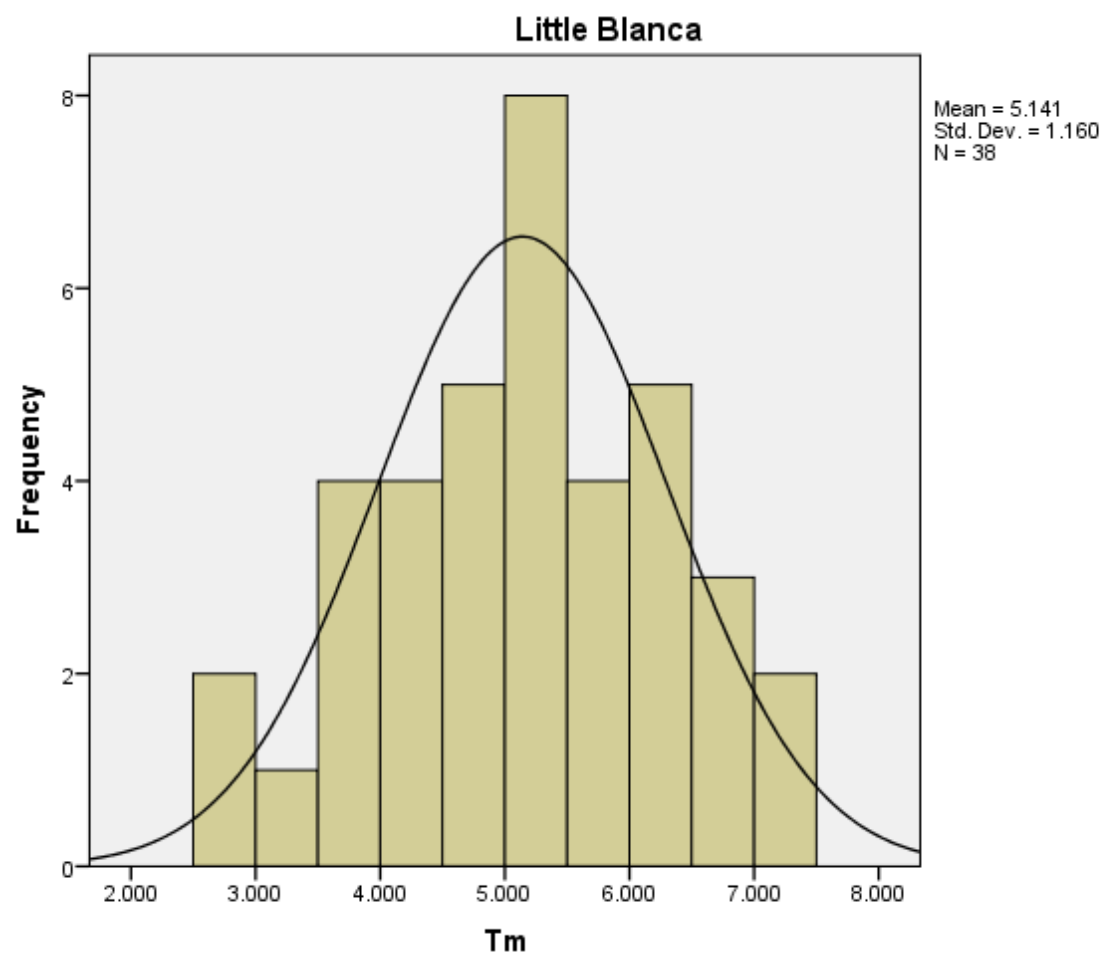


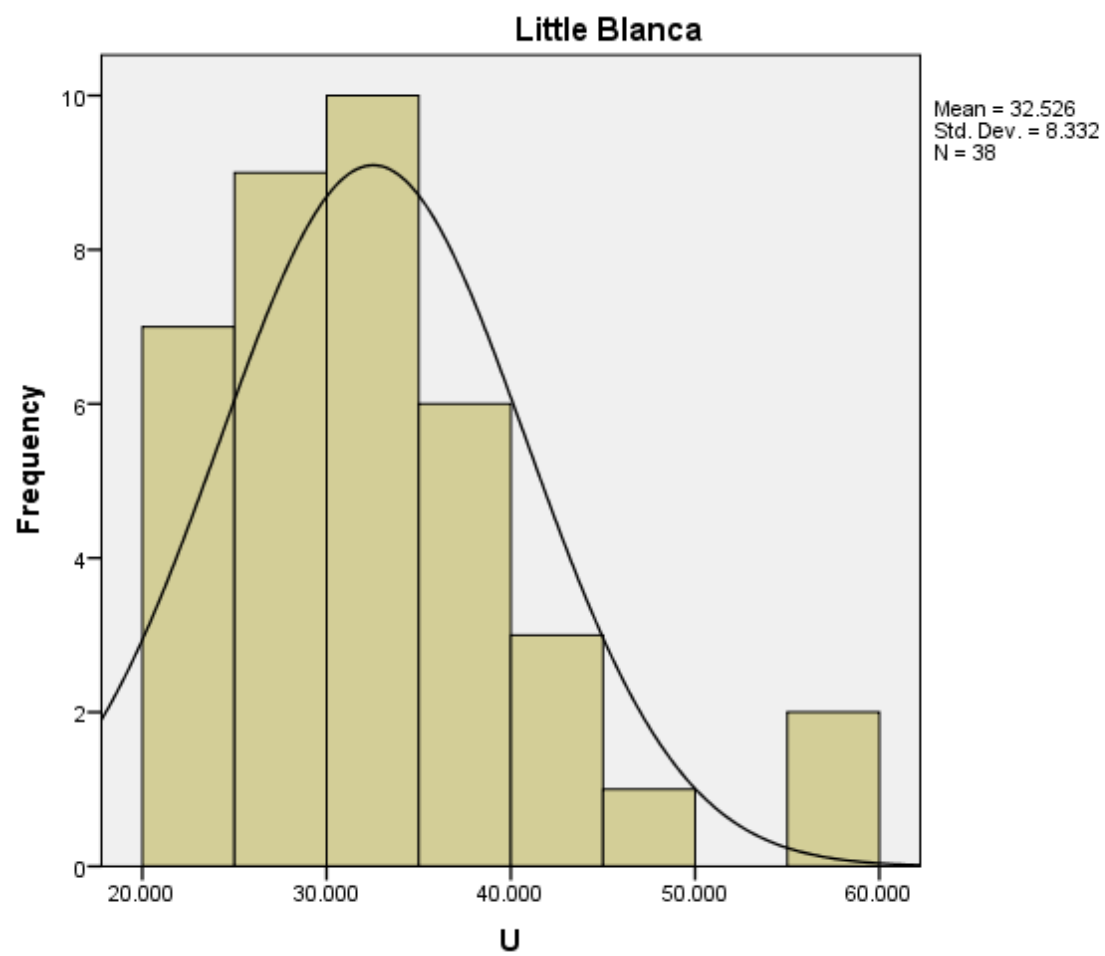


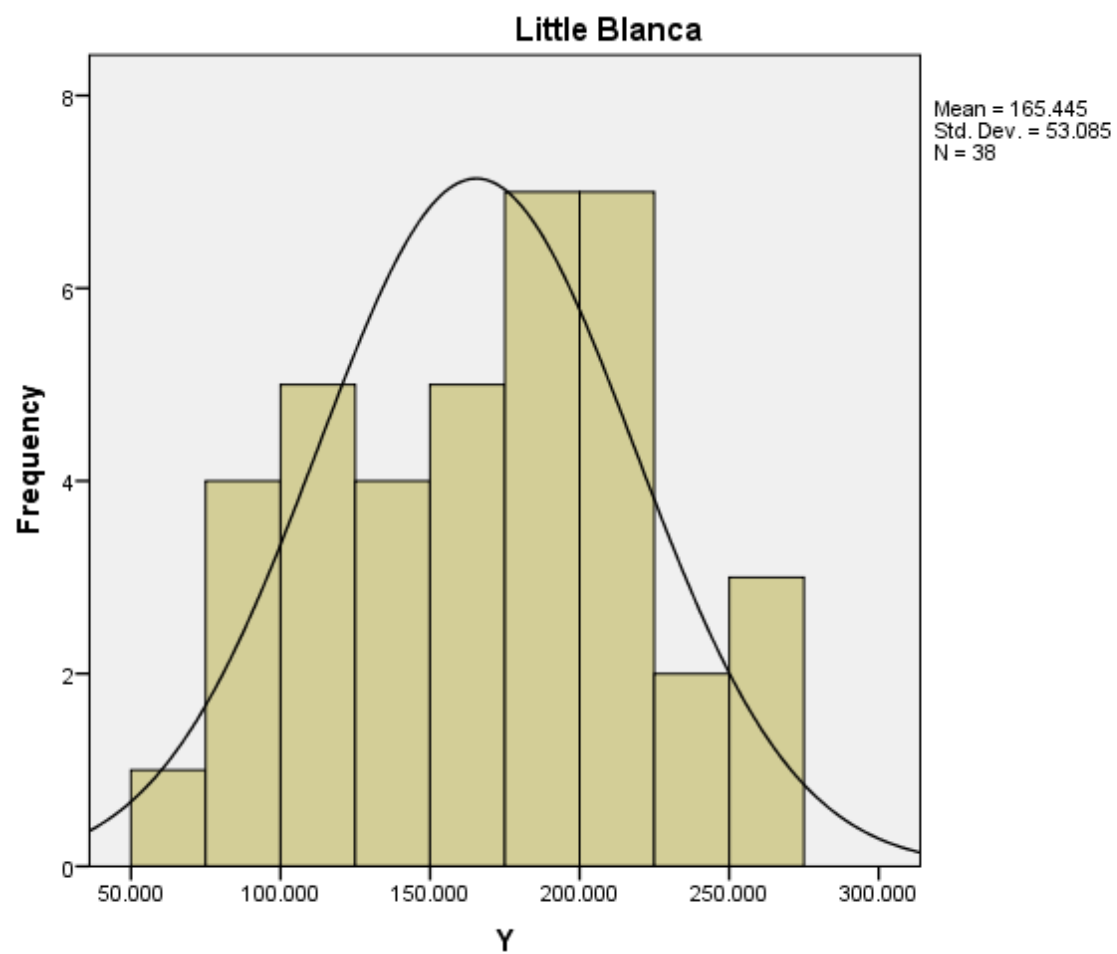


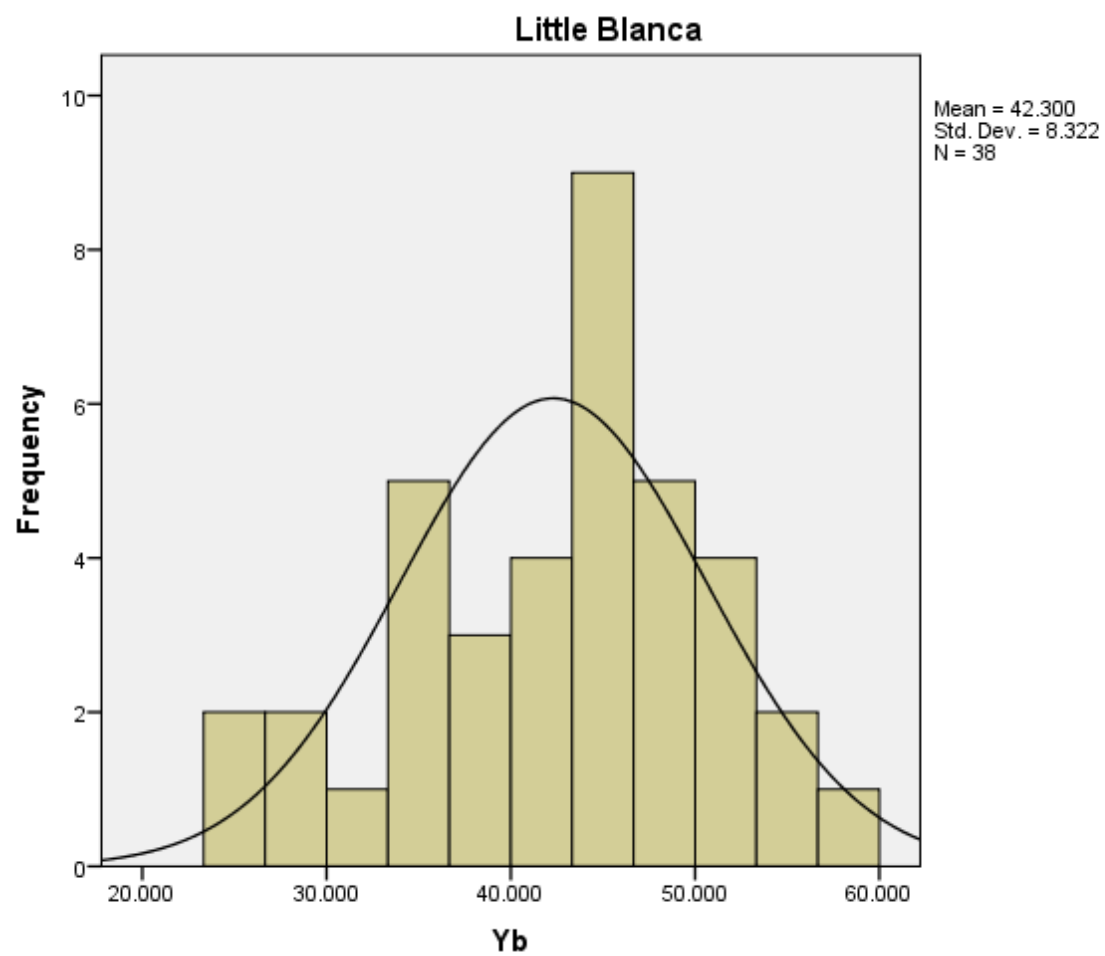


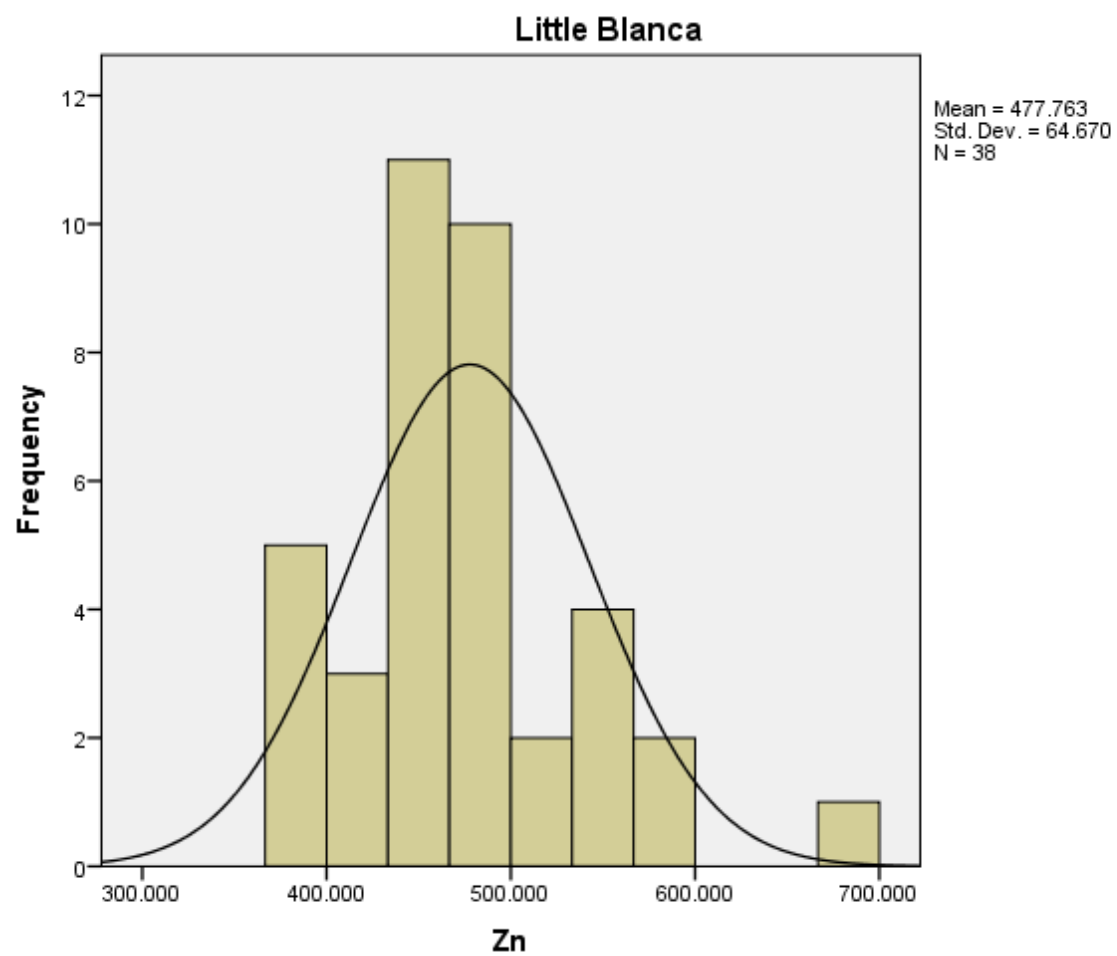


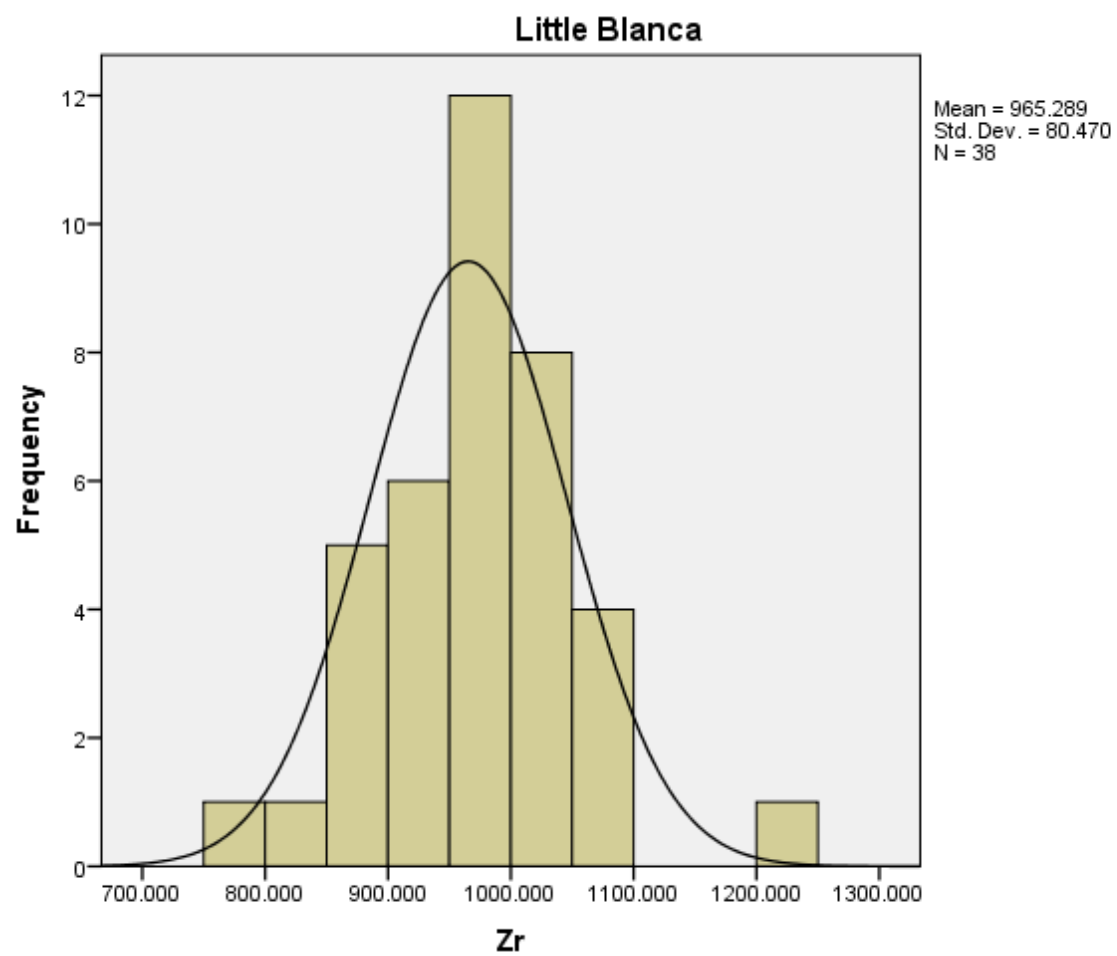


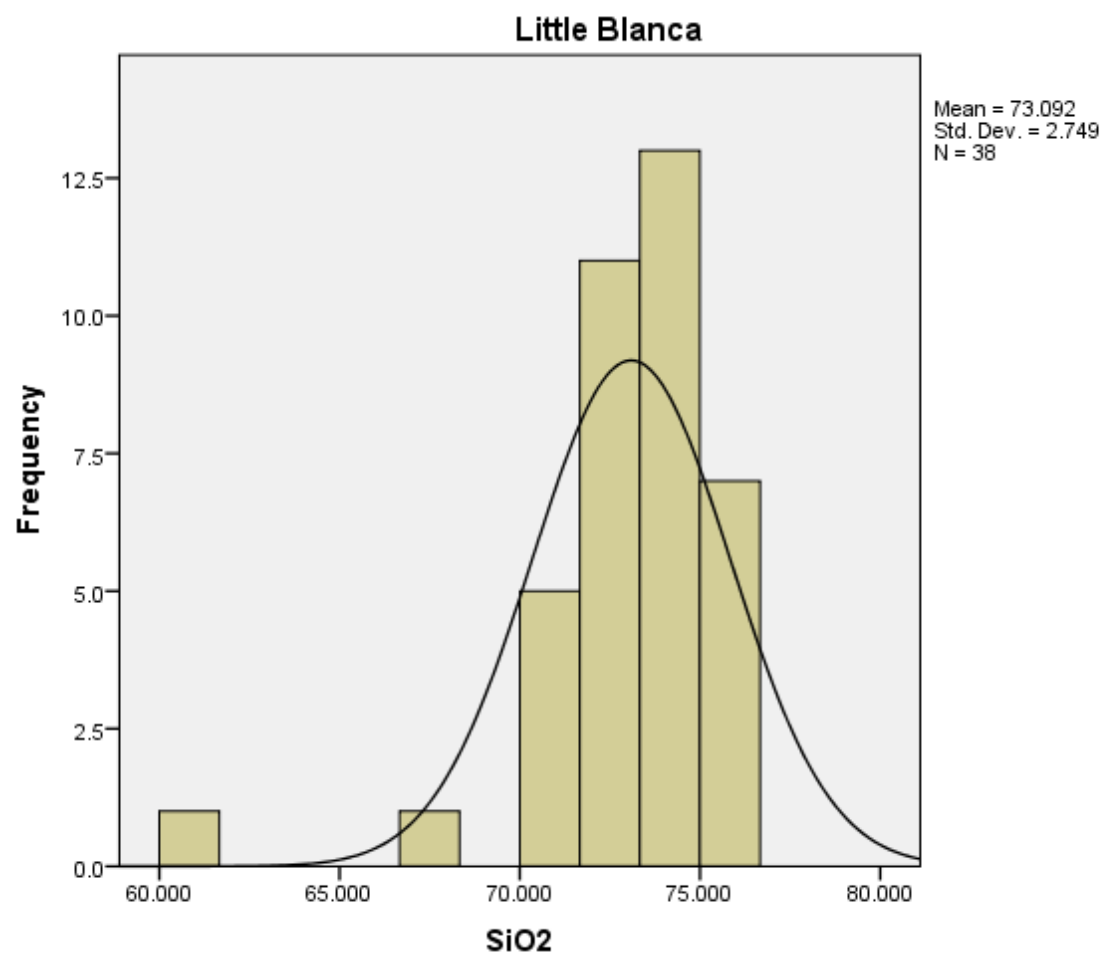


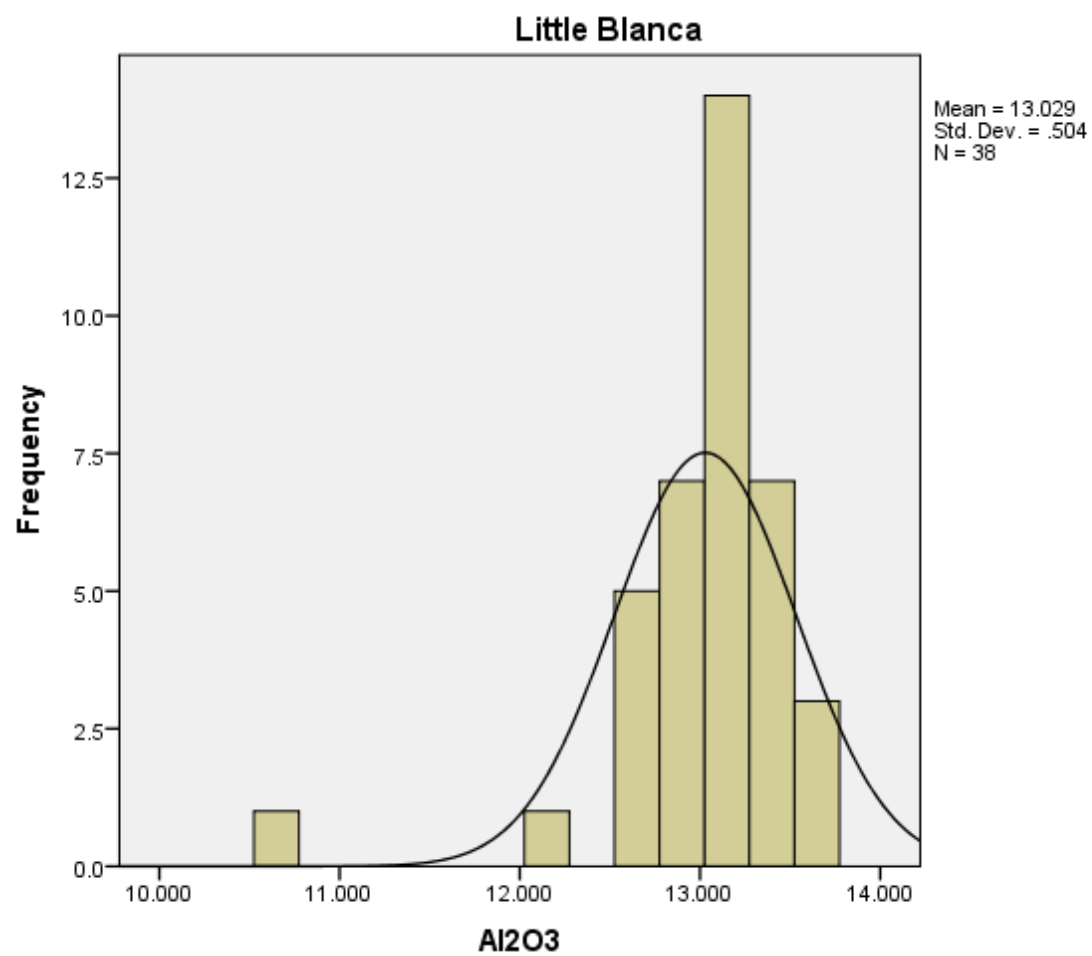


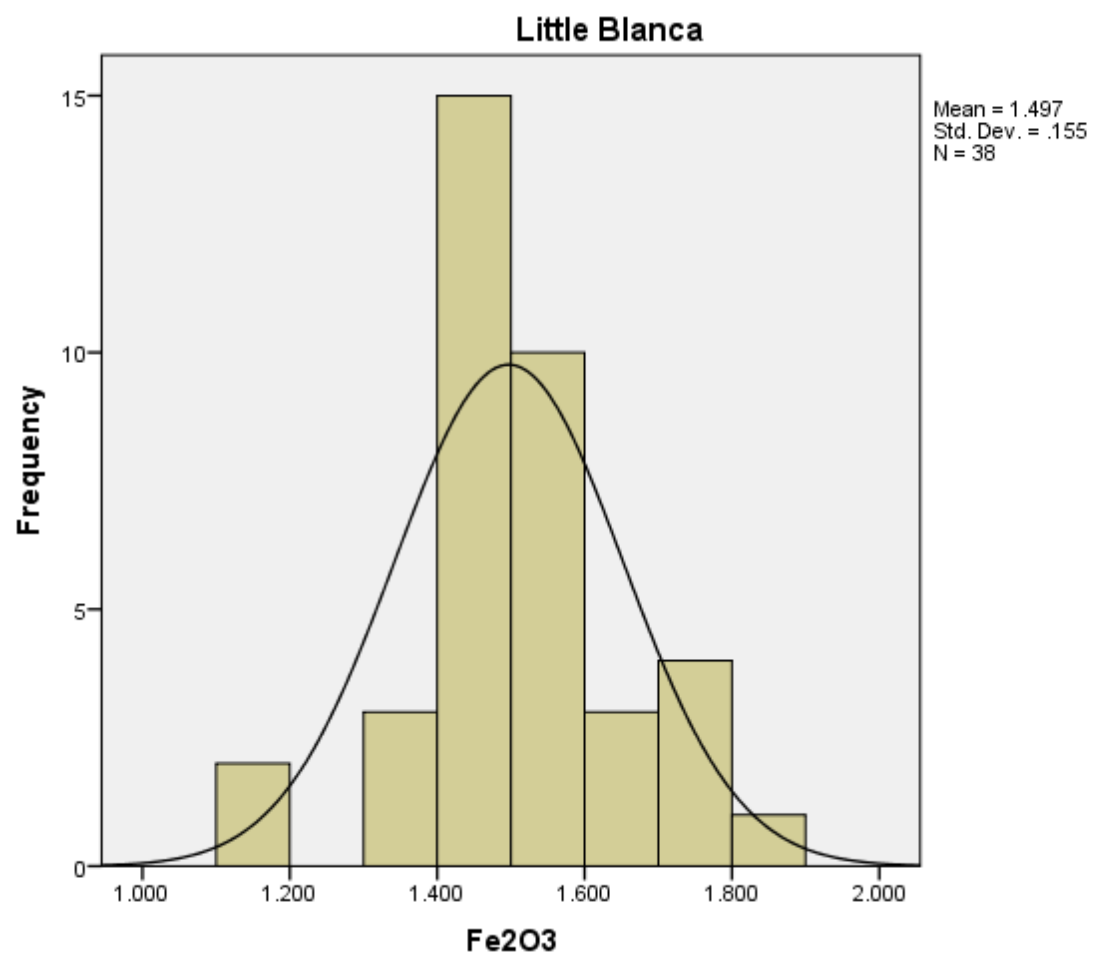


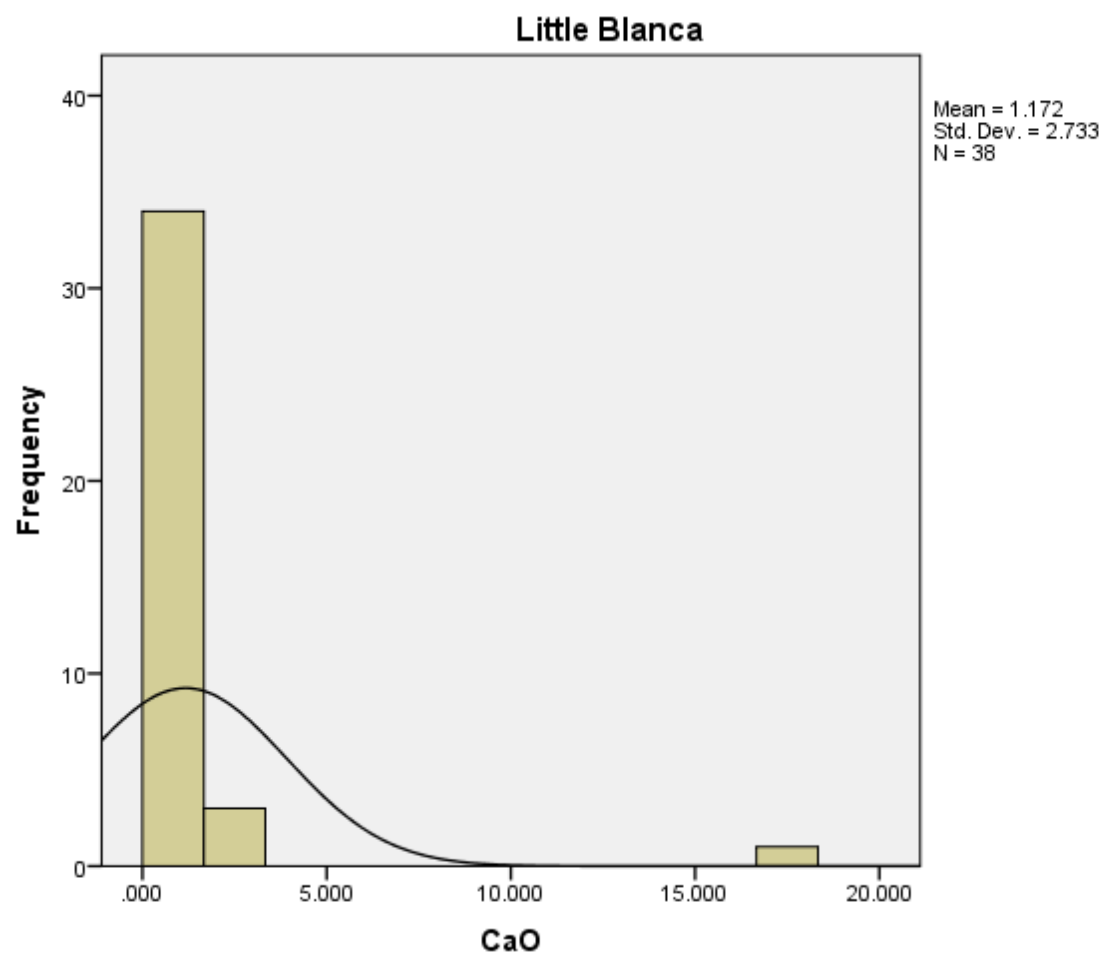


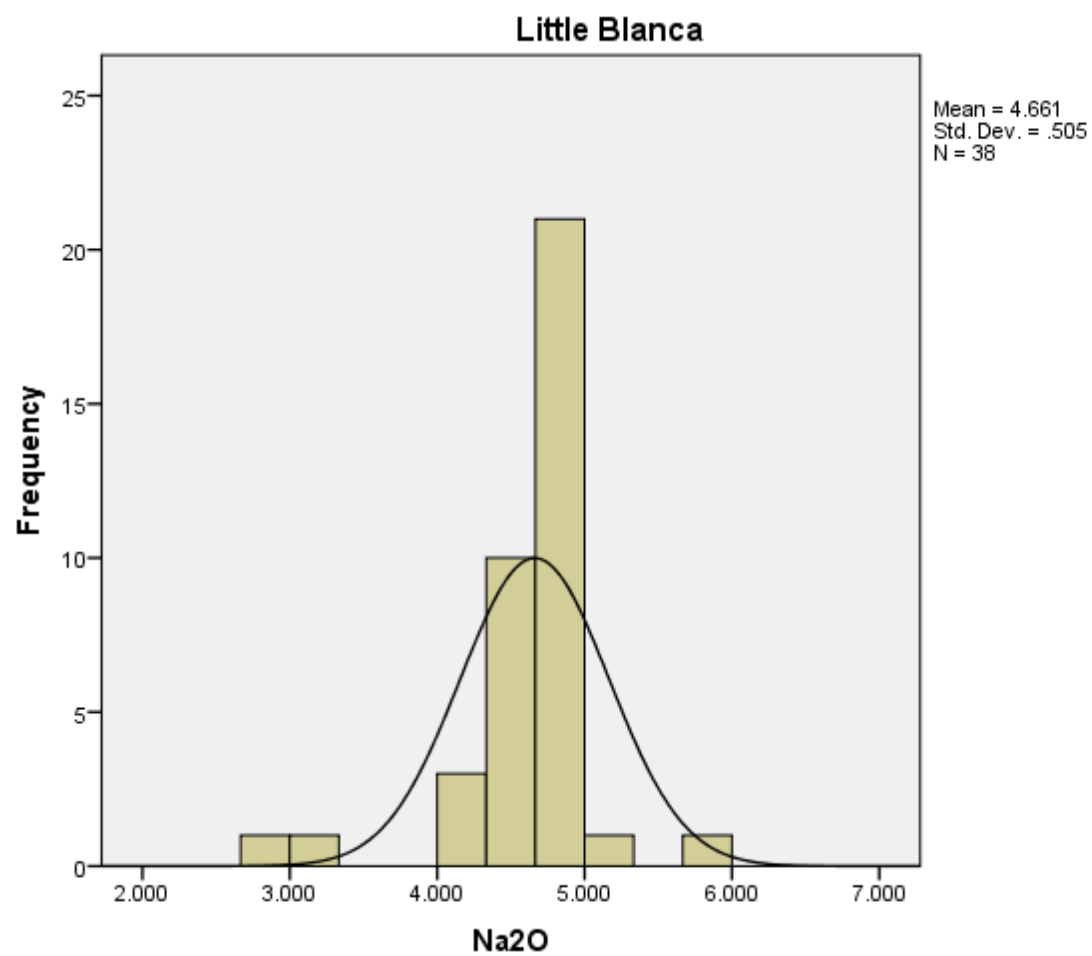


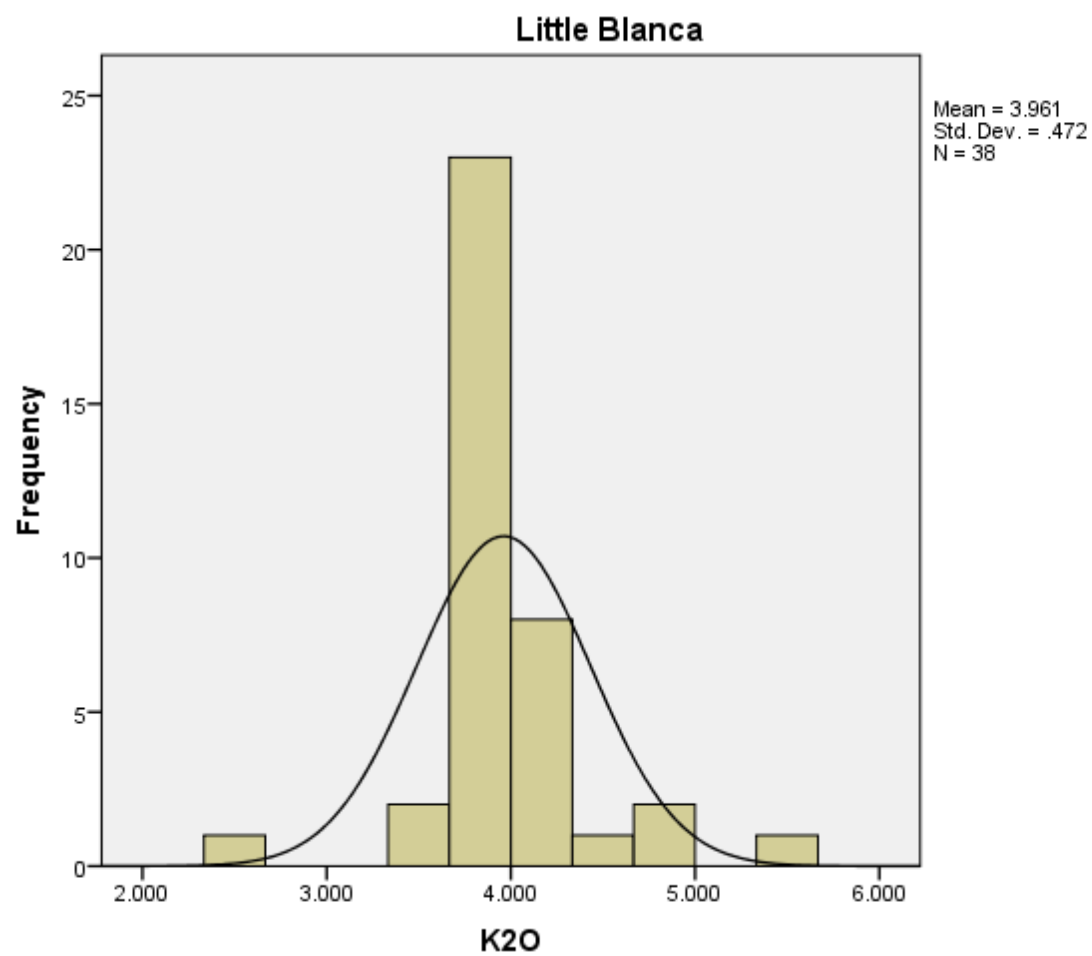


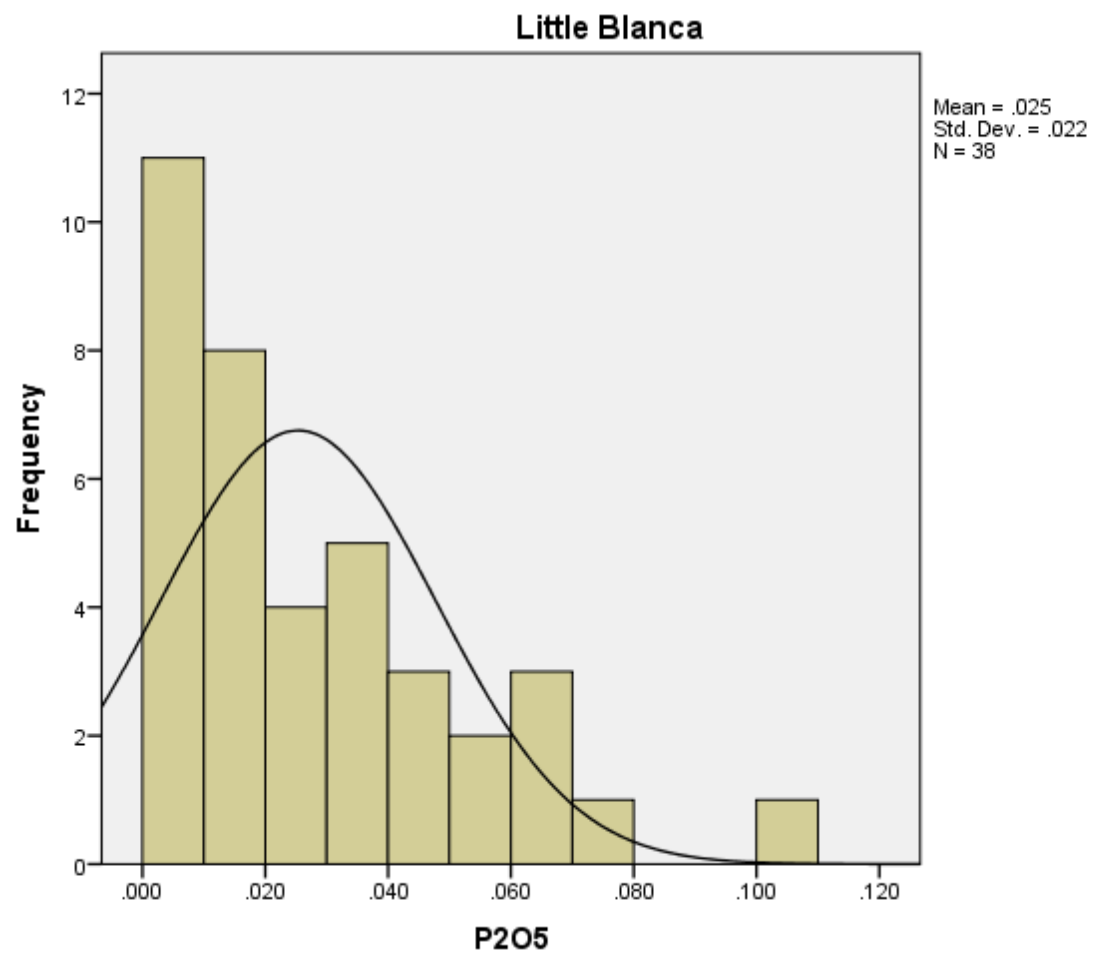


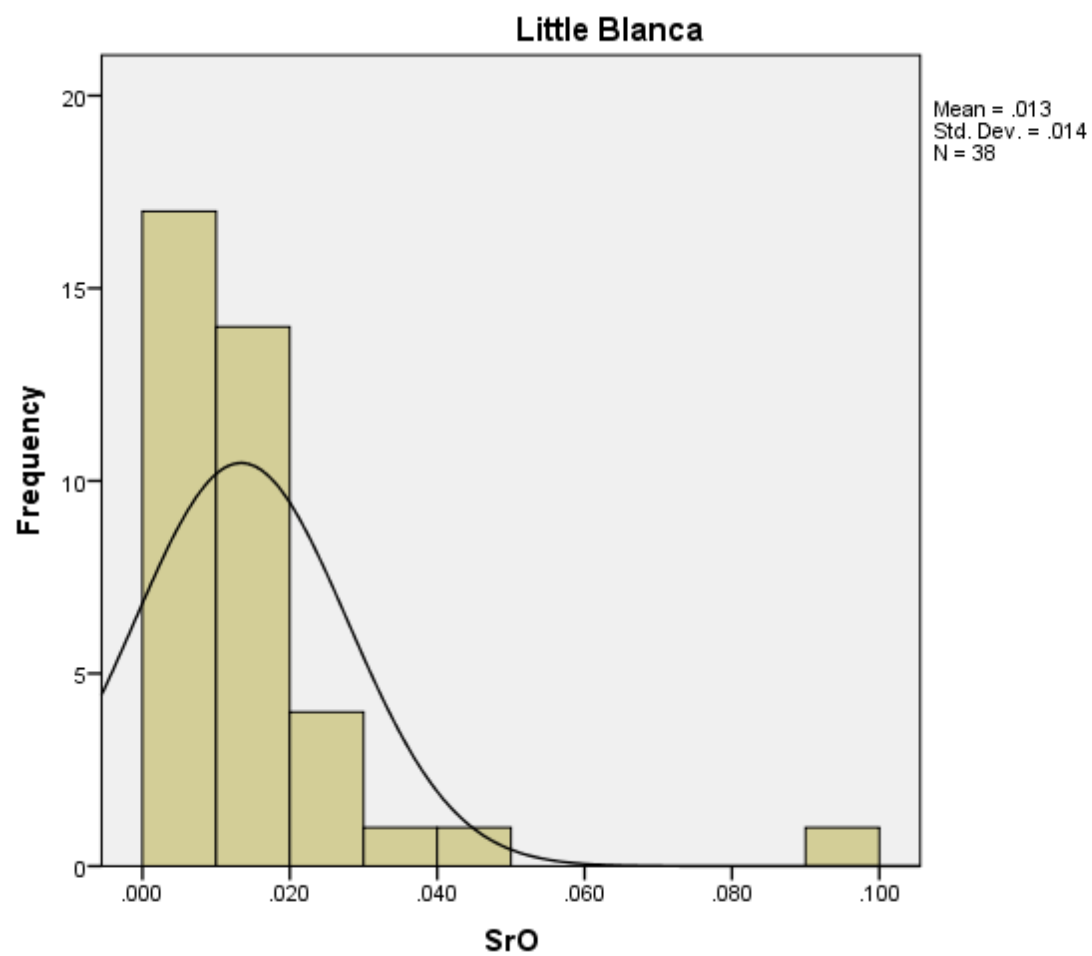


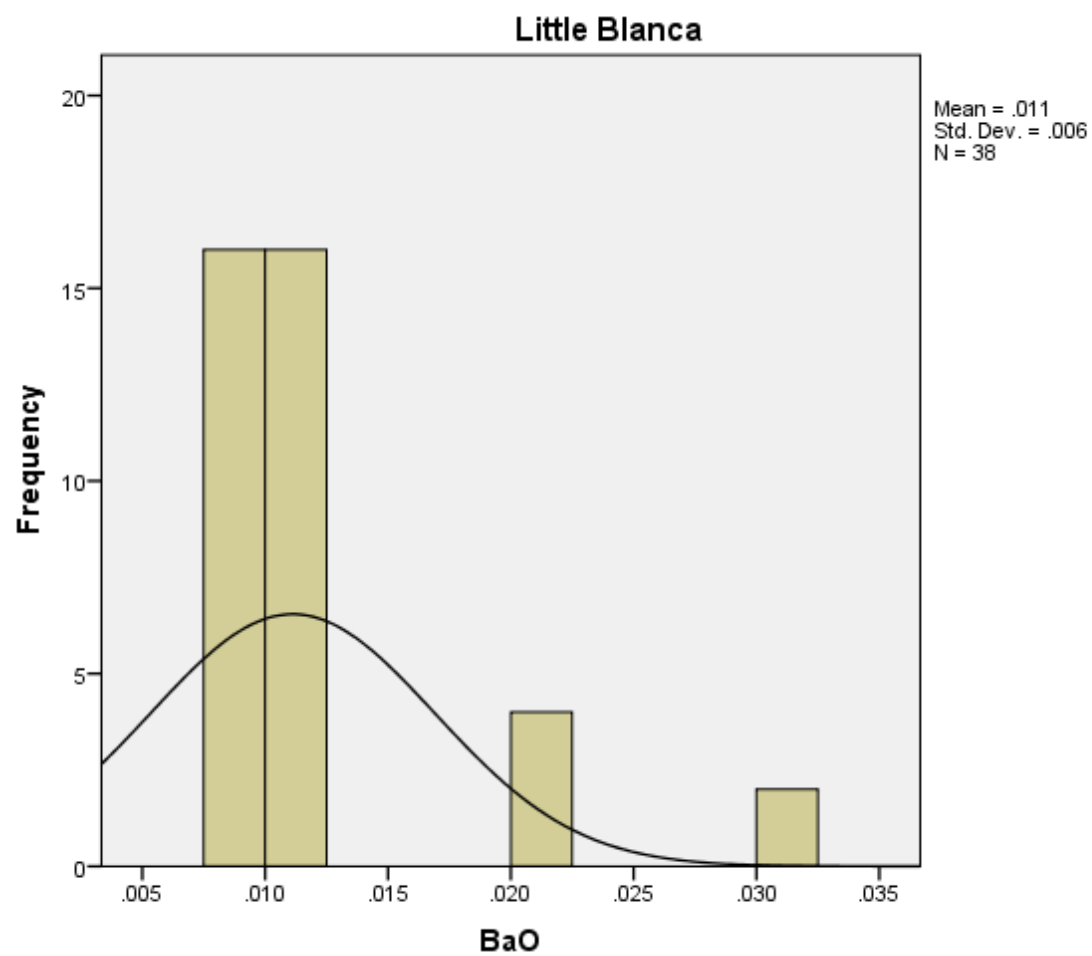




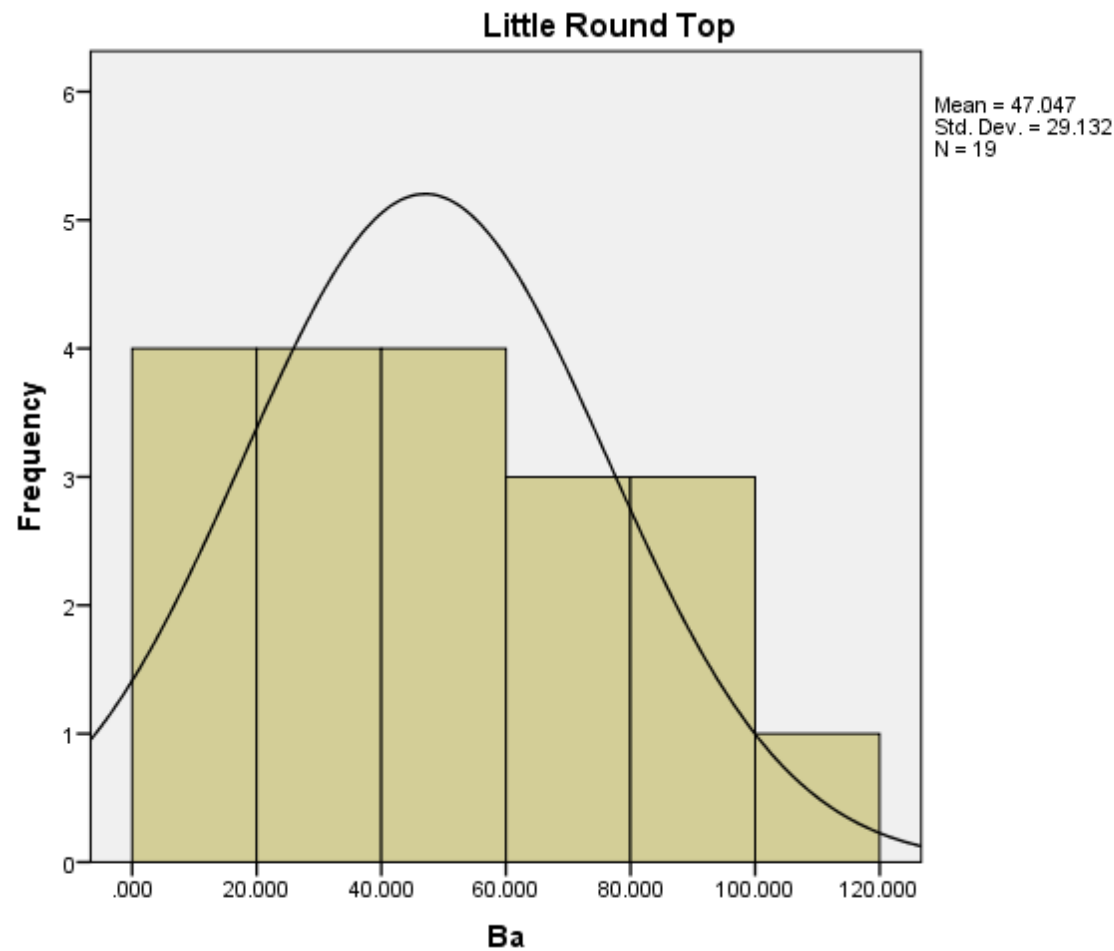


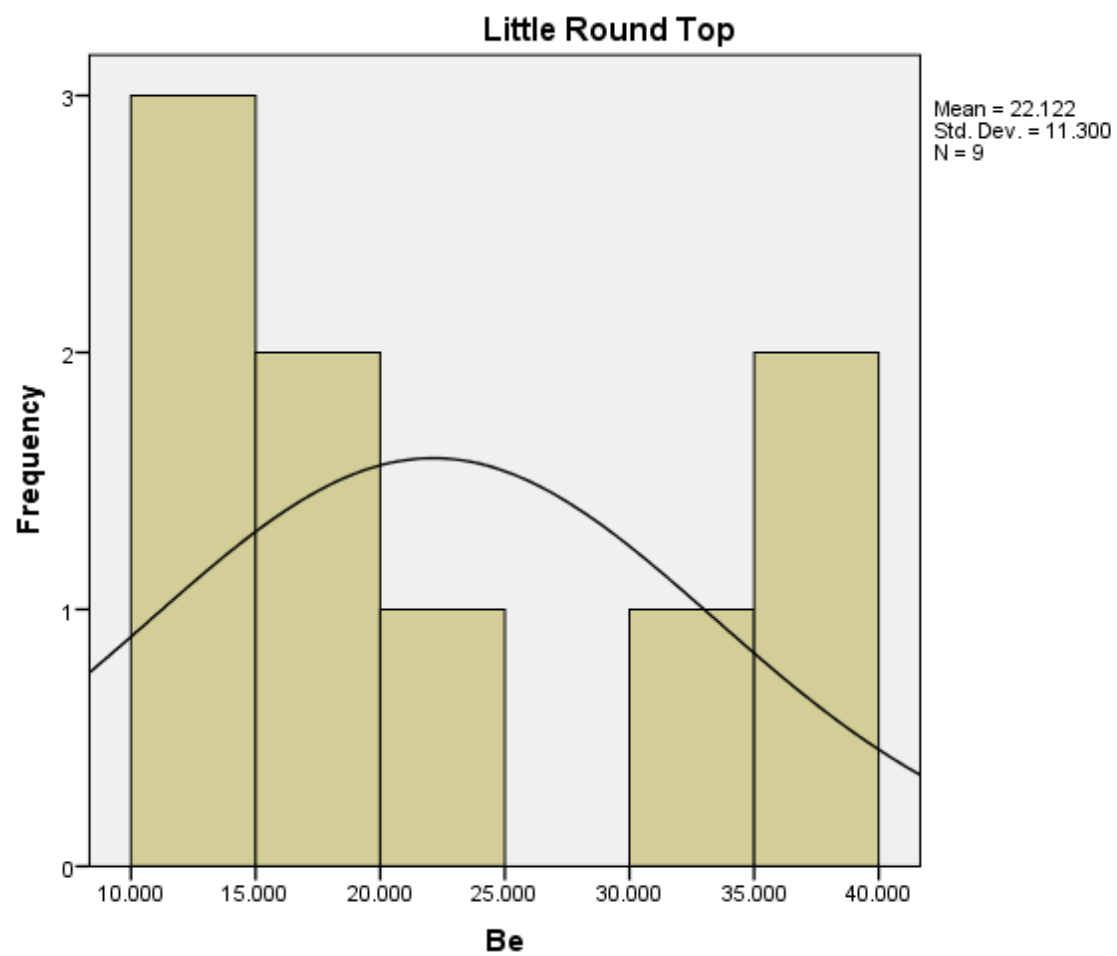


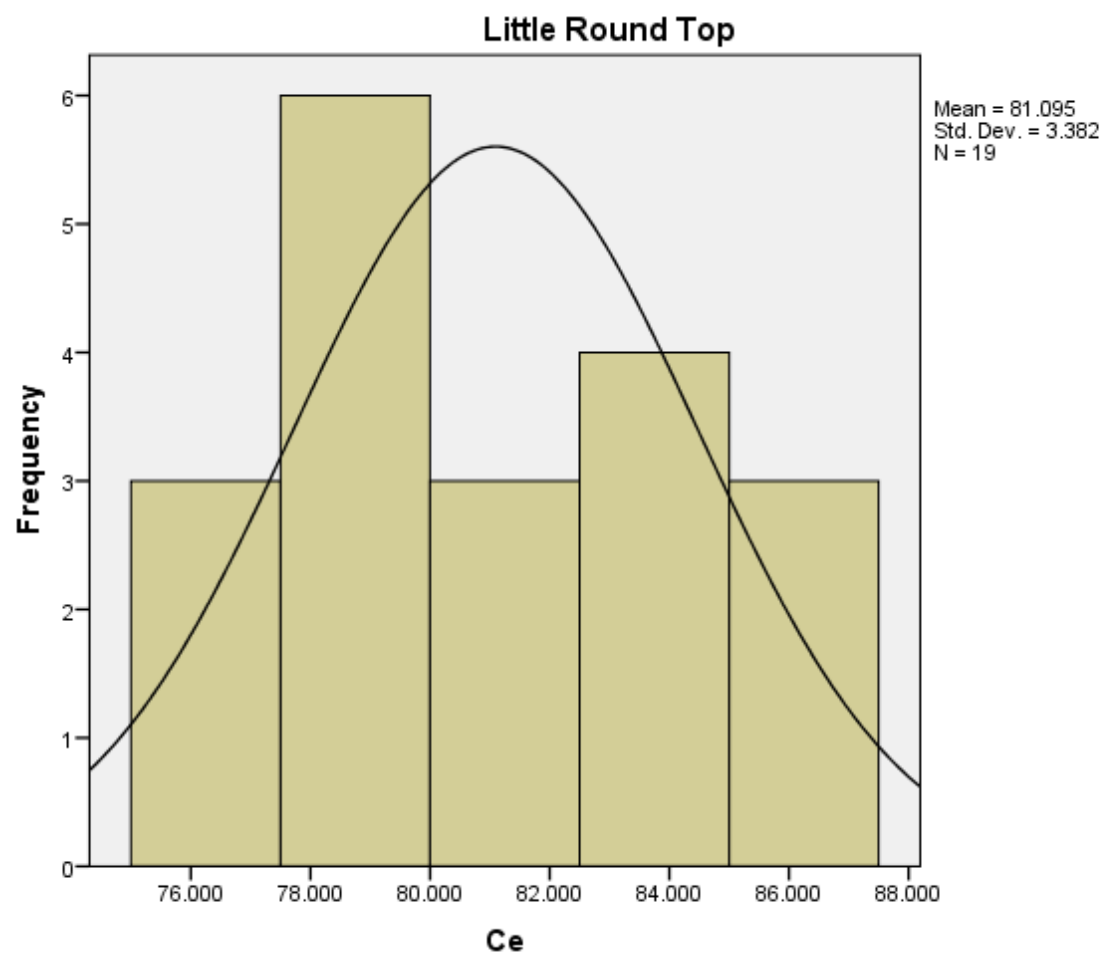


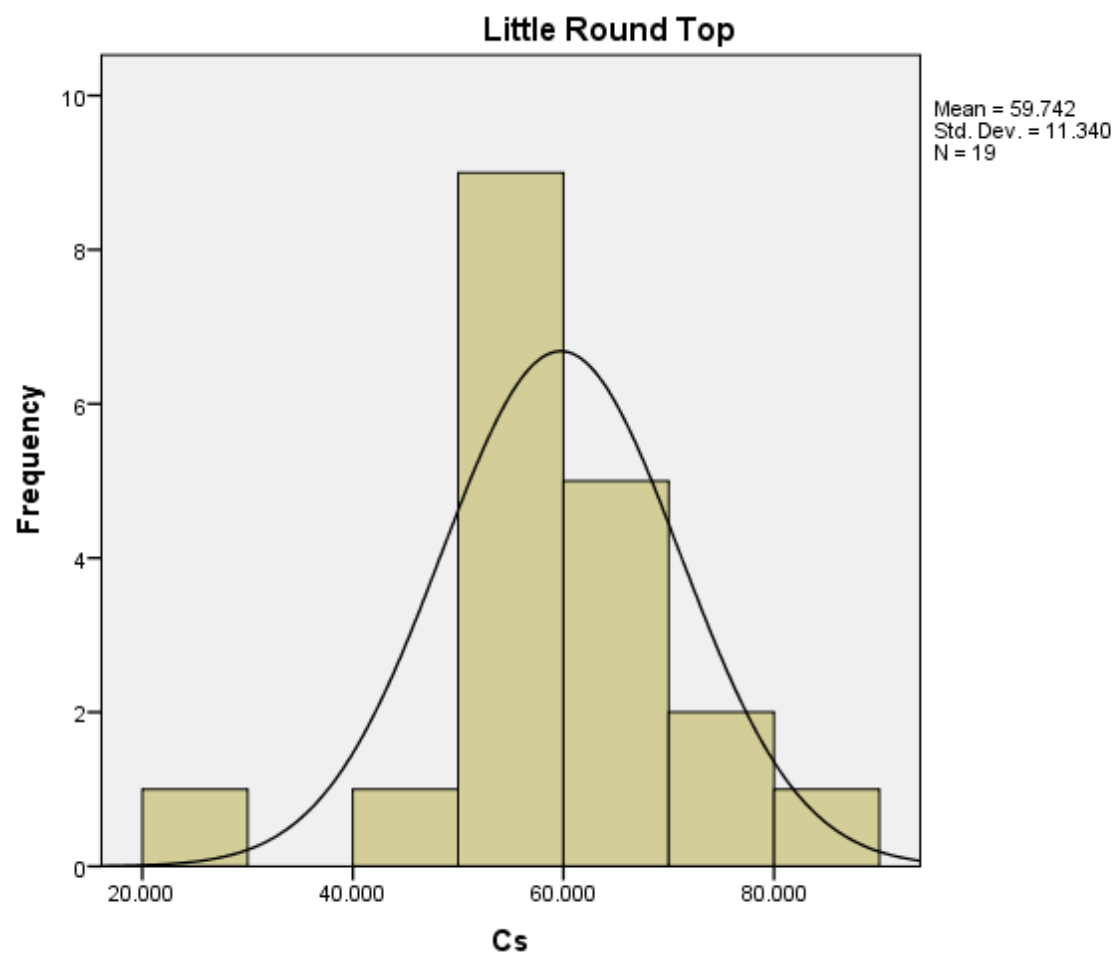


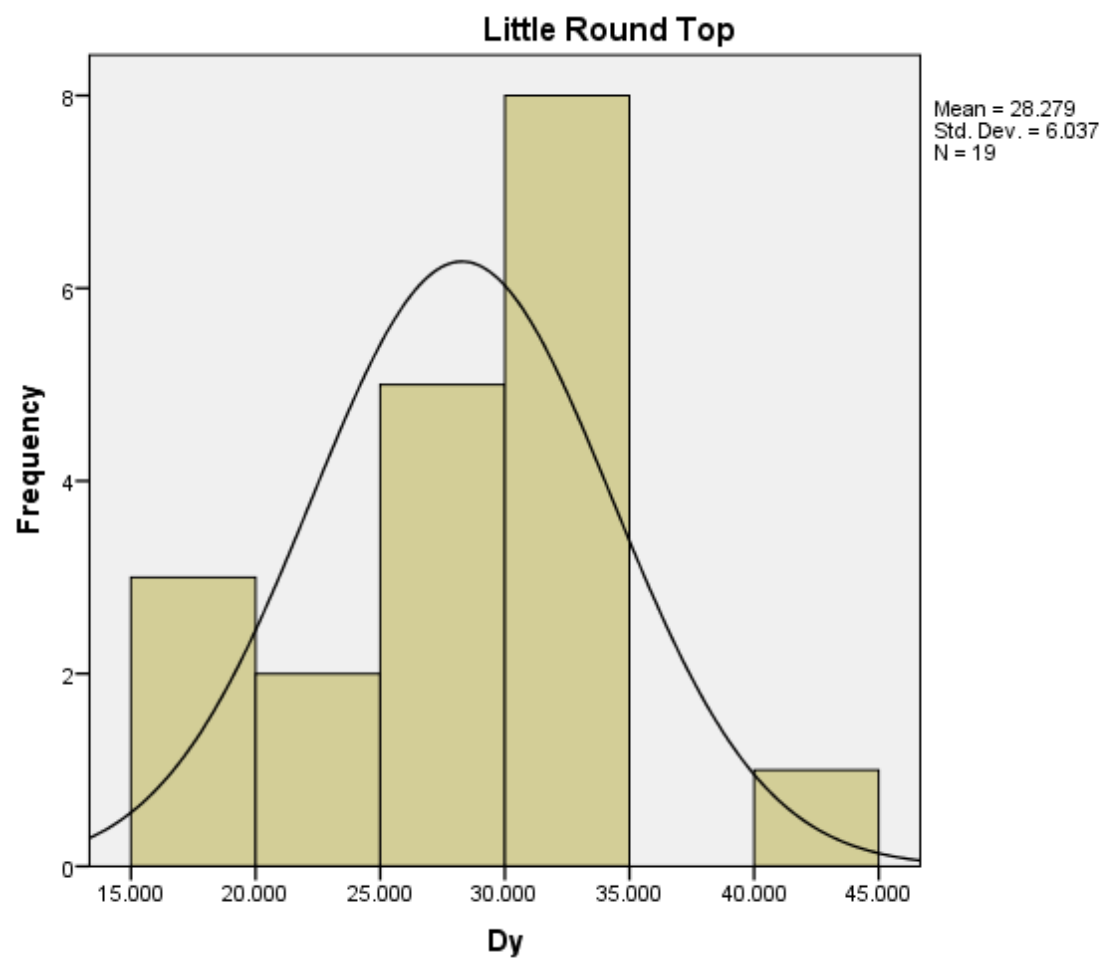
Histograms: Little Round Top

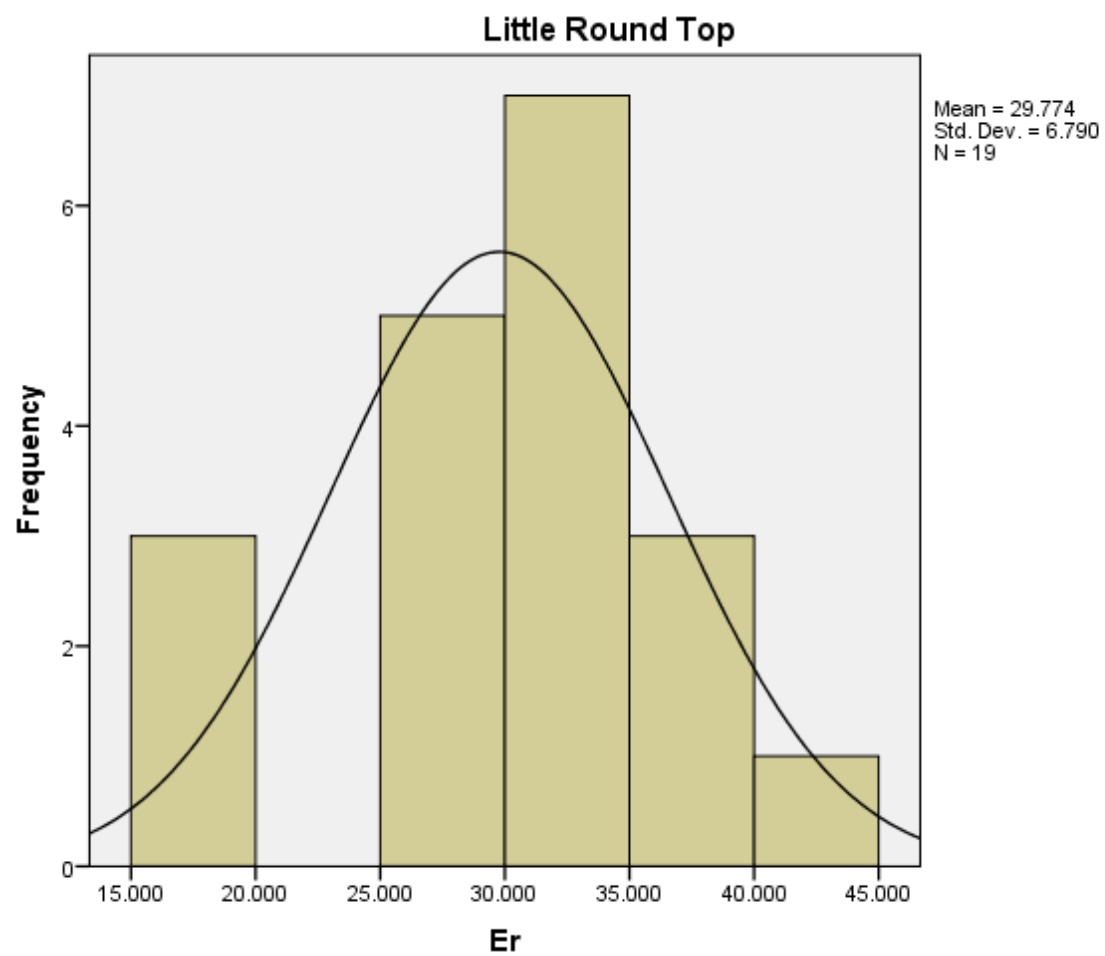


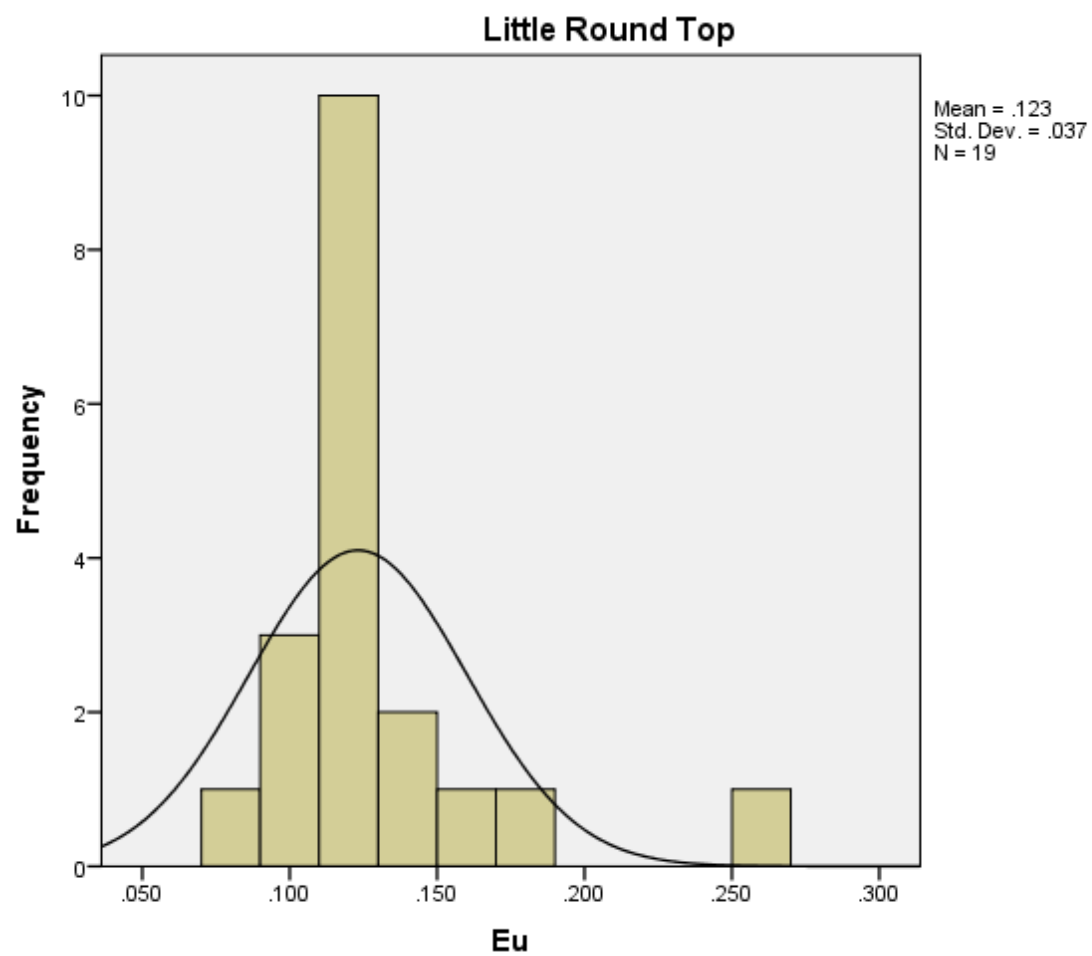


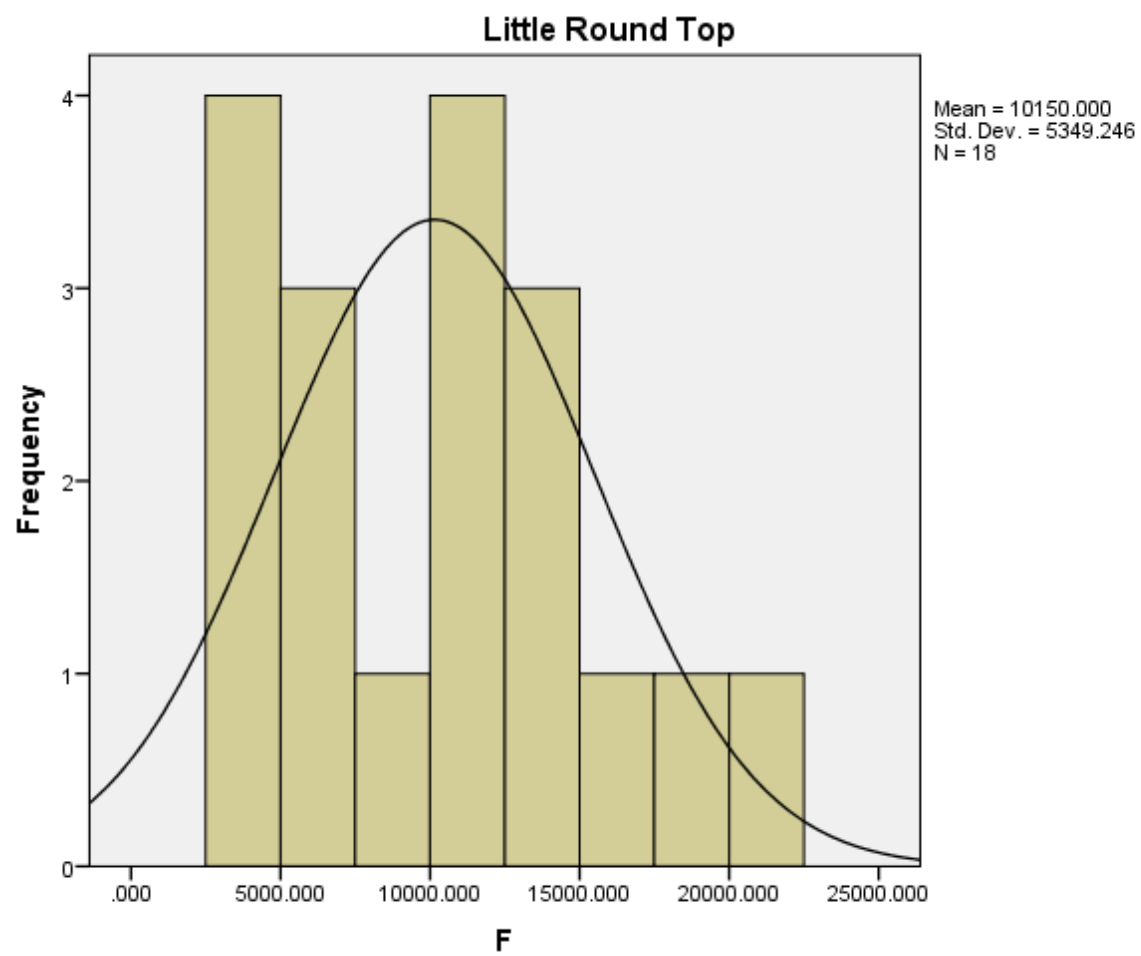


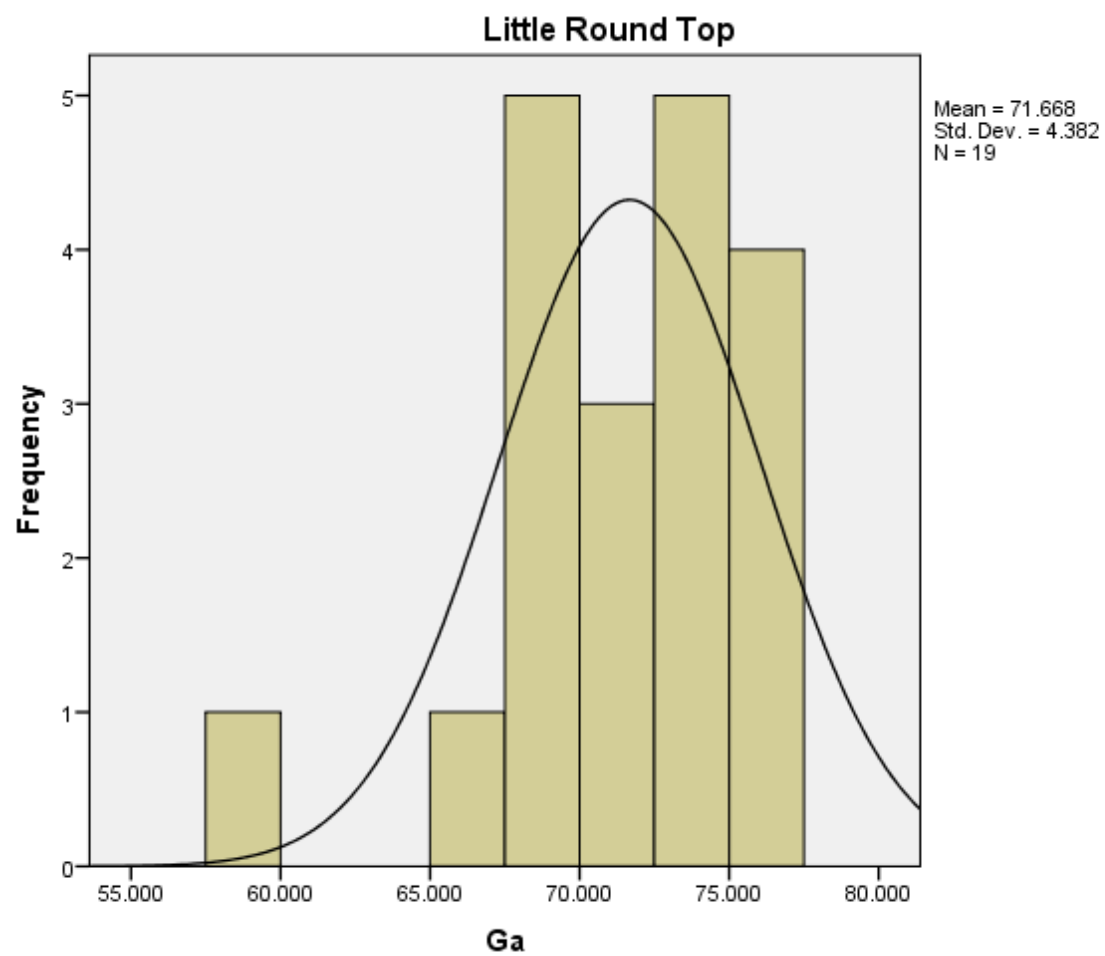


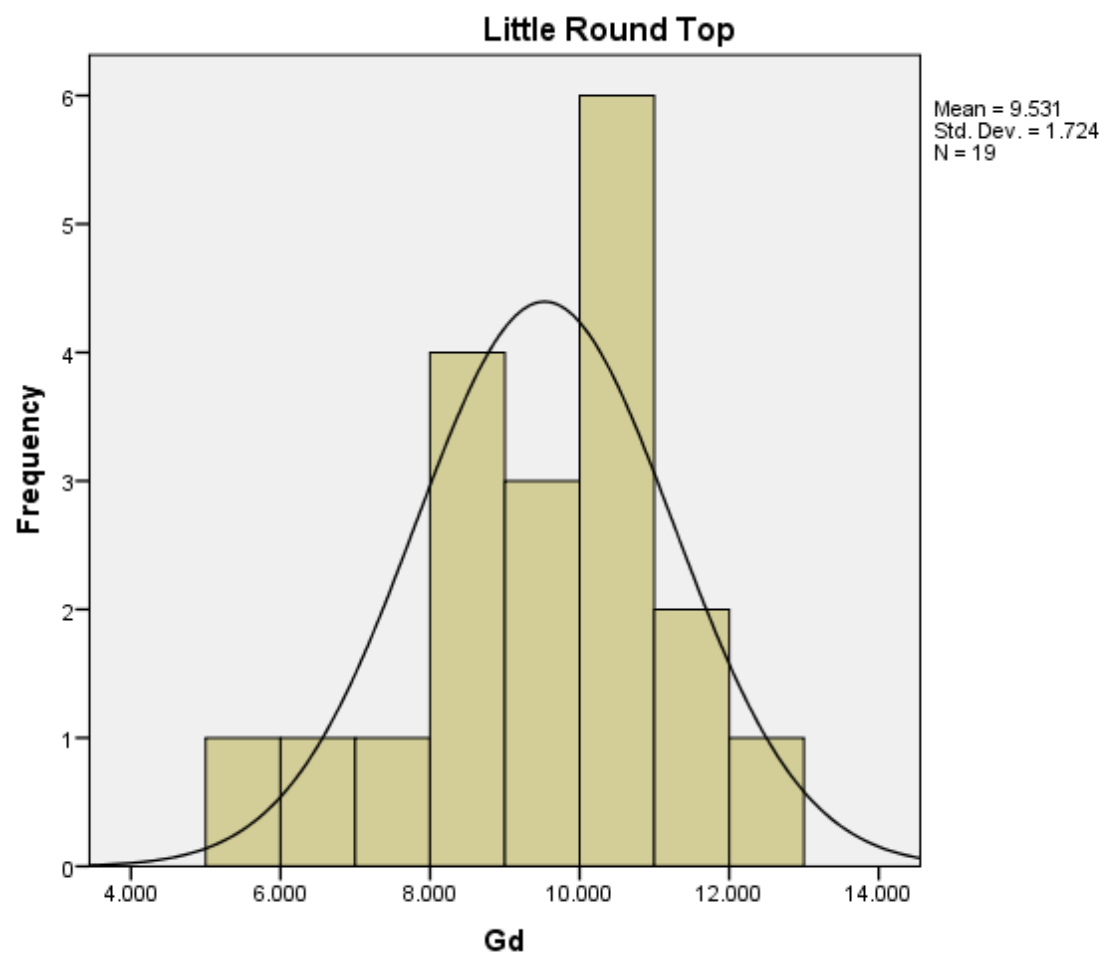


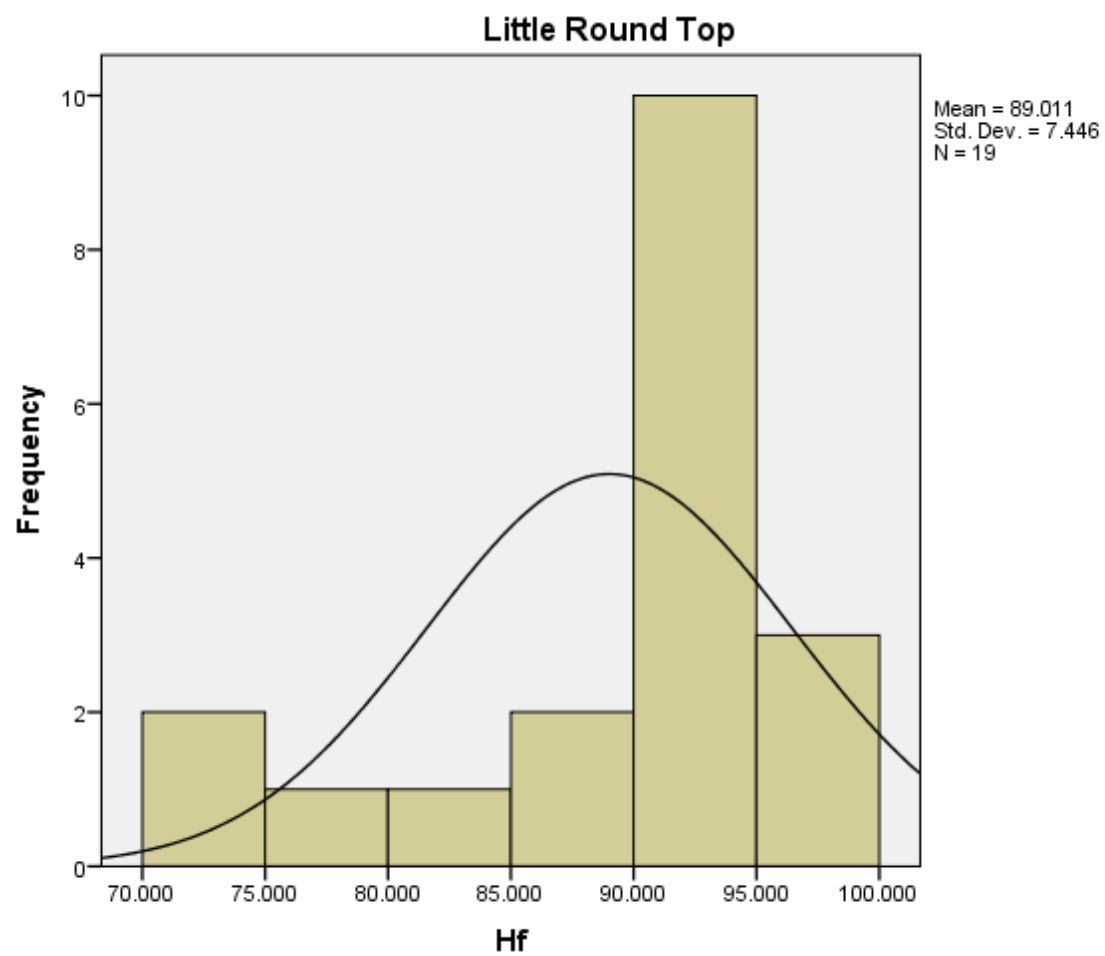


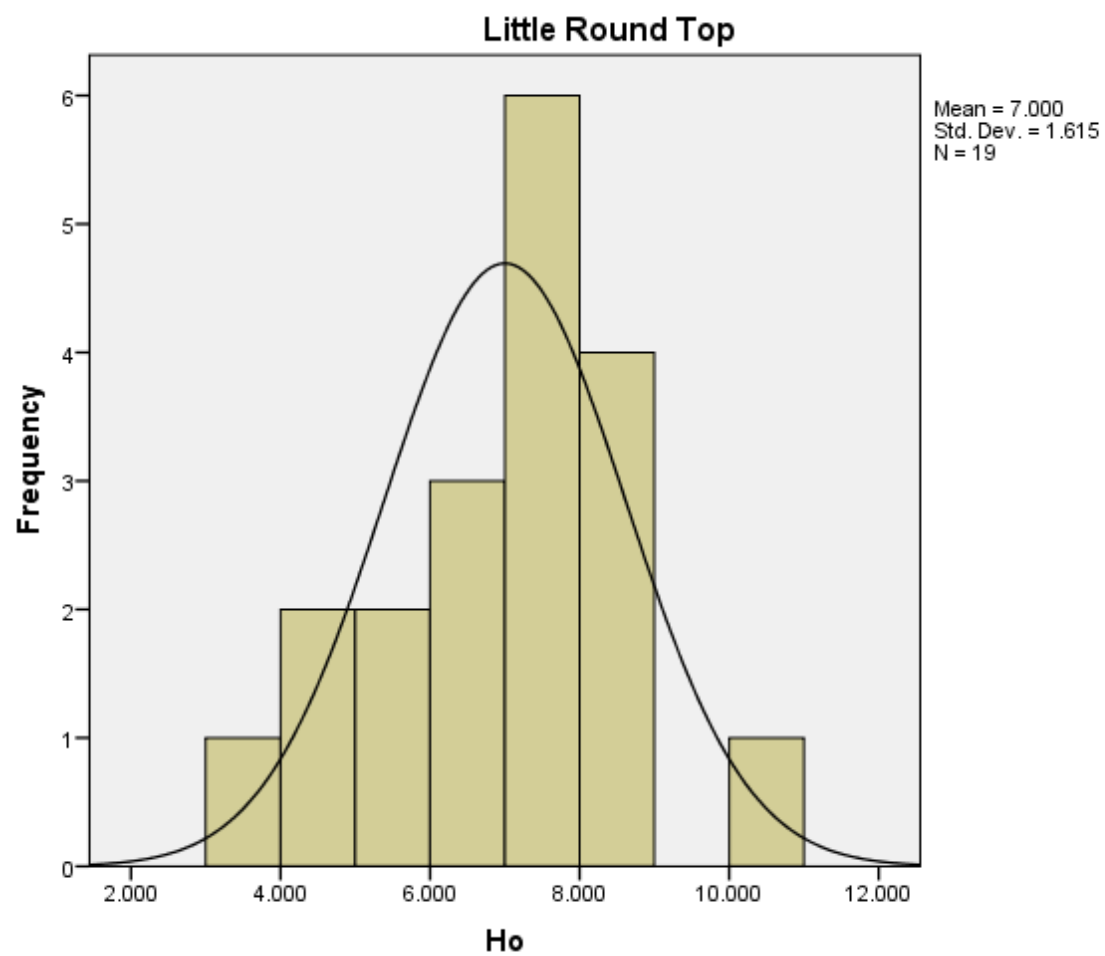


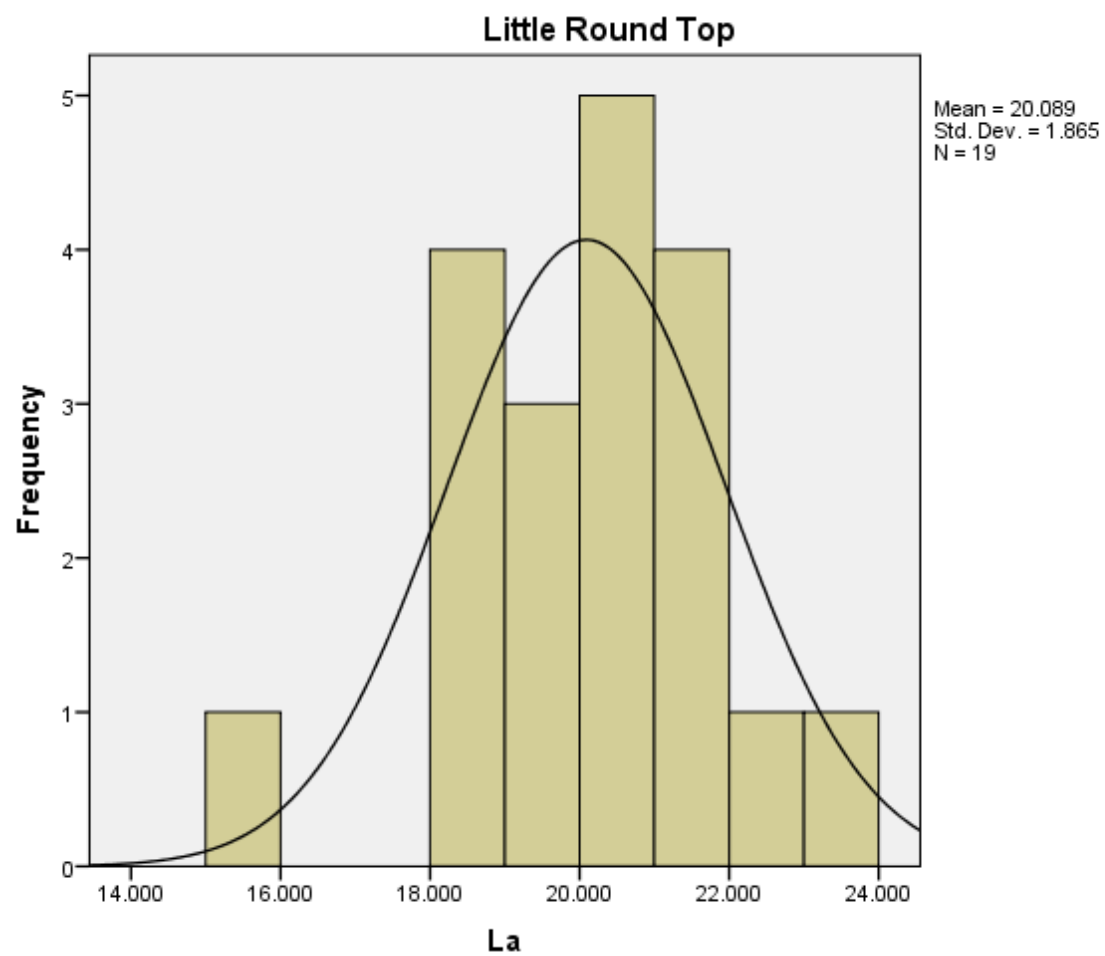


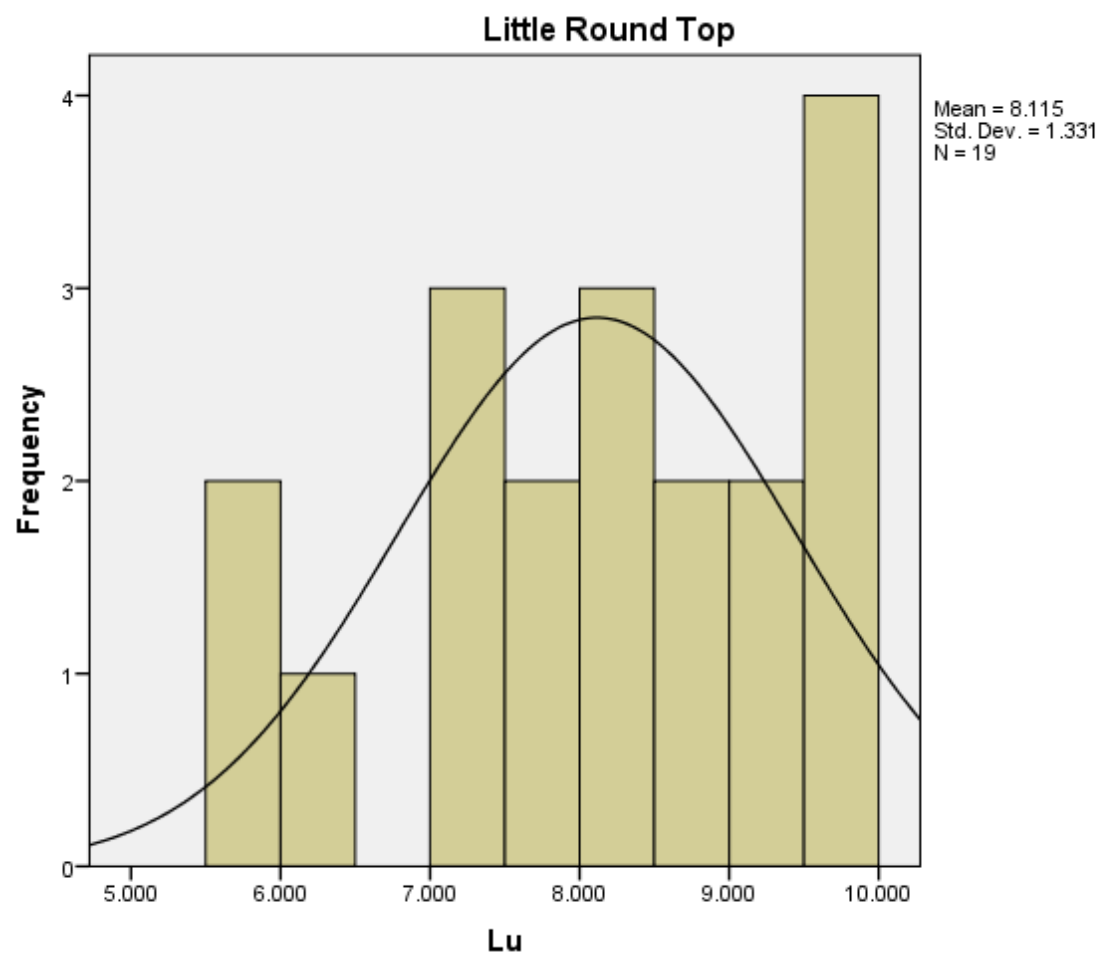


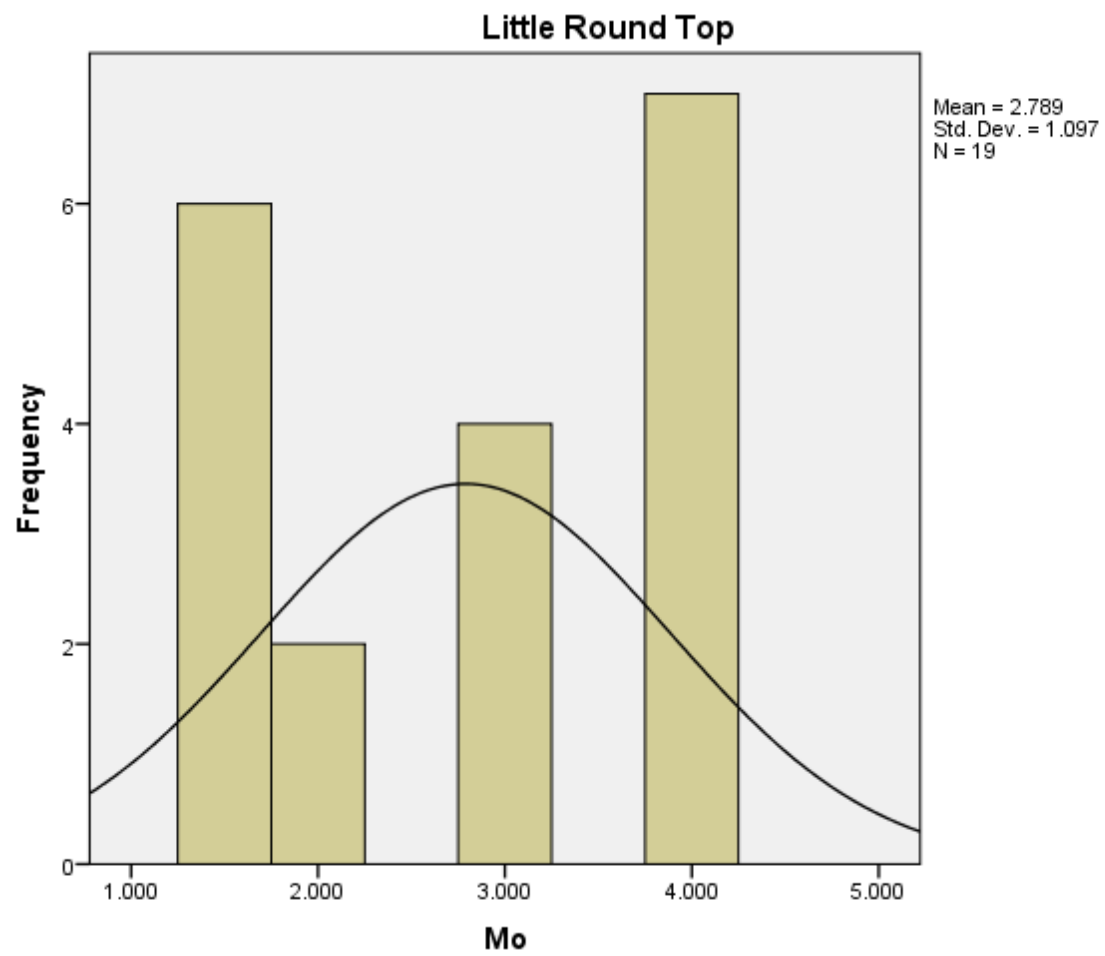


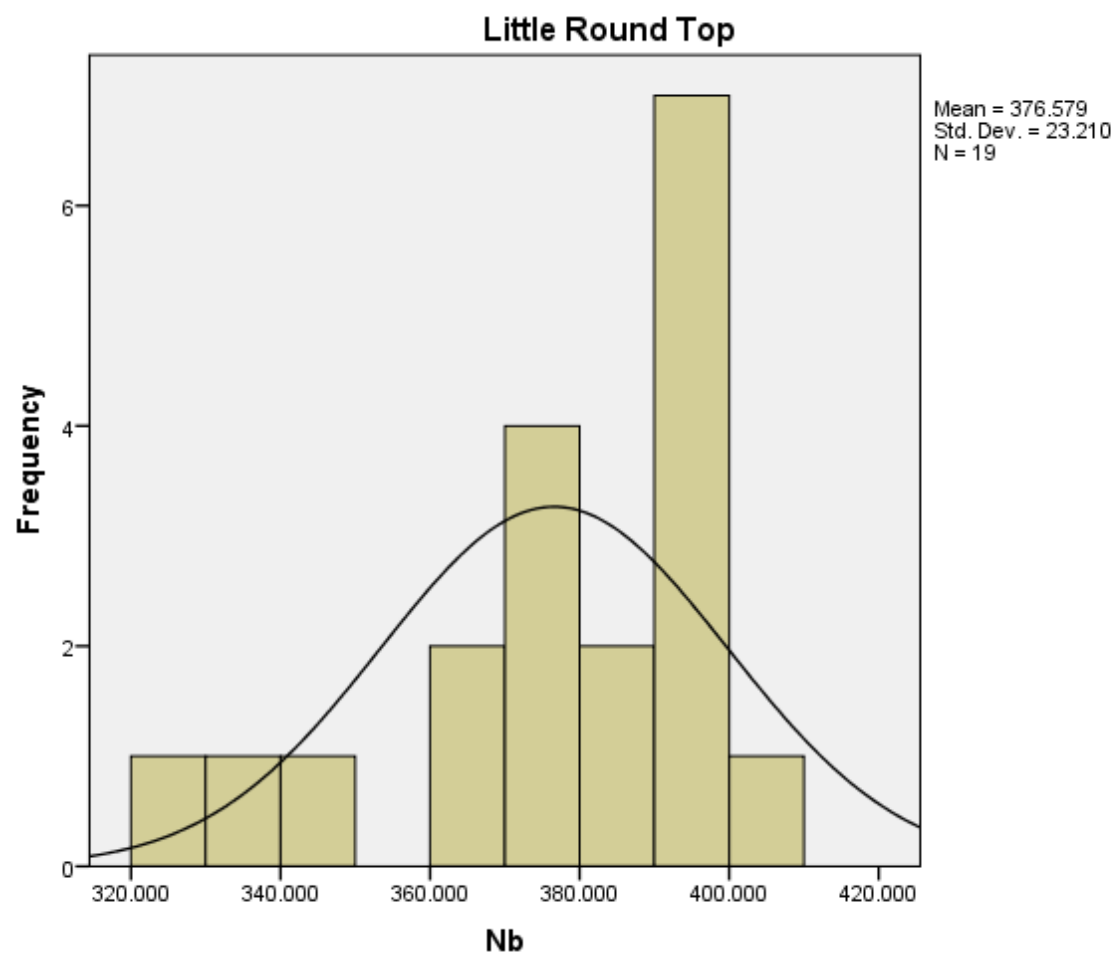


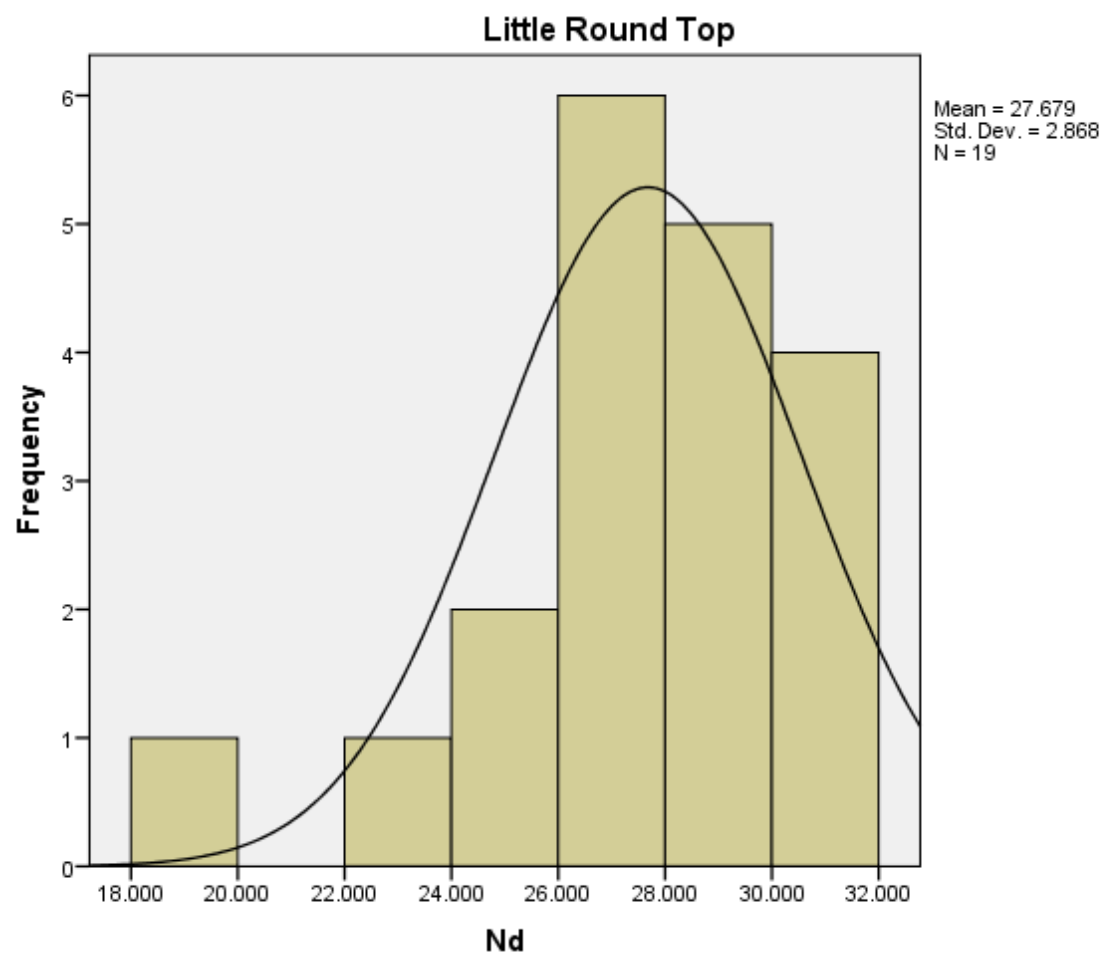


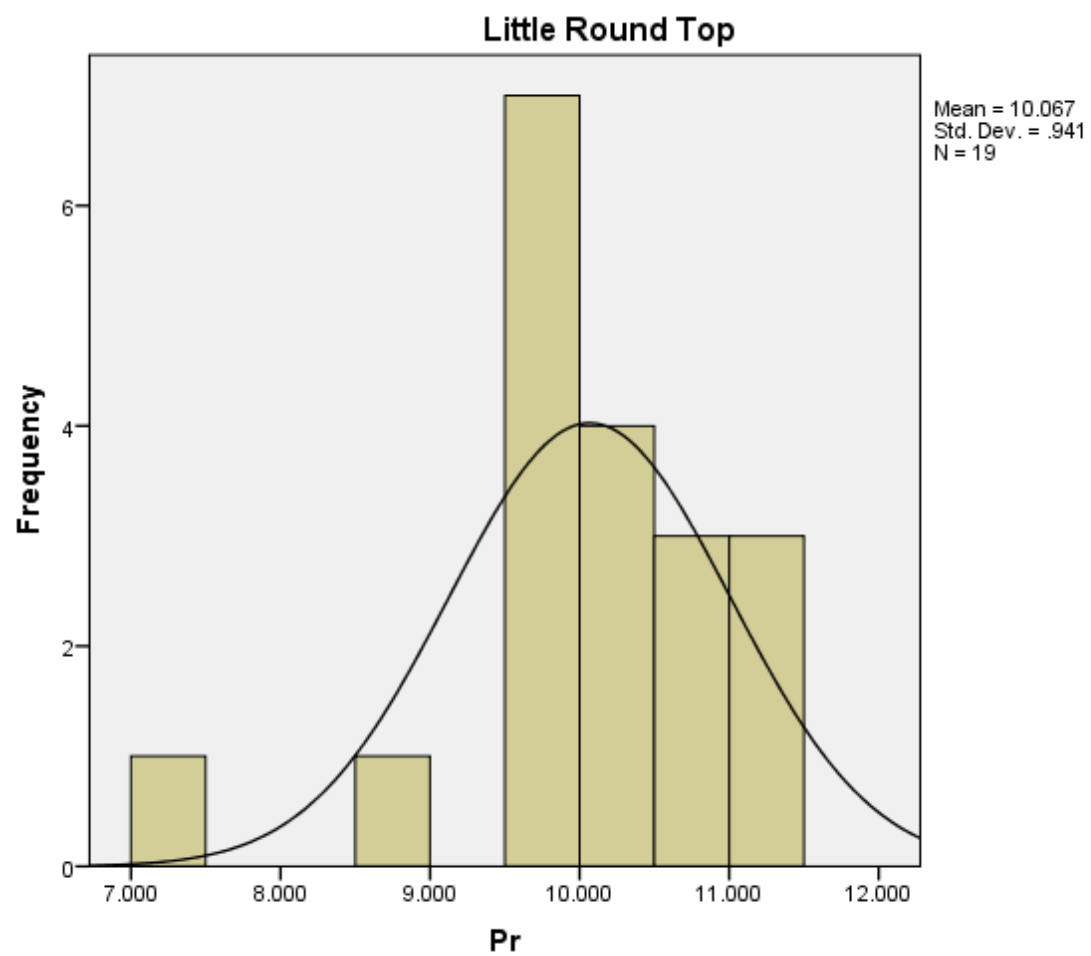


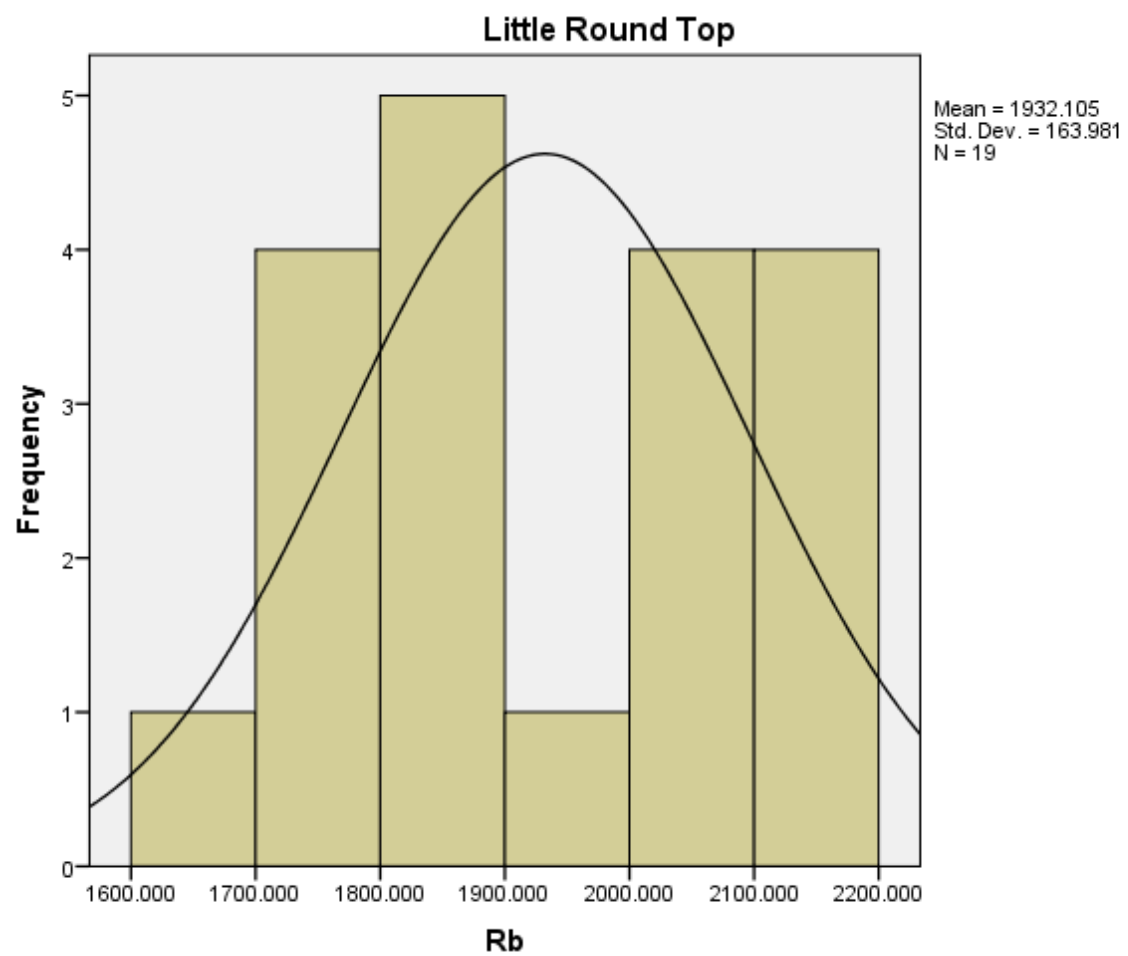


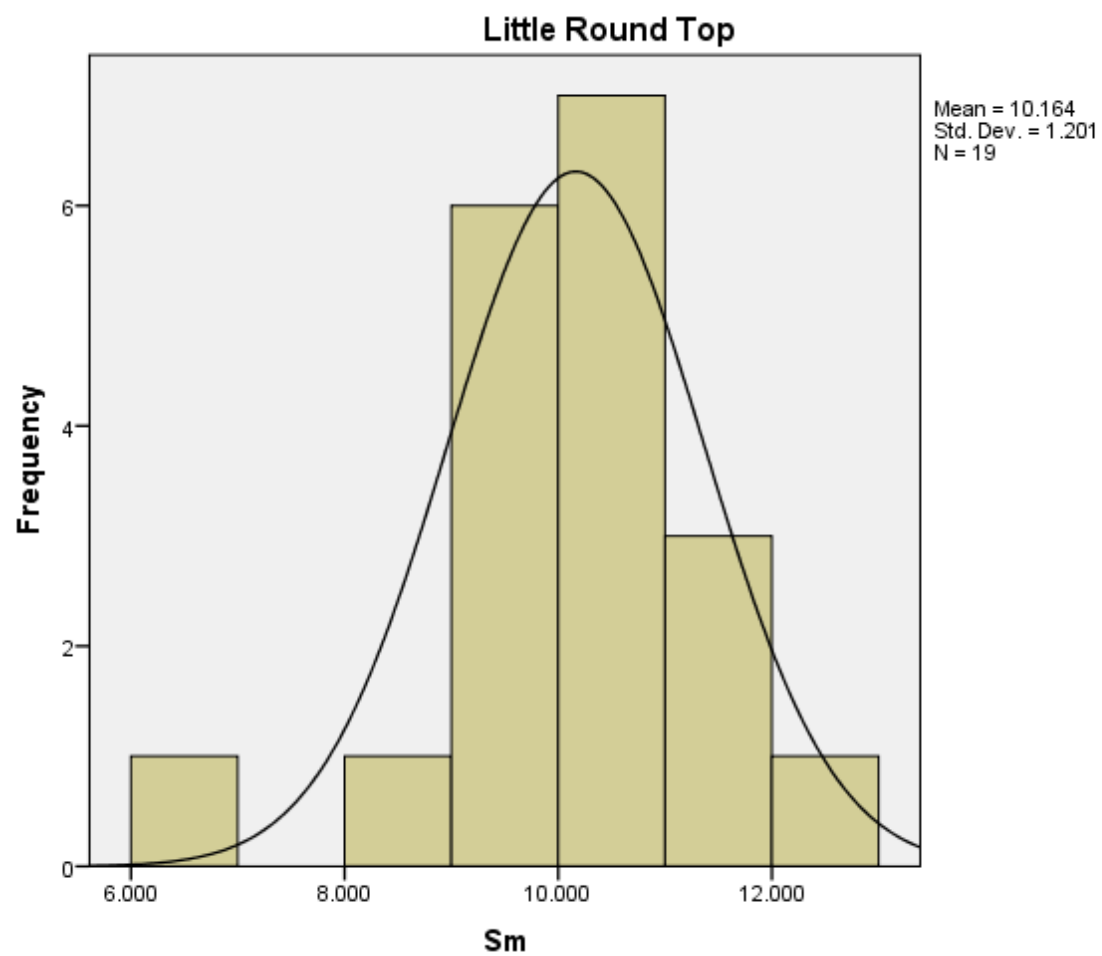


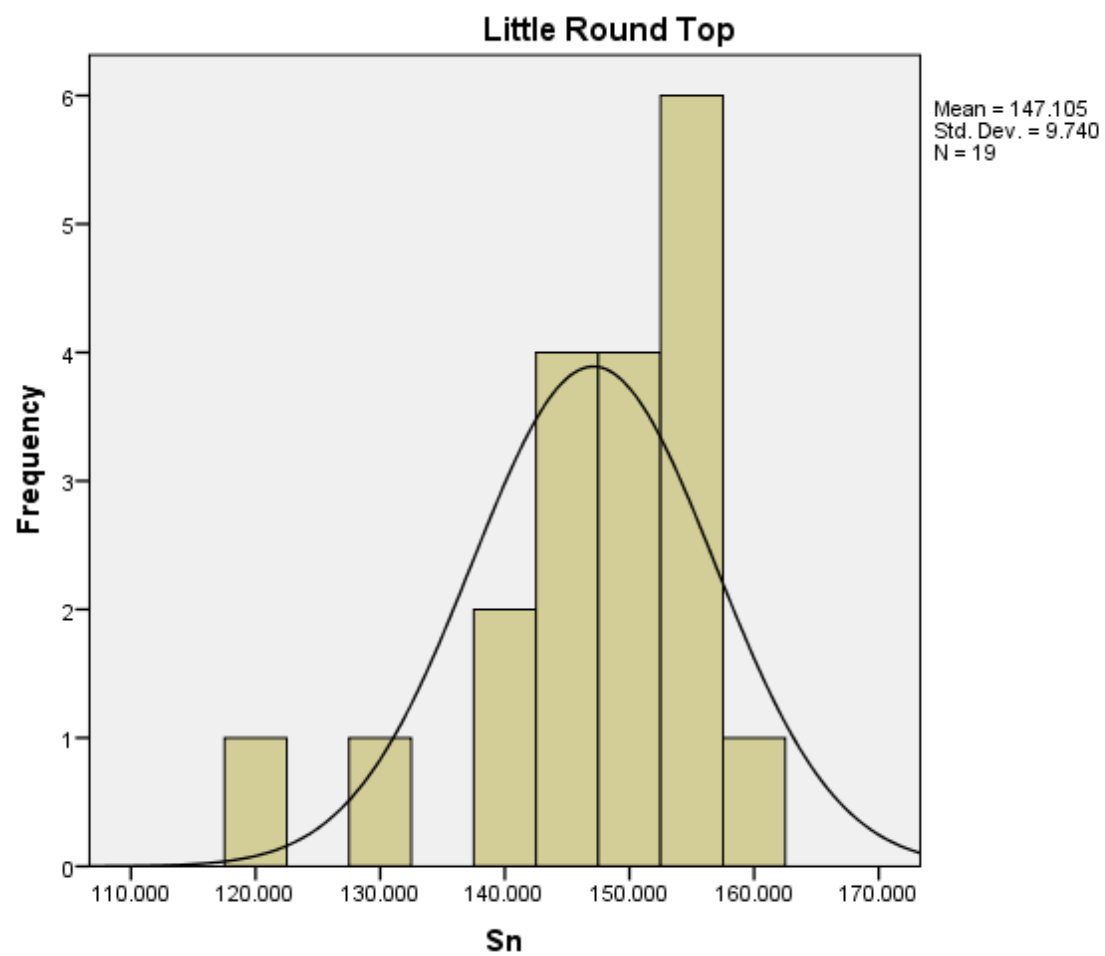


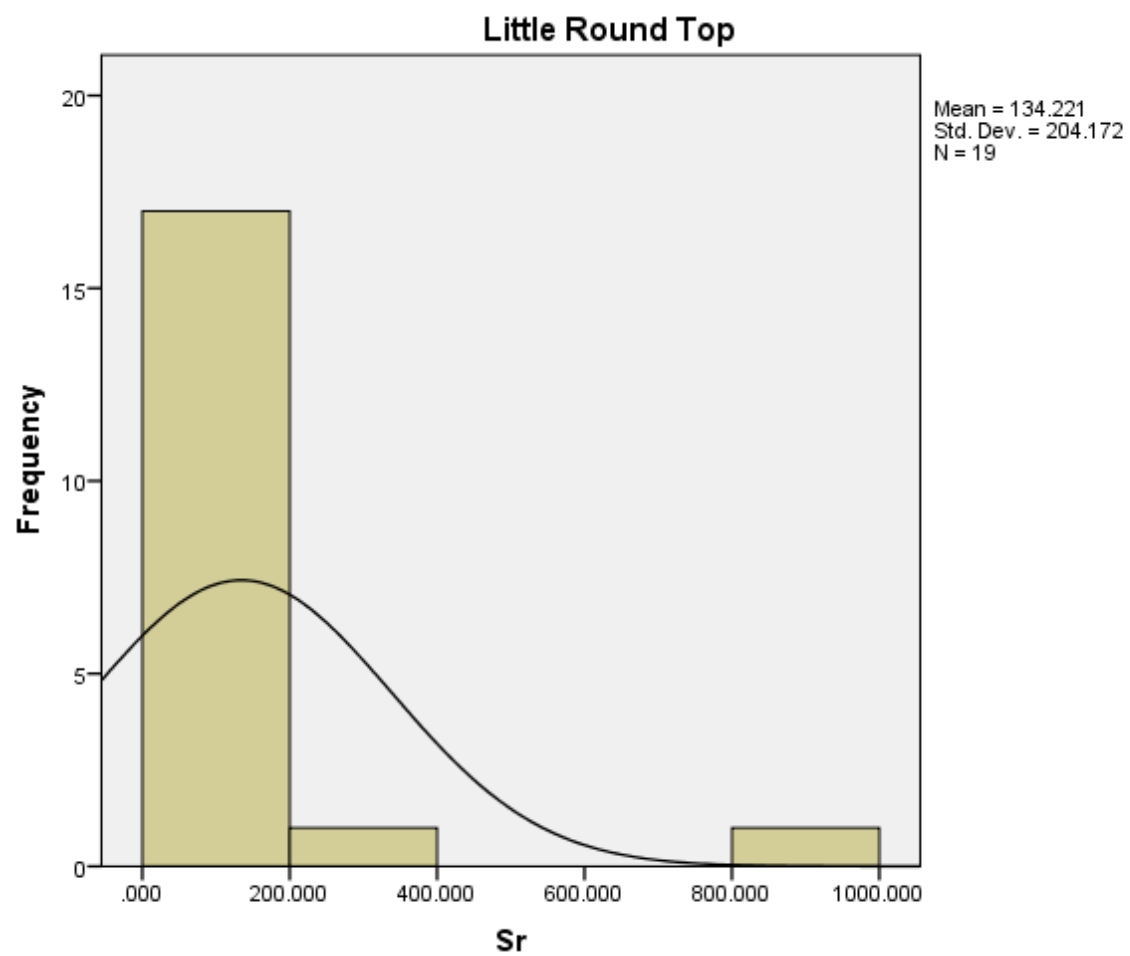


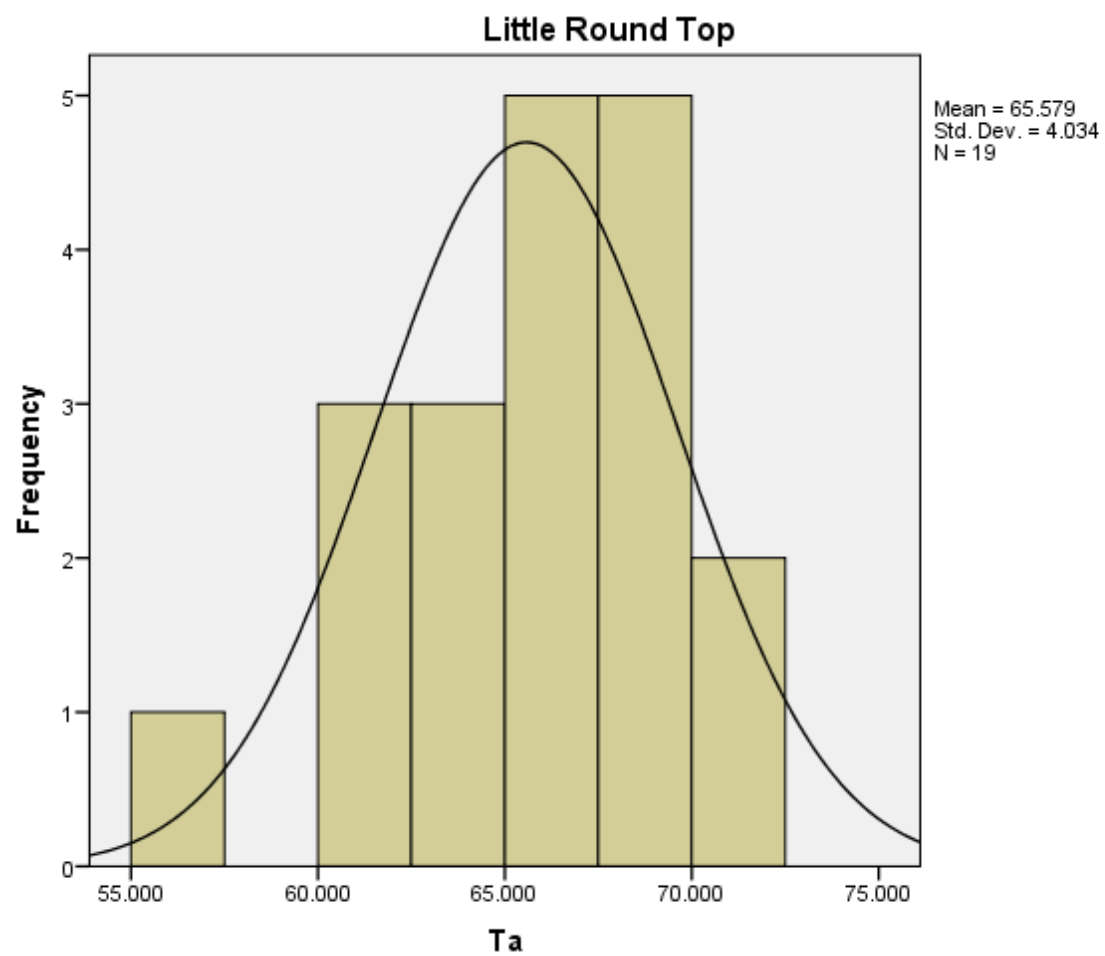


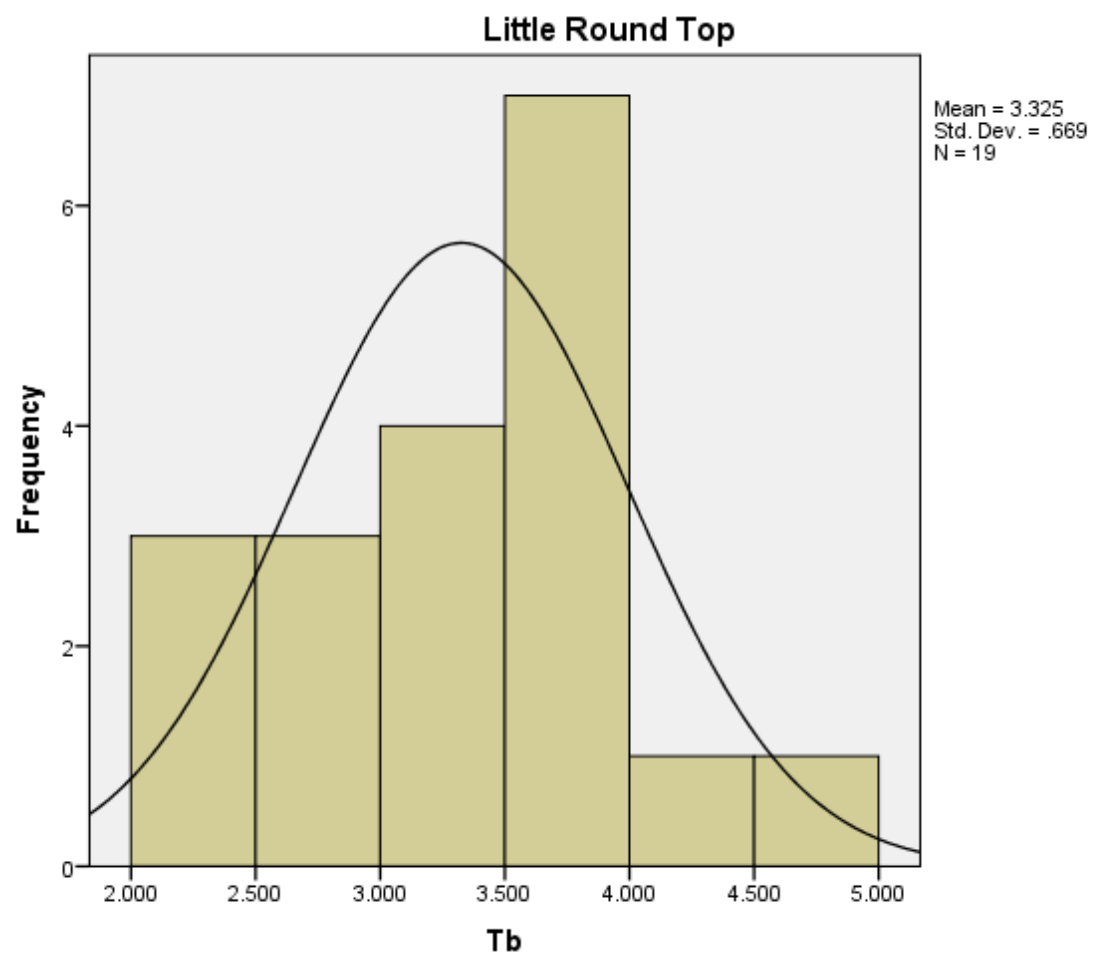


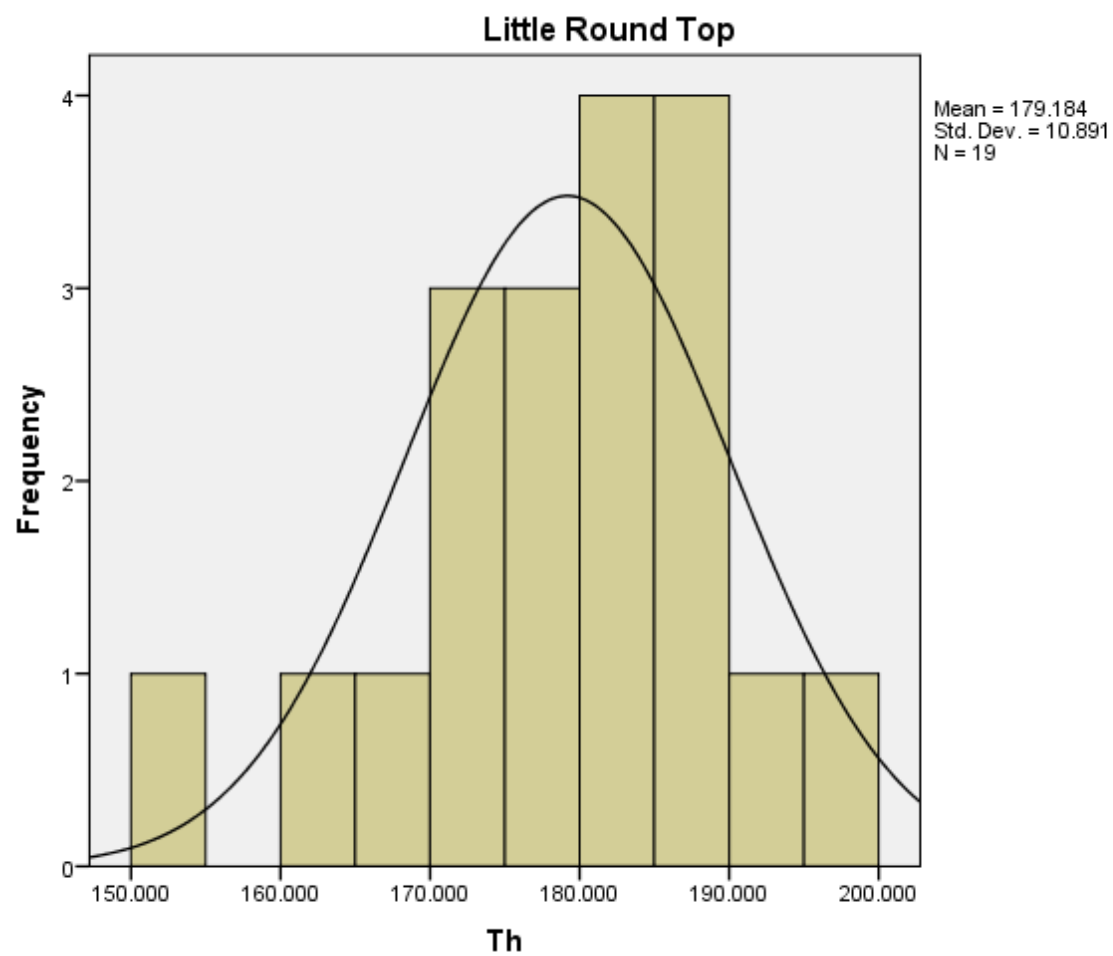


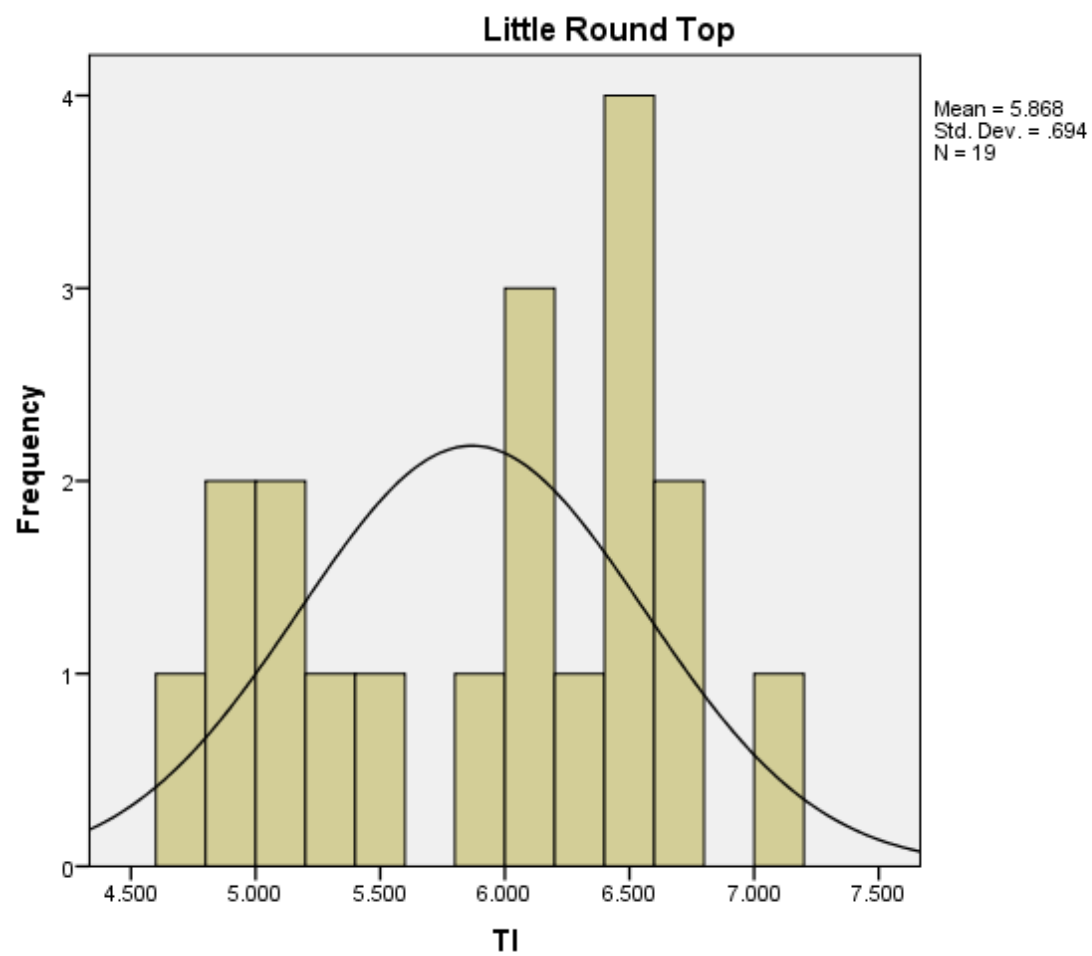


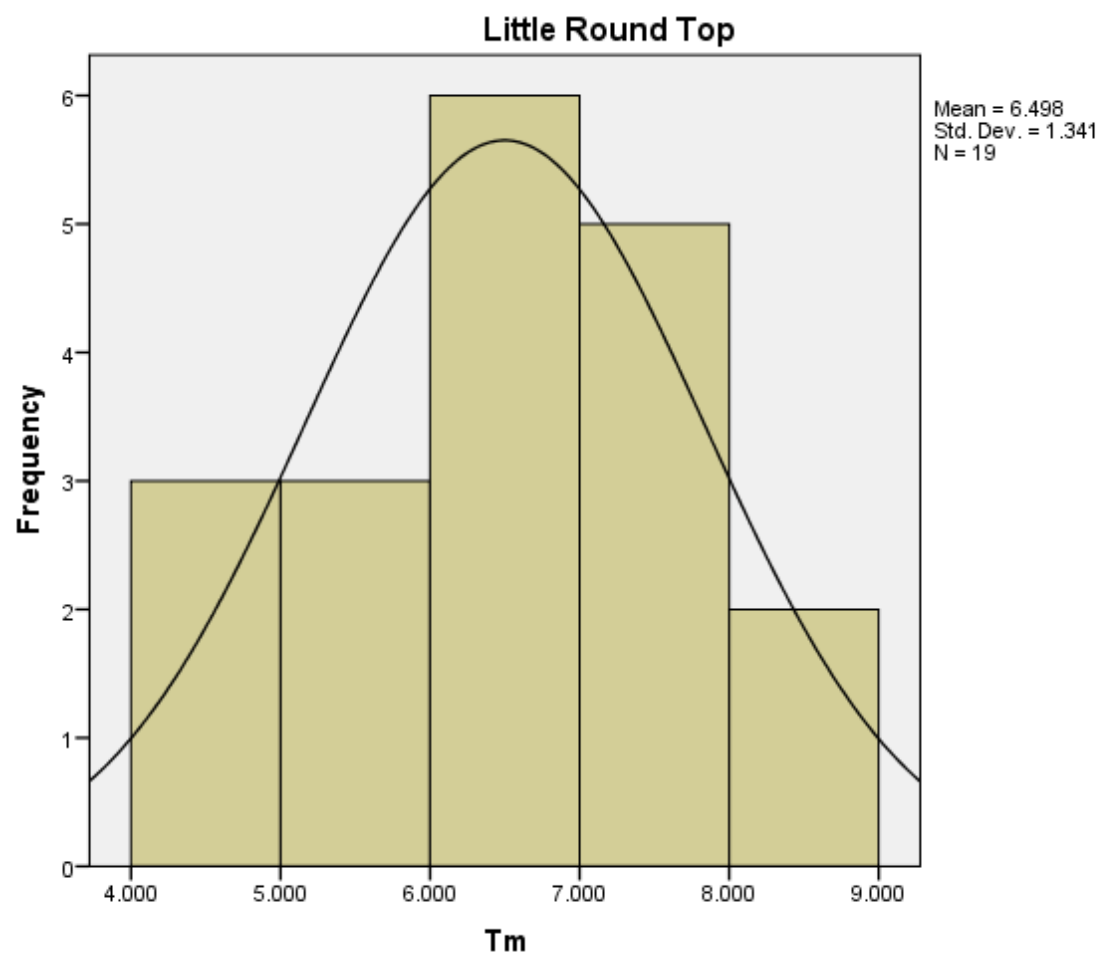


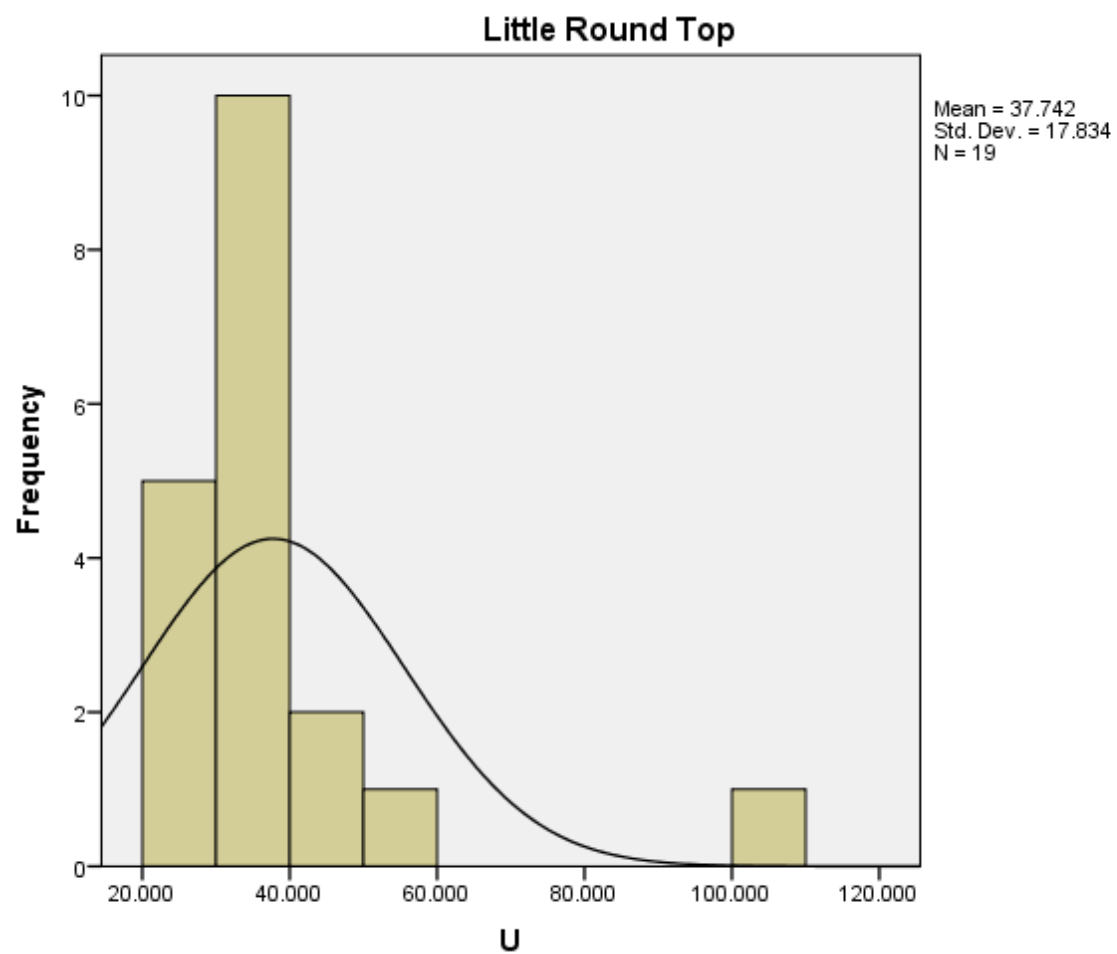


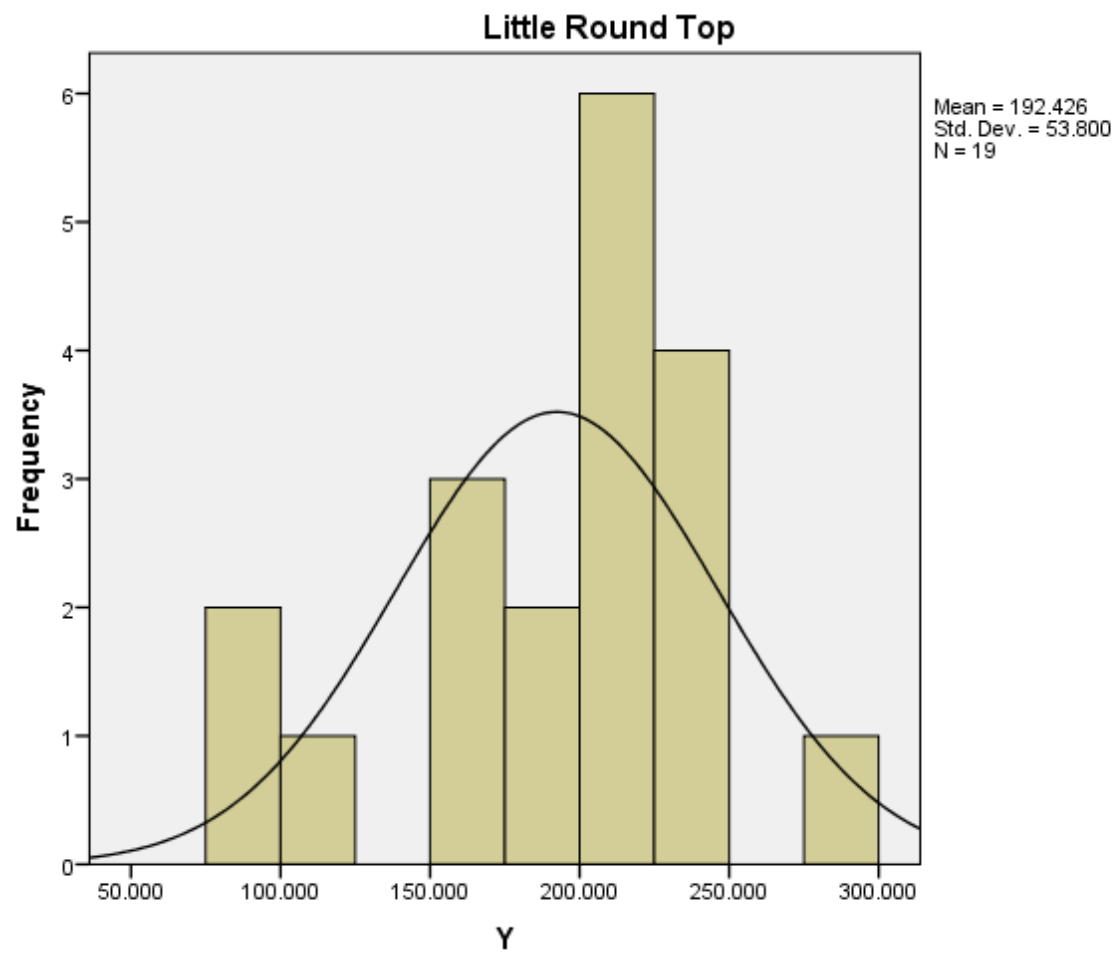


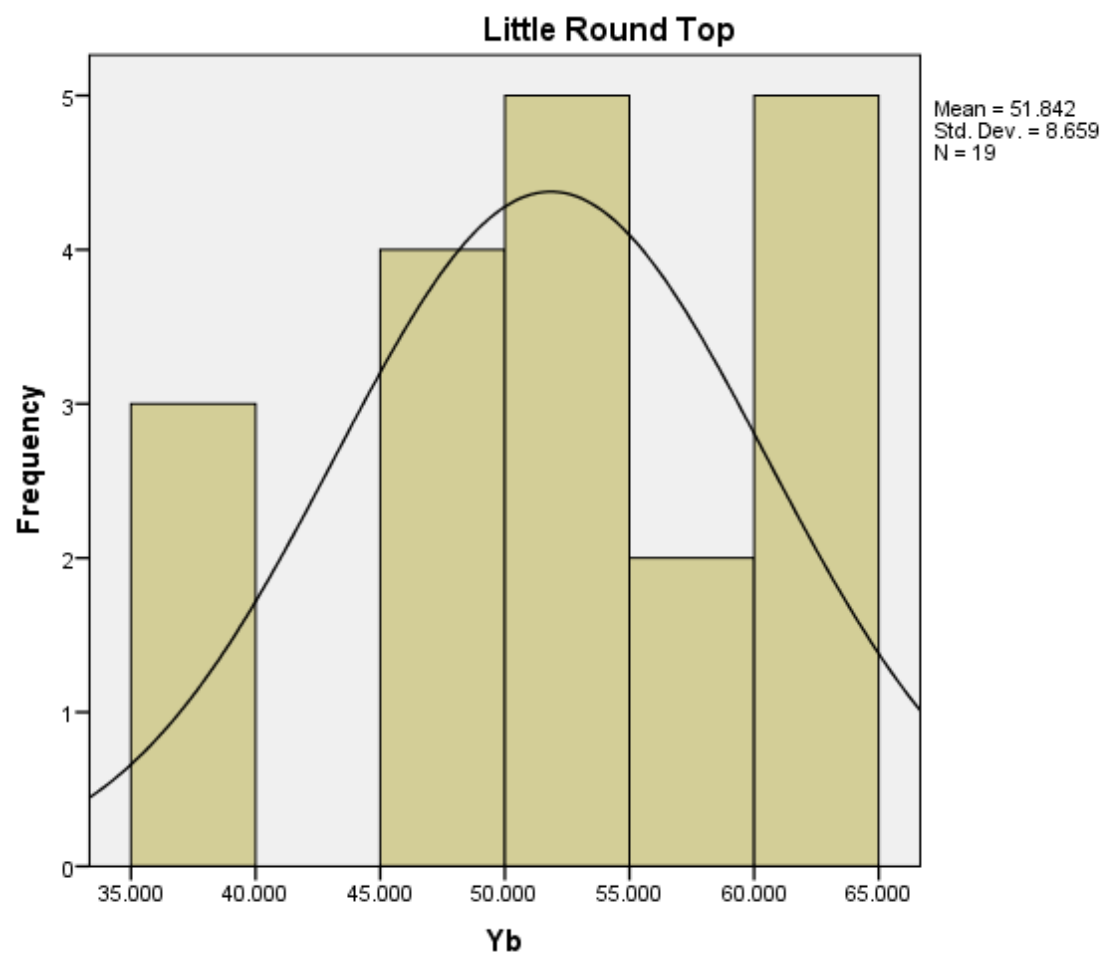


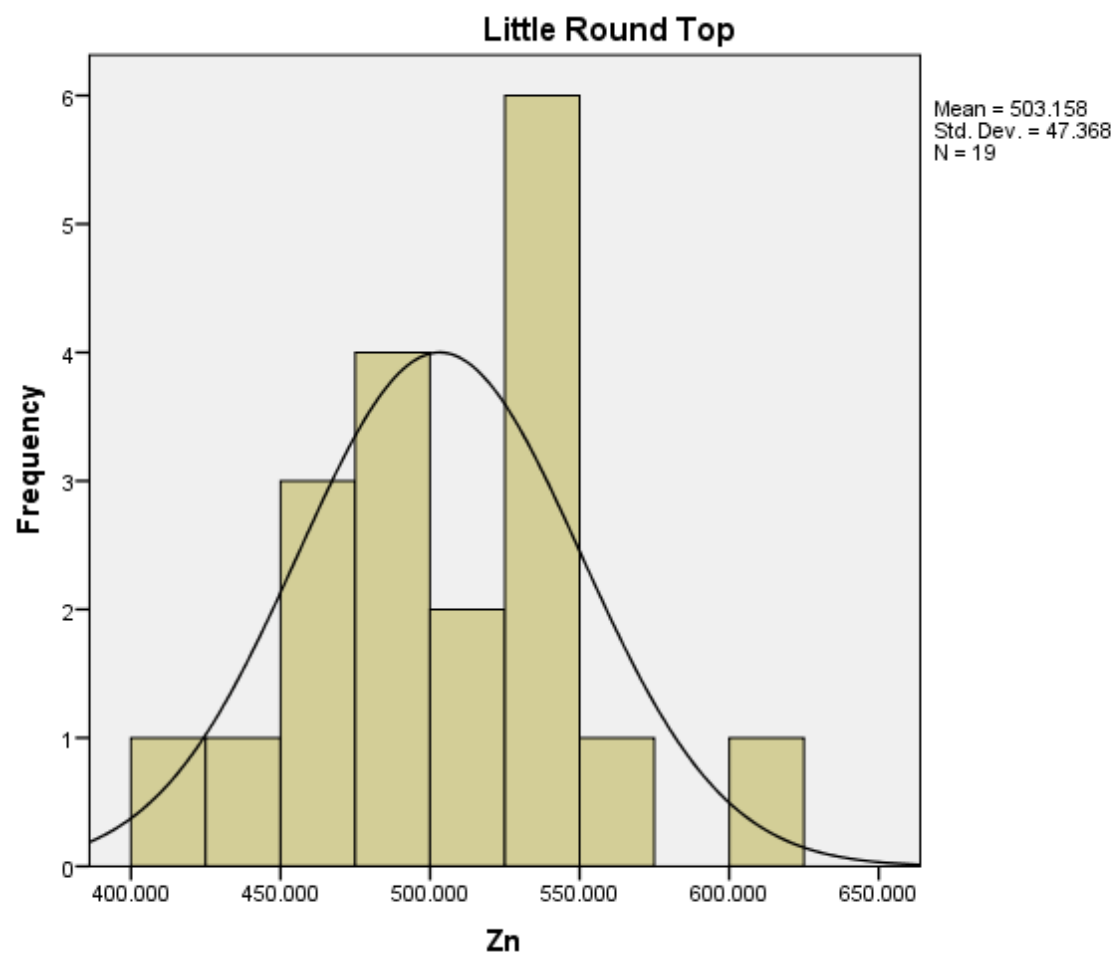


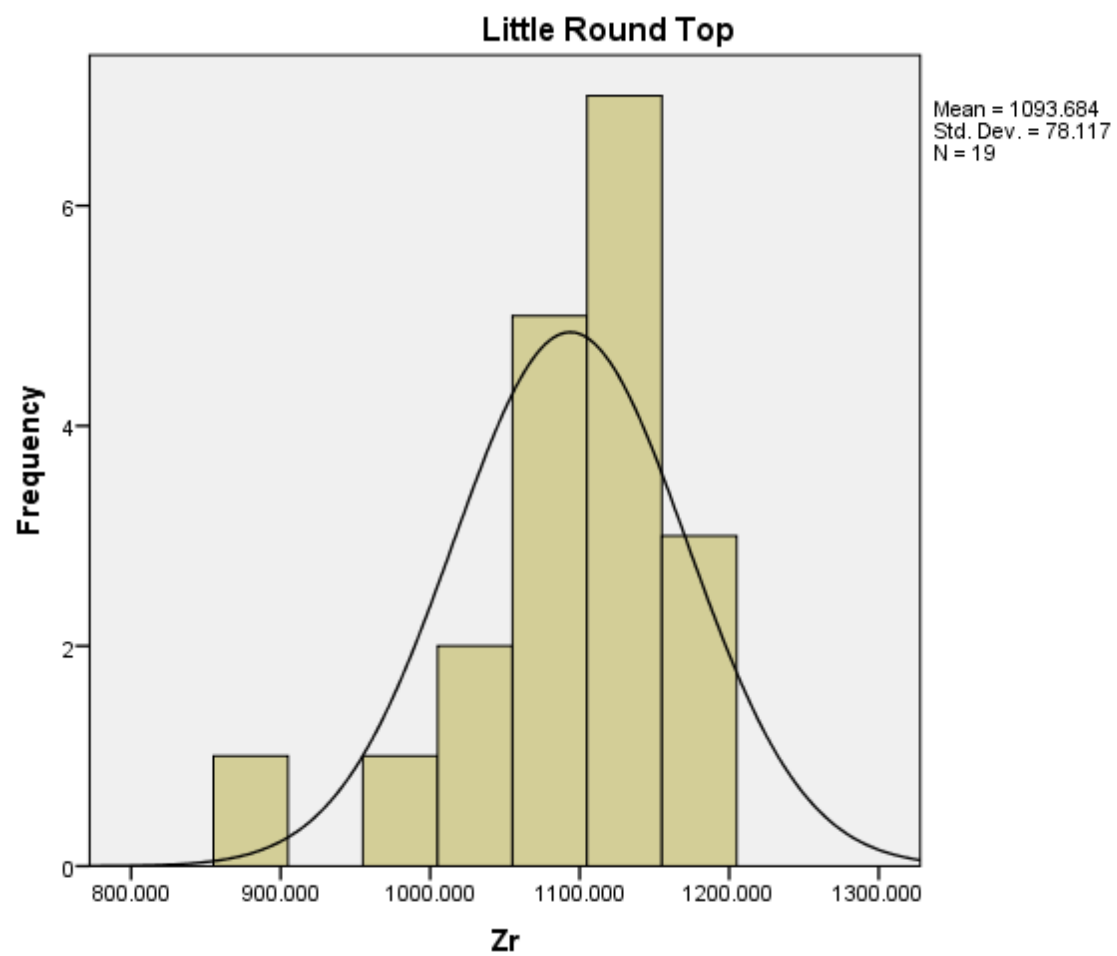


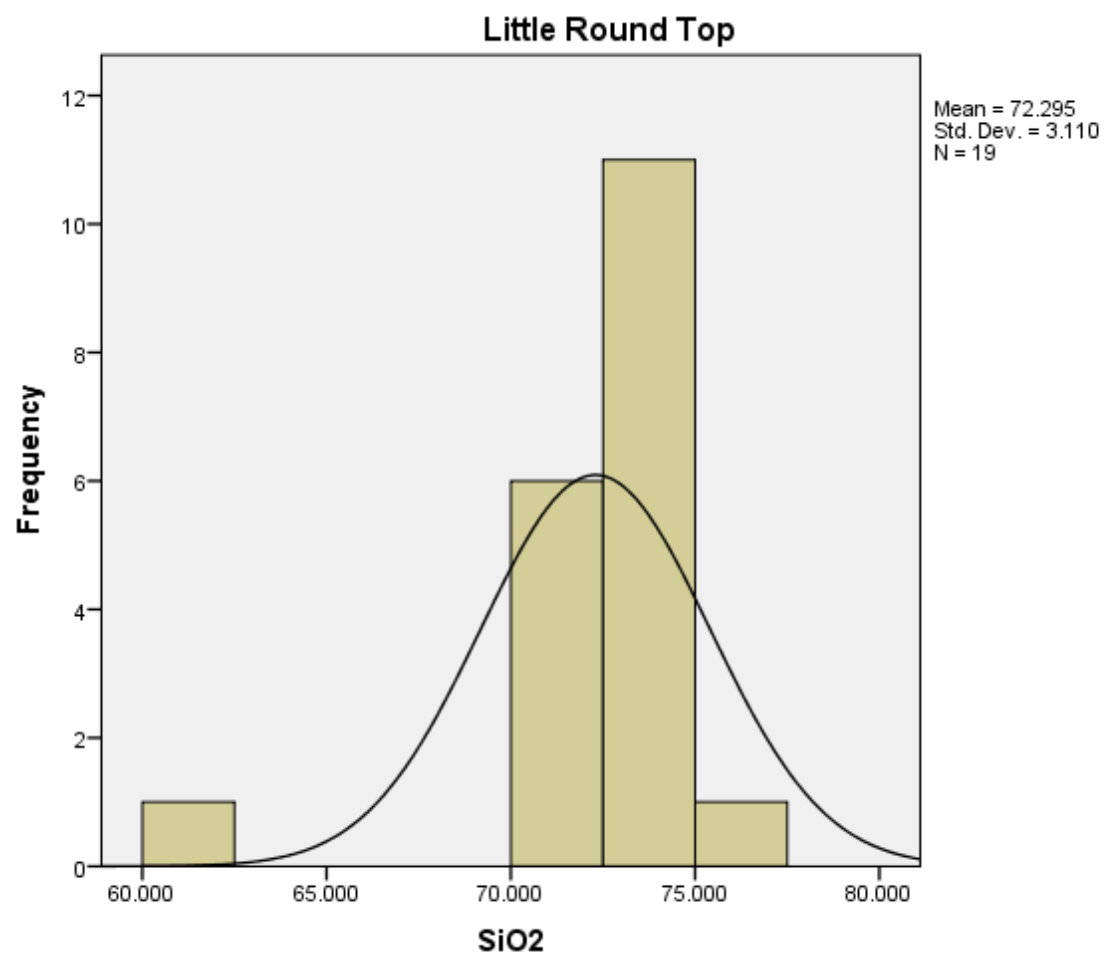


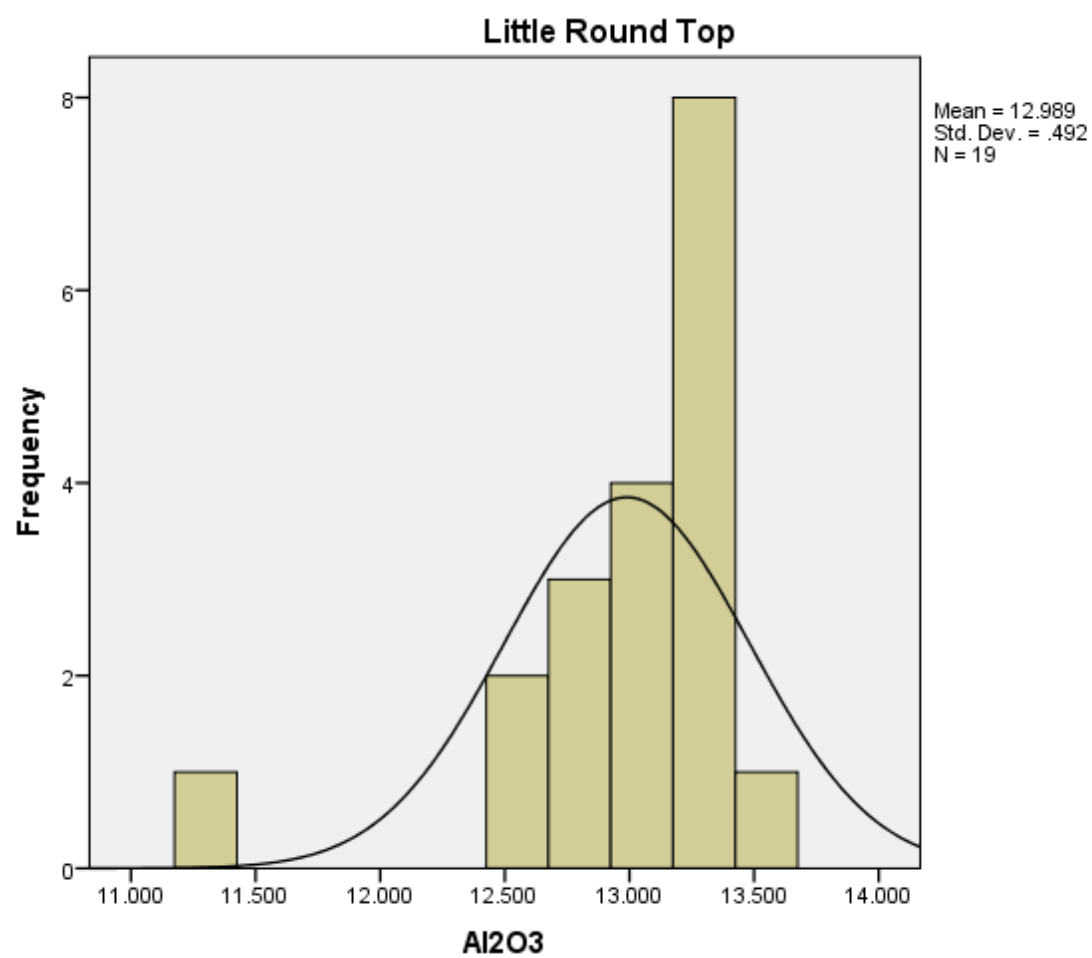


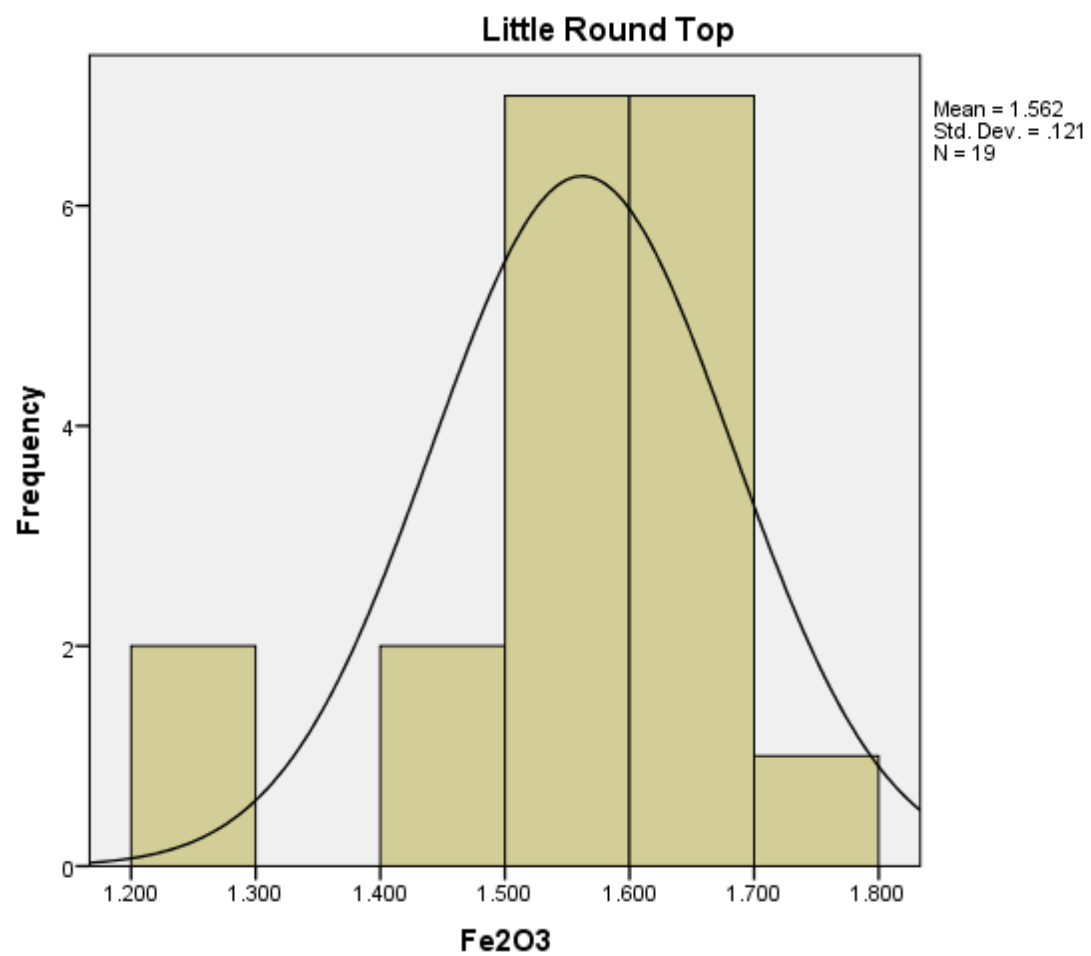


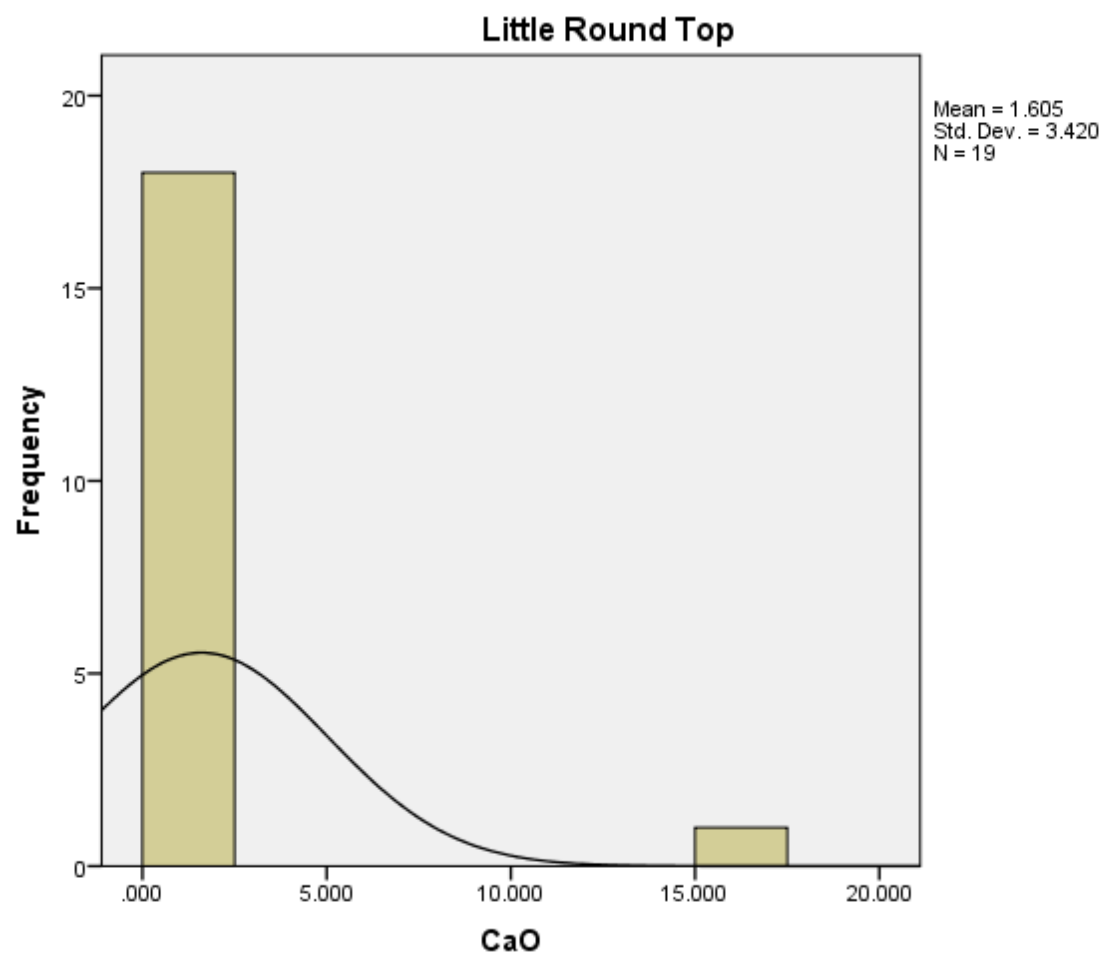


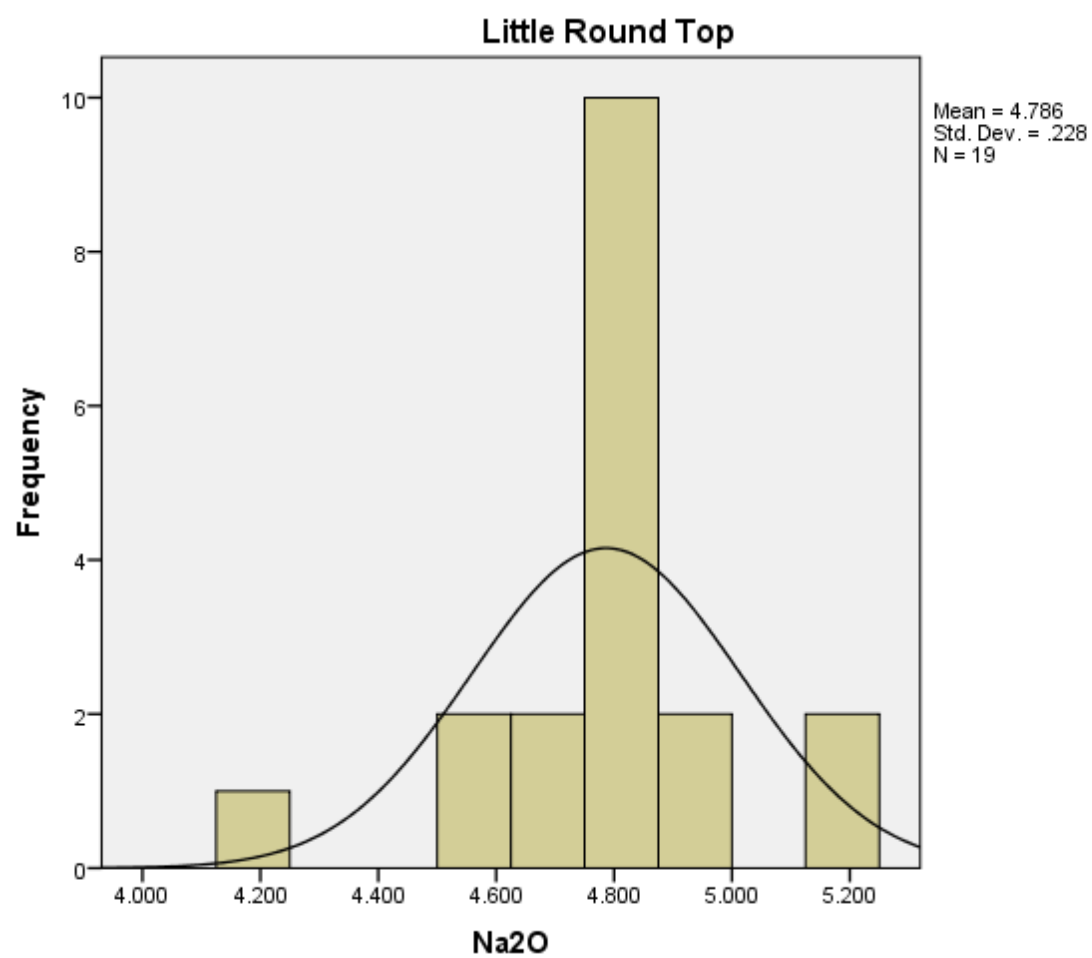


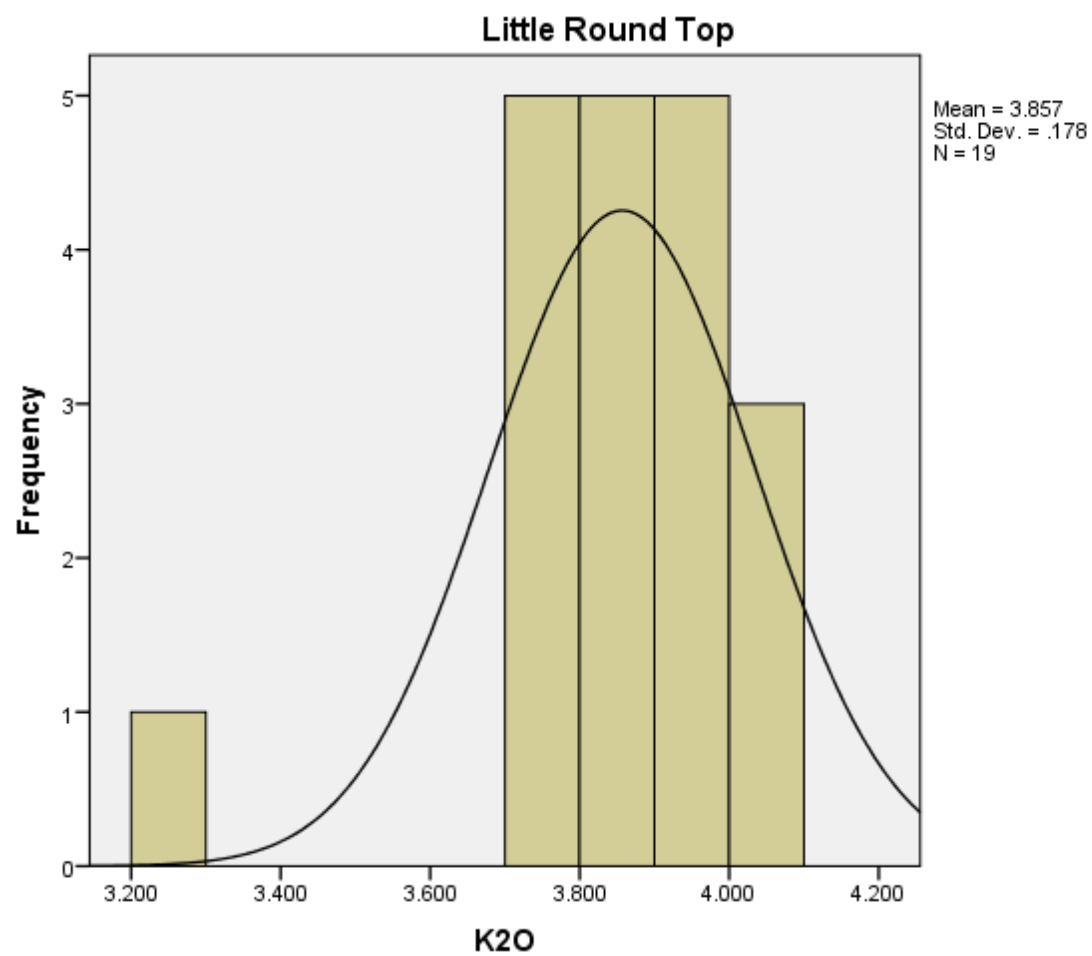


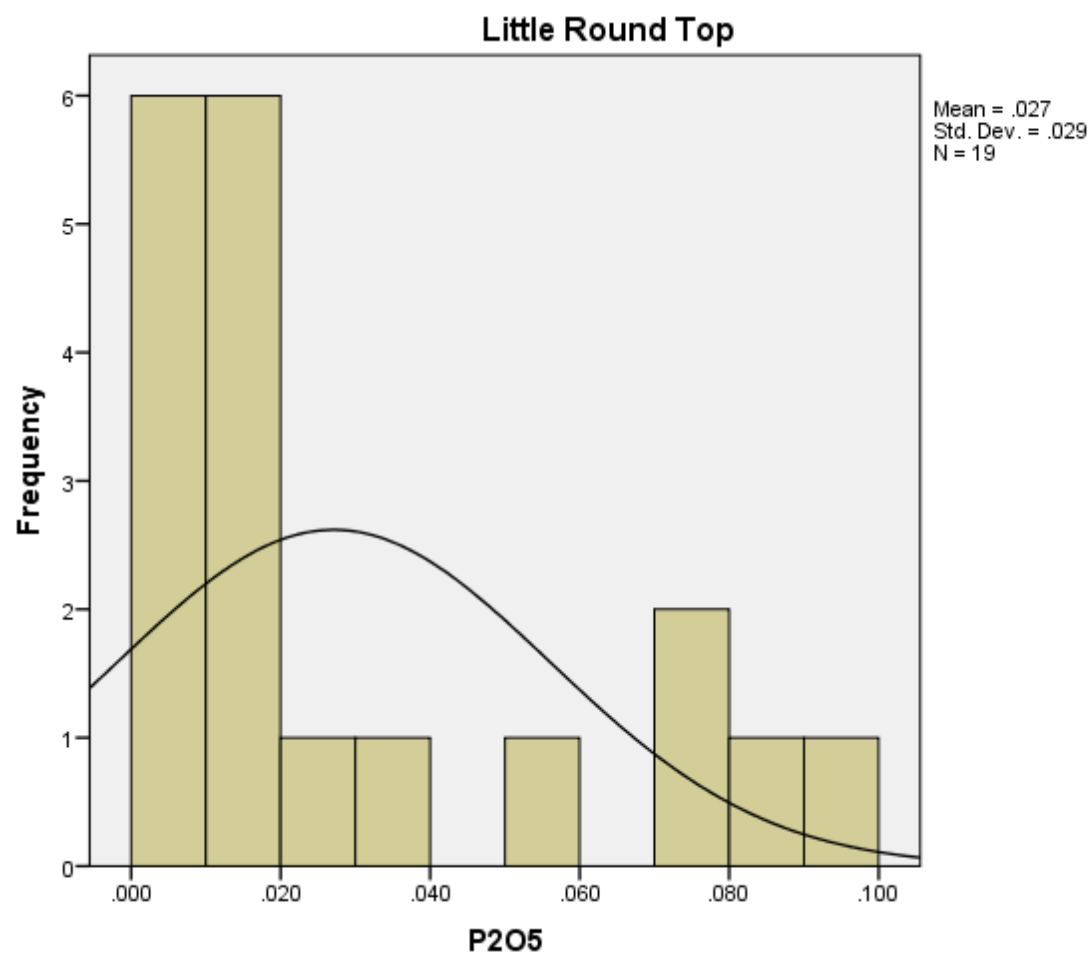


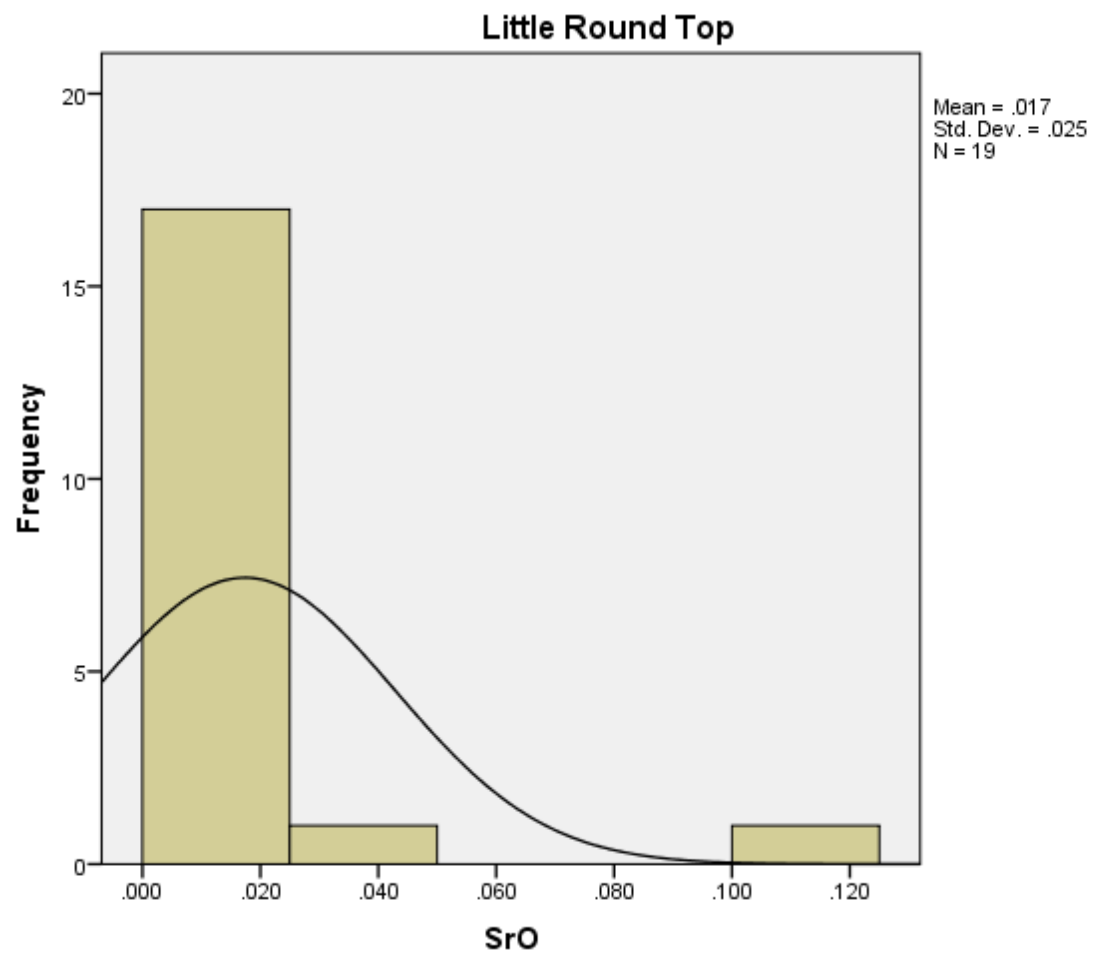


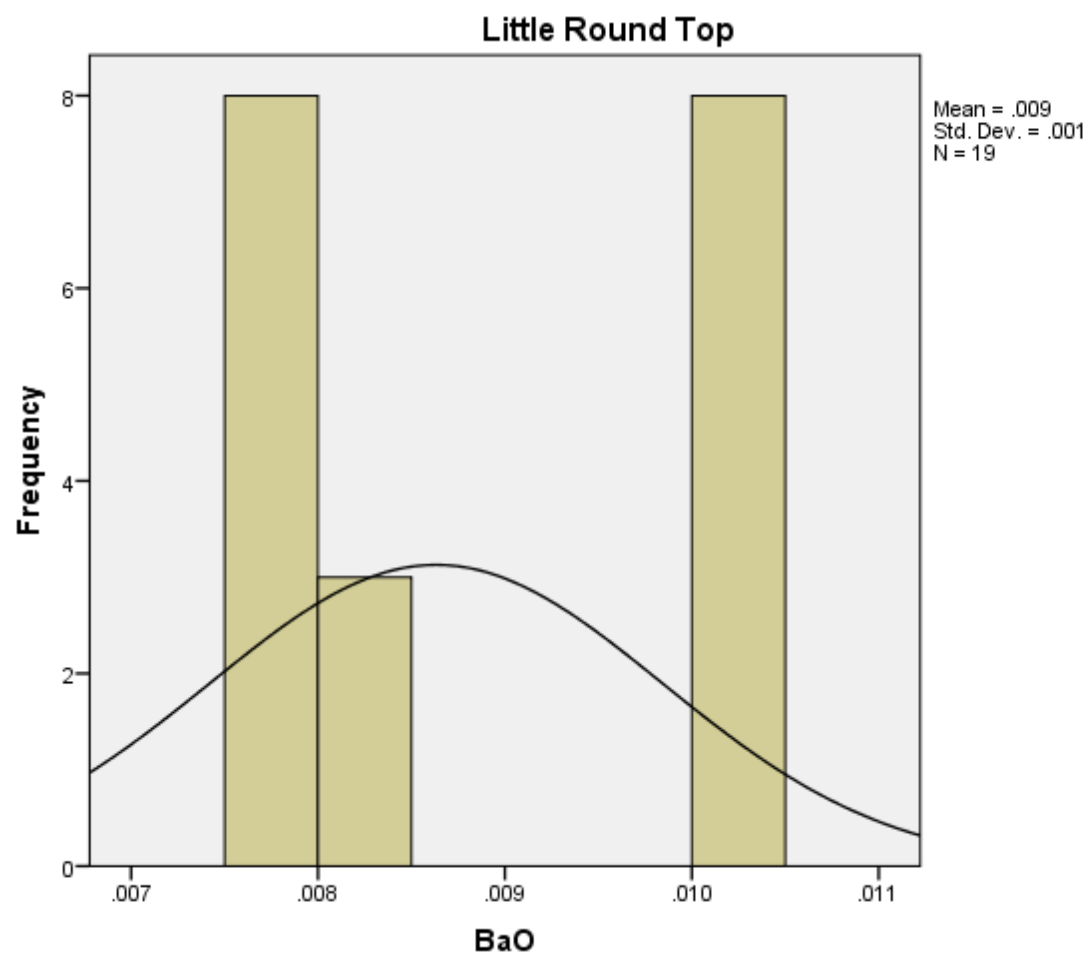




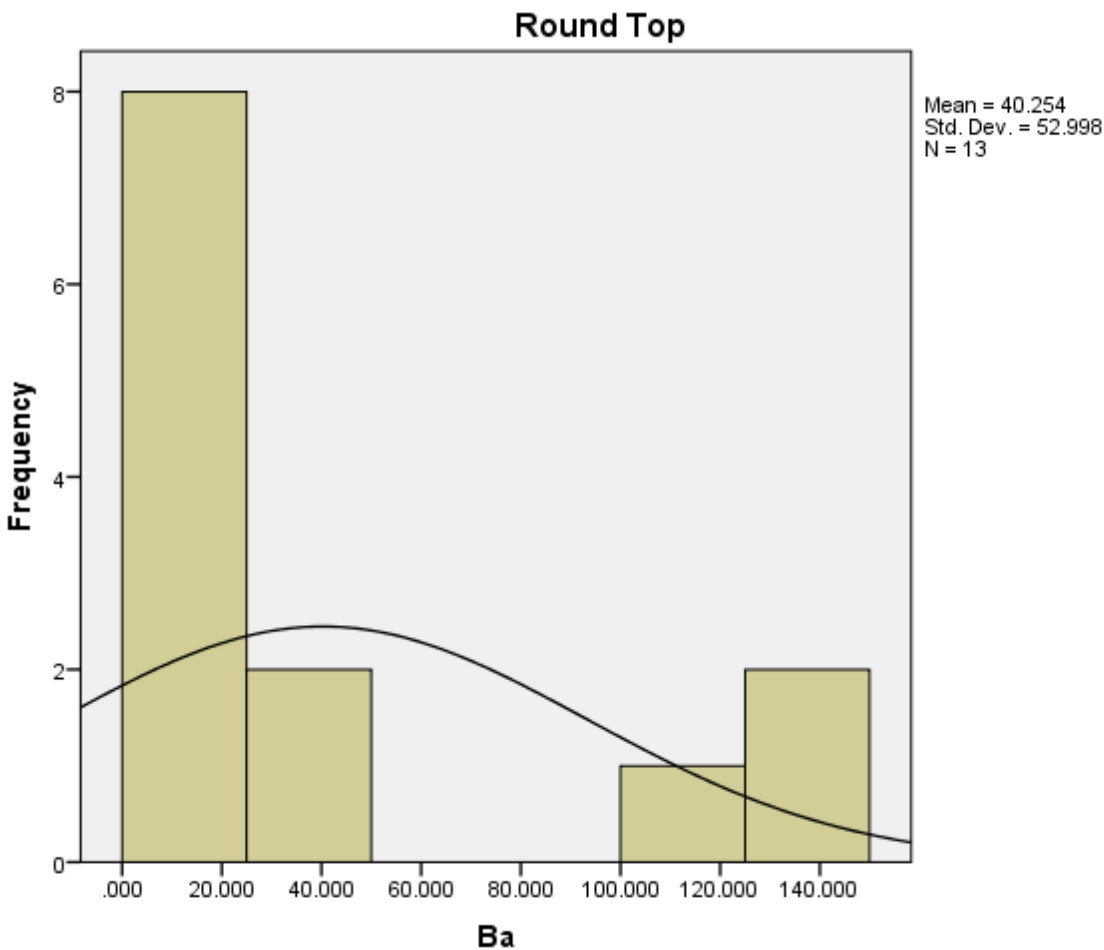


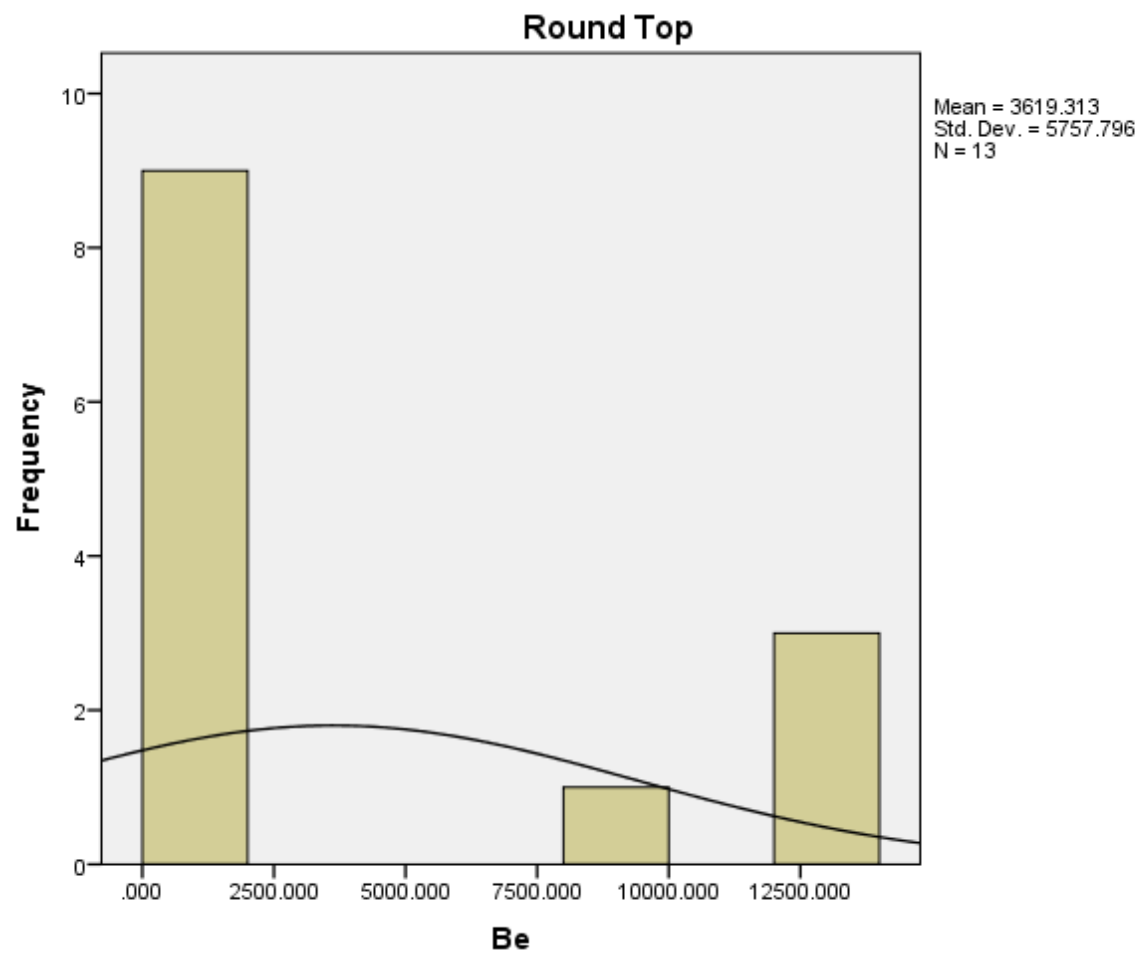


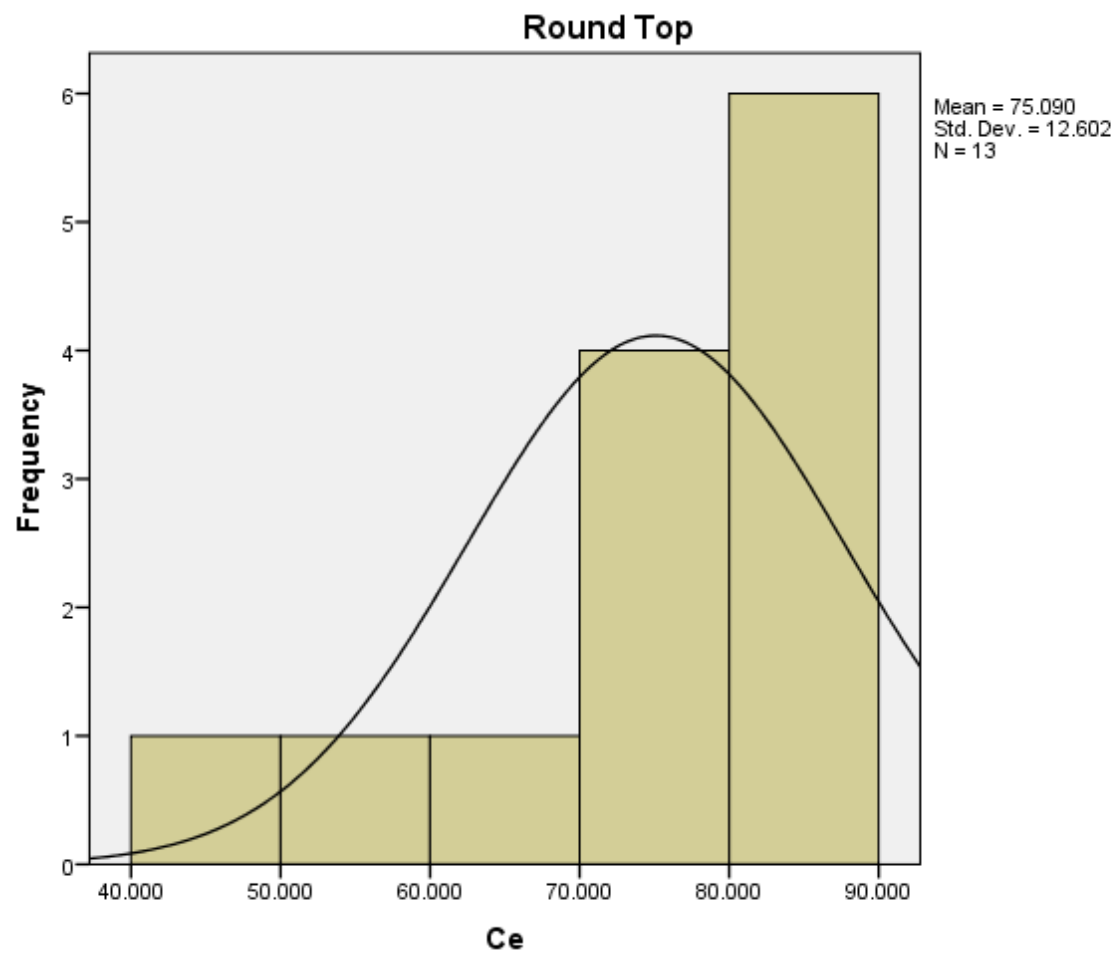


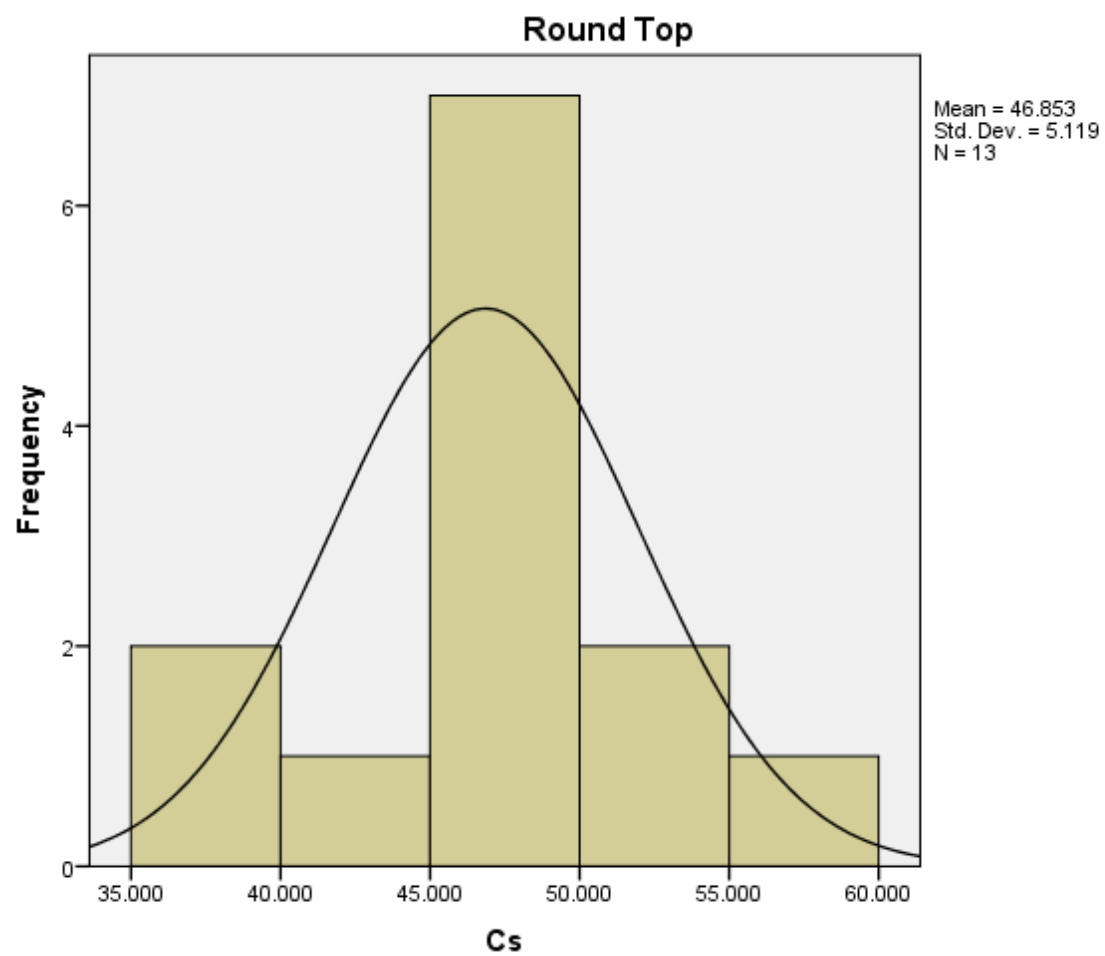


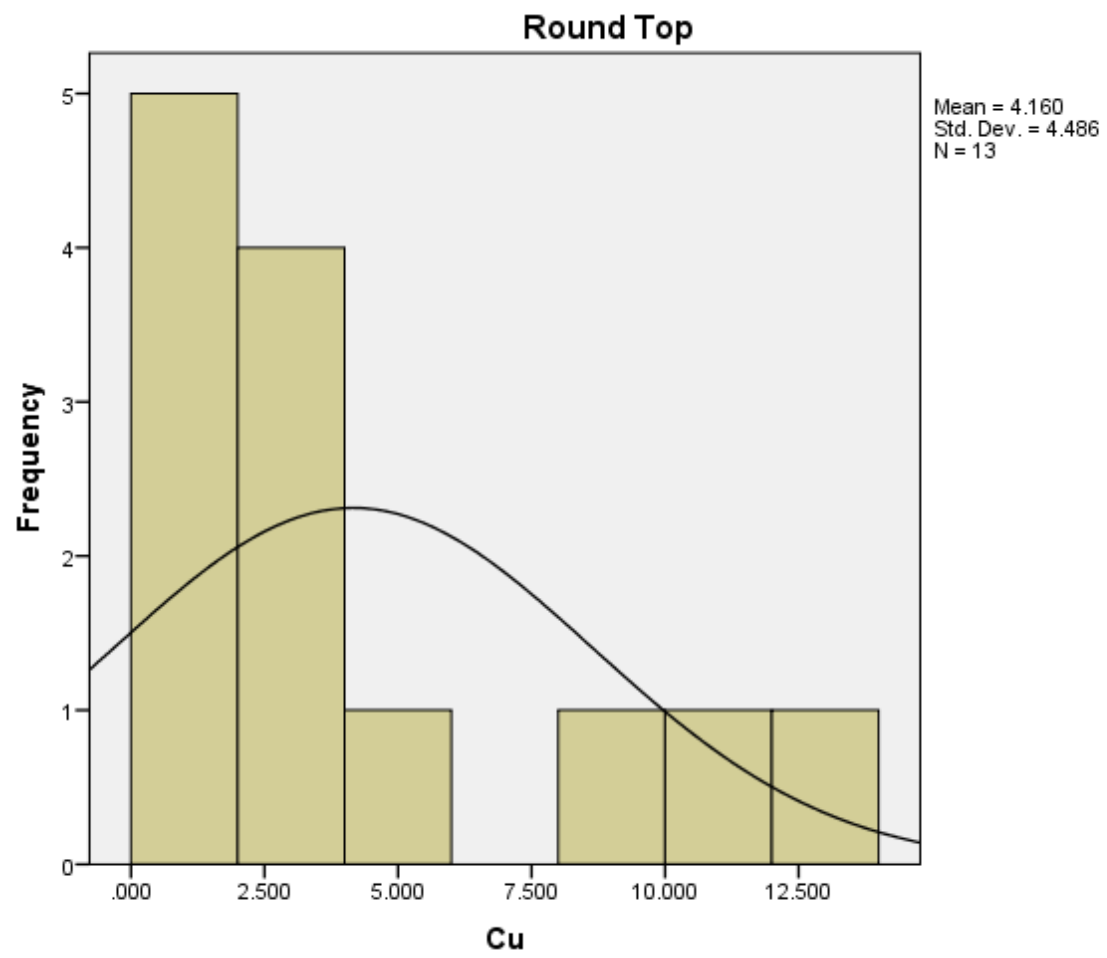
Histograms: Round Top

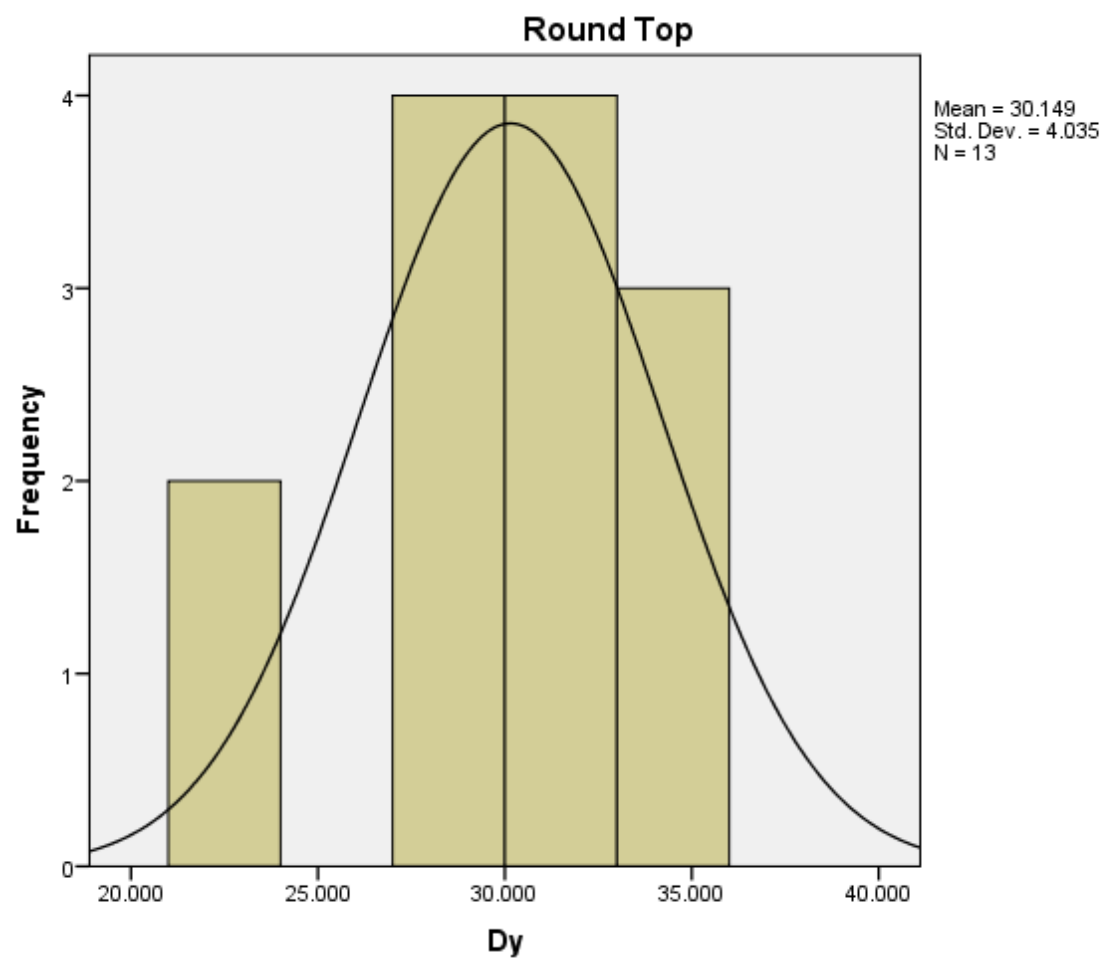


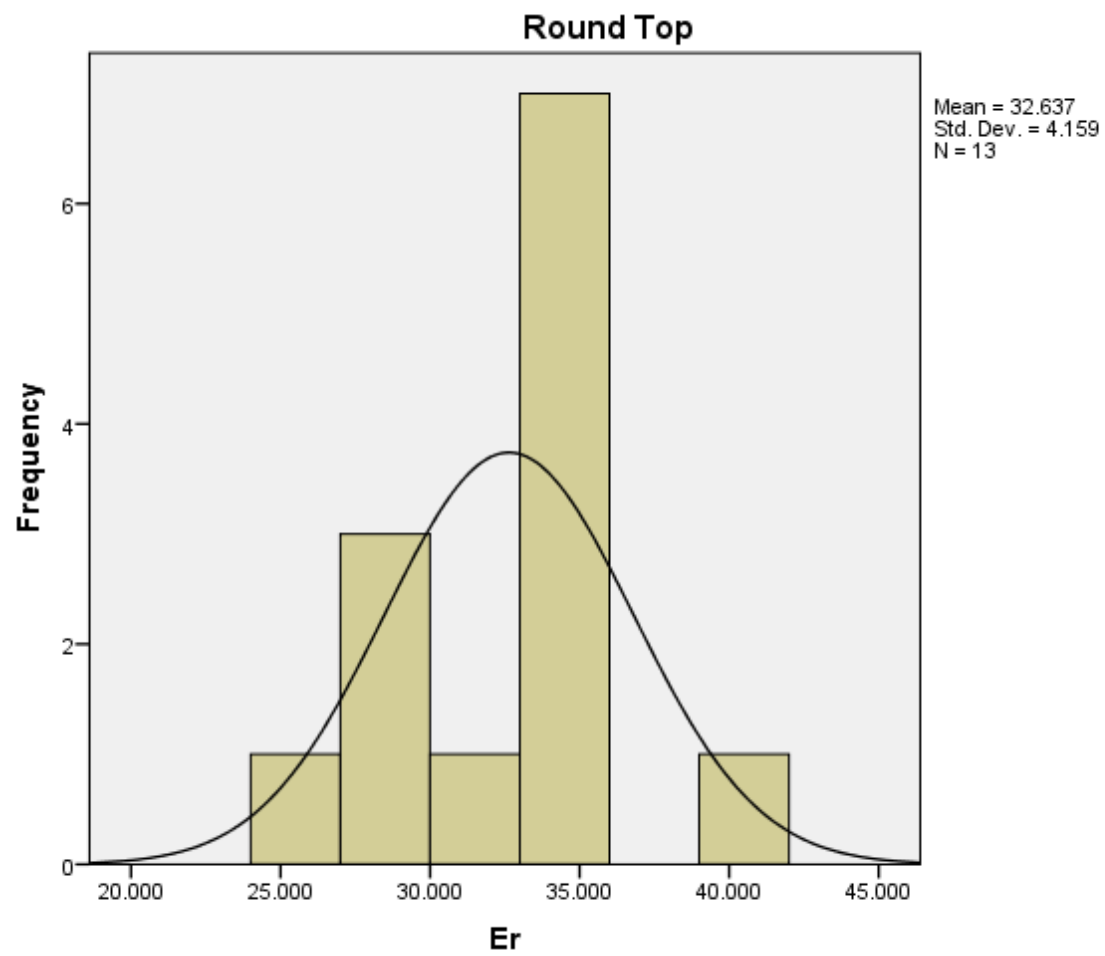


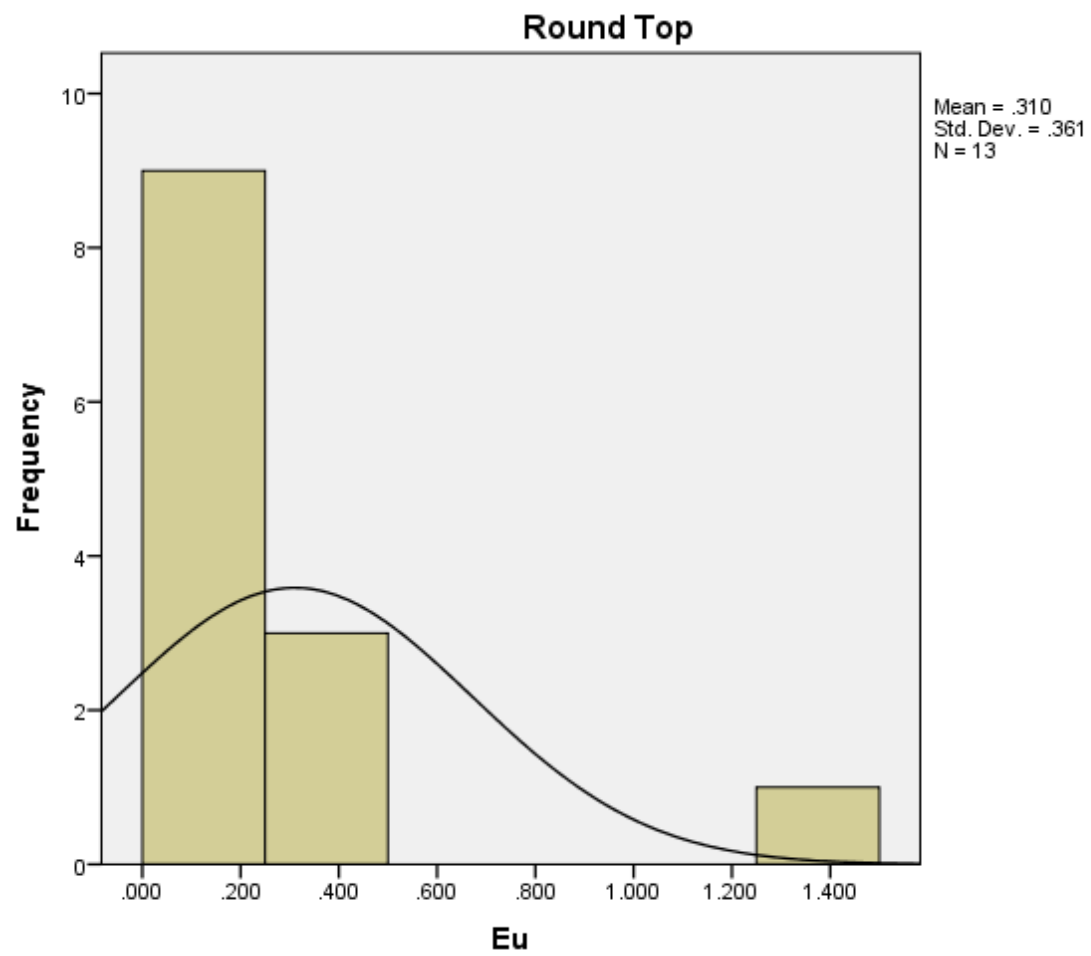


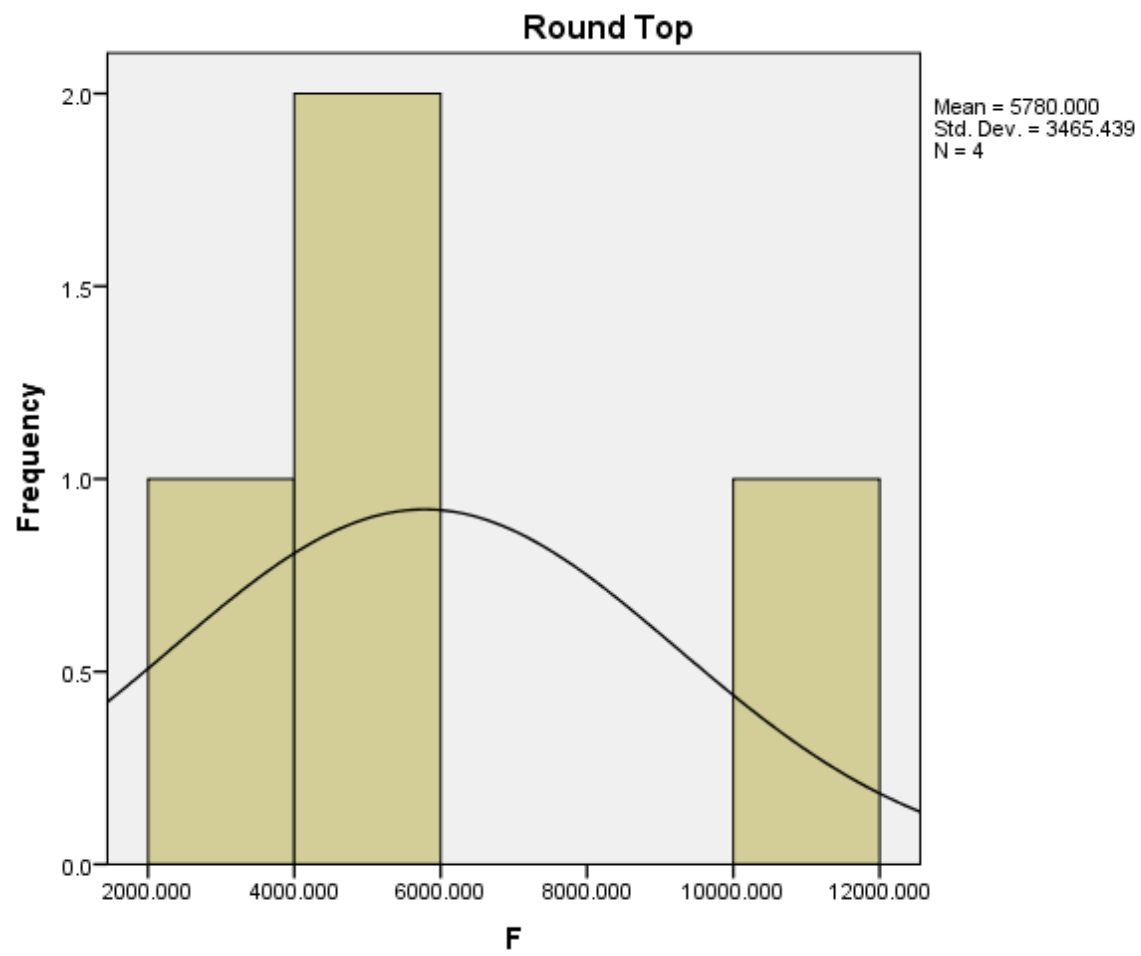


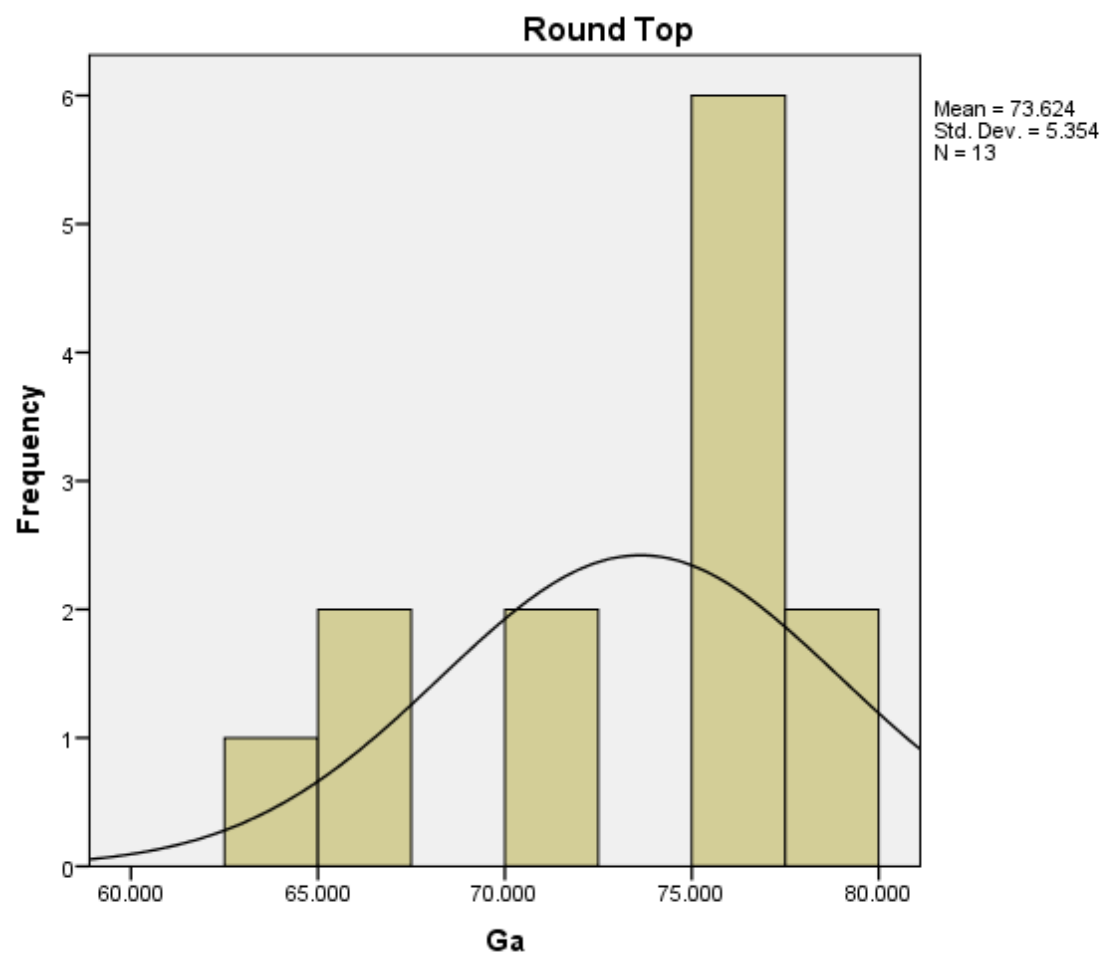


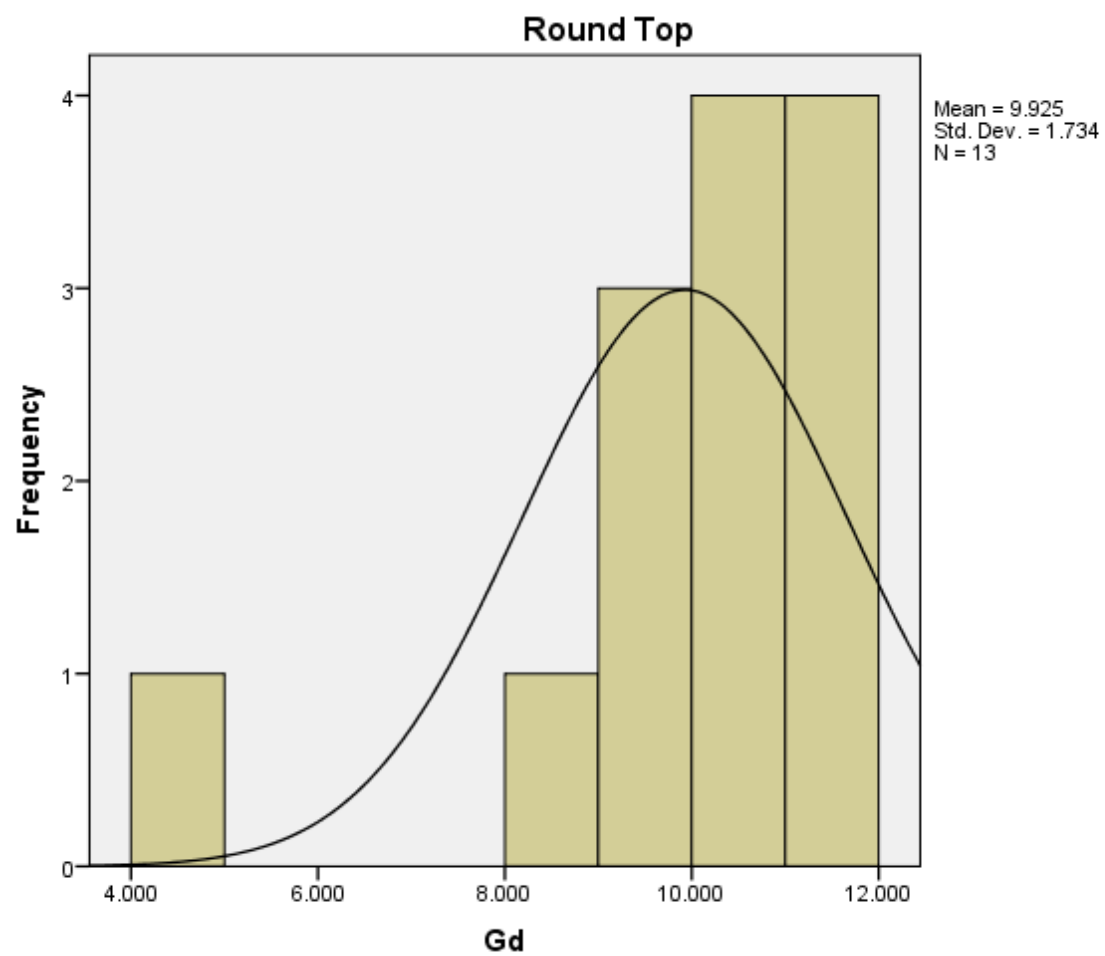


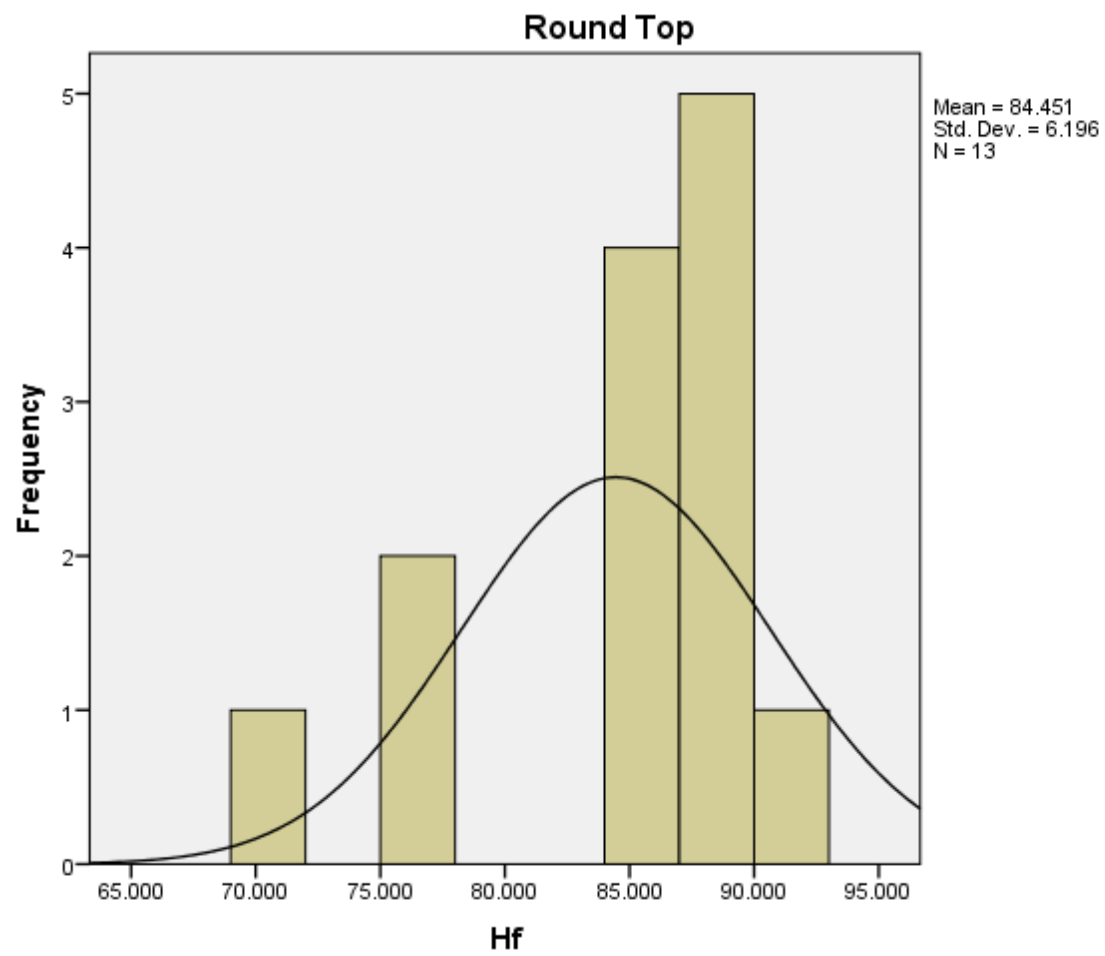


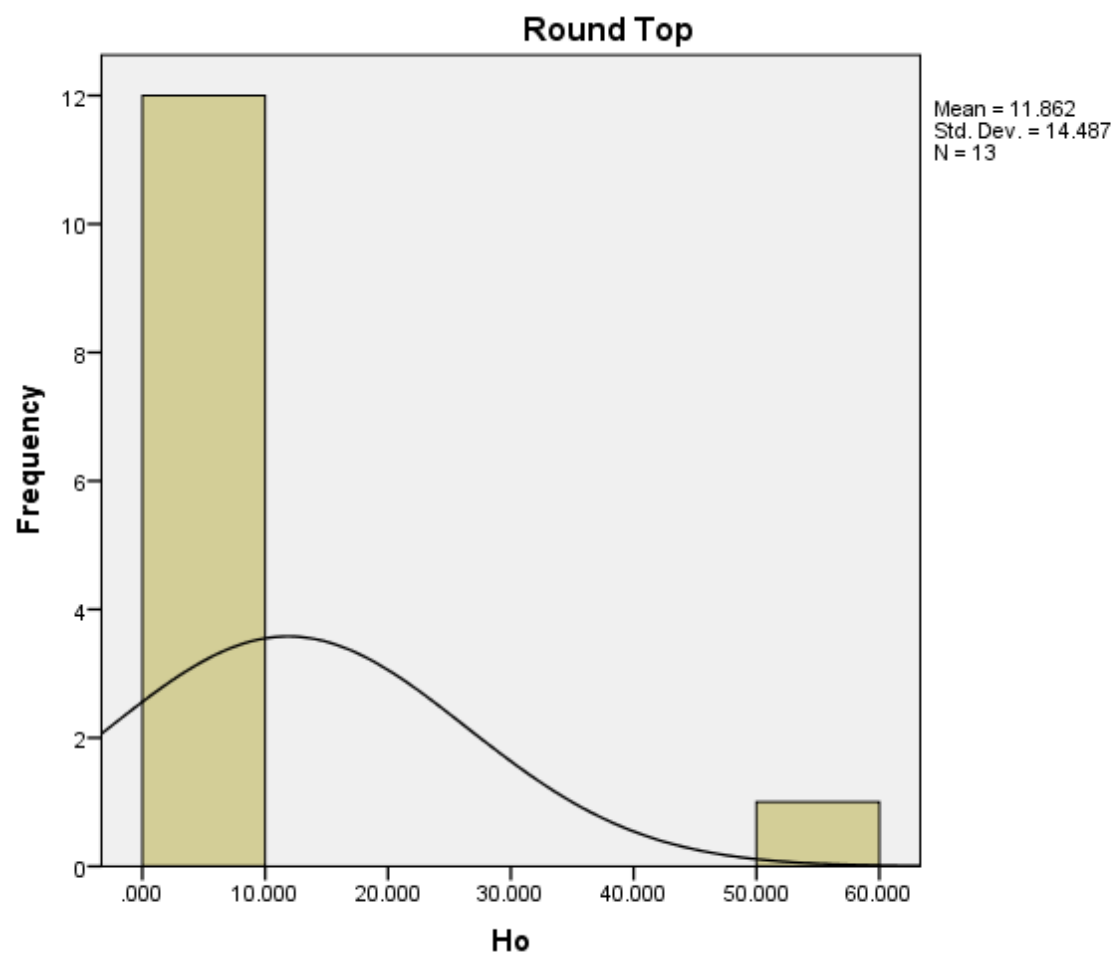


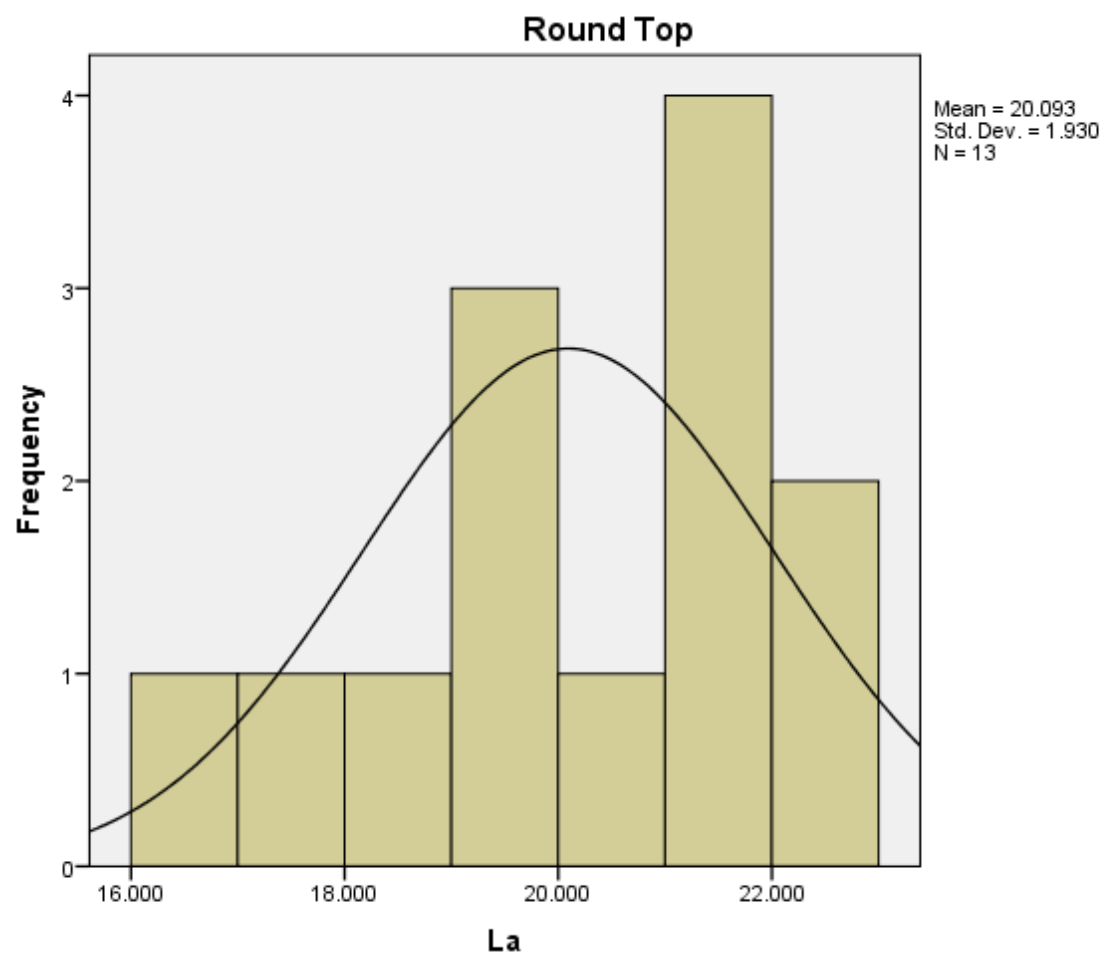


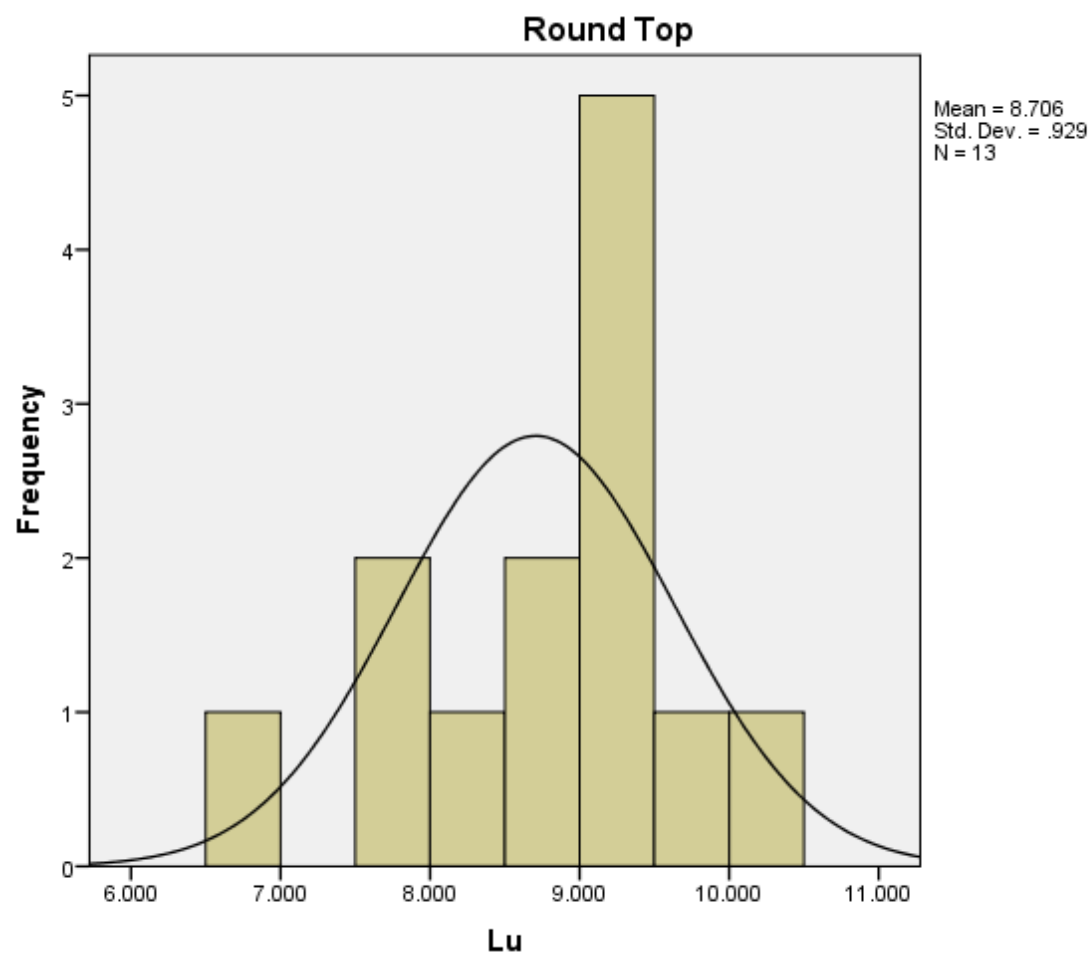


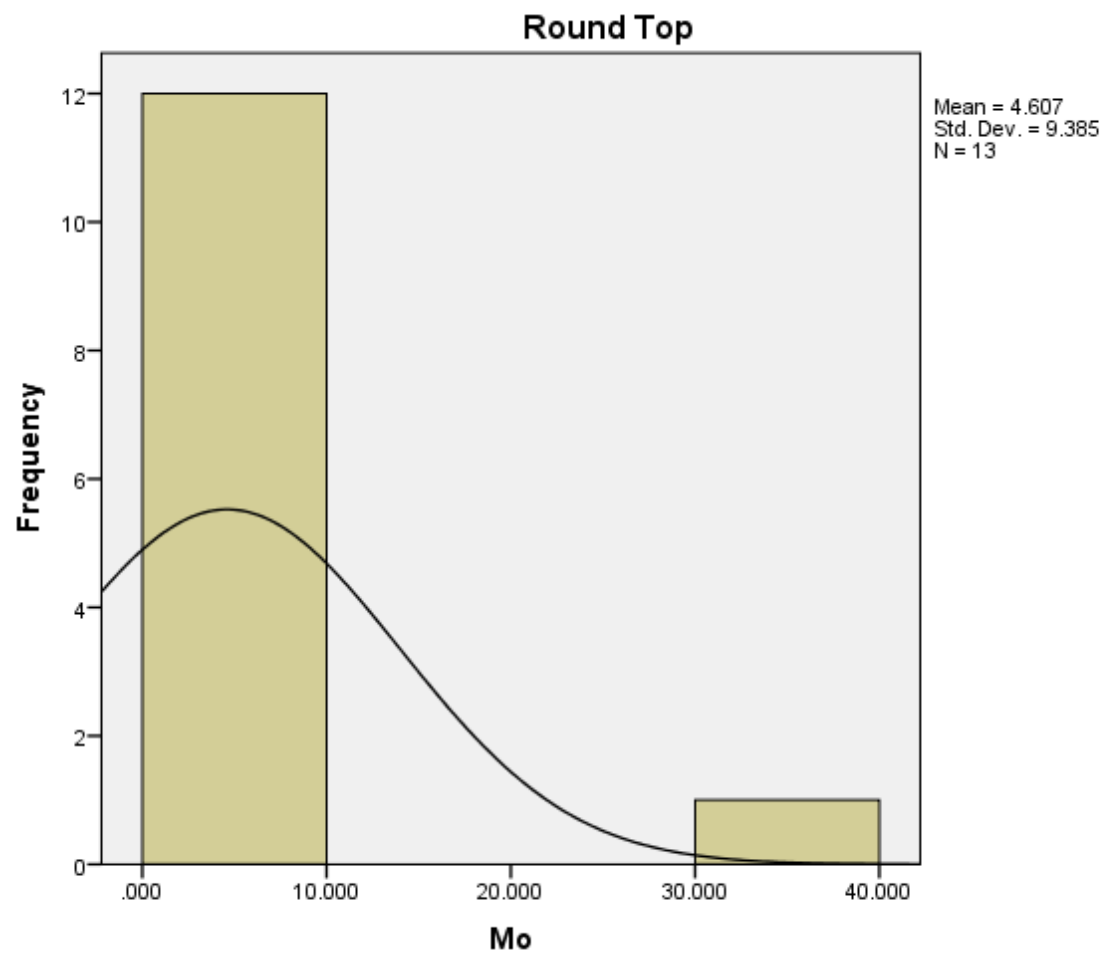


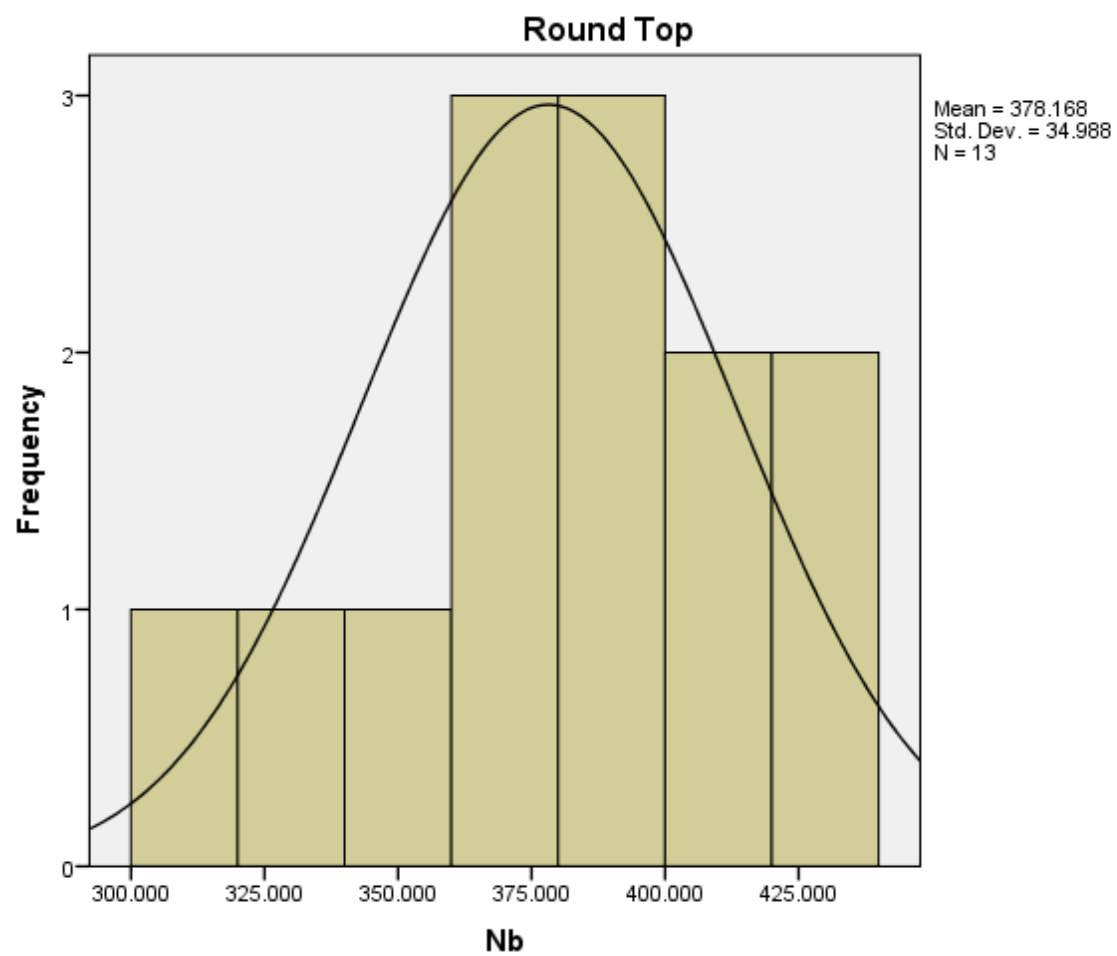


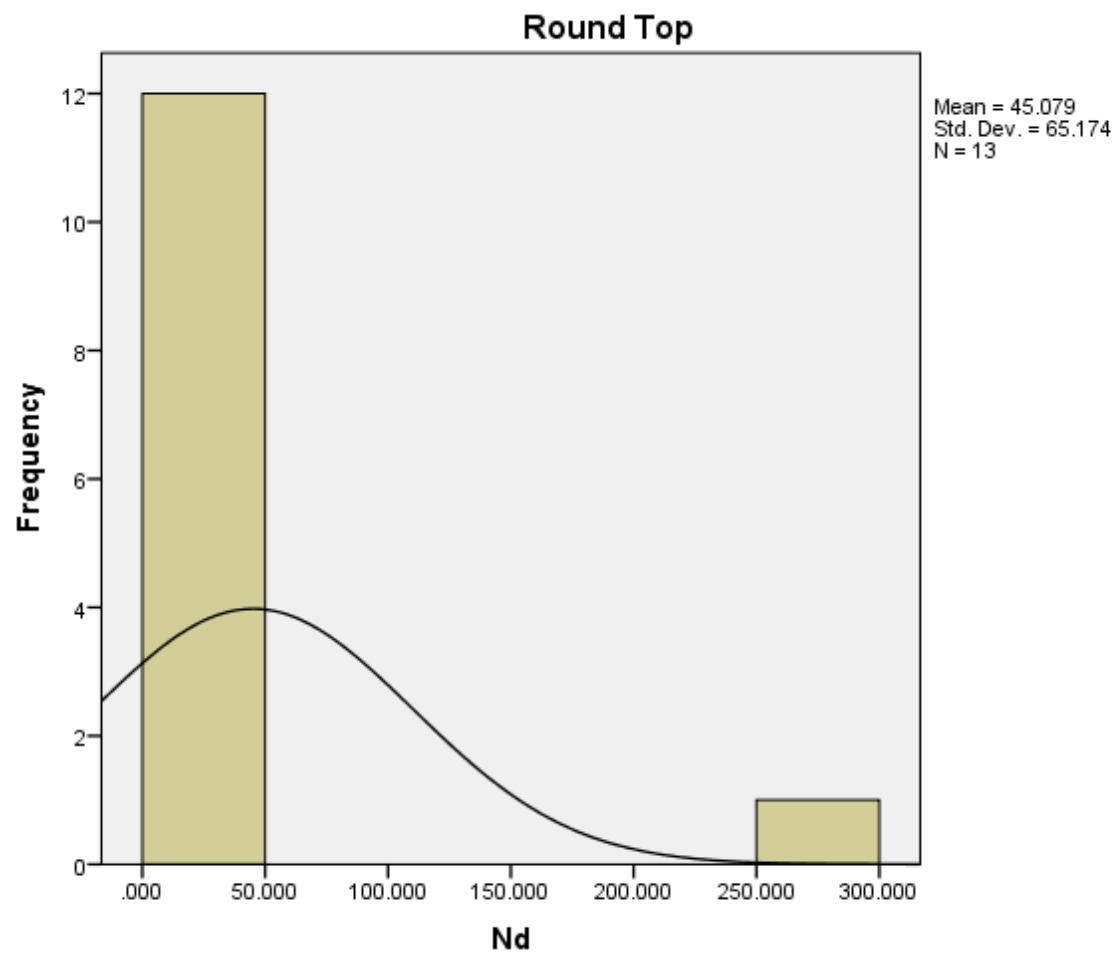


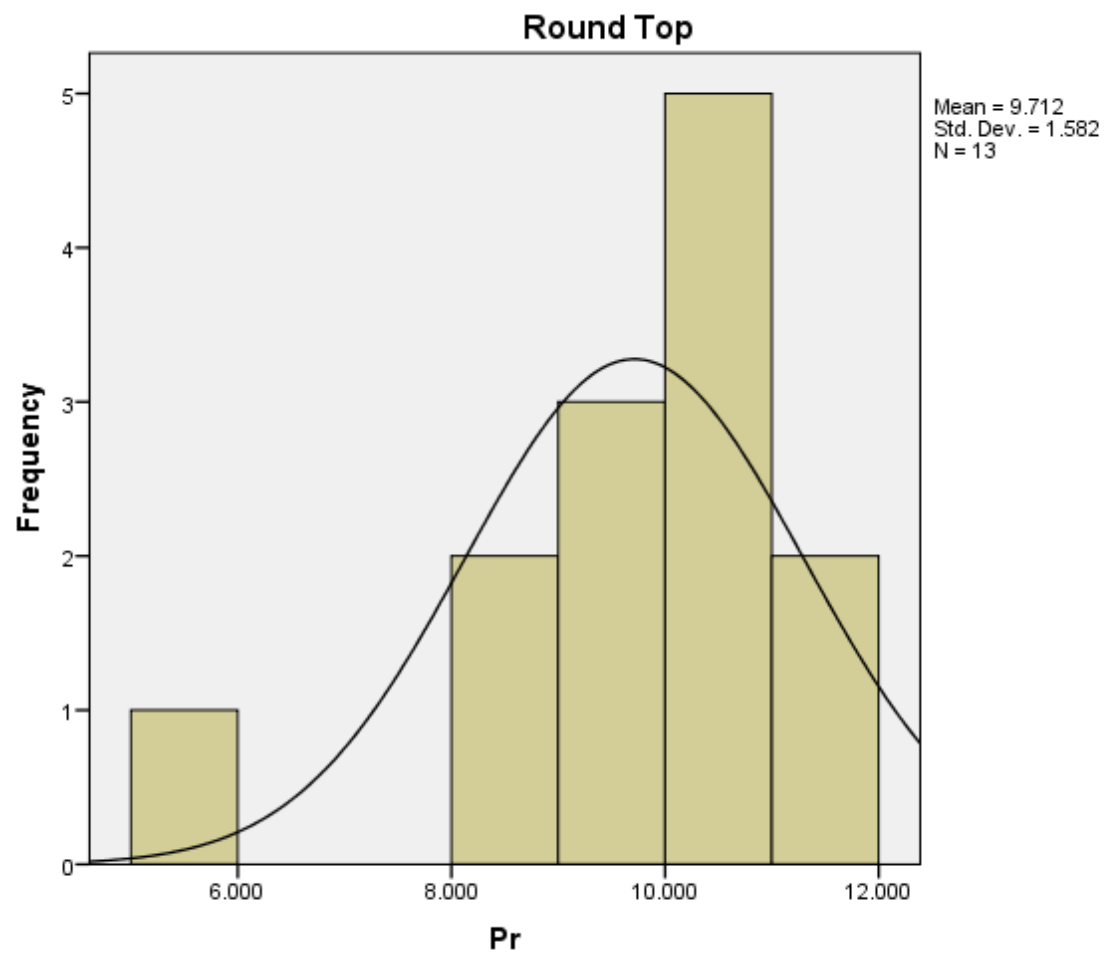


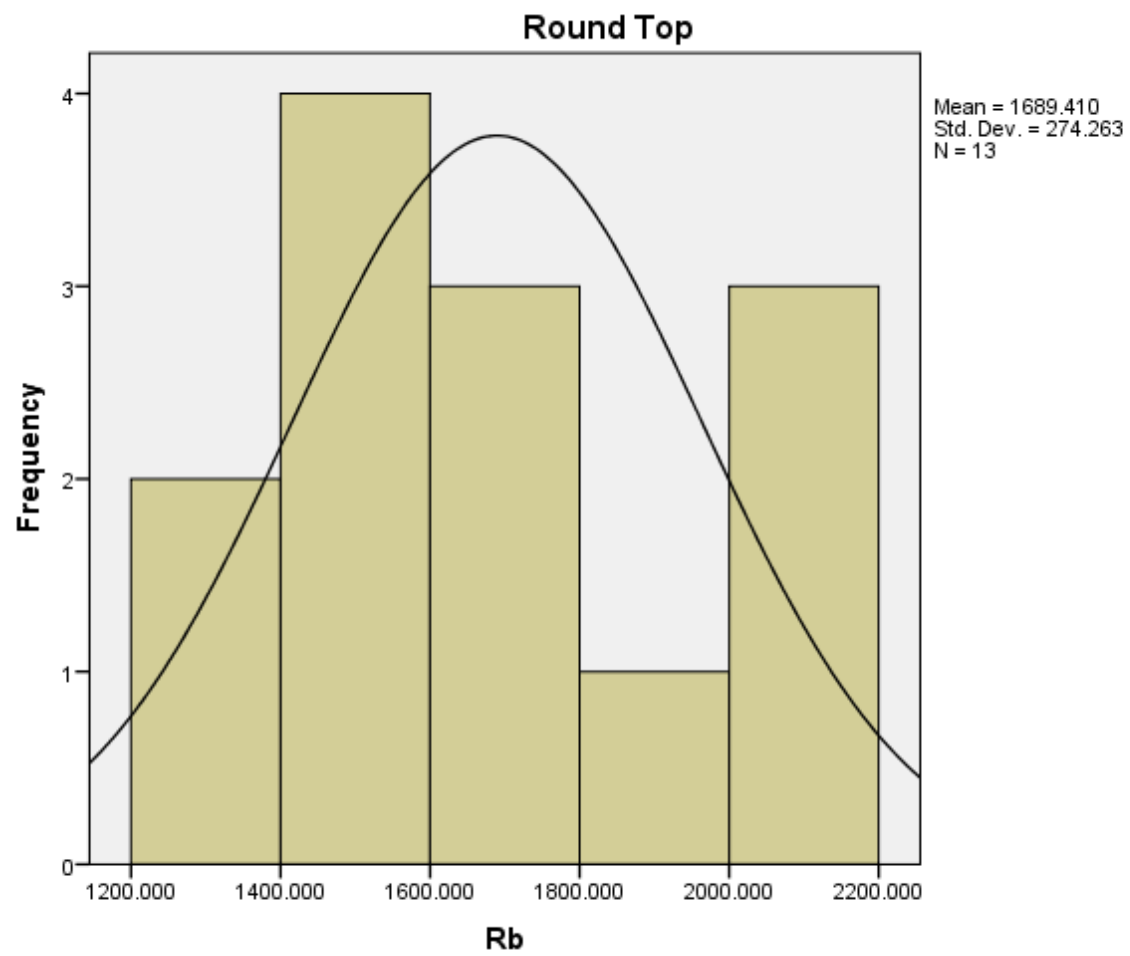


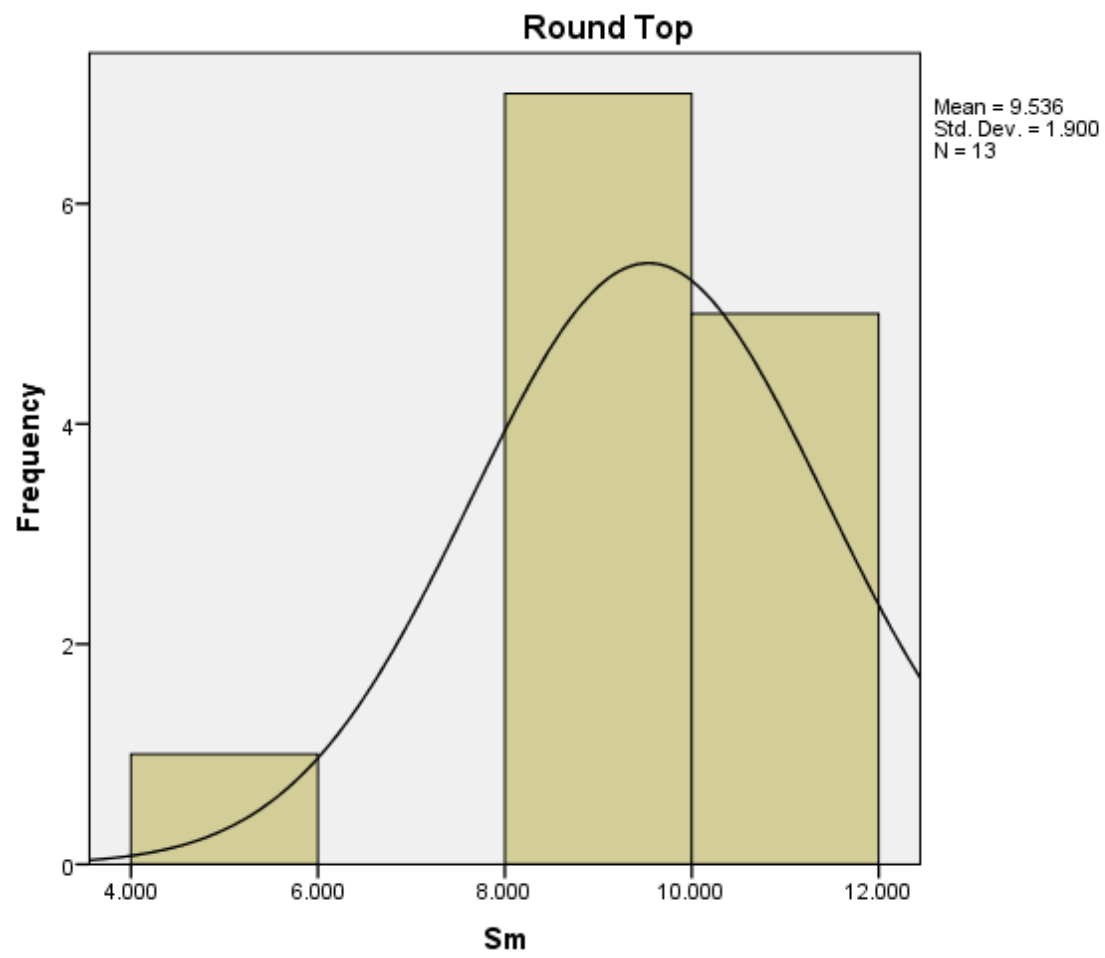


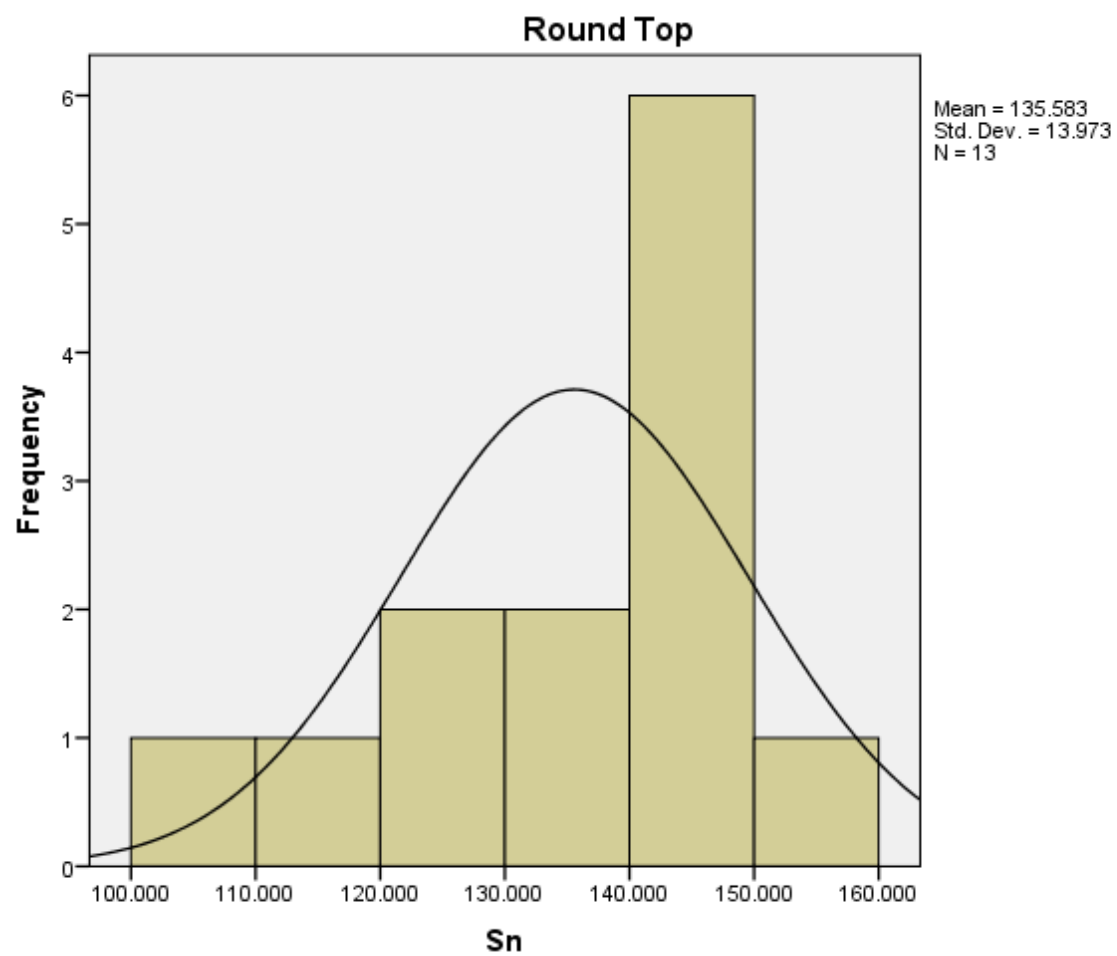


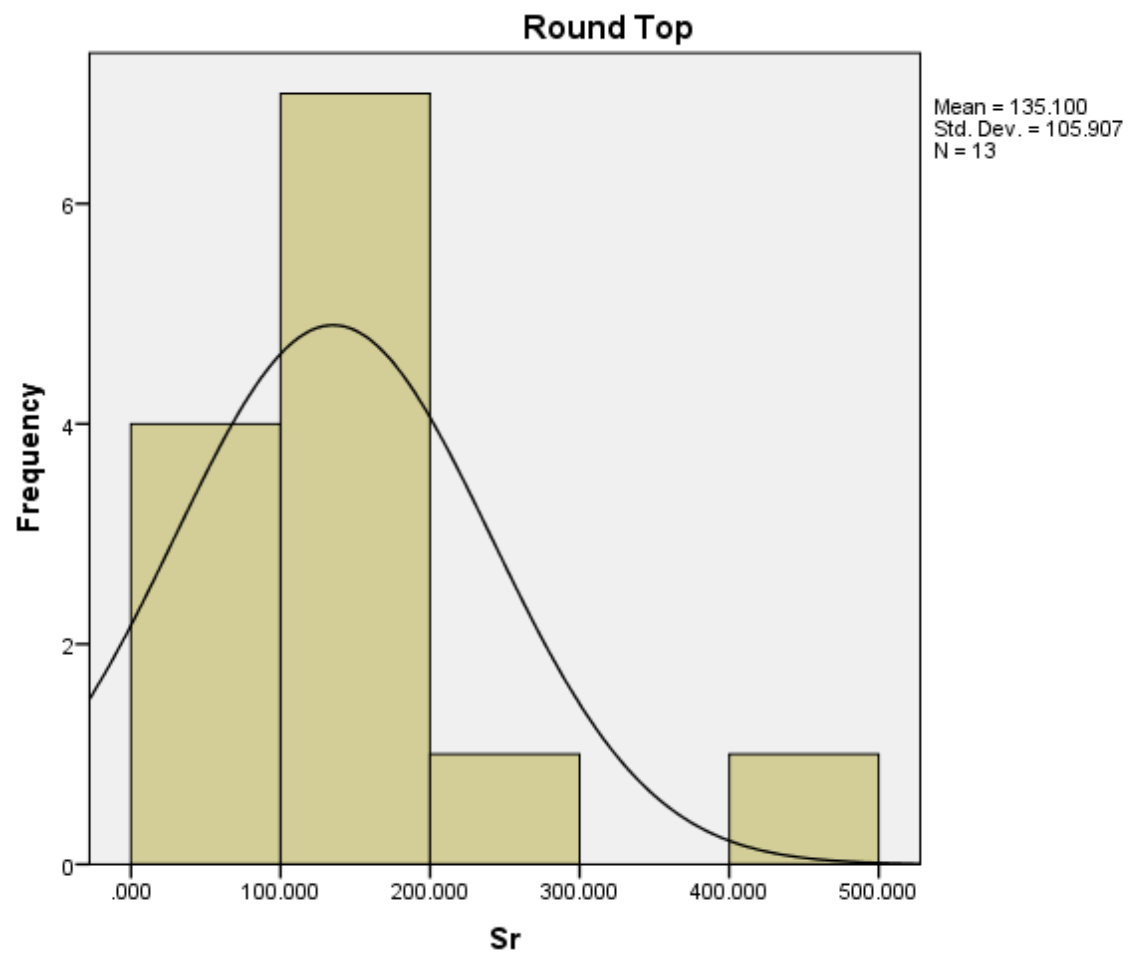


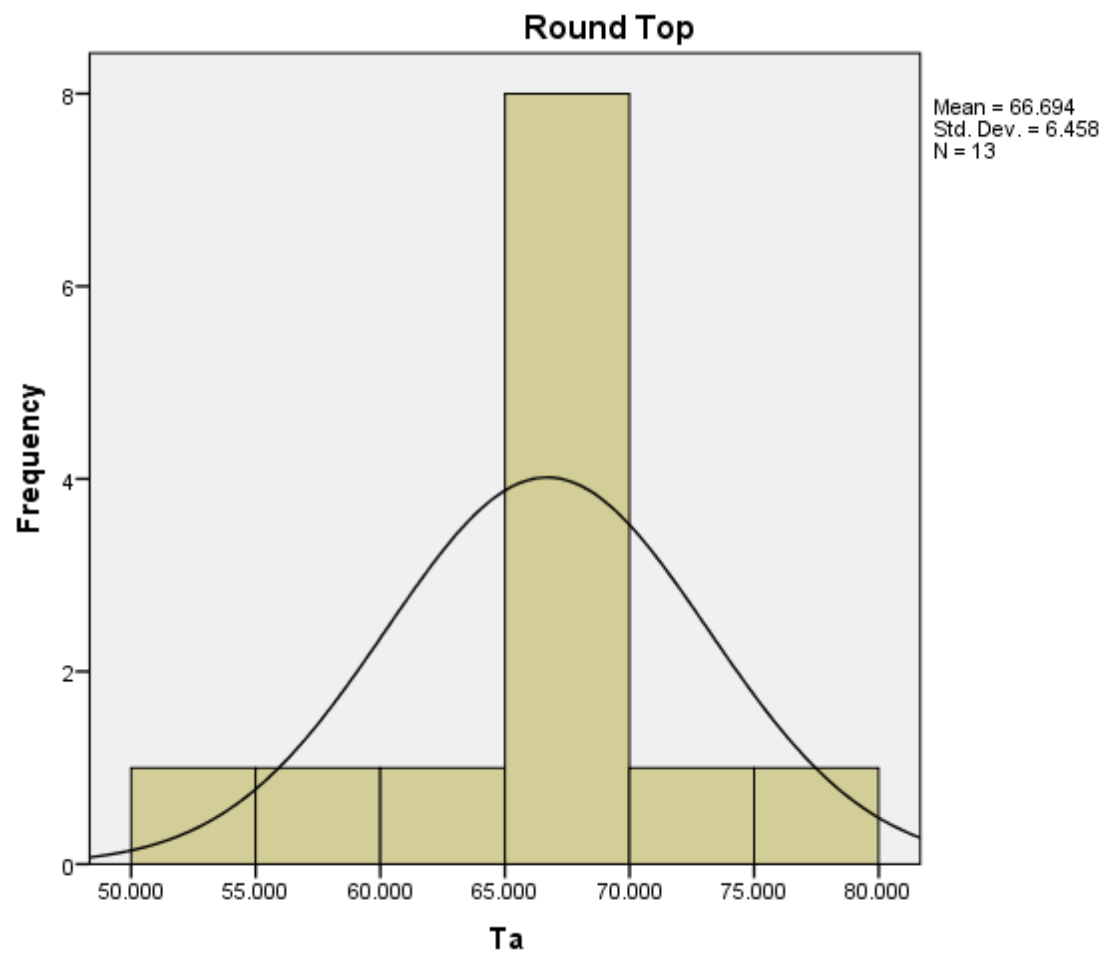


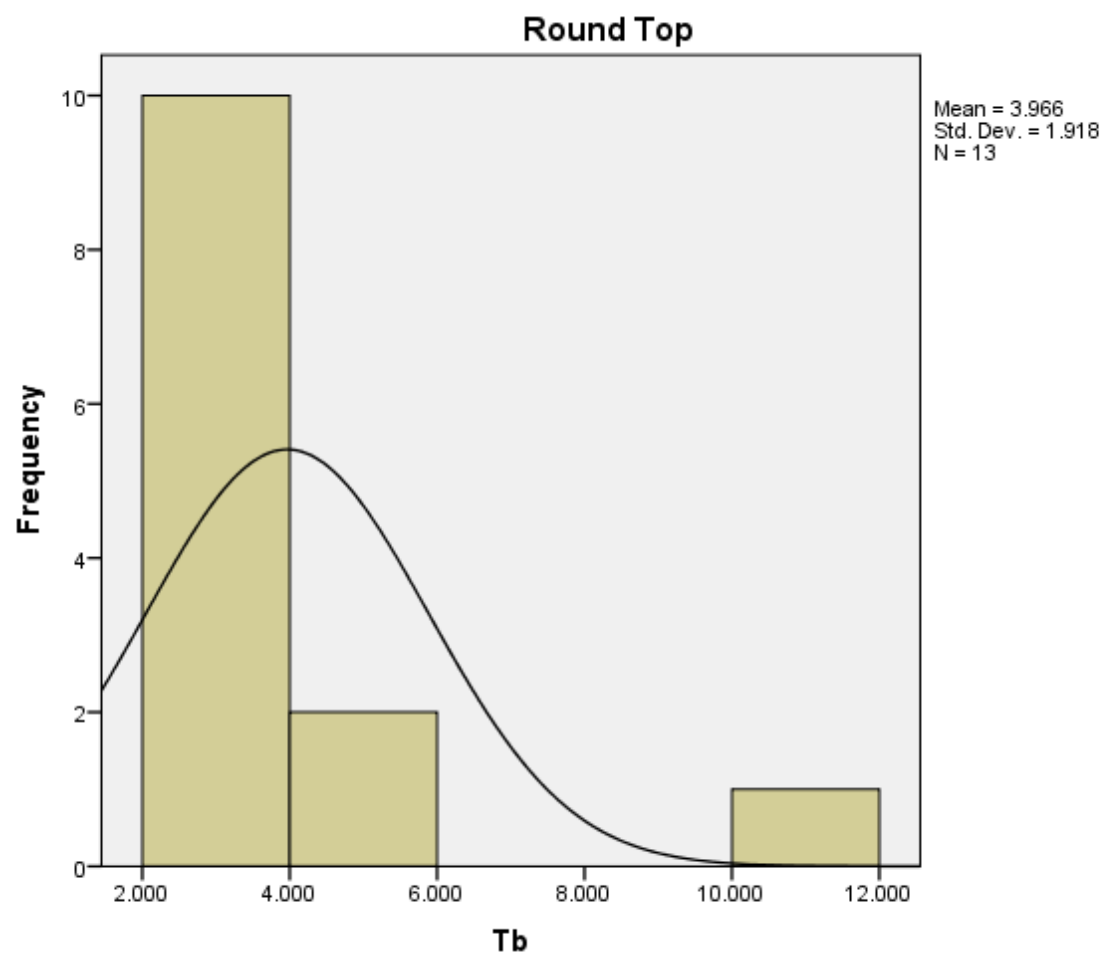


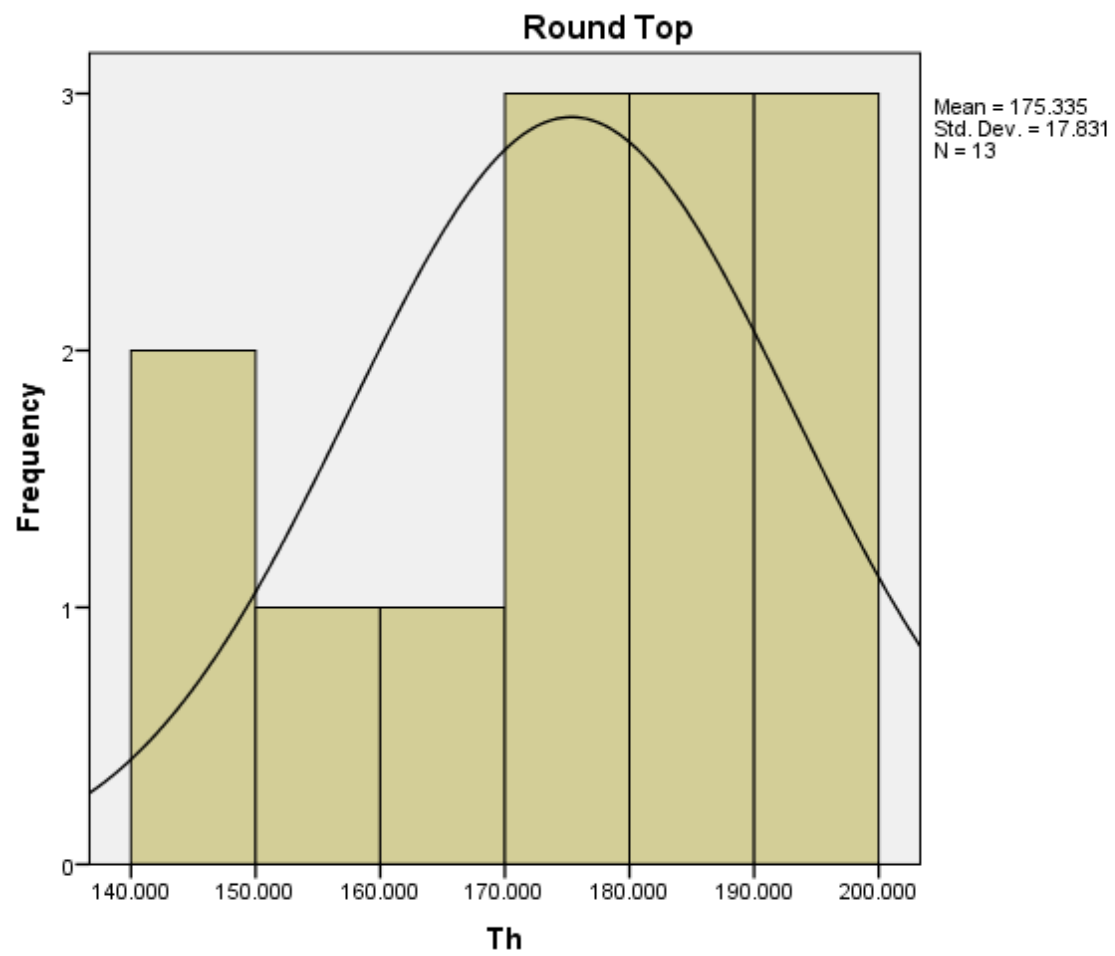


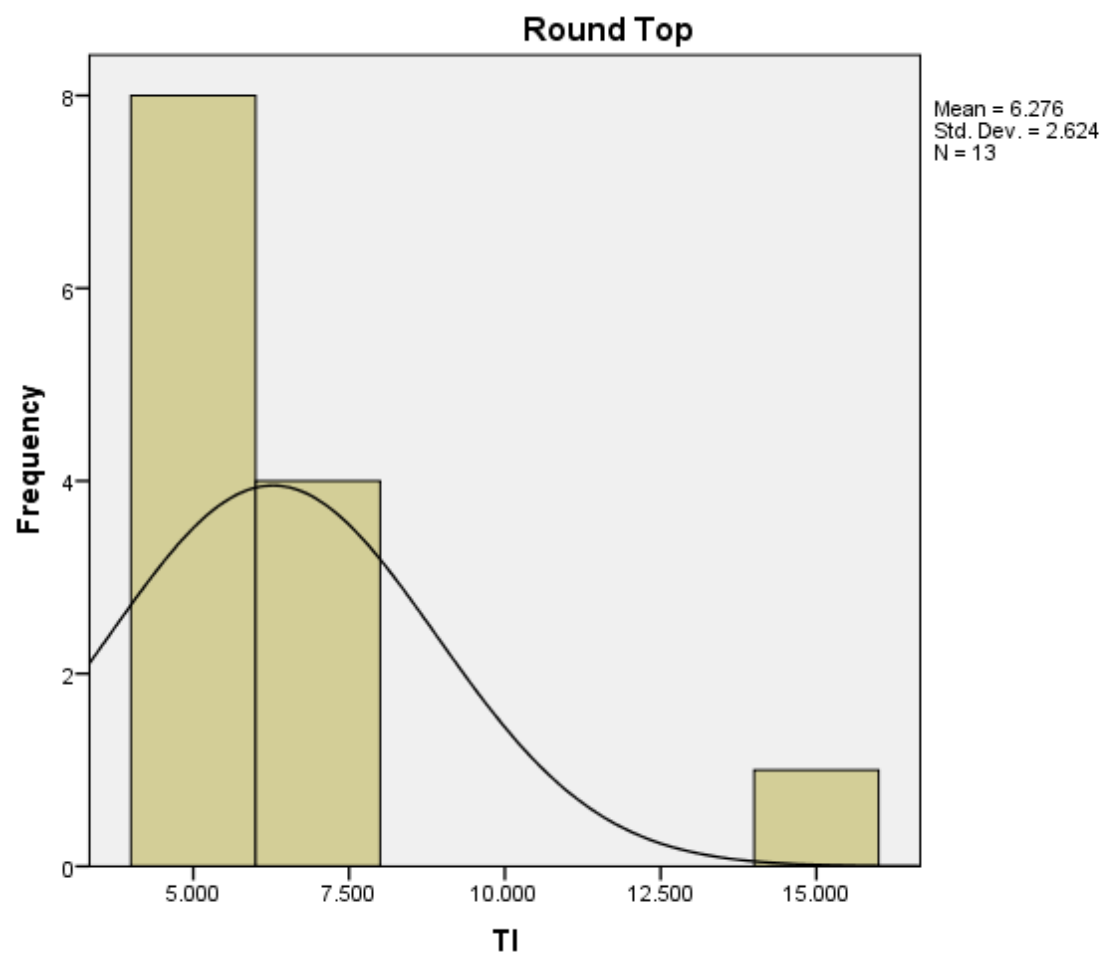


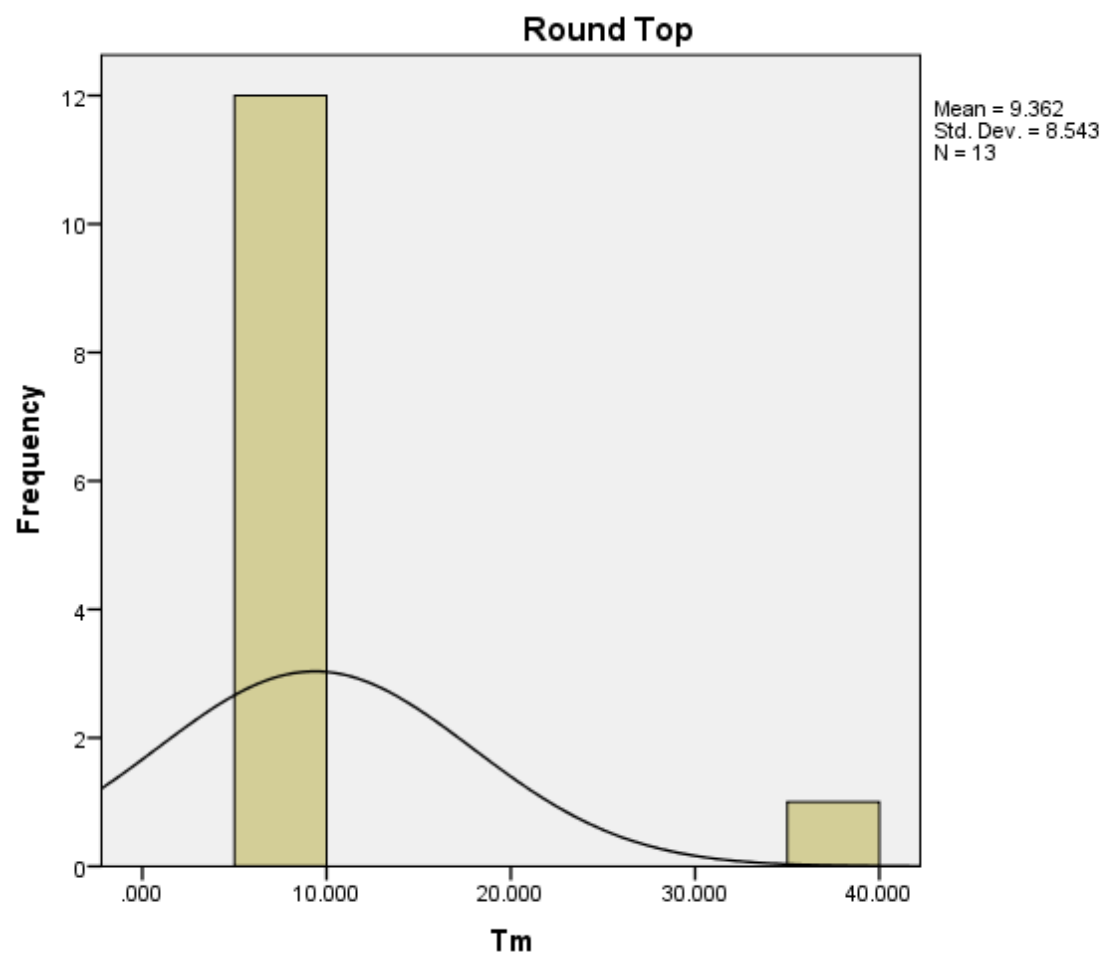


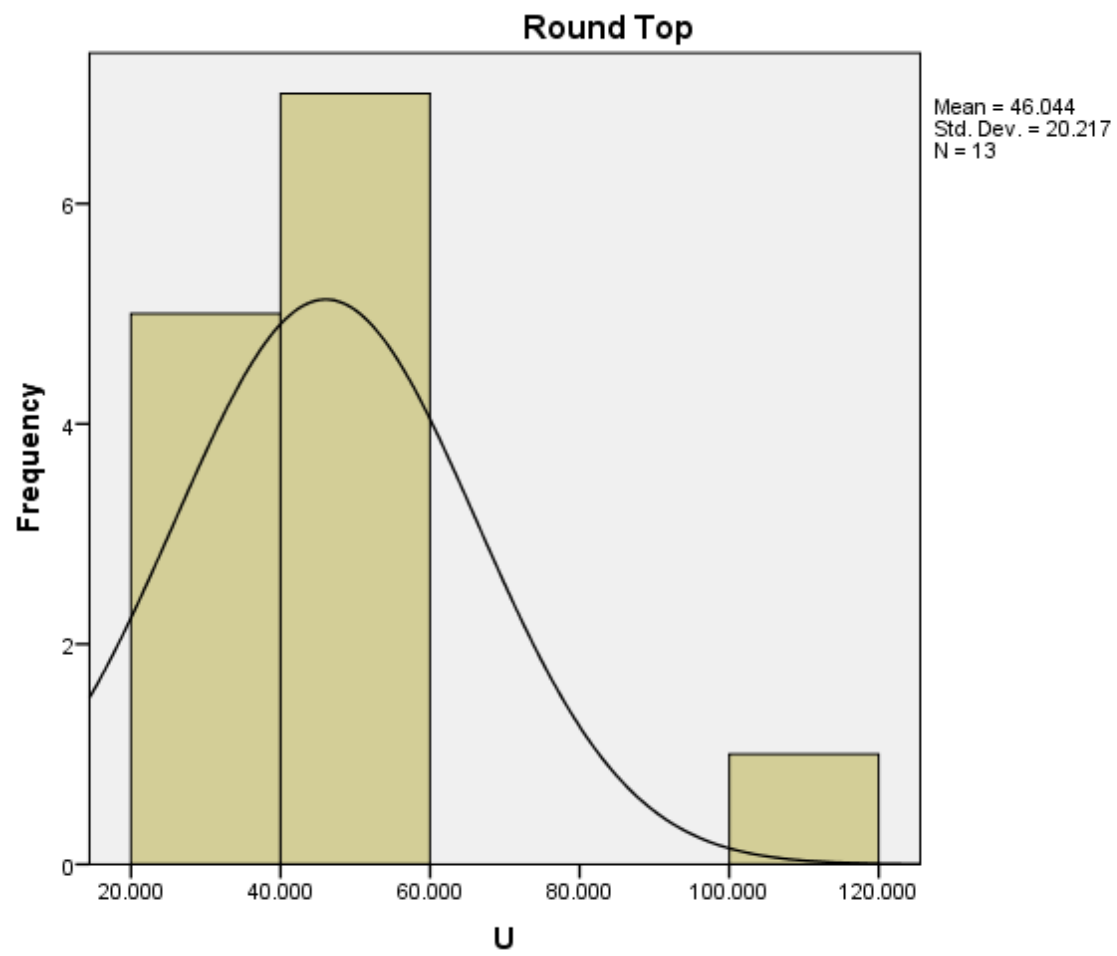


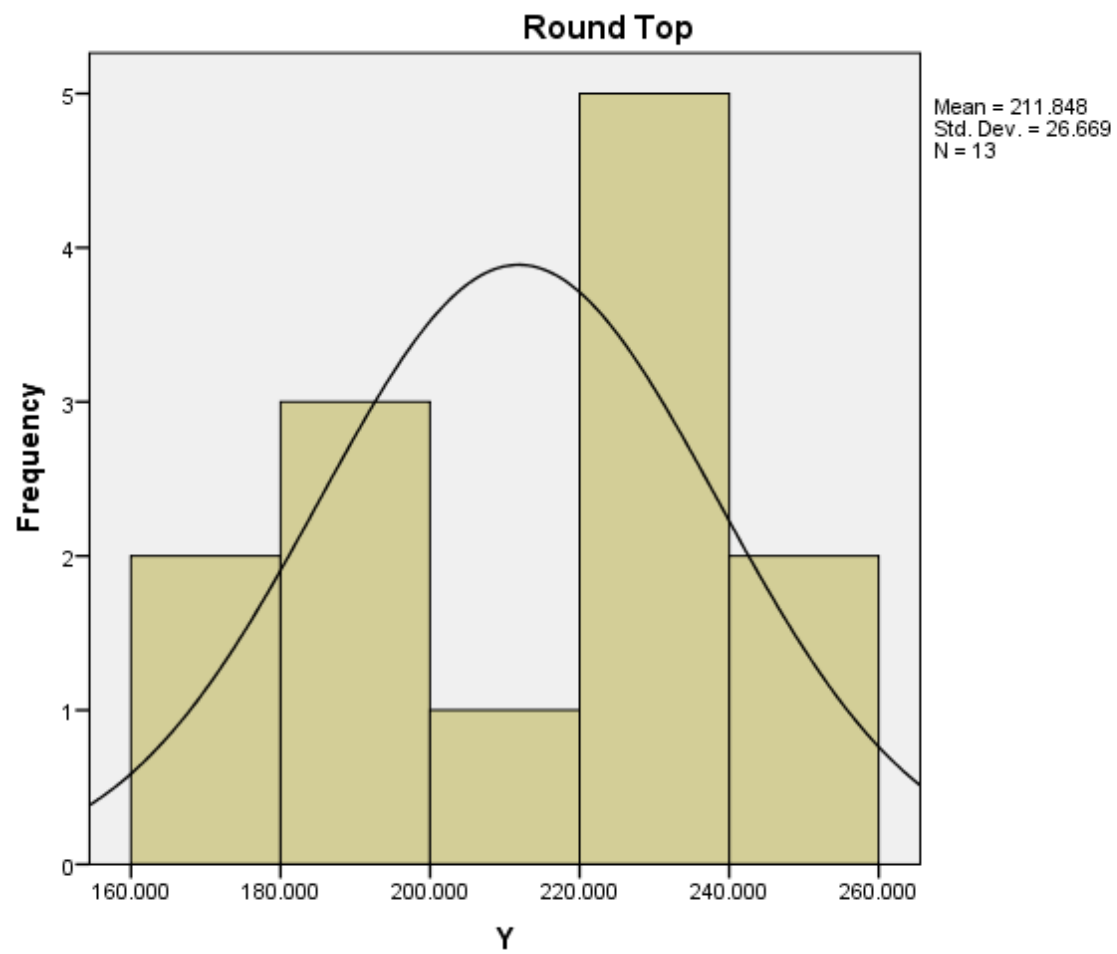


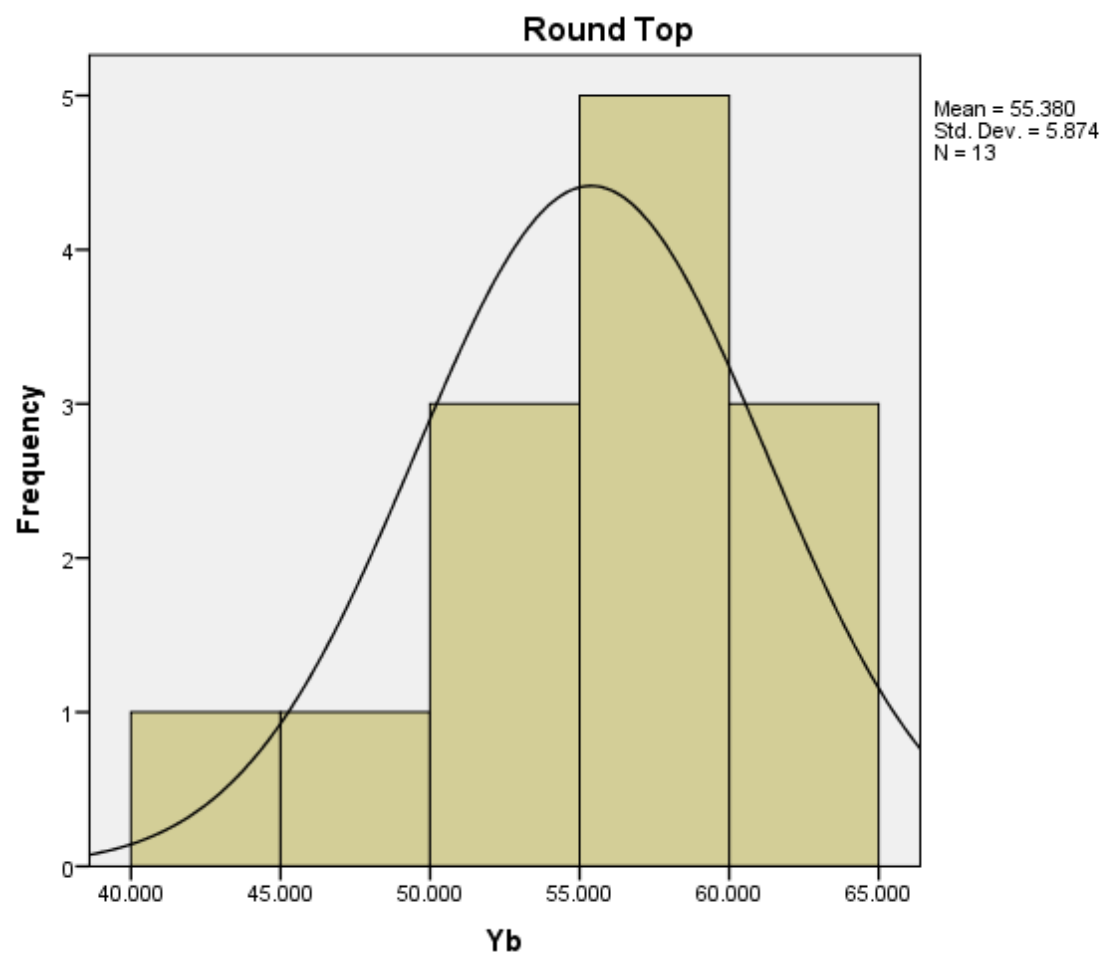


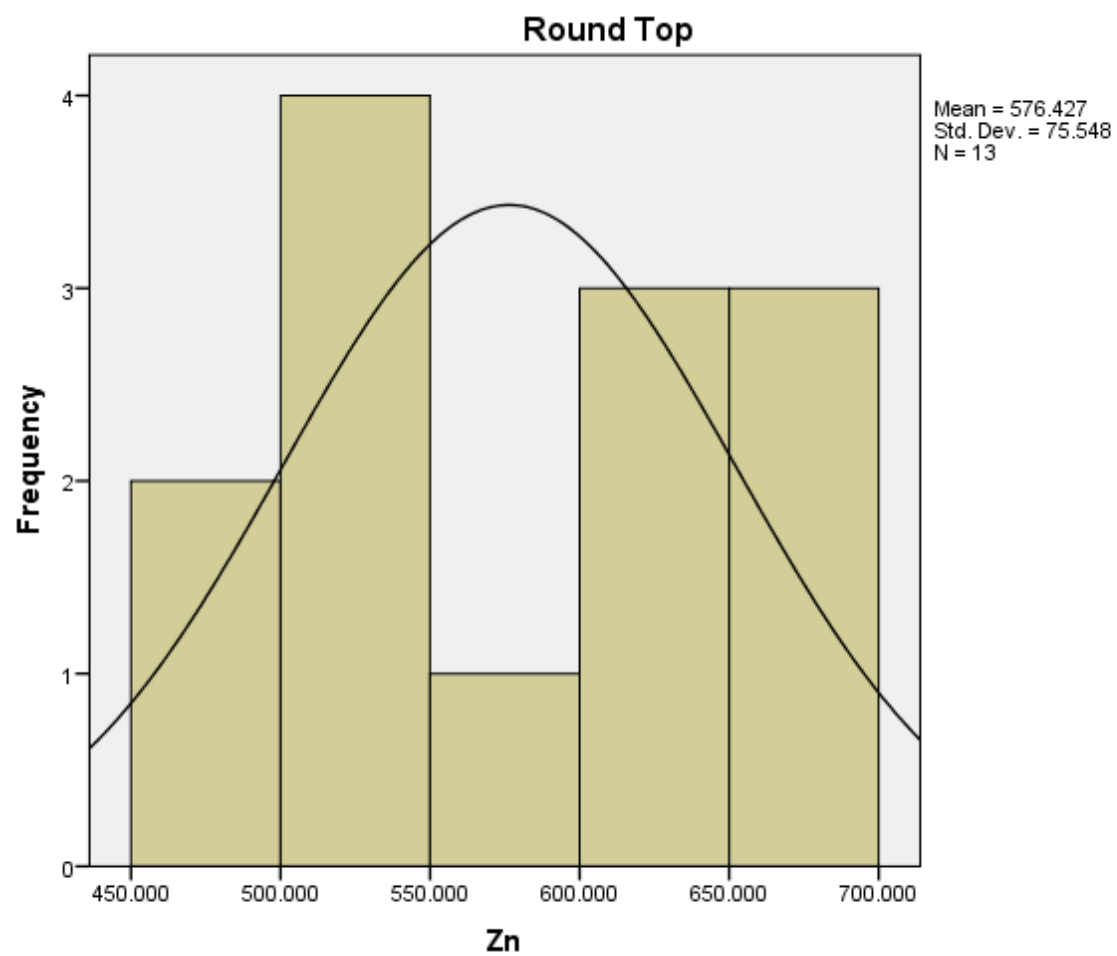


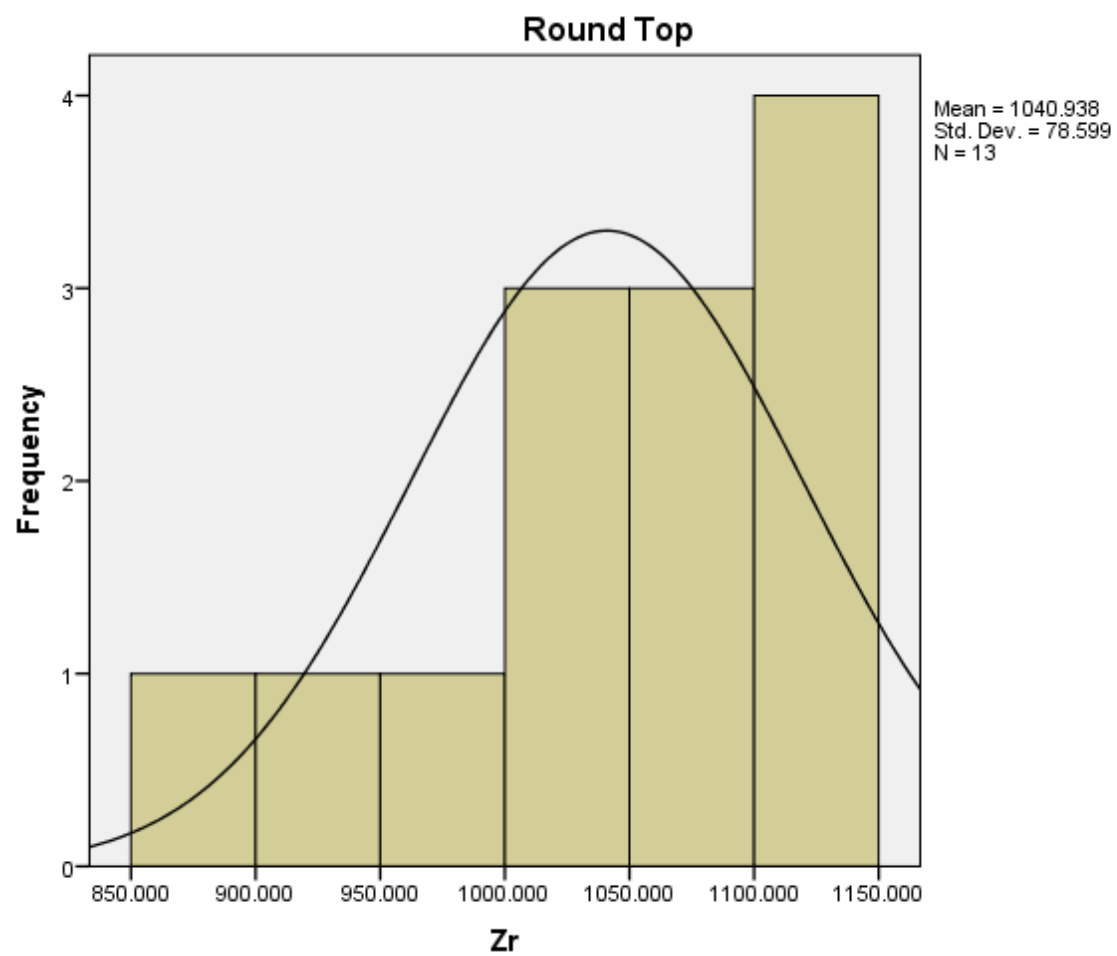


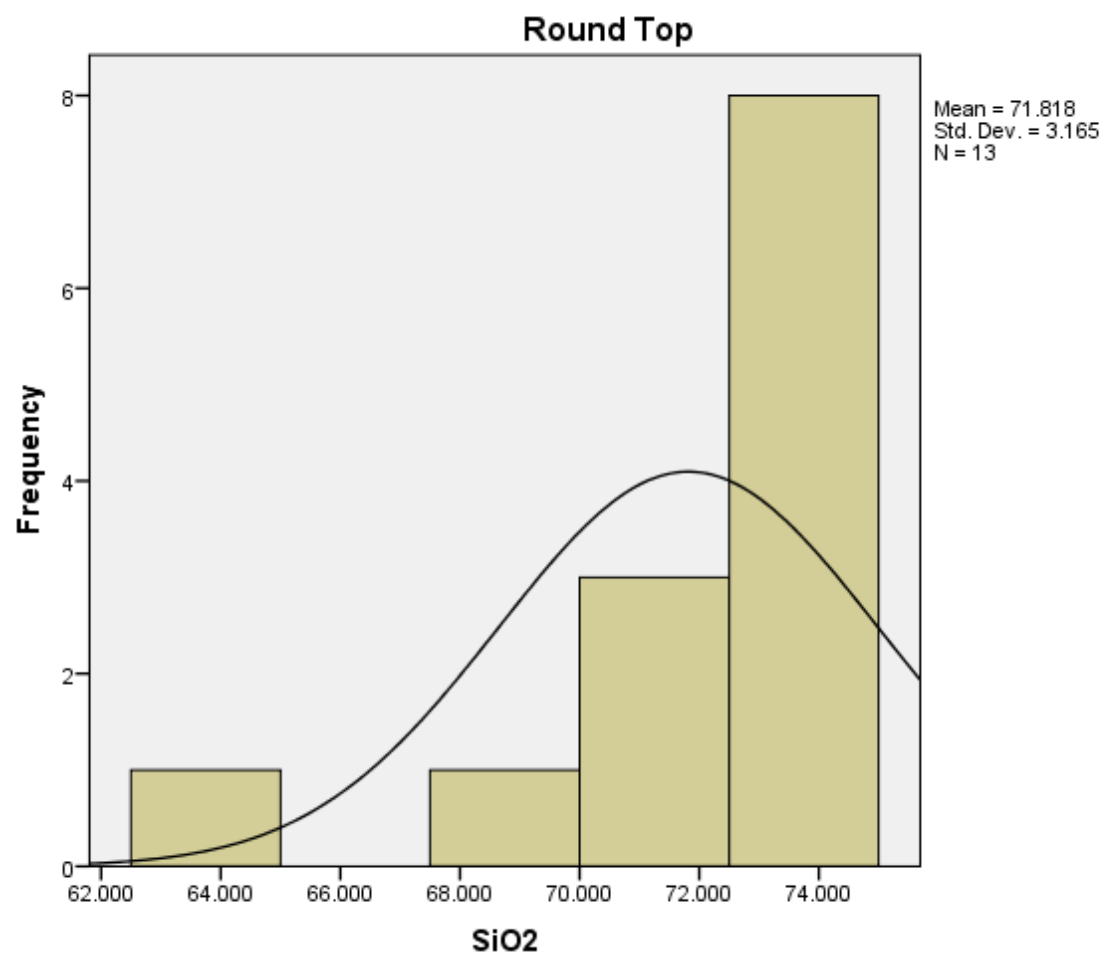


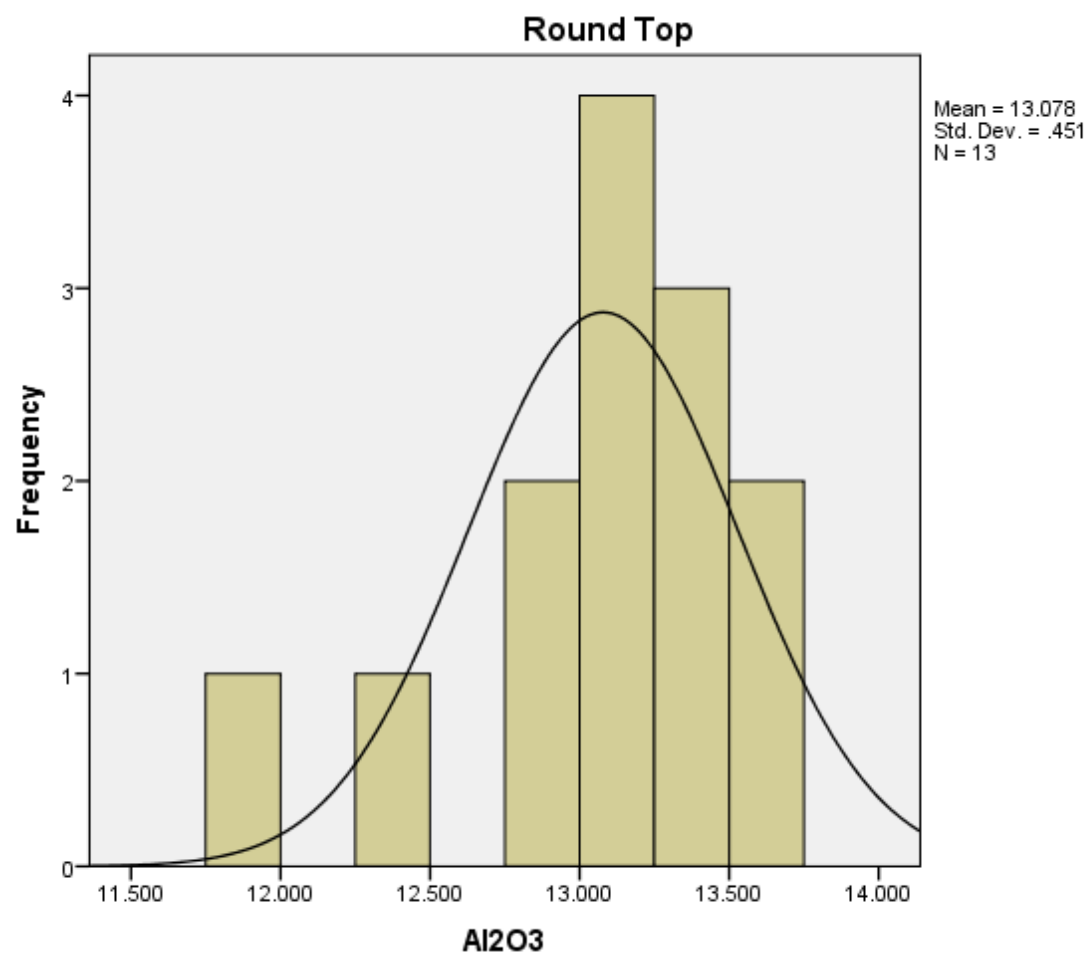


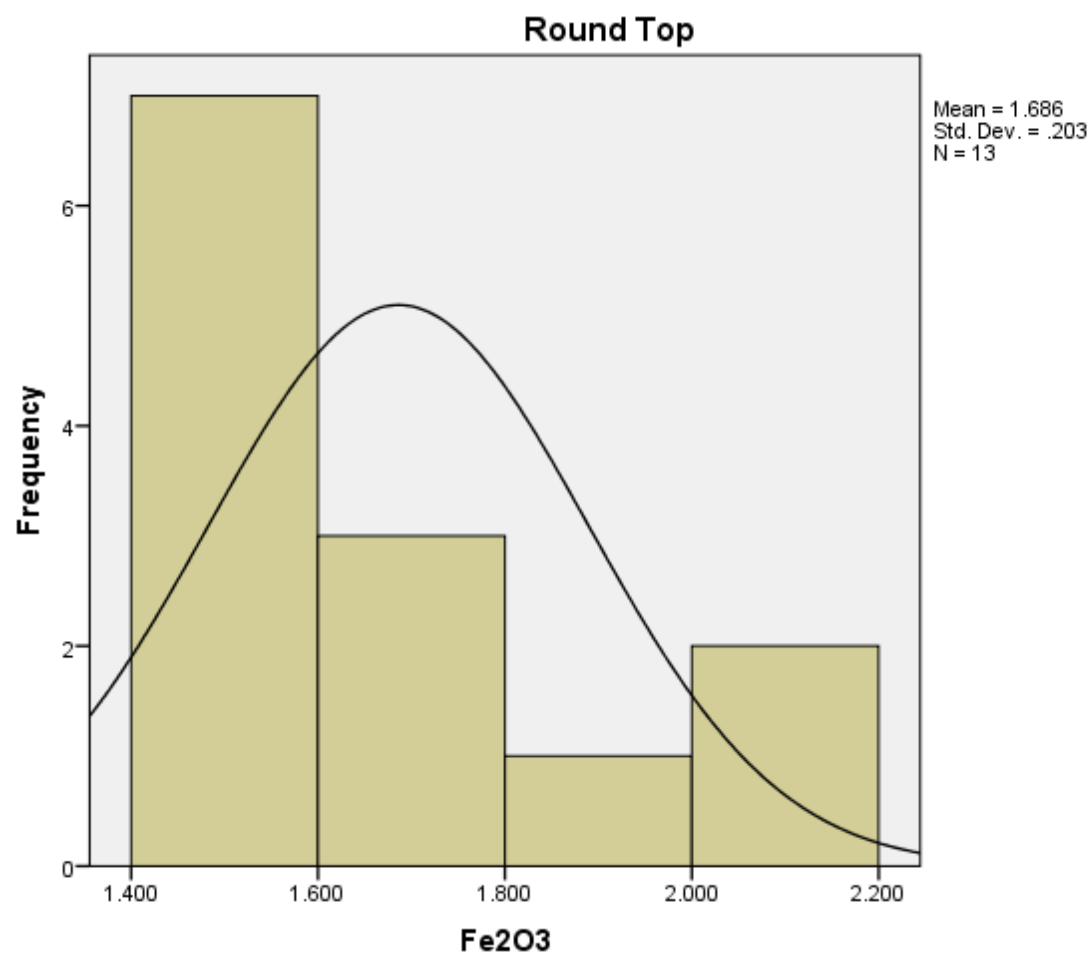


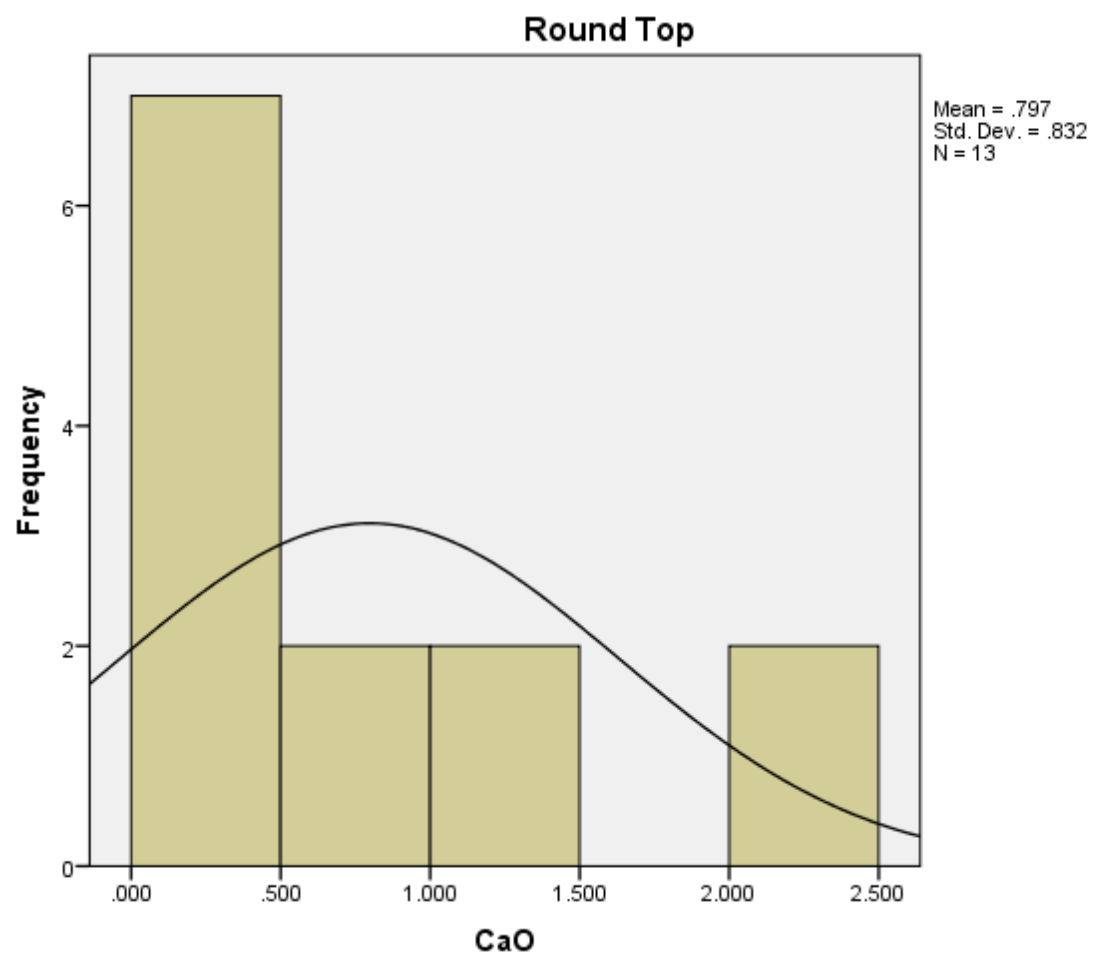


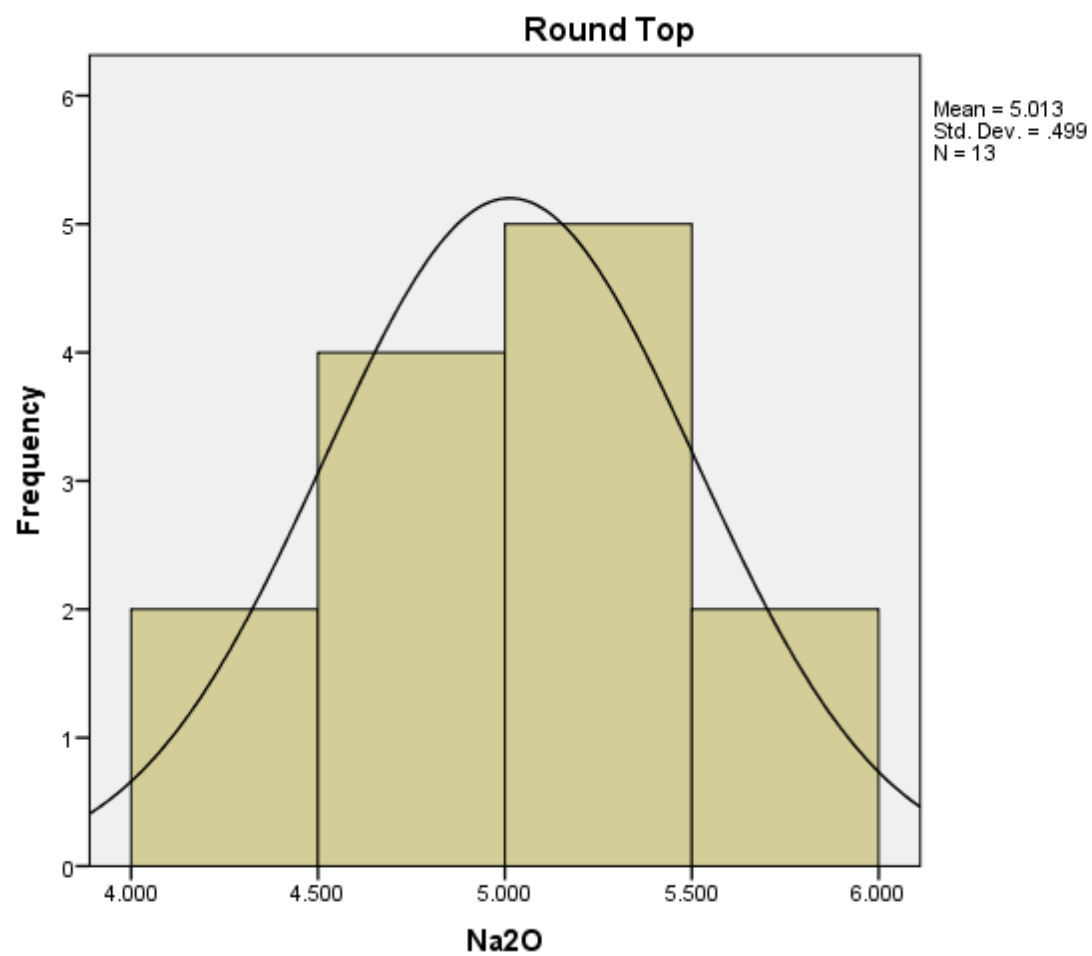


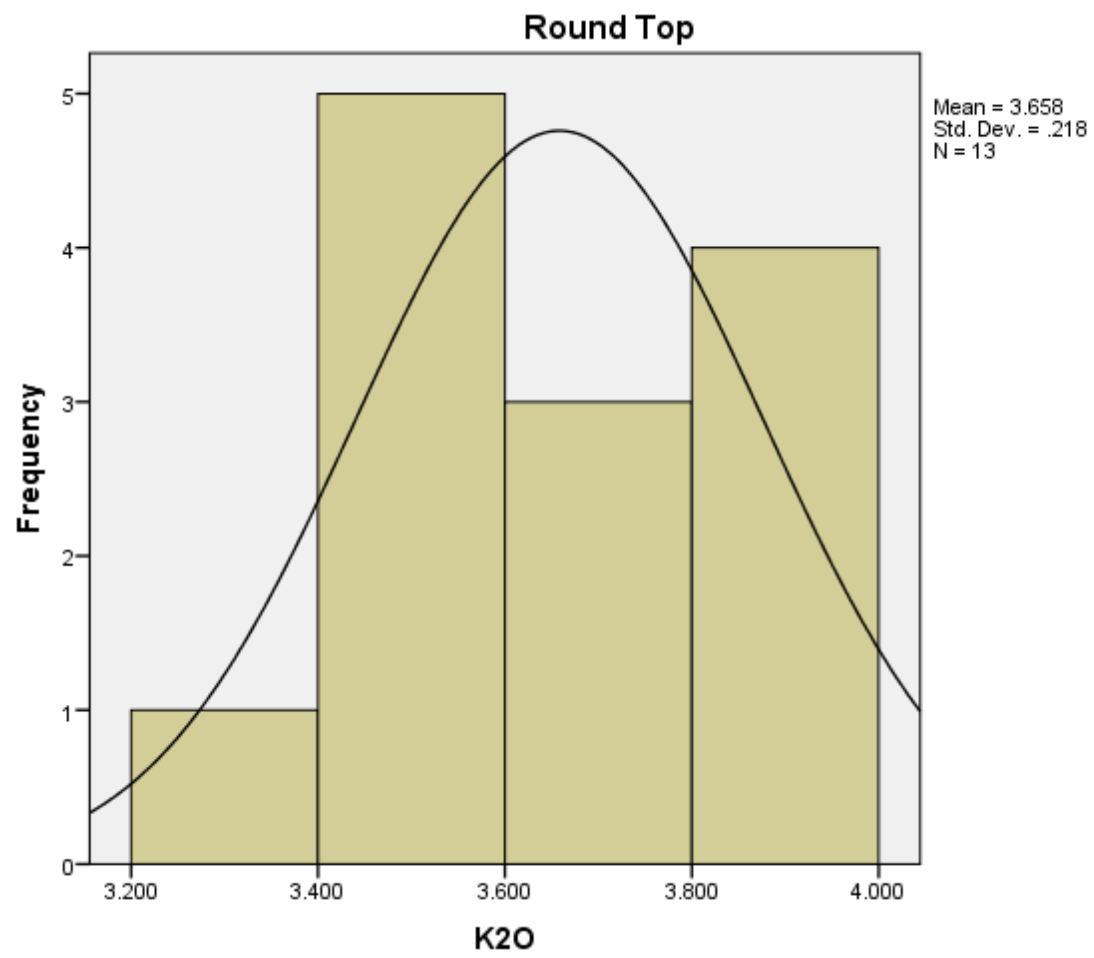


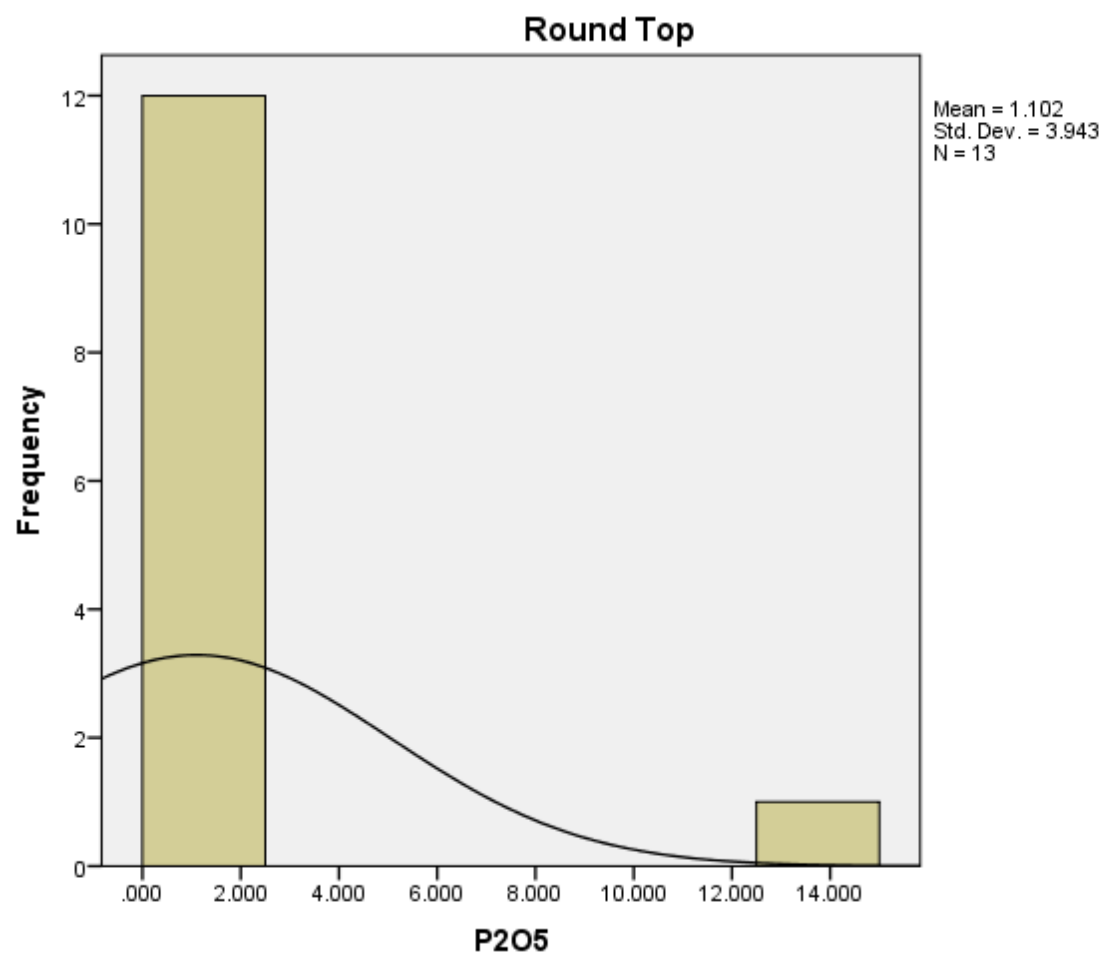


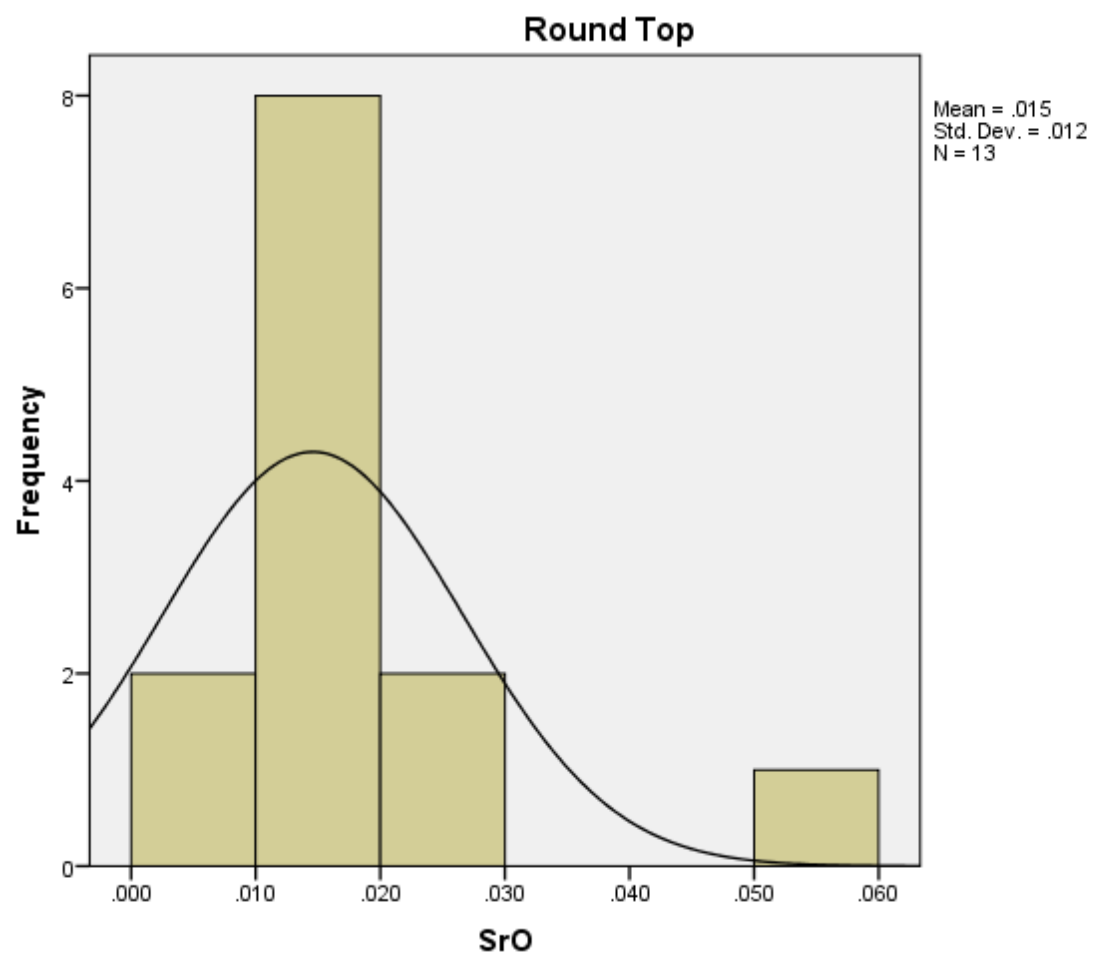


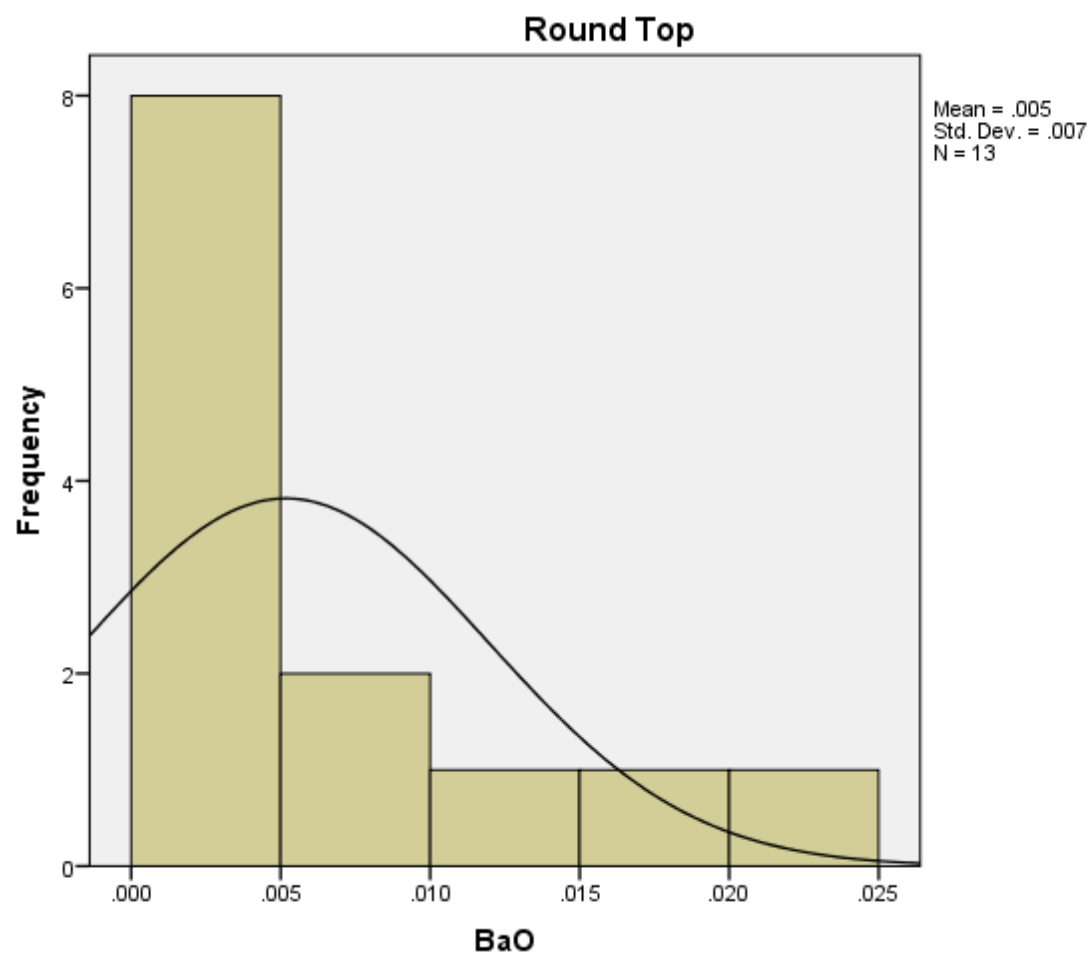












APPENDIX VI: CORRELATION COEFFICIENTS

Correlation Coefficients: Little Blanca

Correlations		Ba	Be	Ce	Cs	Dy	Er	Eu	F	Ga	Gd	Hf
Ba	Pearson Correlation	1	0.293	-0.165	.514**	-0.244	-0.235	0.308	-0.285	-0.238	-0.206	-0.131
	Sig. (2-tailed)		0.411	0.324	0.001	0.14	0.155	0.06	0.083	0.15	0.216	0.434
	N	38	10	38	38	38	38	38	38	38	38	38
Be	Pearson Correlation	0.293	1	0.022	0.616	0.059	0.08	-0.171	0.334	-.886**	0.023	-0.42
	Sig. (2-tailed)	0.411		0.951	0.058	0.871	0.827	0.637	0.346	0.001	0.951	0.227
	N	10	10	10	10	10	10	10	10	10	10	10
Ce	Pearson Correlation	-0.165	0.022	1	-0.03	.501**	.486**	0.094	0.042	.415**	.540**	0.155
	Sig. (2-tailed)	0.324	0.951		0.857	0.001	0.002	0.574	0.804	0.009	0	0.353
	N	38	10	38	38	38	38	38	38	38	38	38
Cs	Pearson Correlation	.514**	0.616	-0.03	1	-0.23	-0.182	0.16	-.375*	-0.089	-0.207	0.01
	Sig. (2-tailed)	0.001	0.058	0.857		0.165	0.273	0.336	0.021	0.597	0.213	0.953
	N	38	10	38	38	38	38	38	38	38	38	38
Dy	Pearson Correlation	-0.244	0.059	.501**	-0.23	1	.986**	0.042	.581**	0.122	.962**	0.109
	Sig. (2-tailed)	0.14	0.871	0.001	0.165		0	0.804	0	0.465	0	0.517
	N	38	10	38	38	38	38	38	38	38	38	38
Er	Pearson Correlation	-0.235	0.08	.486**	-0.182	.986**	1	0.045	.567**	0.153	.934**	0.178
	Sig. (2-tailed)	0.155	0.827	0.002	0.273	0		0.788	0	0.358	0	0.286
	N	38	10	38	38	38	38	38	38	38	38	38
Eu	Pearson Correlation	0.308	-0.171	0.094	0.16	0.042	0.045	1	-0.026	-0.168	0.136	-0.109
	Sig. (2-tailed)	0.06	0.637	0.574	0.336	0.804	0.788		0.878	0.313	0.414	0.515
	N	38	10	38	38	38	38	38	38	38	38	38
F	Pearson Correlation	-0.285	0.334	0.042	-.375*	.581**	.567**	-0.026	1	-0.113	.551**	-0.284
	Sig. (2-tailed)	0.083	0.346	0.804	0.021	0	0	0.878		0.501	0	0.084
	N	38	10	38	38	38	38	38	38	38	38	38
Ga	Pearson Correlation	-0.238	-.886**	.415**	-0.089	0.122	0.153	-0.168	-0.113	1	0.161	0.287
	Sig. (2-tailed)	0.15	0.001	0.009	0.597	0.465	0.358	0.313	0.501		0.333	0.08
	N	38	10	38	38	38	38	38	38	38	38	38
Gd	Pearson Correlation	-0.206	0.023	.540**	-0.207	.962**	.934**	0.136	.551**	0.161	1	-0.003
	Sig. (2-tailed)	0.216	0.951	0	0.213	0	0	0.414	0	0.333		0.987
	N	38	10	38	38	38	38	38	38	38	38	38
Hf	Pearson Correlation	-0.131	-0.42	0.155	0.01	0.109	0.178	-0.109	-0.284	0.287	-0.003	1
	Sig. (2-tailed)	0.434	0.227	0.353	0.953	0.517	0.286	0.515	0.084	0.08	0.987	
	N	38	10	38	38	38	38	38	38	38	38	38
Ho	Pearson Correlation	-0.234	0.035	.491**	-0.223	.996**	.986**	0.041	.607**	0.119	.961**	0.072
	Sig. (2-tailed)	0.157	0.923	0.002	0.179	0	0	0.809	0	0.476	0	0.666
	N	38	10	38	38	38	38	38	38	38	38	38
La	Pearson Correlation	-0.216	0.305	.805**	-0.13	.683**	.670**	0.24	.352*	0.247	.775**	-0.046
	Sig. (2-tailed)	0.193	0.391	0	0.437	0	0	0.147	0.03	0.135	0	0.782
	N	38	10	38	38	38	38	38	38	38	38	38
Lu	Pearson Correlation	-0.23	0.064	.560**	-0.136	.914**	.954**	0.042	.512**	0.183	.864**	0.203
	Sig. (2-tailed)	0.164	0.86	0	0.415	0	0	0.802	0.001	0.273	0	0.222
	N	38	10	38	38	38	38	38	38	38	38	38

Correlation Coefficients: Little Blanca

Correlations		Ho	La	Lu	Mo	Nb	Nd	Pr	Rb	Sm	Sn	Sr
Ba	Pearson Correlation	-0.234	-0.216	-0.23	0.233	-0.025	-0.195	-0.272	0.073	-0.245	-0.055	0.076
	Sig. (2-tailed)	0.157	0.193	0.164	0.159	0.882	0.24	0.098	0.663	0.139	0.742	0.648
	N	38	38	38	38	38	38	38	38	38	38	38
Be	Pearson Correlation	0.035	0.305	0.064	.731*	-.834**	0.378	0.319	.719*	0.391	-.785**	0.611
	Sig. (2-tailed)	0.923	0.391	0.86	0.016	0.003	0.282	0.369	0.019	0.264	0.007	0.061
	N	10	10	10	10	10	10	10	10	10	10	10
Ce	Pearson Correlation	.491**	.805**	.560**	0.033	.328*	.739**	.789**	0.025	.693**	.454**	-0.087
	Sig. (2-tailed)	0.002	0	0	0.846	0.044	0	0	0.882	0	0.004	0.605
	N	38	38	38	38	38	38	38	38	38	38	38
Cs	Pearson Correlation	-0.223	-0.13	-0.136	0.241	0.124	-0.086	-0.134	.332*	-0.135	0.17	-0.132
	Sig. (2-tailed)	0.179	0.437	0.415	0.146	0.458	0.609	0.424	0.042	0.418	0.308	0.429
	N	38	38	38	38	38	38	38	38	38	38	38
Dy	Pearson Correlation	.996**	.683**	.914**	0.104	-0.113	.797**	.778**	-0.149	.900**	0.095	.505**
	Sig. (2-tailed)	0	0	0	0.535	0.498	0	0	0.371	0	0.572	0.001
	N	38	38	38	38	38	38	38	38	38	38	38
Er	Pearson Correlation	.986**	.670**	.954**	0.164	-0.072	.785**	.767**	-0.058	.881**	0.16	.443**
	Sig. (2-tailed)	0	0	0	0.325	0.669	0	0	0.731	0	0.337	0.005
	N	38	38	38	38	38	38	38	38	38	38	38
Eu	Pearson Correlation	0.041	0.24	0.042	0.12	-0.201	0.272	0.141	-0.096	0.125	-0.025	0.009
	Sig. (2-tailed)	0.809	0.147	0.802	0.471	0.227	0.099	0.4	0.568	0.454	0.883	0.959
	N	38	38	38	38	38	38	38	38	38	38	38
F	Pearson Correlation	.607**	.352*	.512**	-0.141	-0.291	.394*	.376*	-.403*	.452**	-.329*	.524**
	Sig. (2-tailed)	0	0.03	0.001	0.398	0.076	0.014	0.02	0.012	0.004	0.044	0.001
	N	38	38	38	38	38	38	38	38	38	38	38
Ga	Pearson Correlation	0.119	0.247	0.183	0.023	.583**	0.235	.343*	.431**	0.195	.570**	-.402*
	Sig. (2-tailed)	0.476	0.135	0.273	0.893	0	0.155	0.035	0.007	0.24	0	0.012
	N	38	38	38	38	38	38	38	38	38	38	38
Gd	Pearson Correlation	.961**	.775**	.864**	0.056	-0.154	.887**	.865**	-0.155	.949**	0.094	.538**
	Sig. (2-tailed)	0	0	0	0.739	0.357	0	0	0.353	0	0.574	0
	N	38	38	38	38	38	38	38	38	38	38	38
Hf	Pearson Correlation	0.072	-0.046	0.203	.332*	.480**	-0.026	-0.001	.364*	-0.029	.616**	-.384*
	Sig. (2-tailed)	0.666	0.782	0.222	0.042	0.002	0.877	0.993	0.025	0.862	0	0.017
	N	38	38	38	38	38	38	38	38	38	38	38
Ho	Pearson Correlation	1	.687**	.925**	0.079	-0.114	.797**	.780**	-0.148	.898**	0.092	.512**
	Sig. (2-tailed)		0	0	0.635	0.496	0	0	0.377	0	0.584	0.001
	N	38	38	38	38	38	38	38	38	38	38	38
La	Pearson Correlation	.687**	1	.730**	0.045	0.055	.961**	.960**	-0.112	.873**	0.261	0.21
	Sig. (2-tailed)	0		0	0.788	0.743	0	0	0.504	0	0.113	0.205
	N	38	38	38	38	38	38	38	38	38	38	38
Lu	Pearson Correlation	.925**	.730**	1	0.145	0.057	.804**	.797**	0.028	.862**	0.302	0.285
	Sig. (2-tailed)	0	0		0.384	0.734	0	0	0.866	0	0.066	0.082
	N	38	38	38	38	38	38	38	38	38	38	38

Correlation Coefficients: Little Blanca

Correlations		Ta	Tb	Th	Tl	Tm	U	Y	Yb	Zn	Zr
Ba	Pearson Correlation	0.014	-0.237	-0.087	0.101	-0.219	0.113	-0.201	-0.245	.321*	-0.049
	Sig. (2-tailed)	0.936	0.152	0.604	0.547	0.187	0.498	0.227	0.138	0.05	0.769
	N	38	38	38	38	38	38	38	38	38	38
Be	Pearson Correlation	-.642*	0.114	-0.583	.771**	0.129	.646*	0.007	0.011	0.564	-0.31
	Sig. (2-tailed)	0.045	0.754	0.077	0.009	0.723	0.044	0.985	0.976	0.09	0.383
	N	10	10	10	10	10	10	10	10	10	10
Ce	Pearson Correlation	0.214	.486**	0.272	0.081	.475**	-0.025	.436**	.537**	-0.186	0.205
	Sig. (2-tailed)	0.196	0.002	0.098	0.629	0.003	0.881	0.006	0.001	0.264	0.217
	N	38	38	38	38	38	38	38	38	38	38
Cs	Pearson Correlation	0.247	-0.224	-0.023	.389*	-0.145	0.035	-0.215	-0.146	.691**	-0.003
	Sig. (2-tailed)	0.135	0.177	0.89	0.016	0.386	0.837	0.194	0.381	0	0.987
	N	38	38	38	38	38	38	38	38	38	38
Dy	Pearson Correlation	-0.045	.993**	.370*	-0.113	.957**	.378*	.972**	.940**	-0.101	0.067
	Sig. (2-tailed)	0.79	0	0.022	0.5	0	0.019	0	0	0.544	0.691
	N	38	38	38	38	38	38	38	38	38	38
Er	Pearson Correlation	0.027	.977**	.395*	-0.05	.990**	.370*	.957**	.975**	-0.035	0.131
	Sig. (2-tailed)	0.873	0	0.014	0.766	0	0.022	0	0	0.836	0.432
	N	38	38	38	38	38	38	38	38	38	38
Eu	Pearson Correlation	-0.149	0.07	-0.062	-0.062	0.061	-0.039	0.041	0.045	0.031	-0.078
	Sig. (2-tailed)	0.371	0.678	0.71	0.71	0.717	0.815	0.806	0.79	0.853	0.641
	N	38	38	38	38	38	38	38	38	38	38
F	Pearson Correlation	-0.31	.578**	-0.2	-.411*	.537**	.341*	.573**	.514**	-0.238	-.325*
	Sig. (2-tailed)	0.058	0	0.228	0.01	0.001	0.036	0	0.001	0.15	0.046
	N	38	38	38	38	38	38	38	38	38	38
Ga	Pearson Correlation	.559**	0.13	.372*	.372*	0.169	-.412*	0.046	0.189	0.069	.358*
	Sig. (2-tailed)	0	0.438	0.021	0.022	0.311	0.01	0.786	0.256	0.681	0.027
	N	38	38	38	38	38	38	38	38	38	38
Gd	Pearson Correlation	-0.081	.973**	.326*	-0.077	.894**	.418**	.920**	.885**	-0.111	-0.036
	Sig. (2-tailed)	0.631	0	0.046	0.647	0	0.009	0	0	0.506	0.828
	N	38	38	38	38	38	38	38	38	38	38
Hf	Pearson Correlation	.701**	0.09	.645**	0.249	0.241	-0.237	0.064	0.25	0.185	.932**
	Sig. (2-tailed)	0	0.591	0	0.131	0.145	0.152	0.703	0.13	0.266	0
	N	38	38	38	38	38	38	38	38	38	38
Ho	Pearson Correlation	-0.044	.986**	.357*	-0.113	.957**	.401*	.973**	.945**	-0.11	0.035
	Sig. (2-tailed)	0.795	0	0.028	0.499	0	0.013	0	0	0.511	0.833
	N	38	38	38	38	38	38	38	38	38	38
La	Pearson Correlation	0.034	.682**	0.158	-0.036	.658**	0.248	.629**	.710**	-0.237	-0.047
	Sig. (2-tailed)	0.84	0	0.344	0.831	0	0.133	0	0	0.151	0.78
	N	38	38	38	38	38	38	38	38	38	38
Lu	Pearson Correlation	0.145	.888**	.387*	0.032	.965**	.350*	.874**	.990**	-0.062	0.167
	Sig. (2-tailed)	0.384	0	0.016	0.847	0	0.031	0	0	0.713	0.318
	N	38	38	38	38	38	38	38	38	38	38

Correlation Coefficients: Little Blanca

Correlations		SiO2	Al2O3	Fe2O3	CaO	Na2O	K2O	P2O5	SrO	BaO
Ba	Pearson Correlation	-0.045	-0.189	0.124	0.107	-.348*	0.12	0.066	0.084	.943**
	Sig. (2-tailed)	0.788	0.255	0.458	0.522	0.032	0.474	0.695	0.616	0
	N	38	38	38	38	38	38	38	38	38
Be	Pearson Correlation	-0.258	-.836**	-.642*	0.477	-.680*	.787**	0.08	.688*	0.243
	Sig. (2-tailed)	0.471	0.003	0.045	0.163	0.031	0.007	0.826	0.028	0.499
	N	10	10	10	10	10	10	10	10	10
Ce	Pearson Correlation	0.237	.334*	-0.02	-0.305	0.281	-0.043	0.203	-0.211	-0.098
	Sig. (2-tailed)	0.152	0.04	0.903	0.063	0.088	0.8	0.222	0.203	0.56
	N	38	38	38	38	38	38	38	38	38
Cs	Pearson Correlation	0.197	0.145	0.15	-0.188	-.331*	.358*	0.17	-0.126	.605**
	Sig. (2-tailed)	0.237	0.386	0.368	0.259	0.043	0.027	0.309	0.452	0
	N	38	38	38	38	38	38	38	38	38
Dy	Pearson Correlation	-0.195	-0.091	-0.287	.352*	0.216	-0.317	-0.013	.412*	-0.264
	Sig. (2-tailed)	0.24	0.587	0.081	0.03	0.194	0.053	0.94	0.01	0.109
	N	38	38	38	38	38	38	38	38	38
Er	Pearson Correlation	-0.122	-0.033	-0.234	0.289	0.196	-0.249	-0.006	.355*	-0.243
	Sig. (2-tailed)	0.465	0.844	0.157	0.079	0.238	0.131	0.97	0.029	0.142
	N	38	38	38	38	38	38	38	38	38
Eu	Pearson Correlation	0.073	-0.148	0.233	0.02	-0.054	-0.18	.344*	-0.01	0.283
	Sig. (2-tailed)	0.661	0.375	0.159	0.904	0.748	0.281	0.035	0.953	0.085
	N	38	38	38	38	38	38	38	38	38
F	Pearson Correlation	-.520**	-0.302	-.347*	.547**	0.319	-.441**	-0.03	.480**	-.339*
	Sig. (2-tailed)	0.001	0.065	0.033	0	0.051	0.006	0.859	0.002	0.038
	N	38	38	38	38	38	38	38	38	38
Ga	Pearson Correlation	.469**	.694**	-0.106	-.500**	0.286	0.035	-0.248	-.465**	-0.194
	Sig. (2-tailed)	0.003	0	0.526	0.001	0.081	0.835	0.133	0.003	0.244
	N	38	38	38	38	38	38	38	38	38
Gd	Pearson Correlation	-0.264	-0.114	-0.306	.370*	0.198	-.354*	-0.047	.434**	-0.245
	Sig. (2-tailed)	0.109	0.495	0.062	0.022	0.234	0.029	0.78	0.007	0.139
	N	38	38	38	38	38	38	38	38	38
Hf	Pearson Correlation	.627**	.473**	0.204	-.427**	0.12	0.175	0.087	-.384*	0.007
	Sig. (2-tailed)	0	0.003	0.219	0.007	0.474	0.295	0.603	0.017	0.965
	N	38	38	38	38	38	38	38	38	38
Ho	Pearson Correlation	-0.222	-0.097	-0.273	.356*	0.196	-0.309	-0.003	.416**	-0.258
	Sig. (2-tailed)	0.181	0.561	0.097	0.028	0.238	0.059	0.984	0.009	0.118
	N	38	38	38	38	38	38	38	38	38
La	Pearson Correlation	-0.014	0.098	-0.071	-0.028	0.317	-0.199	0.168	0.089	-0.204
	Sig. (2-tailed)	0.934	0.557	0.671	0.866	0.053	0.232	0.313	0.596	0.22
	N	38	38	38	38	38	38	38	38	38
Lu	Pearson Correlation	-0.024	0.083	-0.114	0.122	0.163	-0.111	0.057	0.195	-0.228
	Sig. (2-tailed)	0.886	0.62	0.497	0.465	0.329	0.507	0.732	0.24	0.169
	N	38	38	38	38	38	38	38	38	38

Correlation Coefficients: Little Blanca

Correlations		Ba	Be	Ce	Cs	Dy	Er	Eu	F	Ga	Gd	Hf
Mo	Pearson Correlation	0.233	.731*	0.033	0.241	0.104	0.164	0.12	-0.141	0.023	0.056	.332*
	Sig. (2-tailed)	0.159	0.016	0.846	0.146	0.535	0.325	0.471	0.398	0.893	0.739	0.042
	N	38	10	38	38	38	38	38	38	38	38	38
Nb	Pearson Correlation	-0.025	-.834**	.328*	0.124	-0.113	-0.072	-0.201	-0.291	.583**	-0.154	.480**
	Sig. (2-tailed)	0.882	0.003	0.044	0.458	0.498	0.669	0.227	0.076	0	0.357	0.002
	N	38	10	38	38	38	38	38	38	38	38	38
Nd	Pearson Correlation	-0.195	0.378	.739**	-0.086	.797**	.785**	0.272	.394*	0.235	.887**	-0.026
	Sig. (2-tailed)	0.24	0.282	0	0.609	0	0	0.099	0.014	0.155	0	0.877
	N	38	10	38	38	38	38	38	38	38	38	38
Pr	Pearson Correlation	-0.272	0.319	.789**	-0.134	.778**	.767**	0.141	.376*	.343*	.865**	-0.001
	Sig. (2-tailed)	0.098	0.369	0	0.424	0	0	0.4	0.02	0.035	0	0.993
	N	38	10	38	38	38	38	38	38	38	38	38
Rb	Pearson Correlation	0.073	.719*	0.025	.332*	-0.149	-0.058	-0.096	-.403*	.431**	-0.155	.364*
	Sig. (2-tailed)	0.663	0.019	0.882	0.042	0.371	0.731	0.568	0.012	0.007	0.353	0.025
	N	38	10	38	38	38	38	38	38	38	38	38
Sm	Pearson Correlation	-0.245	0.391	.693**	-0.135	.900**	.881**	0.125	.452**	0.195	.949**	-0.029
	Sig. (2-tailed)	0.139	0.264	0	0.418	0	0	0.454	0.004	0.24	0	0.862
	N	38	10	38	38	38	38	38	38	38	38	38
Sn	Pearson Correlation	-0.055	-.785**	.454**	0.17	0.095	0.16	-0.025	-.329*	.570**	0.094	.616**
	Sig. (2-tailed)	0.742	0.007	0.004	0.308	0.572	0.337	0.883	0.044	0	0.574	0
	N	38	10	38	38	38	38	38	38	38	38	38
Sr	Pearson Correlation	0.076	0.611	-0.087	-0.132	.505**	.443**	0.009	.524**	-.402*	.538**	-.384*
	Sig. (2-tailed)	0.648	0.061	0.605	0.429	0.001	0.005	0.959	0.001	0.012	0	0.017
	N	38	10	38	38	38	38	38	38	38	38	38
Ta	Pearson Correlation	0.014	-.642*	0.214	0.247	-0.045	0.027	-0.149	-0.31	.559**	-0.081	.701**
	Sig. (2-tailed)	0.936	0.045	0.196	0.135	0.79	0.873	0.371	0.058	0	0.631	0
	N	38	10	38	38	38	38	38	38	38	38	38
Tb	Pearson Correlation	-0.237	0.114	.486**	-0.224	.993**	.977**	0.07	.578**	0.13	.973**	0.09
	Sig. (2-tailed)	0.152	0.754	0.002	0.177	0	0	0.678	0	0.438	0	0.591
	N	38	10	38	38	38	38	38	38	38	38	38
Th	Pearson Correlation	-0.087	-0.583	0.272	-0.023	.370*	.395*	-0.062	-0.2	.372*	.326*	.645**
	Sig. (2-tailed)	0.604	0.077	0.098	0.89	0.022	0.014	0.71	0.228	0.021	0.046	0
	N	38	10	38	38	38	38	38	38	38	38	38
Tl	Pearson Correlation	0.101	.771**	0.081	.389*	-0.113	-0.05	-0.062	-.411*	.372*	-0.077	0.249
	Sig. (2-tailed)	0.547	0.009	0.629	0.016	0.5	0.766	0.71	0.01	0.022	0.647	0.131
	N	38	10	38	38	38	38	38	38	38	38	38
Tm	Pearson Correlation	-0.219	0.129	.475**	-0.145	.957**	.990**	0.061	.537**	0.169	.894**	0.241
	Sig. (2-tailed)	0.187	0.723	0.003	0.386	0	0	0.717	0.001	0.311	0	0.145
	N	38	10	38	38	38	38	38	38	38	38	38

Correlation Coefficients: Little Blanca

Correlations		Ho	La	Lu	Mo	Nb	Nd	Pr	Rb	Sm	Sn	Sr
Mo	Pearson Correlation	0.079	0.045	0.145	1	-0.02	0.122	0.085	.368*	0.083	0.087	0.012
	Sig. (2-tailed)	0.635	0.788	0.384		0.903	0.467	0.613	0.023	0.619	0.604	0.942
	N	38	38	38	38	38	38	38	38	38	38	38
Nb	Pearson Correlation	-0.114	0.055	0.057	-0.02	1	-0.034	0.024	.358*	-0.129	.735**	-.541**
	Sig. (2-tailed)	0.496	0.743	0.734	0.903		0.84	0.884	0.028	0.44	0	0
	N	38	38	38	38	38	38	38	38	38	38	38
Nd	Pearson Correlation	.797**	.961**	.804**	0.122	-0.034	1	.982**	-0.057	.951**	0.233	0.317
	Sig. (2-tailed)	0	0	0	0.467	0.84		0	0.735	0	0.159	0.052
	N	38	38	38	38	38	38	38	38	38	38	38
Pr	Pearson Correlation	.780**	.960**	.797**	0.085	0.024	.982**	1	-0.014	.948**	0.283	0.262
	Sig. (2-tailed)	0	0	0	0.613	0.884	0		0.934	0	0.085	0.112
	N	38	38	38	38	38	38	38	38	38	38	38
Rb	Pearson Correlation	-0.148	-0.112	0.028	.368*	.358*	-0.057	-0.014	1	-0.085	.516**	-.366*
	Sig. (2-tailed)	0.377	0.504	0.866	0.023	0.028	0.735	0.934		0.614	0.001	0.024
	N	38	38	38	38	38	38	38	38	38	38	38
Sm	Pearson Correlation	.898**	.873**	.862**	0.083	-0.129	.951**	.948**	-0.085	1	0.164	.400*
	Sig. (2-tailed)	0	0	0	0.619	0.44	0	0	0.614		0.324	0.013
	N	38	38	38	38	38	38	38	38	38	38	38
Sn	Pearson Correlation	0.092	0.261	0.302	0.087	.735**	0.233	0.283	.516**	0.164	1	-.498**
	Sig. (2-tailed)	0.584	0.113	0.066	0.604	0	0.159	0.085	0.001	0.324		0.001
	N	38	38	38	38	38	38	38	38	38	38	38
Sr	Pearson Correlation	.512**	0.21	0.285	0.012	-.541**	0.317	0.262	-.366*	.400*	-.498**	1
	Sig. (2-tailed)	0.001	0.205	0.082	0.942	0	0.052	0.112	0.024	0.013	0.001	
	N	38	38	38	38	38	38	38	38	38	38	38
Ta	Pearson Correlation	-0.044	0.034	0.145	0.135	.750**	0.004	0.06	.528**	-0.06	.791**	-.535**
	Sig. (2-tailed)	0.795	0.84	0.384	0.419	0	0.98	0.719	0.001	0.719	0	0.001
	N	38	38	38	38	38	38	38	38	38	38	38
Tb	Pearson Correlation	.986**	.682**	.888**	0.125	-0.175	.807**	.787**	-0.15	.910**	0.072	.531**
	Sig. (2-tailed)	0	0	0	0.455	0.295	0	0	0.37	0	0.667	0.001
	N	38	38	38	38	38	38	38	38	38	38	38
Th	Pearson Correlation	.357*	0.158	.387*	0.219	0.213	0.236	0.268	.402*	0.294	.402*	-0.218
	Sig. (2-tailed)	0.028	0.344	0.016	0.187	0.2	0.155	0.104	0.012	0.073	0.012	0.189
	N	38	38	38	38	38	38	38	38	38	38	38
Tl	Pearson Correlation	-0.113	-0.036	0.032	0.303	0.227	0.037	0.071	.933**	0.016	.470**	-.335*
	Sig. (2-tailed)	0.499	0.831	0.847	0.064	0.171	0.827	0.674	0	0.925	0.003	0.04
	N	38	38	38	38	38	38	38	38	38	38	38
Tm	Pearson Correlation	.957**	.658**	.965**	0.242	-0.033	.769**	.751**	0.016	.850**	0.196	.390*
	Sig. (2-tailed)	0	0	0	0.143	0.843	0	0	0.923	0	0.238	0.015
	N	38	38	38	38	38	38	38	38	38	38	38

Correlation Coefficients: Little Blanca

Correlations		Ta	Tb	Th	Tl	Tm	U	Y	Yb	Zn	Zr
Mo	Pearson Correlation	0.135	0.125	0.219	0.303	0.242	0.104	0.105	0.163	.392*	.384*
	Sig. (2-tailed)	0.419	0.455	0.187	0.064	0.143	0.535	0.531	0.327	0.015	0.017
	N	38	38	38	38	38	38	38	38	38	38
Nb	Pearson Correlation	.750**	-0.175	0.213	0.227	-0.033	-.453**	-0.152	0.052	0.002	.616**
	Sig. (2-tailed)	0	0.295	0.2	0.171	0.843	0.004	0.362	0.755	0.988	0
	N	38	38	38	38	38	38	38	38	38	38
Nd	Pearson Correlation	0.004	.807**	0.236	0.037	.769**	.329*	.735**	.798**	-0.116	-0.038
	Sig. (2-tailed)	0.98	0	0.155	0.827	0	0.044	0	0	0.487	0.822
	N	38	38	38	38	38	38	38	38	38	38
Pr	Pearson Correlation	0.06	.787**	0.268	0.071	.751**	0.293	.707**	.786**	-0.145	-0.018
	Sig. (2-tailed)	0.719	0	0.104	0.674	0	0.075	0	0	0.386	0.913
	N	38	38	38	38	38	38	38	38	38	38
Rb	Pearson Correlation	.528**	-0.15	.402*	.933**	0.016	0	-0.192	0.022	.572**	.396*
	Sig. (2-tailed)	0.001	0.37	0.012	0	0.923	0.999	0.248	0.895	0	0.014
	N	38	38	38	38	38	38	38	38	38	38
Sm	Pearson Correlation	-0.06	.910**	0.294	0.016	.850**	.382*	.835**	.861**	-0.099	-0.079
	Sig. (2-tailed)	0.719	0	0.073	0.925	0	0.018	0	0	0.555	0.638
	N	38	38	38	38	38	38	38	38	38	38
Sn	Pearson Correlation	.791**	0.072	.402*	.470**	0.196	-0.282	-0.014	0.28	0.1	.623**
	Sig. (2-tailed)	0	0.667	0.012	0.003	0.238	0.087	0.935	0.089	0.548	0
	N	38	38	38	38	38	38	38	38	38	38
Sr	Pearson Correlation	-.535**	.531**	-0.218	-.335*	.390*	.746**	.546**	.324*	0.016	-.417**
	Sig. (2-tailed)	0.001	0.001	0.189	0.04	0.015	0	0	0.047	0.922	0.009
	N	38	38	38	38	38	38	38	38	38	38
Ta	Pearson Correlation	1	-0.074	.555**	.444**	0.098	-0.274	-0.12	0.135	0.178	.722**
	Sig. (2-tailed)		0.66	0	0.005	0.557	0.096	0.472	0.418	0.284	0
	N	38	38	38	38	38	38	38	38	38	38
Tb	Pearson Correlation	-0.074	1	.361*	-0.101	.945**	.390*	.959**	.917**	-0.072	0.04
	Sig. (2-tailed)	0.66		0.026	0.547	0	0.015	0	0	0.669	0.81
	N	38	38	38	38	38	38	38	38	38	38
Th	Pearson Correlation	.555**	.361*	1	.411*	.426**	0.004	.369*	.420**	0.171	.602**
	Sig. (2-tailed)	0	0.026		0.01	0.008	0.982	0.023	0.009	0.304	0
	N	38	38	38	38	38	38	38	38	38	38
Tl	Pearson Correlation	.444**	-0.101	.411*	1	0.002	0.063	-0.171	0.014	.576**	0.269
	Sig. (2-tailed)	0.005	0.547	0.01		0.99	0.709	0.306	0.933	0	0.103
	N	38	38	38	38	38	38	38	38	38	38
Tm	Pearson Correlation	0.098	.945**	.426**	0.002	1	.365*	.930**	.983**	0.019	0.198
	Sig. (2-tailed)	0.557	0	0.008	0.99		0.024	0	0	0.91	0.233
	N	38	38	38	38	38	38	38	38	38	38

Correlation Coefficients: Little Blanca

Correlations		SiO2	Al2O3	Fe2O3	CaO	Na2O	K2O	P2O5	SrO	BaO
Mo	Pearson Correlation	0.298	0.04	0.038	-0.098	-0.088	0.157	-0.126	-0.018	0.216
	Sig. (2-tailed)	0.069	0.813	0.823	0.556	0.601	0.345	0.451	0.913	0.192
	N	38	38	38	38	38	38	38	38	38
Nb	Pearson Correlation	.590**	.767**	0.258	-.657**	0.116	.332*	0.076	-.591**	0.105
	Sig. (2-tailed)	0	0	0.118	0	0.487	0.042	0.65	0	0.53
	N	38	38	38	38	38	38	38	38	38
Nd	Pearson Correlation	-0.081	0.041	-0.145	0.09	0.235	-0.216	0.078	0.194	-0.2
	Sig. (2-tailed)	0.631	0.809	0.385	0.592	0.155	0.192	0.641	0.243	0.229
	N	38	38	38	38	38	38	38	38	38
Pr	Pearson Correlation	-0.046	0.118	-0.158	0.022	0.27	-0.192	0.031	0.131	-0.272
	Sig. (2-tailed)	0.785	0.481	0.342	0.897	0.101	0.248	0.853	0.431	0.098
	N	38	38	38	38	38	38	38	38	38
Rb	Pearson Correlation	.509**	.523**	0.259	-.520**	-.585**	.812**	-0.191	-.397*	0.074
	Sig. (2-tailed)	0.001	0.001	0.116	0.001	0	0	0.25	0.013	0.658
	N	38	38	38	38	38	38	38	38	38
Sm	Pearson Correlation	-0.162	-0.038	-0.249	0.209	0.204	-0.246	0.014	0.284	-0.268
	Sig. (2-tailed)	0.332	0.823	0.131	0.207	0.219	0.136	0.932	0.084	0.104
	N	38	38	38	38	38	38	38	38	38
Sn	Pearson Correlation	.593**	.664**	.326*	-.611**	-0.028	.373*	0.03	-.560**	0.049
	Sig. (2-tailed)	0	0	0.046	0	0.867	0.021	0.859	0	0.772
	N	38	38	38	38	38	38	38	38	38
Sr	Pearson Correlation	-.756**	-.676**	-.341*	.876**	-0.071	-.346*	-0.085	.975**	-0.019
	Sig. (2-tailed)	0	0	0.036	0	0.671	0.033	0.613	0	0.908
	N	38	38	38	38	38	38	38	38	38
Ta	Pearson Correlation	.603**	.670**	0.141	-.636**	-0.014	.341*	0.097	-.584**	0.158
	Sig. (2-tailed)	0	0	0.397	0	0.933	0.036	0.563	0	0.344
	N	38	38	38	38	38	38	38	38	38
Tb	Pearson Correlation	-0.226	-0.132	-.324*	.392*	0.22	-.355*	-0.038	.440**	-0.265
	Sig. (2-tailed)	0.172	0.43	0.047	0.015	0.185	0.029	0.819	0.006	0.108
	N	38	38	38	38	38	38	38	38	38
Th	Pearson Correlation	.390*	.396*	-0.011	-0.314	-0.125	0.114	-0.015	-0.272	-0.082
	Sig. (2-tailed)	0.016	0.014	0.946	0.055	0.455	0.496	0.928	0.098	0.626
	N	38	38	38	38	38	38	38	38	38
Tl	Pearson Correlation	.399*	.421**	0.134	-.458**	-.623**	.770**	-0.22	-.365*	0.064
	Sig. (2-tailed)	0.013	0.009	0.423	0.004	0	0	0.185	0.024	0.702
	N	38	38	38	38	38	38	38	38	38
Tm	Pearson Correlation	-0.049	0.011	-0.192	0.228	0.181	-0.191	0.019	0.305	-0.216
	Sig. (2-tailed)	0.772	0.946	0.248	0.169	0.277	0.25	0.91	0.062	0.192
	N	38	38	38	38	38	38	38	38	38

Correlation Coefficients: Little Blanca

Correlations		Ba	Be	Ce	Cs	Dy	Er	Eu	F	Ga	Gd	Hf
Tm	Pearson Correlation	-0.219	0.129	.475**	-0.145	.957**	.990**	0.061	.537**	0.169	.894**	0.241
	Sig. (2-tailed)	0.187	0.723	0.003	0.386	0	0	0.717	0.001	0.311	0	0.145
	N	38	10	38	38	38	38	38	38	38	38	38
U	Pearson Correlation	0.113	.646*	-0.025	0.035	.378*	.370*	-0.039	.341*	-.412*	.418**	-0.237
	Sig. (2-tailed)	0.498	0.044	0.881	0.837	0.019	0.022	0.815	0.036	0.01	0.009	0.152
	N	38	10	38	38	38	38	38	38	38	38	38
Y	Pearson Correlation	-0.201	0.007	.436**	-0.215	.972**	.957**	0.041	.573**	0.046	.920**	0.064
	Sig. (2-tailed)	0.227	0.985	0.006	0.194	0	0	0.806	0	0.786	0	0.703
	N	38	10	38	38	38	38	38	38	38	38	38
Yb	Pearson Correlation	-0.245	0.011	.537**	-0.146	.940**	.975**	0.045	.514**	0.189	.885**	0.25
	Sig. (2-tailed)	0.138	0.976	0.001	0.381	0	0	0.79	0.001	0.256	0	0.13
	N	38	10	38	38	38	38	38	38	38	38	38
Zn	Pearson Correlation	.321*	0.564	-0.186	.691**	-0.101	-0.035	0.031	-0.238	0.069	-0.111	0.185
	Sig. (2-tailed)	0.05	0.09	0.264	0	0.544	0.836	0.853	0.15	0.681	0.506	0.266
	N	38	10	38	38	38	38	38	38	38	38	38
Zr	Pearson Correlation	-0.049	-0.31	0.205	-0.003	0.067	0.131	-0.078	-.325*	.358*	-0.036	.932**
	Sig. (2-tailed)	0.769	0.383	0.217	0.987	0.691	0.432	0.641	0.046	0.027	0.828	0
	N	38	10	38	38	38	38	38	38	38	38	38
SiO2	Pearson Correlation	-0.045	-0.258	0.237	0.197	-0.195	-0.122	0.073	-.520**	.469**	-0.264	.627**
	Sig. (2-tailed)	0.788	0.471	0.152	0.237	0.24	0.465	0.661	0.001	0.003	0.109	0
	N	38	10	38	38	38	38	38	38	38	38	38
Al2O3	Pearson Correlation	-0.189	-.836**	.334*	0.145	-0.091	-0.033	-0.148	-0.302	.694**	-0.114	.473**
	Sig. (2-tailed)	0.255	0.003	0.04	0.386	0.587	0.844	0.375	0.065	0	0.495	0.003
	N	38	10	38	38	38	38	38	38	38	38	38
Fe2O3	Pearson Correlation	0.124	-.642*	-0.02	0.15	-0.287	-0.234	0.233	-.347*	-0.106	-0.306	0.204
	Sig. (2-tailed)	0.458	0.045	0.903	0.368	0.081	0.157	0.159	0.033	0.526	0.062	0.219
	N	38	10	38	38	38	38	38	38	38	38	38
CaO	Pearson Correlation	0.107	0.477	-0.305	-0.188	.352*	0.289	0.02	.547**	-.500**	.370*	-.427**
	Sig. (2-tailed)	0.522	0.163	0.063	0.259	0.03	0.079	0.904	0	0.001	0.022	0.007
	N	38	10	38	38	38	38	38	38	38	38	38
Na2O	Pearson Correlation	-.348*	-.680*	0.281	-.331*	0.216	0.196	-0.054	0.319	0.286	0.198	0.12
	Sig. (2-tailed)	0.032	0.031	0.088	0.043	0.194	0.238	0.748	0.051	0.081	0.234	0.474
	N	38	10	38	38	38	38	38	38	38	38	38
K2O	Pearson Correlation	0.12	.787**	-0.043	.358*	-0.317	-0.249	-0.18	-.441**	0.035	-.354*	0.175
	Sig. (2-tailed)	0.474	0.007	0.8	0.027	0.053	0.131	0.281	0.006	0.835	0.029	0.295
	N	38	10	38	38	38	38	38	38	38	38	38
P2O5	Pearson Correlation	0.066	0.08	0.203	0.17	-0.013	-0.006	.344*	-0.03	-0.248	-0.047	0.087
	Sig. (2-tailed)	0.695	0.826	0.222	0.309	0.94	0.97	0.035	0.859	0.133	0.78	0.603
	N	38	10	38	38	38	38	38	38	38	38	38
SrO	Pearson Correlation	0.084	.688*	-0.211	-0.126	.412*	.355*	-0.01	.480**	-.465**	.434**	-.384*
	Sig. (2-tailed)	0.616	0.028	0.203	0.452	0.01	0.029	0.953	0.002	0.003	0.007	0.017
	N	38	10	38	38	38	38	38	38	38	38	38
BaO	Pearson Correlation	.943**	0.243	-0.098	.605**	-0.264	-0.243	0.283	-.339*	-0.194	-0.245	0.007
	Sig. (2-tailed)	0	0.499	0.56	0	0.109	0.142	0.085	0.038	0.244	0.139	0.965
	N	38	10	38	38	38	38	38	38	38	38	38

Correlation Coefficients: Little Blanca

Correlations		Ho	La	Lu	Mo	Nb	Nd	Pr	Rb	Sm	Sn	Sr
Tm	Pearson Correlation	.957**	.658**	.965**	0.242	-0.033	.769**	.751**	0.016	.850**	0.196	.390*
	Sig. (2-tailed)	0	0	0	0.143	0.843	0	0	0.923	0	0.238	0.015
	N	38	38	38	38	38	38	38	38	38	38	38
U	Pearson Correlation	.401*	0.248	.350*	0.104	-.453**	.329*	0.293	0	.382*	-0.282	.746**
	Sig. (2-tailed)	0.013	0.133	0.031	0.535	0.004	0.044	0.075	0.999	0.018	0.087	0
	N	38	38	38	38	38	38	38	38	38	38	38
Y	Pearson Correlation	.973**	.629**	.874**	0.105	-0.152	.735**	.707**	-0.192	.835**	-0.014	.546**
	Sig. (2-tailed)	0	0	0	0.531	0.362	0	0	0.248	0	0.935	0
	N	38	38	38	38	38	38	38	38	38	38	38
Yb	Pearson Correlation	.945**	.710**	.990**	0.163	0.052	.798**	.786**	0.022	.861**	0.28	.324*
	Sig. (2-tailed)	0	0	0	0.327	0.755	0	0	0.895	0	0.089	0.047
	N	38	38	38	38	38	38	38	38	38	38	38
Zn	Pearson Correlation	-0.11	-0.237	-0.062	.392*	0.002	-0.116	-0.145	.572**	-0.099	0.1	0.016
	Sig. (2-tailed)	0.511	0.151	0.713	0.015	0.988	0.487	0.386	0	0.555	0.548	0.922
	N	38	38	38	38	38	38	38	38	38	38	38
Zr	Pearson Correlation	0.035	-0.047	0.167	.384*	.616**	-0.038	-0.018	.396*	-0.079	.623**	-.417**
	Sig. (2-tailed)	0.833	0.78	0.318	0.017	0	0.822	0.913	0.014	0.638	0	0.009
	N	38	38	38	38	38	38	38	38	38	38	38
SiO2	Pearson Correlation	-0.222	-0.014	-0.024	0.298	.590**	-0.081	-0.046	.509**	-0.162	.593**	-.756**
	Sig. (2-tailed)	0.181	0.934	0.886	0.069	0	0.631	0.785	0.001	0.332	0	0
	N	38	38	38	38	38	38	38	38	38	38	38
Al2O3	Pearson Correlation	-0.097	0.098	0.083	0.04	.767**	0.041	0.118	.523**	-0.038	.664**	-.676**
	Sig. (2-tailed)	0.561	0.557	0.62	0.813	0	0.809	0.481	0.001	0.823	0	0
	N	38	38	38	38	38	38	38	38	38	38	38
Fe2O3	Pearson Correlation	-0.273	-0.071	-0.114	0.038	0.258	-0.145	-0.158	0.259	-0.249	.326*	-.341*
	Sig. (2-tailed)	0.097	0.671	0.497	0.823	0.118	0.385	0.342	0.116	0.131	0.046	0.036
	N	38	38	38	38	38	38	38	38	38	38	38
CaO	Pearson Correlation	.356*	-0.028	0.122	-0.098	-.657**	0.09	0.022	-.520**	0.209	-.611**	.876**
	Sig. (2-tailed)	0.028	0.866	0.465	0.556	0	0.592	0.897	0.001	0.207	0	0
	N	38	38	38	38	38	38	38	38	38	38	38
Na2O	Pearson Correlation	0.196	0.317	0.163	-0.088	0.116	0.235	0.27	-.585**	0.204	-0.028	-0.071
	Sig. (2-tailed)	0.238	0.053	0.329	0.601	0.487	0.155	0.101	0	0.219	0.867	0.671
	N	38	38	38	38	38	38	38	38	38	38	38
K2O	Pearson Correlation	-0.309	-0.199	-0.111	0.157	.332*	-0.216	-0.192	.812**	-0.246	.373*	-.346*
	Sig. (2-tailed)	0.059	0.232	0.507	0.345	0.042	0.192	0.248	0	0.136	0.021	0.033
	N	38	38	38	38	38	38	38	38	38	38	38
P2O5	Pearson Correlation	-0.003	0.168	0.057	-0.126	0.076	0.078	0.031	-0.191	0.014	0.03	-0.085
	Sig. (2-tailed)	0.984	0.313	0.732	0.451	0.65	0.641	0.853	0.25	0.932	0.859	0.613
	N	38	38	38	38	38	38	38	38	38	38	38
SrO	Pearson Correlation	.416**	0.089	0.195	-0.018	-.591**	0.194	0.131	-.397*	0.284	-.560**	.975**
	Sig. (2-tailed)	0.009	0.596	0.24	0.913	0	0.243	0.431	0.013	0.084	0	0
	N	38	38	38	38	38	38	38	38	38	38	38
BaO	Pearson Correlation	-0.258	-0.204	-0.228	0.216	0.105	-0.2	-0.272	0.074	-0.268	0.049	-0.019
	Sig. (2-tailed)	0.118	0.22	0.169	0.192	0.53	0.229	0.098	0.658	0.104	0.772	0.908
	N	38	38	38	38	38	38	38	38	38	38	38

Correlation Coefficients: Little Blanca

Correlations		Ta	Tb	Th	Tl	Tm	U	Y	Yb	Zn	Zr
Tm	Pearson Correlation	0.098	.945**	.426**	0.002	1	.365*	.930**	.983**	0.019	0.198
	Sig. (2-tailed)	0.557	0	0.008	0.99		0.024	0	0	0.91	0.233
	N	38	38	38	38	38	38	38	38	38	38
U	Pearson Correlation	-0.274	.390*	0.004	0.063	.365*	1	.393*	.340*	0.137	-0.286
	Sig. (2-tailed)	0.096	0.015	0.982	0.709	0.024		0.015	0.037	0.411	0.081
	N	38	38	38	38	38	38	38	38	38	38
Y	Pearson Correlation	-0.12	.959**	.369*	-0.171	.930**	.393*	1	.911**	-0.101	0.036
	Sig. (2-tailed)	0.472	0	0.023	0.306	0	0.015		0	0.545	0.829
	N	38	38	38	38	38	38	38	38	38	38
Yb	Pearson Correlation	0.135	.917**	.420**	0.014	.983**	.340*	.911**	1	-0.028	0.203
	Sig. (2-tailed)	0.418	0	0.009	0.933	0	0.037	0		0.865	0.222
	N	38	38	38	38	38	38	38	38	38	38
Zn	Pearson Correlation	0.178	-0.072	0.171	.576**	0.019	0.137	-0.101	-0.028	1	0.104
	Sig. (2-tailed)	0.284	0.669	0.304	0	0.91	0.411	0.545	0.865		0.536
	N	38	38	38	38	38	38	38	38	38	38
Zr	Pearson Correlation	.722**	0.04	.602**	0.269	0.198	-0.286	0.036	0.203	0.104	1
	Sig. (2-tailed)	0	0.81	0	0.103	0.233	0.081	0.829	0.222	0.536	
	N	38	38	38	38	38	38	38	38	38	38
SiO2	Pearson Correlation	.603**	-0.226	.390*	.399*	-0.049	-.582**	-0.225	-0.017	0.198	.628**
	Sig. (2-tailed)	0	0.172	0.016	0.013	0.772	0	0.174	0.922	0.234	0
	N	38	38	38	38	38	38	38	38	38	38
Al2O3	Pearson Correlation	.670**	-0.132	.396*	.421**	0.011	-.530**	-0.14	0.082	0.149	.506**
	Sig. (2-tailed)	0	0.43	0.014	0.009	0.946	0.001	0.403	0.623	0.372	0.001
	N	38	38	38	38	38	38	38	38	38	38
Fe2O3	Pearson Correlation	0.141	-.324*	-0.011	0.134	-0.192	-0.124	-0.26	-0.118	0.105	0.158
	Sig. (2-tailed)	0.397	0.047	0.946	0.423	0.248	0.457	0.115	0.48	0.529	0.344
	N	38	38	38	38	38	38	38	38	38	38
CaO	Pearson Correlation	-.636**	.392*	-0.314	-.458**	0.228	.602**	.386*	0.153	-0.005	-.479**
	Sig. (2-tailed)	0	0.015	0.055	0.004	0.169	0	0.017	0.359	0.976	0.002
	N	38	38	38	38	38	38	38	38	38	38
Na2O	Pearson Correlation	-0.014	0.22	-0.125	-.623**	0.181	-.395*	0.185	0.183	-.363*	0.089
	Sig. (2-tailed)	0.933	0.185	0.455	0	0.277	0.014	0.265	0.273	0.025	0.594
	N	38	38	38	38	38	38	38	38	38	38
K2O	Pearson Correlation	.341*	-.355*	0.114	.770**	-0.191	0.071	-.334*	-0.145	.398*	0.205
	Sig. (2-tailed)	0.036	0.029	0.496	0	0.25	0.673	0.041	0.384	0.013	0.217
	N	38	38	38	38	38	38	38	38	38	38
P2O5	Pearson Correlation	0.097	-0.038	-0.015	-0.22	0.019	0.065	0.048	0.051	-0.171	0.063
	Sig. (2-tailed)	0.563	0.819	0.928	0.185	0.91	0.696	0.773	0.762	0.303	0.707
	N	38	38	38	38	38	38	38	38	38	38
SrO	Pearson Correlation	-.584**	.440**	-0.272	-.365*	0.305	.714**	.461**	0.236	0.059	-.430**
	Sig. (2-tailed)	0	0.006	0.098	0.024	0.062	0	0.004	0.155	0.726	0.007
	N	38	38	38	38	38	38	38	38	38	38
BaO	Pearson Correlation	0.158	-0.265	-0.082	0.064	-0.216	-0.01	-0.234	-0.24	.331*	0.085
	Sig. (2-tailed)	0.344	0.108	0.626	0.702	0.192	0.954	0.157	0.146	0.042	0.611
	N	38	38	38	38	38	38	38	38	38	38

Correlation Coefficients: Little Blanca

Correlations		SiO2	Al2O3	Fe2O3	CaO	Na2O	K2O	P2O5	SrO	BaO
Tm	Pearson Correlation	-0.049	0.011	-0.192	0.228	0.181	-0.191	0.019	0.305	-0.216
	Sig. (2-tailed)	0.772	0.946	0.248	0.169	0.277	0.25	0.91	0.062	0.192
	N	38	38	38	38	38	38	38	38	38
U	Pearson Correlation	-.582**	-.530**	-0.124	.602**	-.395*	0.071	0.065	.714**	-0.01
	Sig. (2-tailed)	0	0.001	0.457	0	0.014	0.673	0.696	0	0.954
	N	38	38	38	38	38	38	38	38	38
Y	Pearson Correlation	-0.225	-0.14	-0.26	.386*	0.185	-.334*	0.048	.461**	-0.234
	Sig. (2-tailed)	0.174	0.403	0.115	0.017	0.265	0.041	0.773	0.004	0.157
	N	38	38	38	38	38	38	38	38	38
Yb	Pearson Correlation	-0.017	0.082	-0.118	0.153	0.183	-0.145	0.051	0.236	-0.24
	Sig. (2-tailed)	0.922	0.623	0.48	0.359	0.273	0.384	0.762	0.155	0.146
	N	38	38	38	38	38	38	38	38	38
Zn	Pearson Correlation	0.198	0.149	0.105	-0.005	-.363*	.398*	-0.171	0.059	.331*
	Sig. (2-tailed)	0.234	0.372	0.529	0.976	0.025	0.013	0.303	0.726	0.042
	N	38	38	38	38	38	38	38	38	38
Zr	Pearson Correlation	.628**	.506**	0.158	-.479**	0.089	0.205	0.063	-.430**	0.085
	Sig. (2-tailed)	0	0.001	0.344	0.002	0.594	0.217	0.707	0.007	0.611
	N	38	38	38	38	38	38	38	38	38
SiO2	Pearson Correlation	1	.796**	.427**	-.821**	0.082	.426**	0.157	-.778**	0.088
	Sig. (2-tailed)		0	0.008	0	0.625	0.008	0.346	0	0.6
	N	38	38	38	38	38	38	38	38	38
Al2O3	Pearson Correlation	.796**	1	0.289	-.802**	0.095	.423**	-0.051	-.744**	-0.071
	Sig. (2-tailed)	0		0.078	0	0.569	0.008	0.76	0	0.674
	N	38	38	38	38	38	38	38	38	38
Fe2O3	Pearson Correlation	.427**	0.289	1	-.397*	-0.253	.422**	0.174	-.349*	0.173
	Sig. (2-tailed)	0.008	0.078		0.014	0.125	0.008	0.297	0.032	0.299
	N	38	38	38	38	38	38	38	38	38
CaO	Pearson Correlation	-.821**	-.802**	-.397*	1	0.008	-.501**	-0.088	.923**	-0.022
	Sig. (2-tailed)	0	0	0.014		0.963	0.001	0.598	0	0.895
	N	38	38	38	38	38	38	38	38	38
Na2O	Pearson Correlation	0.082	0.095	-0.253	0.008	1	-.723**	0.029	-0.057	-0.235
	Sig. (2-tailed)	0.625	0.569	0.125	0.963		0	0.864	0.734	0.156
	N	38	38	38	38	38	38	38	38	38
K2O	Pearson Correlation	.426**	.423**	.422**	-.501**	-.723**	1	-0.014	-.363*	0.136
	Sig. (2-tailed)	0.008	0.008	0.008	0.001	0		0.934	0.025	0.415
	N	38	38	38	38	38	38	38	38	38
P2O5	Pearson Correlation	0.157	-0.051	0.174	-0.088	0.029	-0.014	1	-0.092	0.105
	Sig. (2-tailed)	0.346	0.76	0.297	0.598	0.864	0.934		0.583	0.531
	N	38	38	38	38	38	38	38	38	38
SrO	Pearson Correlation	-.778**	-.744**	-.349*	.923**	-0.057	-.363*	-0.092	1	-0.016
	Sig. (2-tailed)	0	0	0.032	0	0.734	0.025	0.583		0.925
	N	38	38	38	38	38	38	38	38	38
BaO	Pearson Correlation	0.088	-0.071	0.173	-0.022	-0.235	0.136	0.105	-0.016	1
	Sig. (2-tailed)	0.6	0.674	0.299	0.895	0.156	0.415	0.531	0.925	
	N	38	38	38	38	38	38	38	38	38

Correlation Coefficients: Little Round Top

Correlations		Ba	Be	Ce	Cs	Dy	Er	Eu	F	Ga	Gd	Hf
Ba	Pearson Correlation	1	0.443	0.013	0.081	-0.219	-0.248	0.344	-0.034	-0.295	-0.239	-0.11
	Sig. (2-tailed)		0.233	0.959	0.742	0.367	0.306	0.149	0.895	0.22	0.325	0.655
	N	19	9	19	19	19	19	19	18	19	19	19
Be	Pearson Correlation	0.443	1	-0.177	0.312	-0.02	-0.06	0.121	-0.094	-0.506	-0.147	-0.562
	Sig. (2-tailed)	0.233		0.649	0.413	0.96	0.879	0.756	0.811	0.165	0.707	0.115
	N	9	9	9	9	9	9	9	9	9	9	9
Ce	Pearson Correlation	0.013	-0.177	1	0.305	-0.098	-0.047	-0.24	-0.236	.584**	0.004	0.078
	Sig. (2-tailed)	0.959	0.649		0.205	0.69	0.85	0.323	0.345	0.009	0.987	0.75
	N	19	9	19	19	19	19	19	18	19	19	19
Cs	Pearson Correlation	0.081	0.312	0.305	1	-.469*	-0.442	-0.167	-0.378	0.289	-.491*	0.327
	Sig. (2-tailed)	0.742	0.413	0.205		0.043	0.058	0.495	0.122	0.229	0.033	0.172
	N	19	9	19	19	19	19	19	18	19	19	19
Dy	Pearson Correlation	-0.219	-0.02	-0.098	-.469*	1	.991**	0.27	.729**	-0.18	.968**	-0.453
	Sig. (2-tailed)	0.367	0.96	0.69	0.043		0	0.263	0.001	0.461	0	0.051
	N	19	9	19	19	19	19	19	18	19	19	19
Er	Pearson Correlation	-0.248	-0.06	-0.047	-0.442	.991**	1	0.249	.692**	-0.079	.963**	-0.401
	Sig. (2-tailed)	0.306	0.879	0.85	0.058	0		0.303	0.001	0.747	0	0.088
	N	19	9	19	19	19	19	19	18	19	19	19
Eu	Pearson Correlation	0.344	0.121	-0.24	-0.167	0.27	0.249	1	0.168	-0.401	0.249	-0.044
	Sig. (2-tailed)	0.149	0.756	0.323	0.495	0.263	0.303		0.505	0.089	0.304	0.86
	N	19	9	19	19	19	19	19	18	19	19	19
F	Pearson Correlation	-0.034	-0.094	-0.236	-0.378	.729**	.692**	0.168	1	-0.373	.699**	-.600**
	Sig. (2-tailed)	0.895	0.811	0.345	0.122	0.001	0.001	0.505		0.127	0.001	0.008
	N	18	9	18	18	18	18	18	18	18	18	18
Ga	Pearson Correlation	-0.295	-0.506	.584**	0.289	-0.18	-0.079	-0.401	-0.373	1	-0.101	.563*
	Sig. (2-tailed)	0.22	0.165	0.009	0.229	0.461	0.747	0.089	0.127		0.681	0.012
	N	19	9	19	19	19	19	19	18	19	19	19
Gd	Pearson Correlation	-0.239	-0.147	0.004	-.491*	.968**	.963**	0.249	.699**	-0.101	1	-0.445
	Sig. (2-tailed)	0.325	0.707	0.987	0.033	0	0	0.304	0.001	0.681		0.057
	N	19	9	19	19	19	19	19	18	19	19	19
Hf	Pearson Correlation	-0.11	-0.562	0.078	0.327	-0.453	-0.401	-0.044	-.600**	.563*	-0.445	1
	Sig. (2-tailed)	0.655	0.115	0.75	0.172	0.051	0.088	0.86	0.008	0.012	0.057	
	N	19	9	19	19	19	19	19	18	19	19	19
Ho	Pearson Correlation	-0.251	-0.031	-0.07	-.470*	.992**	.985**	0.251	.741**	-0.157	.962**	-.485*
	Sig. (2-tailed)	0.301	0.936	0.777	0.042	0	0	0.299	0	0.521	0	0.035
	N	19	9	19	19	19	19	19	18	19	19	19
La	Pearson Correlation	0.05	-.795*	0.094	-0.241	0.284	0.313	.542*	0.042	0.182	0.408	0.204
	Sig. (2-tailed)	0.837	0.01	0.702	0.319	0.239	0.192	0.017	0.87	0.455	0.083	0.403
	N	19	9	19	19	19	19	19	18	19	19	19
Lu	Pearson Correlation	-0.319	-0.256	0.041	-0.45	.944**	.969**	0.229	.608**	0.073	.946**	-0.258
	Sig. (2-tailed)	0.183	0.507	0.868	0.053	0	0	0.346	0.007	0.768	0	0.287
	N	19	9	19	19	19	19	19	18	19	19	19

Correlation Coefficients: Little Round Top

Correlations		Ho	La	Lu	Mo	Nb	Nd	Pr	Rb	Sm	Sn
Ba	Pearson Correlation	-0.251	0.05	-0.319	-0.138	-0.261	-0.097	-0.098	-0.153	-0.285	-0.394
	Sig. (2-tailed)	0.301	0.837	0.183	0.572	0.281	0.694	0.689	0.531	0.238	0.095
	N	19	19	19	19	19	19	19	19	19	19
Be	Pearson Correlation	-0.031	-.795*	-0.256	0.128	-0.533	-.747*	-.799**	-0.445	-0.632	-.670*
	Sig. (2-tailed)	0.936	0.01	0.507	0.744	0.14	0.021	0.01	0.23	0.068	0.048
	N	9	9	9	9	9	9	9	9	9	9
Ce	Pearson Correlation	-0.07	0.094	0.041	.518*	0.288	0.099	0.176	.598**	0.02	0.393
	Sig. (2-tailed)	0.777	0.702	0.868	0.023	0.232	0.688	0.471	0.007	0.934	0.096
	N	19	19	19	19	19	19	19	19	19	19
Cs	Pearson Correlation	-.470*	-0.241	-0.45	0.016	0.341	-0.346	-0.359	0.195	-.463*	0.253
	Sig. (2-tailed)	0.042	0.319	0.053	0.947	0.153	0.146	0.131	0.423	0.046	0.296
	N	19	19	19	19	19	19	19	19	19	19
Dy	Pearson Correlation	.992**	0.284	.944**	0.372	-0.237	.527*	.486*	-0.022	.751**	-0.254
	Sig. (2-tailed)	0	0.239	0	0.117	0.328	0.02	0.035	0.929	0	0.294
	N	19	19	19	19	19	19	19	19	19	19
Er	Pearson Correlation	.985**	0.313	.969**	0.421	-0.147	.547*	.508*	0.087	.751**	-0.171
	Sig. (2-tailed)	0	0.192	0	0.073	0.547	0.015	0.026	0.722	0	0.483
	N	19	19	19	19	19	19	19	19	19	19
Eu	Pearson Correlation	0.251	.542*	0.229	-0.092	-0.187	0.39	0.291	-0.275	0.299	-0.333
	Sig. (2-tailed)	0.299	0.017	0.346	0.707	0.442	0.098	0.227	0.254	0.214	0.164
	N	19	19	19	19	19	19	19	19	19	19
F	Pearson Correlation	.741**	0.042	.608**	0.315	-0.431	0.266	0.213	-0.278	.498*	-.470*
	Sig. (2-tailed)	0	0.87	0.007	0.203	0.074	0.286	0.396	0.265	0.036	0.049
	N	18	18	18	18	18	18	18	18	18	18
Ga	Pearson Correlation	-0.157	0.182	0.073	0.301	.801**	0.154	0.218	.912**	0.031	.846**
	Sig. (2-tailed)	0.521	0.455	0.768	0.211	0	0.528	0.37	0	0.9	0
	N	19	19	19	19	19	19	19	19	19	19
Gd	Pearson Correlation	.962**	0.408	.946**	.461*	-0.21	.660**	.630**	0.062	.852**	-0.206
	Sig. (2-tailed)	0	0.083	0	0.047	0.389	0.002	0.004	0.8	0	0.398
	N	19	19	19	19	19	19	19	19	19	19
Hf	Pearson Correlation	-.485*	0.204	-0.258	-0.363	.868**	0.028	0.009	0.417	-0.151	.802**
	Sig. (2-tailed)	0.035	0.403	0.287	0.126	0	0.908	0.97	0.075	0.537	0
	N	19	19	19	19	19	19	19	19	19	19
Ho	Pearson Correlation	1	0.259	.943**	0.368	-0.264	.503*	.469*	-0.026	.733**	-0.261
	Sig. (2-tailed)		0.284	0	0.121	0.275	0.028	0.043	0.917	0	0.28
	N	19	19	19	19	19	19	19	19	19	19
La	Pearson Correlation	0.259	1	0.454	0.109	0.287	.933**	.914**	0.267	.749**	0.222
	Sig. (2-tailed)	0.284		0.051	0.657	0.233	0	0	0.268	0	0.361
	N	19	19	19	19	19	19	19	19	19	19
Lu	Pearson Correlation	.943**	0.454	1	0.398	0.015	.665**	.638**	0.201	.829**	0.005
	Sig. (2-tailed)	0	0.051		0.091	0.951	0.002	0.003	0.408	0	0.984
	N	19	19	19	19	19	19	19	19	19	19

Correlation Coefficients: Little Round Top

Correlations		Sr	Ta	Tb	Th	Tl	Tm	U	Y	Yb	Zn	Zr
Ba	Pearson Correlation	0.062	-0.342	-0.23	-.477*	-0.209	-0.255	-0.037	-0.225	-0.289	-0.088	-0.189
	Sig. (2-tailed)	0.801	0.152	0.344	0.039	0.39	0.293	0.881	0.353	0.23	0.719	0.438
	N	19	19	19	19	19	19	19	19	19	19	19
Be	Pearson Correlation	0.451	-0.647	-0.074	-0.623	-0.413	-0.122	0.429	0.049	-0.212	-0.164	-0.474
	Sig. (2-tailed)	0.223	0.059	0.85	0.073	0.269	0.755	0.249	0.9	0.585	0.674	0.198
	N	9	9	9	9	9	9	9	9	9	9	9
Ce	Pearson Correlation	-0.444	.497*	-0.023	.691**	.716**	0.021	-0.365	-0.109	-0.016	0.204	0.44
	Sig. (2-tailed)	0.057	0.03	0.927	0.001	0.001	0.932	0.124	0.658	0.949	0.402	0.059
	N	19	19	19	19	19	19	19	19	19	19	19
Cs	Pearson Correlation	-0.286	0.126	-.486*	0.141	0.063	-0.433	-0.184	-0.418	-0.445	.664**	0.341
	Sig. (2-tailed)	0.236	0.607	0.035	0.564	0.796	0.064	0.45	0.075	0.056	0.002	0.152
	N	19	19	19	19	19	19	19	19	19	19	19
Dy	Pearson Correlation	.604**	-0.088	.992**	0.087	0.068	.971**	.633**	.973**	.953**	-.550*	-0.364
	Sig. (2-tailed)	0.006	0.719	0	0.723	0.783	0	0.004	0	0	0.015	0.126
	N	19	19	19	19	19	19	19	19	19	19	19
Er	Pearson Correlation	.544*	-0.005	.991**	0.145	0.161	.993**	.603**	.971**	.974**	-.495*	-0.269
	Sig. (2-tailed)	0.016	0.983	0	0.554	0.511	0	0.006	0	0	0.031	0.266
	N	19	19	19	19	19	19	19	19	19	19	19
Eu	Pearson Correlation	0.263	-0.26	0.249	-0.383	-0.247	0.226	0.217	0.299	0.276	-0.109	-0.281
	Sig. (2-tailed)	0.277	0.282	0.304	0.106	0.308	0.353	0.372	0.214	0.252	0.656	0.244
	N	19	19	19	19	19	19	19	19	19	19	19
F	Pearson Correlation	.632**	-0.316	.718**	-0.11	-0.103	.653**	.590**	.709**	.608**	-.599**	-.533*
	Sig. (2-tailed)	0.005	0.202	0.001	0.663	0.684	0.003	0.01	0.001	0.007	0.009	0.023
	N	18	18	18	18	18	18	18	18	18	18	18
Ga	Pearson Correlation	-.666**	.924**	-0.115	.779**	.773**	0.015	-.488*	-0.194	0.011	0.419	.913**
	Sig. (2-tailed)	0.002	0	0.638	0	0	0.95	0.034	0.426	0.965	0.074	0
	N	19	19	19	19	19	19	19	19	19	19	19
Gd	Pearson Correlation	.555*	-0.013	.987**	0.218	0.181	.954**	.574*	.918**	.937**	-.614**	-0.295
	Sig. (2-tailed)	0.014	0.957	0	0.369	0.46	0	0.01	0	0	0.005	0.22
	N	19	19	19	19	19	19	19	19	19	19	19
Hf	Pearson Correlation	-.678**	.673**	-0.448	0.327	0.021	-0.346	-.490*	-.496*	-0.24	.762**	.801**
	Sig. (2-tailed)	0.001	0.002	0.054	0.172	0.933	0.147	0.033	0.031	0.323	0	0
	N	19	19	19	19	19	19	19	19	19	19	19
Ho	Pearson Correlation	.565*	-0.073	.986**	0.121	0.114	.965**	.576**	.984**	.945**	-.561*	-0.371
	Sig. (2-tailed)	0.012	0.768	0	0.623	0.642	0	0.01	0	0	0.012	0.118
	N	19	19	19	19	19	19	19	19	19	19	19
La	Pearson Correlation	-0.141	0.223	0.334	0.273	0.184	0.361	-0.088	0.246	0.44	-0.175	0.233
	Sig. (2-tailed)	0.565	0.358	0.162	0.259	0.45	0.129	0.721	0.309	0.059	0.473	0.338
	N	19	19	19	19	19	19	19	19	19	19	19
Lu	Pearson Correlation	0.364	0.151	.959**	0.303	0.264	.985**	0.445	.926**	.993**	-0.421	-0.114
	Sig. (2-tailed)	0.125	0.537	0	0.208	0.275	0	0.056	0	0	0.073	0.641
	N	19	19	19	19	19	19	19	19	19	19	19

Correlation Coefficients: Little Round Top

Correlations		SiO2	Al2O3	Fe2O3	CaO	Na2O	K2O	P2O5	SrO	BaO
Ba	Pearson Correlation	-0.18	-0.194	0.027	0.207	-0.352	0.115	-0.033	0.049	.837**
	Sig. (2-tailed)	0.461	0.427	0.913	0.394	0.139	0.64	0.894	0.841	0
	N	19	19	19	19	19	19	19	19	19
Be	Pearson Correlation	-0.505	-0.598	0.052	0.54	-.714*	-0.506	-0.038	0.418	0.357
	Sig. (2-tailed)	0.166	0.089	0.894	0.133	0.031	0.165	0.922	0.263	0.346
	N	9	9	9	9	9	9	9	9	9
Ce	Pearson Correlation	.470*	.580**	0.375	-.458*	0.265	.460*	-0.403	-0.423	0.002
	Sig. (2-tailed)	0.042	0.009	0.113	0.049	0.273	0.048	0.087	0.071	0.995
	N	19	19	19	19	19	19	19	19	19
Cs	Pearson Correlation	0.246	0.053	0.263	-0.25	-0.025	0.178	0.309	-0.269	0.11
	Sig. (2-tailed)	0.31	0.83	0.277	0.301	0.92	0.466	0.199	0.265	0.653
	N	19	19	19	19	19	19	19	19	19
Dy	Pearson Correlation	-0.433	-0.205	-.512*	.507*	-0.147	-.545*	-0.415	.587**	-0.082
	Sig. (2-tailed)	0.064	0.399	0.025	0.027	0.547	0.016	0.077	0.008	0.737
	N	19	19	19	19	19	19	19	19	19
Er	Pearson Correlation	-0.354	-0.137	-.486*	0.445	-0.076	-.500*	-0.402	.536*	-0.091
	Sig. (2-tailed)	0.137	0.577	0.035	0.056	0.757	0.029	0.088	0.018	0.711
	N	19	19	19	19	19	19	19	19	19
Eu	Pearson Correlation	-0.301	-0.381	-0.21	0.327	-0.169	-0.231	0.301	0.295	.461*
	Sig. (2-tailed)	0.21	0.107	0.387	0.172	0.489	0.341	0.21	0.22	0.047
	N	19	19	19	19	19	19	19	19	19
F	Pearson Correlation	-.509*	-0.181	-.739**	.498*	-0.045	-.619**	-.508*	.591**	-0.118
	Sig. (2-tailed)	0.031	0.472	0	0.035	0.858	0.006	0.031	0.01	0.641
	N	18	18	18	18	18	18	18	18	18
Ga	Pearson Correlation	.785**	.659**	0.215	-.736**	.583**	.549*	-0.079	-.641**	-0.246
	Sig. (2-tailed)	0	0.002	0.378	0	0.009	0.015	0.747	0.003	0.311
	N	19	19	19	19	19	19	19	19	19
Gd	Pearson Correlation	-0.353	-0.131	-.501*	0.443	-0.056	-.462*	-.470*	.541*	-0.088
	Sig. (2-tailed)	0.138	0.592	0.029	0.057	0.82	0.046	0.042	0.017	0.721
	N	19	19	19	19	19	19	19	19	19
Hf	Pearson Correlation	.673**	0.314	0.347	-.618**	.495*	.613**	.554*	-.628**	0.009
	Sig. (2-tailed)	0.002	0.191	0.146	0.005	0.031	0.005	0.014	0.004	0.972
	N	19	19	19	19	19	19	19	19	19
Ho	Pearson Correlation	-0.405	-0.16	-.478*	0.455	-0.136	-.543*	-0.435	.536*	-0.152
	Sig. (2-tailed)	0.085	0.513	0.038	0.05	0.579	0.016	0.063	0.018	0.535
	N	19	19	19	19	19	19	19	19	19
La	Pearson Correlation	0.274	0.193	-0.05	-0.15	.460*	0.298	0.11	-0.089	0.248
	Sig. (2-tailed)	0.256	0.428	0.839	0.54	0.048	0.215	0.655	0.717	0.306
	N	19	19	19	19	19	19	19	19	19
Lu	Pearson Correlation	-0.151	0.043	-0.383	0.256	0.116	-0.322	-0.353	0.361	-0.133
	Sig. (2-tailed)	0.538	0.861	0.106	0.29	0.636	0.178	0.138	0.129	0.588
	N	19	19	19	19	19	19	19	19	19

Correlation Coefficients: Little Round Top

Correlations		Ba	Be	Ce	Cs	Dy	Er	Eu	F	Ga	Gd	Hf
Mo	Pearson Correlation	-0.138	0.128	.518*	0.016	0.372	0.421	-0.092	0.315	0.301	.461*	-0.363
	Sig. (2-tailed)	0.572	0.744	0.023	0.947	0.117	0.073	0.707	0.203	0.211	0.047	0.126
	N	19	9	19	19	19	19	19	18	19	19	19
Nb	Pearson Correlation	-0.261	-0.533	0.288	0.341	-0.237	-0.147	-0.187	-0.431	.801**	-0.21	.868**
	Sig. (2-tailed)	0.281	0.14	0.232	0.153	0.328	0.547	0.442	0.074	0	0.389	0
	N	19	9	19	19	19	19	19	18	19	19	19
Nd	Pearson Correlation	-0.097	-.747*	0.099	-0.346	.527*	.547*	0.39	0.266	0.154	.660**	0.028
	Sig. (2-tailed)	0.694	0.021	0.688	0.146	0.02	0.015	0.098	0.286	0.528	0.002	0.908
	N	19	9	19	19	19	19	19	18	19	19	19
Pr	Pearson Correlation	-0.098	-.799**	0.176	-0.359	.486*	.508*	0.291	0.213	0.218	.630**	0.009
	Sig. (2-tailed)	0.689	0.01	0.471	0.131	0.035	0.026	0.227	0.396	0.37	0.004	0.97
	N	19	9	19	19	19	19	19	18	19	19	19
Rb	Pearson Correlation	-0.153	-0.445	.598**	0.195	-0.022	0.087	-0.275	-0.278	.912**	0.062	0.417
	Sig. (2-tailed)	0.531	0.23	0.007	0.423	0.929	0.722	0.254	0.265	0	0.8	0.075
	N	19	9	19	19	19	19	19	18	19	19	19
Sm	Pearson Correlation	-0.285	-0.632	0.02	-.463*	.751**	.751**	0.299	.498*	0.031	.852**	-0.151
	Sig. (2-tailed)	0.238	0.068	0.934	0.046	0	0	0.214	0.036	0.9	0	0.537
	N	19	9	19	19	19	19	19	18	19	19	19
Sn	Pearson Correlation	-0.394	-.670*	0.393	0.253	-0.254	-0.171	-0.333	-.470*	.846**	-0.206	.802**
	Sig. (2-tailed)	0.095	0.048	0.096	0.296	0.294	0.483	0.164	0.049	0	0.398	0
	N	19	9	19	19	19	19	19	18	19	19	19
Sr	Pearson Correlation	0.062	0.451	-0.444	-0.286	.604**	.544*	0.263	.632**	-.666**	.555*	-.678**
	Sig. (2-tailed)	0.801	0.223	0.057	0.236	0.006	0.016	0.277	0.005	0.002	0.014	0.001
	N	19	9	19	19	19	19	19	18	19	19	19
Ta	Pearson Correlation	-0.342	-0.647	.497*	0.126	-0.088	-0.005	-0.26	-0.316	.924**	-0.013	.673**
	Sig. (2-tailed)	0.152	0.059	0.03	0.607	0.719	0.983	0.282	0.202	0	0.957	0.002
	N	19	9	19	19	19	19	19	18	19	19	19
Tb	Pearson Correlation	-0.23	-0.074	-0.023	-.486*	.992**	.991**	0.249	.718**	-0.115	.987**	-0.448
	Sig. (2-tailed)	0.344	0.85	0.927	0.035	0	0	0.304	0.001	0.638	0	0.054
	N	19	9	19	19	19	19	19	18	19	19	19
Th	Pearson Correlation	-.477*	-0.623	.691**	0.141	0.087	0.145	-0.383	-0.11	.779**	0.218	0.327
	Sig. (2-tailed)	0.039	0.073	0.001	0.564	0.723	0.554	0.106	0.663	0	0.369	0.172
	N	19	9	19	19	19	19	19	18	19	19	19
Tl	Pearson Correlation	-0.209	-0.413	.716**	0.063	0.068	0.161	-0.247	-0.103	.773**	0.181	0.021
	Sig. (2-tailed)	0.39	0.269	0.001	0.796	0.783	0.511	0.308	0.684	0	0.46	0.933
	N	19	9	19	19	19	19	19	18	19	19	19
Tm	Pearson Correlation	-0.255	-0.122	0.021	-0.433	.971**	.993**	0.226	.653**	0.015	.954**	-0.346
	Sig. (2-tailed)	0.293	0.755	0.932	0.064	0	0	0.353	0.003	0.95	0	0.147
	N	19	9	19	19	19	19	19	18	19	19	19

Correlation Coefficients: Little Round Top

Correlations		Ho	La	Lu	Mo	Nb	Nd	Pr	Rb	Sm	Sn	Sr
Mo	Pearson Correlation	0.368	0.109	0.398	1	0.043	0.248	0.258	.528*	0.295	0.041	0.3
	Sig. (2-tailed)	0.121	0.657	0.091		0.86	0.307	0.287	0.02	0.219	0.867	0.212
	N	19	19	19	19	19	19	19	19	19	19	19
Nb	Pearson Correlation	-0.264	0.287	0.015	0.043	1	0.186	0.185	.722**	0.029	.937**	-.618**
	Sig. (2-tailed)	0.275	0.233	0.951	0.86		0.447	0.447	0	0.908	0	0.005
	N	19	19	19	19	19	19	19	19	19	19	19
Nd	Pearson Correlation	.503*	.933**	.665**	0.248	0.186	1	.986**	0.257	.925**	0.164	0.044
	Sig. (2-tailed)	0.028	0	0.002	0.307	0.447		0	0.289	0	0.502	0.859
	N	19	19	19	19	19	19	19	19	19	19	19
Pr	Pearson Correlation	.469*	.914**	.638**	0.258	0.185	.986**	1	0.299	.905**	0.197	-0.038
	Sig. (2-tailed)	0.043	0	0.003	0.287	0.447	0		0.214	0	0.418	0.878
	N	19	19	19	19	19	19	19	19	19	19	19
Rb	Pearson Correlation	-0.026	0.267	0.201	.528*	.722**	0.257	0.299	1	0.115	.704**	-0.428
	Sig. (2-tailed)	0.917	0.268	0.408	0.02	0	0.289	0.214		0.639	0.001	0.068
	N	19	19	19	19	19	19	19	19	19	19	19
Sm	Pearson Correlation	.733**	.749**	.829**	0.295	0.029	.925**	.905**	0.115	1	0.047	0.247
	Sig. (2-tailed)	0	0	0	0.219	0.908	0	0	0.639		0.848	0.308
	N	19	19	19	19	19	19	19	19	19	19	19
Sn	Pearson Correlation	-0.261	0.222	0.005	0.041	.937**	0.164	0.197	.704**	0.047	1	-.696**
	Sig. (2-tailed)	0.28	0.361	0.984	0.867	0	0.502	0.418	0.001	0.848		0.001
	N	19	19	19	19	19	19	19	19	19	19	19
Sr	Pearson Correlation	.565*	-0.141	0.364	0.3	-.618**	0.044	-0.038	-0.428	0.247	-.696**	1
	Sig. (2-tailed)	0.012	0.565	0.125	0.212	0.005	0.859	0.878	0.068	0.308	0.001	
	N	19	19	19	19	19	19	19	19	19	19	19
Ta	Pearson Correlation	-0.073	0.223	0.151	0.199	.825**	0.199	0.231	.821**	0.12	.865**	-.617**
	Sig. (2-tailed)	0.768	0.358	0.537	0.415	0	0.414	0.341	0	0.624	0	0.005
	N	19	19	19	19	19	19	19	19	19	19	19
Tb	Pearson Correlation	.986**	0.334	.959**	0.443	-0.204	.580**	.545*	0.054	.789**	-0.215	.571*
	Sig. (2-tailed)	0	0.162	0	0.057	0.402	0.009	0.016	0.825	0	0.378	0.011
	N	19	19	19	19	19	19	19	19	19	19	19
Th	Pearson Correlation	0.121	0.273	0.303	0.324	.534*	0.369	0.437	.652**	0.378	.649**	-.540*
	Sig. (2-tailed)	0.623	0.259	0.208	0.176	0.018	0.12	0.062	0.002	0.111	0.003	0.017
	N	19	19	19	19	19	19	19	19	19	19	19
Tl	Pearson Correlation	0.114	0.184	0.264	.622**	0.359	0.209	0.279	.827**	0.145	0.426	-0.335
	Sig. (2-tailed)	0.642	0.45	0.275	0.004	0.132	0.39	0.247	0	0.554	0.069	0.161
	N	19	19	19	19	19	19	19	19	19	19	19
Tm	Pearson Correlation	.965**	0.361	.985**	.461*	-0.063	.585**	.552*	0.187	.765**	-0.09	.472*
	Sig. (2-tailed)	0	0.129	0	0.047	0.799	0.009	0.014	0.442	0	0.714	0.041
	N	19	19	19	19	19	19	19	19	19	19	19

Correlation Coefficients: Little Round Top

Correlations		Ta	Tb	Th	Tl	Tm	U	Y	Yb	Zn	Zr
Mo	Pearson Correlation	0.199	0.443	0.324	.622**	.461*	0.379	0.331	0.356	-0.26	0.104
	Sig. (2-tailed)	0.415	0.057	0.176	0.004	0.047	0.109	0.166	0.135	0.282	0.673
	N	19	19	19	19	19	19	19	19	19	19
Nb	Pearson Correlation	.825**	-0.204	.534*	0.359	-0.063	-0.373	-0.272	0.006	.680**	.912**
	Sig. (2-tailed)	0	0.402	0.018	0.132	0.799	0.116	0.261	0.98	0.001	0
	N	19	19	19	19	19	19	19	19	19	19
Nd	Pearson Correlation	0.199	.580**	0.369	0.209	.585**	0.095	.465*	.644**	-0.363	0.12
	Sig. (2-tailed)	0.414	0.009	0.12	0.39	0.009	0.7	0.045	0.003	0.127	0.626
	N	19	19	19	19	19	19	19	19	19	19
Pr	Pearson Correlation	0.231	.545*	0.437	0.279	.552*	-0.004	0.427	.607**	-0.388	0.149
	Sig. (2-tailed)	0.341	0.016	0.062	0.247	0.014	0.987	0.068	0.006	0.101	0.543
	N	19	19	19	19	19	19	19	19	19	19
Rb	Pearson Correlation	.821**	0.054	.652**	.827**	0.187	-0.206	-0.066	0.146	0.279	.849**
	Sig. (2-tailed)	0	0.825	0.002	0	0.442	0.397	0.789	0.551	0.248	0
	N	19	19	19	19	19	19	19	19	19	19
Sm	Pearson Correlation	0.12	.789**	0.378	0.145	.765**	0.282	.679**	.813**	-.493*	-0.077
	Sig. (2-tailed)	0.624	0	0.111	0.554	0	0.242	0.001	0	0.032	0.755
	N	19	19	19	19	19	19	19	19	19	19
Sn	Pearson Correlation	.865**	-0.215	.649**	0.426	-0.09	-.505*	-0.283	-0.02	.650**	.881**
	Sig. (2-tailed)	0	0.378	0.003	0.069	0.714	0.028	0.24	0.935	0.003	0
	N	19	19	19	19	19	19	19	19	19	19
Sr	Pearson Correlation	-.617**	.571*	-.540*	-0.335	.472*	.934**	.558*	0.395	-.580**	-.720**
	Sig. (2-tailed)	0.005	0.011	0.017	0.161	0.041	0	0.013	0.094	0.009	0.001
	N	19	19	19	19	19	19	19	19	19	19
Ta	Pearson Correlation	1	-0.027	.778**	.663**	0.078	-0.436	-0.14	0.103	0.422	.894**
	Sig. (2-tailed)		0.912	0	0.002	0.751	0.062	0.567	0.676	0.072	0
	N	19	19	19	19	19	19	19	19	19	19
Tb	Pearson Correlation	-0.027	1	0.162	0.16	.980**	.606**	.955**	.959**	-.571*	-0.309
	Sig. (2-tailed)	0.912		0.506	0.514	0	0.006	0	0	0.011	0.199
	N	19	19	19	19	19	19	19	19	19	19
Th	Pearson Correlation	.778**	0.162	1	.688**	0.214	-0.407	0.039	0.236	0.153	.632**
	Sig. (2-tailed)	0	0.506		0.001	0.379	0.084	0.875	0.331	0.532	0.004
	N	19	19	19	19	19	19	19	19	19	19
Tl	Pearson Correlation	.663**	0.16	.688**	1	0.247	-0.233	0.073	0.175	0.008	.557*
	Sig. (2-tailed)	0.002	0.514	0.001		0.307	0.336	0.768	0.473	0.973	0.013
	N	19	19	19	19	19	19	19	19	19	19
Tm	Pearson Correlation	0.078	.980**	0.214	0.247	1	.553*	.949**	.983**	-.459*	-0.177
	Sig. (2-tailed)	0.751	0	0.379	0.307		0.014	0	0	0.048	0.469
	N	19	19	19	19	19	19	19	19	19	19

Correlation Coefficients: Little Round Top

Correlations		SiO2	Al2O3	Fe2O3	CaO	Na2O	K2O	P2O5	SrO	BaO
Mo	Pearson Correlation	-0.121	0.055	-0.359	0.197	0.098	-0.259	-.552*	0.342	-0.009
	Sig. (2-tailed)	0.622	0.824	0.131	0.42	0.691	0.283	0.014	0.152	0.97
	N	19	19	19	19	19	19	19	19	19
Nb	Pearson Correlation	.712**	0.45	0.204	-.624**	.639**	.542*	0.322	-.557*	-0.072
	Sig. (2-tailed)	0.001	0.053	0.401	0.004	0.003	0.016	0.179	0.013	0.77
	N	19	19	19	19	19	19	19	19	19
Nd	Pearson Correlation	0.145	0.164	-0.187	-0.021	0.41	0.139	-0.088	0.078	0.107
	Sig. (2-tailed)	0.554	0.502	0.443	0.932	0.081	0.571	0.72	0.75	0.662
	N	19	19	19	19	19	19	19	19	19
Pr	Pearson Correlation	0.223	0.267	-0.117	-0.106	0.432	0.23	-0.157	-0.01	0.088
	Sig. (2-tailed)	0.36	0.27	0.634	0.666	0.065	0.343	0.521	0.969	0.72
	N	19	19	19	19	19	19	19	19	19
Rb	Pearson Correlation	.593**	.493*	0.083	-.465*	.486*	0.389	-0.173	-0.369	-0.049
	Sig. (2-tailed)	0.007	0.032	0.735	0.045	0.035	0.1	0.478	0.12	0.842
	N	19	19	19	19	19	19	19	19	19
Sm	Pearson Correlation	-0.036	0.09	-0.352	0.138	0.296	-0.089	-0.253	0.261	-0.073
	Sig. (2-tailed)	0.885	0.714	0.14	0.573	0.219	0.717	0.295	0.28	0.766
	N	19	19	19	19	19	19	19	19	19
Sn	Pearson Correlation	.748**	.543*	0.319	-.728**	.631**	.617**	0.257	-.650**	-0.225
	Sig. (2-tailed)	0	0.016	0.184	0	0.004	0.005	0.288	0.003	0.355
	N	19	19	19	19	19	19	19	19	19
Sr	Pearson Correlation	-.933**	-.788**	-.672**	.963**	-.616**	-.902**	-0.238	.986**	0.135
	Sig. (2-tailed)	0	0	0.002	0	0.005	0	0.326	0	0.583
	N	19	19	19	19	19	19	19	19	19
Ta	Pearson Correlation	.721**	.566*	0.124	-.682**	.582**	.481*	-0.053	-.597**	-0.29
	Sig. (2-tailed)	0	0.012	0.613	0.001	0.009	0.037	0.828	0.007	0.228
	N	19	19	19	19	19	19	19	19	19
Tb	Pearson Correlation	-0.381	-0.147	-.510*	.468*	-0.087	-.503*	-.466*	.558*	-0.087
	Sig. (2-tailed)	0.107	0.549	0.026	0.043	0.722	0.028	0.044	0.013	0.724
	N	19	19	19	19	19	19	19	19	19
Th	Pearson Correlation	.697**	.734**	0.189	-.643**	.601**	.489*	-0.337	-.535*	-0.419
	Sig. (2-tailed)	0.001	0	0.439	0.003	0.006	0.034	0.159	0.018	0.074
	N	19	19	19	19	19	19	19	19	19
Tl	Pearson Correlation	.481*	.559*	0.048	-0.415	0.352	0.24	-0.437	-0.317	-0.183
	Sig. (2-tailed)	0.037	0.013	0.844	0.077	0.14	0.323	0.062	0.186	0.453
	N	19	19	19	19	19	19	19	19	19
Tm	Pearson Correlation	-0.263	-0.051	-0.453	0.372	0.007	-0.425	-0.409	.471*	-0.084
	Sig. (2-tailed)	0.278	0.834	0.052	0.117	0.978	0.069	0.082	0.042	0.734
	N	19	19	19	19	19	19	19	19	19

Correlation Coefficients: Little Round Top

Correlations		Ba	Be	Ce	Cs	Dy	Er	Eu	F	Ga	Gd	Hf
U	Pearson Correlation	-0.037	0.429	-0.365	-0.184	.633**	.603**	0.217	.590**	-.488*	.574*	-.490*
	Sig. (2-tailed)	0.881	0.249	0.124	0.45	0.004	0.006	0.372	0.01	0.034	0.01	0.033
	N	19	9	19	19	19	19	19	18	19	19	19
Y	Pearson Correlation	-0.225	0.049	-0.109	-0.418	.973**	.971**	0.299	.709**	-0.194	.918**	-.496*
	Sig. (2-tailed)	0.353	0.9	0.658	0.075	0	0	0.214	0.001	0.426	0	0.031
	N	19	9	19	19	19	19	19	18	19	19	19
Yb	Pearson Correlation	-0.289	-0.212	-0.016	-0.445	.953**	.974**	0.276	.608**	0.011	.937**	-0.24
	Sig. (2-tailed)	0.23	0.585	0.949	0.056	0	0	0.252	0.007	0.965	0	0.323
	N	19	9	19	19	19	19	19	18	19	19	19
Zn	Pearson Correlation	-0.088	-0.164	0.204	.664**	-.550*	-.495*	-0.109	-.599**	0.419	-.614**	.762**
	Sig. (2-tailed)	0.719	0.674	0.402	0.002	0.015	0.031	0.656	0.009	0.074	0.005	0
	N	19	9	19	19	19	19	19	18	19	19	19
Zr	Pearson Correlation	-0.189	-0.474	0.44	0.341	-0.364	-0.269	-0.281	-.533*	.913**	-0.295	.801**
	Sig. (2-tailed)	0.438	0.198	0.059	0.152	0.126	0.266	0.244	0.023	0	0.22	0
	N	19	9	19	19	19	19	19	18	19	19	19
SiO2	Pearson Correlation	-0.18	-0.505	.470*	0.246	-0.433	-0.354	-0.301	-.509*	.785**	-0.353	.673**
	Sig. (2-tailed)	0.461	0.166	0.042	0.31	0.064	0.137	0.21	0.031	0	0.138	0.002
	N	19	9	19	19	19	19	19	18	19	19	19
Al2O3	Pearson Correlation	-0.194	-0.598	.580**	0.053	-0.205	-0.137	-0.381	-0.181	.659**	-0.131	0.314
	Sig. (2-tailed)	0.427	0.089	0.009	0.83	0.399	0.577	0.107	0.472	0.002	0.592	0.191
	N	19	9	19	19	19	19	19	18	19	19	19
Fe2O3	Pearson Correlation	0.027	0.052	0.375	0.263	-.512*	-.486*	-0.21	-.739**	0.215	-.501*	0.347
	Sig. (2-tailed)	0.913	0.894	0.113	0.277	0.025	0.035	0.387	0	0.378	0.029	0.146
	N	19	9	19	19	19	19	19	18	19	19	19
CaO	Pearson Correlation	0.207	0.54	-.458*	-0.25	.507*	0.445	0.327	.498*	-.736**	0.443	-.618**
	Sig. (2-tailed)	0.394	0.133	0.049	0.301	0.027	0.056	0.172	0.035	0	0.057	0.005
	N	19	9	19	19	19	19	19	18	19	19	19
Na2O	Pearson Correlation	-0.352	-.714*	0.265	-0.025	-0.147	-0.076	-0.169	-0.045	.583**	-0.056	.495*
	Sig. (2-tailed)	0.139	0.031	0.273	0.92	0.547	0.757	0.489	0.858	0.009	0.82	0.031
	N	19	9	19	19	19	19	19	18	19	19	19
K2O	Pearson Correlation	0.115	-0.506	.460*	0.178	-.545*	-.500*	-0.231	-.619**	.549*	-.462*	.613**
	Sig. (2-tailed)	0.64	0.165	0.048	0.466	0.016	0.029	0.341	0.006	0.015	0.046	0.005
	N	19	9	19	19	19	19	19	18	19	19	19
P2O5	Pearson Correlation	-0.033	-0.038	-0.403	0.309	-0.415	-0.402	0.301	-.508*	-0.079	-.470*	.554*
	Sig. (2-tailed)	0.894	0.922	0.087	0.199	0.077	0.088	0.21	0.031	0.747	0.042	0.014
	N	19	9	19	19	19	19	19	18	19	19	19
SrO	Pearson Correlation	0.049	0.418	-0.423	-0.269	.587**	.536*	0.295	.591**	-.641**	.541*	-.628**
	Sig. (2-tailed)	0.841	0.263	0.071	0.265	0.008	0.018	0.22	0.01	0.003	0.017	0.004
	N	19	9	19	19	19	19	19	18	19	19	19
BaO	Pearson Correlation	.837**	0.357	0.002	0.11	-0.082	-0.091	.461*	-0.118	-0.246	-0.088	0.009
	Sig. (2-tailed)	0	0.346	0.995	0.653	0.737	0.711	0.047	0.641	0.311	0.721	0.972
	N	19	9	19	19	19	19	19	18	19	19	19

Correlation Coefficients: Little Round Top

Correlations		Ho	La	Lu	Mo	Nb	Nd	Pr	Rb	Sm	Sn	Sr
U	Pearson Correlation	.576**	-0.088	0.445	0.379	-0.373	0.095	-0.004	-0.206	0.282	-.505*	.934**
	Sig. (2-tailed)	0.01	0.721	0.056	0.109	0.116	0.7	0.987	0.397	0.242	0.028	0
	N	19	19	19	19	19	19	19	19	19	19	19
Y	Pearson Correlation	.984**	0.246	.926**	0.331	-0.272	.465*	0.427	-0.066	.679**	-0.283	.558*
	Sig. (2-tailed)	0	0.309	0	0.166	0.261	0.045	0.068	0.789	0.001	0.24	0.013
	N	19	19	19	19	19	19	19	19	19	19	19
Yb	Pearson Correlation	.945**	0.44	.993**	0.356	0.006	.644**	.607**	0.146	.813**	-0.02	0.395
	Sig. (2-tailed)	0	0.059	0	0.135	0.98	0.003	0.006	0.551	0	0.935	0.094
	N	19	19	19	19	19	19	19	19	19	19	19
Zn	Pearson Correlation	-.561*	-0.175	-0.421	-0.26	.680**	-0.363	-0.388	0.279	-.493*	.650**	-.580**
	Sig. (2-tailed)	0.012	0.473	0.073	0.282	0.001	0.127	0.101	0.248	0.032	0.003	0.009
	N	19	19	19	19	19	19	19	19	19	19	19
Zr	Pearson Correlation	-0.371	0.233	-0.114	0.104	.912**	0.12	0.149	.849**	-0.077	.881**	-.720**
	Sig. (2-tailed)	0.118	0.338	0.641	0.673	0	0.626	0.543	0	0.755	0	0.001
	N	19	19	19	19	19	19	19	19	19	19	19
SiO2	Pearson Correlation	-0.405	0.274	-0.151	-0.121	.712**	0.145	0.223	.593**	-0.036	.748**	-.933**
	Sig. (2-tailed)	0.085	0.256	0.538	0.622	0.001	0.554	0.36	0.007	0.885	0	0
	N	19	19	19	19	19	19	19	19	19	19	19
Al2O3	Pearson Correlation	-0.16	0.193	0.043	0.055	0.45	0.164	0.267	.493*	0.09	.543*	-.788**
	Sig. (2-tailed)	0.513	0.428	0.861	0.824	0.053	0.502	0.27	0.032	0.714	0.016	0
	N	19	19	19	19	19	19	19	19	19	19	19
Fe2O3	Pearson Correlation	-.478*	-0.05	-0.383	-0.359	0.204	-0.187	-0.117	0.083	-0.352	0.319	-.672**
	Sig. (2-tailed)	0.038	0.839	0.106	0.131	0.401	0.443	0.634	0.735	0.14	0.184	0.002
	N	19	19	19	19	19	19	19	19	19	19	19
CaO	Pearson Correlation	0.455	-0.15	0.256	0.197	-.624**	-0.021	-0.106	-.465*	0.138	-.728**	.963**
	Sig. (2-tailed)	0.05	0.54	0.29	0.42	0.004	0.932	0.666	0.045	0.573	0	0
	N	19	19	19	19	19	19	19	19	19	19	19
Na2O	Pearson Correlation	-0.136	.460*	0.116	0.098	.639**	0.41	0.432	.486*	0.296	.631**	-.616**
	Sig. (2-tailed)	0.579	0.048	0.636	0.691	0.003	0.081	0.065	0.035	0.219	0.004	0.005
	N	19	19	19	19	19	19	19	19	19	19	19
K2O	Pearson Correlation	-.543*	0.298	-0.322	-0.259	.542*	0.139	0.23	0.389	-0.089	.617**	-.902**
	Sig. (2-tailed)	0.016	0.215	0.178	0.283	0.016	0.571	0.343	0.1	0.717	0.005	0
	N	19	19	19	19	19	19	19	19	19	19	19
P2O5	Pearson Correlation	-0.435	0.11	-0.353	-.552*	0.322	-0.088	-0.157	-0.173	-0.253	0.257	-0.238
	Sig. (2-tailed)	0.063	0.655	0.138	0.014	0.179	0.72	0.521	0.478	0.295	0.288	0.326
	N	19	19	19	19	19	19	19	19	19	19	19
SrO	Pearson Correlation	.536*	-0.089	0.361	0.342	-.557*	0.078	-0.01	-0.369	0.261	-.650**	.986**
	Sig. (2-tailed)	0.018	0.717	0.129	0.152	0.013	0.75	0.969	0.12	0.28	0.003	0
	N	19	19	19	19	19	19	19	19	19	19	19
BaO	Pearson Correlation	-0.152	0.248	-0.133	-0.009	-0.072	0.107	0.088	-0.049	-0.073	-0.225	0.135
	Sig. (2-tailed)	0.535	0.306	0.588	0.97	0.77	0.662	0.72	0.842	0.766	0.355	0.583
	N	19	19	19	19	19	19	19	19	19	19	19

Correlation Coefficients: Little Round Top

Correlations		Ta	Tb	Th	Tl	Tm	U	Y	Yb	Zn	Zr
U	Pearson Correlation	-0.436	.606**	-0.407	-0.233	.553*	1	.560*	.479*	-0.408	-.492*
	Sig. (2-tailed)	0.062	0.006	0.084	0.336	0.014		0.013	0.038	0.083	0.032
	N	19	19	19	19	19	19	19	19	19	19
Y	Pearson Correlation	-0.14	.955**	0.039	0.073	.949**	.560*	1	.936**	-.510*	-0.407
	Sig. (2-tailed)	0.567	0	0.875	0.768	0	0.013		0	0.026	0.084
	N	19	19	19	19	19	19	19	19	19	19
Yb	Pearson Correlation	0.103	.959**	0.236	0.175	.983**	.479*	.936**	1	-0.391	-0.151
	Sig. (2-tailed)	0.676	0	0.331	0.473	0	0.038	0		0.097	0.538
	N	19	19	19	19	19	19	19	19	19	19
Zn	Pearson Correlation	0.422	-.571*	0.153	0.008	-.459*	-0.408	-.510*	-0.391	1	.588**
	Sig. (2-tailed)	0.072	0.011	0.532	0.973	0.048	0.083	0.026	0.097		0.008
	N	19	19	19	19	19	19	19	19	19	19
Zr	Pearson Correlation	.894**	-0.309	.632**	.557*	-0.177	-.492*	-0.407	-0.151	.588**	1
	Sig. (2-tailed)	0	0.199	0.004	0.013	0.469	0.032	0.084	0.538	0.008	
	N	19	19	19	19	19	19	19	19	19	19
SiO2	Pearson Correlation	.721**	-0.381	.697**	.481*	-0.263	-.799**	-0.418	-0.193	.477*	.805**
	Sig. (2-tailed)	0	0.107	0.001	0.037	0.278	0	0.075	0.429	0.039	0
	N	19	19	19	19	19	19	19	19	19	19
Al2O3	Pearson Correlation	.566*	-0.147	.734**	.559*	-0.051	-.698**	-0.179	-0.011	0.204	.550*
	Sig. (2-tailed)	0.012	0.549	0	0.013	0.834	0.001	0.463	0.964	0.403	0.015
	N	19	19	19	19	19	19	19	19	19	19
Fe2O3	Pearson Correlation	0.124	-.510*	0.189	0.048	-0.453	-.684**	-0.417	-0.387	.465*	0.282
	Sig. (2-tailed)	0.613	0.026	0.439	0.844	0.052	0.001	0.076	0.102	0.045	0.242
	N	19	19	19	19	19	19	19	19	19	19
CaO	Pearson Correlation	-.682**	.468*	-.643**	-0.415	0.372	.909**	.457*	0.302	-.483*	-.719**
	Sig. (2-tailed)	0.001	0.043	0.003	0.077	0.117	0	0.049	0.209	0.036	0.001
	N	19	19	19	19	19	19	19	19	19	19
Na2O	Pearson Correlation	.582**	-0.087	.601**	0.352	0.007	-0.446	-0.163	0.078	0.228	.634**
	Sig. (2-tailed)	0.009	0.722	0.006	0.14	0.978	0.056	0.506	0.751	0.349	0.004
	N	19	19	19	19	19	19	19	19	19	19
K2O	Pearson Correlation	.481*	-.503*	.489*	0.24	-0.425	-.838**	-.556*	-0.343	0.441	.626**
	Sig. (2-tailed)	0.037	0.028	0.034	0.323	0.069	0	0.013	0.151	0.059	0.004
	N	19	19	19	19	19	19	19	19	19	19
P2O5	Pearson Correlation	-0.053	-.466*	-0.337	-0.437	-0.409	-0.214	-0.336	-0.303	.592**	0.168
	Sig. (2-tailed)	0.828	0.044	0.159	0.062	0.082	0.38	0.16	0.207	0.008	0.491
	N	19	19	19	19	19	19	19	19	19	19
SrO	Pearson Correlation	-.597**	.558*	-.535*	-0.317	.471*	.960**	.528*	0.396	-.526*	-.663**
	Sig. (2-tailed)	0.007	0.013	0.018	0.186	0.042	0	0.02	0.093	0.021	0.002
	N	19	19	19	19	19	19	19	19	19	19
BaO	Pearson Correlation	-0.29	-0.087	-0.419	-0.183	-0.084	0.105	-0.114	-0.083	0.038	-0.126
	Sig. (2-tailed)	0.228	0.724	0.074	0.453	0.734	0.668	0.643	0.735	0.876	0.608
	N	19	19	19	19	19	19	19	19	19	19

Correlation Coefficients: Little Round Top

Correlations		SiO2	Al2O3	Fe2O3	CaO	Na2O	K2O	P2O5	SrO	BaO
U	Pearson Correlation	-.799**	-.698**	-.684**	.909**	-0.446	-.838**	-0.214	.960**	0.105
	Sig. (2-tailed)	0	0.001	0.001	0	0.056	0	0.38	0	0.668
	N	19	19	19	19	19	19	19	19	19
Y	Pearson Correlation	-0.418	-0.179	-0.417	.457*	-0.163	-.556*	-0.336	.528*	-0.114
	Sig. (2-tailed)	0.075	0.463	0.076	0.049	0.506	0.013	0.16	0.02	0.643
	N	19	19	19	19	19	19	19	19	19
Yb	Pearson Correlation	-0.193	-0.011	-0.387	0.302	0.078	-0.343	-0.303	0.396	-0.083
	Sig. (2-tailed)	0.429	0.964	0.102	0.209	0.751	0.151	0.207	0.093	0.735
	N	19	19	19	19	19	19	19	19	19
Zn	Pearson Correlation	.477*	0.204	.465*	-.483*	0.228	0.441	.592**	-.526*	0.038
	Sig. (2-tailed)	0.039	0.403	0.045	0.036	0.349	0.059	0.008	0.021	0.876
	N	19	19	19	19	19	19	19	19	19
Zr	Pearson Correlation	.805**	.550*	0.282	-.719**	.634**	.626**	0.168	-.663**	-0.126
	Sig. (2-tailed)	0	0.015	0.242	0.001	0.004	0.004	0.491	0.002	0.608
	N	19	19	19	19	19	19	19	19	19
SiO2	Pearson Correlation	1	.880**	.501*	-.937**	.755**	.875**	0.098	-.905**	-0.171
	Sig. (2-tailed)		0	0.029	0	0	0	0.689	0	0.484
	N	19	19	19	19	19	19	19	19	19
Al2O3	Pearson Correlation	.880**	1	0.387	-.836**	.743**	.766**	-0.25	-.776**	-0.238
	Sig. (2-tailed)	0		0.102	0	0	0	0.301	0	0.328
	N	19	19	19	19	19	19	19	19	19
Fe2O3	Pearson Correlation	.501*	0.387	1	-.563*	0.134	.630**	0.409	-.674**	-0.038
	Sig. (2-tailed)	0.029	0.102		0.012	0.584	0.004	0.082	0.002	0.877
	N	19	19	19	19	19	19	19	19	19
CaO	Pearson Correlation	-.937**	-.836**	-.563*	1	-.692**	-.830**	-0.156	.967**	0.3
	Sig. (2-tailed)	0	0	0.012		0.001	0	0.523	0	0.212
	N	19	19	19	19	19	19	19	19	19
Na2O	Pearson Correlation	.755**	.743**	0.134	-.692**	1	.578**	0.031	-.562*	-0.34
	Sig. (2-tailed)	0	0	0.584	0.001		0.009	0.901	0.012	0.155
	N	19	19	19	19	19	19	19	19	19
K2O	Pearson Correlation	.875**	.766**	.630**	-.830**	.578**	1	0.141	-.865**	0.127
	Sig. (2-tailed)	0	0	0.004	0	0.009		0.564	0	0.605
	N	19	19	19	19	19	19	19	19	19
P2O5	Pearson Correlation	0.098	-0.25	0.409	-0.156	0.031	0.141	1	-0.206	0.103
	Sig. (2-tailed)	0.689	0.301	0.082	0.523	0.901	0.564		0.398	0.676
	N	19	19	19	19	19	19	19	19	19
SrO	Pearson Correlation	-.905**	-.776**	-.674**	.967**	-.562*	-.865**	-0.206	1	0.176
	Sig. (2-tailed)	0	0	0.002	0	0.012	0	0.398		0.471
	N	19	19	19	19	19	19	19	19	19
BaO	Pearson Correlation	-0.171	-0.238	-0.038	0.3	-0.34	0.127	0.103	0.176	1
	Sig. (2-tailed)	0.484	0.328	0.877	0.212	0.155	0.605	0.676	0.471	
	N	19	19	19	19	19	19	19	19	19

Correlation Coefficients: Round Top

Correlations		Ba	Be	Ce	Cs	Cu	Dy	Er	Eu	F	Ga	Gd	Hf
Ba	Pearson Correlation	1	-0.088	-0.14	-0.203	0.264	-0.434	-0.491	-0.052	-0.461	-0.322	-0.115	-0.382
	Sig. (2-tailed)		0.774	0.647	0.505	0.383	0.139	0.088	0.865	0.539	0.283	0.708	0.198
	N	13	13	13	13	13	13	13	13	4	13	13	13
Be	Pearson Correlation	-0.088	1	0.267	-0.474	0.209	0.101	-0.058	-0.077	-0.457	0.283	0.174	-0.015
	Sig. (2-tailed)	0.774		0.377	0.102	0.494	0.744	0.852	0.803	0.543	0.349	0.571	0.961
	N	13	13	13	13	13	13	13	13	4	13	13	13
Ce	Pearson Correlation	-0.14	0.267	1	-0.351	-0.024	.773**	.568*	0.144	0.703	0.083	.883**	0.071
	Sig. (2-tailed)	0.647	0.377		0.239	0.937	0.002	0.043	0.64	0.297	0.789	0	0.817
	N	13	13	13	13	13	13	13	13	4	13	13	13
Cs	Pearson Correlation	-0.203	-0.474	-0.351	1	-.743**	0.057	-0.147	-0.54	-0.307	0.449	-0.3	.575*
	Sig. (2-tailed)	0.505	0.102	0.239		0.004	0.852	0.631	0.057	0.693	0.124	0.32	0.04
	N	13	13	13	13	13	13	13	13	4	13	13	13
Cu	Pearson Correlation	0.264	0.209	-0.024	-.743**	1	-0.436	0.049	0.499	.c	-0.393	-0.102	-0.493
	Sig. (2-tailed)	0.383	0.494	0.937	0.004		0.137	0.875	0.083	0	0.184	0.74	0.087
	N	13	13	13	13	13	13	13	13	4	13	13	13
Dy	Pearson Correlation	-0.434	0.101	.773**	0.057	-0.436	1	.672*	-0.103	0.737	0.486	.883**	.566*
	Sig. (2-tailed)	0.139	0.744	0.002	0.852	0.137		0.012	0.738	0.263	0.093	0	0.044
	N	13	13	13	13	13	13	13	13	4	13	13	13
Er	Pearson Correlation	-0.491	-0.058	.568*	-0.147	0.049	.672*	1	0.523	0.768	0.265	.611*	0.306
	Sig. (2-tailed)	0.088	0.852	0.043	0.631	0.875	0.012		0.067	0.232	0.382	0.026	0.309
	N	13	13	13	13	13	13	13	13	4	13	13	13
Eu	Pearson Correlation	-0.052	-0.077	0.144	-0.54	0.499	-0.103	0.523	1	0.626	-0.523	0.084	-.568*
	Sig. (2-tailed)	0.865	0.803	0.64	0.057	0.083	0.738	0.067		0.374	0.067	0.785	0.043
	N	13	13	13	13	13	13	13	13	4	13	13	13
F	Pearson Correlation	-0.461	-0.457	0.703	-0.307	.c	0.737	0.768	0.626	1	-0.913	0.684	0.875
	Sig. (2-tailed)	0.539	0.543	0.297	0.693	0	0.263	0.232	0.374		0.087	0.316	0.125
	N	4	4	4	4	4	4	4	4	4	4	4	4
Ga	Pearson Correlation	-0.322	0.283	0.083	0.449	-0.393	0.486	0.265	-0.523	-0.913	1	0.212	.925**
	Sig. (2-tailed)	0.283	0.349	0.789	0.124	0.184	0.093	0.382	0.067	0.087		0.488	0
	N	13	13	13	13	13	13	13	13	4	13	13	13
Gd	Pearson Correlation	-0.115	0.174	.883**	-0.3	-0.102	.883**	.611*	0.084	0.684	0.212	1	0.272
	Sig. (2-tailed)	0.708	0.571	0	0.32	0.74	0	0.026	0.785	0.316	0.488		0.368
	N	13	13	13	13	13	13	13	13	4	13	13	13
Hf	Pearson Correlation	-0.382	-0.015	0.071	.575*	-0.493	.566*	0.306	-.568*	0.875	.925**	0.272	1
	Sig. (2-tailed)	0.198	0.961	0.817	0.04	0.087	0.044	0.309	0.043	0.125	0	0.368	
	N	13	13	13	13	13	13	13	13	4	13	13	13
Ho	Pearson Correlation	-0.096	-0.179	0.076	-0.408	0.466	-0.072	.622*	.968**	0.764	-0.372	0.065	-0.389
	Sig. (2-tailed)	0.755	0.558	0.805	0.166	0.108	0.816	0.023	0	0.236	0.211	0.833	0.189
	N	13	13	13	13	13	13	13	13	4	13	13	13
La	Pearson Correlation	0.234	0.066	.850**	-0.376	0.184	0.443	0.392	0.296	0.659	-0.224	.704**	-0.24
	Sig. (2-tailed)	0.441	0.831	0	0.206	0.547	0.129	0.185	0.326	0.341	0.462	0.007	0.43
	N	13	13	13	13	13	13	13	13	4	13	13	13
Lu	Pearson Correlation	-.564*	0.08	.623*	0.113	-0.215	.828**	.751**	-0.091	0.752	.657*	.631*	.691**
	Sig. (2-tailed)	0.045	0.795	0.023	0.712	0.48	0	0.003	0.768	0.248	0.015	0.021	0.009
	N	13	13	13	13	13	13	13	13	4	13	13	13

Correlation Coefficients: Round Top

Correlations		Ho	La	Lu	Mo	Nb	Nd	Pr	Rb	Sm	Sn	Sr
Ba	Pearson Correlation	-0.096	0.234	-.564*	-0.052	-0.229	-0.062	-0.04	0.152	-0.137	-0.273	0.083
	Sig. (2-tailed)	0.755	0.441	0.045	0.867	0.452	0.84	0.897	0.621	0.656	0.368	0.787
	N	13	13	13	13	13	13	13	13	13	13	13
Be	Pearson Correlation	-0.179	0.066	0.08	-0.149	0.228	-0.177	0.053	-0.229	0.233	-0.019	-0.152
	Sig. (2-tailed)	0.558	0.831	0.795	0.628	0.454	0.563	0.863	0.453	0.445	0.952	0.619
	N	13	13	13	13	13	13	13	13	13	13	13
Ce	Pearson Correlation	0.076	.850**	.623*	0.055	-0.023	0.1	.886**	-0.28	.937**	0.004	0.317
	Sig. (2-tailed)	0.805	0	0.023	0.858	0.941	0.745	0	0.354	0	0.989	0.292
	N	13	13	13	13	13	13	13	13	13	13	13
Cs	Pearson Correlation	-0.408	-0.376	0.113	-0.446	.570*	-0.436	-0.403	0.544	-0.346	.593*	-0.099
	Sig. (2-tailed)	0.166	0.206	0.712	0.126	0.042	0.136	0.172	0.054	0.248	0.033	0.747
	N	13	13	13	13	13	13	13	13	13	13	13
Cu	Pearson Correlation	0.466	0.184	-0.215	0.508	-.572*	0.483	0.108	-0.118	-0.1	-0.429	0.075
	Sig. (2-tailed)	0.108	0.547	0.48	0.076	0.041	0.094	0.724	0.701	0.744	0.143	0.807
	N	13	13	13	13	13	13	13	13	13	13	13
Dy	Pearson Correlation	-0.072	0.443	.828**	-0.141	0.446	-0.075	.737**	0.017	.860**	0.421	0.128
	Sig. (2-tailed)	0.816	0.129	0	0.645	0.127	0.808	0.004	0.955	0	0.152	0.677
	N	13	13	13	13	13	13	13	13	13	13	13
Er	Pearson Correlation	.622*	0.392	.751**	.555*	0.059	.609*	.648*	-0.043	0.542	0.344	-0.022
	Sig. (2-tailed)	0.023	0.185	0.003	0.049	0.848	0.027	0.017	0.89	0.056	0.249	0.944
	N	13	13	13	13	13	13	13	13	13	13	13
Eu	Pearson Correlation	.968**	0.296	-0.091	.970**	-.682*	.975**	0.24	-.564*	0.053	-0.38	-0.076
	Sig. (2-tailed)	0	0.326	0.768	0	0.01	0	0.429	0.045	0.863	0.2	0.806
	N	13	13	13	13	13	13	13	13	13	13	13
F	Pearson Correlation	0.764	0.659	0.752	.c	0.208	0.69	0.694	-0.303	0.687	0.889	.999**
	Sig. (2-tailed)	0.236	0.341	0.248	0	0.792	0.31	0.306	0.697	0.313	0.111	0.001
	N	4	4	4	4	4	4	4	4	4	4	4
Ga	Pearson Correlation	-0.372	-0.224	.657*	-0.412	.928**	-0.406	-0.011	.633*	0.125	.894**	-0.22
	Sig. (2-tailed)	0.211	0.462	0.015	0.161	0	0.169	0.972	0.02	0.684	0	0.471
	N	13	13	13	13	13	13	13	13	13	13	13
Gd	Pearson Correlation	0.065	.704**	.631*	0.015	0.174	0.084	.920**	-0.096	.974**	0.173	0.318
	Sig. (2-tailed)	0.833	0.007	0.021	0.961	0.569	0.786	0	0.755	0	0.573	0.289
	N	13	13	13	13	13	13	13	13	13	13	13
Hf	Pearson Correlation	-0.389	-0.24	.691**	-0.441	.904**	-0.422	0.066	.702**	0.167	.908**	-0.065
	Sig. (2-tailed)	0.189	0.43	0.009	0.131	0	0.151	0.83	0.007	0.586	0	0.833
	N	13	13	13	13	13	13	13	13	13	13	13
Ho	Pearson Correlation	1	0.218	0.013	.989**	-0.552	.999**	0.222	-0.363	-0.006	-0.178	-0.1
	Sig. (2-tailed)		0.473	0.966	0	0.051	0	0.467	0.223	0.986	0.561	0.746
	N	13	13	13	13	13	13	13	13	13	13	13
La	Pearson Correlation	0.218	1	0.267	0.198	-0.291	0.258	.836**	-0.227	.752**	-0.179	0.444
	Sig. (2-tailed)	0.473		0.377	0.517	0.334	0.395	0	0.457	0.003	0.558	0.129
	N	13	13	13	13	13	13	13	13	13	13	13
Lu	Pearson Correlation	0.013	0.267	1	-0.036	0.451	-0.006	0.541	0.209	.602*	.582*	-0.033
	Sig. (2-tailed)	0.966	0.377		0.907	0.122	0.983	0.056	0.493	0.029	0.037	0.915
	N	13	13	13	13	13	13	13	13	13	13	13

Correlation Coefficients: Round Top

Correlations		Ta	Tb	Th	Tl	Tm	U	Y	Yb	Zn	Zr
Ba	Pearson Correlation	-0.5	-0.168	-0.272	0.043	-0.116	-0.452	-0.326	-0.527	-0.464	-0.138
	Sig. (2-tailed)	0.082	0.584	0.368	0.889	0.707	0.121	0.277	0.064	0.11	0.653
	N	13	13	13	13	13	13	13	13	13	13
Be	Pearson Correlation	-0.155	-0.131	0.243	-0.215	-0.174	-0.045	0.271	0.1	0.452	0.027
	Sig. (2-tailed)	0.614	0.669	0.424	0.482	0.569	0.884	0.371	0.745	0.121	0.93
	N	13	13	13	13	13	13	13	13	13	13
Ce	Pearson Correlation	0.236	0.273	0.155	0.042	0.087	0.283	.663*	0.497	0.361	-0.089
	Sig. (2-tailed)	0.437	0.366	0.614	0.893	0.777	0.349	0.014	0.084	0.226	0.773
	N	13	13	13	13	13	13	13	13	13	13
Cs	Pearson Correlation	0.473	-0.443	0.428	-0.307	-0.4	0.109	0.099	0.219	0.016	.603*
	Sig. (2-tailed)	0.103	0.13	0.145	0.307	0.175	0.722	0.747	0.473	0.96	0.029
	N	13	13	13	13	13	13	13	13	13	13
Cu	Pearson Correlation	-0.421	0.398	-0.317	0.472	0.459	-0.42	-0.318	-0.238	-0.407	-0.432
	Sig. (2-tailed)	0.152	0.179	0.291	0.103	0.115	0.153	0.29	0.434	0.167	0.14
	N	13	13	13	13	13	13	13	13	13	13
Dy	Pearson Correlation	.619*	0.153	0.47	-0.051	-0.054	0.375	.886**	.756**	0.409	0.347
	Sig. (2-tailed)	0.024	0.617	0.105	0.868	0.86	0.206	0	0.003	0.165	0.246
	N	13	13	13	13	13	13	13	13	13	13
Er	Pearson Correlation	0.514	.753**	0.188	.635*	.640*	0.163	.569*	.573*	0.013	0.017
	Sig. (2-tailed)	0.072	0.003	0.538	0.02	0.018	0.594	0.043	0.041	0.967	0.957
	N	13	13	13	13	13	13	13	13	13	13
Eu	Pearson Correlation	-0.243	.945**	-.661*	.848**	.964**	-0.014	-0.31	-0.358	-0.243	-.741**
	Sig. (2-tailed)	0.424	0	0.014	0	0	0.965	0.302	0.23	0.423	0.004
	N	13	13	13	13	13	13	13	13	13	13
F	Pearson Correlation	0.763	0.717	0.637	0.487	0.783	0.088	0.751	0.808	-.964*	0.931
	Sig. (2-tailed)	0.237	0.283	0.363	0.513	0.217	0.912	0.249	0.192	0.036	0.069
	N	4	4	4	4	4	4	4	4	4	4
Ga	Pearson Correlation	.745**	-0.288	.910**	-0.188	-0.351	-0.021	.705**	.754**	0.226	.879**
	Sig. (2-tailed)	0.003	0.34	0	0.539	0.239	0.946	0.007	0.003	0.457	0
	N	13	13	13	13	13	13	13	13	13	13
Gd	Pearson Correlation	0.323	0.288	0.243	0.105	0.073	0.2	.779**	0.539	0.215	0.112
	Sig. (2-tailed)	0.281	0.34	0.424	0.733	0.812	0.513	0.002	0.057	0.48	0.717
	N	13	13	13	13	13	13	13	13	13	13
Hf	Pearson Correlation	.823**	-0.29	.895**	-0.203	-0.37	0.088	.725**	.812**	0.128	.925**
	Sig. (2-tailed)	0.001	0.337	0	0.505	0.213	0.775	0.005	0.001	0.677	0
	N	13	13	13	13	13	13	13	13	13	13
Ho	Pearson Correlation	-0.092	.972**	-0.517	.940**	1.000**	-0.063	-0.233	-0.233	-0.347	-.576*
	Sig. (2-tailed)	0.764	0	0.07	0	0	0.839	0.443	0.443	0.245	0.039
	N	13	13	13	13	13	13	13	13	13	13
La	Pearson Correlation	-0.093	0.344	-0.106	0.239	0.219	-0.048	0.368	0.144	-0.003	-0.282
	Sig. (2-tailed)	0.762	0.25	0.73	0.431	0.472	0.877	0.217	0.64	0.991	0.35
	N	13	13	13	13	13	13	13	13	13	13
Lu	Pearson Correlation	.840**	0.186	.619*	0.061	0.038	0.332	.803**	.939**	0.377	0.436
	Sig. (2-tailed)	0	0.543	0.024	0.844	0.903	0.268	0.001	0	0.204	0.136
	N	13	13	13	13	13	13	13	13	13	13

Correlation Coefficients: Round Top

Correlations		SiO2	Al2O3	Fe2O3	CaO	Na2O	K2O	P2O5	SrO	BaO
Ba	Pearson Correlation	-0.035	-0.066	0.227	0.294	-.565*	0.118	-0.061	0.041	.938**
	Sig. (2-tailed)	0.91	0.83	0.456	0.329	0.044	0.701	0.843	0.894	0
	N	13	13	13	13	13	13	13	13	13
Be	Pearson Correlation	0.313	-0.087	0.073	-0.128	0.357	-0.134	-0.189	-0.254	-0.189
	Sig. (2-tailed)	0.298	0.777	0.813	0.676	0.231	0.663	0.537	0.402	0.537
	N	13	13	13	13	13	13	13	13	13
Ce	Pearson Correlation	-0.075	0.012	0.144	-0.045	0.193	-0.133	0.028	0.177	-0.142
	Sig. (2-tailed)	0.809	0.97	0.638	0.885	0.527	0.664	0.928	0.563	0.643
	N	13	13	13	13	13	13	13	13	13
Cs	Pearson Correlation	0.486	.629*	-.770**	-0.404	0.4	.640*	-0.409	-0.016	-0.022
	Sig. (2-tailed)	0.092	0.021	0.002	0.171	0.176	0.019	0.165	0.958	0.943
	N	13	13	13	13	13	13	13	13	13
Cu	Pearson Correlation	-0.46	-.583*	.613*	0.19	-.690**	-0.301	0.487	0.068	0.213
	Sig. (2-tailed)	0.114	0.036	0.026	0.534	0.009	0.317	0.092	0.824	0.485
	N	13	13	13	13	13	13	13	13	13
Dy	Pearson Correlation	0.214	0.393	-0.288	-0.4	.572*	0.11	-0.134	0.037	-0.413
	Sig. (2-tailed)	0.482	0.184	0.34	0.175	0.041	0.721	0.663	0.903	0.161
	N	13	13	13	13	13	13	13	13	13
Er	Pearson Correlation	-0.357	-0.129	0.108	-0.437	0.075	-0.179	.572*	-0.064	-0.43
	Sig. (2-tailed)	0.232	0.674	0.724	0.136	0.807	0.558	0.041	0.835	0.143
	N	13	13	13	13	13	13	13	13	13
Eu	Pearson Correlation	-.906**	-.846**	.832**	0.242	-.596*	-.743**	.969**	-0.073	-0.145
	Sig. (2-tailed)	0	0	0	0.425	0.031	0.004	0	0.812	0.637
	N	13	13	13	13	13	13	13	13	13
F	Pearson Correlation	-0.904	-0.037	0.447	-0.17	0.527	-0.759	.c	.986*	-0.233
	Sig. (2-tailed)	0.096	0.963	0.553	0.83	0.473	0.241	0	0.014	0.767
	N	4	4	4	4	4	4	4	4	4
Ga	Pearson Correlation	.747**	.744**	-.813**	-.910**	.718**	.654*	-0.406	-0.253	-0.206
	Sig. (2-tailed)	0.003	0.004	0.001	0	0.006	0.015	0.168	0.404	0.5
	N	13	13	13	13	13	13	13	13	13
Gd	Pearson Correlation	-0.002	0.149	0.051	-0.178	0.225	-0.063	0.012	0.201	-0.142
	Sig. (2-tailed)	0.995	0.627	0.868	0.562	0.461	0.839	0.969	0.51	0.643
	N	13	13	13	13	13	13	13	13	13
Hf	Pearson Correlation	.687**	.804**	-.876**	-.837**	.691**	.674*	-0.427	-0.071	-0.231
	Sig. (2-tailed)	0.01	0.001	0	0	0.009	0.012	0.146	0.819	0.448
	N	13	13	13	13	13	13	13	13	13
Ho	Pearson Correlation	-.865**	-.740**	.691**	0.06	-.576*	-.607*	.998**	-0.081	-0.134
	Sig. (2-tailed)	0	0.004	0.009	0.846	0.039	0.028	0	0.794	0.662
	N	13	13	13	13	13	13	13	13	13
La	Pearson Correlation	-0.301	-0.175	0.383	0.138	-0.275	-0.126	0.193	0.333	0.261
	Sig. (2-tailed)	0.317	0.568	0.196	0.653	0.364	0.682	0.528	0.267	0.389
	N	13	13	13	13	13	13	13	13	13
Lu	Pearson Correlation	0.246	0.448	-0.423	-.638*	0.546	0.284	-0.046	-0.097	-0.478
	Sig. (2-tailed)	0.419	0.125	0.15	0.019	0.054	0.348	0.881	0.751	0.099
	N	13	13	13	13	13	13	13	13	13

Correlation Coefficients: Round Top

Correlations		Ba	Be	Ce	Cs	Cu	Dy	Er	Eu	F	Ga	Gd	Hf
Mo	Pearson Correlation	-0.052	-0.149	0.055	-0.446	0.508	-0.141	.555*	.970**	.c	-0.412	0.015	-0.441
	Sig. (2-tailed)	0.867	0.628	0.858	0.126	0.076	0.645	0.049	0	0	0.161	0.961	0.131
	N	13	13	13	13	13	13	13	13	4	13	13	13
Nb	Pearson Correlation	-0.229	0.228	-0.023	.570*	-.572*	0.446	0.059	-.682*	0.208	.928**	0.174	.904**
	Sig. (2-tailed)	0.452	0.454	0.941	0.042	0.041	0.127	0.848	0.01	0.792	0	0.569	0
	N	13	13	13	13	13	13	13	13	4	13	13	13
Nd	Pearson Correlation	-0.062	-0.177	0.1	-0.436	0.483	-0.075	.609*	.975**	0.69	-0.406	0.084	-0.422
	Sig. (2-tailed)	0.84	0.563	0.745	0.136	0.094	0.808	0.027	0	0.31	0.169	0.786	0.151
	N	13	13	13	13	13	13	13	13	4	13	13	13
Pr	Pearson Correlation	-0.04	0.053	.886**	-0.403	0.108	.737**	.648*	0.24	0.694	-0.011	.920**	0.066
	Sig. (2-tailed)	0.897	0.863	0	0.172	0.724	0.004	0.017	0.429	0.306	0.972	0	0.83
	N	13	13	13	13	13	13	13	13	4	13	13	13
Rb	Pearson Correlation	0.152	-0.229	-0.28	0.544	-0.118	0.017	-0.043	-.564*	-0.303	.633*	-0.096	.702**
	Sig. (2-tailed)	0.621	0.453	0.354	0.054	0.701	0.955	0.89	0.045	0.697	0.02	0.755	0.007
	N	13	13	13	13	13	13	13	13	4	13	13	13
Sm	Pearson Correlation	-0.137	0.233	.937**	-0.346	-0.1	.860**	0.542	0.053	0.687	0.125	.974**	0.167
	Sig. (2-tailed)	0.656	0.445	0	0.248	0.744	0	0.056	0.863	0.313	0.684	0	0.586
	N	13	13	13	13	13	13	13	13	4	13	13	13
Sn	Pearson Correlation	-0.273	-0.019	0.004	.593*	-0.429	0.421	0.344	-0.38	0.889	.894**	0.173	.908**
	Sig. (2-tailed)	0.368	0.952	0.989	0.033	0.143	0.152	0.249	0.2	0.111	0	0.573	0
	N	13	13	13	13	13	13	13	13	4	13	13	13
Sr	Pearson Correlation	0.083	-0.152	0.317	-0.099	0.075	0.128	-0.022	-0.076	.999**	-0.22	0.318	-0.065
	Sig. (2-tailed)	0.787	0.619	0.292	0.747	0.807	0.677	0.944	0.806	0.001	0.471	0.289	0.833
	N	13	13	13	13	13	13	13	13	4	13	13	13
Ta	Pearson Correlation	-0.5	-0.155	0.236	0.473	-0.421	.619*	0.514	-0.243	0.763	.745**	0.323	.823**
	Sig. (2-tailed)	0.082	0.614	0.437	0.103	0.152	0.024	0.072	0.424	0.237	0.003	0.281	0.001
	N	13	13	13	13	13	13	13	13	4	13	13	13
Tb	Pearson Correlation	-0.168	-0.131	0.273	-0.443	0.398	0.153	.753**	.945**	0.717	-0.288	0.288	-0.29
	Sig. (2-tailed)	0.584	0.669	0.366	0.13	0.179	0.617	0.003	0	0.283	0.34	0.34	0.337
	N	13	13	13	13	13	13	13	13	4	13	13	13
Th	Pearson Correlation	-0.272	0.243	0.155	0.428	-0.317	0.47	0.188	-.661*	0.637	.910**	0.243	.895**
	Sig. (2-tailed)	0.368	0.424	0.614	0.145	0.291	0.105	0.538	0.014	0.363	0	0.424	0
	N	13	13	13	13	13	13	13	13	4	13	13	13
Tl	Pearson Correlation	0.043	-0.215	0.042	-0.307	0.472	-0.051	.635*	.848**	0.487	-0.188	0.105	-0.203
	Sig. (2-tailed)	0.889	0.482	0.893	0.307	0.103	0.868	0.02	0	0.513	0.539	0.733	0.505
	N	13	13	13	13	13	13	13	13	4	13	13	13
Tm	Pearson Correlation	-0.116	-0.174	0.087	-0.4	0.459	-0.054	.640*	.964**	0.783	-0.351	0.073	-0.37
	Sig. (2-tailed)	0.707	0.569	0.777	0.175	0.115	0.86	0.018	0	0.217	0.239	0.812	0.213
	N	13	13	13	13	13	13	13	13	4	13	13	13

Correlation Coefficients: Round Top

Correlations		La	Lu	Mo	Nb	Nd	Pr	Rb	Sm	Sn	Sr
Mo	Pearson Correlation	0.198	-0.036	1	-.602*	.989**	0.163	-0.412	-0.051	-0.225	-0.104
	Sig. (2-tailed)	0.517	0.907		0.029	0	0.594	0.162	0.868	0.46	0.736
	N	13	13	13	13	13	13	13	13	13	13
Nb	Pearson Correlation	-0.291	0.451	-.602*	1	-.580*	-0.071	.666*	0.091	.846**	-0.133
	Sig. (2-tailed)	0.334	0.122	0.029		0.038	0.818	0.013	0.766	0	0.665
	N	13	13	13	13	13	13	13	13	13	13
Nd	Pearson Correlation	0.258	-0.006	.989**	-.580*	1	0.249	-0.38	0.018	-0.21	-0.071
	Sig. (2-tailed)	0.395	0.983	0	0.038		0.412	0.2	0.954	0.491	0.819
	N	13	13	13	13	13	13	13	13	13	13
Pr	Pearson Correlation	.836**	0.541	0.163	-0.071	0.249	1	-0.104	.927**	0.001	0.402
	Sig. (2-tailed)	0	0.056	0.594	0.818	0.412		0.735	0	0.997	0.174
	N	13	13	13	13	13	13	13	13	13	13
Rb	Pearson Correlation	-0.227	0.209	-0.412	.666*	-0.38	-0.104	1	-0.205	.719**	0.043
	Sig. (2-tailed)	0.457	0.493	0.162	0.013	0.2	0.735		0.502	0.006	0.89
	N	13	13	13	13	13	13	13	13	13	13
Sm	Pearson Correlation	.752**	.602*	-0.051	0.091	0.018	.927**	-0.205	1	0.034	0.315
	Sig. (2-tailed)	0.003	0.029	0.868	0.766	0.954	0	0.502		0.913	0.294
	N	13	13	13	13	13	13	13	13	13	13
Sn	Pearson Correlation	-0.179	.582*	-0.225	.846**	-0.21	0.001	.719**	0.034	1	-0.008
	Sig. (2-tailed)	0.558	0.037	0.46	0	0.491	0.997	0.006	0.913		0.979
	N	13	13	13	13	13	13	13	13	13	13
Sr	Pearson Correlation	0.444	-0.033	-0.104	-0.133	-0.071	0.402	0.043	0.315	-0.008	1
	Sig. (2-tailed)	0.129	0.915	0.736	0.665	0.819	0.174	0.89	0.294	0.979	
	N	13	13	13	13	13	13	13	13	13	13
Ta	Pearson Correlation	-0.093	.840**	-0.115	.581*	-0.126	0.126	0.365	0.234	.749**	-0.184
	Sig. (2-tailed)	0.762	0	0.707	0.037	0.681	0.681	0.22	0.442	0.003	0.548
	N	13	13	13	13	13	13	13	13	13	13
Tb	Pearson Correlation	0.344	0.186	.950**	-0.476	.973**	0.409	-0.387	0.216	-0.119	-0.05
	Sig. (2-tailed)	0.25	0.543	0	0.1	0	0.166	0.192	0.478	0.698	0.871
	N	13	13	13	13	13	13	13	13	13	13
Th	Pearson Correlation	-0.106	.619*	-.566*	.892**	-0.541	0.118	.742**	0.197	.803**	-0.001
	Sig. (2-tailed)	0.73	0.024	0.044	0	0.056	0.701	0.004	0.52	0.001	0.998
	N	13	13	13	13	13	13	13	13	13	13
Tl	Pearson Correlation	0.239	0.061	.912**	-0.359	.938**	0.26	-0.056	-0.013	0.054	-0.043
	Sig. (2-tailed)	0.431	0.844	0	0.228	0	0.39	0.856	0.967	0.861	0.89
	N	13	13	13	13	13	13	13	13	13	13
Tm	Pearson Correlation	0.219	0.038	.987**	-0.537	.997**	0.228	-0.357	0.003	-0.16	-0.105
	Sig. (2-tailed)	0.472	0.903	0	0.058	0	0.455	0.231	0.993	0.601	0.733
	N	13	13	13	13	13	13	13	13	13	13

Correlation Coefficients: Round Top

Correlations		Ta	Tb	Th	Tl	Tm	U	Y	Yb	Zn	Zr
Mo	Pearson Correlation	-0.115	.950**	-.566*	.912**	.987**	-0.017	-0.308	-0.29	-0.33	-.624*
	Sig. (2-tailed)	0.707	0	0.044	0	0	0.955	0.306	0.336	0.271	0.023
	N	13	13	13	13	13	13	13	13	13	13
Nb	Pearson Correlation	.581*	-0.476	.892**	-0.359	-0.537	-0.048	.676*	.612*	0.18	.936**
	Sig. (2-tailed)	0.037	0.1	0	0.228	0.058	0.876	0.011	0.026	0.555	0
	N	13	13	13	13	13	13	13	13	13	13
Nd	Pearson Correlation	-0.126	.973**	-0.541	.938**	.997**	-0.072	-0.239	-0.253	-0.355	-.602*
	Sig. (2-tailed)	0.681	0	0.056	0	0	0.815	0.432	0.403	0.234	0.029
	N	13	13	13	13	13	13	13	13	13	13
Pr	Pearson Correlation	0.126	0.409	0.118	0.26	0.228	0.064	.661*	0.458	0.04	-0.065
	Sig. (2-tailed)	0.681	0.166	0.701	0.39	0.455	0.836	0.014	0.115	0.896	0.832
	N	13	13	13	13	13	13	13	13	13	13
Rb	Pearson Correlation	0.365	-0.387	.742**	-0.056	-0.357	-0.453	0.357	0.441	-0.418	.848**
	Sig. (2-tailed)	0.22	0.192	0.004	0.856	0.231	0.12	0.231	0.132	0.155	0
	N	13	13	13	13	13	13	13	13	13	13
Sm	Pearson Correlation	0.234	0.216	0.197	-0.013	0.003	0.256	.742**	0.517	0.338	0.017
	Sig. (2-tailed)	0.442	0.478	0.52	0.967	0.993	0.399	0.004	0.07	0.259	0.957
	N	13	13	13	13	13	13	13	13	13	13
Sn	Pearson Correlation	.749**	-0.119	.803**	0.054	-0.16	-0.078	.610*	.658*	-0.04	.848**
	Sig. (2-tailed)	0.003	0.698	0.001	0.861	0.601	0.8	0.027	0.015	0.896	0
	N	13	13	13	13	13	13	13	13	13	13
Sr	Pearson Correlation	-0.184	-0.05	-0.001	-0.043	-0.105	-0.238	0.16	0.046	-0.34	0.018
	Sig. (2-tailed)	0.548	0.871	0.998	0.89	0.733	0.433	0.602	0.88	0.256	0.955
	N	13	13	13	13	13	13	13	13	13	13
Ta	Pearson Correlation	1	0.024	.594*	-0.018	-0.071	0.409	.564*	.787**	0.312	.586*
	Sig. (2-tailed)		0.939	0.032	0.953	0.818	0.165	0.045	0.001	0.3	0.036
	N	13	13	13	13	13	13	13	13	13	13
Tb	Pearson Correlation	0.024	1	-0.434	.912**	.975**	0.027	-0.039	-0.077	-0.243	-0.523
	Sig. (2-tailed)	0.939		0.139	0	0	0.931	0.898	0.801	0.425	0.067
	N	13	13	13	13	13	13	13	13	13	13
Th	Pearson Correlation	.594*	-0.434	1	-0.313	-0.499	-0.111	.775**	.813**	0.122	.926**
	Sig. (2-tailed)	0.032	0.139		0.298	0.083	0.718	0.002	0.001	0.691	0
	N	13	13	13	13	13	13	13	13	13	13
Tl	Pearson Correlation	-0.018	.912**	-0.313	1	.940**	-0.271	-0.1	-0.13	-0.526	-0.337
	Sig. (2-tailed)	0.953	0	0.298		0	0.371	0.744	0.673	0.065	0.26
	N	13	13	13	13	13	13	13	13	13	13
Tm	Pearson Correlation	-0.071	.975**	-0.499	.940**	1	-0.056	-0.214	-0.21	-0.337	-.563*
	Sig. (2-tailed)	0.818	0	0.083	0		0.856	0.482	0.492	0.261	0.045
	N	13	13	13	13	13	13	13	13	13	13

Correlation Coefficients: Round Top

Correlations		SiO2	Al2O3	Fe2O3	CaO	Na2O	K2O	P2O5	SrO	BaO
Mo	Pearson Correlation	-.868**	-.781**	.717**	0.112	-.594*	-.647*	.991**	-0.09	-0.106
	Sig. (2-tailed)	0	0.002	0.006	0.716	0.032	0.017	0	0.77	0.729
	N	13	13	13	13	13	13	13	13	13
Nb	Pearson Correlation	.832**	.795**	-.868**	-.774**	.748**	.681*	-.579*	-0.152	-0.111
	Sig. (2-tailed)	0	0.001	0	0.002	0.003	0.01	0.038	0.619	0.718
	N	13	13	13	13	13	13	13	13	13
Nd	Pearson Correlation	-.881**	-.756**	.721**	0.095	-.603*	-.621*	.997**	-0.056	-0.104
	Sig. (2-tailed)	0	0.003	0.005	0.758	0.029	0.024	0	0.857	0.736
	N	13	13	13	13	13	13	13	13	13
Pr	Pearson Correlation	-0.241	-0.037	0.237	-0.022	-0.053	-0.118	0.176	0.298	-0.018
	Sig. (2-tailed)	0.427	0.904	0.436	0.944	0.864	0.702	0.565	0.322	0.953
	N	13	13	13	13	13	13	13	13	13
Rb	Pearson Correlation	0.55	.676*	-.721**	-.655*	0.108	.860**	-0.366	0.084	0.373
	Sig. (2-tailed)	0.052	0.011	0.005	0.015	0.725	0	0.219	0.785	0.209
	N	13	13	13	13	13	13	13	13	13
Sm	Pearson Correlation	-0.003	0.118	0.094	-0.048	0.247	-0.096	-0.057	0.19	-0.175
	Sig. (2-tailed)	0.992	0.701	0.761	0.877	0.417	0.755	0.853	0.534	0.568
	N	13	13	13	13	13	13	13	13	13
Sn	Pearson Correlation	0.525	.669*	-.755**	-.898**	0.516	.619*	-0.207	-0.004	-0.076
	Sig. (2-tailed)	0.065	0.012	0.003	0	0.071	0.024	0.497	0.989	0.804
	N	13	13	13	13	13	13	13	13	13
Sr	Pearson Correlation	-0.146	0.001	0.121	0.172	-0.151	-0.114	-0.102	.983**	0.249
	Sig. (2-tailed)	0.633	0.996	0.693	0.574	0.622	0.711	0.74	0	0.411
	N	13	13	13	13	13	13	13	13	13
Ta	Pearson Correlation	0.401	.614*	-.654*	-.731**	.588*	0.447	-0.136	-0.194	-0.423
	Sig. (2-tailed)	0.174	0.026	0.015	0.004	0.034	0.125	0.657	0.525	0.15
	N	13	13	13	13	13	13	13	13	13
Tb	Pearson Correlation	-.819**	-.663*	.656*	0.003	-0.461	-.602*	.957**	-0.056	-0.215
	Sig. (2-tailed)	0.001	0.014	0.015	0.993	0.113	0.03	0	0.855	0.48
	N	13	13	13	13	13	13	13	13	13
Th	Pearson Correlation	.773**	.760**	-.842**	-.788**	.651*	.739**	-0.551	-0.037	-0.083
	Sig. (2-tailed)	0.002	0.003	0	0.001	0.016	0.004	0.051	0.903	0.788
	N	13	13	13	13	13	13	13	13	13
Tl	Pearson Correlation	-.736**	-.560*	0.535	-0.15	-.607*	-0.363	.937**	-0.023	0.067
	Sig. (2-tailed)	0.004	0.047	0.06	0.625	0.028	0.223	0	0.941	0.829
	N	13	13	13	13	13	13	13	13	13
Tm	Pearson Correlation	-.855**	-.729**	.677*	0.039	-.557*	-.600*	.996**	-0.087	-0.15
	Sig. (2-tailed)	0	0.005	0.011	0.898	0.048	0.03	0	0.777	0.624
	N	13	13	13	13	13	13	13	13	13

Correlation Coefficients: Round Top

Correlations		Ba	Be	Ce	Cs	Cu	Dy	Er	Eu	F	Ga	Gd	Hf
U	Pearson Correlation	-0.452	-0.045	0.283	0.109	-0.42	0.375	0.163	-0.014	0.088	-0.021	0.2	0.088
	Sig. (2-tailed)	0.121	0.884	0.349	0.722	0.153	0.206	0.594	0.965	0.912	0.946	0.513	0.775
	N	13	13	13	13	13	13	13	13	4	13	13	13
Y	Pearson Correlation	-0.326	0.271	.663*	0.099	-0.318	.886**	.569*	-0.31	0.751	.705**	.779**	.725**
	Sig. (2-tailed)	0.277	0.371	0.014	0.747	0.29	0	0.043	0.302	0.249	0.007	0.002	0.005
	N	13	13	13	13	13	13	13	13	4	13	13	13
Yb	Pearson Correlation	-0.527	0.1	0.497	0.219	-0.238	.756**	.573*	-0.358	0.808	.754**	0.539	.812**
	Sig. (2-tailed)	0.064	0.745	0.084	0.473	0.434	0.003	0.041	0.23	0.192	0.003	0.057	0.001
	N	13	13	13	13	13	13	13	13	4	13	13	13
Zn	Pearson Correlation	-0.464	0.452	0.361	0.016	-0.407	0.409	0.013	-0.243	-.964*	0.226	0.215	0.128
	Sig. (2-tailed)	0.11	0.121	0.226	0.96	0.167	0.165	0.967	0.423	0.036	0.457	0.48	0.677
	N	13	13	13	13	13	13	13	13	4	13	13	13
Zr	Pearson Correlation	-0.138	0.027	-0.089	.603*	-0.432	0.347	0.017	-.741**	0.931	.879**	0.112	.925**
	Sig. (2-tailed)	0.653	0.93	0.773	0.029	0.14	0.246	0.957	0.004	0.069	0	0.717	0
	N	13	13	13	13	13	13	13	13	4	13	13	13
SiO2	Pearson Correlation	-0.035	0.313	-0.075	0.486	-0.46	0.214	-0.357	-.906**	-0.904	.747**	-0.002	.687**
	Sig. (2-tailed)	0.91	0.298	0.809	0.092	0.114	0.482	0.232	0	0.096	0.003	0.995	0.01
	N	13	13	13	13	13	13	13	13	4	13	13	13
Al2O3	Pearson Correlation	-0.066	-0.087	0.012	.629*	-.583*	0.393	-0.129	-.846**	-0.037	.744**	0.149	.804**
	Sig. (2-tailed)	0.83	0.777	0.97	0.021	0.036	0.184	0.674	0	0.963	0.004	0.627	0.001
	N	13	13	13	13	13	13	13	13	4	13	13	13
Fe2O3	Pearson Correlation	0.227	0.073	0.144	-.770**	.613*	-0.288	0.108	.832**	0.447	-.813**	0.051	-.876**
	Sig. (2-tailed)	0.456	0.813	0.638	0.002	0.026	0.34	0.724	0	0.553	0.001	0.868	0
	N	13	13	13	13	13	13	13	13	4	13	13	13
CaO	Pearson Correlation	0.294	-0.128	-0.045	-0.404	0.19	-0.4	-0.437	0.242	-0.17	-.910**	-0.178	-.837**
	Sig. (2-tailed)	0.329	0.676	0.885	0.171	0.534	0.175	0.136	0.425	0.83	0	0.562	0
	N	13	13	13	13	13	13	13	13	4	13	13	13
Na2O	Pearson Correlation	-.565*	0.357	0.193	0.4	-.690**	.572*	0.075	-.596*	0.527	.718**	0.225	.691**
	Sig. (2-tailed)	0.044	0.231	0.527	0.176	0.009	0.041	0.807	0.031	0.473	0.006	0.461	0.009
	N	13	13	13	13	13	13	13	13	4	13	13	13
K2O	Pearson Correlation	0.118	-0.134	-0.133	.640*	-0.301	0.11	-0.179	-.743**	-0.759	.654*	-0.063	.674*
	Sig. (2-tailed)	0.701	0.663	0.664	0.019	0.317	0.721	0.558	0.004	0.241	0.015	0.839	0.012
	N	13	13	13	13	13	13	13	13	4	13	13	13
P2O5	Pearson Correlation	-0.061	-0.189	0.028	-0.409	0.487	-0.134	.572*	.969**	.c	-0.406	0.012	-0.427
	Sig. (2-tailed)	0.843	0.537	0.928	0.165	0.092	0.663	0.041	0	0	0.168	0.969	0.146
	N	13	13	13	13	13	13	13	13	4	13	13	13
SrO	Pearson Correlation	0.041	-0.254	0.177	-0.016	0.068	0.037	-0.064	-0.073	.986*	-0.253	0.201	-0.071
	Sig. (2-tailed)	0.894	0.402	0.563	0.958	0.824	0.903	0.835	0.812	0.014	0.404	0.51	0.819
	N	13	13	13	13	13	13	13	13	4	13	13	13
BaO	Pearson Correlation	.938**	-0.189	-0.142	-0.022	0.213	-0.413	-0.43	-0.145	-0.233	-0.206	-0.142	-0.231
	Sig. (2-tailed)	0	0.537	0.643	0.943	0.485	0.161	0.143	0.637	0.767	0.5	0.643	0.448
	N	13	13	13	13	13	13	13	13	4	13	13	13

Correlation Coefficients: Round Top

Correlations		Ho	La	Lu	Mo	Nb	Nd	Pr	Rb	Sm	Sn	Sr
U	Pearson Correlation	-0.063	-0.048	0.332	-0.017	-0.048	-0.072	0.064	-0.453	0.256	-0.078	-0.238
	Sig. (2-tailed)	0.839	0.877	0.268	0.955	0.876	0.815	0.836	0.12	0.399	0.8	0.433
	N	13	13	13	13	13	13	13	13	13	13	13
Y	Pearson Correlation	-0.233	0.368	.803**	-0.308	.676*	-0.239	.661*	0.357	.742**	.610*	0.16
	Sig. (2-tailed)	0.443	0.217	0.001	0.306	0.011	0.432	0.014	0.231	0.004	0.027	0.602
	N	13	13	13	13	13	13	13	13	13	13	13
Yb	Pearson Correlation	-0.233	0.144	.939**	-0.29	.612*	-0.253	0.458	0.441	0.517	.658*	0.046
	Sig. (2-tailed)	0.443	0.64	0	0.336	0.026	0.403	0.115	0.132	0.07	0.015	0.88
	N	13	13	13	13	13	13	13	13	13	13	13
Zn	Pearson Correlation	-0.347	-0.003	0.377	-0.33	0.18	-0.355	0.04	-0.418	0.338	-0.04	-0.34
	Sig. (2-tailed)	0.245	0.991	0.204	0.271	0.555	0.234	0.896	0.155	0.259	0.896	0.256
	N	13	13	13	13	13	13	13	13	13	13	13
Zr	Pearson Correlation	-.576*	-0.282	0.436	-.624*	.936**	-.602*	-0.065	.848**	0.017	.848**	0.018
	Sig. (2-tailed)	0.039	0.35	0.136	0.023	0	0.029	0.832	0	0.957	0	0.955
	N	13	13	13	13	13	13	13	13	13	13	13
SiO2	Pearson Correlation	-.865**	-0.301	0.246	-.868**	.832**	-.881**	-0.241	0.55	-0.003	0.525	-0.146
	Sig. (2-tailed)	0	0.317	0.419	0	0	0	0.427	0.052	0.992	0.065	0.633
	N	13	13	13	13	13	13	13	13	13	13	13
Al2O3	Pearson Correlation	-.740**	-0.175	0.448	-.781**	.795**	-.756**	-0.037	.676*	0.118	.669*	0.001
	Sig. (2-tailed)	0.004	0.568	0.125	0.002	0.001	0.003	0.904	0.011	0.701	0.012	0.996
	N	13	13	13	13	13	13	13	13	13	13	13
Fe2O3	Pearson Correlation	.691**	0.383	-0.423	.717**	-.868**	.721**	0.237	-.721**	0.094	-.755**	0.121
	Sig. (2-tailed)	0.009	0.196	0.15	0.006	0	0.005	0.436	0.005	0.761	0.003	0.693
	N	13	13	13	13	13	13	13	13	13	13	13
CaO	Pearson Correlation	0.06	0.138	-.638*	0.112	-.774**	0.095	-0.022	-.655*	-0.048	-.898**	0.172
	Sig. (2-tailed)	0.846	0.653	0.019	0.716	0.002	0.758	0.944	0.015	0.877	0	0.574
	N	13	13	13	13	13	13	13	13	13	13	13
Na2O	Pearson Correlation	-.576*	-0.275	0.546	-.594*	.748**	-.603*	-0.053	0.108	0.247	0.516	-0.151
	Sig. (2-tailed)	0.039	0.364	0.054	0.032	0.003	0.029	0.864	0.725	0.417	0.071	0.622
	N	13	13	13	13	13	13	13	13	13	13	13
K2O	Pearson Correlation	-.607*	-0.126	0.284	-.647*	.681*	-.621*	-0.118	.860**	-0.096	.619*	-0.114
	Sig. (2-tailed)	0.028	0.682	0.348	0.017	0.01	0.024	0.702	0	0.755	0.024	0.711
	N	13	13	13	13	13	13	13	13	13	13	13
P2O5	Pearson Correlation	.998**	0.193	-0.046	.991**	-.579*	.997**	0.176	-0.366	-0.057	-0.207	-0.102
	Sig. (2-tailed)	0	0.528	0.881	0	0.038	0	0.565	0.219	0.853	0.497	0.74
	N	13	13	13	13	13	13	13	13	13	13	13
SrO	Pearson Correlation	-0.081	0.333	-0.097	-0.09	-0.152	-0.056	0.298	0.084	0.19	-0.004	.983**
	Sig. (2-tailed)	0.794	0.267	0.751	0.77	0.619	0.857	0.322	0.785	0.534	0.989	0
	N	13	13	13	13	13	13	13	13	13	13	13
BaO	Pearson Correlation	-0.134	0.261	-0.478	-0.106	-0.111	-0.104	-0.018	0.373	-0.175	-0.076	0.249
	Sig. (2-tailed)	0.662	0.389	0.099	0.729	0.718	0.736	0.953	0.209	0.568	0.804	0.411
	N	13	13	13	13	13	13	13	13	13	13	13

Correlation Coefficients: Round Top

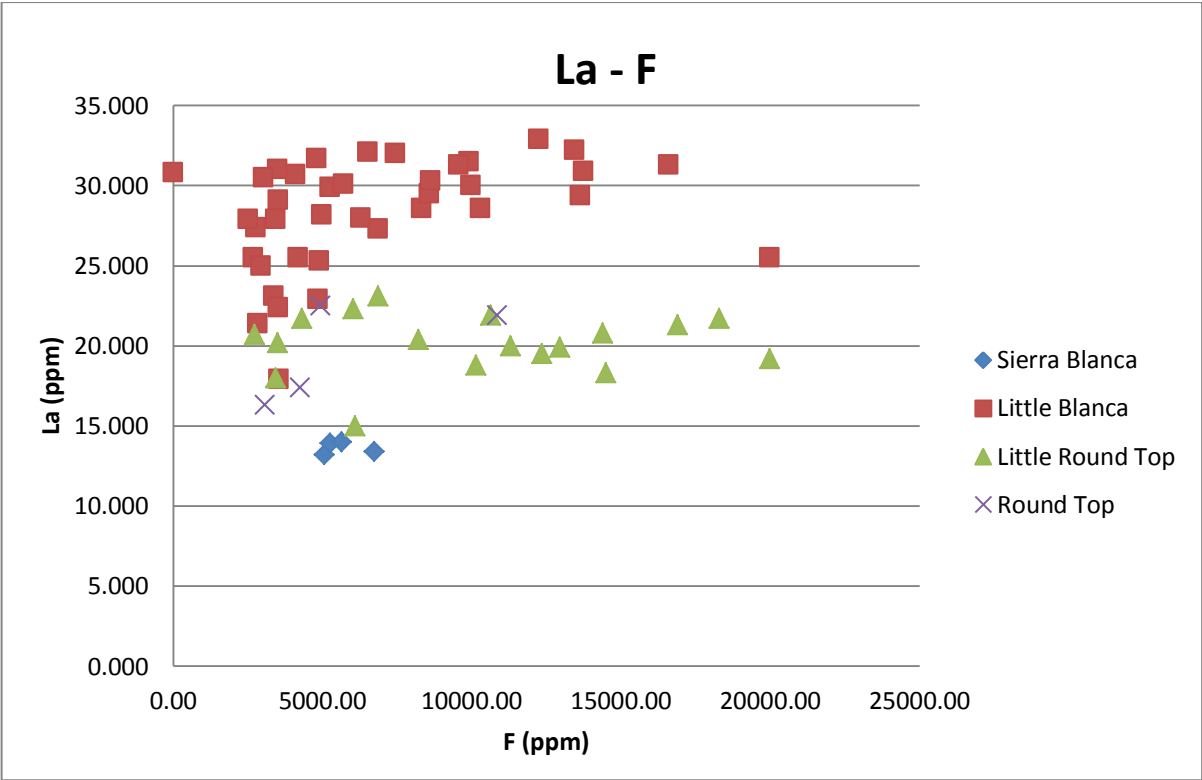
Correlations		Ta	Tb	Th	Tl	Tm	U	Y	Yb	Zn	Zr
U	Pearson Correlation	0.409	0.027	-0.111	-0.271	-0.056	1	0.064	0.202	.722**	-0.176
	Sig. (2-tailed)	0.165	0.931	0.718	0.371	0.856		0.836	0.508	0.005	0.565
	N	13	13	13	13	13	13	13	13	13	13
Y	Pearson Correlation	.564*	-0.039	.775**	-0.1	-0.214	0.064	1	.854**	0.236	.627*
	Sig. (2-tailed)	0.045	0.898	0.002	0.744	0.482	0.836		0	0.437	0.022
	N	13	13	13	13	13	13	13	13	13	13
Yb	Pearson Correlation	.787**	-0.077	.813**	-0.13	-0.21	0.202	.854**	1	0.31	.650*
	Sig. (2-tailed)	0.001	0.801	0.001	0.673	0.492	0.508	0		0.303	0.016
	N	13	13	13	13	13	13	13	13	13	13
Zn	Pearson Correlation	0.312	-0.243	0.122	-0.526	-0.337	.722**	0.236	0.31	1	-0.044
	Sig. (2-tailed)	0.3	0.425	0.691	0.065	0.261	0.005	0.437	0.303		0.886
	N	13	13	13	13	13	13	13	13	13	13
Zr	Pearson Correlation	.586*	-0.523	.926**	-0.337	-.563*	-0.176	.627*	.650*	-0.044	1
	Sig. (2-tailed)	0.036	0.067	0	0.26	0.045	0.565	0.022	0.016	0.886	
	N	13	13	13	13	13	13	13	13	13	13
SiO2	Pearson Correlation	0.401	-.819**	.773**	-.736**	-.855**	-0.007	0.444	0.453	0.33	.815**
	Sig. (2-tailed)	0.174	0.001	0.002	0.004	0	0.982	0.128	0.12	0.27	0.001
	N	13	13	13	13	13	13	13	13	13	13
Al2O3	Pearson Correlation	.614*	-.663*	.760**	-.560*	-.729**	0.023	0.528	.621*	0.24	.845**
	Sig. (2-tailed)	0.026	0.014	0.003	0.047	0.005	0.941	0.064	0.023	0.43	0
	N	13	13	13	13	13	13	13	13	13	13
Fe2O3	Pearson Correlation	-.654*	.656*	-.842**	0.535	.677*	-0.103	-0.478	-.615*	-0.193	-.914**
	Sig. (2-tailed)	0.015	0.015	0	0.06	0.011	0.739	0.099	0.025	0.527	0
	N	13	13	13	13	13	13	13	13	13	13
CaO	Pearson Correlation	-.731**	0.003	-.788**	-0.15	0.039	0.231	-.614*	-.677*	0.062	-.778**
	Sig. (2-tailed)	0.004	0.993	0.001	0.625	0.898	0.447	0.026	0.011	0.84	0.002
	N	13	13	13	13	13	13	13	13	13	13
Na2O	Pearson Correlation	.588*	-0.461	.651*	-.607*	-.557*	0.437	.589*	.613*	.670*	.592*
	Sig. (2-tailed)	0.034	0.113	0.016	0.028	0.048	0.136	0.034	0.026	0.012	0.033
	N	13	13	13	13	13	13	13	13	13	13
K2O	Pearson Correlation	0.447	-.602*	.739**	-0.363	-.600*	-0.209	0.369	0.49	-0.008	.800**
	Sig. (2-tailed)	0.125	0.03	0.004	0.223	0.03	0.492	0.214	0.089	0.979	0.001
	N	13	13	13	13	13	13	13	13	13	13
P2O5	Pearson Correlation	-0.136	.957**	-0.551	.937**	.996**	-0.086	-0.29	-0.287	-0.374	-.598*
	Sig. (2-tailed)	0.657	0	0.051	0	0	0.78	0.337	0.341	0.208	0.031
	N	13	13	13	13	13	13	13	13	13	13
SrO	Pearson Correlation	-0.194	-0.056	-0.037	-0.023	-0.087	-0.254	0.064	-0.003	-0.389	0.017
	Sig. (2-tailed)	0.525	0.855	0.903	0.941	0.777	0.402	0.836	0.992	0.189	0.957
	N	13	13	13	13	13	13	13	13	13	13
BaO	Pearson Correlation	-0.423	-0.215	-0.083	0.067	-0.15	-.570*	-0.218	-0.386	-.603*	0.041
	Sig. (2-tailed)	0.15	0.48	0.788	0.829	0.624	0.042	0.475	0.193	0.029	0.894
	N	13	13	13	13	13	13	13	13	13	13

Correlation Coefficients: Round Top

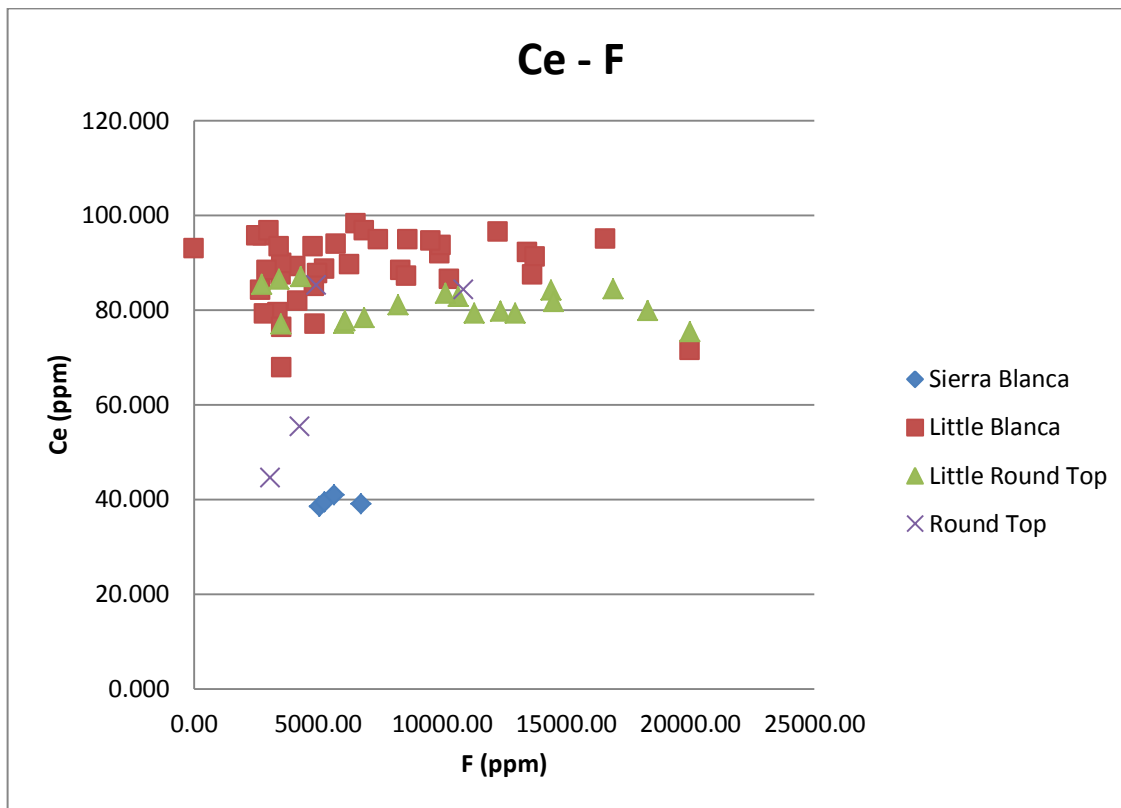
Correlations		SiO2	Al2O3	Fe2O3	CaO	Na2O	K2O	P2O5	SrO	BaO
U	Pearson Correlation	-0.007	0.023	-0.103	0.231	0.437	-0.209	-0.086	-0.254	-.570*
	Sig. (2-tailed)	0.982	0.941	0.739	0.447	0.136	0.492	0.78	0.402	0.042
	N	13	13	13	13	13	13	13	13	13
Y	Pearson Correlation	0.444	0.528	-0.478	-.614*	.589*	0.369	-0.29	0.064	-0.218
	Sig. (2-tailed)	0.128	0.064	0.099	0.026	0.034	0.214	0.337	0.836	0.475
	N	13	13	13	13	13	13	13	13	13
Yb	Pearson Correlation	0.453	.621*	-.615*	-.677*	.613*	0.49	-0.287	-0.003	-0.386
	Sig. (2-tailed)	0.12	0.023	0.025	0.011	0.026	0.089	0.341	0.992	0.193
	N	13	13	13	13	13	13	13	13	13
Zn	Pearson Correlation	0.33	0.24	-0.193	0.062	.670*	-0.008	-0.374	-0.389	-.603*
	Sig. (2-tailed)	0.27	0.43	0.527	0.84	0.012	0.979	0.208	0.189	0.029
	N	13	13	13	13	13	13	13	13	13
Zr	Pearson Correlation	.815**	.845**	-.914**	-.778**	.592*	.800**	-.598*	0.017	0.041
	Sig. (2-tailed)	0.001	0	0	0.002	0.033	0.001	0.031	0.957	0.894
	N	13	13	13	13	13	13	13	13	13
SiO2	Pearson Correlation	1	.835**	-.858**	-0.51	.715**	.744**	-.875**	-0.178	0.016
	Sig. (2-tailed)		0	0	0.075	0.006	0.004	0	0.56	0.958
	N	13	13	13	13	13	13	13	13	13
Al2O3	Pearson Correlation	.835**	1	-.895**	-.561*	.630*	.846**	-.762**	-0.001	0.043
	Sig. (2-tailed)	0		0	0.046	0.021	0	0.002	0.998	0.89
	N	13	13	13	13	13	13	13	13	13
Fe2O3	Pearson Correlation	-.858**	-.895**	1	.642*	-.704**	-.819**	.709**	0.107	0.068
	Sig. (2-tailed)	0	0		0.018	0.007	0.001	0.007	0.727	0.825
	N	13	13	13	13	13	13	13	13	13
CaO	Pearson Correlation	-0.51	-.561*	.642*	1	-0.45	-.571*	0.091	0.188	0.145
	Sig. (2-tailed)	0.075	0.046	0.018		0.122	0.042	0.767	0.538	0.637
	N	13	13	13	13	13	13	13	13	13
Na2O	Pearson Correlation	.715**	.630*	-.704**	-0.45	1	0.29	-.612*	-0.197	-0.542
	Sig. (2-tailed)	0.006	0.021	0.007	0.122		0.337	0.026	0.519	0.056
	N	13	13	13	13	13	13	13	13	13
K2O	Pearson Correlation	.744**	.846**	-.819**	-.571*	0.29	1	-.615*	-0.09	0.279
	Sig. (2-tailed)	0.004	0	0.001	0.042	0.337		0.025	0.769	0.355
	N	13	13	13	13	13	13	13	13	13
P2O5	Pearson Correlation	-.875**	-.762**	.709**	0.091	-.612*	-.615*	1	-0.078	-0.102
	Sig. (2-tailed)	0	0.002	0.007	0.767	0.026	0.025		0.8	0.741
	N	13	13	13	13	13	13	13	13	13
SrO	Pearson Correlation	-0.178	-0.001	0.107	0.188	-0.197	-0.09	-0.078	1	0.22
	Sig. (2-tailed)	0.56	0.998	0.727	0.538	0.519	0.769	0.8		0.47
	N	13	13	13	13	13	13	13	13	13
BaO	Pearson Correlation	0.016	0.043	0.068	0.145	-0.542	0.279	-0.102	0.22	1
	Sig. (2-tailed)	0.958	0.89	0.825	0.637	0.056	0.355	0.741	0.47	
	N	13	13	13	13	13	13	13	13	13

APPENDIX VII: SCATTERGRAMS

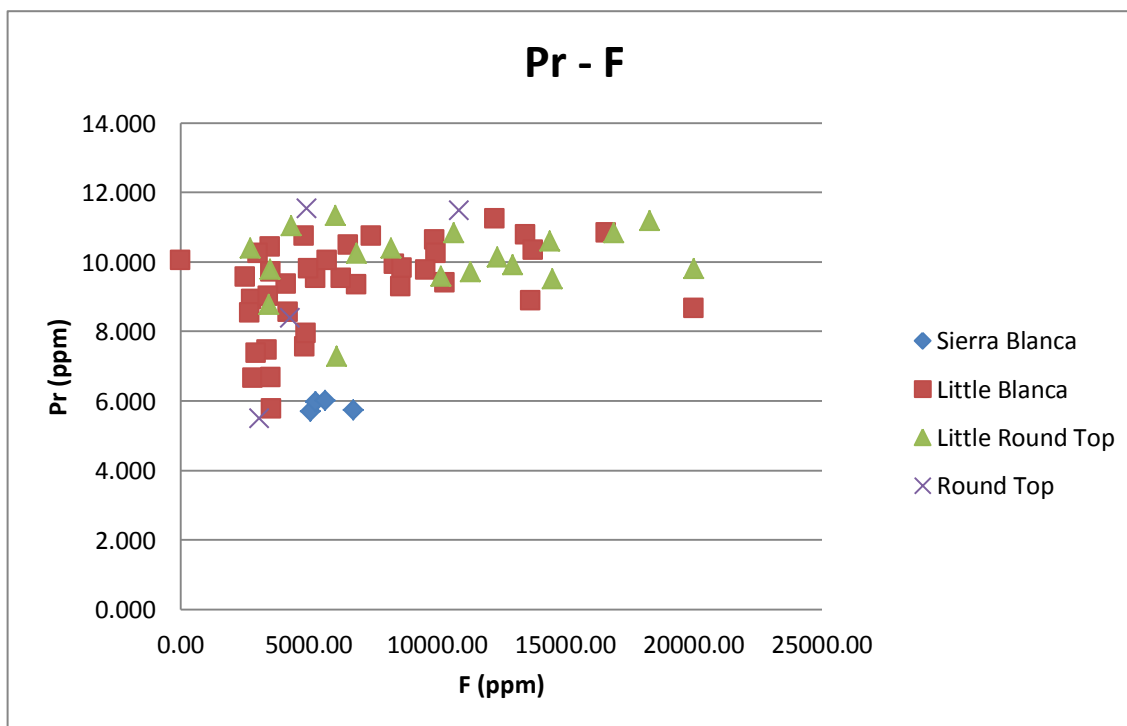
Scattergrams



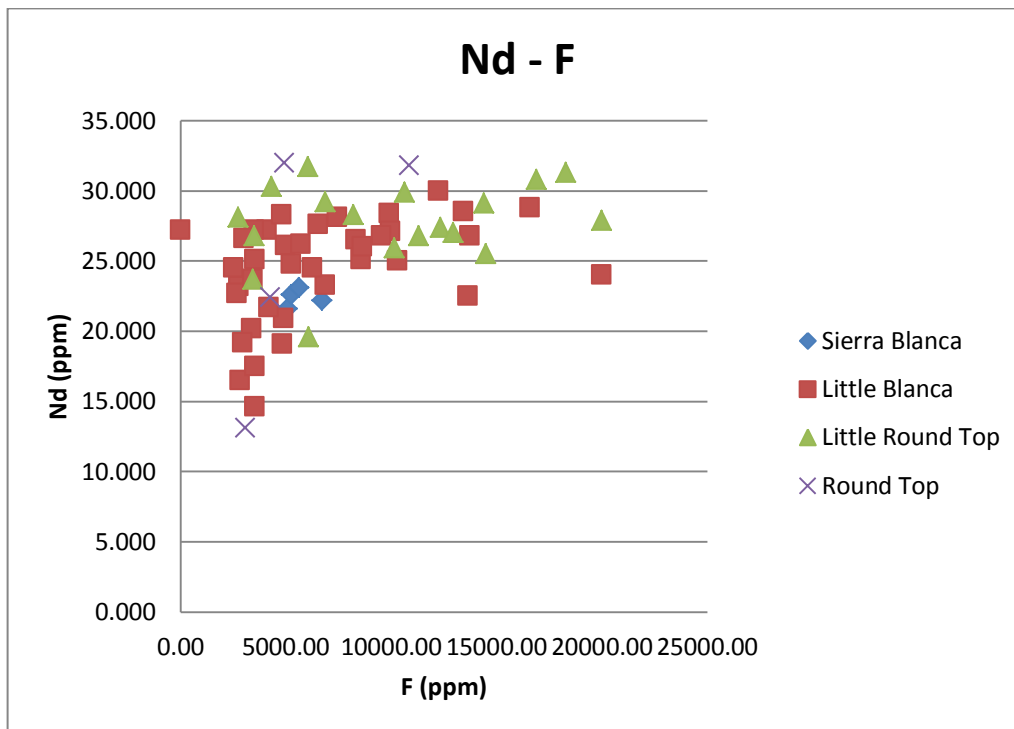
La-F



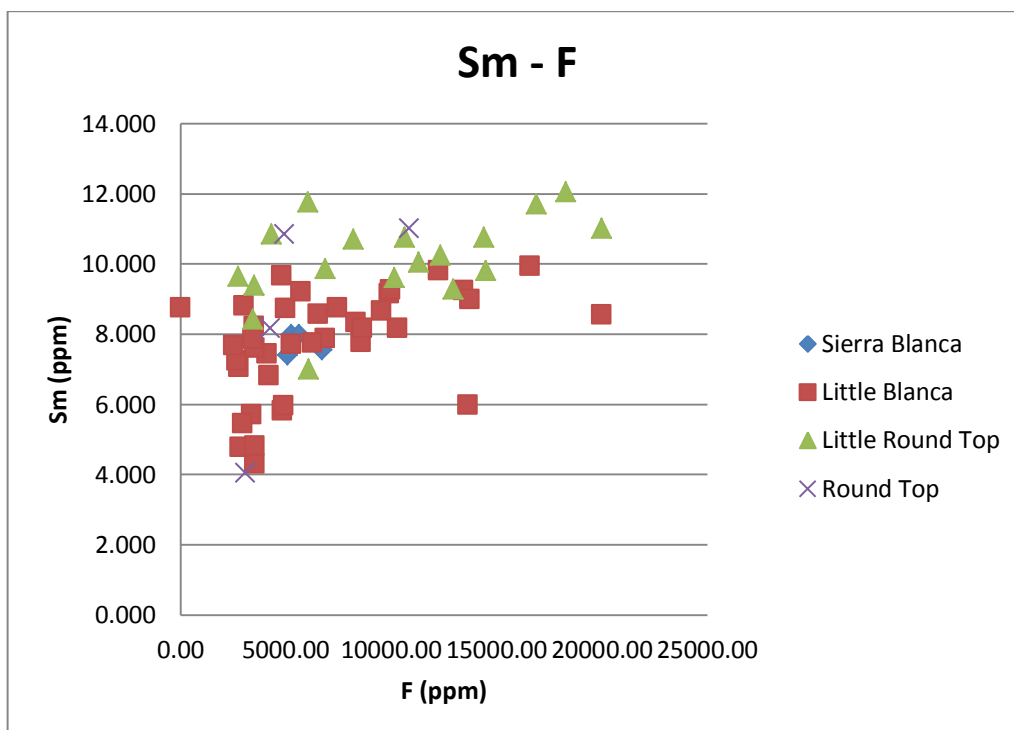
Ce-F



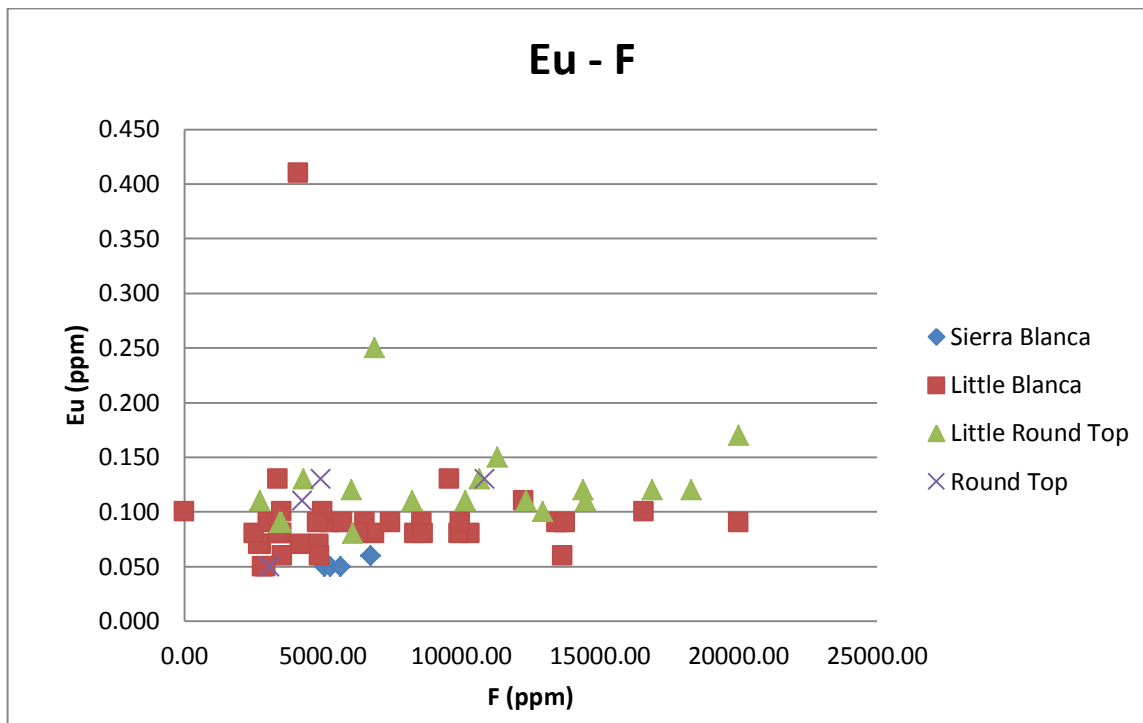
Pr-F



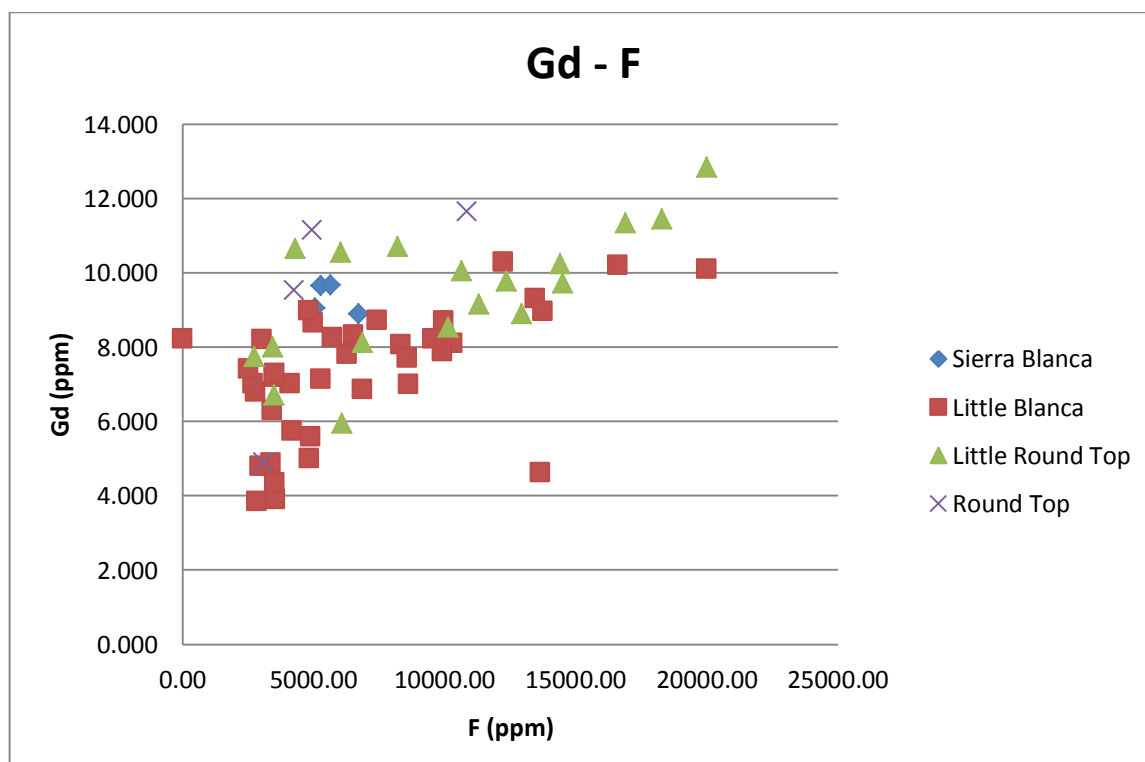
Nd-F



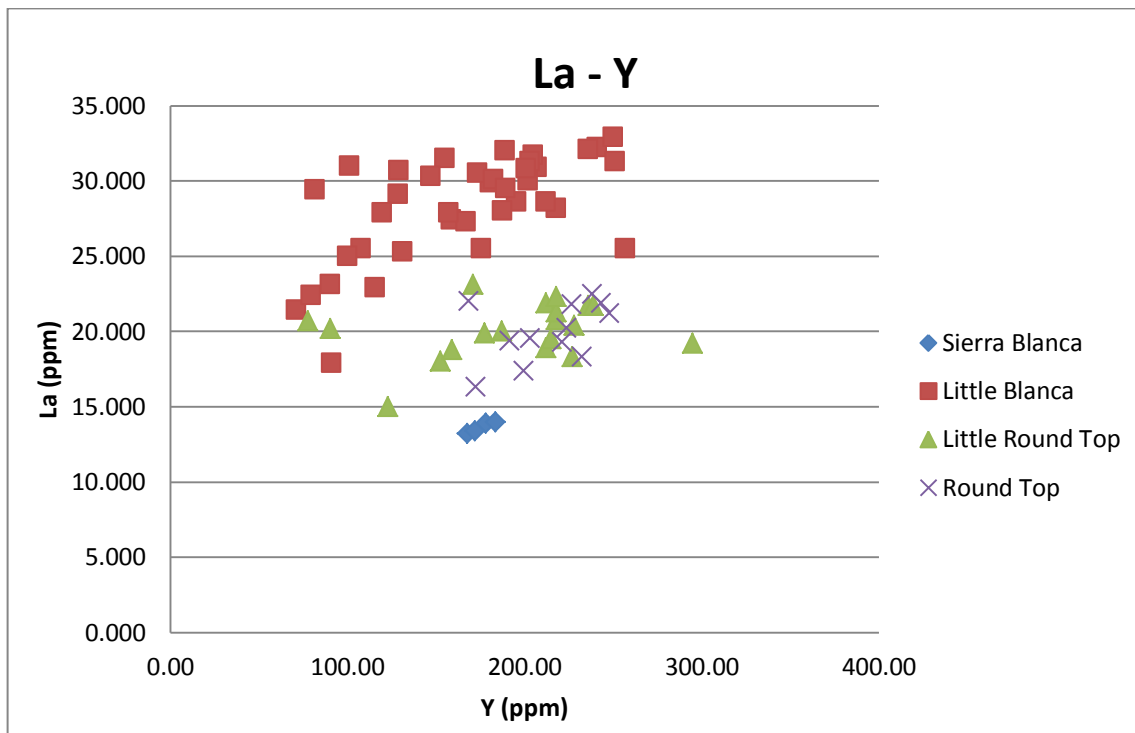
Sm-F



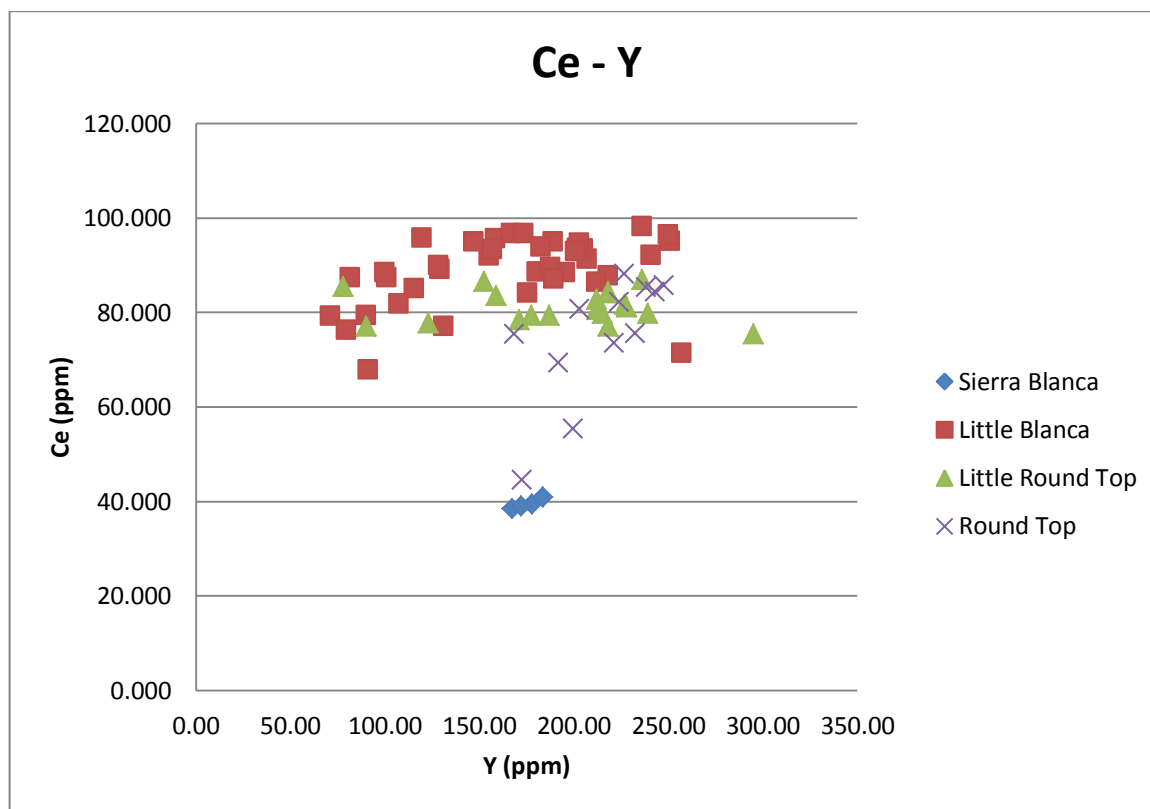
Eu-F



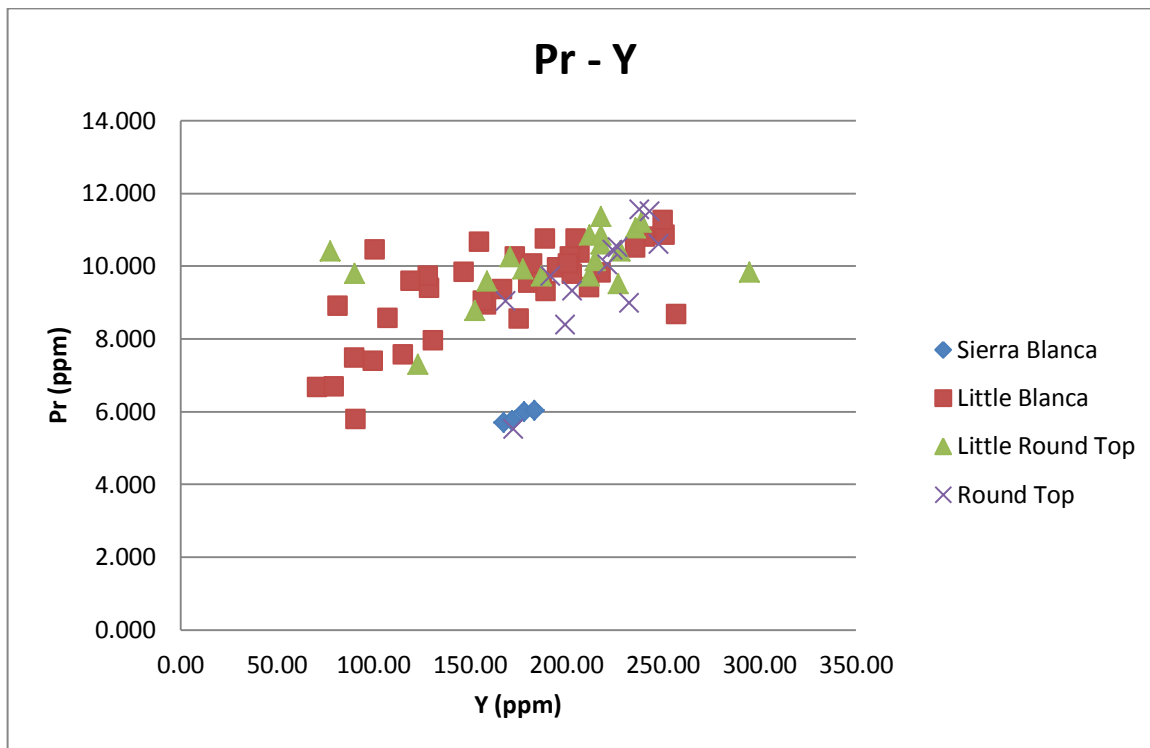
Gd-F



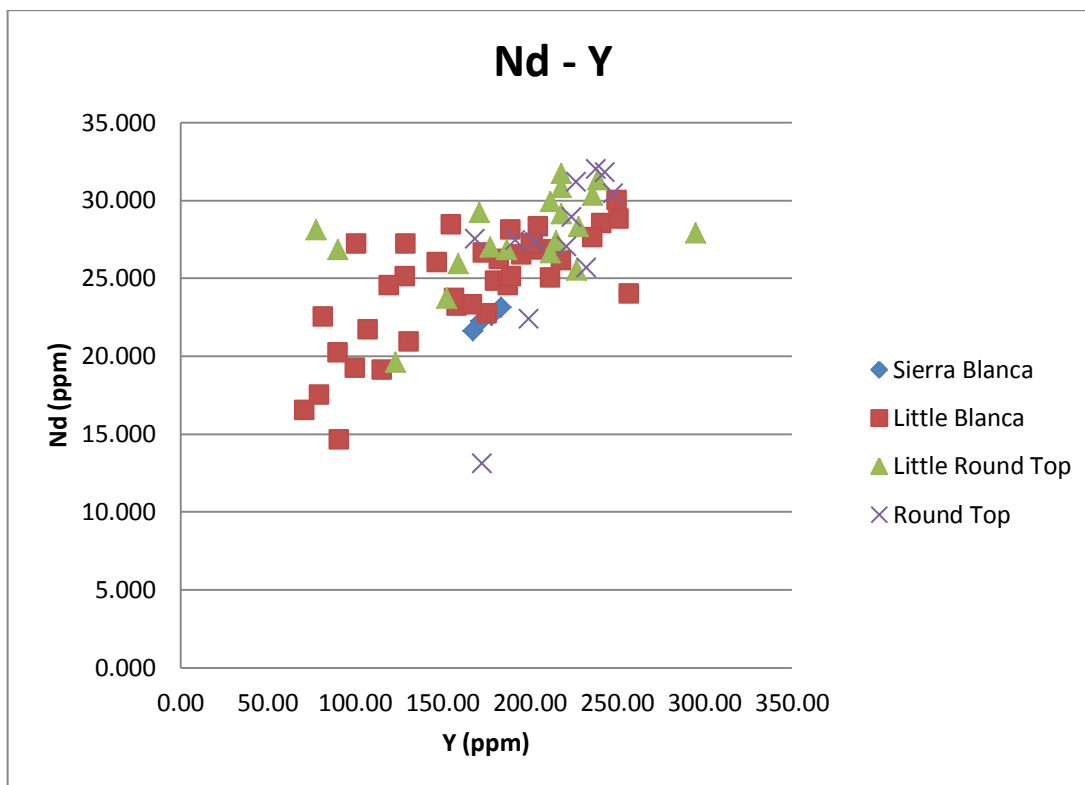
La-Y



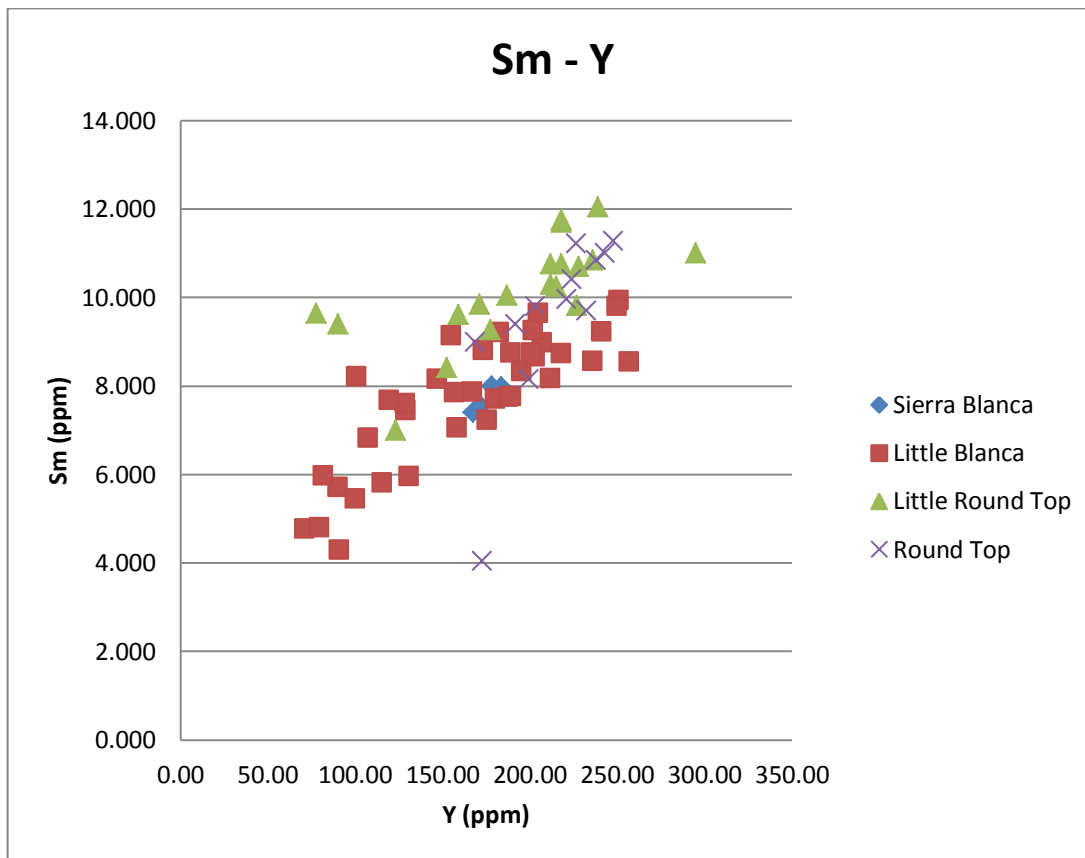
Ce-Y



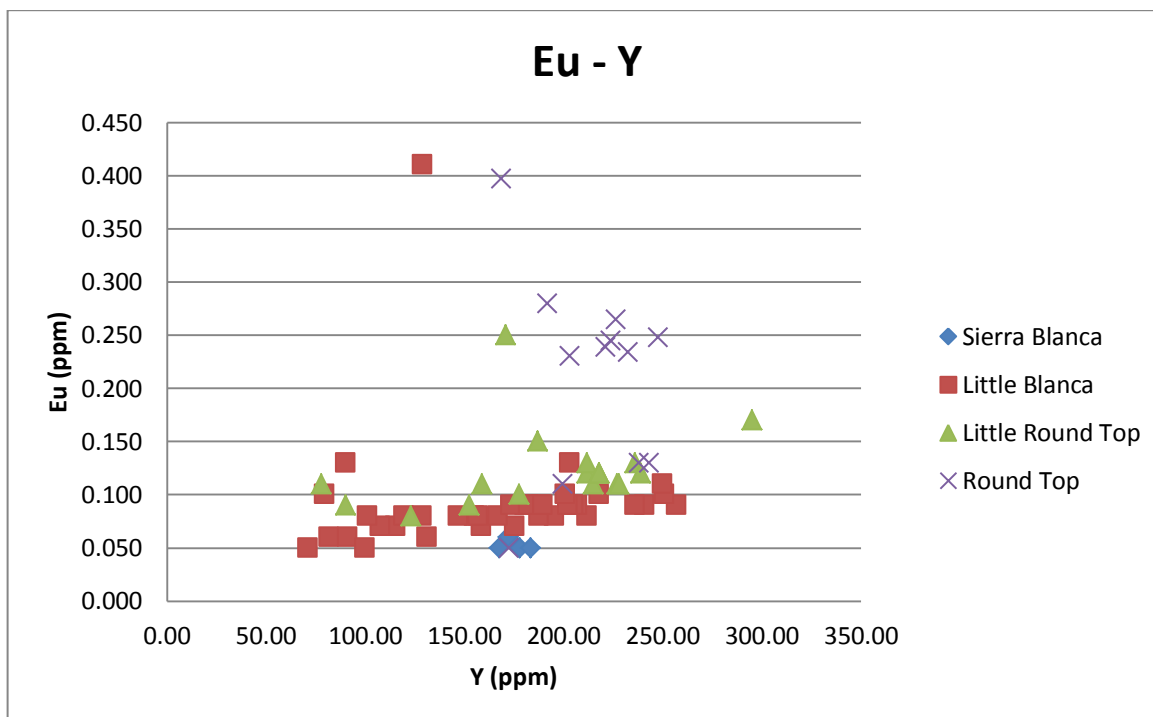
Pr-Y



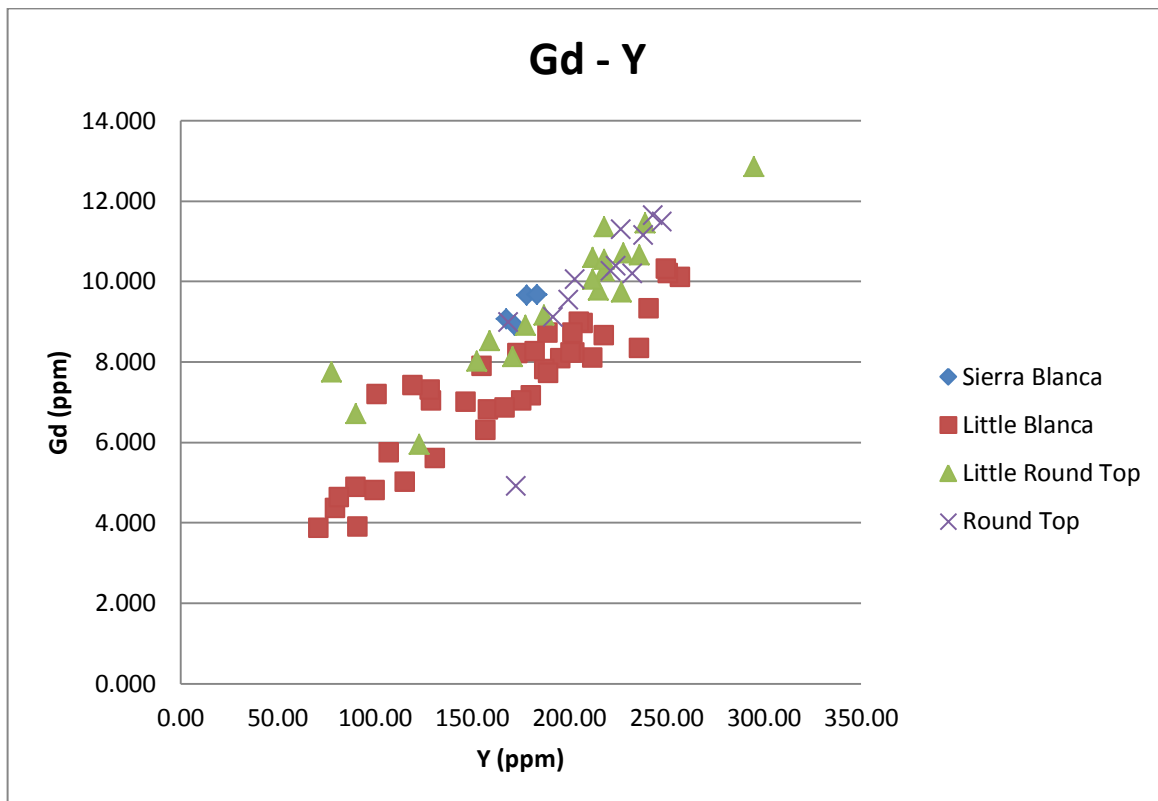
Nd-Y



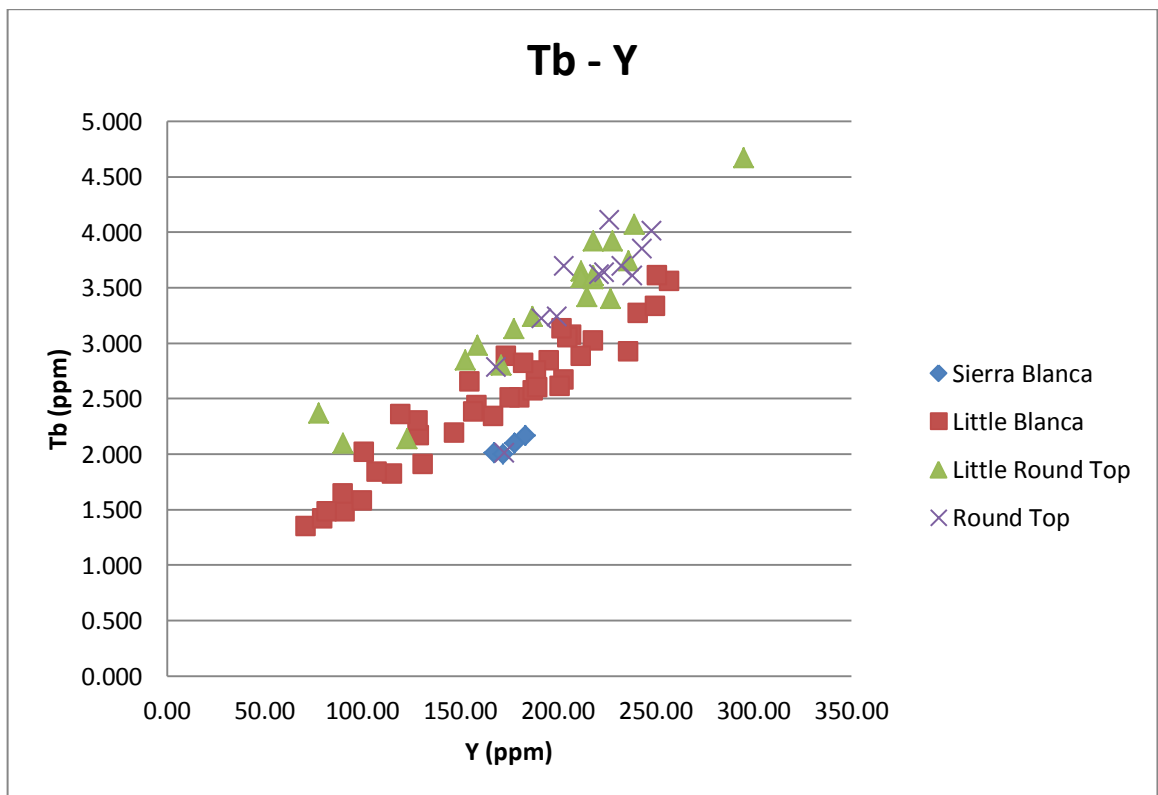
Sm-Y



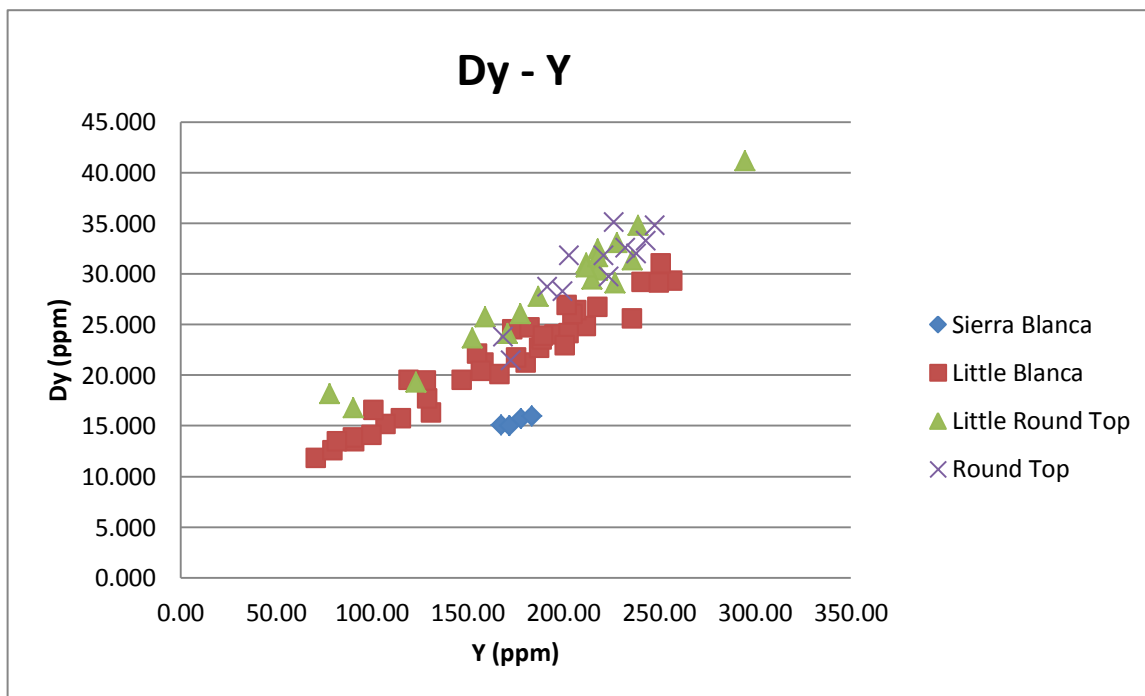
Eu-Y



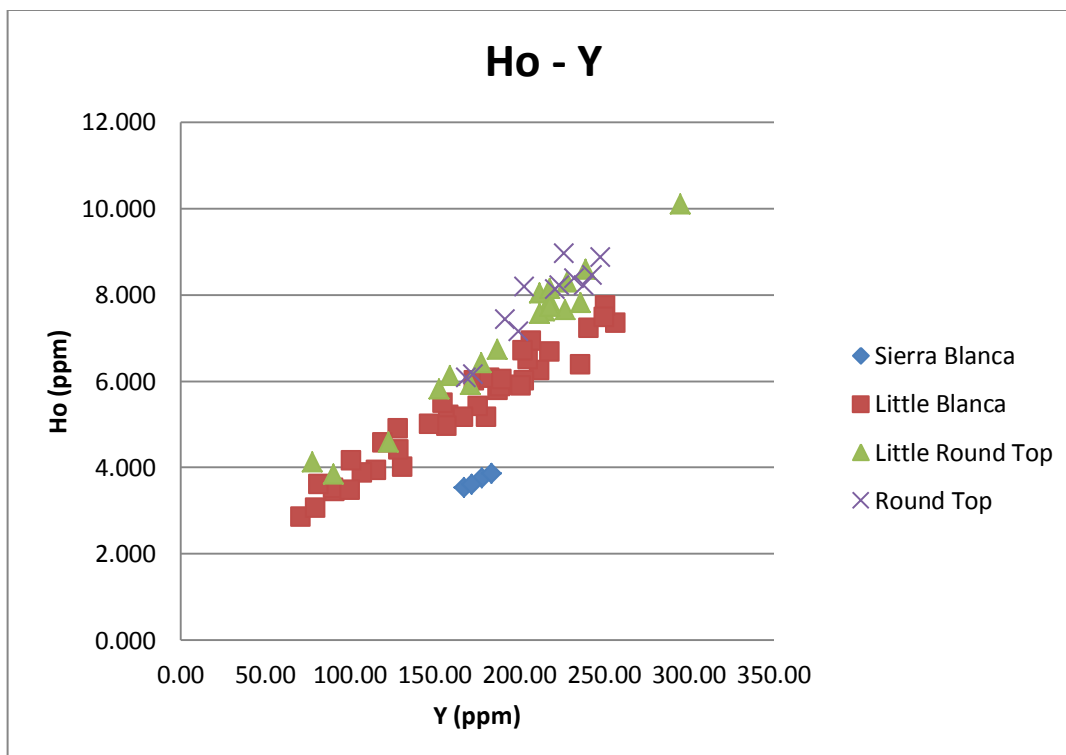
Gd-Y



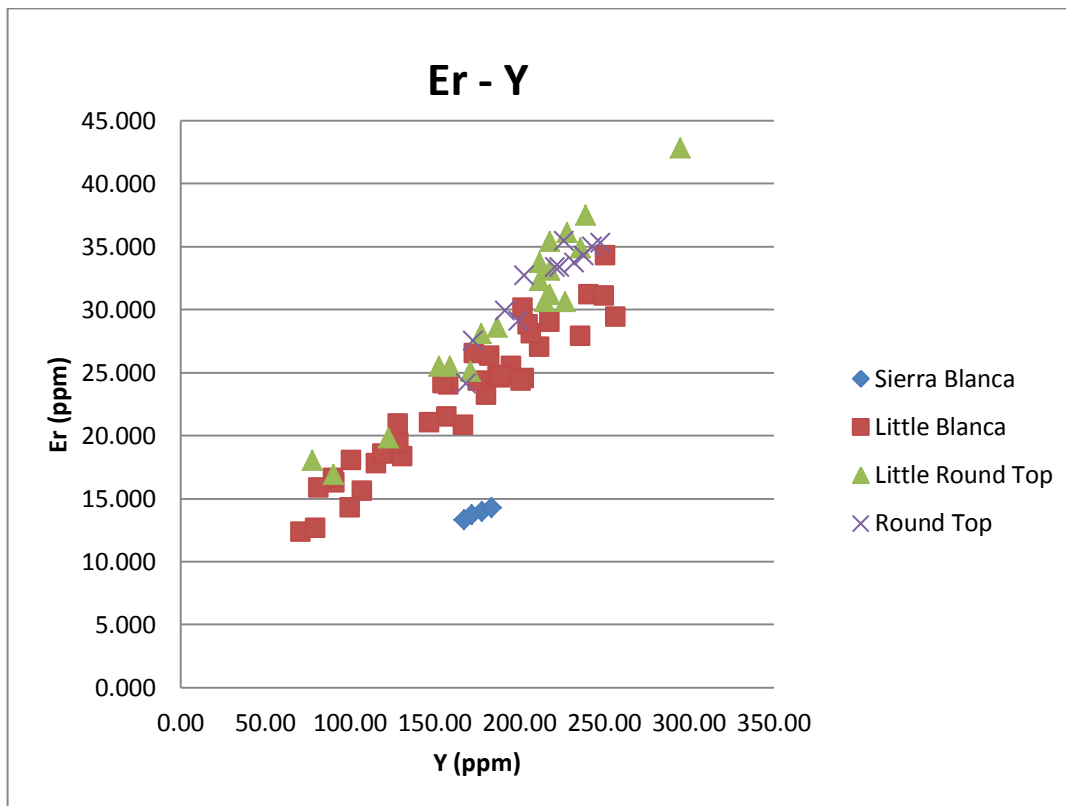
Tb-Y



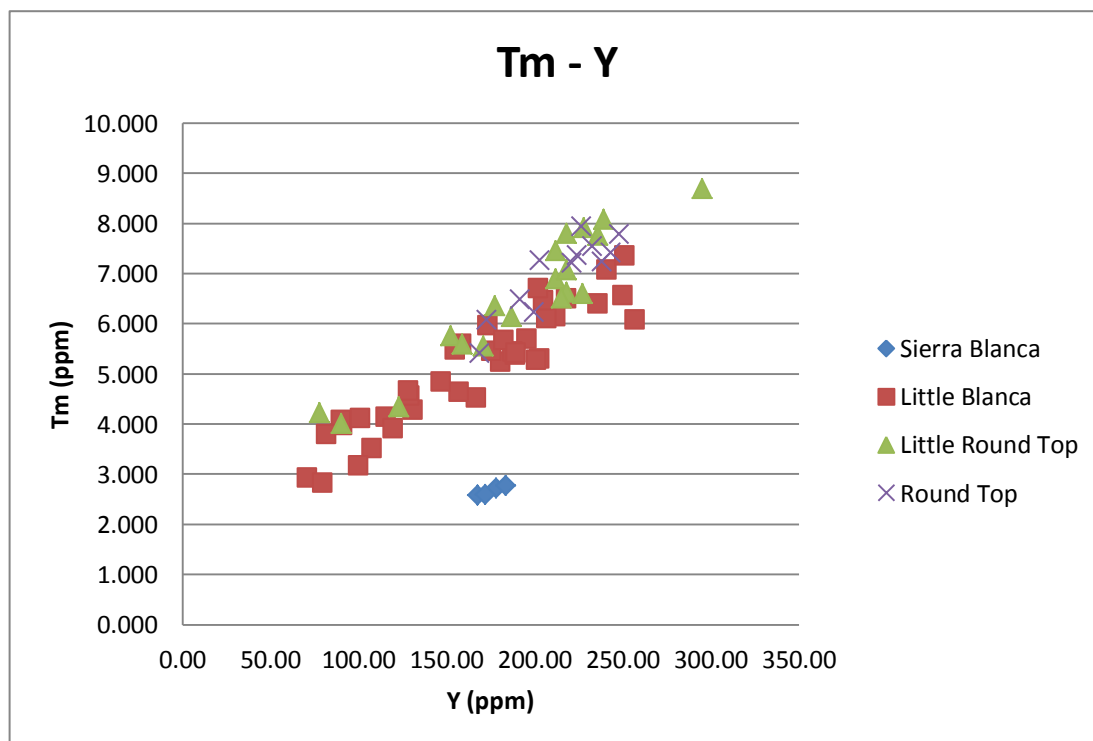
Dy-Y



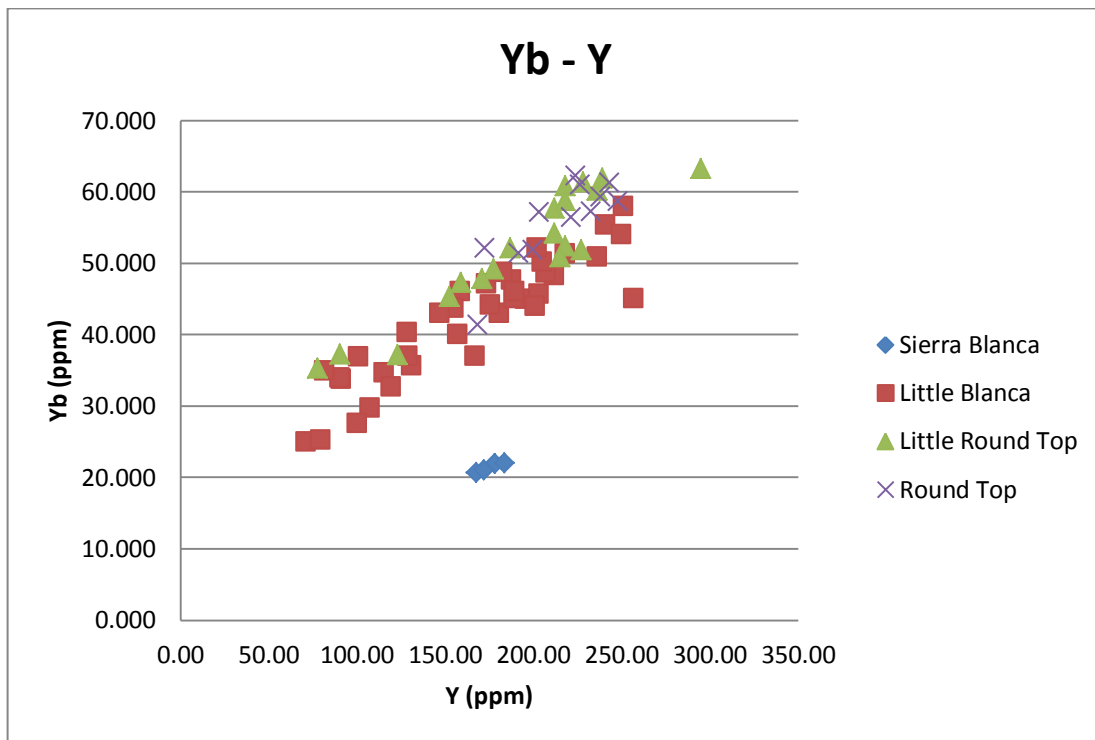
Ho-Y



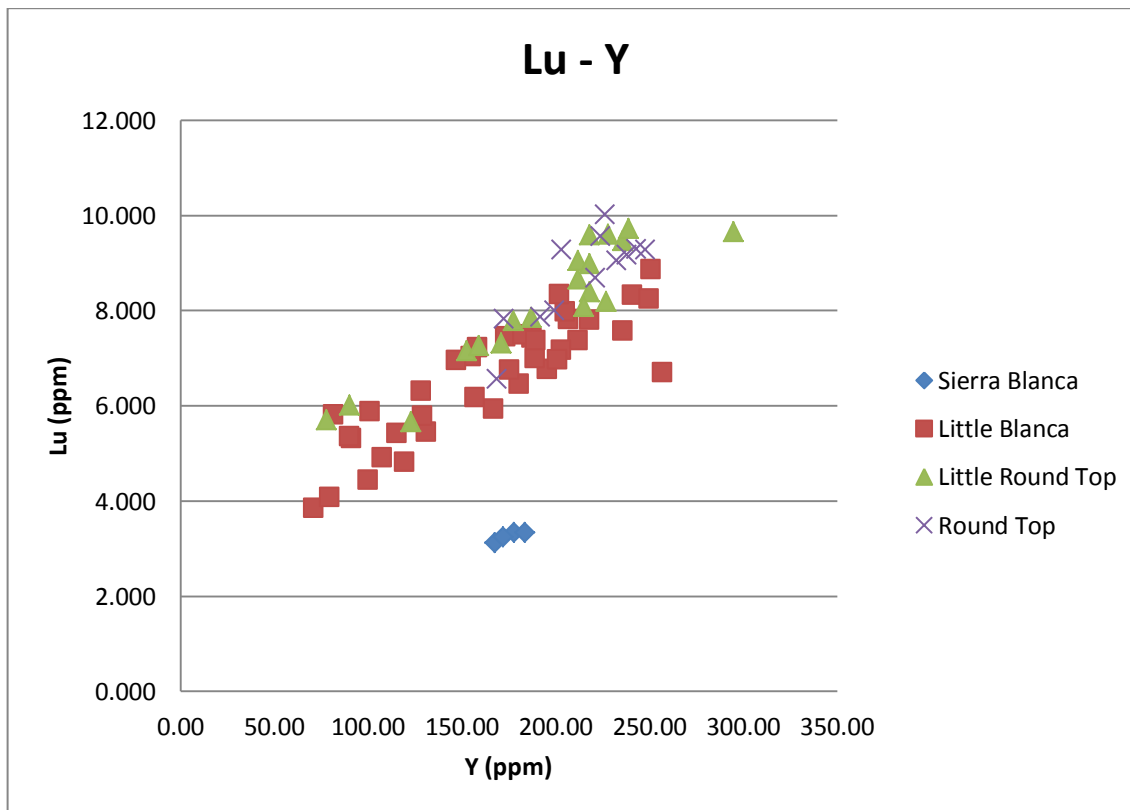
Er-Y



Tm-Y



Yb-Y



Lu-Y

APPENDIX VIII: FACTOR ANALYSIS

Little Blanca

Component Matrix ^a									
	Component								
	1	2	3	4	5	6	7	8	9
Ba	.190	-.507	-.687	.453	-.029	.042	.055	.048	-.146
Be	.575	-.571	.077	-.418	-.261	-.174	.110	.203	-.107
Ce	.415	.496	.566	-.391	.079	-.078	-.138	.276	.014
Cs	.133	-.796	.363	.198	.374	.117	-.143	-.020	.054
Dy	.839	.500	.000	-.113	.060	.075	-.146	.008	-.048
Er	.875	.424	-.111	-.011	.143	.096	-.070	-.082	-.026
Eu	.658	.568	.355	.280	-.126	.023	-.077	.000	.129
F	.802	-.100	-.197	.300	-.104	.223	-.327	.225	.000
Ga	-.481	.676	.157	.437	-.246	-.113	-.030	-.125	.073
Gd	.826	.476	.173	.161	-.163	-.007	-.064	.065	-.015
Hf	-.295	.677	-.010	-.492	.048	.375	.167	.190	.071
Ho	.848	.489	-.050	-.011	.049	.125	-.129	-.025	-.064
La	.694	-.074	.389	.469	-.035	-.028	.359	.100	.034
Lu	.822	.296	-.265	.207	.256	.143	.020	-.179	-.070
Mo	.733	-.295	.083	-.375	.380	-.010	.107	-.228	.140
Nb	-.667	.595	.240	.261	-.224	.058	-.121	-.084	.008
Nd	.800	-.099	.343	.398	-.098	-.053	.218	.076	.095
Pr	.749	-.054	.390	.432	-.110	-.089	.257	.085	.055
Rb	.080	-.822	.370	-.013	.113	.347	.161	-.144	-.015
Sm	.939	.055	.208	.107	.019	-.155	.139	-.047	.121
Sn	-.621	.549	.235	.239	.190	.378	.054	-.135	.031
Sr	.347	-.235	-.092	-.103	-.865	.093	.102	.196	-.005
Ta	-.666	.562	.016	-.123	.054	.200	.420	-.072	.040
Tb	.862	.462	.053	-.145	.064	.040	-.114	.023	-.001
Th	-.148	.737	-.219	.119	.069	.479	.312	.014	-.203
Tl	.024	-.899	.262	.001	.064	.275	.013	.106	-.178
Tm	.882	.350	-.156	.011	.228	.091	.000	-.123	-.023
U	.371	-.578	-.226	.087	-.156	.347	.412	.020	.392
Y	.814	.501	-.091	.018	.002	.110	-.148	.029	-.209
Yb	.823	.386	-.225	.184	.185	.150	-.041	-.153	-.090
Zn	.037	-.854	.224	.229	.383	.096	-.051	-.075	-.044
Zr	-.140	.659	.073	-.560	.028	.405	.084	.223	.075
SiO2	-.104	.296	.199	.001	.685	-.309	.404	.332	-.155
Al2O3	-.606	.451	-.029	.586	.014	-.131	.014	.243	-.094
Fe2O3	-.604	.104	-.146	.443	.193	.298	-.347	.202	.347
CaO	.651	-.296	-.403	-.093	.245	.015	-.326	.338	.192
Na2O	.077	.907	-.024	.146	.150	-.202	.260	.126	.053
K2O	.115	-.922	.182	-.096	.228	.148	.039	.132	-.046
P2O5	.496	.245	-.535	-.299	.110	-.406	.219	-.173	.253
SrO	.747	-.207	.142	-.148	-.514	.204	.129	-.158	-.095
BaO	.059	-.413	-.776	.234	.035	.033	.360	.175	-.077

Extraction Method: Principal Component Analysis.

a. 9 components extracted.

Little Round Top

Component Matrix ^a									
	Component								
	1	2	3	4	5	6	7	8	9
Ba	-.078	-.669	.567	.038	-.370	.230	.051	.175	.000
Be	-.288	-.726	.002	.556	-.185	.163	.116	-.087	.000
Ce	.841	-.007	.195	.369	.290	-.102	-.101	.115	.000
Cs	.309	-.262	.284	.337	.431	.671	-.041	-.056	.000
Dy	-.744	.628	-.070	.195	-.082	.007	-.043	-.032	.000
Er	-.673	.677	-.082	.256	-.120	.033	-.031	-.029	.000
Eu	-.789	.221	.509	-.003	.094	-.047	-.240	-.002	.000
F	-.680	.497	-.180	-.266	-.116	.354	.115	.186	.000
Ga	.931	.326	-.023	.026	-.056	.098	.019	-.116	.000
Gd	-.750	.646	.079	.058	.059	-.074	-.011	.043	.000
Hf	.925	.342	-.151	-.028	-.016	.045	.015	.030	.000
Ho	-.706	.650	-.101	.235	-.106	.020	-.026	-.017	.000
La	.195	.701	.597	-.329	-.008	.064	-.022	-.028	.000
Lu	-.517	.807	-.049	.249	-.131	.011	-.005	.000	.000
Mo	-.130	-.131	.116	.189	.947	-.068	.109	-.054	.000
Nb	.827	.502	-.133	.094	-.035	.144	.055	-.111	.000
Nd	-.120	.763	.522	-.334	.130	.014	.040	.032	.000
Pr	.053	.738	.564	-.355	.054	-.035	.052	-.047	.000
Rb	.943	.284	.037	.103	-.095	.041	.037	-.081	.000
Sm	-.403	.801	.274	-.259	.214	-.072	-.045	.031	.000
Sn	.848	.516	-.033	.022	-.015	-.081	-.038	-.072	.000
Sr	-.888	.119	-.150	-.106	.164	.095	.354	.046	.000
Ta	.877	.438	-.181	-.058	-.020	-.051	.008	.005	.000
Tb	-.736	.651	-.044	.165	-.051	-.034	-.027	-.003	.000
Th	.822	.458	-.044	.062	.315	.020	-.070	.068	.000
Tl	.915	.304	.108	.224	-.048	-.056	-.015	-.049	.000
Tm	-.613	.723	-.073	.270	-.146	.037	-.014	-.017	.000
U	-.908	.094	-.250	.142	.208	.183	-.073	.046	.000
Y	-.642	.636	-.106	.358	-.179	.091	.022	-.052	.000
Yb	-.552	.778	-.056	.259	-.136	.011	-.018	-.004	.000
Zn	.782	.196	.016	.462	.058	.145	-.291	.163	.000
Zr	.961	.236	-.112	-.014	-.018	.072	.040	-.034	.000
SiO2	.943	.292	-.050	-.004	-.086	.127	.011	-.005	.000
Al2O3	.877	.447	-.081	-.026	-.094	.117	.033	.027	.000
Fe2O3	.701	-.116	.192	.536	-.127	-.332	.115	.178	.000
CaO	-.947	-.291	.048	.055	.053	-.047	-.082	.046	.000
Na2O	.649	.577	-.317	-.250	.107	.159	.146	.159	.000
K2O	.949	.113	.193	-.119	-.168	-.020	-.074	.034	.000
P2O5	.160	.342	.596	.605	.081	-.175	.314	.015	.000
SrO	-.967	-.159	.005	-.012	.183	-.027	-.077	-.010	.000
BaO	-.195	-.443	.783	-.016	-.341	.178	.012	-.070	.000
Extraction Method: Principal Component Analysis.									
a. 9 components extracted.									

Round Top

Component Matrix ^a									
	Component								
	1	2	3	4	5	6	7	8	9
Ba	-.002	-.309	-.005	.799	.261	.432	.105	.000	.000
Be	.062	-.314	.423	.136	.700	-.445	.109	.000	.000
Ce	-.385	.606	.638	.174	.124	-.061	-.169	.000	.000
Cs	.712	-.174	-.338	.110	-.560	.051	-.141	.000	.000
Dy	.045	.859	.443	-.035	-.108	.212	.076	.000	.000
Er	-.221	.921	-.228	-.170	-.007	.040	-.140	.000	.000
Eu	-.971	.217	.032	-.041	.071	.016	.048	.000	.000
F	.814	.234	-.235	.390	-.265	.038	.058	.000	.000
Ga	.865	.395	-.181	-.053	.238	-.038	.055	.000	.000
Gd	-.263	.698	.578	.168	.031	.172	.225	.000	.000
Hf	.853	.483	-.133	-.094	-.021	.029	.105	.000	.000
Ho	-.696	.519	-.494	-.046	-.015	.009	-.018	.000	.000
La	-.471	.478	.542	.426	.032	-.101	-.251	.000	.000
Lu	.303	.878	.011	-.275	.193	-.024	-.155	.000	.000
Mo	-.547	.333	-.487	.299	.396	-.305	.114	.000	.000
Nb	.971	.191	-.008	.031	-.025	.063	.122	.000	.000
Nd	-.792	.537	-.285	.044	-.014	.032	.000	.000	.000
Pr	-.352	.726	.564	.117	.002	.133	-.008	.000	.000
Rb	.933	.294	-.174	.104	.008	.046	-.017	.000	.000
Sm	-.323	.606	.689	.107	.044	.162	.122	.000	.000
Sn	.760	.520	-.355	.067	-.108	-.074	.071	.000	.000
Sr	-.240	.318	.750	.228	-.378	-.282	.073	.000	.000
Ta	.622	.653	-.374	-.154	.100	-.004	.112	.000	.000
Tb	-.693	.672	-.238	-.014	-.004	.069	.082	.000	.000
Th	.888	.380	.099	-.070	.151	-.107	-.131	.000	.000
Tl	-.381	.666	-.616	.168	.008	.034	.048	.000	.000
Tm	-.671	.521	-.522	-.059	-.004	-.013	-.045	.000	.000
U	-.459	.029	.250	-.771	-.114	.313	.145	.000	.000
Y	.409	.814	.401	.011	.056	.050	-.056	.000	.000
Yb	.558	.726	.123	-.314	.144	-.044	-.160	.000	.000
Zn	-.056	-.389	.533	-.670	.309	.113	-.068	.000	.000
Zr	.964	.244	-.010	.065	-.008	-.018	.078	.000	.000
SiO ₂	.901	-.239	.241	.072	.240	-.036	.095	.000	.000
Al ₂ O ₃	.954	.066	.209	.004	-.039	.188	.070	.000	.000
Fe ₂ O ₃	-.994	-.025	.050	.015	.051	-.012	.071	.000	.000
CaO	-.661	-.520	.456	-.076	-.214	.173	-.061	.000	.000
Na ₂ O	.838	-.005	.333	-.428	-.038	-.044	-.003	.000	.000
K ₂ O	.978	.024	-.003	.098	.110	.090	-.116	.000	.000
P ₂ O ₅	-.735	.375	-.564	-.011	-.020	-.011	-.009	.000	.000
SrO	.033	.263	.485	.147	-.618	-.526	.120	.000	.000
BaO	.215	-.155	.162	.908	.077	.224	-.152	.000	.000

Extraction Method: Principal Component Analysis.

a. 9 components extracted.

VITA

Nicole Kyger, née Free, was born in Toronto, Ontario to Bernhard and Edith Free, PhD Geology and PhD Geography, respectively. After leaving Toronto the family moved to Calgary, Alberta, for just under two years. Business led Dr. Free to immigrate to the US, and the family found themselves in Denver, Colorado, where Nicole attended first through twelfth grade, graduating with honors from Cherry Creek High School. After high school, Nicole went to Vienna, Austria, attended Modul University, receiving the degree of Hotelkaufmann in Hotel and Restaurant Management. Following several years in the hotel industry, Nicole returned to school and received a bachelor's degree, Summa cum Laude, from the University of Colorado, majoring in archaeology with a minor in geology. Subsequently, Nicole joined the U. S. Marine Corps as an unmanned aerial vehicle (UAV) pilot, eventually being promoted to the non-commissioned officer rank of Corporal. After an honorable discharge from the Marine Corps, Nicole completed a post-baccalaureate certificate course in Geographic Information Systems through Pennsylvania State University. After working for two and a half years at the Texas A&M AgriLife Research Center in El Paso, TX, Nicole returned to school to pursue a master's degree in geology at the University of Texas at El Paso (UTEP). During her time at UTEP, Nicole worked with Texas Rare Earth Resources (TRER) as a geologist, taking part in the exploration and drilling program at the company's Round Top Mountain project. This work with TRER led in part to the preceding dissertation.

Permanent address: 721 Dakota River Ave
El Paso, TX 79932

This thesis was typed by Nicole Kyger